

**The Role of Tissue Transglutaminase in
the Extracellular Matrix Changes
Associated With Kidney Scarring**

**Marie Fisher
Academic Nephrology Unit
School of Medicine and Biomedical Sciences
University of Sheffield**

Thesis submitted for the degree of Doctor of Philosophy

June 2007

Volume 1

**This thesis is dedicated to my parents, Brian and
Carol Fisher, for their love, support and
encouragement**

nil desperandum

Acknowledgements

I would like to acknowledge the contribution of the following individuals and organisations to the completion of this PhD thesis:

Dr Tim Johnson: For his considerable support, encouragement and guidance during the supervision of my PhD and for his invaluable assistance with the preparation of manuscripts and constructive appraisal of the thesis.

Dr John Haylor: For his surgical expertise in performing the Subtotal Nephrectomy (section 3.6.3.3) and aortic perfusion procedures (section 3.6.3.1).

Professor Martin Griffin:

For the synthesis and supply of transglutaminase inhibitors (section 3.6.1) and for the provision of transglutaminase knockout mice for aortic perfusion (section 3.6.2.1).

Dr Rana Rustom: For kindly providing cell lysates and media for analysis from the LLC-PK1 pig proximal tubular cell acidosis model (section 3.1.7).

Dr Richard Jones: For his invaluable contribution to the isolation and characterisation of cells from the transglutaminase knockout mouse (sections 3.1.9 and 3.6.3.2) and for performing *in situ* transglutaminase activity (section 3.3.7.2), hydroxyproline (section 3.5.2.2) and ϵ -(γ -glutamyl) lysine analysis (section 3.3.8.2). Sadly, Richard passed away in June 2006 following a year long battle with a terminal brain tumour and is greatly missed by all who knew him both in a professional and personal capacity.

Dr Linghong Huang: For her technical assistance with the transfection of OK tubular epithelial cells (section 3.2.2).

Miss Zoe Hau: For her technical assistance with the immuno-histochemical and Northern blot analysis of tissue from the Subtotal Nephrectomy study (sections 3.5.2.4 and 3.4.8).

Miss Melissa Vickers: For her technical assistance with the measurement of albuminuria (section 3.6.4.3).

The Sheffield Kidney

Research Foundation: For their invaluable financial support in providing a number of bridging grants and for funding the purchase of laboratory consumables and equipment without which the completion of this thesis would not have been possible.

The work presented in this thesis was supported by generous grants from the National Kidney Research Fund and the Wellcome Trust.

Abstract

The up-regulation and trafficking of tissue transglutaminase (TG2) has been implicated in the development of kidney scarring and the progression of chronic kidney disease (CKD). TG2 is a calcium dependent enzyme that catalyses the crosslinking of proteins via the formation of highly stable $\epsilon(\gamma\text{-glutamyl})$ lysine bonds. It is proposed that the increased formation of these bonds within the extracellular matrix (ECM) contributes to scarring directly by enhancing ECM deposition and impeding proteolytic degradation.

To investigate this, ECM metabolism was studied *in vitro* in tubular epithelial and mesangial cells stably transfected to over-express TG2 and in cells isolated from the TG2 knockout mouse. Further, *in vivo* TG2 inhibition studies were performed in rats subjected to 5/6^{ths} nephrectomy.

Increased expression of TG2 in tubular epithelial cells corresponded to increased extracellular TG2 activity ($p < 0.05$), elevated $\epsilon(\gamma\text{-glutamyl})$ lysine crosslinking in the ECM and higher levels of ECM collagen. Increased ECM collagen was attributable to elevated collagen III and IV. Elevated TG2 levels were associated with accelerated collagen deposition and reduced ECM breakdown by matrix metalloproteinases (MMPs). In contrast, a lack of tubular TG2 was associated with reduced $\epsilon(\gamma\text{-glutamyl})$ lysine crosslinking in the ECM, causing reduced ECM collagen levels and lower ECM per cell.

TG2 over-expressing mesangial cells differed from tubular cells in their handling of TG2 by retaining the enzyme and failing to show increases in extracellular activity, $\epsilon(\gamma\text{-glutamyl})$ lysine crosslinking or ECM levels.

The *in vivo* application of site-directed irreversible TG2 inhibitors strongly supported a causative role for TG2 in the accumulation of ECM associated with scarring. Inhibition of TG2 was effective at preventing a decline in kidney function by reducing glomerulosclerosis and tubulointerstitial fibrosis through a lowering in the accumulation of interstitial collagen.

The data presented here demonstrates a direct pathological role for TG2 in the accumulation of matrix associated with kidney scarring.

Publications

Accepted Papers:

Transglutaminase Inhibition Ameliorates Scarring and Preserves Function in Experimental Chronic Kidney Disease *Johnson T.S., Fisher M., Haylor J.L., Hau Z., Skill N.J., Jones R., Saint R., Coutts I., Vickers M.E., El Nahas A.M. and Griffin M.* Accepted for publication by J Am Soc Nephrol April 2007

Papers in preparation:

Modulation of Tissue Transglutaminase in Tubular Epithelial Cells Alters Extracellular Matrix Levels *in vitro*: a mechanism of kidney scarring *Fisher M., Jones R., Huang L., Haylor J.L., Griffin M., El Nahas A.M. and Johnson T.S.* Awaiting submission

Mesangial Cells: Regulation of Tissue Transglutaminase Cell Export and its Affect on Extracellular Matrix Level and Composition *Fisher M., Jones R., Huang L., Haylor J.L., Griffin M., El Nahas A.M. and Johnson T.S.* Awaiting submission

Abstracts:

Primary Tubular Cells Isolated From the Transglutaminase Knockout Mouse Deposit Less Extracellular Matrix Than Wild Type Cells *Fisher M., Jones R., Griffin M. and Johnson T.S.* Proceedings of the Annual Renal Association Meeting, Harrogate May 2006 Poster presentation RA6395

Over-expression of Tissue Transglutaminase in Proximal Tubular Epithelial Cells Affects Extracellular Matrix Accumulation *in vitro* *Fisher M., Huang L., Hau Z., Griffin M., El Nahas A.M. and Johnson T.S.* Proceedings of the 3rd World Congress of Nephrology meeting June 2005 Poster presentation W-PO20059

Over-expression of Tissue Transglutaminase in Proximal Tubular Epithelial Cells Affects Extracellular Matrix Accumulation *in vitro* *Fisher M., Huang L., Hau Z., Griffin M., El Nahas A. M. and Johnson T.S.* Proceedings of the 8th International Conference on Protein Crosslinking Reactions and Transglutaminases Leubeck, Germany 2005 Poster presentation 2.1

Over-expression of Tissue Transglutaminase in Proximal Tubular Epithelial and Mesangial Cells Leads to a Differential Cell Surface Activity *Fisher M., Huang L., Hau Z., Griffin M., El Nahas A.M. and Johnson T.S.* Proceedings of the Renal Association Spring Meeting, Aberdeen April 2004 Poster Presentation P5

Over-expression of Tissue Transglutaminase Produces Qualitative Changes to the Extracellular Matrix *Fisher M., Huang L., Hau Z., Griffin M., El Nahas A.M. and Johnson T.S.* Proceedings of the Renal Association Spring Meeting, Aberdeen April 2004 Poster Presentation P6

Factors Associated with Renal Scarring that Lead to Changes in Tissue Transglutaminase Expression and Release by Renal Tubular Epithelial Cells *Fisher M., Skill N.J., Huang L., Rustom R., El Nahas A. M., Griffin. M. and Johnson T.S.* Proceedings of the 7th International Conference on Transglutaminases and Protein Crosslinking Reactions, Ferrara, Italy September 2002 Oral presentation

Table of Contents

	Page
Acknowledgements	i
Abstract	ii
Publications	iii
Table of contents	iv
Table of figures	xi
Chapter 1 Introduction	1
1.1 Chronic Kidney Disease (CKD)	2
1.2 Clinical Features of CKD	2
1.3 Progression of CKD	4
1.4 Mechanisms of CKD Progression	4
1.4.1 Systemic and glomerular hypertension	4
1.4.2 Proteinuria	5
1.4.3 Hypoxia	7
1.4.4 Oxidative stress	9
1.4.5 Hypermetabolism	10
1.5 Kidney Scarring	11
1.5.1 Pathology of kidney scarring	11
1.5.2 Pathophysiological events in kidney scarring	11
1.5.2.1 The endothelial response	11
1.5.2.2 Glomerular and interstitial inflammation	13
1.5.2.3 Release of pro-fibrogenic growth factors	14
1.5.2.4 Proliferation and transdifferentiation	15
1.5.2.5 Extracellular matrix accumulation	16
1.6 The Renal ECM	18
1.6.1 Distribution and function of the renal ECM	18
1.6.1.1 Renal interstitium	18
1.6.1.2 Glomerular mesangium	19
1.6.1.3 Glomerular basement membrane (GBM)	19
1.6.2 Major components of the renal ECM	19
1.6.2.1 Collagens	19
1.6.2.1.1 The collagen family	19
1.6.2.1.2 Biosynthesis of collagens	20
1.6.2.1.3 Regulation of collagen synthesis	24
1.6.2.2 Non collagenous glycoproteins	25
1.6.2.2.1 Fibronectin	25
1.6.2.2.2 Assembly of fibronectin	25
1.6.2.2.3 Laminin	26
1.6.2.2.4 Tenascin	29
1.6.2.2.5 SPARC (secreted protein acidic and rich in cysteine)	29
1.6.2.2.6 Thrombospondin	30
1.6.2.3 Proteoglycans	31
1.6.3 Renal ECM degrading enzymes	32
1.6.3.1 Matrix metalloproteinases (MMPs)	32
1.6.3.1.1 Transcriptional regulation of MMPs	33

	Page
1.6.3.1.2 Activation of MMPs	34
1.6.3.1.3 Inhibition of MMPs	35
1.6.3.1.4 MMP cleavage of the ECM	36
1.6.3.1.5 Effects of MMP action on cell function	38
1.6.3.1.6 Renal expression of MMPs and TIMPs	39
1.6.3.2 Plasminogen/ plasmin system	40
1.6.3.3 Cathepsins	41
1.7 Changes in the ECM in Renal Disease	42
1.7.1 Increased synthesis of ECM components	42
1.7.2 Impairment of ECM degradation	43
1.7.3 Stabilisation of the ECM	44
1.8 Transglutaminase	45
1.8.1 Transglutaminase (TG) gene family	45
1.8.2 Tissue transglutaminase (TG2)	47
1.8.2.1 Three dimensional structure of TG2	47
1.8.2.2 Regulation of TG2	49
1.8.2.2.1 Transcriptional regulation of TG2	49
1.8.2.2.2 Regulation of transglutaminase activity	51
1.8.2.3 Expression and localisation of TG2	52
1.8.2.4 Substrate specificity and requirements of TG2	53
1.8.2.5 Multifunctional roles of TG2	55
1.8.2.5.1 Cell growth and proliferation	55
1.8.2.5.2 Cell death	55
1.8.2.5.3 Transmembrane signalling	57
1.8.2.5.4 Cell matrix interactions	57
1.8.2.5.5 Stabilisation of ECM	59
1.8.2.6 TG2 and disease	59
1.8.2.6.1 TG2 in scarring and fibrosis	59
1.9 Thesis Rationale and Hypothesis	60
Chapter 2 Aims	62
Chapter 3 Materials and Methods	64
3.1 Cell Culture	65
3.1.1 Cell lines	65
3.1.2 Cell culture media for cell lines	65
3.1.3 Primary cell culture media	65
3.1.4 Treatment with fibrogenic growth factors/cytokines	66
3.1.5 Treatment with known transglutaminase stimulators	66
3.1.6 Hypoxic treatment of NRK-52E tubular cells	66
3.1.7 Acidic treatment of LLC-PK1 tubular cells	67
3.1.8 Immunofluorescence for tubular cell markers	67
3.1.9 Immunofluorescence for mesangial cell markers	67
3.2 Transfection of Renal Cell Lines	68
3.2.1 Dose response to Geneticin (G418 sulphate)	68
3.2.2 Transfection of OK proximal tubular epithelial cells	69
3.2.3 Transfection of 1097 mesangial cells	69

	Page
3.2.3.1 Preparation of cell suspensions	69
3.2.3.2 Transfection procedure	69
3.2.3.3 Optimisation of the Nucleofection protocol	70
3.2.3.4 Co-transfection with pSVneo/pSG5-htg	70
3.2.3.5 β galactosidase assay	70
3.2.4 Selection of stable clones from transfected cells	72
3.2.5 Growth curves	72
3.3 General and Biochemical Techniques	72
3.3.1 Preparation of tissue homogenates	72
3.3.2 Preparation of cell lysates	73
3.3.3 Acetone precipitation of cell culture media	73
3.3.4 Processing and fixation of tissues	73
3.3.5 Preparation of cryostat sections	73
3.3.6 Western blotting	73
3.3.6.1 Polyacrylamide gel electrophoresis (SDS PAGE)	73
3.3.6.2 Electro-blotting	74
3.3.6.3 Probing of membranes	75
3.3.7 Detection of tissue transglutaminase	76
3.3.7.1 Transglutaminase activity by ^{14}C putrescine incorporation assay	76
3.3.7.2 Detection of <i>in situ</i> transglutaminase activity	78
3.3.7.3 Detection of transglutaminase by Western blot	78
3.3.7.4 TG2 immunocytochemistry	78
3.3.7.5 Extracellular TG activity of cultured cells	79
3.3.7.6 Extracellular TG2 antigen expression by cultured cells	79
3.3.8 Detection of $\epsilon(\gamma\text{-glutamyl})$ lysine crosslink	81
3.3.8.1 Immunofluorescence	81
3.3.8.2 Cation exchange chromatography	81
3.3.9 Quantitation of protein	82
3.3.9.1 Bicinchoninic acid assay	82
3.3.9.2 Lowry assay	82
3.4 Molecular Biology Techniques	83
3.4.1 Expression vectors/ TG2 cDNA	83
3.4.2 Preparation of expression vector pCIneo-htg	83
3.4.2.1 Linearisation of pCIneo plasmid	83
3.4.2.2 Ligation of pCIneo/3.3kb transglutaminase cDNA	83
3.4.3 Bacterial transformation	83
3.4.4 Small scale plasmid preparation	84
3.4.5 Large scale plasmid preparation	84
3.4.6 Ethanol precipitation of the plasmid	84
3.4.7 Agarose gel electrophoresis	86
3.4.8 Northern blotting	86
3.4.8.1 cDNA probes	86
3.4.8.2 RNA extraction	86
3.4.8.3 Electrophoresis of RNA/capillary blotting	87
3.4.8.4 Hybridisation of membranes	87
3.5 ECM Quantitation	88
3.5.1 Quantitation of total ECM protein	88

	Page
3.5.1.1 ³ H-amino acid incorporation	88
3.5.2 Collagen determination	88
3.5.2.1 ³ H-proline incorporation	88
3.5.2.2 Hydroxyproline analysis by gas liquid chromatography	90
3.5.2.2.1 Deoxycholate-insoluble ECM	90
3.5.2.2.2 Tissue homogenates	90
3.5.2.3 Collagen immunofluorescence <i>in vitro</i>	90
3.5.2.4 Immunohistochemical analysis of ECM on paraffin sections	91
3.5.2.5 Immunohistochemical analysis of collagen I on cryostat sections	92
3.5.2.6 Multi-phase image analysis of ECM	93
3.5.2.6.1 Selection of fields	93
3.5.2.6.2 Phase selection	93
3.5.2.6.3 Quantitation of staining	93
3.5.3 Measurement of ECM deposition rate	95
3.5.3.1 ECM labelling in the presence of the MMP inhibitor Galardin	95
3.5.4 ECM degradation	95
3.5.4.1 Activation of matrix metalloproteinase (MMP) enzymes	95
3.5.4.2 ECM degradation assays	95
3.5.4.3 Gelatin zymography	97
3.5.4.4 Fluorescent gelatinase assay	97
3.6 <i>In vivo</i> Experimentation	97
3.6.1 Transglutaminase inhibitors	97
3.6.2 Experimental animals	98
3.6.2.1 Transglutaminase knockout mice	98
3.6.2.2 Wistar rats (subtotal nephrectomy)	98
3.6.3 Experimental procedures	99
3.6.3.1 Retrograde perfusion of mouse kidneys	99
3.6.3.2 Isolation of tubular and mesangial cells from wild type and TG2 ^{-/-} mice	100
3.6.3.3 Subtotal (5/6th) nephrectomy (SNx)	101
3.6.3.4 Renal infusion of transglutaminase inhibitors	102
3.6.3.5 Infusion cannula and preparation of mini-osmotic pump	102
3.6.3.6 Implantation of mini-osmotic pump	102
3.6.4 Biochemical measurement of renal function	102
3.6.4.1 Creatinine	102
3.6.4.2 Proteinuria	103
3.6.4.3 Albuminuria	103
3.6.5 Biochemical measurement of liver function	103
3.6.6 Fibrin clot stability	103
3.6.7 Assessment of kidney scarring	103
3.6.8 Immunohistochemical analysis	104
3.6.8.1 Changes in the ECM	104
3.6.8.2 Interstitial cell infiltration	104
3.7 Statistical Analyses	104

	Page
Chapter 4: Induction of Tissue Transglutaminase in Proximal Tubular Epithelial Cells	105
4.1 Introduction	106
4.2 Results	107
4.2.1 Stimulation of TG2 with fibrogenic growth factors	107
4.2.2 Stimulation of TG2 with the cytokines TNF- α and Il-1 β	107
4.2.3 Stimulation of TG2 with retinoic acid, sodium butyrate and dexamethasone	107
4.2.4 Effect of renal stress factors	111
4.2.4.1 Hypoxia	111
4.2.4.1.1 TG activity	111
4.2.4.1.2 TG2 protein	111
4.2.4.2 Acidosis	111
4.2.4.2.1 TG activity	111
4.2.4.2.2 TG2 protein	112
4.2.4.2.3 TG2 mRNA expression	112
4.2.4.2.4 ϵ (γ -glutamyl) lysine levels	112
4.3 Discussion	120
Chapter 5: Generation and Characterisation of TG2 Over-expressing Tubular Epithelial and Mesangial Cells	126
5.1 Introduction	127
5.2 Results	129
5.2.1 Intracellular TG activity	129
5.2.2 TG2 protein	129
5.2.3 TG2 mRNA expression	133
5.2.4 Effect of TG2 expression on cell morphology	133
5.2.5 Growth characteristics of selected clones	133
5.2.6 Extracellular TG2 expression	138
5.2.6.1 Extracellular TG activity	138
5.2.6.2 Extracellular TG2 antigen	138
5.3 Discussion	141
Chapter 6: Generation and Characterisation of Primary Tubular and Mesangial Cells from the TG2^{-/-} Knockout Mouse	145
6.1 Introduction	146
6.2 Results	147
6.2.1 Morphology of primary tubular and mesangial cells	147
6.2.2 Cell markers	147
6.2.3 Transglutaminase activity	151
6.2.4 TG2 Antigen	151
6.2.5 TG2 mRNA expression	151
6.2.6 ϵ (γ -glutamyl) lysine crosslink levels	151
6.3 Discussion	157

	Page
Chapter 7: Effect of Tissue Transglutaminase Modulation on Tubular Cell ECM	162
7.1 Introduction	163
7.2 Results	165
7.2.1 Preliminary studies	165
7.2.1.1 Optimum concentration of radiolabel	165
7.2.1.2 Removal of non-specific radioactivity	165
7.2.1.3 Cell removal	165
7.2.1.4 ECM recovery	166
7.2.2 Experimental data	169
7.2.2.1 Measurement of total deposited ECM	169
7.2.2.2 Measurement of total ECM collagen	169
7.2.2.3 Analysis of collagen composition by immunofluorescence	174
7.2.2.4 $\epsilon(\gamma\text{-glutamyl})$ lysine levels in the ECM	174
7.2.2.5 Collagen mRNA expression	178
7.2.2.6 Collagen deposition rate	178
7.2.2.7 mRNA expression of MMPs and TIMPs	185
7.2.2.8 MMP activity of OK cells	192
7.2.2.8.1 Gelatin zymography of OK cell medium	192
7.2.2.8.2 MMP activity of TG2 over-expressing OK cell medium	192
7.2.2.9 Enzymatic degradation of tubular ECM	192
7.2.2.10 Degradation of tubular ECM with MMP-1 and MMP-2	194
7.2.2.11 MMP-1/MMP-2 degradation of TG2 over-expressing and TG2 null tubular cell ECM	194
7.3 Discussion	197
Chapter 8: Effect of Tissue Transglutaminase Modulation on Mesangial Cell ECM	203
8.1 Introduction	204
8.2 Results	205
8.2.1 Measurement of total deposited ECM	205
8.2.2 Measurement of total ECM collagen	205
8.2.3 Total ECM collagen following electroporation	205
8.2.4 Collagen mRNA expression	209
8.2.5 Collagen immunofluorescence of WT and TG2 ^{-/-} ECM	209
8.2.6 $\epsilon(\gamma\text{-glutamyl})$ lysine crosslink levels in WT and TG2 ^{-/-} ECM	215
8.2.7 Collagen deposition rate of WT and TG2 ^{-/-} ECM	215
8.2.8 ECM degradation rate	215
8.3 Discussion	219
Chapter 9: Effect of TG2 Inhibition on Disease Progression in the Subtotal Nephrectomy (SNx) Model of Renal Scarring	222
9.1 Introduction	223
9.2 Results	224
9.2.1 Pilot Data	224

	Page
9.2.1.1 Effectiveness of TG inhibitors	224
9.2.1.2 Cellular uptake of TG inhibitors <i>in vitro</i>	224
9.2.1.3 Inhibitor stability study	224
9.2.1.4 Inhibitor dose response curve <i>in vivo</i>	225
9.2.1.5 One month inhibitor pilot study-50mM dose	225
9.2.2 Three month TG inhibitor SNx study	229
9.2.2.1 General observations	229
9.2.2.2 Assessment of renal function	229
9.2.2.3 Quantification of renal scarring	232
9.2.2.4 Inhibition of TG activity	236
9.2.2.5 Inhibition of $\epsilon(\gamma\text{-glutamyl})$ lysine crosslink	236
9.2.2.6 Total collagen levels	240
9.2.2.7 Immunohistochemical analysis of ECM	240
9.2.2.7.1 Collagen I	240
9.2.2.7.2 Collagen III	240
9.2.2.7.3 Collagen IV	241
9.2.2.7.4 Fibronectin	241
9.2.2.8 mRNA expression of ECM components	250
9.2.2.9 Interstitial cells	250
9.2.2.9.1 Myofibroblasts	250
9.2.2.9.2 Monocytes/macrophages	251
9.2.2.10 Correlation analysis	251
9.3 Discussion	257
Chapter 10: General Discussion	264
Chapter 11: References	282
Appendix	337

Table of Figures

Page

Chapter 1: Introduction

Table 1.1	Classification of Chronic Kidney Disease	3
Figure 1.1	Mechanisms of Proteinuric Injury in Tubular Epithelial Cells	7
Figure 1.2	Regulation of Hypoxia Inducible Factor (HIF) Responsive Gene Expression	9
Figure 1.3	Pathology of Glomerular and Tubulointerstitial Scarring	12
Figure 1.4	Proposed Patho-physiological Events in Kidney Scarring	17
Figure 1.5	Subclasses of Collagen Types in the Collagen Superfamily	21
Figure 1.6	Biosynthesis of Fibrillar Collagen	23
Figure 1.7	Domain Structure and Assembly of FN	27
Table 1.2	Proteoglycan Families and their Renal Distribution	32
Figure 1.8	Mechanisms of MMP Activation and Inhibition	37
Figure 1.9	Principle Reactions Catalysed by the Transglutaminase Enzyme Family	46
Table 1.3	Members of the Transglutaminase (TG) Gene Family	47
Figure 1.10	Three Dimensional Structure of TG2	48
Figure 1.11	Schematic Representation of the TG2 Gene Promoter	50
Figure 1.12	Intracellular Localisation of TG2 in Proximal Tubular Epithelial Cells	53
Table 1.4	Major Protein Substrates of TG2	54

Chapter 3: Materials and Methods

Figure 3.1	Geneticin Dose Response Curves for OK and 1097 Cell Lines	68
Table 3.1	Nucleofection Optimisation Programs	71
Table 3.2	Results of Nucleofection Optimisation	71
Table 3.3	Kaleidoscope Pre-stained Protein Markers	75
Table 3.4	Constituents of Reaction Mix for Putrescine Incorporation Assay	76
Figure 3.2	Schematic Diagram of the TG Activity Assay	77
Figure 3.3	Extracellular TG Activity and Extracellular TG2 Antigen Assays	80
Figure 3.4	Expression Vector Plasmid Maps	85
Figure 3.5	Principle of ECM Quantification by ³ H-labelling	89
Table 3.5	Antibodies Used in Immunohistochemical Analysis of ECM	92
Figure 3.6	Phase Selection for Multi-phase Image Analysis	94
Figure 3.7	Principle of the ECM Degradation Assay	96
Figure 3.8	Chemical Structure of Site-Specific Transglutaminase Inhibitors	98

	Page
Figure 3.9 Aortic perfusion of Mouse Kidneys with BSA Inactivated Dynabeads	99
Figure 3.10 Isolation of Primary Tubular Epithelial and Mesangial Cells	100
Figure 3.11 Subtotal Nephrectomy and Implantation of Osmotic Mini-pump	101
Equation 3.1 Calculation of Creatinine Clearance	103
Chapter 4: Induction of Tissue Transglutaminase in Proximal Tubular Epithelial Cells	
Figure 4.1 Effect of Fibrogenic Growth Factors on Intracellular TG Activity in OK Cells	108
Figure 4.2 Effect of Inflammatory Cytokines on Intracellular TG Activity in OK Cells	109
Figure 4.3 Effect of TG Stimulators on Intracellular TG Activity in OK Cells	110
Figure 4.4 Effect of Hypoxia on Transglutaminase Activity in NRK-52E Cells	113
Figure 4.5 Western Blot Analysis of NRK-52E Cells Exposed to Hypoxia	114
Figure 4.6 Effect of pH on TG Activity in LLC-PK1 Cells	115
Figure 4.7 Western Blot Analysis of LLC-PK1 Cells Exposed to low pH	116
Figure 4.8 Western Blot Analysis of TG2 in LLC-PK1 Cell Media Following Exposure to Low pH	117
Figure 4.9 TG2 mRNA Expression in LLC-PK1 Cells Exposed to low pH	118
Figure 4.10 $\epsilon(\gamma\text{-glutamyl})$ lysine ECM Levels in LLC-PK1 Cells Exposed to low pH	119
Chapter 5: Generation and Characterisation of TG2 Over-expressing Tubular Epithelial and Mesangial Cells	
Figure 5.1 TG Activity of TG2 Over-expressing OK Tubular Cell Clones	130
Figure 5.2 TG Activity of TG2 Over-expressing 1097 Mesangial Cell Clones	131
Figure 5.3 Western Blot Analysis of Selected Over-expressing Clones	132
Figure 5.4 Northern Blot Analysis of Selected Over-expressing Clones	134
Figure 5.5 Morphology of TG2 Over-expressing OK Tubular Cells	135
Figure 5.6 Morphology of TG2 Over-expressing 1097 Mesangial Cells	136
Figure 5.7 Growth Curves of Selected Over-expressing Cell Clones	137
Figure 5.8 Extracellular TG2 Activity of Selected Over-expressing Clones	139
Figure 5.9 Extracellular TG2 Antigen Levels of Selected Over-expressing Clones	140

Chapter 6: Generation and Characterisation of Primary Tubular and Mesangial Cells from the TG2^{-/-} Knockout Mouse

Figure 6.1	Morphology of Wild Type and TG2 ^{-/-} Tubular Epithelial and Mesangial Cells	148
Figure 6.2	Immunofluorescent Characterisation of Primary Tubular Epithelial Cells	149
Figure 6.3	Immunofluorescent Characterisation of Primary Mesangial Cells	150
Figure 6.4	Transglutaminase Activity in WT and TG2 ^{-/-} Cells	152
Figure 6.5	Western Blot for Tissue Transglutaminase in TG2 ^{-/-} Tubular Cells	153
Figure 6.6	mRNA Expression (whole kidney)	154
Figure 6.7	$\epsilon(\gamma\text{-glutamyl})$ lysine Crosslink Levels in TG2 ^{-/-} Tubular ECM	155
Figure 6.8	$\epsilon(\gamma\text{-glutamyl})$ lysine Crosslink Levels in TG2 ^{-/-} Mesangial ECM	156
Figure 6.9	Proposed Gene Disruption of TG2 Used in the Generation of the TG2 Knockout Mouse	160

Chapter 7: Effect of Tissue Transglutaminase Modulation on Tubular Cell ECM

Figure 7.1	Determination of Labelling Protocol and Washing Regime for the ECM Labelling Studies	167
Figure 7.2	Evaluation of Cell Removal and ECM Recovery Agents for Use in the ECM Labelling Studies	168
Figure 7.3	Total ECM Levels in TG2 Over-expressing OK Cell Clone ECM	170
Figure 7.4	Total ECM Levels in WT and TG2 ^{-/-} Tubular ECM	171
Figure 7.5	Total ECM Collagen in TG2 Over-expressing OK Cell Clone ECM	172
Figure 7.6	Total ECM Collagen in WT and TG2 ^{-/-} Tubular ECM	173
Figure 7.7	Collagen Immunofluorescence	175
Figure 7.8	Multi-phase Image Analysis of Collagen Immunofluorescence	176
Figure 7.9	Multi-phase Image Analysis of $\epsilon(\gamma\text{-glutamyl})$ lysine Crosslink	177
Figure 7.10	Collagen I mRNA Expression in TG2 Over-expressing OK Cells	180
Figure 7.11	Collagen III mRNA Expression in TG2 Over-expressing OK Cells	181
Figure 7.12	Collagen IV mRNA Expression in TG2 Over-expressing OK Cells	182
Figure 7.13	Collagen mRNA Expression in WT and TG2 ^{-/-} Tubular Cells	183
Figure 7.14	ECM Deposition in the presence of the MMP Inhibitor Galardin	184
Figure 7.15	MMP-1 mRNA Expression in TG2 Over-expressing OK cells	186

	Page
Figure 7.16 MMP-9 mRNA Expression in TG2 Over-expressing OK cells	187
Figure 7.17 TIMP-1 mRNA Expression in TG2 Over-expressing OK cells	188
Figure 7.18 TIMP-3 mRNA Expression in TG2 Over-expressing OK cells	189
Figure 7.19 MMP-1 and MMP-9 mRNA Expression in WT and TG2 ^{-/-} Tubular Cells	190
Figure 7.20 TIMP-1, TIMP-2 and TIMP-3 mRNA Expression in WT and TG2 ^{-/-} Tubular Cells	191
Figure 7.21 MMP Activity of OK Tubular Cells	193
Figure 7.22 Enzymatic Degradation of OK Clone tTg7 ECM	195
Figure 7.23 MMP Degradation of OK Cell Tubular ECM	196

Chapter 8: Effect of Tissue Transglutaminase Modulation on Mesangial Cell ECM

Figure 8.1 Total Mesangial Cell ECM Levels	206
Figure 8.2 Total Collagen in Mesangial Cell ECM	207
Figure 8.3 Total Mesangial ECM Collagen Following Electroporation	208
Figure 8.4 Extracellular TG Levels in Electroporated Mesangial Cells	208
Figure 8.5 Collagen I mRNA Expression in TG2 Over-expressing Mesangial Cells	211
Figure 8.6 Collagen III mRNA Expression in TG2 Over-expressing Mesangial Cells	212
Figure 8.7 Collagen IV mRNA Expression in TG2 Over-expressing Mesangial Cells	213
Figure 8.8 Collagen mRNA Expression in WT and TG2 ^{-/-} Mesangial Cells	214
Figure 8.9 Collagen and ε(γ-glutamyl) lysine Immunofluorescence	216
Figure 8.10 Semi-quantitative Analysis of Collagen Immunofluorescence	217
Figure 8.11 ε(γ-glutamyl) lysine Crosslink Levels	217
Figure 8.12 ECM Deposition in the presence of the MMP Inhibitor Galardin	218
Figure 8.13 Combined MMP-1 and MMP-2 Degradation of WT and TG2 ^{-/-} Mesangial ECM	218

Chapter 9: Effect of TG2 Inhibition on Disease Progression in the Subtotal Nephrectomy (SNx) Model of Renal Scarring

Figure 9.1 Effectiveness of TG Inhibitors	226
Figure 9.2 Cellular Uptake of TG Inhibitors <i>in vitro</i>	226

	Page
Figure 9.3 One Month Inhibitor Stability Study	227
Figure 9.4 One Week Inhibitor Dose Response Curve	228
Figure 9.5 Transglutaminase Activity One Month Study at 50mM	228
Table 9.1 Three Month TG2 Inhibitor SNx Study Renal Function data	230
Table 9.2 Three Month TG2 Inhibitor SNx Study Toxicity Data	230
Figure 9.6 Changes in Renal Function Markers	231
Figure 9.7 Representative Photomicrographs of Masson's Trichrome Staining	233
Figure 9.8 Glomerulosclerosis and Tubulointerstitial Fibrosis at 84 Days Post-SNx	234
Figure 9.9 Assessment of Renal Scarring by Multi-phase Image Analysis	235
Figure 9.10 Changes in Transglutaminase Activity	237
Figure 9.11 TG <i>in situ</i> Activity	238
Figure 9.12 $\epsilon(\gamma\text{-glutamyl})$ lysine Crosslink at 84 Days Post-SNx	239
Figure 9.13 Total Collagen Levels at Day 84 by Hydroxyproline Analysis	239
Figure 9.14 Representative Photomicrographs of Collagen I Immunohistochemistry	242
Figure 9.15 Multi-phase Image Analysis of Collagen I Immunohistochemistry	243
Figure 9.16 Representative Photomicrographs of Collagen III Immunohistochemistry	244
Figure 9.17 Multi-phase Analysis of Collagen III Immunohistochemistry	245
Figure 9.18 Representative Photomicrographs of Collagen IV Immunohistochemistry	246
Figure 9.19 Multi-phase Analysis of Collagen IV Immunohistochemistry	247
Figure 9.20 Representative Photomicrographs of Fibronectin Immunohistochemistry	248
Figure 9.21 Multi-phase Analysis of Fibronectin Immunohistochemistry	249
Figure 9.22 mRNA Expression of Collagens, Fibronectin, MMP-1 and TIMP-1	252
Figure 9.23 Representative Photomicrographs of α -SMA Immunohistochemistry	253
Figure 9.24 Multi-phase Analysis of α -SMA Immunohistochemistry	254
Figure 9.25 Representative Photomicrographs of ED1 Immunohistochemistry	255
Figure 9.26 Multi-phase Analysis of ED1 Immunohistochemistry	256
Figure 9.27 Mechanism of Inhibition by Site-Specific Thioimidazole Inhibitors	258
 Chapter 10: General Discussion	
Figure 10.1 Possible Mechanisms of TG2 Induction in Tubular Epithelial Cells	267
Figure 10.2 Proposed Effects of TG2 on Collagen Accumulation in the Tubular ECM	273
Figure 10.3 Proposed Mechanisms of Tubular Cell TG2 Action in Kidney Scarring	279

Chapter 1

Introduction

1.1 Chronic Kidney Disease (CKD)

Chronic Kidney Disease (CKD) is characterised by a slow, progressive decline in kidney function with time, leading to the development of end stage renal disease (ESRD) and the requirement for renal replacement therapy (RRT). CKD is a major global healthcare problem, with more than 1 million patients on RRT worldwide, expecting to rise to 2 million patients by 2010 (Lysaght, 2002; Xue *et al.*, 2001). In the UK, the prevalence of CKD is estimated to be approximately 5,554 patients per million population (pmp) (John *et al.*, 2004) with 101 new patients pmp requiring RRT every year at a total annual cost in excess of £600 million (Roderick *et al.*, 2005). In addition to the financial implications of CKD, it is a debilitating disease with patients having a significantly reduced quality of life with high levels of morbidity and mortality. Despite a number of available therapeutic strategies aimed at targeting the underlying causes of CKD and delaying the onset of renal replacement, there remains no effective therapy to halt the progression to ESRD. Therefore, research into the mechanisms and pathogenesis of CKD with the ultimate aim of developing an effective therapeutic intervention is crucial if CKD is to be conquered.

1.2 Clinical Features of CKD

Clinically, CKD is characterised by a decline in glomerular filtration rate (GFR) which is a critical determinant of normal renal function (Baylis, 1997). Patients are considered to have CKD if their GFR falls below $60\text{ml}/\text{min}/1.73\text{m}^2$ for greater than 3 months (Levey *et al.*, 2003). The clinical progression of CKD has been classified from Stage 1 to Stage 5 (table 1.1) according to changes in GFR (2002). Stage I represents normal renal function ($\text{GFR} \leq 90\text{ml}/\text{min}/1.73\text{m}^2$), stage II mild renal insufficiency ($60\text{-}89\text{ml}/\text{min}/1.73\text{m}^2$) with end stage renal failure (ESRF) occurring at Stage 5 ($<15\text{ml}/\text{min}/1.73\text{m}^2$).

The decline in GFR to ESRD is characterised by the onset of uraemia, a toxic condition in which nitrogenous metabolites such as uric acid, urea and creatinine accumulate in the blood. The development of uraemia is associated with a number of clinical manifestations including oedema, hypertension, atherosclerosis, metabolic bone disorders, hyperlipidaemia and anaemia (Alvestrand A and P, 1997). Many of these are known to contribute to an increased risk of cardiovascular disease that is a major cause of mortality in patients with CKD (Sarnak, 2003). In addition, some of the physiological effects of uraemia such as hypertension as well as exposure of the damaged kidney to toxic substances are considered to be important factors in promoting the progression of CKD (section 1.3).

Table 1.1 Classification of Chronic Kidney Disease

Classification	Description	GFR (ml/min/1.73m²)
Stage I	Kidney damage* with normal or ↑ GFR	≥ 90
Stage II (mild)	Kidney damage with mild ↓ GFR	60-89
Stage III (moderate)	Moderate ↓ GFR	30-59
Stage IV (severe)	Severe ↓ GFR	15-29
Stage V	Kidney failure (ESRF)	< 15

Chronic Kidney Disease = GFR < 60ml/min/1.73m² for greater than 3 months

*** Kidney damage is defined as pathological abnormalities or markers of damage including abnormalities in blood or urine tests or imaging studies**

Table 1.1 Adapted from National Kidney Foundation K/DOQI Clinical Practice Guidelines for Chronic Kidney Disease: evaluation, classification and stratification (Levey *et al.*, 2003).

1.3 Progression of CKD

The development of CKD and its progression to ESRD is known to arise from a variety of initiating diseases and pathological processes. These include inflammatory diseases such as glomerulonephritis and tubulointerstitial nephritis, diabetic nephropathy and physical factors such as hypertension (Wing and Jones, 2000).

Despite the diversity of these initiating factors and the differences in their pathological mechanisms, the subsequent progression of CKD is considered to proceed via a final common pathway that is characterised by loss of functional renal tissue and the development of kidney scarring and fibrosis. Such events do not require the maintenance of the initiating insult and once instigated occur independently of the underlying disease (Klahr *et al.*, 1988).

The critical common event in the initiation and progression of CKD is a substantial reduction in the number of functioning nephrons. The kidney responds to this by both adaptive and compensatory changes in remaining nephrons in an attempt to maintain normal kidney homeostasis. A loss of functional renal tissue leads to an increase in the single nephron GFR of remaining nephrons (Hostetter *et al.*, 1981) (section 1.4.1) as well as to an increase in kidney growth due to glomerular and tubular hypertrophy (Wesson, 1989). Whilst initially serving to preserve normal kidney function, in the long term, this response is maladaptive and significantly contributes to the perpetuating cycle of further nephron damage and loss (Hostetter *et al.*, 1981). The ultimate consequence of this damage is the development of progressive kidney scarring.

1.4 Mechanisms of CKD Progression

1.4.1 Systemic and glomerular hypertension

It is widely accepted that the presence of systemic hypertension accelerates the progression of both diabetic and non-diabetic CKD (Jacobsen *et al.*, 1999; Klahr *et al.*, 1994) and that it can be both a cause and a consequence of the disease. In the USA for example, hypertension affects 24% of the adult population that rises to around 70% of all patients with CKD (Agarwal, 2005).

Much of the evidence for the role of hypertension in the progression of CKD has come from the study of the subtotal nephrectomy model (Anderson *et al.*, 1985; Brenner *et al.*, 1982; El-Nahas *et al.*, 1983; Jackson *et al.*, 1986; Katoh *et al.*, 1994; Purkerson *et al.*, 1987). For example, in rats subjected to 5/6th nephrectomy, the loss of more than 75% of the renal mass results in the development of hypertension, proteinuria and the progressive loss of GFR consistent with human CKD (El-Nahas *et al.*, 1983). Many of these studies have established a

link between systemic hypertension and the development of glomerular damage and glomerulosclerosis (Anderson *et al.*, 1985; Brenner *et al.*, 1982; El-Nahas *et al.*, 1983). The control of systemic hypertension by anti-hypertensive agents has been demonstrated to be a critical factor in the prevention of disease progression (Anderson, 1989; Griffin *et al.*, 1994; Simons *et al.*, 1994).

The mechanism by which systemic hypertension contributes to glomerular injury is through greater transmission of arterial pressure to the glomerular capillaries, causing alterations to glomerular haemodynamics (Imig and Inscho, 2002). This is mediated mainly through the activation of Angiotensin II, a major effector of the renin-angiotensin system causing constriction of the efferent arteriole (Edwards, 1983). The consequences of this are increased glomerular capillary hydraulic pressure or glomerular hypertension and substantial increases in single nephron GFR leading to hyperfiltration (Hostetter *et al.*, 1981). With time, sustained hyperfiltration is thought to damage the glomerular capillaries by exerting physical forces of mechanical stretch and shear stress (Hostetter, Olson *et al.* 1981) leading to further nephron loss. The exposure of endothelial cells and glomerular mesangial cells to such forces is thought to further promote glomerular damage and glomerulosclerosis by inducing phenotypic changes. In endothelial cells, these include the increased expression of chemokines (Wung *et al.*, 1996) and the altered expression of adhesion molecules (Chien *et al.*, 1998). Mesangial cells respond directly to forces such as mechanical stretch by increasing the expression and accumulation of ECM components such as collagens and FN as well as the expression of growth factors such as TGF- β 1 (Yasuda *et al.*, 1996). In addition, increased exposure of mesangial cells to proteins (section 1.4.2) as a result of glomerular capillary damage is thought to stimulate fibrogenic mechanisms such as proliferation (Greiber *et al.*, 1996; Mondorf *et al.*, 1999) and increased matrix production (Chana *et al.*, 2000; Rovin and Tan, 1993; Wheeler and Chana, 1993).

1.4.2 Proteinuria

A critical consequence of glomerular damage is the abnormal ultra-filtration of plasma proteins leading to the accumulation of medium and high molecular weight proteins in the urine or proteinuria. Numerous studies have demonstrated that the degree of proteinuria correlates with the rate of progression of CKD suggesting that proteinuria is an independent mediator of progression (Remuzzi and Bertani, 1998; Zandi-Nejad *et al.*, 2004).

The abnormal filtration of proteins brings them into contact with both the mesangium and tubular cells instigating injury to the glomerular and tubular compartments. In the mesangium

increased exposure of mesangial cells to lipoproteins is known to play a role in affecting their cell function. The mesangial expression of receptors for low density lipoprotein (LDL) and very low density lipoprotein (vLDL) with the subsequent binding of these proteins stimulates activation of Ras and mitogen activated protein (MAP) kinase signalling pathways leading to increased expression of c-fos and c-jun (Kamanna, 2002). These changes may contribute to glomerular injury by stimulating mesangial cell proliferation (Greiber *et al.*, 1996; Mondorf *et al.*, 1999), monocyte infiltration (Rovin and Tan, 1993), hypertrophy (Wheeler *et al.*, 1990) and mesangial matrix production (Chana *et al.*, 2000; Rovin and Tan, 1993; Wheeler and Chana, 1993).

In tubular cells, the absorption of filtered protein has been attributed to expression of megalin-cubulin complexes on the apical membrane and clathrin mediated endocytosis (Kozyraki *et al.*, 2001). A number of pathways have been proposed by which proteinuria can cause tubular injury (figure 1.1). The sheer quantity of protein to be metabolised by these cells, in itself, can cause injury by overloading the lysosomes resulting in leakage of lysosomal enzymes (Eddy, 1989). Protein ultrafiltration can stimulate the transcription of nuclear factor-kappa B (NF- κ B) -dependent (Mezzano *et al.*, 2004; Mezzano *et al.*, 2001) and -independent genes such as endothelin-1 (Zoja *et al.*, 1995), monocyte chemoattractant protein-1 (MCP-1) (Wang *et al.*, 1997) and osteopontin (Kramer *et al.*, 2005) which are secreted via the basolateral membrane of tubular cells. These factors promote inflammation by attracting mononuclear cells. In addition, increased exposure of tubular cells to albumin can increase the expression of TGF β -1 (Wolf *et al.*, 2004; Yard *et al.*, 2001) which is a major stimulus for epithelial-mesenchymal transformation (Fan *et al.*, 1999) (EMT, section 1.5.2.4) as well as increased matrix production (Eddy and Giachelli, 1995). Release of endothelin-1 can induce renal ischaemia leading to hypoxia (section 1.4.3), stimulate tubular proliferation (Ong *et al.*, 1995) and alter ECM metabolism (Ruiz-Ortega *et al.*, 1994). The increased re-absorption of iron/transferrin complexes may cause tubular injury by increasing the production of reactive oxygen species (ROS) and inducing oxidative stress (Alfrey, 1994). Similarly, increased albumin reabsorption by proximal tubular cells stimulates the generation of ROS, along with the over-expression of chemokines and fibrogenic cytokines (Morigi *et al.*, 2002), all of which may contribute to progressive tubular damage.

Figure 1.1 Mechanisms of Proteinuric Injury in Tubular Epithelial Cells

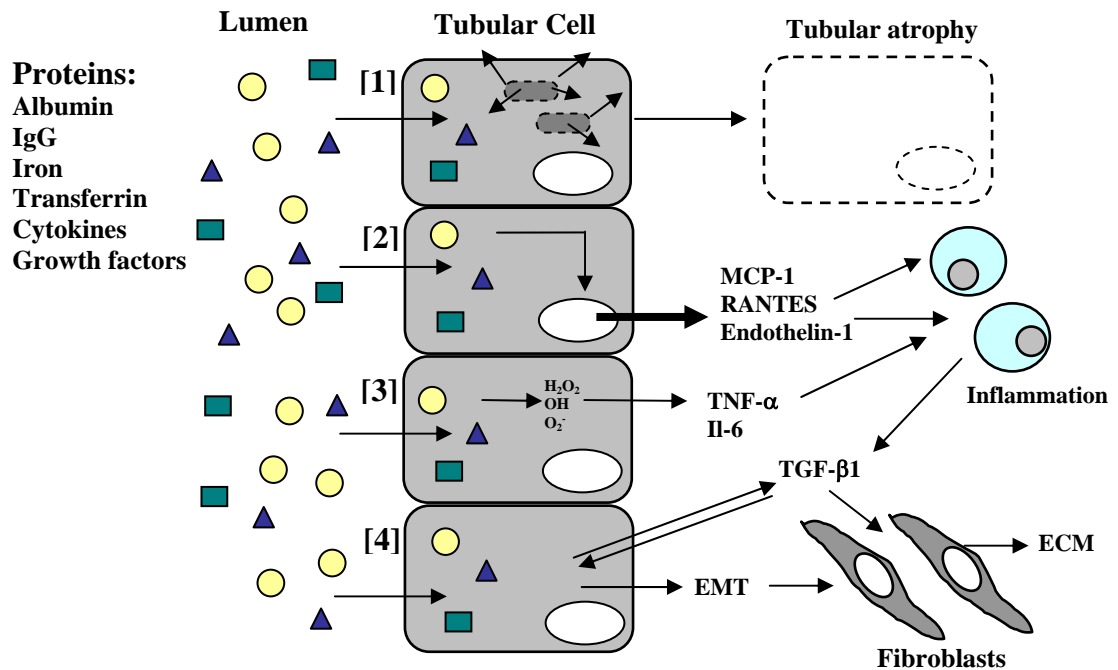


Figure 1.1 Proteinuria can cause damage to tubular epithelial cells by a variety of mechanisms including [1] lysosome overload leading to leakage of lysosomal enzymes and tubular atrophy; [2] expression of chemotactic and inflammatory cytokines; [3] generation of reactive oxygen species and stimulation of NF-kappa-B -dependent cytokines; [4] synthesis and release of TGF-β1 leading to myofibroblast formation, ECM deposition and epithelial mesenchymal transformation (EMT). Adapted from: (Abbate *et al.*, 2006).

1.4.3 Hypoxia

Evidence is accumulating that the loss of tissue oxygen or hypoxia represents an important common pathway in the pathogenesis and progression of CKD. In human renal disease (Bohle *et al.*, 1996) and in experimental models of CKD including experimental glomerulonephritis (Ohashi *et al.*, 2000), the remnant kidney model (Kang *et al.*, 2001) and ureteral obstruction (Ohashi *et al.*, 2002) the number of peritubular capillaries declines with the progressive loss of renal function. The trigger for this loss is unclear but appears to be related to microvascular damage induced by haemodynamic factors. Such damage leads to a cycle of localised ischaemia, peritubular capillary loss and hypoxia (Fine *et al.*, 2000; Fine *et al.*, 1998).

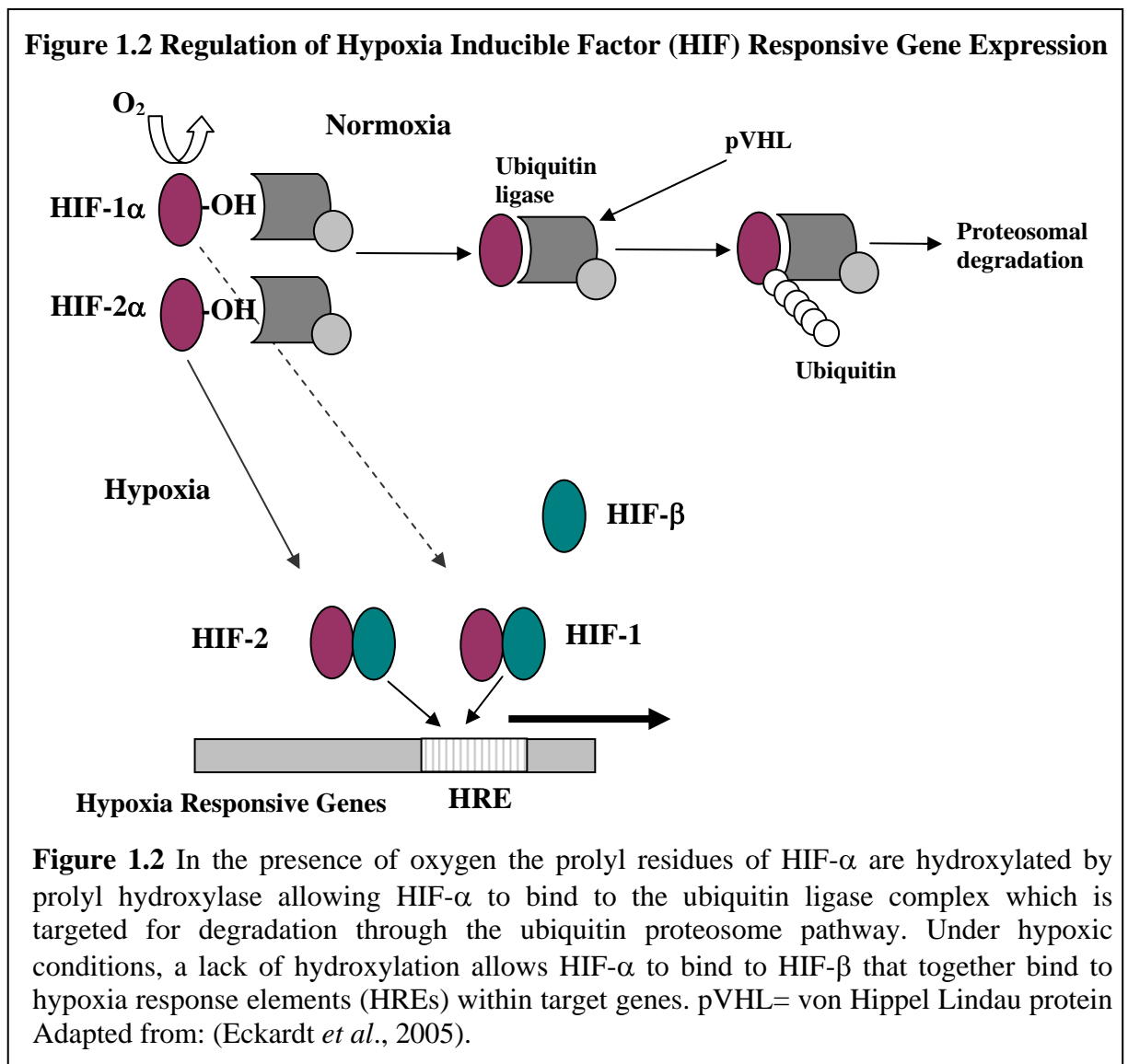
Hypoxia is a potent inducer of gene expression and contributes to tubular injury and fibrogenesis mainly by regulating the expression of a number of pro-fibrogenic genes. This is mediated by the activation of a number of transcription factors including NF-κB (Schreck *et al.*, 1992), AP-1 (Bandyopadhyay *et al.*, 1995) and in particular, the hypoxia inducible

transcription factors (HIFs) (Semenza, 1999b; Wang and Semenza, 1993). HIFs are heterodimers consisting of oxygen regulated α subunit and constitutively expressed β subunit (Wang *et al.*, 1995; Wang and Semenza, 1995). Expression of HIFs is tightly regulated by O₂ concentration and under normoxic conditions they are subject to ubiquitination and proteosomal degradation (Huang *et al.*, 1998; Kallio *et al.*, 1999). Hypoxia leads to increased HIF expression, activity and binding of the heterodimers to hypoxia response elements (HREs) within target genes (Semenza, 1998). The mechanism of oxygen sensing is still unclear but has been suggested to rely on the presence of a global haem-based oxygen sensor (Goldberg *et al.*, 1988) and the activation of protein kinase and tyrosine kinase mediated signalling pathways (Bunn and Poyton, 1996; Morwenna and Ratcliffe, 1997; Norman *et al.*, 2000; Semenza, 1999a). However, recently the oxygen sensing ability of cells has been attributed to prolyl hydroxylase enzymes capable of hydroxylating proline residues within HIF-1 α (Huang *et al.*, 1998; Zhu and Bunn, 2001). Hydroxylation of HIFs under normoxic conditions confers rapid degradation whilst under hypoxic conditions, a lack of hydroxylation serves to stabilise HIFs, allowing them to translocate to the nucleus and dimerise (figure 1.2).

In a number of renal cell types, the expression of pro-fibrogenic factors is increased in response to hypoxia. Endothelial cells have been demonstrated to induce the expression of cytokines including interleukin (IL)-1 (Shreeniwas *et al.*, 1992), IL-6 (Yan *et al.*, 1995) and IL-8 (Karakurum *et al.*, 1994). Similarly, human proximal tubular cells have been shown to up-regulate growth factors such as TGF- β 1 (Orphanides *et al.*, 1997), vascular endothelial growth factor (VEGF) (Nakamura *et al.*, 2006) and platelet derived growth factor (PDGF) (Schweda *et al.*, 2000) in response to hypoxia. Induction of TGF β 1 production has also been demonstrated in interstitial fibroblasts (Norman *et al.*, 2000). The stimulation of cytokine and growth factors by hypoxia may act in an autocrine or paracrine fashion to promote further tubular injury (section 1.5.2.3). In addition, direct or indirect stimulation of epithelial cells under hypoxic conditions may promote de-differentiation and transition to mesenchymal fibroblasts (Haase, 2006).

Hypoxia is also known to promote a fibrogenic phenotype in renal cells by affecting the expression of ECM components. Studies of human proximal tubular epithelial cells and interstitial fibroblasts subjected to hypoxic conditions show a marked increase in Collagen I mRNA and total collagen production by these cells (Norman *et al.*, 2000; Norman *et al.*, 1999; Orphanides *et al.*, 1997). In addition, hypoxia alters the expression of regulators of ECM turnover, in particular, matrix metalloproteinases (MMPs) and their inhibitors (TIMPs). In human proximal tubular cells, hypoxia decreases the expression of MMP-2 and increases

TIMP-1 production (Norman *et al.*, 1999; Orphanides *et al.*, 1997). These *in vitro* effects suggest that hypoxia further contributes to progressive tubular damage by promoting ECM accumulation.



1.4.4 Oxidative stress

In recent years, increasing emphasis has been placed on the role of oxidative stress in the progression and pathogenesis of CKD (Locatelli *et al.*, 2003). Oxidative stress has been implicated in diseases such as glomerulonephritis (Shah, 2004), diabetic nephropathy (Ha and Lee, 2003) and in the pathogenesis of ischaemia-reperfusion injury (Dobashi *et al.*, 2000). An imbalance between the formation of reactive oxygen species (ROS) and anti-oxidant defence mechanisms results in oxidative stress. Generation of ROS including hydrogen peroxide (H_2O_2), superoxide (O_2^-) and hydroxyl radicals (OH) is mediated by both the mitochondrial respiratory chain and the NADPH oxidase systems. These are counteracted by the action of

antioxidant enzyme systems such as superoxide dismutase, catalase and the oxidant scavenger glutathione peroxidase (Locatelli *et al.*, 2003).

In renal disease, a variety of contributing factors have been implicated in increased pro-oxidant activity leading to oxidative stress. Inflammation is considered to be a significant contributory factor with infiltrating and activated neutrophils and monocytes producing elevated levels of ROS (Yasunari *et al.*, 2006). Generation of ROS such as H₂O₂ by inflammatory cells can perpetuate the inflammation by activating the NF-κB pathway, promoting the synthesis of pro-inflammatory cytokines (Haddad, 2002). In mesangial and tubular cells, exposure to high glucose promotes the increased generation of ROS (Allen *et al.*, 2003; Ha and Lee, 2000; Hsieh *et al.*, 2002). Similarly, exposure of tubular cells or embryonic kidney cells to hypoxic conditions increases ROS production (Kim *et al.*, 2002; Mansfield *et al.*, 2004). Proteinuria can also promote ROS production as a result of exposure to increased albumin and iron/transferrin complexes (Harris *et al.*, 1995). In addition, tubular cells exposed to low pH as a result of metabolic acidosis show increases in markers of oxidative stress (Rustom *et al.*, 2003).

The mechanisms by which oxidative stress contributes to progressive glomerular and tubular injury are varied. ROS are known to cause the lipid peroxidation of proteins which if occurring in cell and plasma membranes, results in disruption of structural integrity (Baud and Ardaillou, 1993). In the glomerulus, generation of ROS may affect glomerular basement membrane barrier function through the modulation of MMPs and their inhibitors (Shah *et al.*, 1987). ROS also play an important role in cell signalling and increased generation of ROS is known to activate a number of signalling pathways such as extracellular- regulated kinase (ERK), phosphatidyl inositol-3-kinase (PI3K) and MAP kinase (Wang *et al.*, 1998). Oxidative compounds are also known to cause DNA damage contributing to mutagenesis (Nakabeppu *et al.*, 2006).

1.4.5 Hypermetabolism

A number of studies in the remnant kidney model (Brenner, 1985; Harris *et al.*, 1988; Jarusiripipat *et al.*, 1991; Nath *et al.*, 1990) have demonstrated that the progressive loss of functioning nephrons is associated with a marked increase in the oxidative metabolism of remaining nephrons. This increased oxygen consumption or hypermetabolism has been suggested to provide a further pathway leading to tubular damage and additional nephron loss (Harris *et al.*, 1988). The consequences of increased oxygen metabolism are thought to be two fold. Firstly, tubular cells respond by increasing cellular production of ammonia (Clark *et al.*, 1991; Rustom *et al.*, 1998). This is thought to activate components of the complement

pathway (Clark *et al.*, 1991), in turn promoting inflammation and increased collagen synthesis (Torbohm *et al.*, 1990). Secondly, increased oxygen consumption promotes the increased generation of ROS (Rovin *et al.*, 1990; Yoshioka *et al.*, 1990) which themselves are mediators of progressive renal injury (section 1.4.4).

1.5 Kidney Scarring

1.5.1 Pathology of kidney scarring

The pathological end point of progressive renal disease is the excessive accumulation of ECM leading to scarring and fibrosis of the glomeruli (glomerulosclerosis), the renal interstitium (tubulointerstitial fibrosis) and thickening of the vascular walls (vascular sclerosis) (El Nahas *et al.*, 1997). Glomerulosclerosis, tubulointerstitial fibrosis and vascular sclerosis are normally all present regardless of whether the initial disease originates in the glomeruli, tubules or vessels indicating that their progression and pathogenesis are interrelated (El Nahas, 1995).

Glomerulosclerosis is characterised by localised loss of glomeruli, areas of cell proliferation in remaining glomeruli, expansion of the mesangial matrix, loss of capillaries and a thickened irregular glomerular basement membrane (figure 1.3a). Ultimately there is collapse of the capillary bed. Scarring of the tubulointerstitial compartment is characterised by thickening of the tubular basement membrane, expansion of the interstitial ECM, cellular proliferation and tubular atrophy (figure 1.3b) (Klahr *et al.*, 1988). Vascular sclerosis is seen as thickening and hyalinosis of the arteriolar walls and is considered to be an integral element of the scarring process (Klahr *et al.*, 1988).

The pathophysiological events in the development of glomerulosclerosis and tubulointerstitial scarring are considered to be very similar (Harris and Neilson, 2006). Glomerular and tubular injury stimulates changes to the endothelium promoting infiltration of immune cells and the release of inflammatory cytokines/growth factors, followed by proliferation and trans-differentiation of resident cells and excess accumulation of ECM proteins (figure 1.4) (Harris and Neilson, 2006).

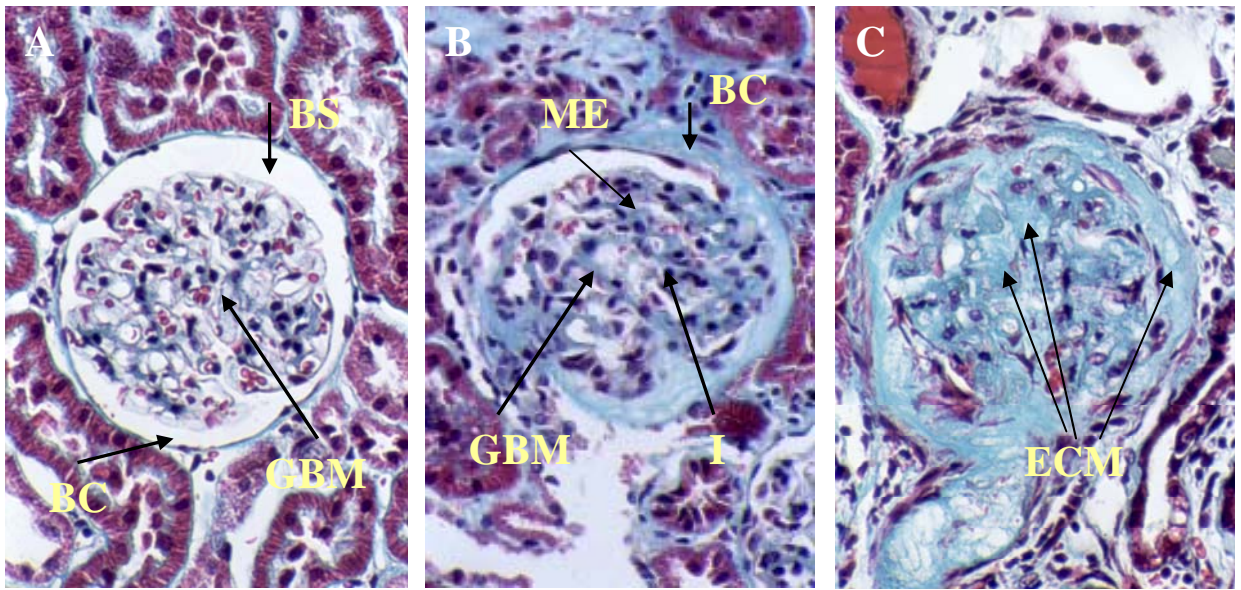
1.5.2 Pathophysiological events in kidney scarring

1.5.2.1 The endothelial response

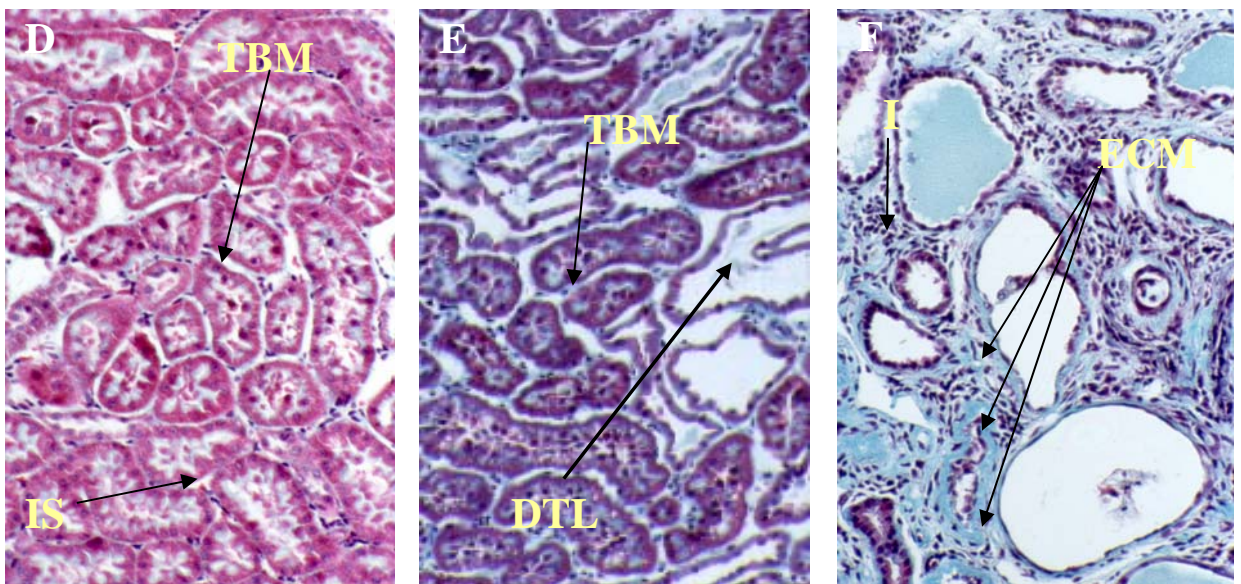
Irrespective of the initial mechanism of injury, damage to the endothelium is an early event in the initiation of kidney scarring (Lee *et al.*, 1995). Endothelial cells respond to injury by losing their anti-coagulant, anti-inflammatory and anti-proliferative characteristics prompted by the increased expression and release of a variety of soluble mediators.

Figure 1.3 Pathology of Glomerular and Tubulointerstitial Scarring

Glomerulosclerosis



Tubulo-Interstitial fibrosis



Normal

Early scarring

ESKD

Figure 1.3 The normal glomerulus (A) comprises the capillary tuft which is situated within a clearly visible Bowman's space (BS) and surrounded by the Bowman's capsule (BC). The endothelium of the capillary tuft is supported by a thin and discrete glomerular basement membrane (GBM). Early glomerular scarring (B) is characterised by thickening of the GBM and Bowman's capsule, cell infiltration (I) and mesangial ECM expansion (ME). As scarring progresses to end stage kidney disease (ESKD) (C), the excess deposition of matrix (ECM) leads to the collapse of the capillary bed. The normal tubulointerstitium (D) comprises tightly packed tubules, surrounded by tubular basement membrane (TBM) and has little interstitial space (IS). Early scarring (E) is characterised by distended tubular lumen (DTL), tubular atrophy and expansion of the tubular basement membrane (TBM). As scarring progresses to ESKD (F) there is substantial cell infiltration (I), excess deposition of interstitial ECM and the collapse of tubular structure.

These include pro-coagulant factors such as platelet activating factor (PAF), pro-inflammatory/ mitogenic cytokines and growth factors [PDGF, interleukins, tumour necrosis factor-alpha (TNF- α)] and chemokines such as monocyte chemoattractant peptide (MCP-1) and macrophage inflammatory protein (MIP-2) (El Nahas *et al.*, 1997). The expression of pro-coagulant factors contributes to the adhesion and aggregation of platelets within glomerular capillaries (Savage, 1994). Release of pro-inflammatory cytokines directly promotes the recruitment of inflammatory cells such as neutrophils and monocytes. The release of chemokines further promotes this by stimulating the expression of cell adhesion molecules (CAMs) such as selectins, ICAM-1 and VCAM-1 (Brady, 1994) that are important in the adhesion of inflammatory cells to the endothelium.

The development of a pro-inflammatory and pro-coagulative phenotype by glomerular endothelial cells may be further promoted by reductions in the level of nitric oxide synthase (NOS) which has been demonstrated to play a role in the maintenance of the glomerular vasculature, by inhibiting both platelet aggregation and leukocyte adhesion (Cattell, 2002).

1.5.2.2 Glomerular and interstitial inflammation

A significant feature of virtually all renal diseases is the infiltration of immune cells and persistent inflammation (Remuzzi and Bertani, 1998). Recruitment of inflammatory cells is promoted by the increased expression of CAMs and chemotactic factors by damaged and activated cells. Initially this is mediated by injured endothelial cells but as inflammation progresses is contributed to by infiltrating cells as well as injured mesangial and tubular cells which sustain the inflammation (Taal *et al.*, 2000). A number of inflammatory cell associated integrins have been identified as mediators in the adhesion of infiltrating cells and locally produced CAMs. In particular, $\alpha 4\beta 1$ integrin (VLA-4) and CD11a/CD18 (LFA-1) have been implicated which interact with VCAM-1 and ICAM-1 on the surface of both endothelial and activated tubular cells (Brady, 1994).

The predominant cell types infiltrating the glomerulus in both clinical and experimental glomerular injury are monocytes and macrophages (Floege *et al.*, 1992c; Nikolic-Paterson *et al.*, 1994). Similarly, in the renal interstitium inflammation is associated with the recruitment of monocytes and macrophages but also the appearance of substantial numbers of cytotoxic T lymphocytes (Alexopoulos *et al.*, 1989).

Infiltration of inflammatory cells may contribute to the progression of glomerular and tubulointerstitial scarring by a number of mechanisms. Activated macrophages produce and release a number of pro-inflammatory mediators including IL-1 and TNF- α which perpetuate

inflammation through autocrine and paracrine induction of CAMs, chemokines and cytokines (Sean Eardley and Cockwell, 2005). In addition, the inflammatory release of such factors in association with growth factors such as TGF- β 1 and PDGF leads to phenotypic and proliferative changes to resident cells such as mesangial cells and fibroblasts inducing increased proliferation and ECM synthesis (Nikolic-Paterson *et al.*, 1994). Cytotoxic T lymphocytes also contribute to scarring through cytokine release (Main and Atkins, 1995) but in addition can cause direct tubular cell destruction through the release of serine esterase and pore-forming proteins which disrupt tubular membrane integrity (Bailey and Kelly, 1997).

1.5.2.3 Release of pro-fibrogenic growth factors

It is now well established that the synthesis and release of a variety of pro-fibrogenic growth factors by both infiltrating immune cells and activated resident cells is a critical event in the development of glomerular and tubular scarring. Of these, TGF- β 1 is considered to play a central role in the pathogenesis of fibrosis, although many studies have highlighted the involvement of factors such as PDGF and connective tissue growth factor (CTGF).

Increases in TGF- β 1 have been observed in a variety of disease models including 5/6th nephrectomy (Coimbra *et al.*, 1996; Junaid *et al.*, 1997), ureteric obstruction (Ishidoya *et al.*, 1996; Wright *et al.*, 1996), protein overload nephropathy (Eddy and Giachelli, 1995) and diabetic nephropathy (Ishidoya *et al.*, 1996; Yamamoto *et al.*, 1993). Macrophages, myofibroblasts and tubular cells have been identified as the major contributors to increased TGF- β 1 production however recent studies have also implicated podocytes in the up-regulation of TGF- β 1 (Abbate *et al.*, 2002). The pro-fibrogenic effects of TGF- β 1 are considerably varied but are mostly associated with phenotypic and proliferative changes to mesangial and tubular cells. In particular, TGF- β 1 stimulates the transdifferentiation of mesangial and tubular cells to myofibroblasts with the associated expression of alpha smooth muscle actin (α -SMA) (Fan *et al.*, 1999; Johnson *et al.*, 1992) (section 1.5.2.4). Such phenotypic changes are known to correspond to the abnormal and increased synthesis of ECM components and thereby serve to promote scar formation.

In addition to the direct effects of TGF- β 1, it has been demonstrated to up-regulate the synthesis and release of supplementary growth factors such as CTGF and basic fibroblast growth factor (bFGF/FGF-2) (Strutz *et al.*, 2001; Yokoi *et al.*, 2001). TGF- β 1 mediated stimulation of CTGF by fibroblasts and tubular cells is capable of increasing both collagen I and FN synthesis which may contribute further to fibrogenesis (Okada *et al.*, 2005; Qi *et al.*, 2005).

Similarly, bFGF is capable of promoting fibroblast proliferation and ECM synthesis (Strutz *et al.*, 2000).

The phenotypic and pro-fibrogenic effects of TGF- β 1 are likely to be mediated through the activation of a number of signal transduction pathways. These include TGF- β 1 mediated phosphorylation of intracellular Smad proteins and activation of the Ras/MEK/ERK kinase pathway (Massague, 2000). Of the Smad proteins, Smad 6 and 7 are up-regulated in glomerular disease where they may participate in the TGF- β 1 mediated up-regulation of collagen I (Schiffer *et al.*, 2002). Stimulation of the Ras/MEK/ERK pathway by TGF- β 1 has been implicated in the increased expression of CTGF (Chen *et al.*, 2002).

Of the other pro-fibrogenic growth factors implicated in the pathogenesis of fibrosis the role of PDGF has also received significant attention. Increased glomerular and tubular expression of PDGF has been observed after 5/6th nephrectomy (Floege *et al.*, 1992c; Kliem *et al.*, 1996; Muchaneta-Kubara *et al.*, 1995), in diabetic rats (Fukui *et al.*, 1994) and in human renal disease (Langham *et al.*, 2003; Matsuda *et al.*, 1997; Uehara *et al.*, 2004). *In vitro* studies suggest that PDGF is pro-fibrogenic in a similar way to TGF- β 1, causing cell proliferation, transdifferentiation into myofibroblasts and promoting collagen synthesis through interactions with TGF- β 1 (Battegay *et al.*, 1990; Haberstroh *et al.*, 1993; Throckmorton *et al.*, 1995).

1.5.2.4 Proliferation and transdifferentiation

The major response of resident cells to pro-fibrotic growth factor and cytokine signals is an increase in their proliferation and the adoption of an activated phenotype that ultimately promotes increased and dysregulated ECM synthesis (Zeisberg *et al.*, 2000).

In the glomerulus, mesangial cells respond to mitogens such as PDGF and TGF- β 1 by trans-differentiating from a pericyte-like phenotype (mesangiocyte) to an embryonic myofibroblastic cell (mesangioblast) (El-Nahas, 2003). Transdifferentiation of mesangial cells is associated with increased proliferation and is characterised by the expression of cytoskeletal proteins including α -SMA (Johnson *et al.*, 1992). The development of a myofibroblastic phenotype and expression of α -SMA by mesangial cells is seen in experimental (Kliem *et al.*, 1996; Zhang *et al.*, 1995a) and human disease (Alpers *et al.*, 1992) and is a predictor of the development of glomerulosclerosis (Goumenos *et al.*, 2001). Glomerular epithelial cells are also capable of transdifferentiating into myofibroblasts by a process termed epithelial-mesenchymal transformation (EMT) (Ng *et al.*, 1999). In these cells, the expression of α -SMA is associated with the loss of epithelial markers such as E-cadherin (Ng *et al.*, 1999).

Similarly, large numbers of myofibroblasts are observed in scarred areas of the tubulointerstitium in experimental (Kliem *et al.*, 1996; Muchaneta-Kubara and El Nahas, 1997; Zhang *et al.*, 1995a) and human disease (Essawy *et al.*, 1997; Goumenos *et al.*, 1998; Goumenos *et al.*, 2001). These are partly derived from resident interstitial fibroblasts that are stimulated to proliferate and become activated by factors such as TGF- β 1, PDGF and FGF-2 (Zeisberg *et al.*, 2000). However a significant number of myofibroblasts may also be derived by EMT of injured tubular epithelial cells (El-Nahas, 2003; Jinde *et al.*, 2001; Ng *et al.*, 1998). This is particularly driven by epithelial release of TGF- β 1, a potent promoter of EMT (Fan *et al.*, 1999). In addition the composition of the underlying basement membrane and ECM are both influential in promoting EMT (Zeisberg *et al.*, 2001a).

1.5.2.5 Extracellular matrix accumulation

The ultimate pathological consequence of phenotypic changes to resident cells is a dysregulation of their ECM metabolism promoting the accumulation of ECM and the development of glomerular and tubulointerstitial scarring.

In the kidney, as in other tissues, continual turnover of the ECM is important for tissue homeostasis and is maintained by a balance between the synthesis and degradation of ECM components. The increased synthesis and decreased breakdown of renal ECM by activated cells has been implicated in scar formation (Eddy, 1996). Quantitative and qualitative changes in ECM synthesis are observed. Activated fibroblasts increase their production of fibronectin and interstitial collagens (Zeisberg *et al.*, 2000) whilst mesangial cells synthesise abnormal glomerular collagens I and III (Floege *et al.*, 1992a; Minto *et al.*, 1993). Changes in the renal expression of ECM degrading enzymes such as MMPs and plasmin and their biological inhibitors favour a reduction in ECM turnover and increased ECM deposition (Jones, 1996). This may be further contributed to by the action of ECM processing enzymes such as lysyl oxidase that serve to stabilise the expanding ECM (section 1.7.3).

The detailed mechanisms by which ECM synthesis, degradation and stabilisation may contribute to the composition and accumulation of the ECM are considered in section 1.7.

Figure 1.4 Proposed Patho-physiological Events in Kidney Scarring

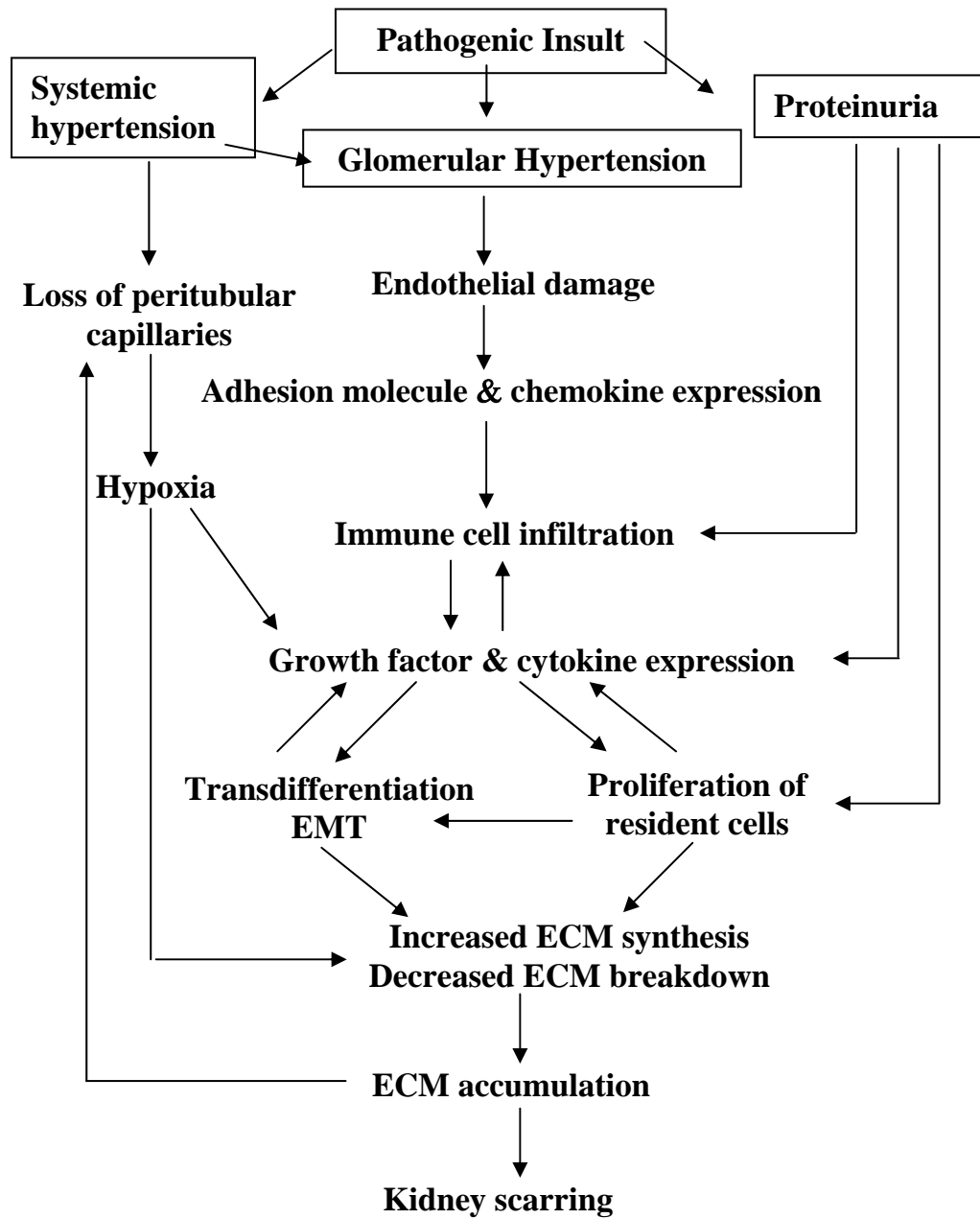


Figure 1.4 The progression of renal disease and the development of kidney scarring proceeds via a common pathway of events driven by glomerular and tubular injury, that stimulates changes to the endothelium promoting infiltration of immune cells and the release of inflammatory cytokines/growth factors, followed by proliferation and transdifferentiation of resident cells and excess accumulation of ECM proteins.

1.6 The Renal ECM

As in most tissues, the renal ECM is composed of an intricate network of macromolecules that together form a complex and dynamic supramolecular scaffold. Secreted locally and then assembled into an organised meshwork, the renal ECM serves to stabilise the structure of the kidney and support normal tissue function. Variation in ECM composition and architecture is critical in determining the kidney's physical properties. However, in addition to providing a structural framework, it has become increasingly clear that the ECM has an active role in regulating cell behaviour and is therefore involved in many cellular processes such as development, attachment and migration, differentiation and proliferation (Lukashev and Werb, 1998). By interacting directly with transmembrane integrin receptors to initiate signal transduction (Boudreau and Jones, 1999) or by immobilising growth factors and their binding proteins (Taipale and Keski-Oja, 1997), the ECM has been shown to act in a dynamic fashion to influence tissue physiology.

1.6.1 Distribution and function of the renal ECM

The renal ECM forms the structural basis for both the renal interstitium and the glomerular mesangium and comprises the specialised matrices of the tubular and glomerular basement membranes where it has distinct structural and functional roles.

1.6.1.1 Renal interstitium

The renal interstitium is composed of predominantly type I and type III collagens that form a fibrillar matrix hydrated by proteoglycans and fibronectin (Lemley and Kriz, 1991). However, it also contains a number of other collagens such types V, VI, VII and XV (Eddy, 2000a). A tubular basement membrane surrounding the outer surface of each nephron separates the tubular epithelium from the renal interstitium. This is composed of mainly type IV collagen as well as laminin, entactin/nidogen and sulphated proteoglycans (Miner, 1999).

The renal interstitium functions to provide structural support to the tubules and vessels, mediated by basement membrane attachment to cell and matrix by glycoproteins such as fibronectin (Leblond and Inoue, 1989) and heparin sulphate proteoglycans (Heremans *et al.*, 1989). It also plays a functional role in regulating differentiation and in the production of hormones such as erythropoietin (Koury and Koury, 1993). The tubular basement membrane, in addition to providing structural support, serves to mediate interaction between the tubules and the interstitium and plays a significant role in regulating epithelial adhesion, migration and differentiation. The composition of the basement membrane is also important for the maintenance of epithelial phenotype and changes in basement membrane architecture are

thought to contribute to the EMT observed in renal disease (Zeisberg *et al.*, 2001b). In addition, the heterogeneous nature of the tubular basement membrane is thought to contribute to the specificity of function in different regions of the nephron (Miner, 1999).

1.6.1.2 Glomerular mesangium

The mesangium is a specialised compartment of the glomerulus containing mesangial cells embedded in mesangial ECM. The most abundant component of the mesangial matrix is fibronectin. It also contains significant amounts of type IV collagen, laminin and entactin (Bender *et al.*, 1981). However, in contrast to the interstitium it lacks both collagen I and III (D'Ardenne *et al.*, 1983). The function of the mesangial matrix is primarily to provide structural support to the glomerular tuft and to maintain the structural integrity of the glomerular capillary network (Kriz *et al.*, 1990) but it is also important in modification of glomerular filtration by influencing mesangial cell contraction. It achieves both by the formation of an interwoven three-dimensional network of fibronectin-coated microfibrils that provide connections between mesangial cells and the glomerular basement membrane (Schwartz *et al.*, 1985).

1.6.1.3 Glomerular basement membrane (GBM)

The GBM is located between the endothelial cells of the glomerular capillaries and the visceral epithelial cells of the urinary space, forming the backbone of the glomerular tuft. Like the tubular basement membrane, the GBM is composed of mainly type IV collagen, laminin and entactin/nidogen (Miner, 1999) but also has a number of heparin sulphate proteoglycans such as agrin and perlecan (Groffen *et al.*, 1998; Groffen *et al.*, 1999). Type IV collagen forms the basis of a three-dimensional lattice-like network that gives the GBM tensile strength and a high degree of elasticity (Timpl and Brown, 1996). The presence of heparin sulphate proteoglycans is important in maintaining the electronegative charge of the GBM, providing a barrier to the loss of protein in the urine (Kanwar *et al.* 1981). In addition, agrin and perlecan have both been demonstrated to mediate cell matrix adhesion in the GBM through their interaction with α -dystroglycan and integrin receptors (Groffen *et al.*, 1999).

1.6.2 Major components of the renal ECM

1.6.2.1 Collagens

1.6.2.1.1 The collagen family

The collagens are a large superfamily of proteins consisting at present of at least 27 identified collagen types with 42 distinct polypeptide chains (Myllyharju and Kivirikko, 2004). Of the major components of the ECM, they are considered to be the most abundant

proteins. All collagens consist of three hydrogen bonded polypeptide α chains wound around one another to form a right handed super helix. In addition they all contain non-collagenous sequences at their termini. Each of the constituent polypeptide chains contain at least one domain composed of repeating Gly-X-Y sequences where X and Y are often proline and 4-hydroxyproline respectively. The presence of numerous glycine and proline residues in each polypeptide chain is important for the formation and stabilisation of the triple helix (Prockop and Kivirikko, 1995).

Depending on the collagen type, the three polypeptide chains can either be identical or the collagen molecule can contain two or three different α chains. For example, collagen I is a heterotrimer of two identical $\alpha 1$ (I) chains and one $\alpha 2$ (I) chain i.e. $[\alpha 1(I)]_2[\alpha 2(I)]$ whereas collagen III is a homotrimer of three $\alpha 1$ chains. In addition, collagen fibrils may also consist of more than one collagen type. For example, collagen I fibrils often contain small amounts of collagen III, V and XII. Some collagens can also form hybrid molecules for example collagen V and XII as they both contain the same α chains.

The superfamily of collagens can be further divided into a number of subfamilies on the basis of the structures they form or other related features (summarised in figure 1.5). The major classes are the fibrillar collagens (types I, II, III, V and XI), the collagens that form network-like structures (types IV, VIII and X) and the fibril-associated collagens with interrupted triple helices (FACITs including types IX, XII, XIV, XVI and XIX) (Myllyharju and Kivirikko, 2004).

The major collagen types present in the normal renal ECM (section 1.6.1) are collagen I and III that are found predominantly in the renal interstitium and collagen IV which is a major constituent of both glomerular and tubular basement membranes and is also present in the mesangial matrix. Interstitial fibroblasts, tubular epithelial and mesangial cells are all key cell types involved in the synthesis of renal collagens.

1.6.2.1.2 Biosynthesis of collagens

The biosynthesis of collagen is a multistep process characterised by a large number of co- and post-translational modifications many of which are unique to collagens and collagen-like proteins [reviewed in (Myllyharju and Kivirikko, 2004; Prockop and Kivirikko, 1995)].

The α chains of fibrillar collagens are synthesised on the ribosomes of the rough endoplasmic reticulum (ER) as large precursor molecules known as pro-collagens that have N and C terminal pro-peptide extensions. These are translocated across the ER membrane into the lumen where they are subject to a number of intracellular modifications that result in the

Figure 1.5 Subclasses of Collagen Types in the Collagen Superfamily


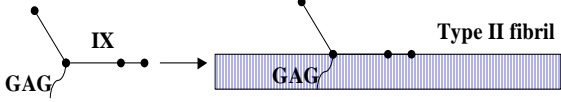
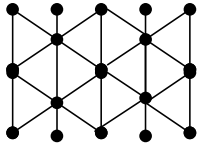
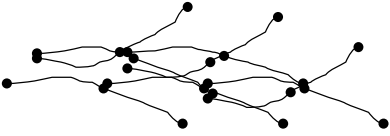
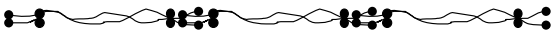
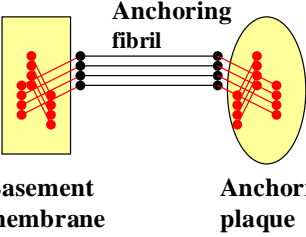
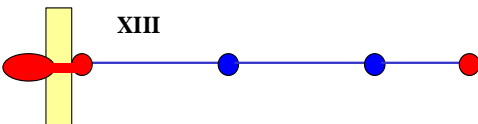
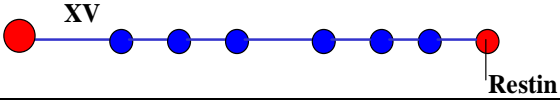
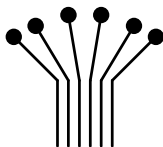
Collagen Subfamily	Collagen types	Structural Features
Fibril forming collagens	I, II, III, V, XI, XXIV, XXVII	
FACIT and related collagens	IX, XII, XIV, XVI, XIX, XX, XXI, XXII, XXVI	
Collagens forming hexagonal networks	VIII, X	
Type IV collagens	IV	
Type VI collagen forming beaded filaments	VI	
Type VII collagen forming anchoring fibrils	VII	
Collagens with transmembrane domains	XIII, XVII, XXIII, XXV	
Type XV and XVIII collagens	XV, XVIII	
Proteins containing triple helical collagenous domains	C1q, adiponectin, collectin, ficolin, acetyl cholesterase, macrophage receptor, ectodysplasin	

Figure 1.5 Collagen types are divided into 9 subfamilies based on the structures they form and other related features. Adapted from: (Myllyharju and Kivirikko, 2004)

formation of the triple helical pro-collagen molecule. Intracellular modifications in the assembly of pro-collagen include the hydroxylation of proline and lysine residues to 4-hydroxyproline, 3-hydroxyproline and hydroxylysine, glycosylation of some of the hydroxylysine residues to galactosyl-hydroxylysine and glucosylgalactosyl-hydroxylysine, glycosylation of certain asparagine residues, the association of polypeptide chains and folding of the triple helix. Once formed, the soluble pro-collagen is secreted from the cell where it undergoes further enzymatic processing to form insoluble collagen fibrils (summarised in figure 1.6). The precise mechanism of pro-collagen secretion is still poorly understood however, it is known to occur through the Golgi via the classical extracellular protein secretion pathway. Studies using fluorescent tagging of pro-collagen suggest that trafficking of pro-collagen through the Golgi occurs via tubular-saccular vesicles and requires the action of protein complexes COPI and COPII (Stephens and Pepperkok, 2002). Once through the Golgi, bundles of pro-collagen are thought to be released to form secretory vacuoles that migrate to the plasma membrane where they are secreted through narrow cellular recesses in the plasma membrane (Birk and Trelstad, 1984; Birk and Trelstad, 1986; Ploetz *et al.*, 1991). Extracellular processing of pro-collagen involves cleavage of the N and C terminal pro-peptide extensions, the self assembly of fibrils by nucleation and propagation and the formation of covalent crosslinks (Prockop and Kivirikko, 1995).

A number of highly specific enzymes have been implicated in the post-translational modification of collagen. Intracellular modifications are mediated by five enzymes: prolyl 4-hydroxylase, prolyl 3-hydroxylase, lysyl hydroxylase, hydroxylysyl galactosyltransferase and galactosyl-hydroxylysyl glucosyltransferase (Myllyharju, 2003; Myllyharju and Kivirikko, 2004). In the extracellular environment, cleavage of the N-terminal and C-terminal pro-peptides is mediated by pro-collagen N proteinase and pro-collagen C proteinase (Prockop *et al.*, 1998) with lysyl oxidase being responsible for the formation of covalent crosslinks (Kagan and Li, 2003).

Additional important enzymes are peptidyl proline cis-trans isomerases and protein disulphide isomerase (Bassuk and Berg, 1989). Collagen synthesis also requires the presence of a specific molecular chaperone Hsp47 which is thought to facilitate the intracellular processing of pro-collagen by the ER (Nakai *et al.*, 1992).

The processing and assembly of non-fibrillar collagens is essentially the same as for fibrillar collagens but with some important exceptions. For example the N and/or C-terminal pro-peptides of many collagens are not cleaved; some collagens undergo N-glycosylation or

Figure 1.6 Biosynthesis of Fibrillar Collagen

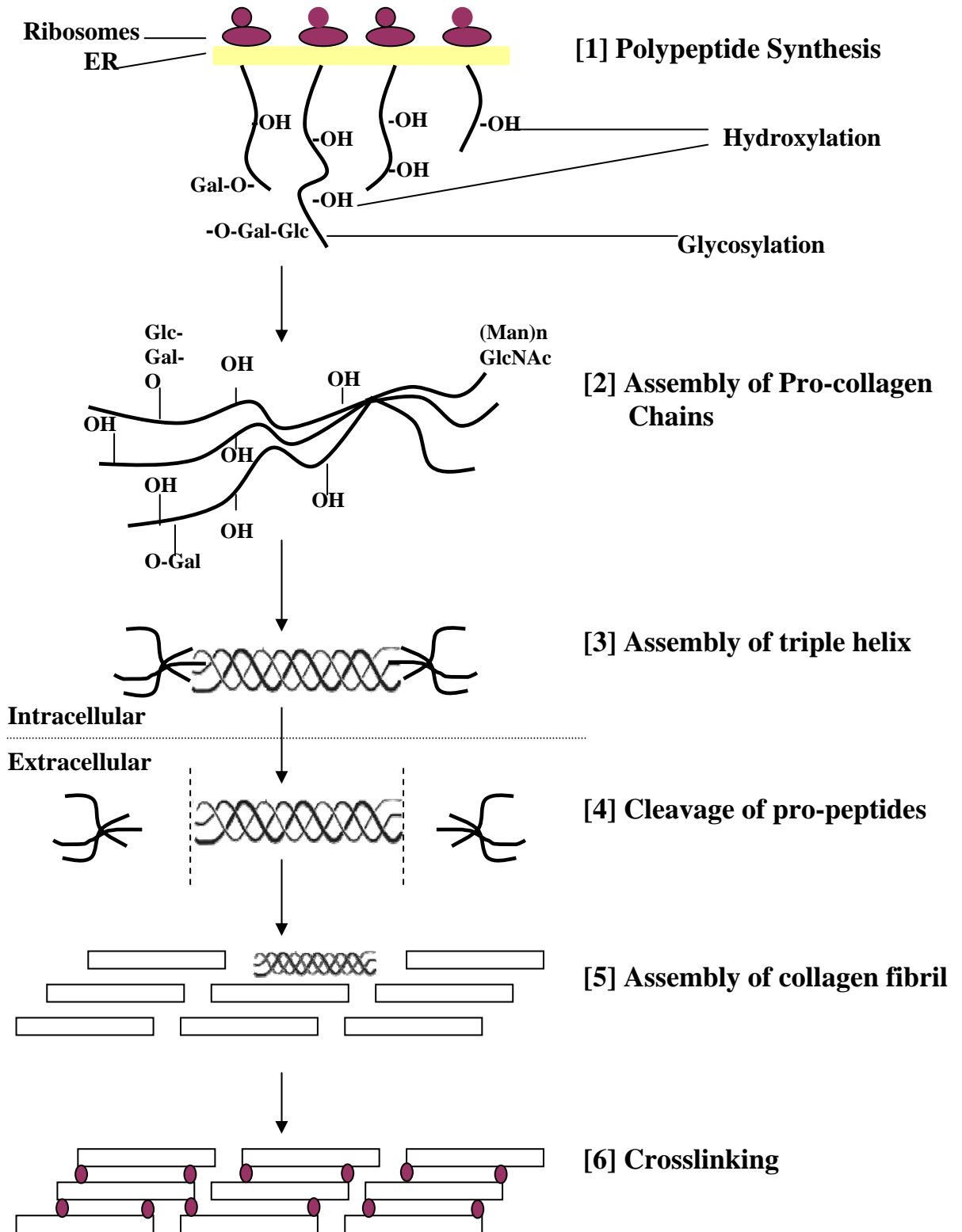


Figure 1.6 Pro-collagen polypeptide chains are synthesised on ribosomes of the rough ER and secreted into the lumen where chains undergo hydroxylation of prolyl and lysyl residues and glycosylation [1] before chain association [2] and triple helix formation [3]. The pro-collagen molecules are secreted into the extracellular space where the N and C pro-peptides are cleaved [4], collagen molecules are assembled into fibrils [5] and stabilised by crosslinking [6]. Adapted from: (Myllyharju and Kivirikko, 2001).

have additional processing steps such as the addition of glycosaminoglycan side chains (Myllyharju and Kivirikko, 2004; Prockop and Kivirikko, 1995).

1.6.2.1.3 Regulation of collagen synthesis

Much of the information regarding the regulation of collagen synthesis has been obtained from the study of pro-collagen I [reviewed by (Ghosh, 2002; Ramirez *et al.*, 2006; Rossert *et al.*, 2000)]. This has demonstrated that control occurs primarily at the transcriptional level. Extensive studies of the pro-collagen I gene have identified a number of regulatory regions within the proximal promoters of the COL1A1 and COL1A2 genes that control basal (Ihn *et al.*, 1996), tissue specific (Goldberg *et al.*, 1992; Simkevich *et al.*, 1992) and cytokine mediated gene expression (Rossert *et al.*, 2000). Basal collagen I transcription from the proximal promoter is under the control of a number of *cis* acting elements that bind positively or negatively acting transcription factors (Ghosh, 2002). These *cis* elements include a CCAAT box motif recognised by the heterotrimeric CCAAT binding factor (CBF) (Hu and Maity, 2000; Maity *et al.*, 1988; Saitta *et al.*, 2000), GC rich consensus regions that bind Sp-1 and Sp-3 (Chen *et al.*, 1998; Tamaki *et al.*, 1995) and a number of distinct DNA sequences that are bound by CCAAT enhancer binding protein (C/EBP), Ets and AP-1 (Ghosh, 2002). In addition, transcription can be modulated by the methylation of responsive CpG sites within the promoter that result in downregulation of collagen I (Thompson *et al.*, 1991).

The *cis*-acting elements are also involved in mediating the transcriptional response to cytokines such as TGF- β and TNF- α which are implicated in tissue remodeling and scarring (Verrecchia and Mauviel, 2004). Activated TGF- β 1 has been shown to regulate COL1A1 expression via the TGF- β activator signalling pathway and binding to the TGF- β *cis* element within the distal promoter region (Jimenez *et al.*, 1994). Modulation of COL1A2 by TGF- β 1 occurs through the activation of transmembrane serine/threonine signalling and the Smad pathway (Chen *et al.*, 1999). Ligand-induced phosphorylation of Smad2 and Smad3 promotes formation of complexes with Smad4, which translocate to the nucleus and activate gene transcription by binding the CAGAC consensus sequence, and by interacting with promoter-specific transcription factors and co-activators (Zhang *et al.*, 2000). TNF- α is in general a negative regulator of collagen I gene expression. TNF- α signals through the TNFR1 and TNFR2 receptors to activate the transcription factors AP-1 and NF- κ B and subsequently inhibit collagen I expression (Kouba *et al.*, 2001; Riches *et al.*, 1996).

1.6.2.2 Non-collagenous glycoproteins

1.6.2.2.1 Fibronectin

Fibronectin (FN) is a high molecular mass glycoprotein that is an abundant component of the renal ECM where it is found in polymerised form as a network of multimeric fibrils. It is secreted as a disulphide bonded dimer composed of two similar 200-250 kDa subunits. Each subunit consists of type I, type II and type III repeating modules (figure 1.7a) that themselves form large functional domains capable of interacting with cells as well as with other matrix components such as collagen, heparin and FN itself (Pankov and Yamada, 2002). Interaction of FN with cells occurs via binding of the Arg-Gly-Asp (RGD) domain to $\alpha_5\beta_1$ integrin receptors on the cell surface (Ruoslahti, 1996). Such binding is known to play a role in regulating cell adhesion and adhesion-mediated signalling in turn modulating processes such as cell growth and migration. In addition, interaction between $\alpha_5\beta_1$ integrin receptor and FN is crucial in initiating the assembly of FN dimers into fibrils (Sechler *et al.*, 1998), a multistep process which is cell mediated and occurs at the cell surface (section 1.6.2.2.2).

As well as insoluble ECM FN, several other isoforms exist such as plasma FN, that result from alternative splicing of the EIIIA, EIIIB and V regions of the FN gene and vary in their biological properties (Kornblihtt *et al.*, 1996). Isoforms containing the EIIIA and EIIIB splice variants have been implicated in the regulation of cell proliferation and migration whereas isoforms containing the full-length V region are ligands for the VLA-4 integrin (Alonso *et al.*, 1999). Changes in the splicing patterns of FN in renal disease (section 1.7.1) may play a role in altering cell behaviour and the physiological properties of the ECM to promote fibrosis.

1.6.2.2.2 Assembly of FN

The assembly of FN into fibrillar matrix is tightly regulated *in vivo* and involves initiation, elongation and stabilisation steps (figure 1.7b) (Schwarzbauer and Sechler, 1999). Initiation of FN assembly is dependent on the activation of soluble FN dimers. This is induced by the interaction between FN and so-called “matrix assembly sites” on the cell surface [step 1] that possess the $\alpha_5\beta_1$ integrin receptor (Sechler *et al.*, 1998). In endothelial cells and fibroblasts, these matrix assembly sites are localised to focal adhesions and cell matrix contacts (Christopher *et al.*, 1997). Binding of FN to $\alpha_5\beta_1$ receptor is known to be critical for fibril assembly and antibodies against $\alpha_5\beta_1$ strongly inhibit fibril formation (Fogerty *et al.*, 1990). In addition, a number of other integrins are able to initiate FN assembly including $\alpha_v\beta_3$, $\alpha_{IIb}\beta_3$ and $\alpha_4\beta_1$ (Sechler *et al.*, 2000; Wennerberg *et al.*, 1996; Wu *et al.*, 1996; Yang and Hynes, 1996). Interestingly, the presence of tissue transglutaminase at matrix assembly sites has been implicated in FN fibrillogenesis (section 1.8.2.5.4). The enzyme has been

shown to act as an integrin co-receptor for FN (Akimov *et al.*, 2000) and its presence at the cell surface enhances FN matrix formation mediated by the $\alpha 5\beta 1$ integrin (Akimov and Belkin, 2001a).

Binding of soluble FN to $\alpha 5\beta 1$ via the RGD sequence in the type III₉ module results in a conformational change that activates FN and promotes fibril assembly [Step 2]. This involves the expansion and unfolding of the N-terminal assembly region exposing FN-binding domains that are hidden in the compact form allowing them to participate in FN-FN interactions (Schwarzbauer and Sechler, 1999; Sechler *et al.*, 1996; Wierzbicka-Patynowski and Schwarzbauer, 2003). A number of other domains contained within this region may also participate in FN interactions including the repeat III₁ domain (Hocking *et al.*, 1999) and the heparin-binding domain (Bultmann *et al.*, 1998).

The interaction of FN dimers with more than one integrin receptor and with other FN dimers leads to integrin receptor clustering [Step 3] and promotes further self association to form FN multimers (Schwarzbauer and Sechler, 1999). Integrin clustering also recruits intracellular signalling and cytoskeletal proteins that themselves serve to regulate the FN matrix assembly process. In particular, the recruitment of Src and PI3 kinase is implicated in initiating and maintaining the propagation of FN fibrils (Wierzbicka-Patynowski and Schwarzbauer, 2002). In addition, activation of the Ras pathway may suppress the ability of $\alpha 5\beta 1$ integrin to mediate FN assembly (Hughes *et al.*, 1997).

Continued self-association of FN dimers gradually leads to the formation of mature FN fibrils [Step 4] that accumulate into a dense detergent-insoluble matrix (Chen and Mosher, 1996; McKeown-Longo and Mosher, 1983). This property of mature FN matrix is thought to result in part from disulphide bond formation by disulphide isomerase that serves to stabilise the matrix (Langenbach and Sottile, 1999) but also from stable protein-protein interactions (Chen and Mosher, 1996).

1.6.2.2.3 Laminin

Laminin is a major component of both the glomerular and tubular basement membrane and is a multidomain heterotrimer composed of three polypeptide chains termed α , β and γ . At present there are 15 reported heterotrimers in the laminin family assembled from five α , four β and three γ chains (Hallmann *et al.*, 2005). All laminin chains share common structural features including a small globular domain involved in chain polymerisation and a series of epidermal growth factor (EGF)-like repeats that host a nidogen binding site (Beck *et al.*, 1990).

Figure 1.7 Domain Structure and Assembly of FN

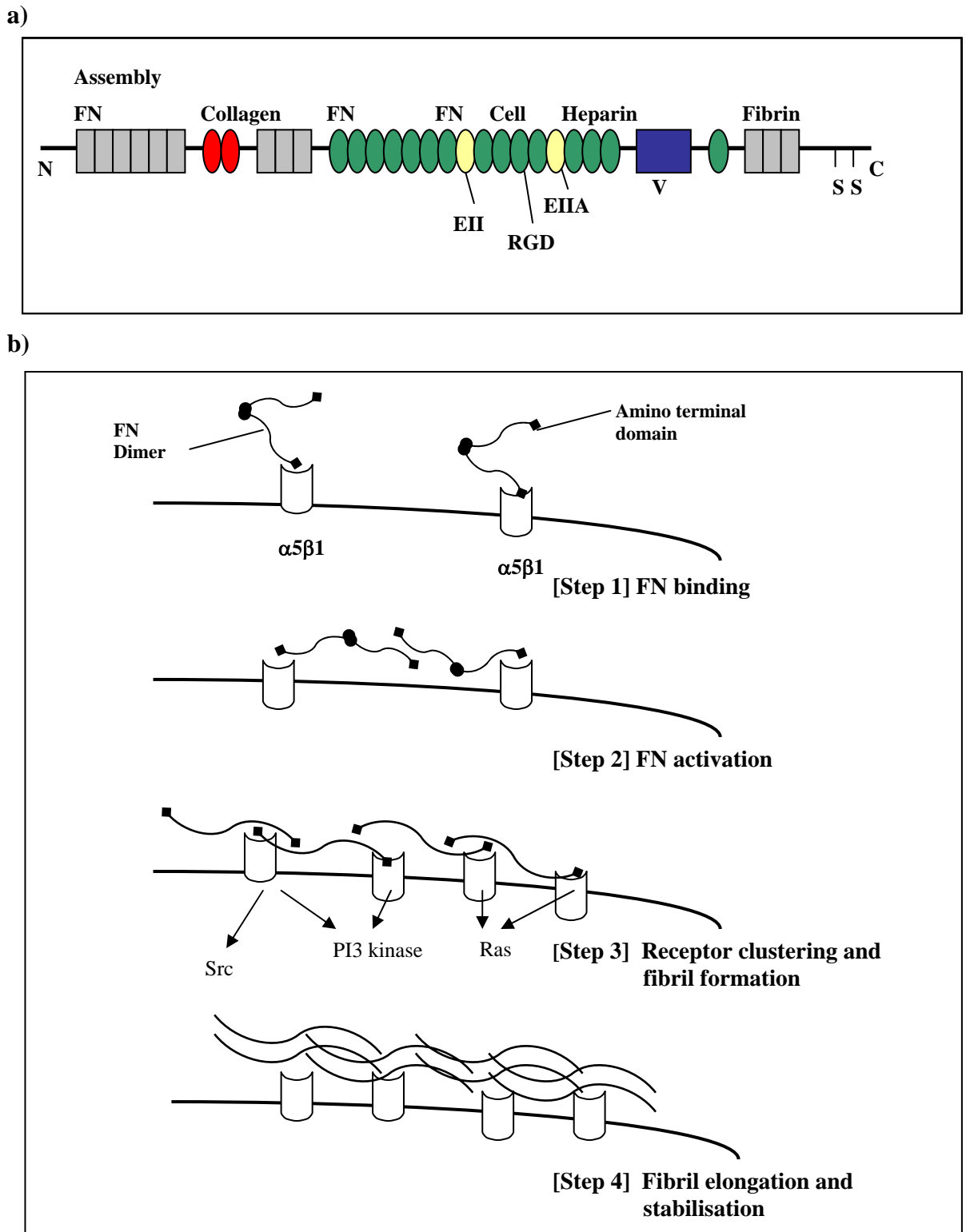


Figure 1.7 (a) Each FN monomer is composed of a domain structure consisting of type I (grey rectangle), type II (red oval) and type III (green oval) repeating modules. Dimers are formed through disulphide bonds at the C-terminus. Repeating modules form a series of domains capable of interaction with cells, ECM components and FN. (b) Assembly of FN fibrils occurs in a stepwise manner at matrix assembly sites on the cell surface that possess specific integrin receptors and involves initiation, elongation and stabilisation stages. Adapted from: (Schwarzbauer and Sechler, 1999).

Interaction of nidogen with this site via its C-terminal globular domain and with the collagenous domain of collagen IV allows linkage between these network-forming proteins. Other structural features are more chain-specific such as the large C terminal domain of the α chain that contains a number of integrin binding sites.

Laminins have the ability to self assemble into polymers to form a polygonal network. The co-ordinated assembly of laminin is considered to follow a mechanism analogous to that of FN assembly (Cheng *et al.*, 1997; Colognato *et al.*, 1999; Yurchenco and Cheng, 1993). Laminin secreted at the cell surface is prompted to self-interact by receptor binding to cell surface integrins and dystroglycans (Colognato *et al.*, 1999; Henry and Campbell, 1998; Henry *et al.*, 2001). Interaction between laminins is thought to occur through the N-terminal laminin domains of the short arm (Schittny and Yurchenco, 1990; Yurchenco and Cheng, 1993). Binding of laminin to receptors causes receptor clustering, the organisation of the actin cytoskeleton and subsequent assembly of the laminin network (Colognato *et al.*, 1999). This forms a scaffold for the recruitment of other basement membrane components such as collagen IV and proteoglycans (Timpl and Brown, 1996).

Most laminin chains have been localised to the kidney by immunohistochemical analysis and co-localisation studies allowing the prediction of predominant trimers. Of these, laminin-1, -10 and -11 are the predominant types in the mature kidney ECM and are synthesised mainly by epithelial and endothelial cells (Miner, 1999). Laminin-1 is found in proximal tubular basement membrane and Loop of Henle basement membrane (Klein *et al.*, 1988; Sorokin *et al.*, 1992). Laminin-10, which is the most abundant trimer in the kidney, is found throughout the length of the tubular and collecting duct basement membranes (Miner *et al.*, 1997; Sorokin *et al.*, 1992). Laminin-11 has a highly restricted distribution and is only found in the GBM and arteriolar basement membranes (Miner *et al.*, 1997).

The role of laminins in the basement membrane is thought to be dynamic and they serve to provide interaction between cells and the ECM thereby influencing cell function by affecting cell adhesion, cell migration and differentiation. They exert these effects through integrins, many of which recognise the integrin binding domain of the α chain. Of relevance to the kidney, laminin-1 has been shown to induce the differentiation of epithelial cells whilst laminin-11 is critical for renal function and if mutated results in the development of proteinuria (Noakes *et al.*, 1995).

1.6.2.2.4 Tenascin

Tenascin (TN) is part of a larger group of secreted “matricellular” glycoproteins that participate in cell matrix interactions. The TN family consists of five large oligomeric glycoproteins: TN-C, TN-R, TN-W, TN-X and TN-Y that share a common domain structure comprising an N-terminal TN assembly (TA) domain, a series of EGF like repeats, FN-III binding domains, an integrin-specific cell binding sequence and calcium binding domains (Sage and Bornstein, 1991). TNs are mainly expressed in embryonic tissues where they participate in tissue remodelling and morphogenesis. In adult tissues they are not abundant but are up-regulated in response to wound healing and tissue injury. In the kidney, TNs are strongly expressed during embryogenesis where they are detected in the interstitium but are absent from immature glomeruli (Okada *et al.*, 1996; Truong *et al.*, 1996). In adult tissue, TN expression is localised to the mesangial matrix (Truong *et al.*, 1994b) where it is synthesised by mesangial cells (Truong *et al.*, 1994a) and is also found in the medullary interstitium (Truong *et al.*, 1996). Increased TN expression during renal disease has been shown to be associated with mesangial expansion and is found in areas of tubulointerstitial damage regardless of the disease pathology (Truong *et al.*, 1996).

The role of TNs within the ECM, as with other ECM glycoproteins, is a dynamic one and they act as adhesive proteins capable of interacting with both cells and the ECM thereby influencing cell behaviour. A number of cell surface receptors exist for TNs including integrins and immunoglobulin-like cell adhesion molecules and they are able to interact with other ECM proteins such as FN and chondroitin sulphate proteoglycans through ECM binding domains. Such a role in cell-matrix interaction is important in the developing kidney in promoting epithelial differentiation and nephrogenesis whilst in the adult kidney it contributes to processes that are important for tissue homeostasis such as growth and cell migration.

1.6.2.2.5 SPARC (Secreted Protein Acidic and Rich in Cysteine)

SPARC formally known as osteonectin, is an acidic cysteine-rich matricellular protein consisting of three modular domains that act independently to bind to cells and the ECM. It is highly expressed in embryonic tissues where it appears to be restricted to areas where there is a high rate of cellular proliferation and remodelling such as limb buds and invasive embryonic cells (Holland *et al.*, 1987; Sage *et al.*, 1989a). In adult tissues it is much less abundant and like TN is up-regulated in response to wound healing and tissue injury. In the normal kidney, SPARC has been found in many species and has been localised to the distal cortical tubule and the medullary tubules of murine kidney (Kopp *et al.*, 1992). *In vivo*, SPARC is constitutively expressed by glomerular epithelial cells (podocytes) (Floege *et al.*, 1992b) and

in vitro is also expressed by a number of proximal tubular cell lines including LLC-PK1 and OK cells (Kopp *et al.*, 1992). In the diseased kidney, SPARC protein and mRNA are up-regulated at sites of glomerular and tubulointerstitial fibrosis and contribute to matrix expansion (section 1.7.1).

A variety of functions for SPARC have been demonstrated within the ECM that are likely to contribute to its role within the renal matrix. SPARC has been shown to directly influence cell shape by interfering with cell-matrix interactions (Sage *et al.*, 1989a; Sage *et al.*, 1989b). In the glomerulus this may play a role in controlling glomerular permeability. In addition, SPARC regulates the activity of a number of growth factors including VEGF (Kupprion *et al.*, 1998), FGF (Hasselaar and Sage, 1992), PDGF (Gohring *et al.*, 1998; Raines *et al.*, 1992) and TGF- β 1 (Francki *et al.*, 2004) which has important implications for the control of cell proliferation and matrix synthesis. SPARC also interacts with a number of ECM proteins including collagens (Sage *et al.*, 1989b) and influences the secretion of matrix-degrading enzymes including MMPs (Shankavaram *et al.*, 1997) thereby playing an important role in ECM homeostasis.

1.6.2.2.6 Thrombospondin

The thrombospondins are calcium binding multi-domain glycoproteins that are divided into two subfamilies A and B according to their molecular organisation. The subgroup A proteins are thrombospondins 1 and 2 (TSP-1 and -2) which are found as trimers (Lawler and Hynes, 1986) with each subunit comprising a number of key domains. These include a pro-collagen homology domain, a type 1 repeat domain that binds a number of ECM proteins and TGF- β and a type 3 domain that binds calcium ions and a number of integrins (Adams, 2001). The subgroup B thrombospondins [TSP-3, -4 and 5/Cartilage Oligomeric Matrix Protein (COMP)] exist as homopentamers, have distinct N-terminal regions and lack the pro-collagen homology domain and the type 1 repeats (Adams, 2001).

Each of the thrombospondins has a distinct pattern of tissue distribution. Little is known about the normal distribution of TSP-1 and TSP-2 in adult kidney however, TSP-2 and TSP-3 are present in the embryonic kidney and TSP-3 has been found in adult kidney (Adolph, 1999). Human mesangial cells in culture produce thrombospondin and it is likely that thrombospondin is a component of the normal mesangial matrix (Raugi and Lovett, 1987). Increased expression of thrombospondin, in particular TSP-1 has been associated with the development of glomerular and tubulointerstitial fibrosis (Hugo *et al.*, 2002) and is demonstrated to increase in human glomerular disease (McGregor *et al.*, 1994). TSP-1 may have a number of roles in renal disease although these have yet to be fully defined. TSP-1 has

been shown to induce adhesion and migration of mesangial cells (Taraboletti *et al.*, 1992) and to stimulate proliferation and ECM production (Tada *et al.*, 1995). In addition TSP-1 has been shown to be an important regulator of TGF- β 1 by binding to and activating the latent TGF- β 1 complex (Sasaki *et al.*, 2001; Schultz-Cherry *et al.*, 1994).

1.6.2.3 Proteoglycans

Proteoglycans are a heterogeneous group of complex macromolecules, consisting of sulphated polysaccharide side chains (glycosaminoglycans) covalently linked to a backbone core protein. The different glycosaminoglycans can be distinguished by their sugar residues and the number and location of sulphate groups. These include (1) hyaluronan (hyaluronic acid), (2) chondroitin sulphate and dermatan sulphate, (3) heparin sulphate and heparin and (4) keratin sulphate. Several families of proteoglycans have emerged based on their structural properties and are summarised in table 1.2. Of these, a number have been identified in the kidney as components of the normal renal ECM. These include the heparin sulphate proteoglycans agrin and perlecan, the chondroitin/dermatan sulphate proteoglycans decorin, biglycin and bamacan (Miner, 1999) and the keratin sulphate proteoglycans fibromodulin and lumican (Schaefer *et al.*, 2000).

Many of these proteoglycans are found as constituents of the tubular and glomerular basement membranes. The glycosaminoglycan side chains are highly negatively charged and this contributes to the overall negative charge of the membranes. In the GBM this is essential for maintenance of the charge barrier and the ultrafiltration properties of the membrane (Miner, 1999).

As well as their important function in basement membranes, a number of other roles have been identified for proteoglycans. Decorin, fibromodulin and lumican all appear to be important for normal collagen fibril formation (Ezura *et al.*, 2000; Neame *et al.*, 2000). Targeted disruption of the genes for these proteoglycans leads to abnormal collagen fibril morphology (Danielson *et al.*, 1997; Chakravarti *et al.*, 1998; Svensson *et al.*, 1999). A number of studies have also identified a role for proteoglycans in modulation of cytokine activity. Decorin, biglycan and fibromodulin have been shown to form complexes with TGF- β 1 (Hildebrand *et al.*, 1994). Heparin sulphate proteoglycans have been shown to be important in the response of cells to FGF-2. The expression of cell-surface heparin sulphate proteoglycans appears to be essential for the proliferation of renal fibroblasts in response to FGF-2 (Clayton *et al.*, 2001). Therefore these molecules have an important role in regulating both cell function and in modulating the cell response to cytokines.

Table 1.2 Proteoglycan Families and their Renal Distribution

Proteoglycan Family	Major Family Members	Renal Distribution
Heparin Sulphate PGs		
-Matrix Associated	Perlecan	MM, GBM, TBM ^{a,b,c}
	Agrin	GBM, TBM ^{d,e}
- Membrane Associated	Syndecans	Glomeruli, EK ^{f,g}
	Glypicans	Glomeruli, EK ^{f,g,h}
Lecticans	Aggrecan	Unknown
	Versican	EK ^g
	Neurocan	Not present
	Brevican	Not present
Small leucine rich PGs (SLRP's)	Decorin	
	Biglycan	IM, MM, GBM ⁱ
	Fibromodulin	
	Lumican	
Cell Associated PGs	Serglycin	Unknown
	Betaglycan	Mesangial cells and PTEC ^{j,k}
	CD44 family	PTEC ^{l,m}
	Thrombomodulin	Glomerular endothelial and mesangial cells ^{n,o}

Table 1.2 Proteoglycans (PGs) can be divided into a number of families according to their structural features and other properties (Bosman and Stamenkovic, 2003). A number have been localised to the renal ECM where they participate in a variety of functions including maintenance of ultrafiltration, collagen fibril formation and modulation of the cell response to cytokine signalling. EK=embryonic kidney, MM = mesangial matrix, IM = interstitial matrix, GBM = glomerular basement membrane, TBM = tubular basement membrane and PTEC = proximal tubular epithelial cell. References: ^a Groffen *et al.*, 1997. ^b(Groffen *et al.*, 1999) ^c (Murdoch *et al.*, 1994) ^d (Groffen *et al.*, 1998) ^e (Raats *et al.*, 1998) ^f (Pyke *et al.*, 1997) ^g (Steer *et al.*, 2004) ^h (Hartwig *et al.*, 2005) ⁱ (Schaefer *et al.*, 2000) ^j (Riser *et al.*, 1999) ^k (Eickelberg *et al.*, 2002) ^l (Selbi *et al.*, 2004) ^m (Selbi *et al.*, 2006) ⁿ (Mizutani *et al.*, 1993) ^o (Pruna *et al.*, 1997).

1.6.3 Renal ECM-degrading enzymes

1.6.3.1 Matrix metalloproteinases (MMPs)

The MMPs are a large superfamily of zinc dependent enzymes that together are capable of processing and degrading most ECM proteins. Members of the MMP family include the “classical” MMPs, the membrane-bound MMPs (MT-MMPs), the ADAMS (a disintegrin and

metalloproteinase; adamalysins) and the ADAMTS (a disintegrin and metalloproteinase with thrombospondin motif). There are now at least 20 members of the MMP and ADAMT family that are further subdivided according to their substrate specificity into collagenases, gelatinases, stromelysins, elastases and aggrecanases (Malemud, 2006).

The MMPs consist of a single polypeptide comprising several domain motifs, many of which are common to all members. Most MMPs possess a regulatory pro-peptide domain with a conserved PRCGxPD motif that contains a critical Cys responsible for maintaining latency in MMPs (Becker *et al.*, 1995; Van Wart and Birkedal-Hansen, 1990). The catalytic domain contains a zinc-binding motif HEXGHXXXXXHS and a conserved methionine that form a “Met-turn” structure (Bode *et al.*, 1993). At the C-terminal a haemopexin-like domain is present that has an ellipsoidal disk shape with four antiparallel β -sheets and an α helix (Gomis-Ruth *et al.*, 1996). The haemopexin domain is known to be required for the cleavage of triple helical collagen (Clark and Cawston, 1989; Knauper *et al.*, 1996; Knauper *et al.*, 1993; Ohuchi *et al.*, 1997; Patterson *et al.*, 2001).

1.6.3.1.1 Transcriptional regulation of MMPs

MMP expression is tightly regulated at the transcriptional, translational and post-translational level. At the transcriptional level, MMP gene expression can be induced by variety of stimuli including growth factors and cytokines such as PDGF, TNF- α and IL-1, chemical agents such as phorbol esters, physical stress and oncogenic transformation (Nagase and Woessner, 1999). Expression can also be down-regulated by suppressive factors such retinoic acid and glucocorticoids (Nagase and Woessner, 1999). Some factors both stimulate and down-regulate MMP expression depending on the cell type, for example, TGF- β 1 (Edwards *et al.*, 1996; Edwards *et al.*, 1987; Hui *et al.*, 2001; Kim *et al.*, 2004; Lechuga *et al.*, 2004; Martin *et al.*, 1998; Overall *et al.*, 1991; White *et al.*, 2000). In addition, MMP expression can be regulated by the composition of the ECM via the interaction of ECM proteins with cell membrane-associated receptors (Langholz *et al.*, 1995; Norman and Lewis, 1996; Takahra *et al.*, 2004; Wang *et al.*, 2004). In particular, interaction of the ECM with integrins has an important role in MMP induction. For example, signaling via the α 2 β 1 integrin has been shown to induce MMP-1 expression in several studies (Dumin *et al.*, 2001; Langholz *et al.*, 1995; Riikonen *et al.*, 1995). MMP-9 expression can also be modulated by α 2 β 1 integrin as well as by α 5 β 1 and α 5 β 6 signalling (Agrez *et al.*, 1999; Vo *et al.*, 1998; Xie *et al.*, 1998).

The transcriptional regulation of MMPs requires the activation of a number of intracellular signalling pathways. Most inducible MMPs share common features in their regulatory regions including a TATA box and a number of AP-1 regulatory elements (Matrisian, 1994). Many extracellular stimulators of MMP expression activate the Fos and Jun family of AP-1 transcription factors that bind to the AP-1 *cis* element and activate transcription [reviewed in (Chakraborti *et al.*, 2003)]. However, the inflammatory cytokines TNF- α and IL-1 also activate the ceramide signalling pathways that are mediated by the MAP kinases ERK1/2, JNK and p38 (Reunanen *et al.*, 1998; Westermarck *et al.*, 1998).

Post transcriptional mechanisms also play a role in regulating MMP expression. The stability of MMP-1 and MMP-13 mRNA transcripts can be regulated by a variety of growth factors and cytokines (Delany *et al.*, 1995; Vincenti *et al.*, 1996) whilst TGF- β 1 has been implicated in the stabilisation of MMP-2 and -9 mRNA (Van den Steen *et al.*, 2002).

1.6.3.1.2 Activation of MMPs

As well as being subject to transcriptional regulation, MMPs also require activation for their function. Most MMPs are secreted as pro-enzymes that contain an N-terminal pro-domain. Latency of the pro-MMPs is maintained by the interaction between Cys⁷³ contained within the pro-domain and a Zn²⁺ atom within the catalytic domain that serves to block the active site (Springman *et al.*, 1990; Van Wart and Birkedal-Hansen, 1990). Proteolytic cleavage of the pro-domain is a critical step in the activation of MMPs and leads to the dissociation of Cys⁷³ from the Zn²⁺ atom allowing the binding of a water molecule and exposure of the active site (fig 1.8a). This has been termed the “cysteine-switch” mechanism of activation (Springman *et al.*, 1990; Van Wart and Birkedal-Hansen, 1990). Cleavage of the pro-domain occurs in a stepwise manner with proteases attacking a susceptible “bait” region within the pro-domain. A conformational change in the pro-domain is induced which renders the pro-domain susceptible to further proteolysis. The complete cleavage of the pro-domain is thought to require the additional action of MMP intermediates or active MMPs (Nagase, 1997).

Some of the MMPs have subtle differences in their conformation that have important implications for substrate binding. In pro-MMP-1 for example, the pro-domain interacts with the haemopexin domain which results in a “closed” conformation. Cleavage of the pro-domain releases the haemopexin domain allowing an open conformation and exposure of the active site (Jozic *et al.*, 2005).

In vivo, physiological activators of pro-MMPs are tissue and plasma proteinases and bacterial proteinases. The most significant of these is thought to be proteinases of the urokinase plasminogen activator (uPA)/ plasmin system although trypsin, stromelysin, cathepsins B and L and polymorphonuclear (PMN) elastins have all been implicated in MMP activation (Chakraborti *et al.*, 2003). *In vitro*, pro-MMPs can also be activated by non-proteolytic agents such as SH-reactive agents, mercurial compounds, reactive oxygen and denaturants (Nagase and Woessner, 1999). In most cases, activation is thought to result from perturbation of the pro-MMP structure inducing a conformational change that leads to autoprocessing of the pro-peptide and dissociation of Cys⁷³ (Stack *et al.*, 1996). However, ROS are thought to activate pro-MMPs by directly interacting with Cys⁷³ (Gu *et al.*, 2002; Peppin and Weiss, 1986).

A number of the MMPs, in particular, membrane-associated MMPs are thought to be activated intracellularly and secreted or bound at the cell surface as active enzymes. These share a furin-like pro-peptide recognition sequence RX[KR/R] at the end of the pro-peptide that appears to target intracellular activation (Remacle *et al.*, 2006).

1.6.3.1.3 Inhibition of MMPs

Once in the active form, MMPs are subject to further physiological regulation by endogenous inhibitors such as α_2 macroglobulin and TIMPs. α_2 macroglobulin is the major plasma inhibitor of MMPs and acts by interacting with the cleavable “bait” region of the pro-peptide causing a conformational change that entraps the MMP allowing it to be covalently anchored to α_2 macroglobulin. Such α_2 macroglobulin/MMP complexes are then cleared by scavenger receptor-mediated endocytosis (Hahn-Dantona *et al.*, 2001).

TIMPs are the specific tissue regulators of MMP activity and currently four TIMPs (TIMPs -1 to -4) have been identified (Gomez *et al.*, 1997). TIMPs are 20-30 kDa proteins with a variably glycosylated two-domain structure. TIMP-1, -2 and -4 are secreted in soluble form whilst TIMP-3 is sequestered to the ECM (Gomez *et al.*, 1997). The mechanism of TIMP inhibition involves non-covalent interaction between critical residues located around the disulphide bond between Cys¹ and Cys⁷⁰ located in the N-terminal region of TIMP and the active site of the MMP (fig 1.8b). Cys¹ bidentally coordinates the Zn²⁺ through its α -amino and carbonyl groups while the side chain of residue 2 (Thr or Ser) inserts into the mouth of the enzyme (Gomis-Ruth *et al.*, 1997). Blocking of the N-terminal amino group by carbonylation (Higashi and Miyazaki, 1999), acetylation (Troeborg *et al.*, 2002) or the addition of extra residues (Troeborg *et al.*, 2002; Wingfield *et al.*, 1999) blocks the inhibitory action of TIMPs.

In addition to physiological inhibitors of MMPs, a number of synthetic inhibitors have been generated some of which have been used in a clinical setting. These comprise the peptidyl hydroxamate inhibitors, Batimastat, Marimastat (Coussens *et al.*, 2002), Galardin (Ilomastat) (Grobelny *et al.*, 1992), 1,10 phenanthroline (Benyon and Bond, 1994) and non-peptidyl inhibitors such as tetracycline (Hidalgo and Eckhardt, 2001). The peptidyl hydroxamate compounds are broad spectrum reversible MMP inhibitors that block MMP action by chelating the active site Zn^{2+} ion. The hydroxamate acts as a bidentate ligand with each oxygen at an optimum distance from the Zn^{2+} ion (Grams *et al.*, 1995). Tetracycline can inhibit MMP action by a number of mechanisms including: chelation of active site cations, interference with pro-enzyme processing and increasing MMP susceptibility to degradation (Rifkin *et al.*, 1993; Smith *et al.*, 1999; Sorsa *et al.*, 1994).

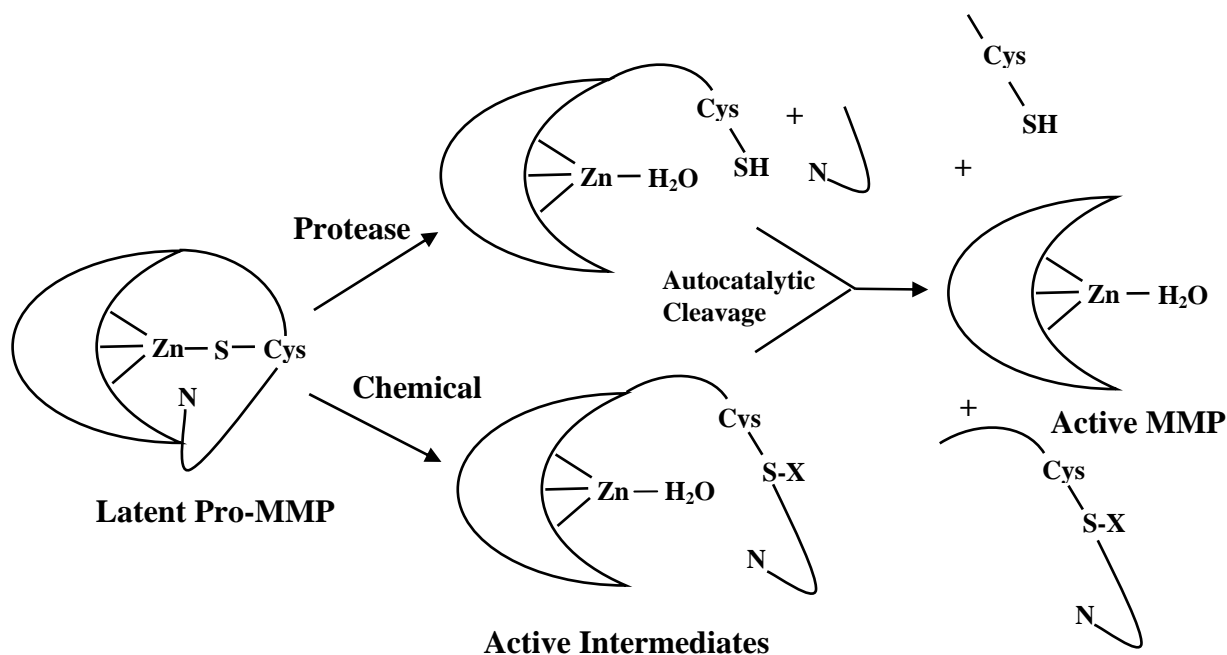
1.6.3.1.4 MMP cleavage of the ECM

The primary physiological role of MMPs is in the degradation of the ECM that is an important process in tissue remodelling and repair, morphogenesis and embryonic development. In particular, many MMPs participate in the breakdown of interstitial collagens (I, II and III) and denatured collagen (gelatin) degradation. These include the collagenases (MMP-1, -8, -13 and 18), MMP-2 (gelatinase A) and membrane type MMP-1 (Chakraborti *et al.*, 2003). The mechanisms by which MMPs, in particular MMP-1, degrade collagen matrix have been the subject of intense study in recent years and details of this process are beginning to emerge.

The triple helical structures of the interstitial collagens are arranged into tightly packed fibrils (section 1.6.2.1) that are highly resistant to proteolytic degradation. Initiation of collagen cleavage is thought to require MMP binding to the fibrils and destabilisation of the fibrillar structure revealing the individual triple helices. The MMP C-terminal domain appears to be important for this process (Lauer-Fields *et al.*, 2000). Studies of MMP-1 suggests that MMP interaction occurs at the outer edges of the fibrils and that once associated, MMP-1 may move along by a process of biased diffusion until it encounters specific cleavage recognition sites (Saffarian *et al.*, 2004). In order for collagen to be cleaved it is thought that the triple helix must be unwound prior to hydrolysis since triple helical collagen is too large to be accommodated in the substrate binding site (Lauer-Fields *et al.*, 2000). In the case of MMP-1, unwinding of the helix has been demonstrated to occur locally at specific cleavage sites and requires the helical peptidase action of the catalytic domain (Chung *et al.*, 2004). The ability of this domain to unwind the triple helix is thought to be separate from its collagen cleavage activity (Lauer-Fields *et al.*, 2002). Once unwinding of the helix has occurred the MMP is

Figure 1.8 Mechanisms of MMP Activation and Inhibition

a) Activation of pro-MMPs



b) Inhibition by TIMP-1

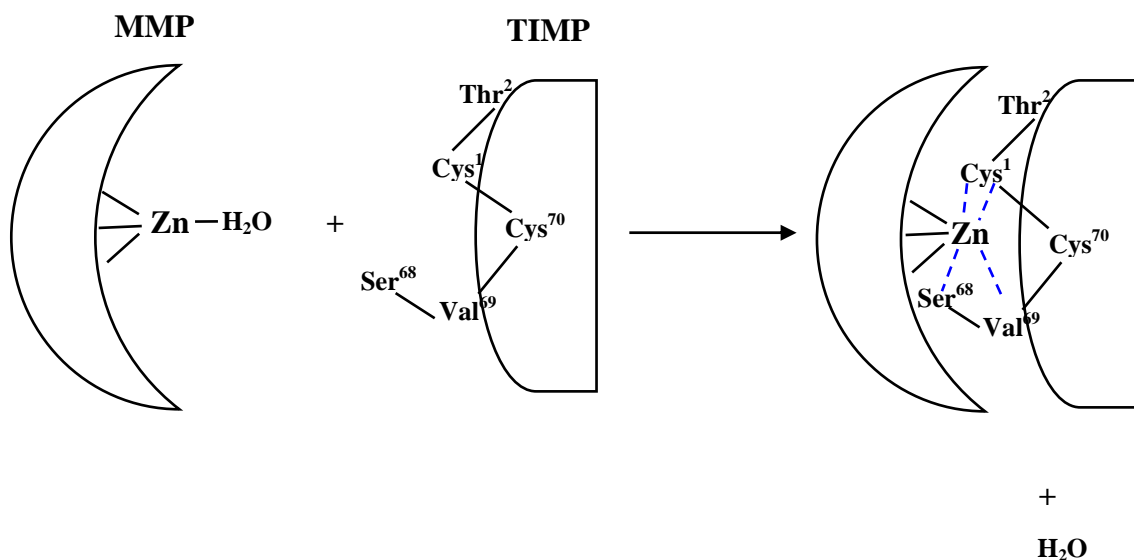


Figure 1.8 (a) Activation of pro-MMPs is by a cysteine switch mechanism. The latency of MMPs is maintained by contact between the cysteine of the pro-domain and the catalytic zinc. Chemical agents and proteolytic enzymes cause disruption of the Cys-Zn interaction leading to the formation of active intermediates. These are then autocatalytically cleaved, removing the pro-peptide and generating fully active enzyme. Adapted from: (Chakraborti *et al.*, 2003). (b) Inhibition of MMP by TIMP-1 involves the binding of Cys¹ and Ser⁶⁸-Val⁶⁹ to either side of the catalytic zinc (blue dotted lines) and the displacement of the zinc bound water molecule. The α -amino and carbonyl groups of Cys¹ bidentately co-ordinate the catalytic zinc (Gomis-Ruth *et al.*, 1997).

able to cleave the individual α chains by peptide bond hydrolysis.

Studies of collagen I cleavage by MMP-1 suggest that cleavage requires both the catalytic and haemopexin domains and that they bind cooperatively in succession (Chung *et al.*, 2004). Similarly, the haemopexin domain has also been shown to be important for collagen cleavage by MMP-2, -8 and -13 (Knauper *et al.*, 1997; Knauper *et al.*, 1993; Patterson *et al.*, 2001). In all cases, cleavage of collagens I, II and III occurs after Glycine at residues 772-773 located three quarters away from the N-terminus of the collagen and results in the generation of $\frac{3}{4}$ and $\frac{1}{4}$ fragments (Aimes and Quigley, 1995; Fields, 1991; Miller *et al.*, 1976). These thermally-unstable fragments then unfold and are subject to further degradation by gelatinases and other non specific tissue proteinases.

1.6.3.1.5 Effects of MMP action on cell function

It has become increasingly clear that the proteolytic action of MMPs on the ECM not only results in clearance of ECM components but can also alter their biological function such that MMPs play a role in regulating cell behaviour. A number of non-matrix substrates for MMPs have also been identified that have the potential to influence cell function.

The cleavage of ECM substrates by MMPs can reveal cryptic sites within the ECM protein or yield bioactive fragments that have physiological effects not associated with the parent protein. For example, cleavage of fibrillar collagen by MMPs exposes cryptic RGD sites that can then interact with $\alpha 5 \beta 3$ integrin and this interaction promotes the survival and growth of melanoma cells (Petitclerc *et al.*, 1999). Similarly, cleavage of basement membrane Collagen IV by MMP-2 and MMP-9 exposes a cryptic epitope that promotes angiogenesis (Hangai *et al.*, 2002; Xu *et al.*, 2001). Studies of laminin 5 cleavage by MMP-2 show that this releases a $\gamma 2$ chain fragment exposing an otherwise inaccessible site that induces epithelial cell migration (Giannelli *et al.*, 1997). Proteolytic cleavage of FN can also release bioactive fragments that influence cell proliferation, differentiation and migration (Schor *et al.*, 2003).

MMPs also influence cell behaviour by releasing ECM-associated growth factors such as VEGF and TGF- $\beta 1$ thereby increasing their bioavailability. VEGF is found tightly bound to heparin sulphate proteoglycans within the ECM (Park *et al.*, 1993). MMP-9 has been implicated in the release of ECM-bound VEGF in a number of tumour models which promotes angiogenesis and tumour progression (Bergers *et al.*, 2000). In renal cell carcinoma, increased expression of MMP-2 and MMP-9 occurs in areas of elevated VEGF suggesting that they may affect its bioavailability (Zhang *et al.*, 2002).

MMPs can also cause the release and activation of TGF- β 1 which is normally sequestered within the ECM as part of the TGF- β 1 complex comprising TGF β 1, LAP (latency- associated peptide) and LTBP (latent TGF- β 1 binding protein). MMPs -2, -9, -13 and -14 have been shown to activate TGF- β 1 via the cleavage of LAP (Yu *et al.*, 2000; Dangelo *et al.*, 2001; Mu *et al.*, 2002). MMP-2, -3 and -9 have been implicated in the cleavage of LTBP (Yu *et al.*, 2000; Dallas *et al.*, 2002; Maeda *et al.*, 2002) however, MMP-2 is the only MMP to cleave ECM-bound LTBP (Dallas *et al.*, 2002). TGF- β 1 can also be found bound in its active form to the proteoglycan decorin and this may form an additional reservoir of TGF- β 1 within the ECM. MMP-2, -3 and -7 have been shown to cleave decorin thereby releasing TGF- β 1 from the complex (Imai *et al.*, 1997).

The affect of MMPs on cell behaviour can also be mediated through the proteolysis of cell surface proteins that are involved in cell adhesion and transmembrane signal transduction. MMP cleavage of β -dystroglycan, a transmembrane component that interacts with the cytoskeleton results in the disruption of cell-ECM contact (Yamada *et al.*, 2001). Similarly, MMP-dependent cleavage of syndecans results in a loss of cell-ECM interaction that is likely to affect cell shape and motility (Fitzgerald *et al.*, 2000, Endo *et al.*, 2003). The cleavage of E-cadherin by MMP-3 and -7 results in the release of a soluble extracellular fragment that disrupts cell aggregation and promotes tumour invasion (Lochter *et al.*, 1997; Noe *et al.*, 2001).

MMPs also release a number of additional cell surface proteins. These include the MMP-3 release of leukocyte L-selectin and heparin binding EGF-like growth factor and the MMP-7 release of active soluble Fas ligand resulting in receptor mediated apoptosis (Powell *et al.*, 1999).

1.6.3.1.6 Renal expression of MMPs and TIMPs

The renal expression of a number of MMPs has been extensively studied and MMP-1, -2, -3, -8, -9 and -13 are all found within the kidney (Lenz *et al.*, 2000). Low levels of MMPs are expressed within adult kidney tissue but expression is substantially altered during renal development and in renal disease (section 1.7.2).

In embryogenesis, the expression of MMP-2, MMP-9 and MT1-MMP is predominant along with their corresponding inhibitors TIMP-1, TIMP-2 and TIMP-3 (Barasch *et al.*, 1999; Lelongt *et al.*, 1997; Ota *et al.*, 1998; Reponen *et al.*, 1995; Tanney *et al.*, 1998). MMP-2 and MMP-9 are localised to the mesenchyme and MMP-2 is weakly expressed in the ureteric bud (Lelongt *et al.*, 1997; Ota *et al.*, 1998). Both are thought to act sequentially on branching

morphogenesis of the ureteric bud with MMP-9 being expressed early in embryogenesis and MMP-2 playing a role from day 13 onwards (Lelongt *et al.*, 2001). MT1-MMP is found predominantly in the ureteric bud early in embryogenesis and later appears in the mesenchyme where it is also thought to contribute to ureteric bud branching (Lelongt *et al.*, 2001).

In the adult kidney, there is significant expression of MMP-1, -2, -3, -8, -9 and -13 (Lenz *et al.*, 2000) as well as TIMP-1, -2 and -3 (Engelmyer *et al.*, 1995; Johnson *et al.*, 2002). Expression of MMP-2, -3 and -9 and TIMP has been demonstrated in the collecting duct epithelia (Norman *et al.*, 1995; Piedagnel *et al.*, 1999). Similarly, MMP-2 as well as TIMP-1 and -2 have been detected in glomerulus (Carome *et al.*, 1993; Jalalah *et al.*, 2000; Nakamura *et al.*, 1994) and MMP-2 and -9 in the proximal and distal tubule although their expression in the tubule remains controversial (Lelongt *et al.*, 2001).

Characterisation of the cellular expression of MMPs has shown that they are produced by a variety of renal cell types including tubular cells, fibroblasts, glomerular epithelial and mesangial cells (Knowlden *et al.*, 1995; Martin *et al.*, 1994; Norman *et al.*, 1995). Tubular cells mainly produce gelatinases (MMP-2 and -9) and also some interstitial collagenases (MMP-1, -8 and -13). Fibroblasts mainly produce MMP-2 and some MMP-1, -8 and -13 (Norman *et al.*, 1995). Glomerular epithelial cells and mesangial cells have both been shown to produce MMP-2 and MMP-9 along with TIMP-1 and TIMP-2 (Knowlden *et al.*, 1995; Martin *et al.*, 1994).

1.6.3.2 Plasminogen/ plasmin system

The second major enzyme system involved in the degradation of the ECM is the plasminogen/plasmin system. This comprises two serine proteases: tissue-type plasminogen activator (t-PA) and urokinase-type plasminogen activator (u-PA) that both catalyse the activation of plasminogen to plasmin (Vassalli *et al.*, 1991). These activators are localised at the cell surface by interaction with membrane-bound receptors that also act as co-receptors for plasminogen and facilitate its cell surface activation to plasmin. uPA is bound by uPAR (urokinase-type plasminogen activator receptor) (Blasi and Carmeliet, 2002) whilst Annexin II has been shown to be a plasminogen/tPA co-receptor at least in endothelial cells (Hajjar and Acharya, 2000). Once plasminogen is converted to plasmin it is capable of degrading a variety of ECM substrates including collagens III, IV, V, laminin, FN and proteoglycans (Werb, 1997). Components of the plasminogen/plasmin cascade may also activate MMPs providing interaction between the two enzyme pathways (Baricos *et al.*, 1995; Cai *et al.*, 2005; Hu *et al.*, 2006; Kazes *et al.*, 1998).

Like MMPs, the plasminogen activators are also subject to physiological regulation at a number of levels. The synthesis of plasminogen activators is subject to transcriptional control and can be modulated by growth factors and cytokines such as IL-1, TNF- α , PDGF and TGF- β 1 as well as glucocorticoids and other steroid hormones (Nagamine *et al.*, 2005). At the post-transcriptional level, cytokines can also modulate the stability of u-PA and t-PA mRNA leading to a prolonged half life (Nagamine *et al.*, 2005). Once secreted, cleavage of the pro-peptide is required for conversion to the active plasminogen activator in a similar manner to that of pro-MMPs (Ichinose *et al.*, 1986; Ichinose *et al.*, 1984). Finally, plasminogen activators are regulated by endogenous inhibitors with both u-PA and t-PA being inhibited by plasminogen activator inhibitors (PAI)-1 and -2 (Kawano *et al.*, 1970; Loskutoff and Edgington, 1977).

Characterisation of the distribution of plasminogen activators in renal cells has demonstrated that t-PA is present in endothelial cells and epithelial cells of the collecting duct (Rerolle *et al.*, 2000; Sappino *et al.*, 1991) while u-PA has been localised to proximal and distal tubular epithelial cells (Kristensen *et al.*, 1991; Larsson *et al.*, 1984; Sappino *et al.*, 1991; Wagner *et al.*, 1996). In addition, both u-PA and t-PA have been detected in the glomeruli (Angles-Cano *et al.*, 1985; Bergstein *et al.*, 1988) where they are thought to be derived from both glomerular epithelial (Brown *et al.*, 1994; Iwamoto *et al.*, 1990; Kanalas, 1995) and mesangial cells (Baricos *et al.*, 1995; Glass *et al.*, 1993; Wilson *et al.*, 1996; Wilson *et al.*, 1993). Plasminogen activator inhibitor -1 (PAI-1) is largely absent the normal kidney (Xu *et al.* 1996) however, it is synthesised by endothelial, tubular and mesangial cells in culture and shown to be up-regulated in a number of renal diseases (Rerolle *et al.*, 2000) (section 1.7.2).

1.6.3.3 Cathepsins

Cathepsins are cysteine proteases that comprise cathepsin B, L, N and S and are found intracellularly as lysosomal enzymes. Whilst they are not present in the ECM, these enzymes play a general role in the degradation of protein and have been shown to degrade ECM substrates. In particular, cathepsins B and L have been shown *in vitro* to degrade collagen I, laminin and proteoglycans at acid pH (Davies *et al.*, 1980). It is likely that cathepsins play an intracellular role in the degradation of matrix components. Some cathepsins such as cathepsin B are also able to activate collagenases and may play an indirect role in ECM metabolism (Davies *et al.*, 1992).

1.7 Changes in the ECM in Renal Disease

1.7.1 Increased synthesis of ECM components

The development of a pro-fibrogenic phenotype by renal cells during the course of renal disease is characterised by their increased synthesis of ECM components. In the interstitium, activated fibroblasts are the key players in increased matrix synthesis although *in situ* hybridisation shows that tubular cells and other interstitial cells also contribute to matrix production (Zeisberg *et al.*, 2000). In the glomerulus, mesangial cells have been identified as the major ECM synthesising cell type (Haralson *et al.*, 1987).

There is significant up-regulation of a number of normal ECM components, in particular, interstitial collagens I and III as well as collagen IV, FN and laminin. Increased synthesis of interstitial collagens has been observed in both disease models (Floege *et al.*, 1992a; Floege *et al.*, 1991; Floege *et al.*, 1992d; Johnson *et al.*, 2002; Jones *et al.*, 1991; Minto *et al.*, 1993; Yamamoto *et al.*, 1994) and human disease (Razzaque *et al.*, 1995; Stokes *et al.*, 2000; Stokes *et al.*, 2001). Similarly, an increase in collagen IV is seen in various disease models including experimental glomerulonephritis (Floege *et al.*, 1992a) and subtotal nephrectomy (Johnson *et al.*, 2002; Kliem *et al.*, 1996). FN mRNA expression is increased in experimental glomerulonephritis (Sady *et al.*, 1995; Yamamoto *et al.*, 1994) and its protein is increased in the remnant kidney model (Floege *et al.*, 1992a). Interestingly, the increased synthesis of FN is considered to be an early event in matrix accumulation and is thought to form a scaffold for the deposition of other ECM proteins (Eddy, 2000).

This increase in normal matrix synthesis is coupled with qualitative changes to the ECM that favour the abnormal deposition of matrix proteins. In particular, increases in collagen I and III levels are significantly contributed to by glomerular synthesis of collagen I and III mRNA and protein that is not observed in the normal kidney (Floege *et al.*, 1992a; Minto *et al.*, 1993). Alterations in the splicing pattern of FN also give rise to novel forms of the protein which are observed in both experimental and human renal disease (Alonso *et al.*, 1999; Van Vliet *et al.*, 2001). Similarly, novel isotypes of laminin normally found in the developing kidney but absent from the mature kidney have been shown to be re-expressed during renal disease (Fischer *et al.*, 2000; Kootstra *et al.*, 1995).

In addition to the major ECM proteins, a number of less abundant ECM proteins are up-regulated including proteoglycans and glycoproteins such as SPARC. The proteoglycans decorin and biglycan have both been shown to accumulate during renal disease (Diamond *et al.*, 1997; Kuroda *et al.*, 2004; Schaefer *et al.*, 2001; Stokes *et al.*, 2000). Similarly, increases in SPARC protein and mRNA are observed at sites of matrix expansion and fibrosis in a

number of disease models including the remnant kidney model, Heyman nephritis and chronic cyclosporin nephropathy (Pichler *et al.*, 1996a; Pichler *et al.*, 1996b). The role of these accumulating proteins in renal disease is uncertain however SPARC can participate in the modulation of cytokine activity such as TGF- β 1 and has been shown to stimulate collagen I and FN synthesis (Bassuk *et al.*, 2000; Francki *et al.*, 1999; Kamihagi *et al.*, 1994).

1.7.2 Impairment of ECM degradation

The net accumulation of ECM that is characteristic of renal disease is further contributed to by alterations in the abundance of proteolytic ECM degrading enzymes such as MMPs and plasmin and their corresponding physiological inhibitors. The consequence of this is the impairment of ECM degradation favouring increased deposition of matrix proteins.

Many studies have focused on changes in the expression and activity of MMPs and TIMPs in renal disease. Several *in vivo* studies have shown decreases in the levels of MMPs that are consistent with the fibrogenic phenotype. For example in a model of unilateral ureteral obstruction, a decrease in the activity of MMP-1 and MMP-9 is observed (Gonzalez-Avila 1998). Similarly, in streptozotocin-induced diabetic nephropathy, there is an overall down-regulation of MMP activity coupled with an up-regulation of TIMP-1 (Nakamura *et al.*, 1994; Reckelhoff *et al.*, 1993; Reckelhoff *et al.*, 1994). A number of *in vitro* studies also suggest a down-regulation of MMPs in response to pro-fibrogenic stimuli such as TGF- β 1 or elevated glucose. For example, human mesangial cells subjected to TGF- β 1 show a reduction in MMP-2 activity (Baricos *et al.*, 1999). Similarly, a decrease in the activity of MMP-2 and -9 is observed in mesangial cells exposed to elevated glucose (Caenazzo *et al.*, 1997; Leehey *et al.*, 1995; McLennan *et al.*, 2000; Singh *et al.*, 2001a). However, not all the experimental data supports a decrease in MMPs with some studies reporting no change or even an increase. For example, in a model of unilateral nephrectomy, the expression of MMP-1 and -3 immediately increases but later returns to control levels, whilst the expression of MMP-2 and -9 remain unchanged (Koide *et al.*, 1997). Similarly, in the subtotal nephrectomy model an increase in MMP-1 and MMP-2 mRNA and active enzyme is reported whilst MMP-3 and MMP-9 remained unchanged (Johnson *et al.*, 2002). Interestingly, studies of Alport syndrome, a chronic nephropathy characterised by tubulointerstitial scarring, suggest that up- and down-regulation of MMP activity may accompany different stages of renal disease thereby fulfilling different functions (Zeisberg *et al.*, 2006), which may, in part, explain the apparent differences observed in MMP expression.

The conflicting data regarding changes in MMPs has shifted the focus onto the role of TIMPs in the impairment of matrix degradation and in particular, TIMP-1. A wide variety of

experimental disease models show an increase in TIMP-1 levels including unilateral nephrectomy (Koide *et al.*, 1997), protein overload model (Eddy and Giachelli, 1995), diabetic nephropathy (Schaefer *et al.*, 1997; Wu *et al.*, 1997) and subtotal nephrectomy (Johnson *et al.*, 2002). TIMP-1 inhibits all of the latent pro-MMPs and increases in TIMP-1 may be important in contributing to an overall decrease in matrix turnover. However, studies of obstructive nephropathy (Kim *et al.*, 2001) and protein overload (Eddy *et al.*, 2000b) in TIMP-1 deficient mice, indicate that interstitial fibrosis is unaffected by TIMP-1 levels suggesting that TIMP-1 may have an MMP independent role.

Changes in the expression and activity of components of the plasminogen/plasmin system are also likely to play a role in modulating ECM turnover in disease. Increases in u-PA and its receptor (u-PAR) have been demonstrated in a number of renal diseases including diabetic nephropathy (Kenichi *et al.*, 2004) and in human crescentic glomerulonephritis (Lee *et al.*, 2001). Changes in t-PA in renal disease appear less well documented although levels of t-PA correlate with the degree of fibrosis in ureteral obstructive nephropathy (Yang *et al.*, 2002). However, it is the expression of plasminogen activator inhibitor-1 in renal disease that has received the most attention (Rerolle *et al.*, 2000). The increased expression and deposition of PAI-1 has been demonstrated in a number of experimental and human nephropathies including crescentic glomerulonephritis (Feng *et al.*, 1993; Malliaros *et al.*, 1993; Rondeau *et al.*, 1990), diabetic nephropathy (Yamamoto *et al.*, 1993) and focal segmental glomerulosclerosis (Hamano *et al.*, 2002). The importance of PAI-1 in promoting fibrosis is supported by studies in PAI-1 deficient mice in which the fibrogenic response is attenuated (Oda *et al.*, 2005). However, interestingly a number of studies also report that a deficiency in PAI-1 is a determinant of early glomerular injury (Hertig *et al.*, 2003; Kitching *et al.*, 2003) suggesting a multifunctional role for PAI-1.

1.7.3 Stabilisation of the ECM

The formation of covalent crosslinks both within and between adjacent ECM proteins by processing enzymes is an important step in the generation of mature matrix. In particular, the enzymes lysyl oxidase and tissue transglutaminase (TG2) are known to be involved in the crosslinking of ECM proteins. Lysyl oxidase catalyses the formation of pyridinoline crosslinks that stabilise the collagen fibril during the synthesis of mature collagen (Kagan and Li, 2003). TG2 is involved in the formation of $\epsilon(\gamma\text{-glutamyl})$ lysine crosslinks between glutamine and lysine residues on a variety of ECM substrates (Griffin *et al.*, 2002) (section 1.8.2).

The up-regulation of ECM crosslinking enzymes and an increase in ECM crosslinking has been suggested to further contribute to ECM accumulation by increasing its resistance to degradation (Johnson *et al.*, 1999; Kleman *et al.*, 1995). Such resistance has been put forward as a contributing factor in the accumulation of ECM associated with lung and liver fibrosis as well as atherosclerosis (Bowness and Tarr, 1990; Bowness *et al.*, 1989a; Bowness *et al.*, 1994; Griffin *et al.*, 1979; Mirza *et al.*, 1997). In the kidney, TG2 and its crosslinked product are increased in areas of matrix expansion in subtotal nephrectomy, streptozotocin-induced diabetic nephropathy and in human renal disease (Johnson *et al.*, 2003; Johnson *et al.*, 1997; Johnson *et al.*, 1999; Skill *et al.*, 2001) suggesting a role in the accumulation of renal matrix.

The potential role of TG2 in ECM stabilisation and fibrosis will be discussed further in sections 1.8.2.5.5 and 1.8.2.6.1 respectively.

1.8 Transglutaminase

Transglutaminases are a family of calcium-dependent enzymes that catalyse the post-translational modification of proteins by the formation of iso-peptide bonds. They mediate the acyl transfer between the γ carboxamide group of a peptide bound glutaminy residue and the ϵ -amino group of peptide bound lysine forming a covalent ϵ -(γ -glutamyl) lysine bond (Lorand and Conrad, 1984). They are also responsible for the incorporation of primary amines at selected peptide-bound glutamine residues (figure 1.9). The resultant iso-peptide bonds are extremely stable and resistant to proteolytic cleavage as well as chemical and mechanical disruption (Parameswaran *et al.*, 1997).

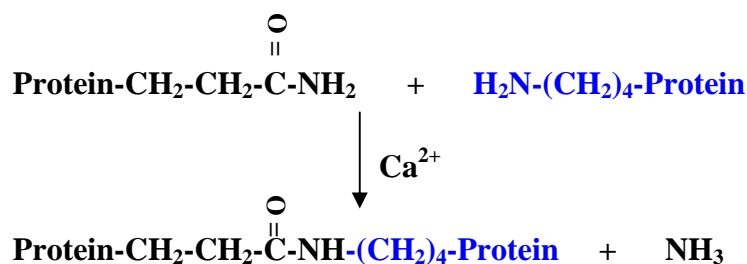
1.8.1 Transglutaminase (TG) gene family

In mammals, the TG gene family consists of nine members, eight of which encode active enzymes. Of these, six have been isolated and characterised at the protein level (Lorand and Graham, 2003). The members of the TG family are summarised in table 1.3. The TG enzymes show a high degree of structural homology and are members of the papain-like superfamily of cysteine proteases which share a catalytic triad of Cys-His-Asp or Cys-His-Asn residues at their active site (Pedersen *et al.*, 1994). However, each TG is the product of a distinct gene and has distinct physiological functions.

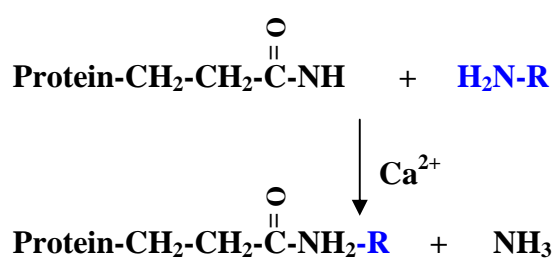
Particularly well characterised members of the TG family include; Factor XIIIa which is responsible for crosslinking fibrin during wound healing and keratinocyte TG (TG1) involved in the formation of the cornified envelope during terminal differentiation.

Figure 1.9 Principle Reactions Catalysed by the Transglutaminase Enzyme Family

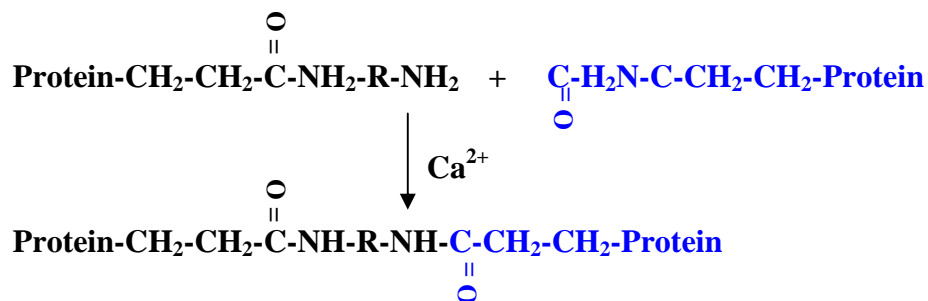
a) ϵ (γ -glutamyl) lysine di-peptide bond



b) N' (γ -glutamyl) amine bond



c) N'N'-bis(γ -glutamyl) polyamine linkage



d) Deamidation of glutamine

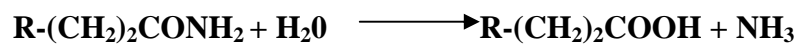


Figure 1.9 Acyl transfer reactions catalysed by transglutaminases, involving peptidyl glutamine residues and a variety of primary amines, lead to the post-translational modification of proteins.

However, the most widespread member of the TG family is tissue transglutaminase (TG2), a ubiquitously expressed enzyme that has multifunctional properties and has been implicated in a variety of physiological processes (Griffin *et al.*, 2002).

Table 1.3 Members of the Transglutaminase (TG) Gene Family

Enzyme Name	Synonyms	kDa	Gene	Prevalent Function
Factor XIIIa	Plasma TG	83	F13A1	Blood clotting and wound healing
TG1	Keratinocyte TG	90	TGM1	Cell envelope formation in the differentiation of keratinocytes
TG2	Tissue TG	80	TGM2	Cell death, differentiation, matrix stabilisation, adhesion protein
TG3	Epidermal TG	77	TGM3	Cell envelope formation in the differentiation of keratinocytes
TG4	Prostate TG	77	TGM4	Semen coagulation
TG5	TG _x	81	TGM5	Epidermal differentiation
TG6	TG _y	unknown	TGM6	Not characterised
TG7	TG _z	80	TGM7	Not characterised
Band 4.2	Erythrocyte protein band 4.2	77		Maintenance of erythrocyte membrane integrity

Adapted from: (Griffin *et al.*, 2002).

1.8.2 Tissue transglutaminase (TG2)

1.8.2.1 Three dimensional structure of TG2

High resolution X-ray crystallography of the A subunit of Factor XIIIa (Fox *et al.*, 1999; Yee *et al.*, 1996; Yee *et al.*, 1994) and the latent guanosine diphosphate (GDP) form of TG2 (Liu *et al.*, 2002) has provided extensive information regarding the structural features of the TG enzymes. Both the Factor XIIIa subunit and TG2 share a four-sequential domain structure comprising an N-terminal β sandwich, a core domain containing both the catalytic and regulatory sites and two C-terminal β barrel domains (figure 1.10). This four domain structure is thought to be highly conserved among the TG isoforms.

The active site of the enzyme, containing the Cys-His-Asp catalytic triad required for transamidation (crosslinking) is buried within the catalytic core domain (Cys²⁷⁷, His³³⁵ and Asp³⁵⁸). The core domain also contains a conserved tryptophan which is essential for catalytic

Figure 1.10 Three Dimensional Structure of TG2

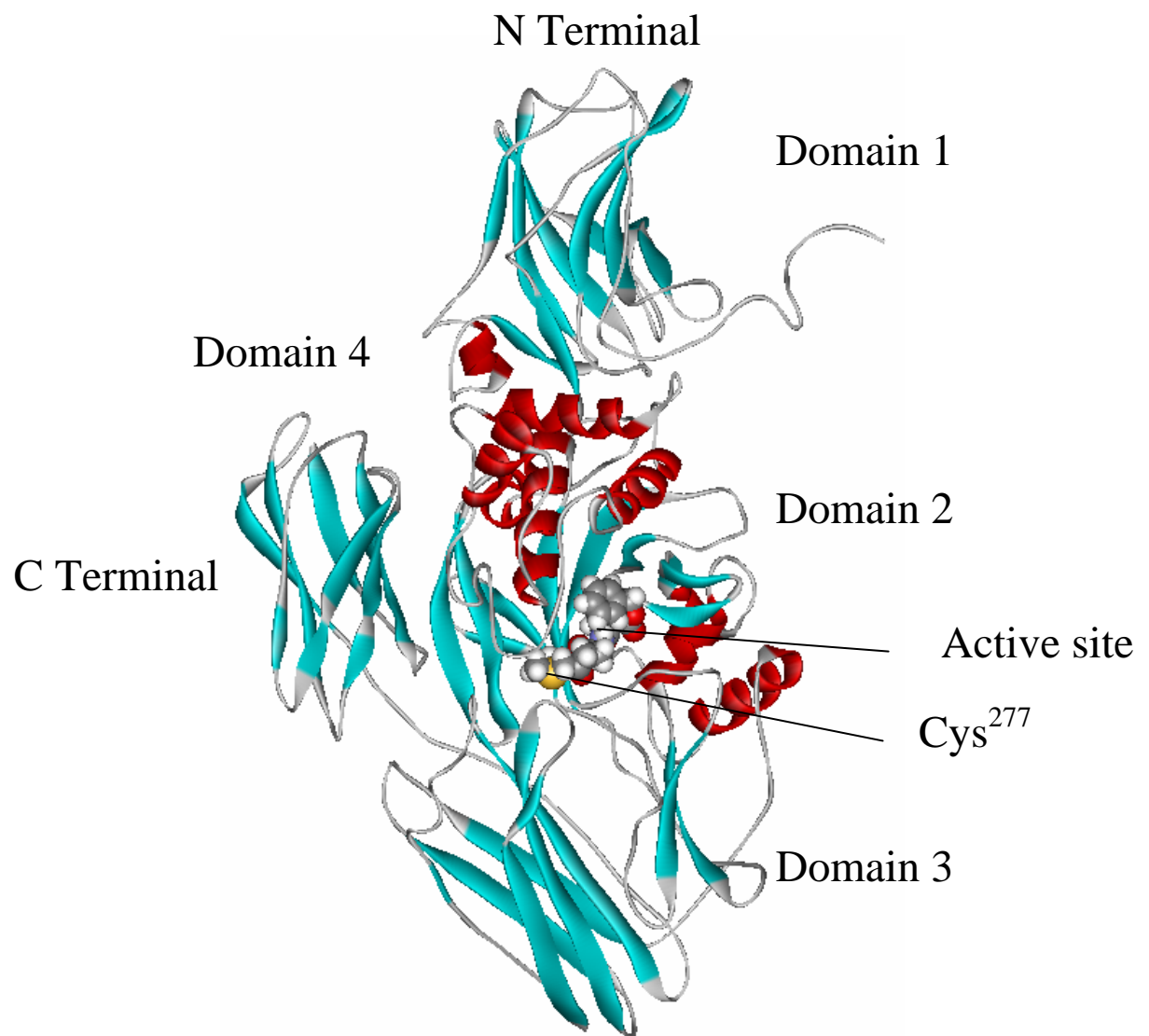


Figure 1.10 The structure of TG2 is closely related to that of Factor XIIIa and consists of four sequential domains. Domain 1 comprises the N terminal β sandwich and contains binding sites for FN and integrins. Domain 2 is the core domain which contains the catalytic active site including Cys²⁷⁷ which is critical for transamidation. Domains 3 and 4 are composed of a β barrel structure and contain important regulatory and GTP binding sites. Reproduced with kind permission from Professor Martin Griffin.

activity (Murthy *et al.*, 2002). The N-terminal β sandwich contains both FN and integrin binding sites (Akimov *et al.*, 2000; Gaudry *et al.*, 1999a), whilst the second C-terminal domain is able to bind phospholipase C (Hwang *et al.*, 1995).

Catalytic activity of TG2 is positively regulated by calcium binding and negatively regulated by guanosine triphosphate (GTP) (section 1.2.2.2.2). Multiple Ca²⁺ binding sites are

thought to exist on TG2 although the critical Ca^{2+} binding site is Cys²⁷⁷ located within the catalytic triad of the core domain (Liu *et al.*, 2002). TG2 is unique among the TGs in its ability to bind GTP. Regulation of TG2 by GTP is thought to occur through GTP binding to a site localised to a hydrophobic pocket between the catalytic core and first β barrel (Liu *et al.*, 2002).

1.8.2.2 Regulation of TG2

1.8.2.2.1 Transcriptional regulation of TG2

The cellular levels of TG2 are tightly regulated at the level of gene expression. In many cell types such as endothelial cells, vascular smooth muscle cells and lens epithelial cells TG2 is expressed constitutively and there are high levels of active enzyme (Greenberg *et al.*, 1991). In cells such as monocytes and tissue macrophages the enzyme is inducible and the basal expression of TG2 is very low (Chiocca *et al.*, 1988; Murtaugh *et al.*, 1984). Studies of the TG2 gene promoter have given important insights into the pathways regulating TG2 gene expression. The human TG2 promoter has been demonstrated to contain a number of regulatory sequences within the 1.7 kilobase flanking region (figure 1.11) including a TATA box element (TATAA), a CAAT box element (GGACAAT), a series of potential transcription factor binding sites (AP-1, Sp-1 and IL-6 response element) and a glucocorticoid response element (Lu *et al.*, 1995). Transfection studies show this promoter to be functional and to account for constitutive expression in a number of transfected cell lines. However, cell type-specific expression is not accounted for by this region suggesting that distal regions of the promoter are required (Lu *et al.*, 1995). The flanking region of the human TG2 promoter shares a high degree of homology with both mouse and guinea pig TG2 promoters (Ikura *et al.*, 1988a; Nanda *et al.*, 1999). However, there is little homology between the TG2 promoter and those of other members of the transglutaminase family, reflecting their diversity.

A number of previous studies have identified regulators of TG2 expression including growth factors, glucocorticoids (Johnson *et al.*, 1998) and retinoids (Chiocca *et al.*, 1988). Growth factors known to affect TG2 expression include TGF- β 1 (George *et al.*, 1990), IL-6 (Ikura *et al.*, 1994; Suto *et al.*, 1993), TNF- α (Kuncio *et al.*, 1998) and EGF (Katoh *et al.*, 1996). Studies of the mouse TG2 gene promoter localise a TGF- β 1 response element to a position 868 nucleotides upstream of the transcriptional start site (Ritter and Davies, 1998). In the human TG2 promoter, a potential IL-6 site is localised to nucleotide 1196 of the flanking region (Lu *et al.*, 1995) whilst TNF- α is known to regulate TG2 expression via an NF- κ B site located 1338 nucleotides upstream of the transcription initiation site (Kuncio *et al.*, 1998).

Figure 1.11 Schematic Representation of the TG2 Gene Promoter

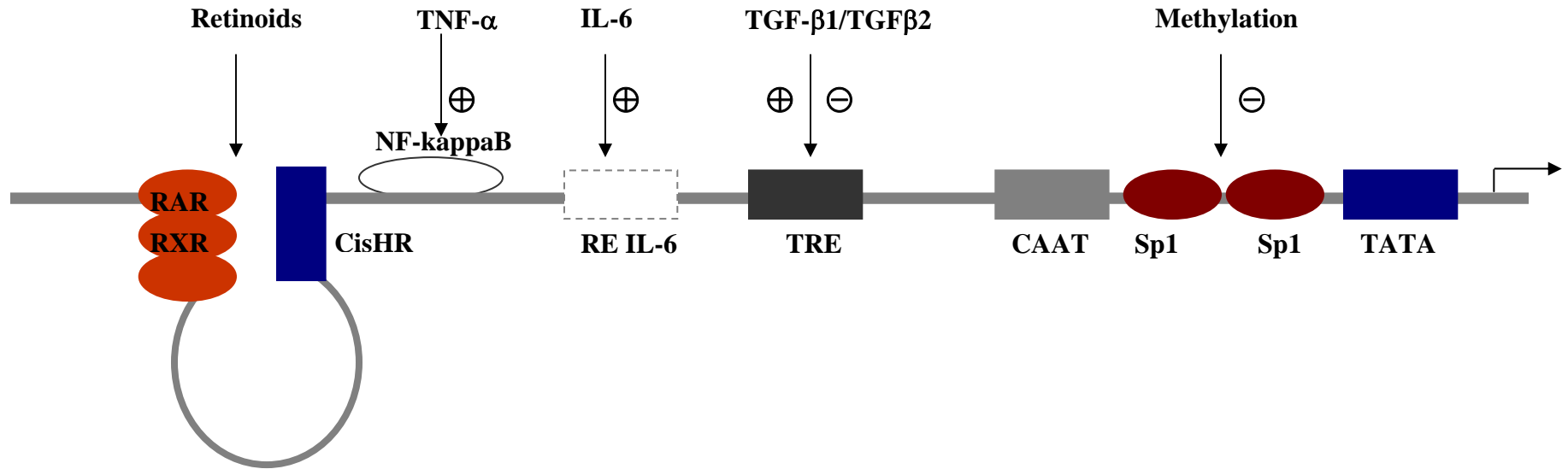


Figure 1.11 The proximal promoter of the TG2 gene comprises a number of regulatory sequences including a TATA box element and a number of upstream Sp1 binding sites that drive constitutive expression. In addition, differential expression is regulated by a variety of response elements including those for TGF β 1/TGF- β 2, TNF- α , IL-6 and retinoids. Adapted from: (Aeschlimann and Thomazy 2000).

In many cell types including peritoneal macrophages (Chiocca *et al.*, 1988), myeloid cells (Davies *et al.*, 1988), endothelial cells (Fesus *et al.*, 1991) and hepatocytes (Piacentini *et al.*, 1992) retinoic acid is considered to be an important regulator of TG2. Studies of the mouse TG2 promoter show the presence of a retinoid response element contained within 4 kilobases of the 5'-end of the gene (Nagy *et al.*, 1996). Co-transfection studies with retinoid receptor expression vectors in CV-1 (kidney fibroblast) cells demonstrate that the mouse TG2 promoter is activated by ligand activation of either retinoic acid receptor-retinoid X receptor (RAR.RXR) heterodimers or RXR homodimers that bind to a core receptor binding motif (Nagy *et al.*, 1996).

Methylation of the TG2 promoter is considered to be a further level of gene regulation and may account for tissue-specific gene expression (Lu and Davies, 1997). Studies of the TG2 promoter demonstrate that hypo-methylation and de-methylation increase TG2 activity whilst hyper-methylation suppresses TG2 (Lu and Davies, 1997).

1.8.2.2.2 Regulation of transglutaminase activity

In addition to transcriptional regulation of the TG2 gene, the TG2 protein is subject to tight post-translational regulation of its enzyme activity.

A critical activator of TG2 catalytic activity is the binding of calcium to Cys²⁷⁷ contained within the core domain. A number of techniques including crystallography (Liu *et al.*, 2002), small angle scattering (Mariani *et al.*, 2000) and site-directed mutagenesis (Murthy *et al.*, 2002) have provided structural information regarding the activation of TG2 by calcium. They suggest that the transamidating activity of TG2 involves a shift in protein domains that changes the reactivity of the active site and its accessibility to substrates. In its inactive state, the active site of TG2 is buried within domain 2 where domains 3 and 4 shield it from interacting with potential substrates. Binding of calcium to Cys²⁷⁷ in domain 2 is thought to initiate the breakdown of interactions between the core domain and the C-terminal barrels 1 and 2 allowing the opening of the active site for substrate binding. This permits the formation of a thioester bond between Cys²⁷⁷ of the active site and a glutamyl residue of the substrate (Folk, 1983; Lorand and Conrad, 1984), a reaction which is essential for crosslinking to occur.

The activation of TG2 by Ca²⁺ binding can be inhibited by GTP binding which under physiological conditions is thought to maintain TG2 as a latent enzyme. Recent studies have identified a critical Arginine residue (Arg⁵⁷⁹) located close to the catalytic site which is important in the GTP regulation of TG2 activity (Begg *et al.*, 2006b). Binding of GTP to TG2 is thought to mask this residue preventing the destabilisation of the enzyme and the

conformational switch to calcium-dependent crosslinking activity. In addition, binding of GTP has been shown to stabilise a bond between Cys²⁷⁷ and Tyr⁵¹⁶ that further promotes an inactive conformation (Begg *et al.*, 2006a). As well as stabilising interactions that prevent conformational change, binding of GTP is also thought to spatially interfere with Cys²⁷⁷ reactivity which itself prevents calcium binding. GTP has also been suggested to reduce TG2 activation by modulating the affinity of additional calcium binding sites as well as interfering with conformational changes induced by calcium (Bergamini, 1988; Iismaa *et al.*, 2000a).

A number of studies have also demonstrated that TG2 activity can be regulated by other factors such interaction with phospholipids (Fesus *et al.*, 1983) or nitric oxide (Bernassola *et al.*, 1999; Lai *et al.*, 2001). Interaction of TG2 with the membrane phospholipid lysophosphatidylcholine has been demonstrated to increase the sensitivity of TG2 to calcium enabling it to become active at physiological levels of calcium. Release of nitric oxide from NO donors is able to inhibit the activity of TG2 by nitrosylating cysteine residues including the critical active site Cys²⁷⁷ (Lai *et al.*, 2001).

1.8.2.3 Expression and localisation of TG2

TG2 is a ubiquitously expressed enzyme with varying levels of expression depending on the tissue type. During development and differentiation, induction of TG2 is widespread and contributes to such processes as embryo implantation (Piacentini and Autuori, 1994) and organogenesis (Iwai *et al.*, 1995; Schittny *et al.*, 1997; Thomazy and Davies, 1999). In mature organs, TG2 is also widely distributed due to constitutive expression in endothelium, smooth muscle cells and fibroblasts [reviewed in (Iismaa, 2002)]. In addition, a number of organ-specific cell types express TG2 constitutively, for example, stromal cells of the endometrium and thymic subcapsular epithelial cells [reviewed in (Iismaa, 2002)].

At the cellular level, TG2 is predominantly a soluble cytoplasmic enzyme although fractionation studies show that TG2 is also associated with both plasma (Slife *et al.*, 1985; Tyrrell *et al.*, 1986) and nuclear membranes (Singh *et al.*, 1995). A number of studies have also demonstrated an association with cytoskeletal proteins such as actin (Eligula *et al.*, 1998; Nemes *et al.*, 1997), desmin, tropomyosin (Derrick and Laki, 1966; Gard and Lazarides, 1979) and tubulin (Cohen and Anderson, 1987) and shown that they are substrates for TG2 (table 1.4). Interestingly, renal cells in culture that have been stained for TG2 show preferential staining around the nuclear membrane extending outwards to and apparently associated with the cytoskeleton (figure 1.12, M Fisher unpublished observation).

Figure 1.12 Intracellular Localisation of TG2 in Proximal Tubular Epithelial Cells

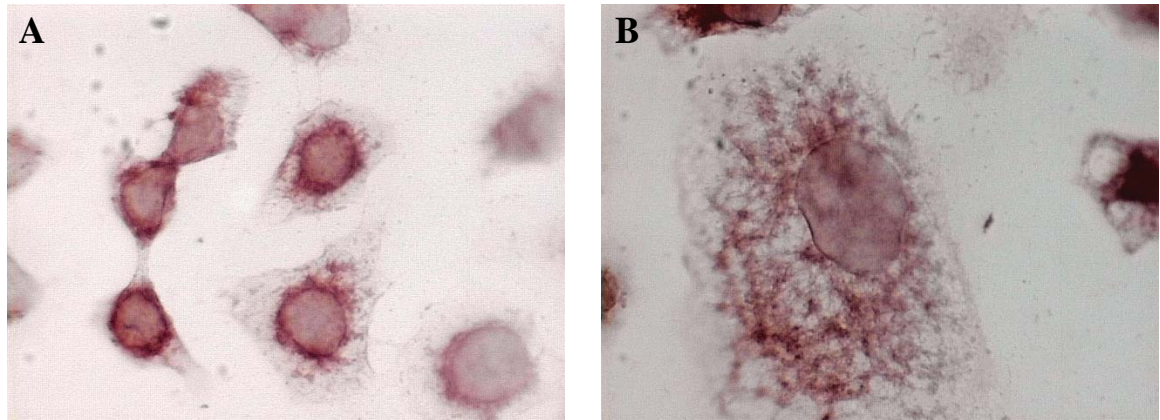


Figure 1.12 Opossum (OK) proximal tubular cells stained for TG2 with 1:750 dilution of TG100 mouse monoclonal anti-TG2 antibody and detected with AEC reagent. Cells shown at 400x magnification (A) and 1000x magnification (B). Staining is localised around the nuclear membrane and associated with the cytoskeleton.

In addition to its intracellular localisation, TG2 is also unique among the TG enzymes in its ability to be secreted and deposited into the surrounding ECM. An increasing number of studies show TG2 to be present on the cell surface and in the surrounding pericellular matrix (Aeschlimann *et al.*, 1995; Gaudry *et al.*, 1999b; Verderio *et al.*, 1998). At the cell surface TG2 is localised to distinct domains where it has been demonstrated to associate with FN and integrins (Akimov and Belkin, 2001a; Akimov *et al.*, 2000; Gaudry *et al.*, 1999a). The precise mechanism by which TG2 is externalised remains to be determined since it lacks the classical signal peptide required for secretion and is therefore not secreted by the ER/Golgi-dependent pathway. Secretion of TG2 does however require the enzyme to be in its active state and appears to be dependent on the presence of an intact N-terminal FN binding site since removal of this domain prevents secretion (Gaudry *et al.*, 1999a).

1.8.2.4 Substrate specificity and requirements of TG2

The identification of protein substrates for TG2 has proved to be a complex process given that most protein products accumulate *in vivo* as part of large insoluble polymers, making the identification of individual proteins difficult. However, a variety of biochemical and functional proteomic studies have been successful in identifying potential *in vitro* and *in vivo* substrates for TG2 (summarised in table 1.4). Both intracellular and extracellular proteins are post-translationally modified by TG2. Examples of intracellular TG2 protein substrates include; cytoskeletal proteins such as actin (Eligula *et al.*, 1998; Nemes *et al.*, 1997) and myosin (Eligula *et al.* 1998), histone and heat shock proteins (Ballestar and Franco, 1997; Boros *et al.*, 2006; Boros *et al.*, 2004; Cooper *et al.*, 2000) and cytosolic enzymes such as

phosphorylase kinase (Nadeau *et al.*, 1998). In the extracellular environment, TG2 interacts with many ECM proteins including FN (Mosher, 1984), a major TG2 substrate, collagens (Kleman *et al.*, 1995), vitronectin (Sane *et al.*, 1988) and laminin (Aeschlimann and Paulsson, 1991).

Table 1.4 Major Protein Substrates of TG2

Protein Classification	Substrates	Reference
Cytoplasmic proteins	Aldolase A Phosphorylase kinase Crystallins Glutathione S-transferase Tau Rho A	(Lee <i>et al.</i> , 1992) (Nadeau <i>et al.</i> , 1998) (Groenen <i>et al.</i> , 1992; Lorand <i>et al.</i> , 1991) (Ikura <i>et al.</i> , 1998) (Murthy <i>et al.</i> , 1998; Tucholski <i>et al.</i> , 1999) (Singh <i>et al.</i> , 2001b)
Cytoskeletal proteins	Actin Myosin Troponin β -tubulin Desmin Vimentin	(Eligula <i>et al.</i> , 1998; Nemes <i>et al.</i> , 1997) (Eligula <i>et al.</i> , 1998) (Bergamini <i>et al.</i> , 1995) (Cohen and Anderson, 1987) (Gard and Lazarides, 1979) (Clement <i>et al.</i> , 1998)
ECM- Associated Proteins	Collagen FN Vitronectin Osteopontin Nidogen Laminin LTBP-1 Osteonectin Osteocalcin	(Kleman <i>et al.</i> , 1995) (Jones <i>et al.</i> , 1997a; Mosher, 1984) (Sane <i>et al.</i> , 1988) (Kaartinen <i>et al.</i> , 1997) (Aeschlimann and Thomazy, 2000) (Aeschlimann and Thomazy, 2000) (Verderio <i>et al.</i> , 1999) (Aeschlimann <i>et al.</i> , 1995) (Kaartinen <i>et al.</i> , 1997)
Miscellaneous proteins	Heat Shock proteins Histone proteins Cytochromes Phospholipase A ₂	(Boros <i>et al.</i> , 2006; Boros <i>et al.</i> , 2004) (Ballestar and Franco, 1997; Cooper <i>et al.</i> , 2000) (Butler and Landon, 1981) (Cordella-Miele <i>et al.</i> , 1990)

Table 1.4 Protein substrates of TG2 have been identified by both structural and functional proteomics. Many more proteins have been identified but only the major substrates are listed here. LTBP-1 = Latent TGF- β 1 binding protein -1. Table adapted from: (Griffin *et al.*, 2002) and (Esposito and Caputo, 2005).

A number of *in vitro* studies have suggested that recognition of target amino acids within protein substrates by TG enzymes is dependent on the sequence of adjacent residues. In particular, the presence of positively-charged residues either two or four residues from an available glutamine appear to promote recognition whereas flanking of glutamine by positively-charged residues discourages binding (Aeschlimann *et al.*, 1992; Coussons *et al.*, 1992). Similarly, the nature of amino acids directly preceding lysine residues may influence TG reactivity (Grootjans *et al.*, 1995).

The presence of uncharged, basic polar and small aliphatic residues promotes TG reactivity whereas aspartic acid, glycine, proline and histidine residues reduce reactivity (Groenen *et al.*, 1994).

The accessibility of target residues is also an important determinant for TG reactivity. For example, exposure of glutamine residues at the surface of the protein in its folded conformation is important for interaction with TG enzymes (Coussons *et al.*, 1992).

1.8.2.5 Multifunctional roles of TG2

The multifunctional properties of TG2 including its protein crosslinking, GTP binding and adhesion activities have implicated this enzyme in a diverse range of physiological events. Extensive studies have indicated that TG2 may play a significant role in processes such as proliferation (Birckbichler *et al.*, 1981), cell death (Akimov and Belkin, 2001a; Gaudry *et al.*, 1999a; Ikura *et al.*, 1988b) transmembrane signalling (Iismaa *et al.*, 2000b), cell-matrix interactions (Gentile *et al.*, 1991; Jones *et al.*, 1997b) and stabilisation of extracellular matrix (Greenberg *et al.*, 1991). It is therefore not surprising that de-regulated expression and activity of TG2 is considered to be an important contributory factor in the changes in cellular homeostasis associated with a number of human diseases including neurodegenerative diseases (Lesort *et al.*, 2000), autoimmune disorders (Dieterich *et al.*, 1997), neoplasia (Barnes *et al.*, 1985; Birckbichler *et al.*, 1977) and tissue fibrosis (Griffin *et al.*, 1979; Malyankar *et al.*, 1997; Mirza *et al.*, 1997).

1.8.2.5.1 Cell growth and proliferation

A number of studies have demonstrated a correlation between TG2 activity and proliferation. Cells treated with cystamine to inhibit their TG activity have been demonstrated to increase proliferation in response to decreased TG2 (Birckbichler *et al.*, 1981). This is consistent with previous studies in which cells expressing low levels of TG2 showed an undifferentiated phenotype and increased proliferation compared to cells with high TG2 (Birckbichler and Patterson, 1978). TG2 may also be involved in regulation of the cell cycle. Transfection studies using hamster fibrosarcoma Met B cells transfected with full length or truncated TG2 cDNA demonstrate that inactivating TG2 crosslinking activity delays progression into the G2/M phase of the cell cycle (Mian *et al.*, 1995).

1.8.2.5.2 Cell death

The involvement of TG2 in the mechanisms of cell death or apoptosis is now widely accepted and it is thought to play both pro- and anti-apoptotic roles depending on a variety of physiological factors.

A number of *in vitro* and *in vivo* studies have reported an association between TG2 and the apoptotic pathway. For example, in neuroblastoma cells induced to over-express TG2 by transfection, an increase in cell death is observed with cells showing the cytoplasmic and nuclear characteristics of apoptosis (Melino *et al.*, 1994). Similarly, in hepatocyte hyperplasia induced by lead nitrite, an increase in TG activity and expression correlates with apoptosis of hepatocytes (Fesus *et al.*, 1987). Increased induction of TG also correlates with apoptosis in tracheobronchial epithelial (Zhang *et al.*, 1995b) and myeloid leukaemia cells (Nagy *et al.*, 1995). Conversely, a reduction in TG2 expression in monocytic U937 cells transfected with anti-sense TG2 cDNA prevents retinoic acid-induced apoptosis (Oliverio *et al.*, 1999). Interestingly, however, not all studies support such an association. For example, the stable transfection of Swiss 3T3 fibroblasts (Verderio *et al.*, 1998) with TG2 leading to increased expression does not increase the rate of apoptosis in these cells although activation with ionomycin results in a novel form of cell death. Similarly, studies of renal scarring *in vivo* also suggest that TG2 may participate in a novel form of cell death in which epithelial cells die through extensive crosslinking of their intracellular proteins as a result of accumulating levels of TG2 (Johnson *et al.*, 1997). In keeping with 3T3 fibroblasts, such cell death occurs in the absence of features consistent with either apoptosis or necrosis.

The pro-apoptotic role of TG2 is thought to be mediated through both upstream and downstream events in the apoptotic pathway. The induction of TG2 is regulated by a number of factors such as retinoic acid and TGF- β 1 that are also able to regulate apoptosis suggesting that TG2 is able to act as an early effector “death” protein (Melino and Piacentini, 1998). Similarly, the GTP binding ability of TG2 may also contribute to the regulation of apoptosis (Melino and Piacentini, 1998) since GTP availability affects second messengers that are known to inhibit apoptosis such as 1,2 diacylglycerol (DAG) (Leszczynski *et al.*, 1994; Nakaoka *et al.*, 1994). TG2 may also promote apoptosis by direct interaction with proteins of the apoptotic pathway such as Bax. Recently it has been demonstrated that interaction of Bax with the BH3 domain of TG2 can cause conformational changes in Bax leading to translocation of Bax to the mitochondria, the release of cytochrome c and cell death (Rodolfo *et al.*, 2004).

In the downstream stages of apoptosis, the activation of TG2 leads to extensive crosslinking of intracellular proteins and the formation of detergent-insoluble protein polymers. These may serve to stabilise apoptotic cells and prevent leakage of intracellular components prior to clearance by phagocytes, thereby reducing inflammation (Fesus, 1998; Fesus *et al.*, 1987). TG2 may also protect cells from apoptosis via non-classical adhesion-

dependent mechanisms. Studies on osteoblasts and dermal fibroblasts demonstrate that TG2 is able to form complexes with FN and heparin sulphate leading to the activation of RhoA and stimulation of the cell survival focal adhesion kinase (FAK) (Verderio *et al.*, 2003).

1.8.2.5.3 Transmembrane signalling

The ability of TG2 to bind and hydrolyse GTP classifies it as part of the heterotrimeric G protein family that are broadly involved in hormone receptor signalling. Its function as a GTPase and role in receptor signalling are distinctly separate from its transamidating function (Chen and Mehta, 1999). The heterotrimeric G proteins consist of a GTP-binding α subunit ($G\alpha$) and regulatory β and γ subunits. However, the TG2 α subunit $G\alpha_h$ does not possess common heterotrimeric GTP binding motifs suggesting that $G\alpha_h$ is a new class of GTP-binding protein (Nakaoka *et al.*, 1994). Despite this, the GTPase cycle of $G\alpha_h$ is similar to that for other heterotrimeric G proteins. TG2 facilitates the signalling response to α_1 adrenergic receptor stimulation resulting from the binding of ligands such as catecholamines, norepinephrine and epinephrine (Im *et al.*, 1997). The association of TG2/ $G\alpha_h$ with the plasma membrane appears to be mediated by the presence of a fatty acid anchor on TG2 (Harsfalvi *et al.*, 1987).

In common with all G proteins the TG2/ $G\alpha_h$ subunit is in its inactive form when bound to GDP. Interaction between the receptor and $G\alpha_h$ results in the activation and release of GDP allowing GTP to bind. This facilitates a conformational change in $G\alpha_h$ and the dissociation of the α and β subunits. Once in the GTP-bound state, TG2 effects the transmembrane signal by interacting with phospholipase C δ , via its binding site located on the C terminal domain, in turn influencing phosphatidylinositol metabolism (Chen *et al.*, 1996; Hwang *et al.*, 1995).

The identity of the $G\beta$ subunit has until recently been unclear. However, studies suggest that it corresponds to the 50kDa Ca^{2+} binding protein calreticulin (Feng *et al.*, 1999). Calreticulin negatively regulates the GTP binding and transglutaminase activity of TG2 by interacting with the GDP bound form of the enzyme.

1.8.2.5.4 Cell matrix interactions

Perhaps the most extensively studied functions of TG2 relate to its involvement in the assembly of the ECM and its role in cell-matrix interactions. Both roles are dependent on the cell surface expression of TG2 and have a profound effect on cell proliferation, adhesion, migration and cell survival.

The matrix assembly role of TG2 mostly relates to its association with FN and its involvement in FN polymerisation (Gaudry *et al.*, 1999a). The enzyme has a high affinity binding site for FN, localised to the first 7 N-terminal amino acids (Jeong *et al.*, 1995). This appears to interact with the 42kDa gelatin binding region of FN (Akimov and Belkin, 2001a; Radek *et al.*, 1993; Turner and Lorand, 1989). In endothelial cells and fibroblasts, TG2 has been demonstrated to crosslink FN polymers at the cell surface (Jones *et al.*, 1997b; Martinez *et al.*, 1994; Verderio *et al.*, 1998). Reduced expression of TG2 in endothelial cells leads to an inhibition of the crosslinking of FN (Jones *et al.*, 1997b). Conversely, an up-regulation of TG2 in Swiss 3T3 fibroblasts increases the amount of crosslinked FN (Verderio *et al.*, 1998).

The precise mechanism by which TG2 promotes FN assembly remains unclear. However, the enzyme is known to act as an integrin co-receptor for FN (Akimov *et al.*, 2000) and to associate with several $\beta 1$ and $\beta 3$ integrins whilst simultaneously binding to FN. The presence of cell surface TG2 enhances FN matrix formation mediated by the $\alpha 5\beta 1$ integrin (Akimov and Belkin, 2001a). Therefore, the role of TG2 in promoting FN assembly appears to be in facilitating the association of FN with $\beta 1$ integrins.

The expression of TG2 at the cell surface and association with integrins and FN also has important implications for cell adhesion and migration. A number of studies have suggested a role for cell surface TG2 in both of these processes. For example, over-expression of TG2 in fibroblast cell lines by transfection with either active or inactive TG2 constructs increases cell attachment and decreases migration on FN (Balklava *et al.*, 2002; Verderio *et al.*, 1998). Reduced expression of TG2 by anti-sense silencing in a human endothelial cell line reduces adhesion and spreading (Jones *et al.*, 1997a). Similarly, blocking of cell surface TG2 with anti-TG2 antibodies in Swiss 3T3 fibroblasts leads to a loss of cell adhesion (Verderio *et al.*, 1998). In a monocytic cell line, TG2 has been shown to be expressed at the cell surface and to be involved in the adhesion and migration of monocytes on FN which particularly requires the gelatine-binding fragment of FN (Akimov and Belkin, 2001b). The adhesive function of TG2 is independent of its crosslinking activity but requires the formation of ternary complexes with FN and $\beta 1$ and $\beta 3$ integrins (Akimov *et al.*, 2000). The formation of such complexes may influence adhesion by causing the enlargement of focal adhesions and amplifying the integrin mediated activation of FAK (Akimov *et al.*, 2000).

The association of TG2 with matrix associated FN appears to promote cell adhesion by RGD-independent mechanisms (Verderio *et al.*, 2003). RGD-mediated cell adhesion plays an important role in cell survival and RGD-containing peptides can induce apoptosis in a number of cell types. However, adhesion via TG2-FN has been suggested to promote cell survival in

the presence of RGD peptides and probably plays such a role in the response to cell stress (Verderio *et al.*, 2003).

1.8.2.5.5 Stabilisation of ECM

The ability of TG2 to form highly stable and proteolytically resistant $\epsilon(\gamma\text{-glutamyl})$ lysine crosslinks between extracellular proteins including those of the ECM, has implicated the enzyme in tissue maintenance and matrix stabilisation. TG2 has been shown to crosslink and stabilise the fibrin clot both during wound healing and in human umbilical vein endothelial cells in which TG2 is up-regulated by thrombin (Auld *et al.*, 2001; Haroon *et al.*, 1999). In human dermal fibroblasts exposed to UVA radiation, increased TG2 activity in the extracellular environment leads to increased polymerisation of FN and stabilisation of the ECM (Gross *et al.*, 2003; Nicholas *et al.*, 2003). Similarly, a number of other studies show that TG2-mediated formation of FN multimers leads to its stabilisation (Gross *et al.*, 2003; Jones *et al.*, 1997a; Martinez *et al.*, 1994; Verderio *et al.*, 1998). Studies also show that TG2 is able to stabilise collagen-rich matrix. In rhabdomyosarcoma cells expressing TG2, crosslinking of collagen fibrils occurs in the absence of the collagen crosslinking enzyme lysyl oxidase (Kleman *et al.*, 1995). This results in the formation of a highly insoluble collagen matrix that is resistant to the action of MMPs. Inhibition of the TG2 activity in these cells by putrescine drastically increases the solubility of this matrix (Kleman *et al.*, 1995). Similarly, in opossum proximal tubular cells stimulated to over-express TG2 by elevated glucose an accumulation in collagen and FN matrix is observed that is suggested to be due to increased ECM crosslinking (Skill *et al.*, 2004).

The potential role of TG2 in the stabilisation of the ECM is likely to be important in maintaining tissue integrity by influencing the balance between matrix deposition and breakdown. For that reason, TG2 has attracted significant interest in its potential role in diseases for which altered tissue homeostasis is a characteristic feature, in particular wound healing and fibrosis.

1.8.2.6 TG2 and disease

1.8.2.6.1 TG2 in scarring and fibrosis

TG2 has been implicated in a number of diseases in which inflammation and the accumulation of ECM are prevalent features. In the lung, up-regulation of TG2 was first shown to be associated with progressive scarring in an experimental model of pulmonary fibrosis induced by the herbicide paraquat (Griffin *et al.*, 1979). Several studies of liver fibrosis have also suggested the involvement of TG2. In rats treated with carbon tetrachloride

(CCL4) to induce hepatic injury, increased expression of TG2 is observed early after injury and correlates with the development of fibrosis (Mirza *et al.*, 1997). Increases in TG2 expression in this model appear to be mediated by NF- κ B. In another study, TG2-mediated crosslinking is associated with the early inflammatory stage of liver fibrosis (Grenard *et al.*, 2001). TG2 has also been implicated in cardiovascular disease. An increase in TG2 is reported to be found in atherosclerotic plaques where increased crosslinking is associated with stabilisation of the collagen III-lipoprotein interface surrounding the plaque (Bowness *et al.*, 1987; Bowness and Tarr, 1990; Bowness *et al.*, 1989b; Bowness *et al.*, 1994). Studies using transgenic mice with increased cardiac TG2 expression also show that TG2 is associated with the development of cardiomyopathy (Small *et al.*, 1999).

Perhaps the most extensive evidence for a role of TG2 in progressive scarring has come from studies of experimental and human kidney disease. An elevation in TG2 activity, coupled with increased $\epsilon(\gamma$ -glutamyl) crosslinking has been demonstrated in the subtotal nephrectomy model of renal scarring (Johnson *et al.*, 1997; Johnson *et al.*, 1999). Both increases were found predominantly in the tubulointerstitium and correlated with the development of scarring. Similarly, in the streptozotocin model of early diabetic nephropathy increased levels of $\epsilon(\gamma$ -glutamyl) crosslink were found in the interstitium and in the expanding mesangial matrix (Skill *et al.*, 2001).

Increases in TG2 and $\epsilon(\gamma$ -glutamyl) crosslink have also been implicated in human renal disease. In human diabetic nephropathy, elevated TG2 and its crosslinked product are found to be associated with progressive expansion of the tubulointerstitial and glomerular compartments (El Nahas *et al.*, 2004). Analysis of renal biopsies from diabetic patients with type 2 diabetes show a correlation between the level of scarring and increases in the peritubular and peri-glomerular distribution of TG2 and $\epsilon(\gamma$ -glutamyl) crosslink. This study has been taken further with the analysis of scarring in human renal biopsies from 136 patients with a range of chronic kidney diseases (Johnson *et al.*, 2003). In this study, changes in TG2 and $\epsilon(\gamma$ -glutamyl) crosslink also correlated well with the degree of scarring and were independent of the original disease. Finally, TG2 has been demonstrated to be associated with scarring resulting from chronic allograft nephropathy (Johnson *et al.*, 2004).

1.9 Thesis Rationale and Hypothesis

The study of both experimental and human renal disease has clearly established the involvement of the protein crosslinking enzyme TG2 in the development of scarring. The up-regulation and release of TG2 occurs predominantly from injured tubular cells and results in

the increased presence of crosslinking in the extracellular environment (Johnson *et al.*, 1997; Johnson *et al.*, 1999; Skill *et al.*, 2001). However, to date, the precise pathological role of TG2 crosslinking in kidney scarring and fibrosis has yet to be determined. It is likely that TG2 has the potential to act via a number of mechanisms that contribute to and perpetuate renal disease. These may include an indirect role in the activation of latent TGF- β 1 (Nunes *et al.*, 1997). However, recent evidence suggests that the most significant influence of TG2 on the scarring process is likely to be its potential effect on ECM homeostasis. Previous studies have demonstrated the ability of TG2 to stabilise both collagen and FN fibrils suggesting that TG2 may influence the rate of ECM deposition (Gross *et al.*, 2003; Jones *et al.*, 1997a; Kleman *et al.*, 1995; Martinez *et al.*, 1994; Verderio *et al.*, 1998). Similarly, TG2 mediated crosslinking of isolated collagen fibrils has been shown to increase their resistance to MMP-1 degradation (Johnson *et al.*, 1999). Thus TG2 has the potential contribute to ECM expansion and scarring through a direct effect on the rate of ECM deposition and breakdown.

Whilst these studies have suggested a causative role for TG2 in the accumulation of ECM, much of the previous *in vitro* work in the kidney has been performed on isolated collagen or investigated the effects of exogenous TG2 on the ECM. It therefore remains to be determined whether TG2 at physiological levels, produced by and exported from tubular cells exerts similar effects on the ECM. The *in vitro* studies performed in this thesis therefore aim to test the hypothesis that TG2 up-regulated by and released from tubular cells contributes to the scarring process by directly affecting the rate of ECM deposition and breakdown and thus facilitating the accumulation of matrix.

Previous *in vivo* studies, whilst demonstrating a link between TG2 and the development of scarring have yet to establish whether elevated TG2 and $\epsilon(\gamma\text{-glutamyl})$ lysine are crucial in driving the scarring process or whether they are accompanying factors. The ultimate objective of this thesis is therefore to investigate whether *in vivo* inhibition of TG2 can directly prevent the development of scarring and halt the progression of renal disease. It is hoped that the findings of these studies will provide definitive evidence to support the pathological role of TG2 in driving the accumulation of ECM as well as to establish whether TG2 inhibition has the potential as a therapeutic intervention to prevent progressive renal disease.

Chapter 2

Aims

It is hypothesised that TG2 up-regulated and released by tubular cells drives the development of kidney scarring by directly affecting the rate of ECM deposition and breakdown and thus facilitating the accumulation of matrix.

The principle aims of these studies are to determine:

- 1) **What fibrogenic factors associated with renal disease cause TG2 to be up-regulated and released from tubular epithelial cells.** Proximal tubular epithelial cells will be treated with growth factors and cytokines *in vitro* to study their effects on TG2 expression and activity. Cell culture models of hypoxia and acidosis will be used to assess the effect of cell stress on TG2 expression.
- 2) **Whether TG2 can be modulated in tubular and mesangial cells.** Opossum (OK) proximal tubular cells and 1097 mesangial cells will be stably transfected with expression vectors containing the 3.3 kb human TG2 gene, the resultant cell clones selected and characterised. TG2 null tubular and mesangial cells will be isolated and characterised from the TG2 knockout mouse.
- 3) **If modulation of TG2 affects ECM accumulation *in vitro*.** The ECM from TG2 over-expressing tubular and mesangial cells and TG2 null cells will be radiolabelled and the levels of ECM determined along with the rates of deposition and breakdown by MMPs.
- 4) **If TG2 inhibition *in vivo* can prevent the accumulation of ECM thus halting the progression of renal disease and maintaining kidney function.** Non-competitive irreversible inhibitors of TG2 will be administered via osmotic mini-pump for up to 84 days to the kidneys of rats subjected to 5/6th subtotal nephrectomy. Markers of kidney function and scarring will be used to assess the progression of renal disease. Changes to the ECM will be analysed by immunohistochemistry and Northern blotting.

Chapter 3

Materials and Methods

3.1 Cell Culture

3.1.1 Cell lines

Opossum proximal tubular epithelial cells (OK cells), rat proximal tubular epithelial cells (RPT) and NRK-52E tubular epithelial cells were obtained from the European Collection of Cell Cultures (ECACC). 1097 rat mesangial cells were a gift from Dr. Robert Atkins (Department of Nephrology, Monash Medical Centre, Victoria, Australia). LLC-PK1 pig proximal tubular cells were cultured by Dr. Rana Rustom (Medical School, Liverpool University, UK).

3.1.2 Cell culture media for cell lines

OK cells were cultured in Dulbecco's Modified Eagles Medium (DMEM, Cambrex Bioscience, Wokingham, UK) containing 2mM L-glutamine, 5% (v/v) heat-inactivated foetal calf serum, 100 IU/ml penicillin and 100 µg/ml streptomycin (Sigma, Poole, UK).

RPT cells were cultured in DMEM/ Ham's F12 (Cambrex Bioscience) containing 2mM L-glutamine, 10% heat-inactivated foetal calf serum, 100 IU/ml penicillin, 100µg/ml streptomycin supplemented with 5µg/ml insulin, 5µg/ml transferrin and 10ng/ml EGF (Sigma).

NRK-52E and 1097 cells were cultured in DMEM (Cambrex Bioscience) containing 2mM L-glutamine, 10% heat-inactivated foetal calf serum, 100 IU/ml penicillin and 100 µg/ml streptomycin.

LLC-PK1 cells were cultured in Medium 199 (Sigma) containing 10% heat-inactivated foetal calf serum, 15mM HEPES, 100 IU/ml penicillin, 100 µg/ml streptomycin, 2mM L-glutamine, 4µg/ml hydrocortisone, 10µg/ml insulin, 5.5µg/ml and 5ng/ml sodium selenite (ITS media supplement, Sigma).

All cultures were maintained at 37°C and in a humidified atmosphere of 5% CO₂ in air (Ig500 incubator, Jouan, Saint-Herblain, France).

3.1.3 Primary cell culture media

Primary tubular epithelial cells were cultured in DMEM/F12 (Cambrex Bioscience) containing 0.5-5% (v/v) foetal calf serum, 100 IU/ml penicillin, 100µg/ml streptomycin, 2mM L-glutamine and supplemented with 10µg/ml insulin, 5.5µg/ml transferrin, 5ng/ml sodium selenite (ITS supplement, Sigma), 10ng/ml epidermal growth factor, 5pg/ml tri-iodothyramine, 5µg/ml dexamethasone, 12.5µg/ml each of adenosine, cytosine, guanosine, uridine and 0.25µg/ml amphotericin B (Fungizone™, Life Technologies, Paisley, UK).

Primary mesangial cells were cultured in RPMI 1640 medium (Cambrex Bioscience) containing 20% foetal calf serum, 2mM L-glutamine, 100 IU/ml penicillin, 100 µg/ml streptomycin, 1mM sodium pyruvate (Sigma), 15mM HEPES, sodium bicarbonate and 0.25µg/ml amphotericin-B (Fungizone™, Life Technologies). In addition media was supplemented with 50-100µg/ml of dithiothreitol (DTT) activated guinea pig liver transglutaminase (Sigma) at the time of initial plating to facilitate attachment of mesangial cells.

3.1.4 Treatment with fibrogenic growth factors/cytokines

OK cells were seeded in complete growth medium (section 3.1.2) supplemented with 10-100ng/ml of TGF-β1 (Life Technologies), IGF-1 (Kabi, Uppsala, Sweden), PDGF, IL-1β or TNF-α (Sigma) and cultured for up to 48 hours. Cells were trypsinised with 0.25% (v/v) trypsin/1mM EDTA (Life Technologies), centrifuged at 13,000rpm for 2 mins (Jouan A14 centrifuge, 5.5cm rotor) and the subsequent cell pellet snap frozen in liquid nitrogen. Cell lysates were prepared as described in section 3.3.2 and transglutaminase (TG) activity determined using the putrescine incorporation assay (section 3.3.7.1).

3.1.5 Treatment with known transglutaminase stimulators

OK cells were seeded in complete growth medium supplemented with 10-100µg of; all *trans* retinoic acid, sodium butyrate or dexamethasone (Sigma) and cultured for a total of 48 hours. Cells were harvested as described in section 3.1.4 and cell lysates prepared as described in section 3.3.2. Intracellular TG activity was determined by the putrescine incorporation assay.

3.1.6 Hypoxic treatment of NRK-52E tubular cells

NRK-52E cells were plated in 100mm² petri dishes (Iwaki, Japan) and allowed to attach overnight at 37°C. After this time period cells had reached approximately 50% confluency. Cells were cultured for a further 6, 12, 24 or 48 hours under either normoxic conditions of 21% oxygen or hypoxic conditions of 1% oxygen, in a multigas incubator (Ig750, Jouan). Oxygen levels were constantly monitored using an oxygen probe (Oxycheck 2, David Bishop Instruments, Leamington Spa, UK). Cells were harvested as described in section 3.1.4 and intracellular TG activity measured by the putrescine incorporation assay or TG2 antigen measured by Western blotting (sections 3.3.6 and 3.3.7.3). In addition, extracellular TG activity was determined after exposure to hypoxia by plating cells into 96 well plates and measuring biotin cadaverine incorporation as described in section 3.3.7.5

3.1.7 Acidic treatment of LLC-PK1 tubular cells

The acidic treatment of LLC-PK1 tubular cells was performed by Dr. Rana Rustom at Liverpool University, UK. Porcine LLC-PK1 cells were seeded at a density of 2×10^4 - 2×10^5 in T25 flasks and cultured under standard conditions for 72 hours until 30% confluent. At this stage, the medium was modified by substituting HEPES with BIS-TRIS buffer (final concentration 12.5mM). Three different buffer concentrates were prepared such that the ratio of acid and base components differed giving final extracellular pHs of 7.4 (control), 7.0 and 6.7. Media pH levels were monitored throughout the experimental period using a standard pH electrode. After 48 hours growth in BIS-TRIS buffered serum containing medium, the medium was changed to serum free, again with BIS-TRIS buffer. After 24 hours in serum free conditions cells grown in pH 7.4 and pH 7.0 were confluent and those grown in pH 6.7 were 95% confluent. At this stage cells were harvested for analysis by putrescine incorporation assay, biotin cadaverine ELISA, Western and Northern blotting (section 3.4.8). Cell culture media was removed and analysed for TG2 protein following acetone precipitation (section 3.3.3)

3.1.8 Immunofluorescence for tubular cell markers

Tubular epithelial cells were plated onto 22mm^2 glass coverslips at a density of 1×10^6 and cultured for 48 hours. Cells were washed in phosphate buffered saline (PBS) and fixed in methanol for 10 mins at room temperature. Cells were blocked for 30 mins with 5% BSA/0.1% TBS-tween 20 and immunoprobed for either β -catenin (1:250 dilution, Abcam, Cambridge, UK) or α -smooth muscle actin (1:100 dilution, Dako, High Wycombe, UK). Antibody binding was revealed by incubation with FITC conjugated anti-mouse IgG (Dako). Cells were washed and mounted with Vectashield fluorescent mount (Vector Labs, Peterborough, UK). Fluorescence was visualised using an Olympus BX61 microscope at 494nm with excitation at 518nm.

3.1.9 Immunofluorescence for mesangial cell markers

Immunofluorescence for mesangial cell markers was performed by Dr. Richard Jones at Nottingham Trent University, Nottingham, UK. Cells were plated onto 8 well chamber slides (Nunc, Naperville, IL, USA) and cultured for 72 hours. Cells were washed in PBS and fixed in methanol for 10 mins. Cells were immunoprobed for fibroblast cell surface antigen (monoclonal clone 1B10, Sigma), CD31 endothelial cell marker (rat monoclonal, Abcam, UK), vimentin (mouse monoclonal, Abcam) and cytokeratin (monoclonal anti-pan cytokeratin mixture, Sigma). Antibody binding was revealed by incubation with FITC conjugated anti-mouse IgG (fibroblast antigen, vimentin, cytokeratin) or TRITC conjugated anti-rat IgG

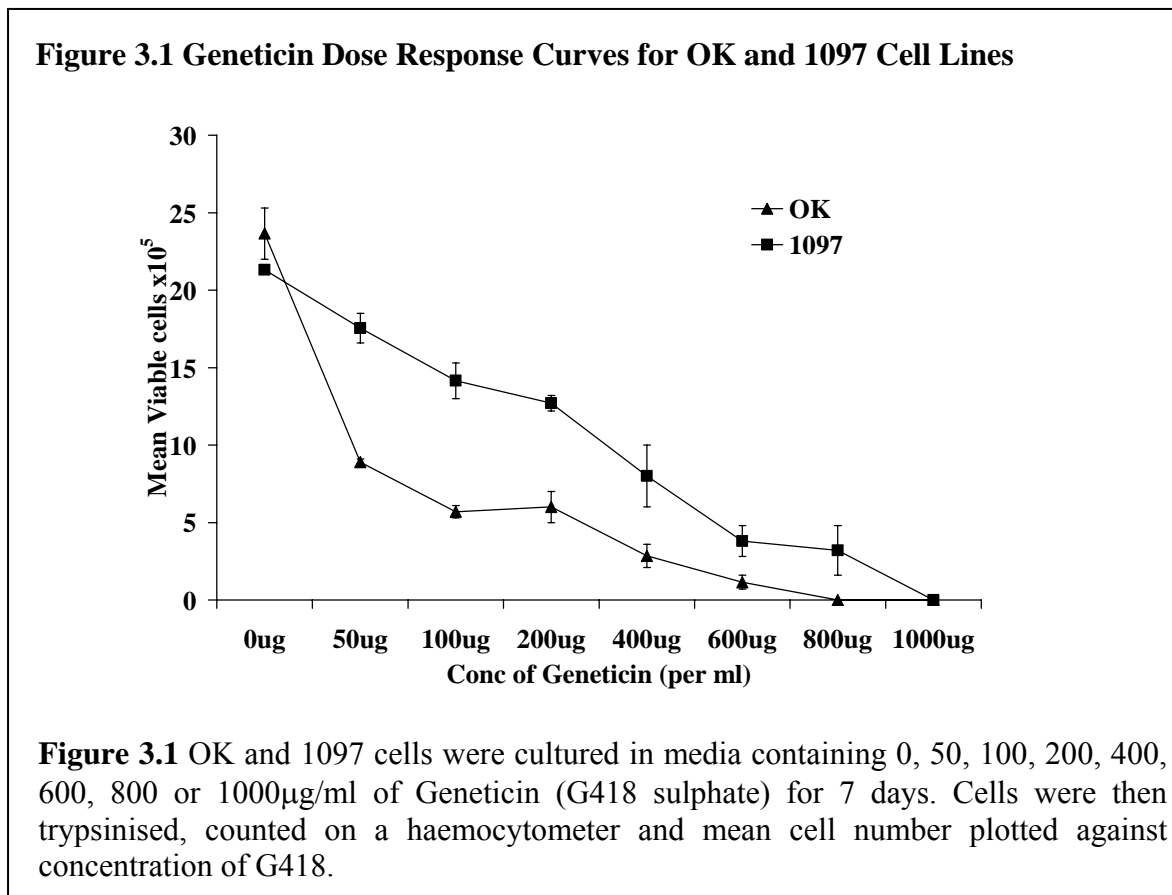
(CD31). Cells were washed and mounted with Vectashield mounting medium containing propidium iodide (Vector Labs). Fluorescence was visualised using a Leica TS NT confocal microscope (Leica, Wetzlar, Germany) with FITC excitation at 494nm and TRITC excitation at 560nm.

3.2 Transfection of Renal Cell Lines

3.2.1 Dose response to geneticin (G418 sulphate)

Cells were seeded in duplicate into T25 flasks such that they reached 30% confluency after 24 hours at 37°C. A 10mg/ml stock of Geneticin (G418, Life Technologies) was prepared in sterile distilled water. Using this stock solution, concentrations of 0, 50, 100, 200, 400, 600, 800 and 1000µg/ml were prepared in 2.5mls of media and added to duplicate flasks.

Media was changed every 2 days and fresh Geneticin added. Cells were cultured for a maximum of 7 days. Following 7 days in culture, cells were trypsinised using 0.25% (v/v) trypsin/1mM EDTA (Invitrogen, UK) and counted on a haemocytometer (Weber Scientific, Hamilton, NJ, USA). The mean cell number for each flask was calculated and plotted against the concentration of geneticin as shown in figure 3.1. A concentration of 800µg/ml (OK) and 1000µg/ml (1097) was chosen to select for stably transfected cells, since this killed 100% of untransfected cells within 7 days.



3.2.2 Transfection of OK proximal tubular cells with pCIneo-htg

Cells were seeded into a 100mm² petri dish (Iwaki) and allowed to attach overnight at 37°C after which they had reached 50% confluency. Transfection was performed using 63µl of lipofectin® reagent (Life Technologies) and 15µg of either pCIneo or pCIneo-htg vector (section 3.4.1). Tubes were prepared, containing 750µl of Optimem low serum medium (Life Technologies) and either 63µl of lipofectin® or 15µg of either pCIneo or pCIneo-htg. All tubes were allowed to stand at room temperature for 45 mins. The lipofectin and DNA solutions were combined, the resultant lipofectin®/DNA mixtures vortexed and incubated at room temperature for 15 mins. Meanwhile, cells to be transfected were washed for 2x 5 mins with 10mls per dish of Optimem medium. The lipofectin®/DNA mixtures were made up to 7.5mls with Optimem medium and added to the cells. Cells were incubated for 7 hours at 37°C. Following transfection, the lipofectin®/DNA mixture was removed and replaced with 10mls of complete media. Cells were incubated for 36 hours prior to the selection of stable clones (section 3.2.4).

3.2.3 Transfection of 1097 mesangial cells

All transfections were performed using the Nucleofector™ system (Amaxa Biosystems, Cologne, Germany). This is a highly efficient electroporation technique that uses a combination of optimised electrical parameters and specific Nucleofector™ solutions to allow the direct delivery of DNA into the nucleus. Transfection using the Nucleofector system™ was chosen in preference to cationic lipid transfection in order to overcome the problem of low transfection efficiency observed in 1097 cells.

3.2.3.1 Preparation of cell suspensions

6 well plates were prepared containing 1ml/well of pre-warmed RPMI 1640 medium (Cambrex Bioscience) supplemented with 10% foetal calf serum, 100 IU/ml penicillin and 100 µg/ml streptomycin (Sigma). These were pre-incubated at 37°C/5% CO₂ prior to transfection. Cells were harvested using trypsin-EDTA and counted on a haemocytometer. The cell pellet was re-suspended in the appropriate Nucleofector solution to a final concentration of 1.5x10⁶ cells/100µl.

3.2.3.2 Transfection procedure

A cell suspension of 1097 cells was prepared as described in section 3.2.3.1. Plasmid DNA was added to a 100µl aliquot of cell suspension, transferred to an Amaxa cuvette and the cuvette capped. The cuvette was inserted into the cuvette holder and the turning wheel rotated clockwise to the final position. Transfection was performed by selecting the program

on the Nucleofector device and pressing the “X” key to start the program. On completion of the program, 500µl of pre-warmed culture medium was added to the cuvette and the cells transferred to the prepared 6 well plate.

3.2.3.3 Optimisation of the nucleofection protocol

6 well plates and cell pellets were prepared as described in section 3.2.3.1. Cell pellets were re-suspended in either Nucleofector solution T, solution R or solution V to a final concentration of 1.5×10^6 cells/100µl. Each 100µl of cells were transfected with 5µg of pSVgal control plasmid (Promega, Southampton, UK) using a range of Nucleofector programs (table 3.1). Following transfection, cells were made up to 500µl with pre-warmed complete RPMI 1640 medium, plated and allowed to grow for 24 hours. Efficiency of the transfection was determined by the β-galactosidase assay as described in section 3.2.3.5 and expressed as a percentage compared to un-transfected cells. Visual inspection of the cells was used to determine the % viability of cells post transfection. The results of the optimisation are shown in table 3.2. Program T27 and Nucleofector solution V were chosen for subsequent transfections.

3.2.3.4 Co-transfection of 1097 mesangial cells with pSVneo and pSG5-htg vectors

1097 cells at a final concentration of 1.5×10^6 /100µl were co- transfected with either 2µg pSV₂neo/4µg pSG5-htg or 2µg pSV₂neo/8µg pSG5-htg using program T27. On completion of the program, 500µl of pre-warmed culture medium was added to the cuvette and the cells transferred to the prepared 6 well plate. Cells were allowed to grow for 48 hours, after which time media was replaced with DMEM containing 10% foetal calf serum, 100IU/ml penicillin, 100 µg/ml streptomycin (Sigma) and 1mg/ml of Geneticin (Life Technologies). Resistant colonies were picked and transferred to 96 well plates as described in section 3.2.4

3.2.3.5 β-Galactosidase assay

The efficiency of 1097 cell transfection with pSVgal vector was determined using the Promega β-Galactosidase enzyme assay system. Cells transfected in 6 well plates were washed once with 1x PBS followed by lysis of the cells with 150µl/well of 1x reporter lysis buffer for 15 mins at room temperature with gentle rocking. The lysates were removed and vortexed for 15 secs, followed by centrifugation at 13,000 rpm for 2 mins (Jouan A14 centrifuge, 5.5cm rotor). The supernatant was removed and transferred to a fresh tube. 120 µl of 2x assay buffer was added and sample left overnight (16 hours) at 37°C for colour to

Table 3.1 Nucleofector Optimisation Programs

Program	Solution R	Solution T	Solution V
w/o nucleofection	+	+	+
T-16 no plasmid	-	-	-
A23	+	+	+
A27	+	+	+
G16	+	+	+
O17	+	+	+
T01	+	+	+
T16	+	+	+
T20	+	+	+
T24	+	+	+
T27	+	+	+

Table 3.2 Results of Nucleofector Optimisation

Program	Solution R		Solution T		Solution V	
	Efficiency	% Viable	Efficiency	% Viable	Efficiency	% Viable
w/o	0	98	0	98	0	98
no plasmid	0	70	0	60	0	95
A23	1.2	85	13.5	90	8.7	90
A27	4.8	85	8.1	90	4.9	95
G16	14.6	80	2.3	80	0	80
O17	40.2	70	3.2	85	25.4	85
T01	8.5	85	27.3	90	7.0	95
T16	39	60	8.3	80	24.2	85
T20	120.7	50	0	50	35.8	85
T24	20	60	0	60	98	60
T27	39	50	0	95	49.5	50

Table 3.1 and 3.2 1097 cells were re-suspended in either Nucleofector solution T, solution R or solution V to a final concentration of 1.5×10^6 cells/100 μ l. Each 100 μ l of cells were transfected with 5 μ g of pSVgal control plasmid using a range of pre-set Nucleofector programs. The efficiency of 1097 transfection with each program was determined by the β -galactosidase assay (section 3.2.3.5) and expressed as a percentage increase in OD compared to un-transfected 1097 cells. Visual inspection of the cells post transfection was used to determine the percentage viability.

develop. Samples were transferred to a 96 well plate and the optical density read at 405nm (Multiskan Ascent plate reader, Thermo Labsystems, Helsinki, Finland).

3.2.4 Selection of stable clones from transfected cells

36 hours post transfection, media was replaced with fresh complete medium containing 800µg/ml of geneticin. Cells were cultured for 4 days after which time 100% of control cells were killed. The media was replaced and the geneticin concentration dropped to 400µg/ml. Colonies of cells were selected and picked from the petri dishes using a 200µl pipette and transferred into a 96 well plate. The pipette tip was placed next to the colony and dragged across it at the same time sucking cells up with the pipette. A colony plus 200µl of media was deposited in each well.

Upon reaching confluency in 96 well plates, cell clones were amplified by culture in 6 well plates, followed by transfer to T25 flasks. The transglutaminase activity of each cell clone was determined in three consecutive T25 flasks by the putrescine incorporation assay (section 3.3.7.1).

3.2.5 Growth curves

OK and 1097 cell clones were seeded at 1×10^6 in T25 flasks. Attached cells were harvested at 24, 48, 72 and 96 hours post plating using trypsin-EDTA and re-suspended in 1ml of complete medium prior to counting on a haemocytometer. Duplicate counts were taken from each flask and the growth curves were repeated 3 times. Since growth was found to be exponential, the log of cell number was used to obtain linear plots from which the gradient was calculated and used to determine growth rates and doubling times of individual clones.

3.3 General and Biochemical Techniques

3.3.1 Preparation of tissue homogenates

100-200mg of snap frozen rat kidney tissue was weighed and transferred to a small tube. To this was added 9 times the volume of STE buffer (0.32M sucrose, 5mM Tris, 2mM EDTA) containing protease inhibitors [1mM leupeptin, 5mM benzamidine and 1mM phenylmethylsulphonylfluoride (Sigma)] and the tissue homogenised using an Ultra Turrax T25 homogeniser (Merck, Darmstadt, Germany). This produced a 10% (w/v) tissue homogenate. The homogenate was aliquoted and either used directly in the putrescine incorporation assay (section 3.3.7.1) or stored at -80°C for Western blot analysis (section 3.3.6.1).

3.3.2 Preparation of cell lysates

Cells were trypsinised using 0.25% (v/v) trypsin/1mM EDTA for 5mins at 37°C. These were re-suspended in 10mls of complete media and centrifuged at 800rpm (Jouan A14 centrifuge, 5.5cm rotor) for 5 mins at room temperature. The media was removed and cells centrifuged at 13,000 rpm for 2 mins (Jouan A14 centrifuge, 5.5cm rotor) to produce a cell pellet. Any excess media was removed and the cell pellet snap frozen in liquid nitrogen for analysis. On thawing, cells were re-suspended in 100µl of STE buffer containing protease inhibitors (section 3.3.1). A cell lysate was produced by sonicating the cells for 3x 5 secs on ice.

3.3.3 Acetone precipitation of cell culture media

The media was collected and any residual cells removed by centrifugation at 800rpm (Jouan A14 centrifuge, 5.5cm rotor) for 2 mins. Proteins in the remaining media were precipitated by the addition of an equal volume of acetone and incubation on ice. The protein pellet was air dried and re-suspended in 1/10 volume of STE buffer containing protease inhibitors prior to Western blot analysis.

3.3.4 Processing and fixation of tissues

Kidneys were halved, fixed overnight in 10% formalin and rinsed in PBS before being embedded in paraffin. Sections 4µm thick were cut from the paraffin blocks using a rotatory microtome by the Histopathology Department, Northern General Hospital, Sheffield, UK and mounted onto poly L-lysine coated microscope slides (VWR, Poole, UK). These were stored at room temperature prior to performing immunohistochemistry.

3.3.5 Preparation of cryostat sections

Kidney tissue was snap frozen in liquid nitrogen and then mounted in OCT mounting media (Raymond Lamb, Eastbourne, UK). Cryostat sections, 10µm thick, were cut at -12°C, mounted onto poly L-lysine coated microscope slides (VWR) and stored at -20°C prior to use.

3.3.6 Western blotting

3.3.6.1 Polyacrylamide gel electrophoresis (SDS-PAGE)

Polyacrylamide gel electrophoresis was performed using either the mini-protean 2 electrophoresis system (Sample size 1-10) (Biorad, Hemel Hemstead, UK) or the Geneflow OmniPAGE system (sample size 10-24) (Geneflow, Fradley, UK). The electrophoresis method is a modification of that described by Laemmli (Laemmli, 1970).

A 10% resolving gel was prepared by the addition of 7.5ml resolving buffer (1.5M Tris

pH8.8), 5ml of acrylamide:bis acrylamide stock (37.5:1, Biorad), 0.5ml of 1% ammonium persulphate, 150 μ l of 10% SDS (sodium dodecyl sulphate) and 2.2ml distilled water to a Buchner flask. The resolving gel was degassed by attaching the flask to a vacuum line for 10 mins, prior to the addition of 20 μ l of TEMED (*N,N,N',N'*-tetramethylethylenediamine, Sigma). The resolving gel was then pipetted carefully into the space between the glass plates of the electrophoresis apparatus, overlaid with a small volume of butanol and allowed to set for 30 mins at 37°C. Once the resolving gel had set, a 5% stacking gel was prepared containing 5ml 0.75M Tris pH6.8, 1.5ml of acrylamide stock, 0.25ml 2% ammonium persulphate, 100 μ l 10% SDS, 3.5ml distilled water and 35 μ l of TEMED. The butanol was carefully rinsed off the resolving gel with distilled water and residual water removed with tissue paper. The stacking gel was pipetted onto the resolving gel and a plastic comb inserted in the space between the two plates. The stacking gel was allowed to set at 37°C for 30 mins.

Protein samples were prepared by transferring 20 μ g of protein as determined by the Lowry assay (section 3.3.9.2) to a microfuge tube and adding an equal volume of sample buffer [10mM Tris pH 6.8, 2.5% (w/v) SDS, 10% (w/v) glycerol, 0.02% (w/v) bromophenol blue and 5% (v/v) 2-mercaptoethanol]. Samples were then heated to 95°C for 5 mins, cooled to room temperature and briefly centrifuged to bring to the bottom of the tube. The comb was removed from the stacking gel and the resultant wells filled with 1 x Tris-glycine SDS PAGE buffer (Geneflow). Samples were loaded, gels transferred to the gel tank and Tris-glycine buffer poured between and around the gels. Gels were run at 100V for 1.5 to 2 hours.

3.3.6.2 Electro-blotting

Proteins previously separated by SDS PAGE (section 3.3.6.1) were electroblotted onto Hybond C membrane (Amersham Biosciences, Buckingham, UK) using the Trans-Blot[®] SD semi-dry electrophoretic transfer cell (Biorad). Eight pieces of filter paper slightly larger than the resolving gel and the Hybond C membrane were soaked for at least 30 mins in a small volume of transfer buffer [25mM (w/v) Tris, 150mM (w/v) glycine, 20% (v/v) methanol]. After electrophoresis was complete, the glass plates containing the gel were removed from the apparatus, separated and the stacking gel removed with a scalpel blade. The gel was transferred to a small volume of transfer buffer to equilibrate the gel. The Trans blot anode was wetted with a small volume of distilled water and 4 pieces of filter paper placed onto the anode. A glass pipette was rolled over the filter paper to remove any air bubbles and the pre-wetted membrane placed on top. After removing the air bubbles, the gel was placed on top of the membrane followed by the remaining filter paper to form a sandwich. The cathode was carefully placed onto the stack and the blot run at 15V for 30 mins.

Following electroblotting, the top filter paper was carefully removed and the position of the markers impressed onto the membrane using a sharp needle. The membrane was then immersed briefly in Ponceau Red Solution (Sigma) to stain protein bands and confirm successful transfer. Ponceau Red was removed by rinsing the membrane in distilled water followed by incubation for 15 mins in 1 x Tris Buffered Saline/ 0.1% Tween 20 (TBST) at room temperature.

3.3.6.3 Probing of membranes

Following incubation with TBST membranes were blocked overnight with 5% (w/v) non fat dried milk (Marvel) diluted in 1 x TBST at 4°C. After overnight incubation, membranes were washed with 1 x TBST for 3 x 5 min washes. Membranes were then probed with primary antibody in TBST for 2 hours at room temperature followed by 3 x 5 min washes in 1 x TBST. Primary antibody binding was revealed by probing with secondary antibody diluted in 1 x TBST for 1 hour at room temperature. Membranes were again washed 3 x 5 mins with 1x TBST and protein bands detected by chemiluminescence using ECL reagent (Amersham Biosciences). ECL reagents 1 and 2 were mixed in equal volumes and applied to the membrane for 1 min, the reagent tipped off the blots and wrapped in cling film to form an envelope. Blots were then placed protein side up in a Biomax® film cassette (Perkin Elmer Life Sciences, Waltham, MA,USA).

In a dark room, a sheet of autoradiographic film (Kodak Biomax light, Sigma) was placed over the top of the membrane and the cassette closed. After the appropriate exposure time, the film was removed and developed using Kodak GBX developer (Sigma) for 2 mins, followed by fixing for 2 mins with Kodak GBX fixer (Sigma) and rinsing for 30 secs with water. Bands were quantified by volume densitometry using a Biorad GS-690 imaging densitometer and Multi-Analyst version 3.2 software (Biorad). Determination of band size was by reference to Kaleidoscope protein markers (Control 85303, Biorad). Sizes of protein markers are shown in table 3.3

Table 3.3 Kaleidoscope Pre-stained Protein Markers

Protein	Colour	MW kDa
Myosin	Blue	217
β-galactosidase	Magenta	126
Bovine serum albumin	Green	73
Carbonic anhydrase	Violet	43.5
Soybean trypsin inhibitor	Orange	31.6
Lysozyme	Red	18
Aprotinin	Blue	7.5

3.3.7 Detection of tissue transglutaminase

3.3.7.1 Transglutaminase activity by ^{14}C putrescine incorporation assay

Transglutaminase enzyme activity levels were measured as described previously by Lorand (Lorand *et al.*, 1972). In this assay, active transglutaminase in the presence of calcium incorporates $[1,4-^{14}\text{C}]$ -putrescine into N,N-dimethylcasein forming a radioactive TCA-insoluble material capable of being detected by scintillation counting (figure 3.2).

Samples were set up containing 50 μl of cell lysate, tissue homogenate or re-suspended freeze dried media, and 50 μl of TG activity reaction mix (table 3.4). A control in which calcium was replaced with EDTA was used to determine non-enzymatic incorporation. Samples and control were incubated at 37°C for 60 mins. At set time points after initiation of the reaction, 10 μl aliquots, in duplicate, were removed from the reaction tubes and spotted on to 1 cm^2 Whatman 3MM filter papers. These were immediately dropped into a beaker containing 10% (w/v) trichloroacetic acid (TCA) to stop the reaction and to precipitate ^{14}C labelled N, N'-dimethylcasein. Filters were further washed with 10 % (w/v) ice cold TCA for 10 mins, 5 % (w/v) ice cold TCA for 3 x 5 mins, 1:1 acetone:ethanol for 5 mins and 100% acetone for 5 mins. To determine efficiency of counting 10 μl of the sample/reaction mixture was spotted on to a filter paper square and not washed. These filter papers represent the total counts in the reaction mixture. Filter papers were allowed to air dry before being placed in 4ml of Ultima Gold XR liquid scintillation fluid (Perkin Elmer, Beaconsfield, UK) and radioactive incorporation measured by scintillation counting on a Rack-beta liquid scintillation counter (Packard Instrument Co, Downers Grove, IL, USA). Using only the linear part of the graph, the gradient (change in CPM per minute) was calculated which was subsequently used to calculate transglutaminase activity. Values were corrected for protein and expressed as nmol of putrescine incorporated per hour [Unit of activity per mg of protein (U/mg protein)].

Table 3.4 Constituents of Reaction Mix for Putrescine Incorporation Assay

Sample		Background Control	
Reagent	Vol (μl)	Reagent	Vol (μl)
2.5mM CaCl_2	10	EDTA	10
3.8mM dithiothreitol	10	3.8mM dithiothreitol	10
$[1,4,^{14}\text{C}]$ putrescine	10	$[1,4,^{14}\text{C}]$ putrescine	10
N,N' Dimethylcasein	20	N,N' Dimethylcasein	20

Figure 3.2 Schematic Diagram of the Transglutaminase Activity Assay

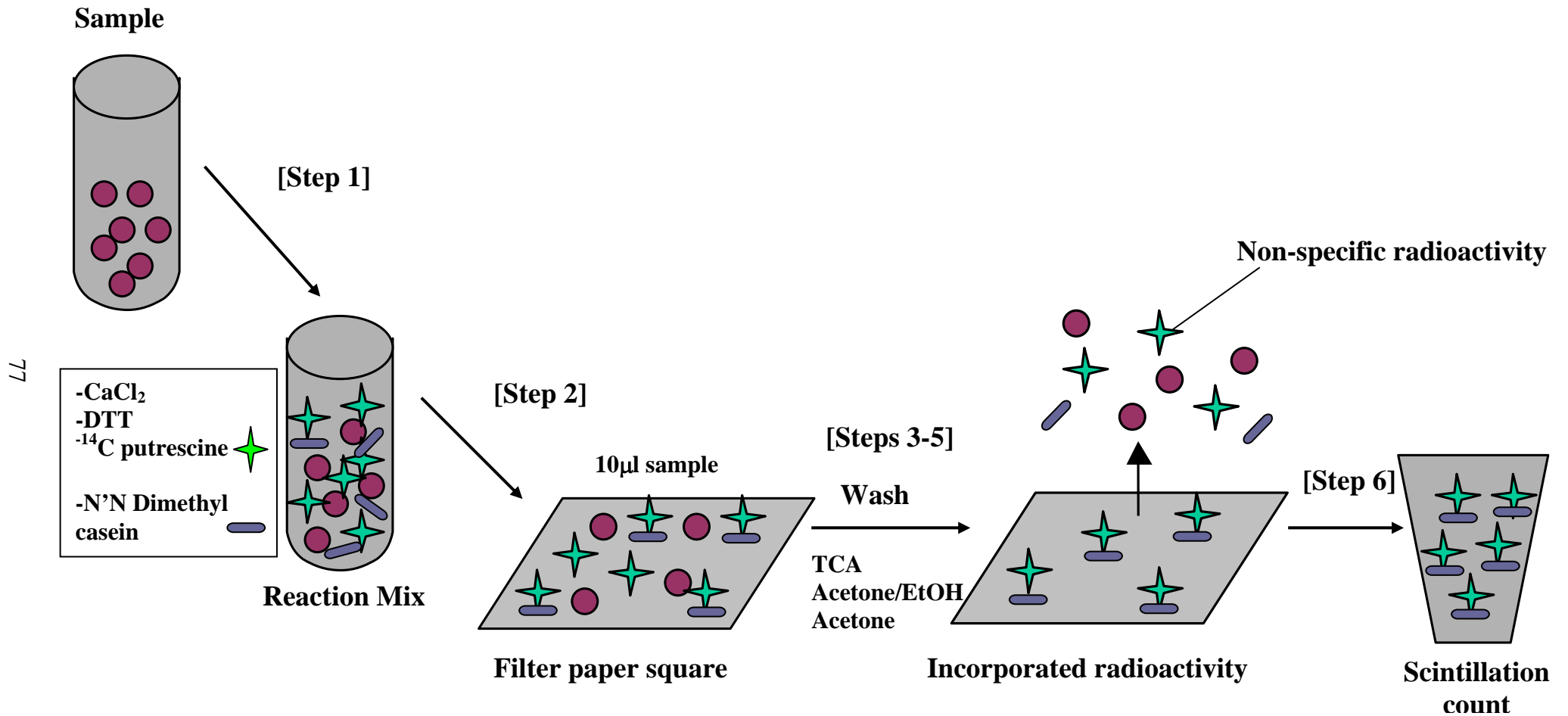


Figure 3.2 [Step1] 50µl of cell lysate, tissue homogenate or media is added to reaction mix containing ¹⁴C-putrescine and the TG substrate N’N dimethyl casein. [Step2] 10µl of reaction mix is dotted onto 1cm² filter paper squares. [Step3-5] Filter papers are washed sequentially with 5% TCA, 1:1 acetone: ethanol and acetone to remove non-incorporated label and air dried. [Step 6] Incorporation of ¹⁴C-putrescine into N’N dimethylcasein (TG activity) is measured by scintillation counting.

3.3.7.2 Detection of *in situ* transglutaminase activity

Determination of *in situ* TG activity was performed on cryostat sections (section 3.3.5) by Dr Richard Jones at Nottingham Trent University. Unfixed sections were incubated with fluorescein (FITC) cadaverine (Molecular Probes, Eugene, OR, USA) in 50mM Tris-HCl pH7.4 containing either 10mM CaCl₂ or 10mM EDTA (negative control) for 1 hour at 37°C. Sections were washed, fixed in 100% methanol for 10 mins and blocked for 1 hour at room temperature with 3% (w/v) bovine serum albumin, 0.01% (v/v) triton X-100 in PBS, pH 7.4 containing 5% (v/v) goat serum. After washing, sections were incubated with mouse anti-FITC antibody (Sigma) overnight at 4°C and probed with goat anti-mouse Cy5-conjugated antibody (Stratech Scientific, Luton, UK) for 1 hour at room temperature. Sections were visualised using confocal microscopy (Leica CLSM confocal laser microscope) using an argon/krypton laser adjusted to 647nm and 488nm for both Cy5 and FITC emissions. Semi-quantitation of activity was obtained using the mean Cy5 emissions per field (mV/μm²) from at least ten 200x magnification fields.

3.3.7.3 Detection of transglutaminase by western blot

Transglutaminase antigen levels were measured by immuno-probing of Western blots. Cell lysates were separated on a 10 % (w/v) polyacrylamide denaturing gel by SDS-PAGE and proteins electroblotted for 30 mins at 15V onto Hybond C membrane as described in sections 3.3.6.1 and 3.3.6.2. Membranes were blocked overnight at 4°C with 5% (w/v) non-fat milk protein (Marvel) in 1 x TBST followed by probing with monoclonal mouse anti-transglutaminase antibody (TG100, Neomarkers, Fremont, CA, USA) in TBST at 1:750 dilution. Following 3 washes with TBST, primary antibody was revealed with goat anti-mouse HRP (Dako) in TBST at 1:1000 dilution. Transglutaminase bands were visualised using ECL chemiluminescence and quantified by volume densitometry as described in section 3.3.6.3. Typical exposure times for the visualisation of TG2 bands were 10-20 seconds.

3.3.7.4 TG2 immunocytochemistry

Cells were plated at 0.5×10^6 on 22mm² coverslips and allowed to attach overnight at 37°C prior to staining. The media was removed and cells washed twice gently with 1 x PBS. Cells were fixed in 100% methanol for 20 mins at room temperature. After fixing, cells were washed 3 x 5 mins with 1xPBS/1% (v/v) tween 20 (PBST) and the cells permeabilised with 0.1% triton in PBS for 5 mins at room temperature. Following 3 x 5 min washes with PBST, endogenous peroxidase was quenched with 3% H₂O₂ in PBS for 5 mins at room temperature. Cells were washed a further 3 x 5 mins with PBST and blocked with 150μl of horse serum (ABC Vectastain Kit, Vector Labs) in 10mls of 0.1% BSA/PBS for 30 mins at room

temperature. The block was rinsed off in PBST and incubated for 1 hour at room temperature with mouse monoclonal TG2 antibody (TG100, Neomarkers) at 1:200 dilution in blocking solution. Cells were then washed 3 x 5 mins with PBST and incubated with 50µl biotinylated anti-mouse IgG (ABC Vectastain kit) in 10mls of 0.1% BSA/PBS for 30 mins at room temperature. Following secondary antibody probing, cells were washed for 3 x 5 mins with PBST and incubated for 30 mins with ABC reagent at room temperature. Cells were washed for 3 x 5 mins and incubated with AEC substrate (Vector Labs) for 10 mins at room temperature followed by 2 washes with distilled water and counterstaining with haematoxylin solution (Gill's no 2, Fisher Scientific, Loughborough, UK) for 2 mins. Coverslips were mounted using glycerol (Dako) and staining visualised on an Olympus BH-2 microscope.

3.3.7.5 Extracellular TG activity of cultured cells

Extracellular TG activity was determined by modified cell ELISA as described previously by Verderio *et al.*, 1998. Cells were plated at a density of 8×10^4 cells/well in serum free medium onto a 96 well plate that had been coated overnight with 100µl/well of 5µg/ml fibronectin (Sigma) in 50mM Tris-HCl pH 7.4. Cells were allowed to attach for 2.5 hours at 37°C in the presence of 0.1mM biotin cadaverine [N-(5 amino pentyl biotinamide) trifluoroacetic acid] (Molecular Probes, Eugene, OR, USA). Plates were washed twice with 3mM EDTA/PBS and cells removed by incubating for 20 mins at 37°C with 0.1% (w/v) sodium deoxycholate in 5mM EDTA/PBS. The supernatant was collected and used for protein determination. The remaining deoxycholate insoluble material was washed 3 times with 50mM Tris-HCl. Incorporated biotin cadaverine was revealed with 1:5000 dilution of extravidin HRP conjugate (Sigma) for 1 hour at room temperature followed by 30 mins with TMB (3,3',5,5'-tetramethylbenzidine) substrate (Sigma). The reaction was stopped with 50µl 2.5M H₂SO₄ and the absorbance read at 450nm (Multiskan Ascent, Thermo Labsystems). The principle stages of the assay are represented in figure 3.3a

3.3.7.6 Extracellular TG2 antigen expression by cultured cells

Extracellular TG2 antigen was determined using a modified cell ELISA as described previously (Verderio *et al.*, 1998, Skill *et al.*, 2004). Cells were seeded at a density of 8×10^4 /well of a 96 well plate in serum free medium and allowed to attach for 3 hours. After 3 hours, the media was changed to complete media and extracellular TG2 detected by incubating cells with 100µl of 1:1000 dilution of anti-TG2 monoclonal antibody Cub 7402 (Strattech Scientific) overnight at 37°C. A parallel plate was used to correct for protein by the Lowry assay (section 3.3.9.2). Media was removed, cells washed gently once with PBS pH 7.4 and the PBS discarded. Cells were fixed with 4% (w/v) paraformaldehyde (Sigma) in PBS

Figure 3.3 Principle Steps of the Extracellular TG Activity and Extracellular TG2 Antigen Assays

a) Extracellular TG activity

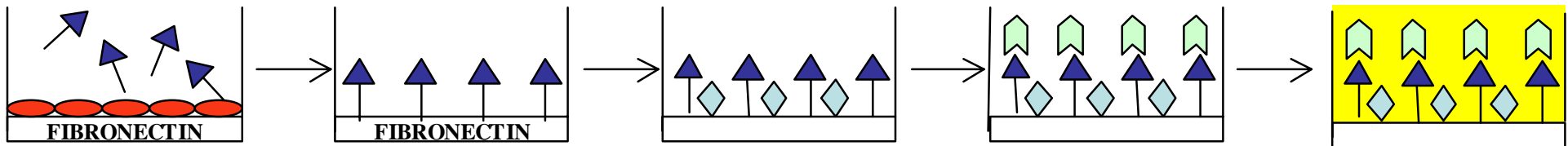
Step1: Incubate cells with biotin cadaverine, 2 hours @ 37°C

Step2: Remove cells (0.1% DC, 10mins @ 37°C)

Step3: Block non-specific sites (3% BSA/PBS, 30mins @ 37°C)

Step4: Incubate with extravidin-HRP (1:5000, 1 hour @ 37°C)

Step5: Add TMB substrate, 30 mins R°. Read 450nm



b) Extracellular TG2 Antigen

Step1: Incubate cells with anti-TG2 1° (Cub7402)

Step2: Fix cells (4% paraformaldehyde, 15 mins R°)

Step3: Block non-specific sites (5% milk/PBS, 30mins R°)

Step4: Incubate with anti-mouse HRP 2° (1:1000, 2 hours R°)

Step5: Add TMB substrate, 30 mins R°. Read 450nm

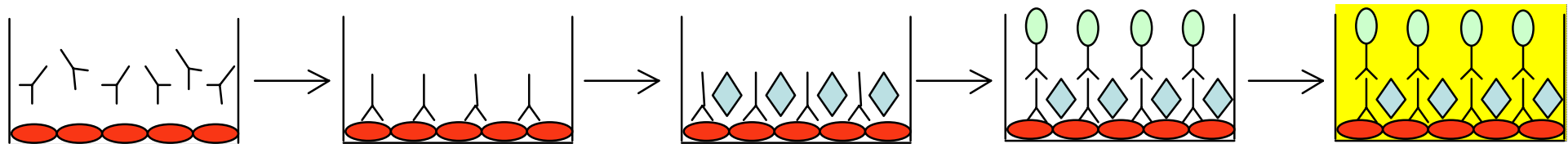


Figure 3.3 a) Extracellular TG activity was determined in cultured cells by the TG mediated incorporation of biotin cadaverine into fibronectin. b) Extracellular TG2 antigen levels were determined in cultured cells by incubation with the anti-TG2 antibody CUB7402 and antibody binding revealed with anti-mouse HRP. DC= sodium deoxycholate, R°= room temperature, 1° = primary antibody, 2°= secondary antibody.

for 15 mins at room temperature and washed 3 times with PBS prior to blocking with 5% non-fat dried milk in PBS for 30 mins at room temperature. Primary antibody binding was revealed with 100µl/well of 1:1000 dilution of goat anti-mouse HRP (Dako) in blocking solution for 2 hours at room temperature using a TMB substrate. The reaction was stopped with 50µl 2.5M H₂SO₄ and the absorbance read at 450nm. The principle stages of the assay are represented in figure 3.3b.

3.3.8 Detection of ε(γ-glutamyl) lysine crosslink

3.3.8.1 Immunofluorescence

Cells were plated at a density of 1x 10⁶ cells on 22mm² glass coverslips and cultured for 48 hours prior to staining for ε(γ-glutamyl) lysine crosslink. After 48 hours, the media was removed and cells gently washed with PBS for 5 mins. Cells were fixed in ice-cold methanol for 10 mins at room temperature. Coverslips were air dried for 10 mins at room temperature followed by re-hydration for 10 mins with PBS. After a further wash with PBS, coverslips were incubated in PBS at 42°C for 10 mins to open up the epitopes. Blocking was performed using 5% (w/v) BSA in PBS for 30 mins at room temperature. ε(γ-glutamyl) lysine was detected by incubating overnight with mouse monoclonal anti ε(γ-glutamyl) lysine antibody (Clone 153-81D4, Covalab, Lyon, France) at 1:50 dilution in blocking solution. Primary antibody binding was revealed by incubation with anti-mouse FITC (Dako) at 1:50 dilution in blocking solution for 30 mins at room temperature. Cells were washed and mounted with Vectashield fluorescent mount containing DAPI (Vector Labs). Fluorescence was visualised using an Olympus BX61 microscope at 494nm with excitation at 518nm.

3.3.8.2 Cation exchange chromatography

ε(γ-glutamyl) lysine crosslink levels were determined in tissue samples subjected to exhaustive proteolysis using a method originally described by Griffin and Wilson (Griffin and Wilson, 1984) and was performed by Dr Richard Jones at Nottingham Trent University.

Approximately 10mg of protein was precipitated from a 20% (w/v) tissue homogenate (section 3.3.1) by adding TCA to a final concentration of 10% (w/v). After rehydration in 0.1M ammonium carbonate, extracted proteins were subject to exhaustive proteolytic digestion with subtilisin (EC 3.4.21.61, Sigma), pronase (EC 3.4.24.31, Sigma), activated leucine amino peptidase (EC 3.4.11.2, Sigma), activated prolidase (EC 3.4.14.9, Sigma) and carboxypeptidase Y (EC 3.4.16.1, Sigma). Samples were then freeze dried and resuspended in 0.1 N HCl and stored at -20°C. The amount of ε(γ-glutamyl) lysine in the tissue digests was analysed by cation exchange chromatography using an LKB 4151 amino acid analyser

(Pharmacia, Cambridge, UK) by a modification of a lithium citrate buffer method (Griffin and Wilson, 1984). Separation of $\epsilon(\gamma\text{-glutamyl})$ lysine was achieved using Ultrapac 8 cation exchange resin ($8 \pm 0.5\mu\text{m}$ particle size) at a constant temperature of 25°C and a stepwise gradient of increasing molarity and pH of lithium citrate buffers. The detection of amino acids and peptides was undertaken by a post column reaction with 600mg/litre *o*-phthalaldehyde/5ml/litre 2-mercaptoethanol and the fluorescence was observed at 450nm after excitation at 360nm using an LS1 detector (Perkin Elmer). Quantitation was achieved by computer integration of the chromatograms obtained using a Nelson 9000 A-D integrator and software (Nelson Analytical, Cupertino, CA, USA). The amount of $\epsilon(\gamma\text{-glutamyl})$ lysine in each sample was quantified by standard addition of 1 nmol of $\epsilon(\gamma\text{-glutamyl})$ lysine di-peptide.

3.3.9 Quantitation of protein

3.3.9.1 Bicinchoninic acid assay

Total protein was determined in solubilised cells and ECM collected from ECM deposition studies using a modification of the bicinchoninic acid assay (Gates, 1991).

Cells were solubilised for 10 mins with 2 mls of 0.25M (v/v) ammonium hydroxide in 50mM Tris pH 7.4. This was collected and the protein allowed to precipitate at -20°C . Samples were thawed and centrifuged at $10,000 \times g$ (Jouan MR22i, 24 x 1.5ml rotor) for 15 mins to produce a protein pellet. The supernatant was discarded and the protein pellet resuspended in 100 μl per sample of 0.1M NaOH/2% (w/v) SDS. To facilitate solubilisation of the protein, samples were boiled for 5 mins and pipetted gently to resuspend. A standard curve was prepared of 0, 0.4, 0.8, 1.2, 1.6, 2.0 mg/ml BSA in distilled water. A volume of 1ml of BCA working solution [(25 parts solution A (1% bicinchoninic acid, 2% sodium carbonate, 0.16% sodium tartrate, 0.4% sodium hydroxide, 0.95% sodium hydrogen carbonate): 1 part solution B (4% copper sulphate)] was added to samples and standards and all tubes vortexed prior to incubation at 37°C for 30 mins. 200 μl of standards and samples were pipetted in duplicate into a 96 well plate and the optical density read at 600nm (Multiskan Ascent, Labsystems). Protein concentrations were calculated using Genesis version 3 software (Labsystems).

3.3.9.2 Lowry assay

Total protein was determined in cell lysates and rat urine using a modification of the Lowry method (Lowry *et al.*, 1951). A standard curve of 0, 0.4, 0.8, 1.2, 1.6 and 2.0mg/ml BSA in PBS was used. Samples were diluted 1:10 with PBS. 100 μl of 2% (w/v) SDS in distilled water was added to samples and standards. Tubes were vortexed prior to the addition

of 1ml of Folin's reagent [49 parts solution A (0.4% sodium hydroxide, 2% sodium carbonate, 0.02% sodium tartrate): 1part solution B (0.5% copper sulphate)]. Tubes were vortexed again and incubated at room temperature for 20 mins. 100µl of Folin and Ciocalteu reagent (Sigma) that had previously been diluted 1:1 with distilled water was added to each tube. Samples were vortexed and incubated at room temperature for 20 mins. 200µl of each sample was transferred to a 96 well plate and the optical density read at 750nm (Multiskan Ascent, Labsystems). Protein concentrations were calculated using Genesis version 3 software (Labsystems).

3.4 Molecular Biology Techniques

3.4.1 Expression vectors/ TG2 cDNA

The pCIneo vector (figure 3.4a) was obtained from Promega, UK. The pSG5 expression vector (figure 3.4b) and the pSVneo resistance vectors were obtained from Stratagene, La Jolla, CA, USA. The 3.3kb TG2 cDNA corresponding to the 2.1kb coding region of human TG2 (Gentile *et al.*, 1991) plus 1.2kb of upstream non coding sequence was ligated into these vectors to produce the 8.7kb pCIneo-htg and the 7.4kb pSG5-htg expression vectors. TG2 cDNA and the pSG5-htg expression vector were a kind gift from Dr Peter Davies (University of Texas, Houston, TX, USA).

3.4.2 Preparation of expression vector pCIneo-htg

3.4.2.1 Linearisation of pCIneo plasmid

A restriction enzyme digest was prepared containing 30µg of pCIneo plasmid, 36U *EcoRI* (12U/µl, Oncor Appligene, Durham, UK), 5µl Buffer III (10x stock, Oncor Appligene) and 7µl ultra-pure water. This was incubated at 37°C for 2 hours and the digestion stopped by heating for 15 mins at 65°C. Successful digestion was determined by running 1µg of digested plasmid on a 1% (w/v) agarose gel as described in section 3.4.7.

3.4.2.2 Ligation of pCIneo and 3.3kb transglutaminase cDNA

A ligation reaction was set up containing 200ng of pCIneo vector (8µl), 375ng (1µl) of the 3.3 kb TG2 cDNA, 2.1 units (0.7µl) of T₄ DNA ligase (Promega) and 2µl of 10x ligase buffer (Promega) and 1µl of calf intestine alkaline phosphatase (CIAP, dephosphorylates 5' ends). This was made up to a final volume of 20µl with nuclease-free water and kept at 4°C overnight to allow ligation to occur.

3.4.3 Bacterial transformation

The DH5α *Escherichia Coli* (*E.Coli*) bacterial strain was used for transformation and

competent bacteria prepared using a procedure based on the Hanrahan method (Hanrahan, 1983).

15ng (0.5µl) of ligated pCIneo-htg plasmid was added to competent bacteria and placed on ice for 30 mins. The bacteria were heat shocked at 42°C for 90 seconds and immediately transferred to ice for 2 mins. 800µl of SOC medium (2% (w/v) Peptone 140, 0.5% (w/v) yeast extract, 10mM NaCl, 2.5mM KCl, 40mM D-glucose, 20mM Mg²⁺) was added at room temperature and the culture incubated at 37°C for 1 hour with shaking at 200rpm. 1µl, 10µl and 100µl aliquots of transformed bacteria were plated onto LB agar containing 50µg/ml of ampicillin as a selection agent. Plates were incubated overnight at 37°C to allow the formation of discrete colonies. A single colony of transformed bacteria was used to inoculate 5mls of LB medium [1% (w/v) Bacto-tryptone, 0.5% (w/v) yeast extract, 1% NaCl, 0.5% (v/v) NaOH] containing 50µg/ml of ampicillin. The culture was incubated at 37°C overnight with shaking at 250rpm. 850µl of this culture was added to 150µl of sterile glycerol, mixed by vortexing and stored at -80°C. The remainder of the culture was used to prepare a small scale plasmid preparation to verify successful transformation.

3.4.4 Small scale plasmid preparation

Small scale plasmid preparation was performed using the Wizard™ Miniprep DNA purification system (Promega) as per the manufacturer's instructions.

3.4.5 Large scale plasmid preparation

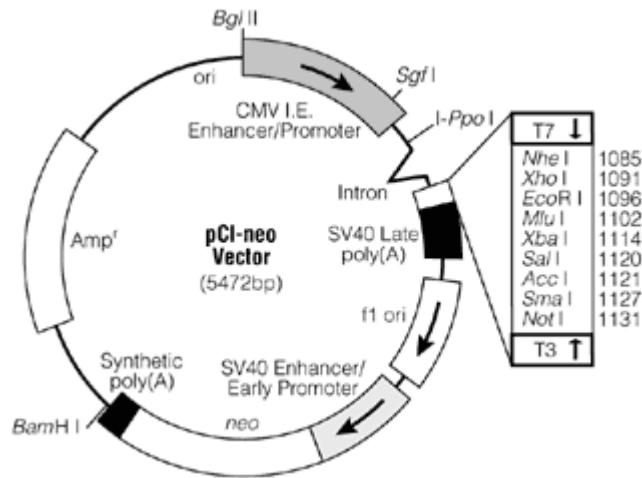
Large scale purification of pCIneo and pCIneo-htg plasmid DNA was performed using the Wizard™ Maxiprep DNA Purification System (Promega) as per the manufacturer's instructions.

3.4.6 Ethanol precipitation of the plasmid

0.1 volumes of 4M sodium acetate was added to the vector along with an equal volume of 100% ice cold ethanol. This was placed at -20°C overnight then centrifuged at 12,000 x g for 15 mins (Jouan MR22i, 24 x 1.5ml rotor). The subsequent pellet was re-suspended in 1ml of endonuclease free 70% ethanol and vortexed. This was centrifuged at 8,000 x g for 5mins (Jouan MR22i). The supernatant was removed and the sample centrifuged again at 8,000 x g for 1 min. The remainder of the supernatant was removed and the DNA pellet re-suspended in sterile water. The DNA concentration was determined by 260nm/280nm ratio.

Figure 3.4 Expression Vector Plasmid Maps

a) pCIneo



b) pSG5

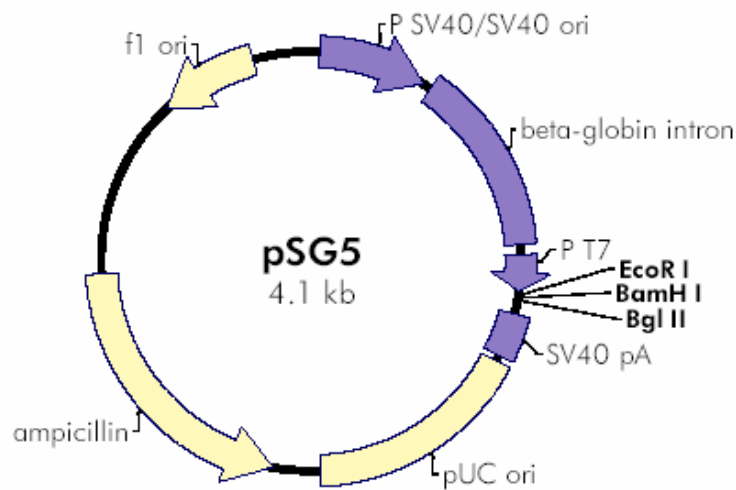


Figure 3.4 (a) The pCIneo expression vector carries the human cytomegalovirus (hCMV) promoter/enhancer to promote constitutive expression of cDNA inserts and the neomycin phosphotransferase gene as a selectable marker. (b) The pSG5 expression vector carries the T7 bacteriophage promoter which facilitates the *in vitro* expression of cloned cDNA but lacks the neomycin gene and requires transfection with the resistance vector pSVneo for selection. pCIneo-htg and pSG5-htg were constructed by inserting the full length human TG2 cDNA into the *EcoR*I site within the multiple cloning region in a sense orientation.

3.4.7 Agarose gel electrophoresis

All DNA was separated on a 1% (w/v) agarose gel prepared in 1x TAE buffer (diluted from a 50x stock containing 2M Tris, 5% (v/v) glacial acetic acid, 0.05M EDTA, pH8.0) Ethidium bromide was added to a final concentration of 0.5µg/ml prior to pouring. 1µg of DNA was mixed with 6x DNA loading dye [10% (w/v) ficoll 400, 0.25% (w/v) bromophenol blue, 0.25% (v/v) xylene cyanol FF, 0.4% orange G, 10mM Tris-HCl pH 7.5 , 50 mM EDTA (Promega)] and the mixture loaded onto the gel. 7.5µl of 1kb DNA marker (Promega) was loaded and the gel electrophoresed at 100V until the bromophenol blue front had run $\frac{3}{4}$ of the length of the gel. The DNA was visualised on a transilluminator.

3.4.8 Northern blotting

3.4.8.1 cDNA probes

The preparation of cDNA probes for use in the Northern blot analysis was performed previously as described in (Douthwaite *et al.*, 1999). Specific random primed DNA probes were labelled from the following DNA sequences: mouse tissue transglutaminase (Johnson *et al.*, 1997), rat collagen (α 1) I (Vuorio *et al.*, 1987), rat collagen (α 1) III (Virolainen *et al.*, 1995), human collagen (α 1) IV (Kurkinen *et al.*, 1987), rat fibronectin (Schwarzbauer *et al.*, 1983), rat interstitial collagenase (MMP-1) (Quinn *et al.*, 1990), rat gelatinase A (MMP-2) (Marti *et al.*, 1993), rat gelatinase B (MMP-9) (Quinn *et al.*, 1990), rat TIMP-1 (Iredale *et al.*, 1996), rat TIMP-2 (Cook *et al.*, 1994) and human TIMP-3 (Uria *et al.*, 1994).

3.4.8.2 RNA extraction

Total RNA was extracted using Trizol™ (Life Technologies). For tissue samples, 100-200mg of tissue was homogenised on ice in 2ml of Trizol™ reagent until completely homogenised. For cell samples, a confluent T75 flask of cells that had previously been washed twice with 1 x PBS was immersed in 2 mls of Trizol™ reagent and the cells lysed by passing through a small guage needle. Typically, 2 T75 flasks were pooled to gain enough RNA for analysis. RNA was phase separated by the addition of 400µl of chloroform (200µl/ml of Trizol™), the tubes capped and shaken vigorously by hand for 15 secs. Samples were incubated at room temperature for 2-3 mins and centrifuged at 12,000 x g (Jouan MR22i, 10 x 10ml rotor) for 15 mins at 4°C. The upper aqueous layer containing RNA was removed and transferred to a fresh tube. To this was added 1ml of isopropanol (0.5ml/ml of Trizol™) and samples incubated at 4°C for at least 30 mins or stored overnight at -20°C. Samples were then centrifuged at 12, 000 x g (Jouan MR22i, 10 x 10ml rotor) for 10 mins at 4°C. The supernatant was discarded and the RNA pellet washed with 2mls of 70% ethanol with vortexing to loosen the pellet. Samples were centrifuged at 7,500 x g (Jouan

MR22i, 10 x 10ml rotor) for 5 mins at 4°C and the wash procedure repeated. The supernatant was removed and the pellet air dried. RNA pellets were resuspended in a small volume of DEPC (diethylpyrocarbonate)-treated water and incubated for 10 mins at 65°C to ensure that the pellet was completely dissolved. Concentration and purity of the RNA was assessed by scanning spectrophotometer at 260nm and 280nm.

3.4.8.3 Electrophoresis of RNA/capillary blotting

Twenty micrograms of total RNA was separated on a 1.2% (w/v) agarose/ 4-morpholinepropanesulphonic acid (MOPS)/ 2% (v/v) formaldehyde gel. The desired amount of RNA was transferred to a fresh tube to which was added an equal volume of sample buffer (ethidium bromide, deionised formamide, 10 x MOPS, 37% formaldehyde, DEPC H₂O, 30% Ficoll, 10mM EDTA and 0.05% (w/v) bromophenol blue). Samples were incubated at 65°C for 15 mins to abolish secondary structure prior to loading. Gels were electrophoresed at 100V until the bromophenol blue dye front had travelled $\frac{3}{4}$ the length of the gel. The loading and integrity of the RNA was verified by viewing the gel under ultraviolet light on a transilluminator.

RNA was transferred to Hybond N nylon membrane (Amersham) by capillary blotting with 20 x SSC (3.0M NaCl, 0.3M sodium citrate pH 7.0). A wick was prepared using filter paper that was soaked in SSC and extended into a tray containing 1 litre of SSC. Onto this was placed the inverted gel that had previously been rinsed in 20 x SSC. A pipette was used to roll out any air bubbles and a piece of pre-soaked Hybond N placed over the gel. This was covered with 2 pieces of pre-soaked Whatmann 3MM filter paper, a 10-15cm stack of absorbant paper towels and finally weighted with approximately 1kg. Transfer was allowed to occur overnight. After overnight transfer, the blot was dismantled, the nylon membrane dried between 3MM filter papers at 80°C for 10 mins and the RNA fixed by UV irradiation (70mJ/cm²) using a UV crosslinker (Amersham).

3.4.8.4 Hybridisation of membranes

Purified cDNA probes (section 3.4.8.1) were random primed with ³²P-labelled dCTP (3000 Ci/mmole, Amersham) using the Prime-a-Gene system (Promega). A mixture was set up containing 12.5ng of cDNA template, 5µl labelling buffer, 1µl each of dATP, dGTP and dTTP and the mixture made up to 15µl with DEPC H₂O. The mixture was heated at 100°C for 3 mins and placed on ice to denature the DNA. To this was added 1µl BSA, 1µl Klenow fragment and 25µCi [α -³²P] dCTP and the reaction allowed to proceed at room temperature for 3 hours. Unincorporated nucleotides were removed by passing the probe through a Sephadex G50 Nick column™ (Pharmacia, Uppsala, Sweden).

Membranes were pre-hybridised by incubating for 5 mins at 68°C with 6 x SSC followed by 30 mins at the same temperature with pre-hybridisation buffer (Amersham). After 30 mins the probe was added and hybridisation allowed to proceed for either 1 hour or overnight at 68°C. Membranes were then washed with 2 x SSPE [3.6M NaCl, 0.2M NaH₂PO₄, 0.02M EDTA, pH7.4 /0.5% SDS] (room temperature, 4 washes) followed by 0.2 x SSPE/0.5% SDS (50°C, 2 washes). Membranes were dried between 3MM filter paper and exposed to Kodak Biomax MS film for up to 7 days with intensifying screens. Developed films were analysed by volume densitometry using the Biorad GS-690 scanning densitometer and Multi-Analyst Version 3.2. Loading was corrected by reference to the housekeeping gene cyclophilin.

In the case of re-probing, the membranes were stripped with boiling 0.1% SDS in DEPC H₂O, with shaking until the SDS had cooled, dried and stored between clean 3MM filter papers.

3.5 ECM Quantitation

3.5.1 Quantitation of total ECM protein

3.5.1.1 ³H-Amino acid incorporation

Cells were seeded in 100mm² Petri dishes at a density of 3.75x10⁶ per dish or in 6 well plates at a density of 1 x 10⁶ per well. Deposited ECM was labelled by the addition of 20μCi of ³H amino acid mixture (Amersham) at the time of plating prior to the recovery and analysis of ECM as described in section 3.5.2.1.

3.5.2 Collagen determination

3.5.2.1 ³H-Proline incorporation

Cells were seeded at a density of 3.75x10⁶/100mm² petri dish or 1x 10⁶/well of a 6 well plate. Deposited collagens were labelled by the addition of 10μCi (6 well plate) or 20μCi (10cm² dish) of ^{3,4}H proline (1.0mCi /ml, ICN Biomedicals, Morgan Irvine, CA, USA) at the time of plating. After 72 hours the media was removed and cells washed once for 5 mins with 1x PBS. Cells were then removed with 0.25M ammonium hydroxide in 50mM Tris pH 7.4 at 37°C for 10 mins. The soluble fraction was collected and protein concentration determined using the bicinchoninic acid assay as described in section 3.3.9.1. The dishes were washed extensively with increasing volumes of PBS before the ECM was solubilised with 2.5% (w/v) SDS in 50mM Tris pH6.8 for 1 hour at 37°C. The dish was scraped to ensure complete removal of the ECM and 200μl measured for radioactivity in a Rack-beta liquid scintillation counter (Packard Instruments). The principle of this assay is outlined in figure 3.5.

Figure 3.5 Principle of ECM Quantification by ^3H labelling

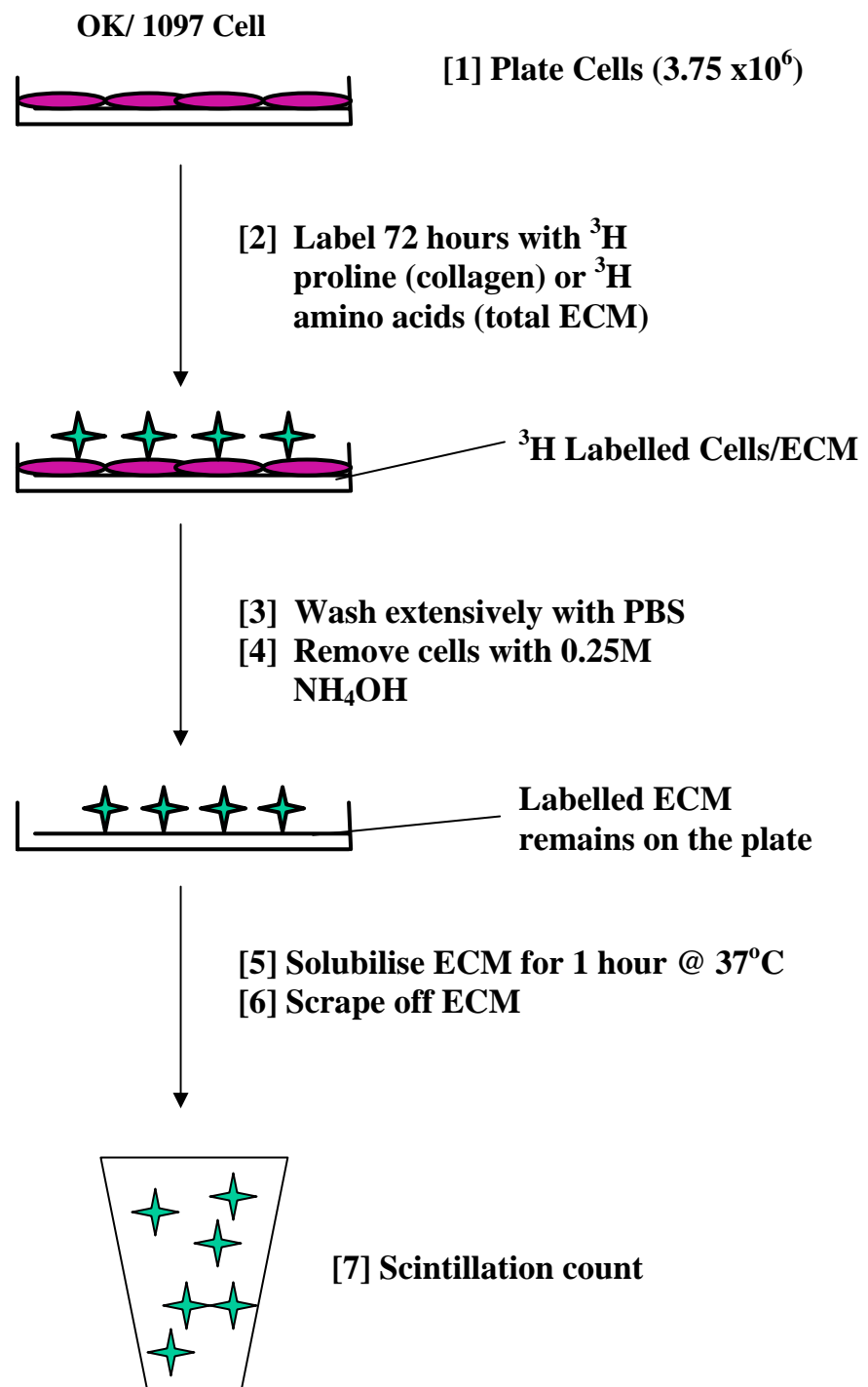


Figure 3.5 Total ECM and total collagen levels were determined in cell derived ECM *in vitro* by labelling with $20\mu\text{Ci}$ of ^3H -amino acid mixture (total ECM) or $20\mu\text{Ci}$ of ^3H -proline (total collagen). Cells were solubilised with 0.25M ammonium hydroxide (NH_4OH) and the remaining ECM recovered. Incorporation of label into the ECM was measured by scintillation counting.

3.5.2.2 Hydroxyproline analysis by gas liquid chromatography

3.5.2.2.1 Deoxycholate- insoluble ECM

Cells were seeded at 3.75×10^6 in 100mm^2 petri dishes for 72 hours prior to the removal of cells with 0.1% (w/v) deoxycholate-2mM EDTA for 10 mins at 37°C . The remaining deoxycholate-insoluble ECM proteins were partially digested with 0.2mg/ml trypsin/1mM EDTA, scraped off and freeze dried. The deoxycholate-insoluble ECM was acid hydrolysed in 6N HCl overnight at 110°C in an oxygen-free environment. After freeze drying and re-suspending in H_2O , the hydrolysates were assayed for hydroxyproline by Gas Chromatography using a 9890N Network GC system (Agilent Technologies, Queensferry, West Lothian, UK), by Dr Richard Jones at Nottingham Trent University. Hydroxyproline content was measured against internal amino acid standards.

3.5.2.2.2 Tissue homogenates

10% kidney homogenates (section 3.3.1) were hydrolysed overnight in 6M HCl at 110°C in an oxygen free environment and amino acids recovered using the EZ:Fast amino acid analysis kit (Phenomenex, Torrance, CA, USA) according to the manufacturer's instructions. The amino acid and hydroxyproline content was measured against internal amino acid standards by Gas Chromatography using a 9890N Network GC system (Agilent Technologies) which was performed by Dr Richard Jones at Nottingham Trent University.

3.5.2.3 Collagen immunofluorescence in vitro

Cells were plated at a density of 0.5×10^6 cells on 22mm^2 glass coverslips and cultured for 72 hours prior to collagen staining. After 72 hours, the media was removed and cells gently washed with PBS for 5 mins. Cells were fixed in methanol for 10 mins at room temperature. Coverslips were air dried for 10 mins at room temperature followed by re-hydration for 10 mins with PBS. Blocking was performed using 5% (w/v) BSA in PBS for 30 mins at room temperature. Collagens were detected by incubating overnight with either mouse monoclonal anti-Collagen I at 1:50 dilution (Abcam, Cambridge, UK), goat anti-collagen III polyclonal (Southern Biotech, Birmingham, AL, USA) at 1:10 dilution or rabbit anti-Collagen IV polyclonal (ICN, Irvine, CA, USA) at 1:35 dilution in blocking solution (table 3.5). Primary antibody binding to tubular collagens was revealed by incubation with FITC conjugated anti-mouse IgG (Dako) at 1:50 dilution (Collagen I), FITC conjugated anti-goat IgG (Dako) at 1:50 dilution (Collagen III) or TRITC conjugated anti-rabbit IgG (Dako) at 1:40 dilution (Collagen IV) in blocking solution for 30 mins at room temperature. Primary antibody binding to mesangial collagens was revealed by incubation the same secondary antibodies except for collagen IV which was detected with Cy5 conjugated anti-rabbit IgG.

Cells were washed and mounted with Vectashield fluorescent mount containing DAPI (tubular epithelial cells) (Vector Labs) or propidium iodide (mesangial cells). Tubular cell fluorescence was visualised using an Olympus BX61 microscope at 527nm with excitation at 541nm (TRITC) and 494nm with excitation at 518nm (FITC). Mesangial cell fluorescence was visualised using confocal microscopy (Leica CLSM confocal laser microscope) using an argon/krypton laser adjusted to 647nm and 488nm for both Cy5 and FITC emissions. Collagen immunofluorescence was quantified by multiphase image analysis as described in detail in section 3.5.2.6

3.5.2.4 Immunohistochemical analysis of ECM in paraffin sections

Immunohistochemistry for Collagen III, IV and fibronectin was performed on paraffin embedded sections prepared by the Histology Department, Northern General Hospital, Sheffield, UK.

Paraffin sections were de-waxed by incubating in xylene for 10 mins followed by graded alcohols (100% for 5 mins, 90% for 5 mins, 75% for 5 mins and 50% for 5 mins) then washed for 5 mins in distilled water. After washing for a further 10 mins with PBS, endogenous peroxidase was quenched with 3% H₂O₂ in methanol for 10 mins. Sections were washed again for 10 mins with PBS followed by treatment with basic tissue unmasking fluid (TUF, Zymed Labs, San Francisco, CA, USA) at 92°C for 10 mins and were allowed to cool to room temperature. Sections were washed with PBS twice for 5 mins and subjected to trypsin digest (Zymed “Digest all 2” solution) for 15 mins at 37°C. Sections were washed twice with PBS and blocked for 30 mins in blocking solution containing 5% serum in 0.1% BSA/PBS. After blocking, sections were incubated with primary antibody overnight at 4°C in 1% BSA/PBS according to dilutions set out in table 3.5. Sections were then incubated twice for 5 mins in 0.1% IGEPAL/PBS followed by 2 x 5 min washes with PBS. Primary antibody binding was revealed by incubation with secondary antibody (table 3.5) in 0.1% BSA/PBS for 30 mins at 37°C. Sections were then washed with 0.1% IGEPAL/PBS twice for 5 mins followed by 2 x 5 min washes with PBS. Where biotinylated secondary antibody was used, sections were incubated with 1:1000 dilution of extravidin-HRP conjugate for 1 hour followed by washing in 0.1% IGEPAL/PBS. Secondary antibody binding was revealed by incubation for 10 mins at room temperature with AEC substrate (Vector Labs). Sections were then washed twice for 5 mins with distilled water followed by 2 washes with PBS and counterstaining with haematoxylin (Fisher Scientific) for 5 mins. Sections were washed with distilled water and mounted using glycerol (Dako). Collagen immunofluorescence was quantified by multiphase image analysis as described in detail in section 3.5.2.6

3.5.2.5 Immunohistochemical analysis of collagen I on cryostat sections

Cryostat sections from snap-frozen tissue were prepared as described in section 3.3.5. Sections were incubated for 10 mins in blocking buffer of 1 x PBS/0.1% Tween 20 containing 3% BSA, 5% rabbit serum, 10mM EDTA, 1mM leupeptin, 1mM benzamidine and 1mM PMSF. After 10 mins, the blocking solution was replaced and this step repeated twice. The sections were then blocked for a further hour at room temperature with fresh blocking solution. Collagen I was detected by incubation with 1:50 goat polyclonal Collagen I antibody (table 3.5) in blocking solution overnight at 4°C. The sections were then washed gently in washing solution [1 x PBS/0.1% Tween 20 containing 3% BSA 10mM EDTA, 1mM leupeptin, 1mM benzamidine and 1mM PMSF] for 3 x 5 mins. Primary antibody binding was revealed by incubation with 1:100 rabbit anti-goat HRP secondary antibody diluted in washing solution for 1 hour at room temperature. Sections were then washed for 3 x 5 mins in washing solution prior to incubation with AEC substrate for 15 mins at room temperature. Sections were then washed for 3 x 5 mins with 1 x PBS and counterstained with haematoxylin for 5 mins. Sections were fixed with 4% paraformaldehyde/PBS for 10 mins, washed once with PBS and mounted with glycergel. Collagen immunofluorescence was quantified by multiphase image analysis as described in detail in section 3.5.2.6

Table 3.5 Antibodies Used in Immunohistochemical Analysis of ECM

Antibody Used	Serum in blocking step	Primary Antibody	Secondary Antibody
Collagen I (Santa Cruz SC8784)	Rabbit	1:50 Col I goat pAb	1:100 rabbit anti-goat HRP
Collagen III (Southern Biotech 1330-01)	Rabbit	1:10 Coll III goat pAb	1:400 anti-goat biotinylated
Collagen IV (ICN 10760)	Goat	1:35 Col IV rabbit pAb	1:500 goat anti-rabbit biotinylated
Fibronectin (Sigma F6140)	Goat	1:50 fibronectin mouse mAb	1:100 goat anti-mouse HRP

Table 3.5 Collagen I immunohistochemistry was performed on cryostat sections (3.5.2.5). All other immunohistochemistry was performed on paraffin sections (3.5.2.4). mAb=monoclonal antibody, pAb=polyclonal antibody, HRP=Horse Radish Peroxidase.

3.5.2.6 Multi-phase image analysis of ECM

Multi-phase image analysis utilises a pseudo-colour overlay system in which areas of a slide can be differentiated by the assignment of representative colours or phases. The area covered by each phase as defined by upper and lower wavelength thresholds and intensity settings can then be quantified by image analysis software to give a percentage area value. A typical example of phase selection is shown in figure 3.6.

Multi-phase analysis was performed on cells cultured on 22mm² coverslips and immunoprobed for ECM collagen (section 3.5.2.3), paraffin sections stained for components of the ECM (3.5.2.4) cryostat sections stained for collagen I (3.5.2.5) and for the assessment of renal scarring by Masson's Trichrome staining (section 3.6.7).

3.5.2.6.1 Selection of fields

To quantify the degree of collagen and ECM staining, ten random non-overlapping fields at 400x magnification were acquired from each coverslip or section using a CC-12 digital camera controlled by Analysis 3.2TM software (Soft Imaging Systems, Muenster, Germany) on an Olympus BX 61 microscope. For determination of tubulointerstitial scarring, ten non-overlapping cortical fields were acquired at 100x magnification to ensure complete coverage of the cortex and 10 glomeruli at 400x magnification.

3.5.2.6.2 Phase selection

For each field, the degree of positive staining was assessed by carrying out multi-phase analysis with 3 phases [phase 1 (positive stain), phase 2 (nuclei and/or cytoplasm) and phase 3 (no stain)] using Analysis 3.2TM software (Soft Imaging Systems) ensuring that total phase coverage was in excess of 95% of the slide or section. Overlay colours were chosen for each representative phase that were deliberately in contrast to that of the original staining to aid the setting of phase thresholds. For *in vitro* analysis of the ECM, phases were represented by: yellow (collagen/ECM), pink (DAPI stained nuclei) and blue (no stain or background). For the *in vivo* analysis of ECM and the assessment of scarring, phases were represented by: green (ECM or scar tissue), yellow (cell cytoplasm/nuclei combined) and blue (tubular lumen/vacuolation).

3.5.2.6.3 Quantitation of staining

For the *in vitro* analysis of the ECM, the degree of positive staining was determined by dividing the % area of phase 1 [yellow (collagen/ECM)] by the % area of phase 2 [pink (DAPI stained nuclei) to correct for differences in cell number. Similarly, *in vivo* analysis of ECM staining and tubulointerstitial scarring was determined by dividing the areas represented

Figure 3.6 Phase Selection for Multi-phase Image Analysis

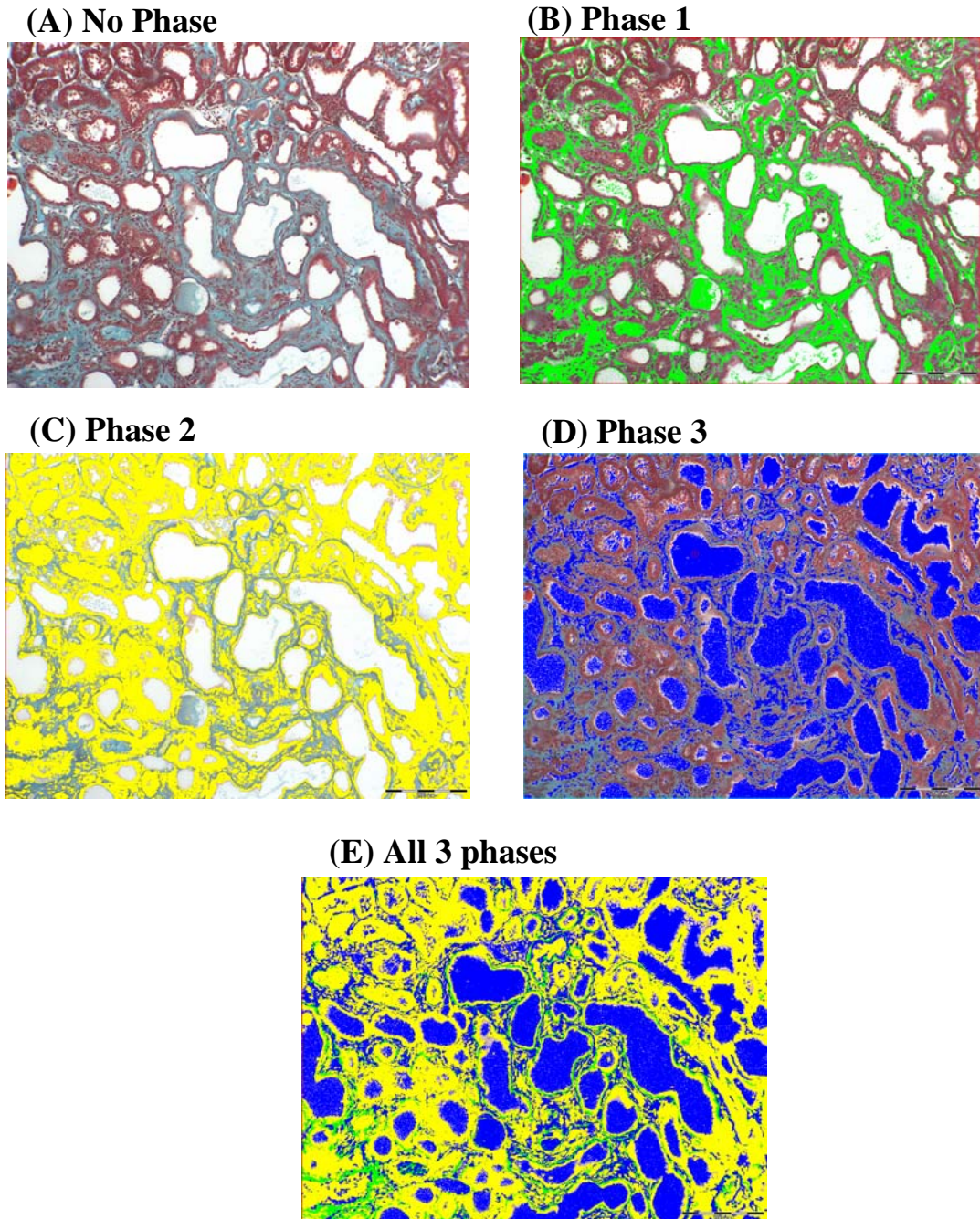


Figure 3.6 Example of the various phases used in the analysis of Masson's Trichrome and ECM stained paraffin sections. (A) Normal Masson's Trichrome stain. (B) Phase 1 (green) representing areas of fibrosis. (C) Phase 2 (yellow) representing cell cytoplasm/ nuclei. (D) Phase 3 (blue) representing tubular lumen and vacuolation. (E) Combination of all 3 phases with total phase coverage in excess of 95% of the section.

by green (ECM or scar tissue) by those represented by yellow (cell cytoplasm/nuclei combined) to correct for cell number and tubular dilatation. Glomerulosclerosis was calculated by dividing the areas represented by green (ECM or scar tissue) by the blue area (no stain) to take account of changes in Bowmans space, hypercellularity and inter-capillary area.

3.5.3 Measurement of ECM deposition rate

3.5.3.1 ECM labelling in the presence of the MMP inhibitor Galardin

Cells were plated in 6 well plates at a density of 1×10^6 cells/well and labelled for 72 hours by the addition of $10 \mu\text{Ci}$ /well of $^3,^4 \text{H}$ proline ($1.0 \text{mCi} / \text{ml}$, ICN) to complete media at the time of plating. Duplicate wells were incubated with $10 \mu\text{M}$ of the MMP inhibitor Galardin [GM6001, Calbiochem, Nottingham, UK ($1 \text{mg} / \text{ml}$ stock diluted in DMSO)]. After 72 hours, the label was removed by extensive washing with PBS. Cells were removed with 0.25M ammonium hydroxide and the ECM solubilised with 2.5% SDS/ 50mM Tris pH 6.8. Incorporation of ^3H proline label into the ECM was determined by scintillation counting.

3.5.4 ECM degradation

3.5.4.1 Activation of matrix metalloproteinase (MMP) enzymes

Pro-matrix metalloproteinase 1 (human MMP-1, Biogenesis, Poole UK) and pro-matrix metalloproteinase 2 (human MMP-2, Biogenesis) were activated in $1 \times$ activation buffer containing 5mM Tris, 20mM NaCl, 1mM CaCl_2 , 0.005% Brij, $0.1 \mu\text{M}$ ZnCl_2 pH 7.6 with 2mM amino phenylmercuric acetate (APMA, Sigma) for 2 hours at 37°C prior to use in matrix degradation assays (section 3.5.4.2) and gelatin zymography (section 3.5.4.3).

3.5.4.2 ECM degradation assays

Cells were plated in 6 well plates at a density of 1×10^6 cells/well and labelled by the addition of $10 \mu\text{Ci}$ of $^3,^4 \text{H}$ -proline ($1.0 \text{mCi} / \text{ml}$, ICN) to complete media at the time of plating. After 72 hours the media was removed and cells washed with PBS. Cells were then removed with 2mls of 0.25M ammonium hydroxide in 50mM Tris pH 7.4 at 37°C for 10 mins. The soluble fraction was collected and protein concentration determined using the bicinchoninic acid assay (section 3.3.9.1). The dishes were washed extensively with increasing volumes of PBS and the remaining ECM degraded by the addition of $1 \text{ml} / \text{well}$ of; $20 \mu\text{g} / \text{ml}$ trypsin (Life Technologies) in PBS, $0.01 \text{U} / \text{ml}$ Collagenase (from *Clostridium histolyticum*, Sigma) in reaction buffer (0.5M Tris-HCl, 1.5M NaCl, 50mM CaCl_2 pH 7.6) or $1 \mu\text{g} / \text{ml}$ MMP-1+ $1 \mu\text{g} / \text{ml}$ MMP-2 (Biogenesis) in reaction buffer. MMPs were activated as described in section 3.5.4.1. Fifty microlitre samples of the supernatant were removed at designated time points

Figure 3.7 Principle of the ECM Degradation Assay

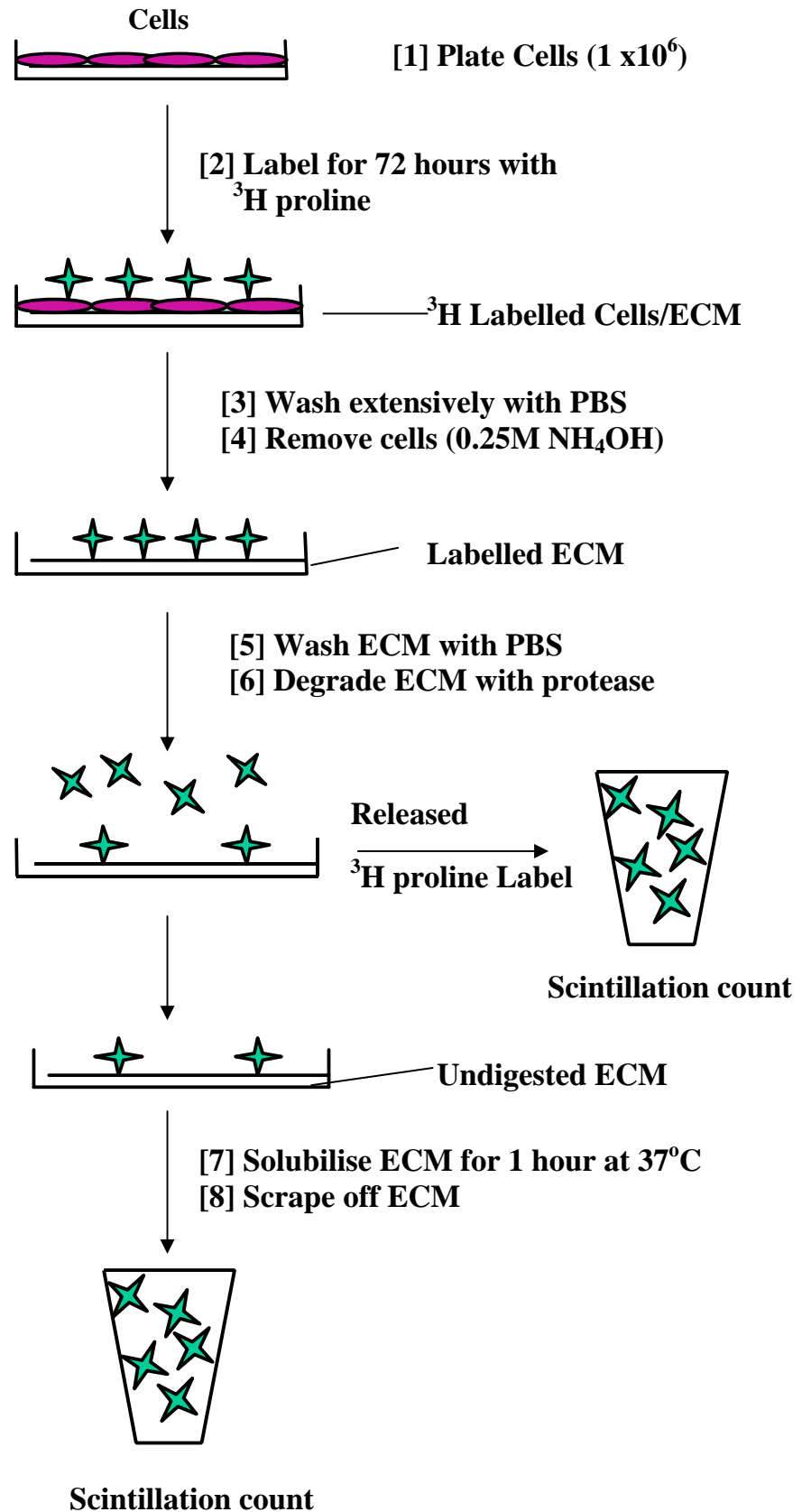


Figure 3.7 The degradation rate of cell-derived ECM was determined by labelling for 72 hours with $10\mu\text{Ci } ^3\text{H}$ -proline, cells solubilised with 0.25M ammonium hydroxide (NH_4OH) and the remaining ECM digested with a range of proteolytic enzymes. The degradation of matrix was calculated as a % of total labelled ECM.

and radioactivity determined by scintillation counting. At the end of the time course the remaining deposited ECM was solubilised as described in section 3.5.2.1. Values were corrected to express the data as % degradation of the total ³H-proline labelled ECM. The principle of the ECM degradation assay is outlined in figure 3.7.

3.5.4.3 Gelatin zymography

The successful activation of commercially obtained pro-MMP enzymes and measurement of OK cell MMP activity was determined by gelatin zymography. Pro-MMP-1 and MMP-2 enzymes (Biogenesis) were activated with APMA as described in section 3.5.4.1 and electrophoresed on a 10% polyacrylamide non-denaturing gel containing 1mg/ml of gelatin. After electrophoresis, gels were placed in 1x activation buffer (5mM Tris, 20mM NaCl, 1mM CaCl₂, 0.005% Brij, 0.1µM ZnCl₂ pH 7.6) for 15 mins at 37°C. The activation buffer was replaced and the gel activated overnight at 37°C. The gel was then stained for 1 hour at 37°C with Coomassie Brilliant Blue dye followed by de-staining in 10% methanol/10% acetic acid for 30 mins at 37°C. The presence of white bands was indicative of enzyme activity. Size of MMP bands was confirmed by reference to kaleidoscope pre-stained standards (Biorad).

3.5.4.4 Fluorescent gelatinase assay

Proteolytic enzyme activity in OK cell media was determined using the EnzChek® Gelatinase/Collagenase assay kit (Molecular Probes, Leiden, The Netherlands) A 1mg/ml solution of fluorescein-labelled DQ gelatin (in distilled water) was diluted 4 fold in 1x reaction buffer (0.05M Tris-HCl, 0.15M NaCl, 5mM CaCl₂, 0.2mM sodium azide pH 7.6) to give a 25µg/ml solution. 20µl of this solution was diluted with 80µl of reaction buffer in a well of a 96 well plate. To test the proteolytic activity of OK cell media, 20µl of media was made up to 100µl with reaction buffer and added to each well. Samples were incubated at 25°C, protected from light and the fluorescent intensity measured at 585nm at 1 hour intervals on a Fluoroskan II microplate reader (Thermo Labsystems).

3.6 In vivo Experimentation

3.6.1 Transglutaminase inhibitors

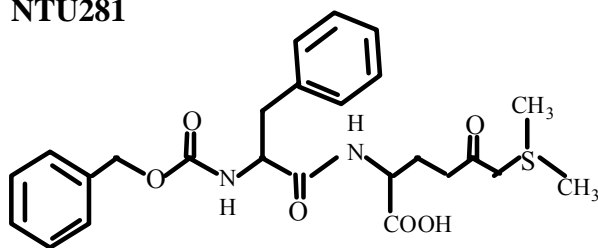
NTU283 (1,dimethyl-2[(oxopropyl)thio]imidazolium) (Syntex, 1990) and NTU281(N-benzyloxycarbonyl-L-phenylalanyl-6-dimethylsulfonium-5-oxo-L-norleucine) (Griffin M, 2004) were synthesised according to published methods (Griffin M, 2004) at Nottingham Trent University. The chemical structure of the inhibitors is shown in figure 3.8.

The purity of both compounds was determined by NMR and mass spectrometry (Nottingham Trent University). Efficacy of the inhibitors against renal transglutaminase was

determined by the application of inhibitors at 100 μ M to a 20% kidney homogenate and the transglutaminase activity measured by the [14 C] putrescine incorporation assay (Chapter 9, section 9.2.1.1).

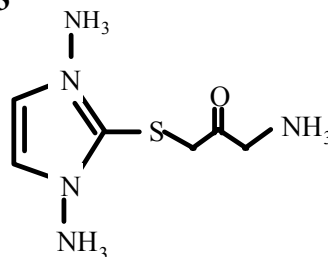
Figure 3.8 Chemical Structure of Site-Specific Transglutaminase Inhibitors

NTU281



N-benzyloxycarbonyl-L-phenylalanyl-6-dimethylsulfonium-5-oxo-L-norleucine

NTU283



1, dimethyl-2[(oxopropyl)thio]imidazolium

Figure 3.8 NTU281 and NTU283 are structurally distinct transglutaminase inhibitors that irreversibly interact with the cysteine residue located within the enzyme active site.

3.6.2 Experimental animals

3.6.2.1 *Transglutaminase knockout mice*

Wild type (WT) C57/b16J strain mice which fully express TG2 and TG2 knockout C57 mice (TG2^{-/-}) which have deletion of most of exons 5 and 6 of the TG2 gene (containing the TG2 active site) were used for the isolation of primary tubular epithelial and mesangial cells. TG2^{-/-} mice were originally generated by De Laurenzi and Melino using homologous recombination techniques (De Laurenzi and Melino, 2001) and obtained for this study from Nottingham Trent University.

3.6.2.2 *Wistar rats (subtotal nephrectomy)*

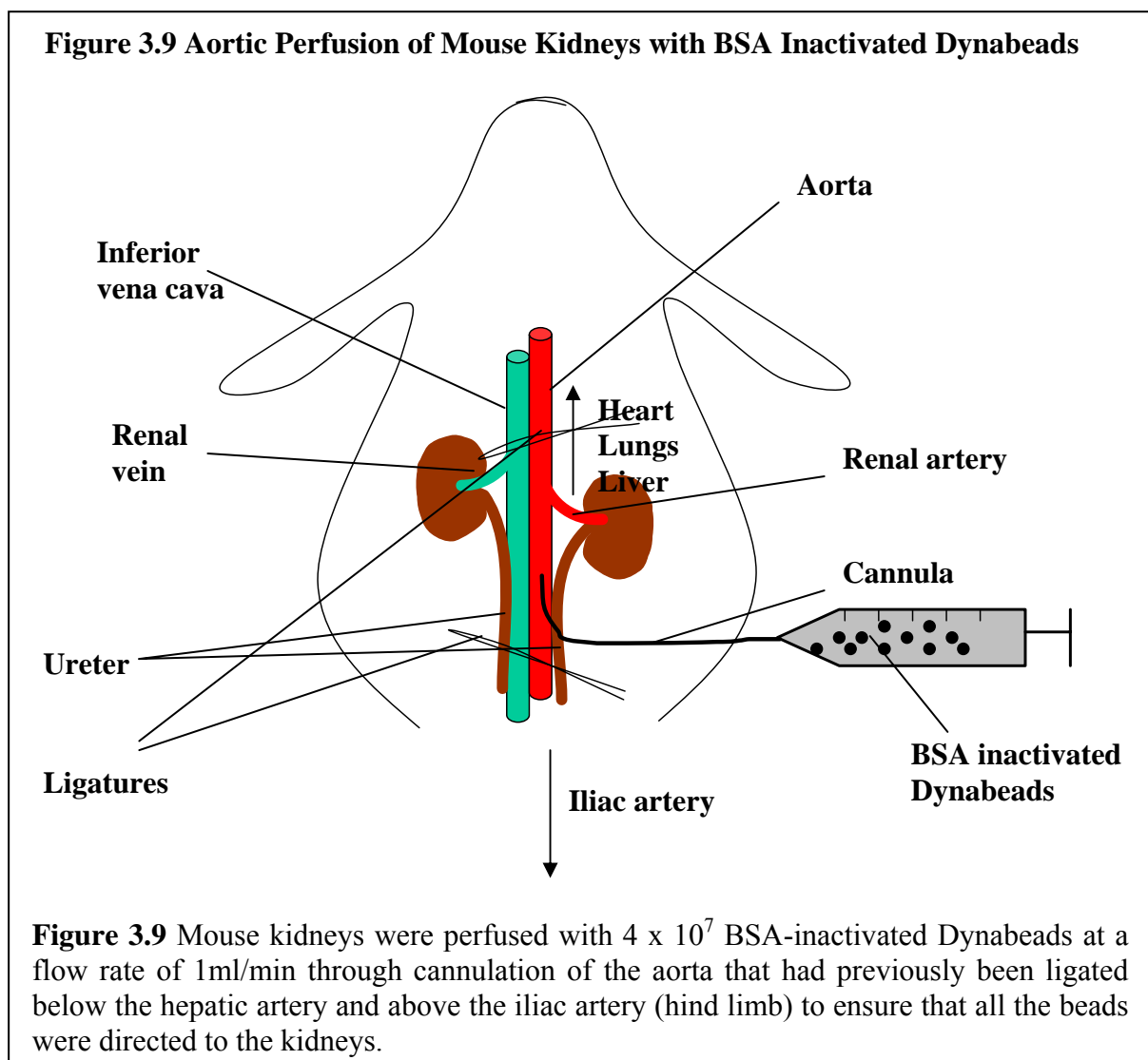
Male Wistar rats (Sheffield University strain) of approximately similar weight (200-250g) and age (8-10 wk) were used for the subtotal (5/6th) nephrectomy model. Rats were allowed free access to standard rat chow (Labsure Ltd, Cambridge, UK) and tap water and were housed 2-4 to a cage at 20-22°C and 45% humidity on a 12h light/dark cycle.

3.6.3 Experimental procedures

3.6.3.1 Retrograde perfusion of mouse kidneys

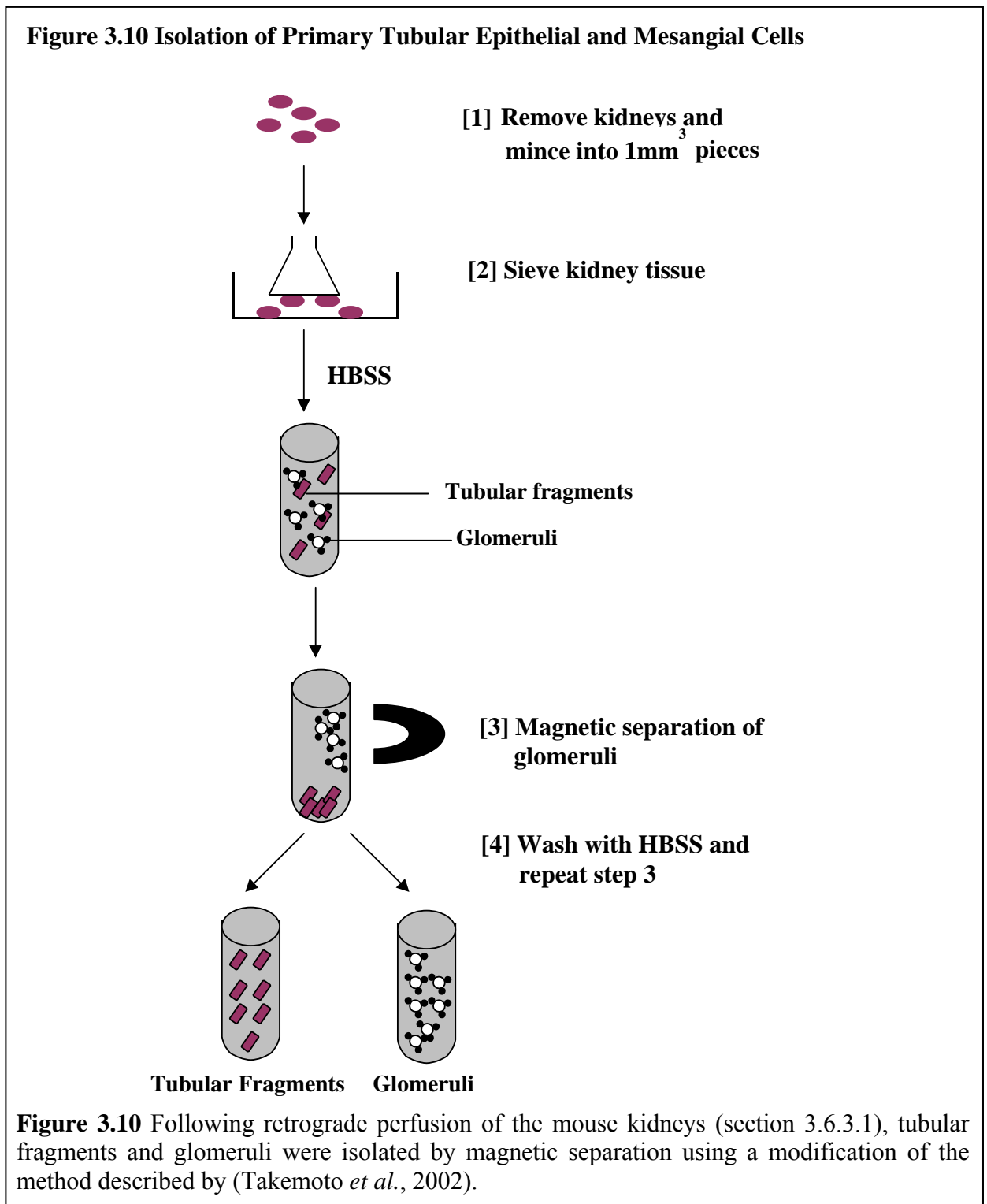
Kidneys from wild type and TG2^{-/-} mice were perfused using a modification of the method described by Takemoto *et al* (Takemoto *et al.*, 2002) for the magnetic separation of tubular and glomerular compartments from the mouse kidney. The perfusion procedure was performed by Dr John Haylor.

Mice were anaesthetised by an intra-peritoneal injection of 0.1ml/10g body weight of 25% Hypnorm and 25% Hypnovel [Hypnorm: Fentanyl citrate 0.315mg/ml, fluanisone 10mg/ml (Janssen Pharmaceutica, Beersel, Belgium), Hypnovel: midazolam 5mg/ml (Roche Products Ltd, Welwyn Garden City, UK)] and kidneys perfused with 4×10^7 BSA-inactivated Dynabeads (M450, Dynal Biotech, Oslo, Norway) at a flow rate of 1ml/min through cannulation of the abdominal aorta. This had previously been ligated below the hepatic artery and above the iliac artery (hind limb) to ensure that all the beads were directed to the kidneys (figure 3.9).



3.6.3.2 Isolation of tubular and mesangial cells from wild type and TG2^{-/-} mice

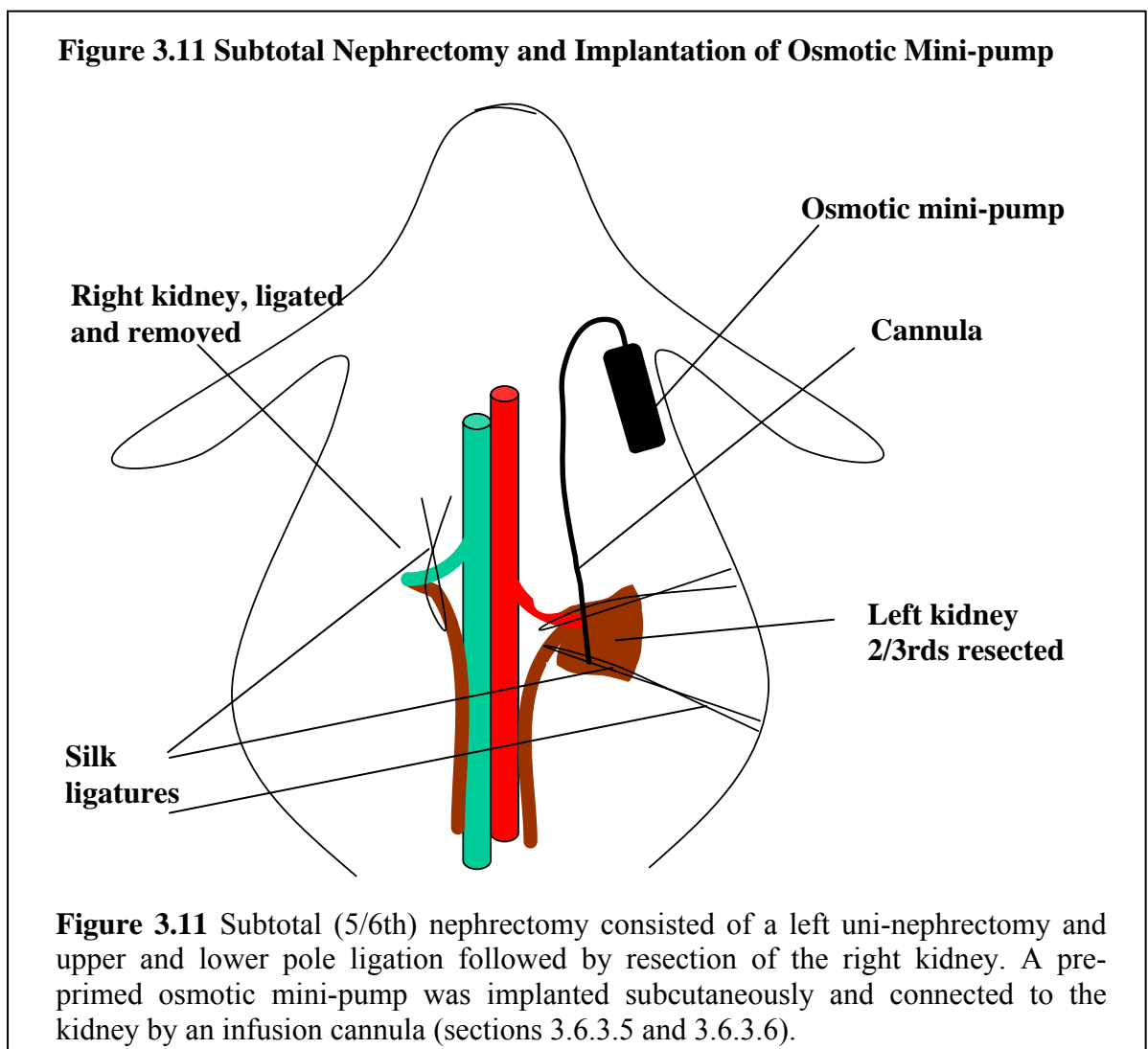
Following retrograde perfusion of the mouse kidneys (section 3.6.3.1) both kidneys were removed, minced into 1mm² pieces and the tissue passed through a 100µm sieve using a flattened pestle. The filtered cells were passed through a second sieve without pressing and the sieve washed with 10ml of Hank's buffered saline solution (HBSS). The cell suspension was centrifuged at 200 x g for 5 mins. The supernatant was discarded, the cell pellet resuspended in 10mls of HBSS and the glomeruli isolated using a magnet.



The glomeruli were washed 3 times and the HBSS containing the tubular fragments pooled. The tubular fragments were centrifuged and plated in primary tubular media as described in section 3.1.3. The HBSS washed glomeruli were plated in primary mesangial cell media as described in section 3.1.3. Isolated glomeruli were allowed to attach for at least one week prior to the addition of fresh media. The principles of the technique are shown in figure 3.10.

3.6.3.3 Subtotal (5/6th) nephrectomy (SNx)

Subtotal nephrectomy was performed by Dr. John Haylor. Male Wistar rats were anaesthetised with halothane (4% halothane, 4L/min O₂) via inhalation in a sealed induction chamber. Once anaesthetised, rats were transferred to a heated mat to maintain body temperature and anaesthesia was maintained via a nose cone (2.5% halothane, 1.5 L/min O₂). The right kidney was ligated, removed and weighed to give an estimation of initial kidney weight. The left kidney was externalised and decapsulated. A ligature was placed around the upper and lower poles of the kidney, which were slowly tightened and the poles excised leaving one third of the kidney remaining (figure 3.11). The poles were weighed to determine the degree of resection.



3.6.3.4 Renal infusion of transglutaminase inhibitors

Direct infusion of transglutaminase inhibitor into the kidneys of rats subjected to subtotal nephrectomy was achieved using a custom made infusion cannula and 2ml4 Azlet® osmotic minipump (Charles River, Maidstone, UK) with a flow rate of 0.5µl/hr for 28 days.

3.6.3.5 Infusion cannula and preparation of mini-osmotic pump

A 9 cm long, 0.58mm diameter polythene cannula was prepared by heat-sealing one end and then fenestrating a 9 mm section inset by 2 mm from the sealed end. The open end was attached to the regulator of the osmotic minipump that had been loaded with either PBS pH7.4 or 50mM solutions of TG inhibitor NTU281 or NTU283 in PBS. The flow moderator was inserted and the pumps primed overnight in a beaker of 0.9% saline at room temperature prior to implantation.

3.6.3.6 Implantation of mini-osmotic pump.

Implantation of mini-osmotic pumps was performed at the same time as subtotal nephrectomy (section 3.6.3.3). An 18 gauge guide needle was placed over the end of the infusion cannula, inserted into the kidney at the bottom pole and passed up through the kidney. The guide needle was passed completely through the kidney, exiting at the top pole leaving the cannula in place. The cannula was positioned such that the fenestrated area was within the renal parenchyma and secured in place using a combination of tissue glue and silk tie at each pole. The osmotic mini pump was then attached to the opposing end of the cannula that had been run through the muscle wall to the scruff of the rat, secured subcutaneously and the skin wound closed using discontinuous silk sutures. Pumps were replaced after 28 days by a small subcutaneous incision under halothane anaesthetic.

3.6.4 Biochemical measurement of renal function

3.6.4.1 Creatinine

Urine creatinine measurements were performed on 24 hour urine samples collected from rats placed in metabolic cages immediately prior to termination. Serum creatinine measurements were performed on blood that had been obtained from the heart at sacrifice. This was allowed to stand for 30 mins and centrifuged at 1500 x g (Heraeus 6000, Heraeus, Brentwood, UK) prior to the removal of serum. The serum was stored at -20°C. Both serum and urine creatinine were analysed by the standard autoanalyser technique (by the Clinical Chemistry Department, Northern General Hospital, Sheffield, UK) and expressed as µmol/l. Serum and urine creatinine measurements were used to calculate creatinine clearance (equation 3.1) which was then used to assess renal function.

Equation 3.1 Calculation of Creatinine Clearance

$$C_{Cr} = \frac{U_{Cr} \times V}{S_{Cr}}$$

Where: U_{Cr} = Urine creatinine ($\mu\text{mol/l}$)
 V = Urine flow (ml/min)
 S_{Cr} = Serum creatinine ($\mu\text{mol/l}$)

3.6.4.2 Proteinuria

Measurements of proteinuria were obtained from 24 hour urine samples collected and measured from rats by placing them in metabolic cages. Protein was determined by the Lowry protein assay as described in section 3.3.9.2 and expressed as mg/24hrs.

3.6.4.3 Albuminuria

Albuminuria was determined in 24 urine samples using the Bethyl Laboratories rat albumin ELISA kit (BioGnosis, Hailsham, UK) as per the manufacturer's instructions.

3.6.5 Biochemical measurement of liver function

Liver function measurements were performed on serum samples prepared from blood obtained at sacrifice as described in section 3.6.4.1. Serum was analysed for alanine aminotransferase (ALT), aspartate aminotransferase (AST) and bilirubin by standard autoanalyser technique by the Clinical Chemistry Department, Northern General Hospital, UK and expressed as units/litre.

3.6.6 Fibrin clot stability

The assessment of clot stability was performed by the Haematology Department, Northern General Hospital, UK, on citrated plasma obtained from blood collected at sacrifice using a semi-quantitative method (Jakobsen and Godal, 1974). Plasma was clotted by the addition of thrombin and incubation at 37°C for 30 mins. The resultant clot was treated with 5M urea and left at room temperature for 24 hours after which time the presence of the clot was assessed visually.

3.6.7 Assessment of kidney scarring

Analysis of kidney scarring was determined on 4 μm thick formalin-fixed paraffin-embedded sections (section 3.3.4) that had been stained with Masson's Trichrome, a widely

used stain for ECM, by the Histopathology Department, Northern General Hospital. The degree of scarring was assessed by carrying out multi-phase image analysis using 3 phases as described in section 3.5.2.6.

3.6.8 Immunohistochemical analysis

3.6.8.1 Changes in the ECM

Immunohistochemistry for collagens III, IV and fibronectin was performed on paraffin-embedded sections as described in section 3.5.2.4. Immunohistochemistry for collagen I was performed on cryostat sections as described in section 3.5.2.5. Staining was quantified by multi-phase image analysis as described in section 3.5.2.6.

3.6.8.2 Interstitial cell infiltration

Immunohistochemistry was performed on paraffin-embedded sections as described in section 3.5.2.4. Myofibroblasts were detected by immunoprobng with mouse monoclonal anti alpha smooth muscle actin (α -SMA) primary antibody (M0851, Dako) at 1:100 dilution followed by incubation with goat anti-mouse HRP (Dako). Monocyte infiltration was detected by immunoprobng with mouse monoclonal anti-ED1 (CD68+, MCA341R, Serotec, Oxford, UK) at 1:100 dilution followed by goat anti-mouse HRP. The level of staining was determined by multi-phase analysis as described in section 3.5.2.6.

3.7 Statistical Analyses

Results are given as mean \pm standard error of the mean (mean \pm SEM). The significant difference in the mean values of more than two groups was determined by one way analysis of variance (ANOVA) followed by Bonferroni post hoc analysis to compare individual groups with the control if ANOVA showed $p < 0.05$. Comparison of two groups was determined by unpaired student t-test and a value of $p < 0.05$ taken as significant. Correlation analysis between variables was determined by performing Pearson's correlation. Statistical analysis was performed using Microsoft Excel 2000 and SPSS version 14.0.

Chapter 4

Induction of Tissue Transglutaminase in Proximal Tubular Epithelial Cells

4.1 Introduction

Numerous studies have demonstrated a link between the development of chronic renal scarring and elevated TG2 expression by tubular epithelial cells (Johnson *et al.*, 1997; Johnson *et al.*, 1999; Skill *et al.*, 2001). To date, the factors that may be responsible for the stimulation of TG2 in tubular cells remain largely unknown. Previous studies have investigated the induction of TG2 in OK tubular cells by elevated glucose and demonstrated a dose-dependent increase in TG2 activity corresponding to elevated levels of $\epsilon(\gamma\text{-glutamyl})$ lysine crosslink (Skill *et al.*, 2004). However, the effect of numerous fibrosis promoting factors on the regulation of TG2 expression has yet to be investigated.

Studies of TG2 expression in numerous non-renal cell types has demonstrated that TG2 is subject to regulation at the transcriptional level by growth factors such as TGF- β 1, IL-6 and TNF- α (George *et al.*, 1990; Suto *et al.*, 1993; Ikura *et al.*, 1994; Kuncio *et al.*, 1998), glucocorticoids (Johnson *et al.*, 1998) and retinoids (Chiocca *et al.*, 1988) and at the post-translational level by calcium (Casadio *et al.*, 1999) and GTP binding (Liu *et al.*, 2002). Such data suggests that similar factors may be involved in the regulation of TG2 expression by tubular cells.

There are many potential candidate factors associated with chronic renal disease that may stimulate TG2 expression by tubular cells. These include fibrosis promoting growth factors such as TGF- β 1, PDGF and insulin-like growth factor-1 (IGF-1) and pro-fibrogenic cytokines such as TNF- α and IL-1 β . In addition, cellular stress imposed by a chronic loss of tissue oxygen (hypoxia) or the effects of metabolic acidosis (lowering of blood pH) may also be key regulators of TG2 in the diseased kidney.

In this chapter, a preliminary screening of a number of growth factors, cytokines and TG2 stimulatory compounds will be performed to determine their effect on the induction and cellular release of TG by tubular cells. In addition the effect of exposure to chronic hypoxia (1% oxygen) and metabolic acidosis (pH below 7.0) will be investigated to determine if either of these stress factors plays a role in the control of TG2 expression. TG expression in response to stress factors will be characterised in terms of changes in intracellular and extracellular TG activity, TG2 protein and mRNA.

4.2 Results

4.2.1 Stimulation of TG2 with fibrogenic growth factors

In the kidney, a number of growth factors are known to be significant in promoting fibrosis including PDGF, IGF-1 and TGF- β 1 (Klahr and Morrissey 2000). To determine if these factors are able to act via up-regulation of TG2, opossum proximal tubular cells (OK cells) were stimulated for 48 hours with either 10ng/ml or 100ng/ml of PDGF (fig 4.1a), IGF-1 (fig 4.1b) or TGF- β 1 (fig 4.1c). Their intracellular transglutaminase (TG) activity was measured by the putrescine incorporation assay. No significant change in intracellular TG activity was observed with any of these factors at the concentrations used.

4.2.2 Stimulation of TG2 with the cytokines TNF- α and IL-1 β

TNF- α and IL-1 β have previously been demonstrated to regulate TG2 transcription and are also considered to be important pro-inflammatory cytokines. To determine if they are able to regulate TG2 in tubular cells, opossum tubular epithelial cells were treated for 48 hours with 10ng/ml or 100ng/ml of either TNF- α (fig 4.2a) or IL-1 β (fig 4.2b).

Stimulation with either of these cytokines failed to produce a significant change in intracellular TG activity.

4.2.3 Stimulation of TG2 with retinoic acid, sodium butyrate and dexamethasone

To determine if well-recognised stimulators of TG2 are able to induce TG in proximal tubular cells, OK cells were treated for 48 hours with 1 μ M and 100 μ M of either all *trans*-retinoic acid (fig 4.3a), sodium butyrate (fig 4.3b) or dexamethasone (fig 4.3c). Intracellular TG activity was determined by putrescine incorporation assay. Treatment with either retinoic acid, sodium butyrate or dexamethasone was found to have no stimulatory effect on intracellular TG activity at these concentrations.

Figure 4.1 Effect of Fibrogenic Growth Factors on Intracellular TG Activity in OK Cells

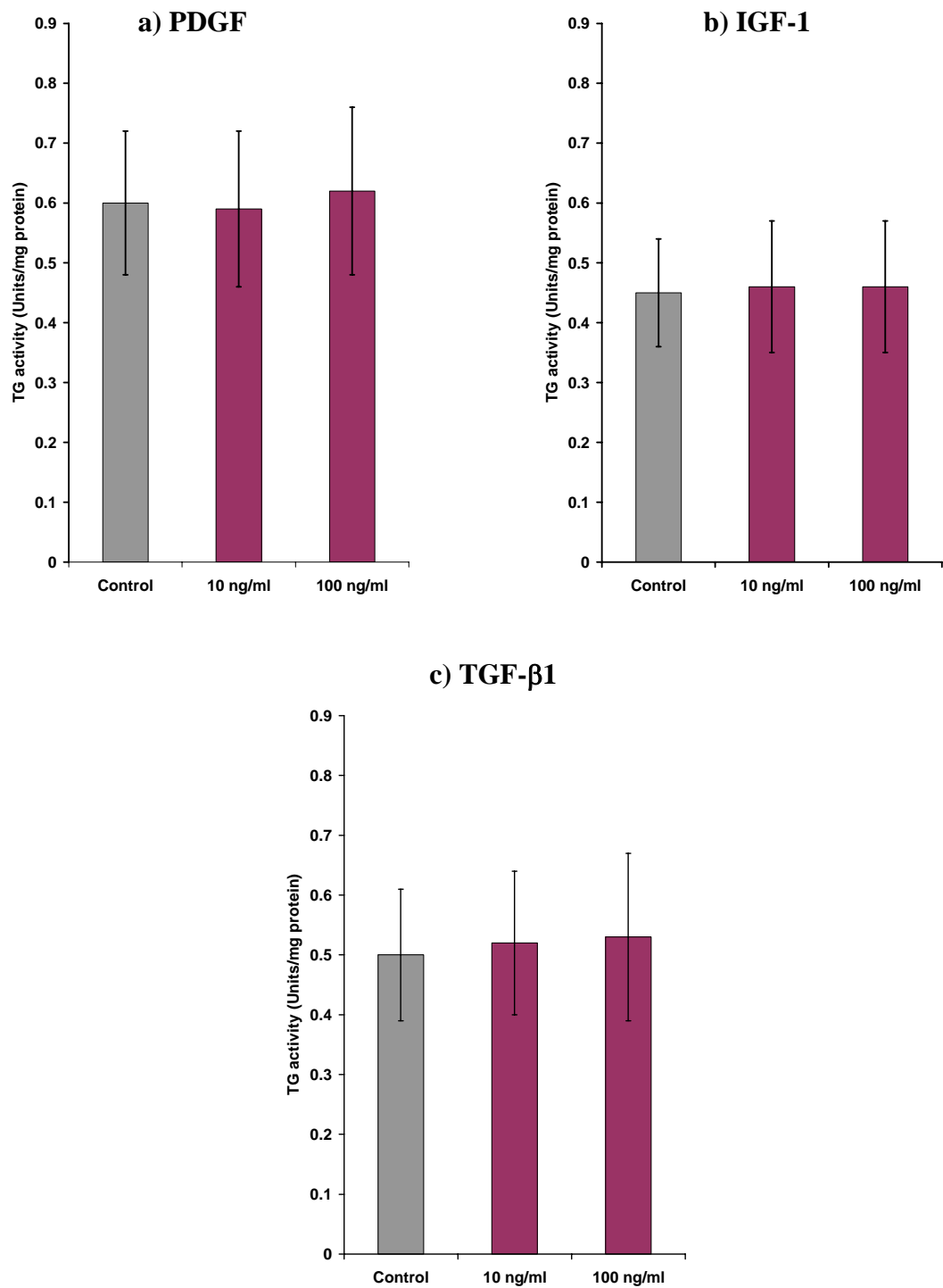


Figure 4.1 Cells were treated for 48 hours with 10ng/ml or 100ng/ml of PDGF (a), IGF-1 (b) or TGF-β1 (c). Cells were harvested using 0.25% trypsin, sonicated and TG activity determined by the putrescine incorporation assay as described in section 3.3.7.1 Data represents mean ± SEM from three separate experiments performed in triplicate.

Figure 4.2 Effect of Inflammatory Cytokines on Intracellular TG activity in OK Cells

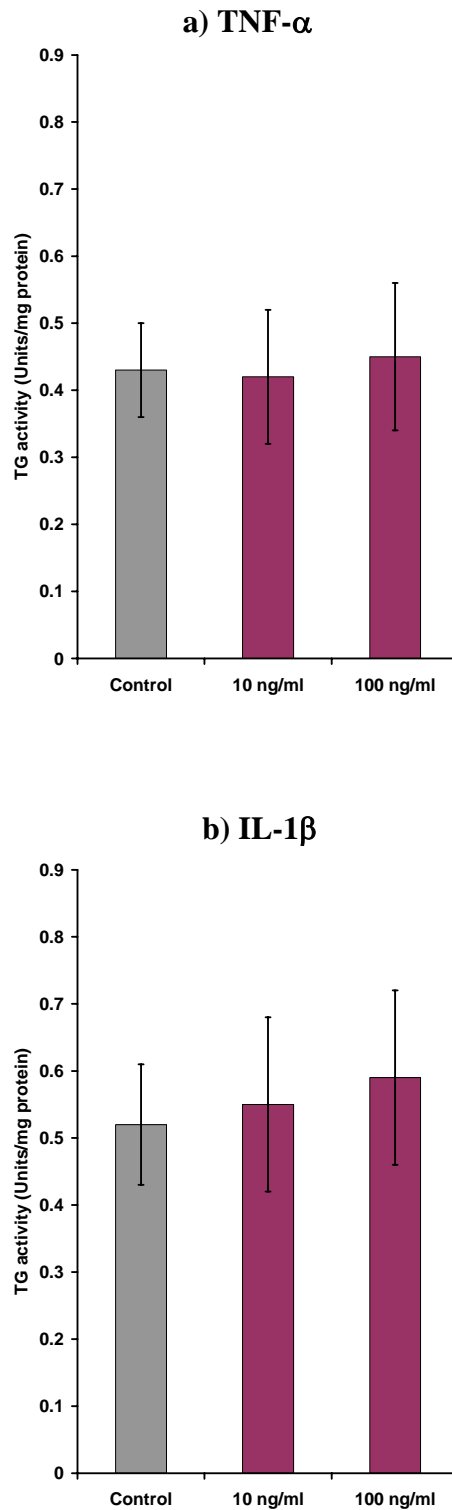


Figure 4.2 Cells were treated for 48 hours with 10ng/ml and 100ng/ml of TNF- α (a) or IL-1 β (b). After treatment, cells were harvested using 0.25% trypsin, sonicated and TG activity determined by the putrescine incorporation assay. Data represents mean \pm SEM from three separate experiments performed in triplicate.

Figure 4.3 Effect of TG Stimulators on Intracellular TG Activity in OK Cells

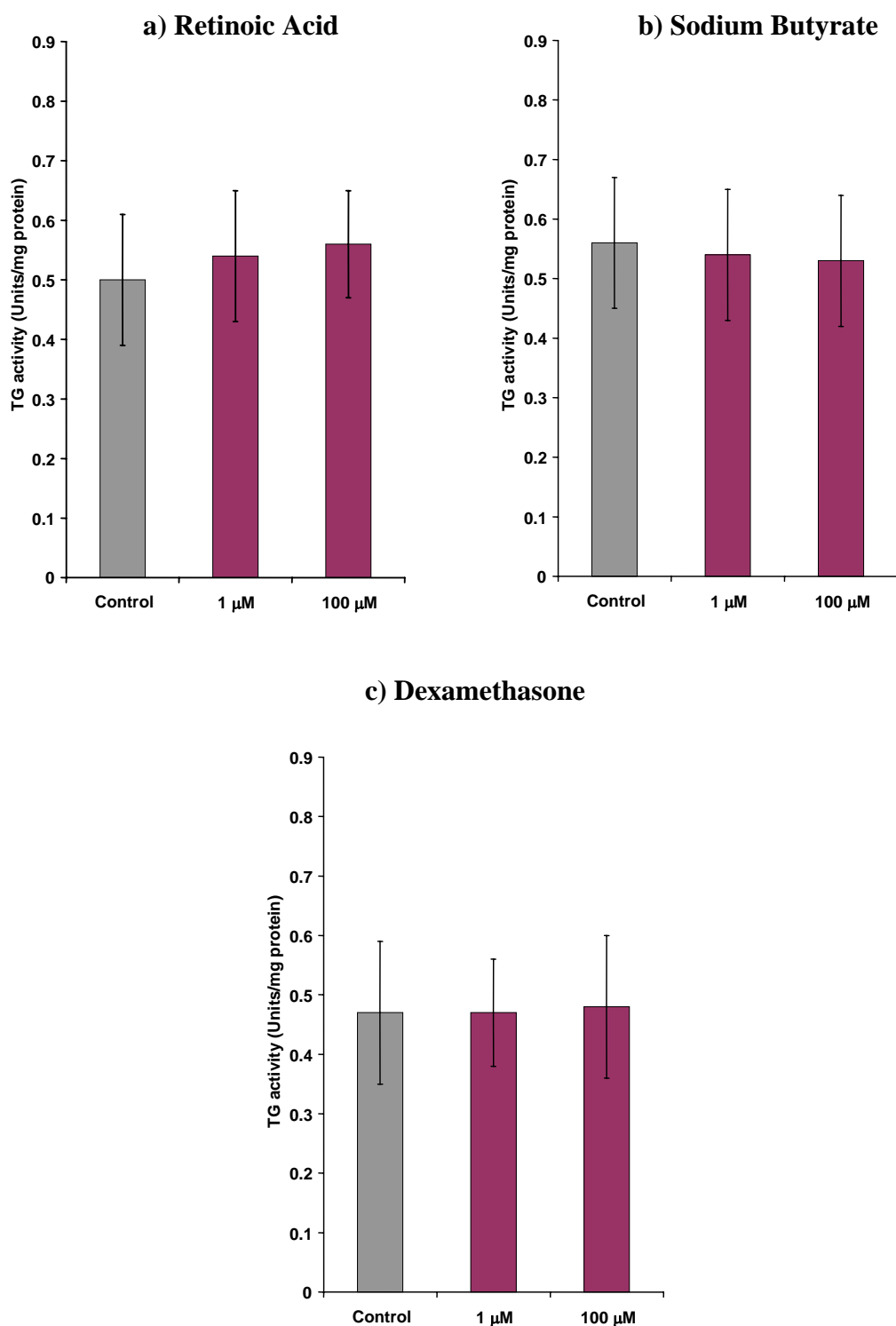


Figure 4.3 Cells were treated for 48 hours with 1μM and 100μM of either all trans retinoic acid (a), sodium butyrate (b) or dexamethasone (c). Cells were harvested with 0.25% trypsin, sonicated and analysed for TG activity by putrescine incorporation assay. Data represents mean ± SEM from three separate experiments performed in triplicate.

4.2.4 Effect of renal stress factors

4.2.4.1 Hypoxia

4.2.4.1.1 TG activity

To determine if chronic hypoxia (1% oxygen) is capable of regulating TG2 in tubular cells, NRK-52E cells were cultured for 6, 12, 24 and 48 hours under normoxic (21% oxygen) or hypoxic (1% oxygen) conditions (fig 4.4a). Hypoxia produced a biphasic increase in intracellular TG activity at 6 hours ($p < 0.05$; one way ANOVA with Bonferroni post hoc test) and 24 hours, with no change at 12 and 48 hours. Measurement of extracellular TG activity at 6 and 24 hours (fig 4.4b) demonstrated a corresponding increase in extracellular TG activity ($p < 0.05$ and $p < 0.001$ respectively; students t-test) at these time points.

4.2.4.1.2 TG2 protein

TG2 protein levels in NRK-52E cells exposed to 1% oxygen were determined after 6, 12, 24 and 48 hours culture by Western blot analysis (fig 4.5). Initially blots were probed with the mouse monoclonal anti-TG antibody TG100. However, no bands were observed that corresponded to TG2 in any of the lysates analysed despite repeated probing (data not shown). Blots were then repeated and probed with polyclonal anti-TG2 antibody (Abcam).

Probing with the polyclonal antibody revealed a band at 85 kDa as indicated by comparison to kaleidoscope markers (section 3.3.6.3), that was present in both normoxic and hypoxic samples and which would be consistent with full length TG2 (fig 4.5a). However, a number of smaller bands were also present in particular, a band at approximately 65 kDa. Unfortunately, due to the high background signal it was difficult to obtain reliable volume densitometry analysis of the 85 kDa band despite pooling the data from 3 separate blots (fig 4.5b) and is included for evaluation only.

4.2.4.2 Acidosis

To determine if acidosis is able to influence TG2 expression and its cellular release, a model of chronic acidosis was used in which media pH was modified using Bis-Tris buffer as a replacement for bicarbonate buffer. LLC-PK1 cells were exposed to increasing acidic conditions of pH 7 and 6.7 for 72 hours including 24 hours in serum free media, to mimic mild and chronic metabolic acidosis, prior to analysis for TG2 expression and activity.

4.2.4.2.1 TG activity

Intracellular, extracellular (cell surface) and free TG enzyme activities were determined in LLC-PK1 cells subjected to normal pH (7.4), pH 7.0 and pH 6.7. At pH 7.4, intracellular TG activity (fig 4.6a) was 0.015 ± 0.004 units/mg protein. Reducing the pH to 7.0 increased this

by 168% and by pH 6.7 intracellular activity had increased 3 fold ($p < 0.05$; Bonferroni post hoc test). Increased intracellular TG activity corresponded with increases in both cell surface TG (fig 4.6b) and TG released into the cell culture media (fig 4.6c). However, these increases only became significant for media TG at pH 6.7 ($p < 0.05$; Bonferroni post hoc test).

4.2.4.2.2 TG2 protein

TG2 protein levels in LLC-PK-1 cells and media following culture at pH 7.4, 7.0 and 6.7 were determined by Western blotting analysis (fig 4.7 and 4.8). Lowering the pH from 7.4 to 7.0 and 6.7 resulted in a decrease in cellular TG2 protein expression of 72% and 60% respectively ($p < 0.05$; Bonferroni post hoc test) (fig 4.7b).

Analysis of TG2 protein levels in acetone precipitated media from the same cells (fig 4.8a) revealed the presence of multiple protein bands, including a band at 85kDa that appeared to correspond to TG2. Volume densitometry of this band (fig 4.8b) showed a significant increase in this protein in the media at pH 7.0 ($p < 0.001$) and 6.7 ($p < 0.0001$; Bonferroni post hoc test).

4.2.4.2.3 TG2 mRNA expression

TG2 mRNA expression in LLC-PK1 cells following culture at pH 7.4, 7.0 and 6.7 was determined by Northern blotting (fig 4.9). Lowering the pH from 7.4 to pH 7.0 increased TG2 mRNA expression although this was not significant. Reducing the pH further to pH 6.7 produced a highly significant increase in TG2 expression ($p < 0.0001$; Bonferroni post hoc test), elevating TG2 by greater than 5 fold compared to control.

4.2.4.2.4 $\epsilon(\gamma\text{-glutamyl})$ lysine levels

Immunoprobings of the ECM from LLC-PK1 cells subjected to low pH with a mouse monoclonal $\epsilon(\gamma\text{-glutamyl})$ lysine antibody followed by multiphase image analysis (fig 4.10) was used to assess the levels of extracellular TG2 crosslinking. Increases in $\epsilon(\gamma\text{-glutamyl})$ lysine crosslink were observed in the ECM of LLC-PK-1 cells cultured at both pH 7.0 ($p < 0.01$; Bonferroni post hoc test) and pH 6.7.

Figure 4.4 Effect of Hypoxia on Transglutaminase Activity in NRK-52E Cells

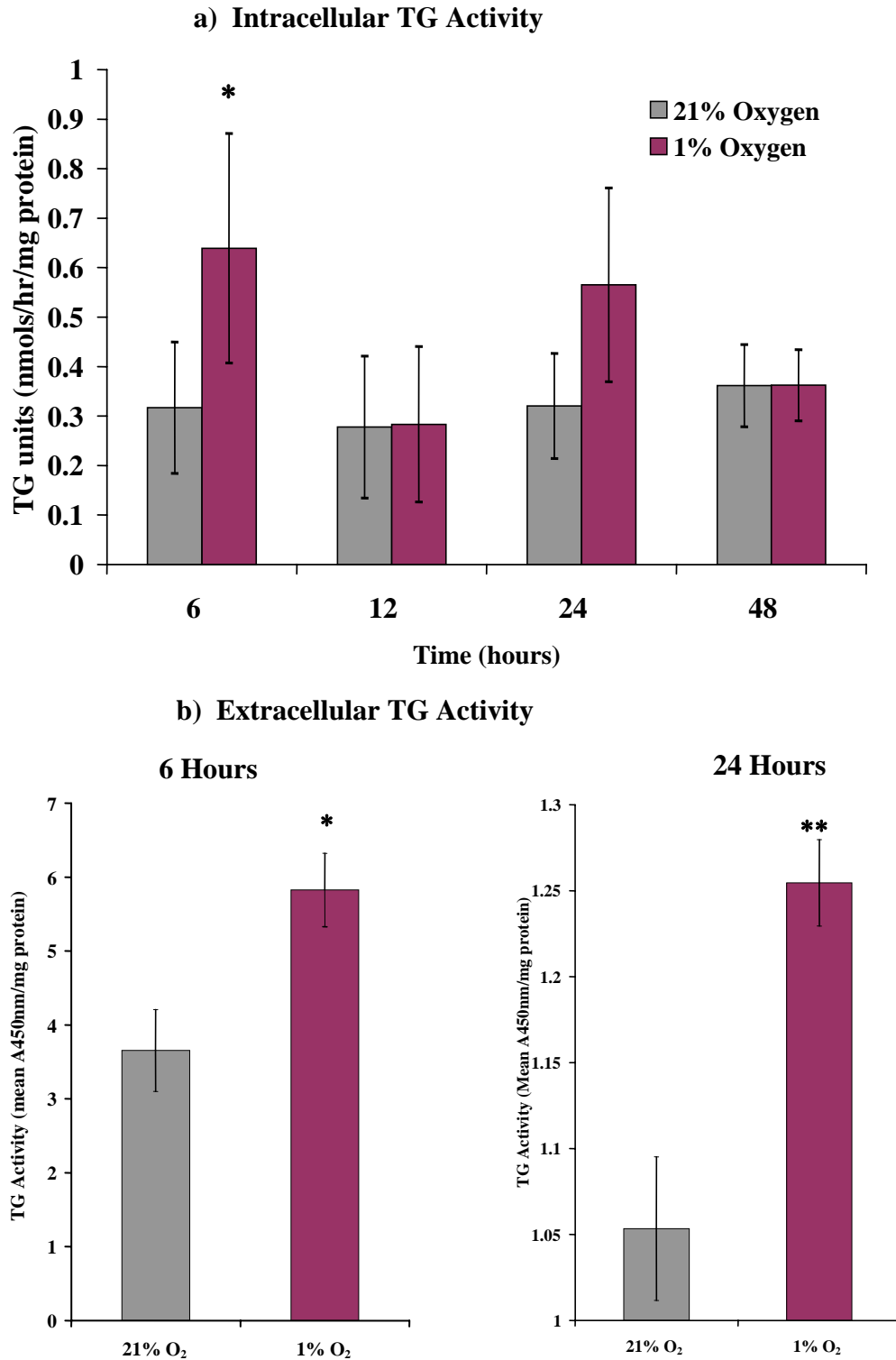
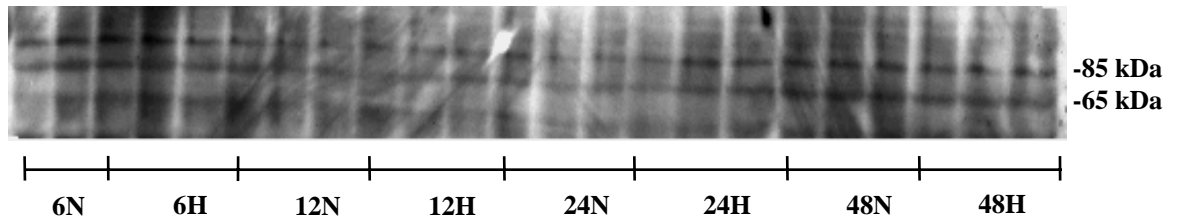


Figure 4.4 Intracellular transglutaminase activity (a) was determined using the putrescine incorporation assay. Cells were cultured under either normoxic conditions of 21% oxygen (grey bars) or 1% oxygen (purple bars) for 6, 12, 24 and 48 hours prior to harvest. Data represents mean \pm SEM from three separate experiments performed in triplicate * = $p < 0.05$ compared to control (one way ANOVA with Bonferroni post hoc test). Extracellular TG activity was determined using the biotin cadaverine ELISA (b) as described in section 3.3.7.5. Cells were cultured for 6 or 24 hours under normoxic or hypoxic conditions prior to assay. Data represents mean \pm SEM from three separate experiments, $n = 10$ wells per experiment. * = $p < 0.05$, ** = $p < 0.001$ compared to control by students t-test.

Figure 4.5 Western Blot Analysis of NRK-52E Cells Exposed to Hypoxia

a) TG2 Western Blot



b) β -Actin



c) Volume densitometry of 85kDa band

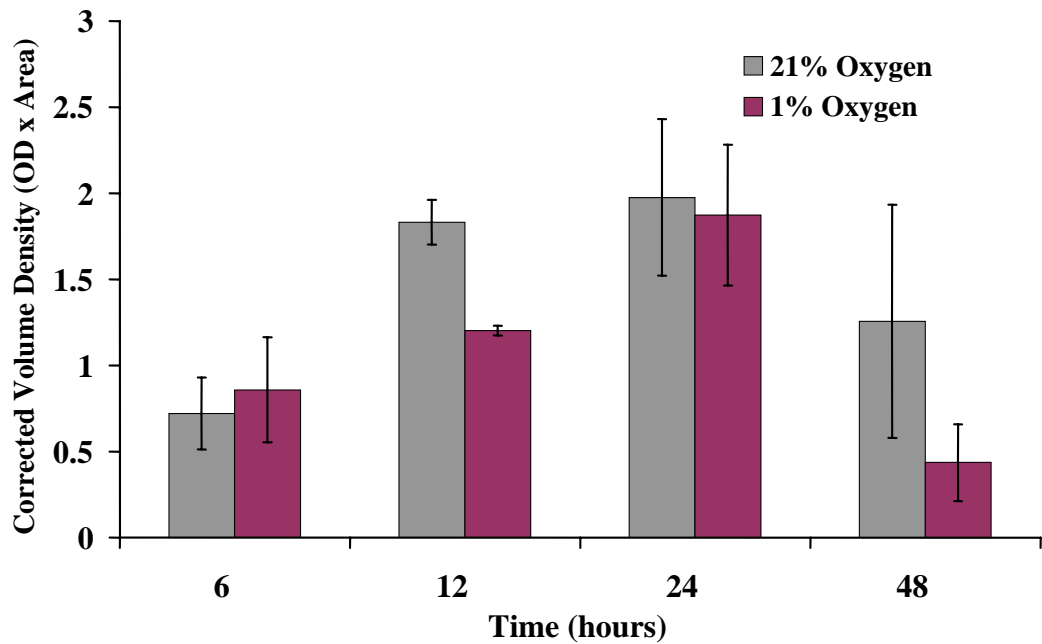


Figure 4.5 Cell lysates from NRK-52E cells exposed to 1% oxygen for 6, 12, 24 and 48 hours were separated on a 10% polyacrylamide gel and blotted onto PVDF membrane (section 3.3.6). Western blots were immunoprobed for TG2 using a polyclonal anti-TG2 antibody (Abcam) and revealed by chemiluminescence (a) as described in section 3.3.7.3. TG2 protein was quantitated by volume densitometry using Multi-Analyst version 3.2 and corrected for loading using β -actin (c). Data represents mean \pm SEM from 3 separate experiments n=2-3 samples per experiment.

Figure 4.6 Effect of pH on TG Activity in LLC-PK1 Cells

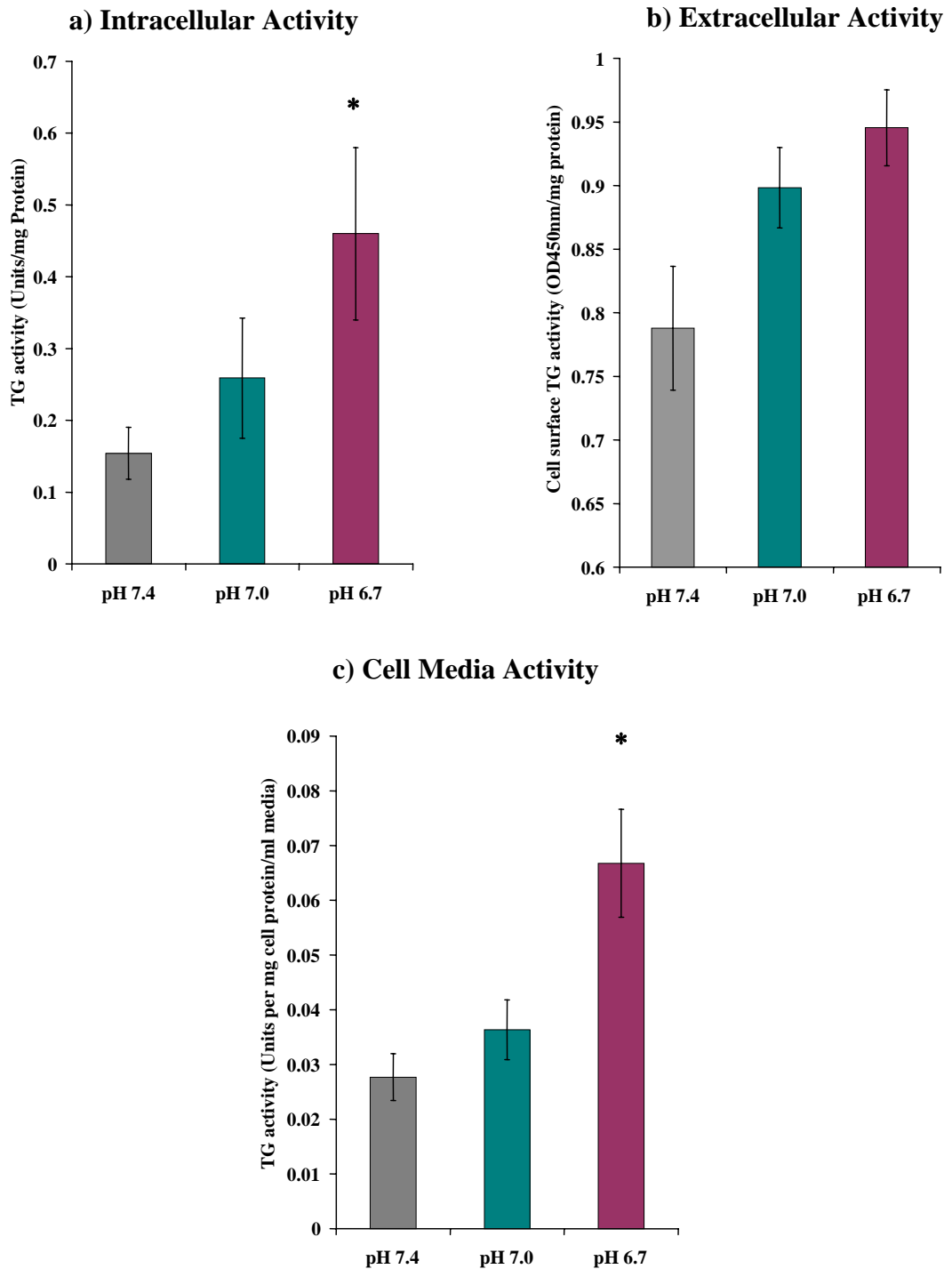
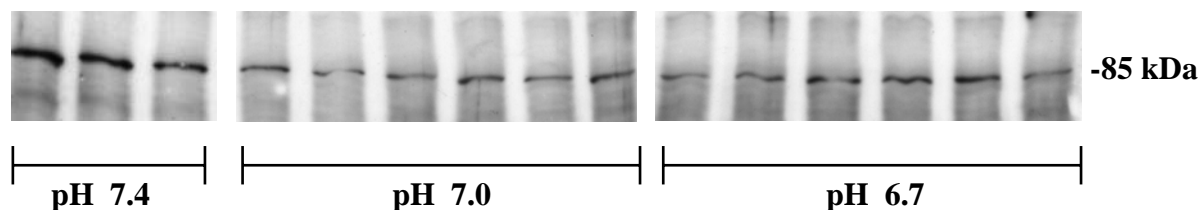


Figure 4.6 Cells were cultured under modified acidic pH conditions of pH 7.4, 7.0 and 6.7 for a total of 72 hours prior to assay for TG activity. Intracellular and cell media TG activity (a and c) were measured by the putrescine incorporation assay. Extracellular TG activity (b) was determined using the biotin cadaverine ELISA. Data represents mean \pm SEM from 2 separate experiments performed in triplicate. *= $p < 0.05$ compared to control, by one way ANOVA with Bonferroni post hoc test.

Figure 4.7 Western Blot Analysis of LLC-PK1 Cells Exposed to low pH

a) TG2 Western Blot



b) Volume Densitometry

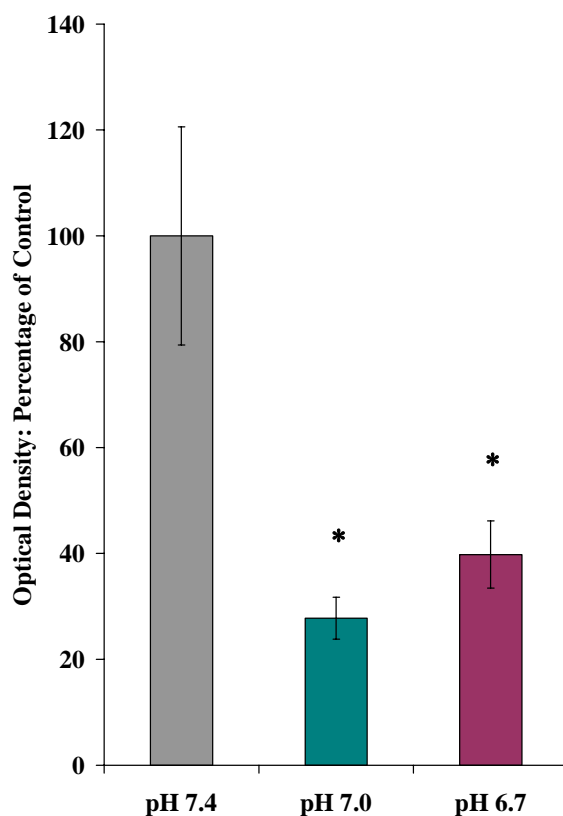
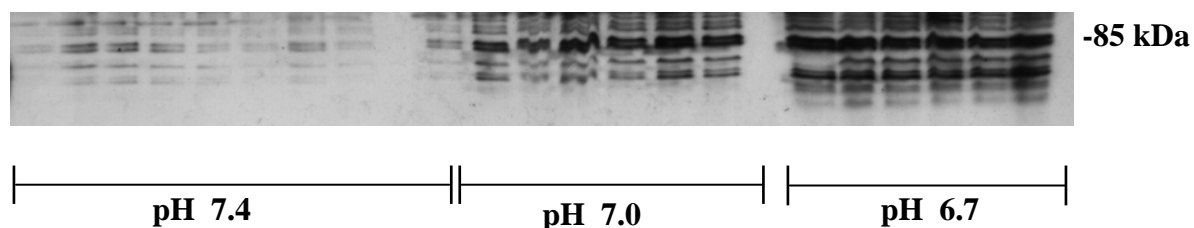


Figure 4.7 Cell lysates from LLC-PK1 cells exposed to pH 7.4, 7.0 and 6.7 for 72 hours were separated on a 10% polyacrylamide gel and blotted onto PVDF membrane. Western blots were immunoprobed for TG2 using a monoclonal anti-TG2 antibody and revealed by chemiluminescence (a). TG2 protein was quantified by volume densitometry using Multi-Analyst version 3.2 (b). *= $p < 0.05$ compared to control (pH 7.4) by one way ANOVA with Bonferroni post hoc test.

Figure 4.8 Western Blot Analysis of TG2 in LLC-PK1 Cell Media Following Exposure to Low pH

a) TG2 Western Blot



b) Volume Densitometry

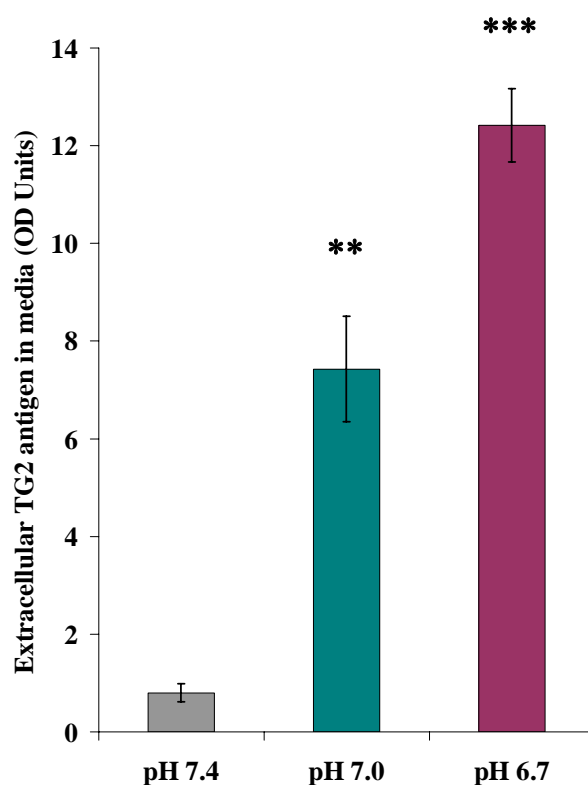
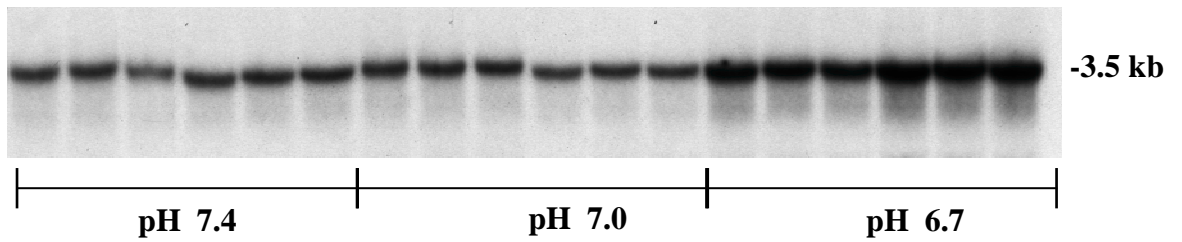


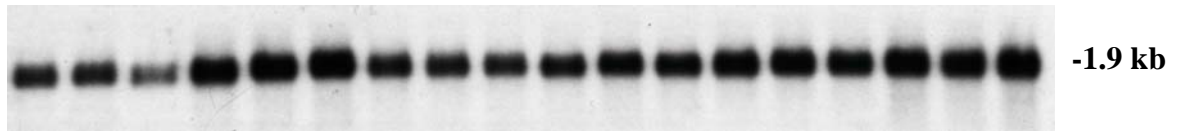
Figure 4.8 LLC-PK1 cells were cultured for 72 hours at pH 7.4, pH 7.0 and pH 6.7 prior to the collection and acetone precipitation of the culture media as described in section 3.3.3. Re-suspended media was separated on a 10% polyacrylamide gel and blotted onto PVDF membrane. Western blots were immunoprobed for TG2 using a monoclonal anti-TG2 antibody and revealed by chemiluminescence (a). TG2 protein was quantified by volume densitometry using Multi-Analyst version 3.2 (b). Data represents mean \pm SEM from 2 separate experiments. ** = $p < 0.001$, *** = $p < 0.001$ compared to control by one way ANOVA with Bonferroni post hoc test.

Figure 4.9 TG2 mRNA Expression in LLC-PK1 Cells Exposed to low pH

a) TG2 Northern Blot



b) Cyclophilin



c) Volume Densitometry

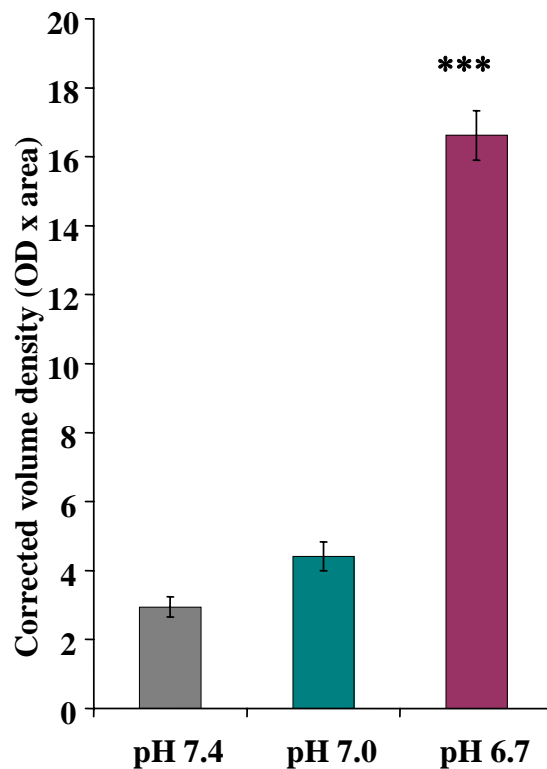
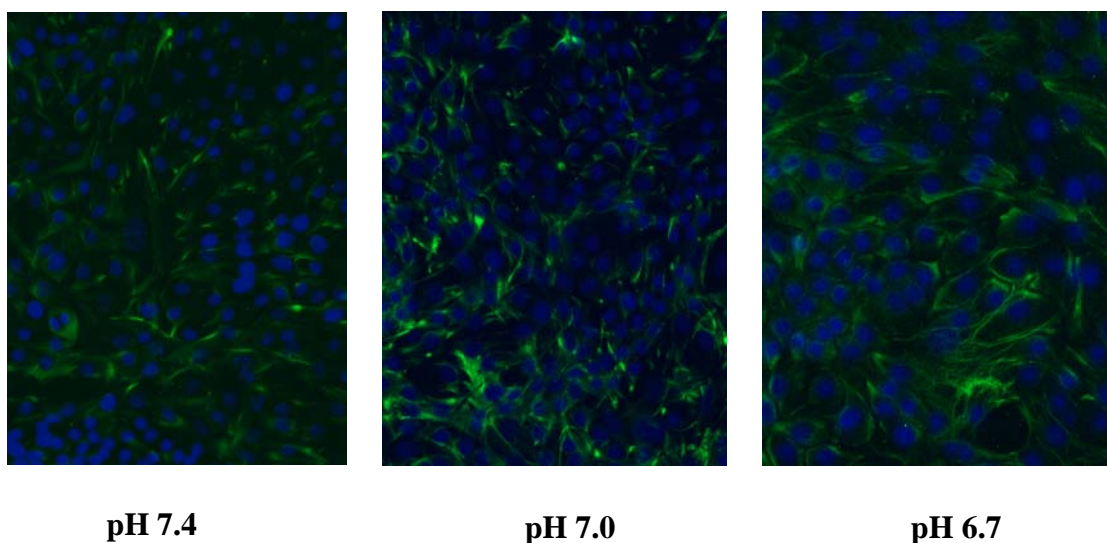


Figure 4.9 Total RNA extracted from LLC-PK1 cells exposed to pH 7.4, 7.0 and 6.7 for 72 hours was separated on a 1.2% agarose/formaldehyde gel, blotted onto Hybond N membrane and probed with a random primed 32 P-dCTP labelled TG2 specific cDNA probe (section 3.4.8). Films were analysed by volume densitometry and transcript size determined by comparison to RNA molecular weight markers. Values were corrected for loading by repeat probing with the housekeeping gene cyclophilin. Data represents mean \pm SEM from 2 separate experiments, n=6 samples experiment. *** = $p < 0.001$ compared to control by one way ANOVA with Bonferroni post hoc test.

Figure 4.10 $\epsilon(\gamma\text{-glutamyl})$ lysine ECM Levels in LLC-PK1 Cells Exposed to Low pH

a) Photomicrographs



b) Multi-phase Image Analysis

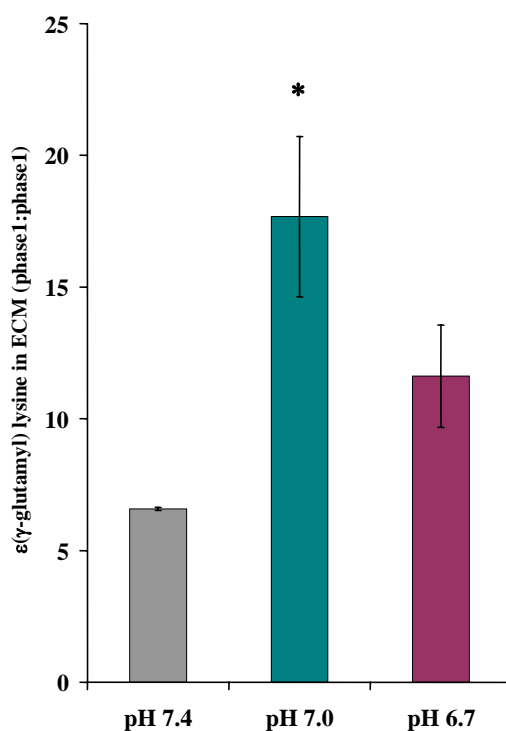


Figure 4.10 The ECM from LLC-PK1 cells cultured at pH 7.4, 7.0 and 6.7 for 72 hours was immunoprobed with monoclonal anti $\epsilon(\gamma\text{-glutamyl})$ lysine antibody and revealed with anti mouse FITC (a). Photomicrographs are shown at 200x magnification. 10 random fields were analysed by multi-phase image analysis (b) as described in section 3.5.2.6. Immunofluorescence was expressed as a ratio of $\epsilon(\gamma\text{-glutamyl})$ lysine (phase1): DAPI staining (phase2) to correct for cell number. Data represents mean \pm SEM of 10 fields. *= $p < 0.001$, compared to control by one way ANOVA with Bonferroni post hoc test.

4.3 Discussion

At the present time, the factors associated with chronic renal disease that may stimulate the up-regulation and cellular release of TG2 by tubular cells are largely unknown. Recently, elevated glucose has been suggested to be a candidate factor (Skill *et al.*, 2004) however, other such stimuli remain to be investigated. In this chapter, TG2 activity both intracellular and extracellular, protein and mRNA expression was determined in tubular epithelial cells exposed to growth factors, cytokines, TG stimulators, hypoxia and acidosis.

The effect of pro-fibrogenic growth factor and cytokine stimulation on intracellular TG activity was investigated in OK proximal tubular cells which were stimulated for 48 hours with 10 or 100ng/ml of TGF- β 1, PDGF, IGF-1, TNF- α or IL-1 β . The data shows that OK tubular cells do not alter their levels of TG activity in response to 48 hour stimulation with 10 or 100ng/ml of TGF- β 1, PDGF, IGF-1, TNF- α or IL-1 β . This is surprising given that a number of previous studies have implicated these factors in the up-regulation of TG2. For example, TGF- β 1 has been shown to up-regulate TG2 expression and activity in dermal fibroblasts and cells of the trabecular network (Welge-Lussen *et al.*, 2000; Quan *et al.*, 2005). Similarly, TNF- α stimulation of liver cells results in an increase in TG2 activity (Kuncio *et al.*, 1998). In addition TG2 activity in mouse chondrocytes can be induced by IL-1 β stimulation (Johnson *et al.*, 2003).

The reason for a lack of response in OK cells to growth factor and cytokine stimulation is unclear. It may be an issue of concentration since the observed stimulation of TG2 by TGF- β 1 and TNF- α in other cells occurs at 1ng/ml rather than the 10 and 100ng/ml described here. A potential criticism of this investigation may be that the doses used were far in excess of those routinely used to study stimulation by these factors. However, the rationale was to stimulate with strong doses within the ng range to see if any response was possible and if so, to titrate out to determine a threshold dose for these factors. Given that no response was obtained even at the 10ng dose suggests that stimulation with a lower dose may also have been ineffective. A further criticism could be that OK cells need either a shorter or more prolonged exposure to these factors than the 48 hours used here and it is acknowledged that more than one time-point should have been investigated. It could also be argued that the lack of response is a reflection of performing these experiments in the presence of serum. However, it was felt that serum starvation prior to stimulation with pro-fibrogenic factors in these experiments was not wholly representative of the *in vivo* situation in which up-regulation of TG2 occurs against a background of competing growth factors.

Interestingly, an examination of the literature reveals that the OK cell line has not been widely used for the study of growth factor stimulation. The small number of studies that been performed have concentrated on the action of EGF (Kribben *et al.*, 1998; Sauvant *et al.*, 2001; Sauvant *et al.*, 2002), HGF (Liu *et al.*, 1998) or IGF-1 (Fawcett and Rabkin 1995). This suggests that OK cells might be unresponsive to some of the growth factors examined here. However, OK cells do appear to be capable of responding to TGF- β 1 as previous work indicates that they can modulate collagen and TIMP production in response to TGF- β 1 (T.S. Johnson, unpublished observations). TGF- β 1 has also been demonstrated to reduce megalin-cubulin mediated endocytosis of albumin by OK proximal tubular cells (Gekle *et al.*, 2003).

Stimulation of OK cells with either retinoic acid, dexamethasone or sodium butyrate at 1 μ M and 100 μ M for 48 hours similarly failed to effect TG activity. Again this is contrary to previous studies that have shown these factors to be inducers of TG2 in other cell types, particularly in response to 48 hour stimulation with 1 μ M. For example, retinoic acid has been shown to up-regulate TG2 in both murine peritoneal macrophages and promyelocytic leukemia cells (Murtaugh *et al.*, 1986; Chiocca *et al.*, 1989). Dexamethasone can elevate TG2 in hamster fibroblast and fibrosarcoma cell lines (Johnson *et al.*, 1998). Similarly, sodium butyrate stimulation of human embryonic lung fibroblasts results in increased TG2 activity (Birckbichler *et al.*, 1983; Lee *et al.*, 1987).

Retinoic acid and dexamethasone are known to regulate TG2 expression via the binding of nuclear receptors to specific response elements located within the TG2 gene promoter (Chiocca *et al.*, 1988; Lu *et al.*, 1995). Previous studies suggest that increased expression of retinoid or glucocorticoid receptors is critical for an increase in TG2 gene expression (Johnson, Scholfield *et al.* 1998). Whilst the lack of response to these factors could simply reflect the inappropriate selection of concentration and time-point, it may also imply that they lack such receptors or that they are subject to negative regulation. However, this seems unlikely given that OK cells possess the receptors for glucocorticoids as several studies have demonstrated modulation of angiotensin and parathyroid hormone (PTH) gene expression in OK cells by dexamethasone (Abou-Samra *et al.*, 1994; Ming *et al.*, 1996).

Previous studies have implicated hypoxia or the loss of tissue oxygen resulting from injury and obliteration of the microvasculature as a pro-fibrogenic stimulus in renal cells (Norman *et al.*, 1999; Norman *et al.*, 2000). Hypoxia is capable of increasing the expression of a wide variety of genes including growth factors (Shweiki *et al.*, 1992; Gleadle *et al.*, 1995), cytokines (Shreeniwas *et al.*, 1992; Yan *et al.*, 1995), cell adhesion molecules (Combe *et al.*, 1997) and ECM proteins (Falanga *et al.*, 1993; Norman *et al.*, 1999). It would therefore

be a strong candidate for the induction of TG2 in tubular cells. To examine this, the NRK-52E cell line was used in preference to OK cells since it has previously been used in the study of hypoxia/re-oxygenation injury and is capable of responding to hypoxic conditions (Sakai *et al.*, 2001; Basnakian *et al.*, 2002). Cells were exposed to 1% O₂ for up to 96 hours with the degree and duration of hypoxia being selected on the basis of previous work on hypoxia induced collagen synthesis by human proximal tubular cells (Norman *et al.*, 1999).

Exposure of NRK-52E cells to hypoxia produced a biphasic increase in intracellular TG2 activity at 6 and 24 hrs that was paralleled by an increase in extracellular TG2. This differs from our previous observations in NRK-49F fibroblasts exposed to low O₂ which show a reduction in TG2 activity at these time points (M Fisher, unpublished observations). It was difficult to establish however, whether the changes in TG2 activity were as a direct consequence of increased TG2 protein expression given the high background of Western blots and the apparent detection of multiple smaller bands. This is likely to reflect a specificity problem with the polyclonal TG2 antibody given that the monoclonal TG2 antibodies TG100 and CUB7402 are highly specific for the TG2 isoform (M Griffin, personal communication) and give a single band at 85 kDa. However, it was not possible to detect any bands with either of these two antibodies. Interestingly, it has previously been noted from Western blot analysis of TG2 expression in NRK-52E cells following glucose stimulation (Huang 2006) that a number of discrete bands are detectable with this antibody, in the absence of high background, whose sizes correspond to other TG isoforms. If this is the case, then the 65 kDa band detected here may indicate the presence of an additional isoform such as TG3 (epidermal TG) suggesting that the increased TG activity in response to hypoxia may be contributed to by different isoforms of TG.

The early effect of hypoxia on TG2 may be mediated by induction of the hypoxia-inducible transcription factor HIF-1 α . Increased expression and binding of HIF-1 α to the hypoxia response element (HRE) is an important mechanism of hypoxia-regulated gene expression (Semenza 1999). In support of this, a previous study of gene expression in human proximal tubular cells (HK-2) exposed to hypoxia demonstrates the early up-regulation of 48 genes in response to hypoxia, the majority of which are HIF-1 α responsive (Leonard *et al.*, 2003). Early peaks in HIF-1 mRNA (2 hours post hypoxia) are also demonstrated to occur in renal fibroblasts and have been shown to precede the hypoxia induced increase in TIMP-1 and collagen I expression (Norman *et al.*, 1999). Whilst the HIF-1 responsiveness of TG2 has yet to be established, the wider induction of HIF-1 responsive genes in tubular epithelial cells and fibroblasts by hypoxia suggests that a rapid induction of HIF-1 in NRK-52E cells may

account for the early changes in TG2 expression observed here. Clearly, analysis of HIF-1 mRNA expression in this study would have helped to determine its role in early TG2 induction in these cells.

The later induction of TG2 at 24 hours may indicate activation of alternate pathways independent of HIF-1 α . Hypoxia is known to activate a variety of signal transduction pathways including protein kinase C-, protein kinase A- and tyrosine kinase-mediated pathways (Sahai *et al.*, 1997a; Sahai *et al.*, 1997b; Norman *et al.*, 1999; Norman *et al.*, 2000; Sodhi *et al.*, 2000). Interestingly, studies of VEGF expression by NRK-52E tubular cells in response to hypoxia demonstrate that induction of VEGF can be blocked by protein kinase C inhibitors, indicating that this pathway is active in these cells at least for VEGF regulation (Nakagawa *et al.*, 2004). Similarly in renal fibroblasts, protein kinase C inhibitors were seen to block hypoxia induced increases in TIMP-1 mRNA expression (Norman *et al.*, 1999; Norman *et al.*, 2000). Since protein kinase C activation is also capable of increasing TG2 expression in other cells types (Ishii and Ui 1994), this may represent a potential mechanism of hypoxic TG2 regulation in tubular cells.

The parallel increases in extracellular TG2 are likely to represent an increase in export since a link has been demonstrated between increased intracellular expression and externalisation of TG2 in a number of previous studies (Gaudry *et al.*, 1999; Verderio *et al.*, 1999; Skill *et al.*, 2004). However, it cannot be ruled out that the cellular stress imposed on the tubular cells by the hypoxic environment is responsible for its release. Studies of HK-2 cells cultured under hypoxic conditions demonstrate an increase in cell permeability in response to hypoxia (Leonard *et al.*, 2003). It has been suggested that re-distribution of phospholipids within the plasma membrane may underlie such changes (Zager *et al.*, 1999). In this study, extracellular TG2 was only measured at 6 and 24 hours since these were the time-points at which intracellular activity was increased however, if examination of the other time points had been performed it may have revealed a consistent release of the enzyme. Measurement of lactate dehydrogenase (LDH) release into the media is clearly required to confirm whether cell integrity is compromised by culture under hypoxic conditions.

Chronic metabolic acidosis is a common feature of chronic renal failure (Kraut and Kurtz 2005) and refers to a significant lowering of normal blood pH from pH 7.4 to below pH 7. Such changes in pH have previously been demonstrated to have downstream pathogenic effects on proximal tubular cells by increasing oxidative stress via the increased generation of ROS (Rustom *et al.*, 2003). The effect of lowering pH on the expression of TG2 was examined in a well established model of metabolic acidosis (Rustom *et al.*, 2003) that utilises

the LLC-PK1 cell line. Reducing the media pH to below pH 7 significantly increased levels of intracellular TG activity although these changes did not appear to be associated with an increase in intracellular protein as indicated by a reduction in the 85 kDa band. This was surprising given that increases were observed in the mRNA expression of TG2 suggesting that an increase in protein might also have been expected. However, given that an appropriate loading control was not used, it is difficult to be certain of the validity of this finding and the Western blot should be repeated with correction to β -actin.

A reduction in media pH was also associated with increases in extracellular (cell surface) TG activity as well as the TG activity in the media of LLC-PK1 tubular cells. This corresponded to apparent increases in the presence of TG2 protein in the media as indicated by increases in the expression of the 85 kDa band, suggesting the increased externalisation of TG2, although again correction for loading was not performed. Interestingly, the increased detection of a number of other bands was also observed in response to low pH. Whilst, the appearance of multiple bands may indicate non-specific binding, the high specificity of the TG100 antibody for TG2 suggests that this is unlikely. Additional bands larger than TG2 may indicate the presence of post-translationally modified forms of TG2 although previous work on the externalisation of TG2 from 3T3 fibroblasts (Balklava *et al.*, 2002) demonstrates that the molecular weight of externalised TG2 is unaltered. Alternatively, they may simply represent the interaction of TG2 with serum proteins present in the media. The presence of numerous smaller bands is likely to reflect proteolytic breakdown of TG2 either by factors present in the media or by intrinsic endopeptidase activity. Interestingly, previous studies of glucose stimulated OK cells show that increases in extracellular TG2 activity and protein are also associated with elevated endopeptidase activity leading to the detection of numerous antigenic fragments by Western blot (Skill 2001). For this reason, it may have been better to analyse changes in TG2 media protein levels by an alternative method such as fibronectin binding TG2 ELISA (Skill *et al.*, 2004) to eliminate some of this interference.

The data presented on LLC-PK1 cells clearly indicates that metabolic acidosis is a stimulator of TG2 and this may act by a variety of mechanisms. For example, pH-dependent changes in a number of transcription factors that have the potential to control TG2 expression have been demonstrated. In particular, low pH is able to stimulate the transcription and increase the DNA binding activity of Sp-1 (Torigoe *et al.*, 2003). A number of Sp-1 binding sites have been located within the TG2 gene promoter (Lu *et al.*, 1995) that have been linked to the gene response to retinoic acid (Shimada *et al.*, 2001). Increasing evidence suggests that acidosis may also elicit its effect on gene expression by modulating components of the

hypoxia response pathway, thus increasing HIF-1 α (Mekhail *et al.*, 2004). Low pH has been demonstrated to neutralise the function of Von Hippel Lindau tumour suppressor protein, which is the recognition component of an E3 ubiquitin protein ligase that targets HIF-1 α for proteasomal degradation (Mekhail *et al.*, 2004). Clearly this would lead to an accumulation of HIF-1 and activation of hypoxia-responsive genes. Since data presented in this chapter suggests that tubular TG2 is also capable of being modulated by hypoxia, acidosis has the potential to act via this pathway.

Recent studies by other groups of metabolic acidosis in LLC-PK1 cells have highlighted the role of oxidative stress in the response to low pH. A reduction in cellular glutathione and the generation of ROS have been implicated in the downstream pathogenic effects on tubular cells (Rustom *et al.*, 2003). Interestingly, increased ROS generation and subsequent alteration in cell redox state in primary astrocytes exposed to glutamine is known to stimulate TG2 expression (Campisi *et al.*, 2004) suggesting that induction of TG2 may be part of a broader biochemical response to oxidative stress.

The data presented in this chapter has suggested that common pro-fibrogenic stimuli such as growth factors and cytokines may not be effective at stimulating the tubular expression and activity of TG2 although further clarification is clearly required. However, cellular stress factors such as chronic hypoxia and acidosis have the potential to contribute to the increased TG2 expression observed in chronic renal disease. Such data may be important in developing strategies aimed at controlling the elevated expression of TG2 in CKD.

Chapter 5

Generation and Characterisation of TG2 Over-expressing Tubular Epithelial and Mesangial Cells

5.1 Introduction

The increased expression and cellular release of TG2 by tubular epithelial and mesangial cells is a consistent feature of both experimental and human renal disease (Johnson *et al.*, 1997; Johnson *et al.*, 1999; Johnson *et al.*, 2003b; Skill *et al.*, 2001). In tubular epithelial cells, elevated intracellular TG2 levels are associated with cytoplasmic increases in the $\epsilon(\gamma$ -glutamyl) lysine product of the enzyme and increased levels of TG2 and crosslink in the peritubular space (Johnson *et al.*, 1997; Johnson *et al.*, 1999). In the glomerulus, increases in TG2 expression and its $\epsilon(\gamma$ -glutamyl) lysine product are predominantly extracellular and are directly related to increased TG2 production (Skill *et al.*, 2001). In both compartments, elevated TG2 expression is paralleled by the development of scarring. This has led to the hypothesis that over-expression and cellular release of TG2 by tubular and mesangial cells is the driving force for the development of fibrosis. Once in the extracellular environment TG2 may play a direct role in influencing ECM accumulation.

In order to investigate this hypothesis and examine the role of TG2 in matrix changes associated with fibrosis, a suitable cell culture model is required which allows the modulation of TG2 expression. As chapter 4 demonstrates, TG2 can be stimulated in tubular cells by both hypoxia and acidosis suggesting that these could be used to modulate TG2. However, these stimuli are known to affect a number of ECM regulating systems including growth factors, MMPs and TIMPs making the interpretation of TG2-specific ECM changes difficult.

To address this, over-expression of TG2 in tubular epithelial cells (OK cell line) and mesangial cells (1097 cell line) by stable transfection will be utilised. Cells will be transfected with the commercially-available constitutive expression vectors pCIneo (OK) and pSG5 (1097) into which have been inserted the 3.3kb human TG2 gene. Such an approach has been used successfully in the study of the role of TG2 in a number of other processes including cell-matrix interactions (Gentile *et al.*, 1992; Jones *et al.*, 1997) and apoptosis (Melino *et al.*, 1994).

Once generated, stable OK and 1097 cell clones showing increased TG2 activity will be selected for further study. These selected clones will be characterised in terms of their TG2 protein and mRNA expression. To ensure that over-expression of TG2 does not alter other cellular characteristics, changes in cell morphology and growth rates will be investigated.

An important consideration in this part of the study is whether TG2 over-expression in these two cell lines is able to influence the cell surface expression of TG2. A number of studies have shown that increasing the intracellular expression of TG2 by transfection is

associated with elevated levels of TG2 at the cell surface (Gaudry *et al.*, 1999a; Gaudry *et al.*, 1999b; Verderio *et al.*, 1998). This is important since TG2 appears to have a predominantly extracellular role in the scarring process. Therefore the extracellular TG2 expression and enzyme activity will be determined in selected clones using specific cell culture-based ELISA assays.

5.2 Results

5.2.1 Intracellular TG activity

Transfection of OK cells with the expression vector pCIneo-htg yielded 50 stable clones, 43 of which showed increased TG activity compared to wild type cells. Increases ranged from double to 15 times basal TG activity (fig 5.1a). Of these, three clones were chosen to use in subsequent experiments tTg 18, tTg21 and tTg7 that had TG activities of double, 5.5 and 7 times that of control cells respectively (fig 5.1b).

Twenty eight stable clones were generated as the result of transfecting 1097 cells with the pSG5-htg expression vector. Of these, 15 showed elevated TG activity compared to wild type cells (fig 5.2a). Three clones were chosen from the 15 for use in subsequent experiments: tTg 34, tTg 36 and tTg 37 that had TG activities of 1.3, 5 and 14 times that of untransfected 1097 cells (fig 5.2b).

5.2.2 TG2 protein

Western blot analysis of cell homogenates from the selected OK and 1097 clones was used to determine whether increased intracellular TG activity was associated with elevated levels of TG2 protein. Blots were immunoprobed using a highly specific mouse monoclonal anti-TG2 antibody (TG100). In OK proximal tubular cell clones, increased TG2 protein expression (fig 5.3a) was indicated by an increase in a single band of around 85 kDa. All three clones showed increased expression compared to wild type (Con) and transfection control (TF Con) cells. Densitometry of Western blots (in parentheses) indicated that in all three clones the increase in TG2 antigen was greater than that observed for TG activity. Transglutaminase protein expression was increased 5 fold for tTg 18, 25 fold for tTg 21 and 27 fold for tTg 7 compared to expression in the transfection control.

In 1097 mesangial cells, endogenous TG2 expression was indicated by a single band at 85kDa in controls, tTg34 and tTg36 cells (fig 5.3b). In tTg 37 cells, this appeared to become a doublet of 77-85 kDa. An additional band at 90 kDa was present in all three selected clones and was weakly detected in control cells and the pSVneo transfection control. The intensity of this band was found to correspond to increased intracellular TG activity. Densitometry analysis of this 90kDa band indicated a 10 fold increase in protein expression in tTg 34, 9 fold in tTg 36 and 40 fold in tTg 37 compared to the pSVneo transfection control.

Figure 5.1 TG Activity of TG2 Over-expressing OK Tubular Cell Clones

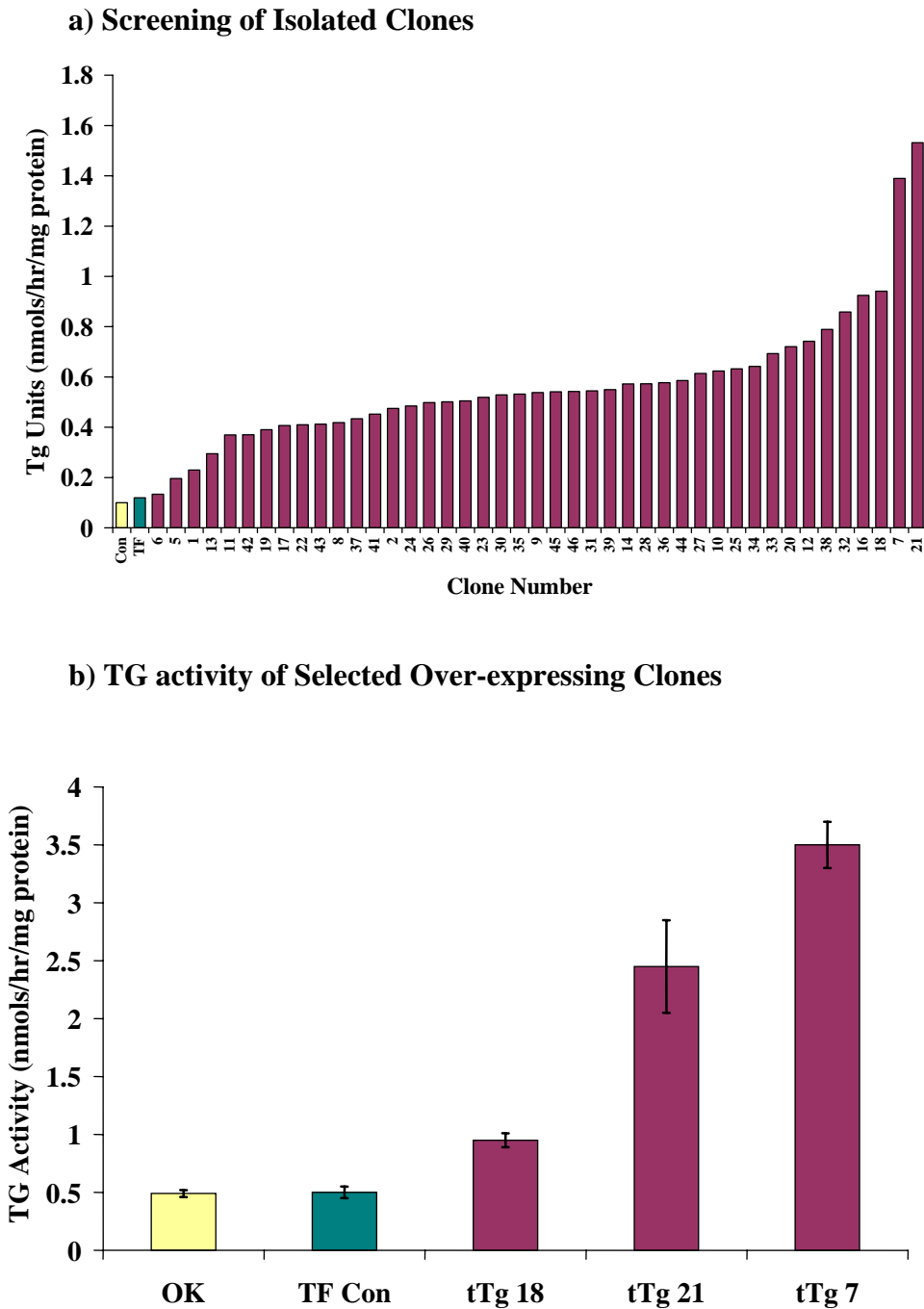
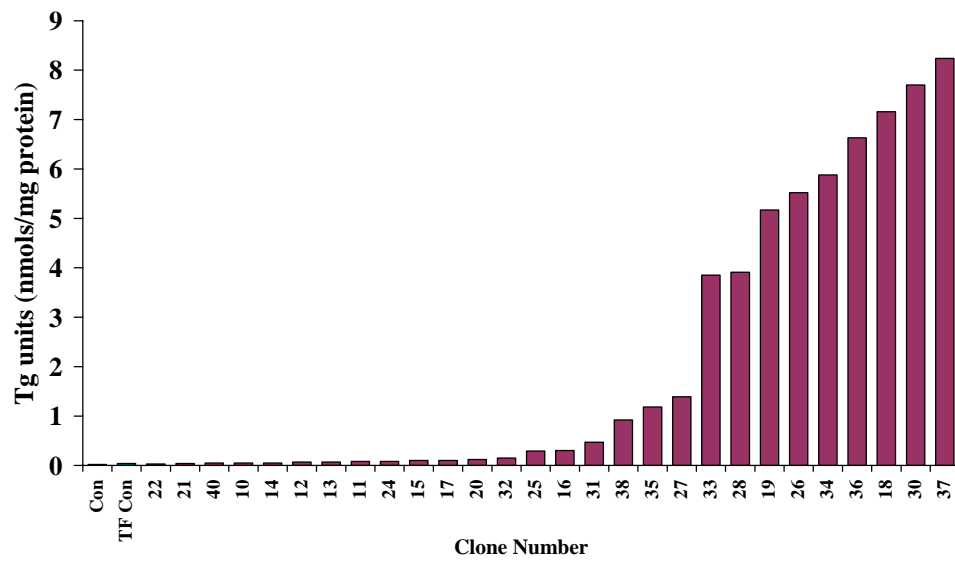


Figure 5.1 OK cells were transfected with pCIneo-htg using Lipofectin® reagent as described in section 3.2.2. 50 stable clones were generated and screened for intracellular TG activity by the putrescine incorporation assay (a). Of the 50 clones, 43 showed increased TG activity (purple) compared to wild type cells (yellow) and cells transfected with pCIneo empty vector (green). From the 43 clones, 3 were chosen for further characterisation (b), tTg 18, tTg 21 and tTg 7 that had 2, 5.5 and 7 times basal TG activity respectively. TG activity is expressed as nmols/hour/mg protein and represents mean \pm SEM from three separate experiments performed in triplicate.

Figure 5.2 TG Activity of TG2 Over-expressing 1097 Mesangial Cell Clones

a) Screening of Isolated Clones



b) TG Activity of Selected Over-expressing Clones

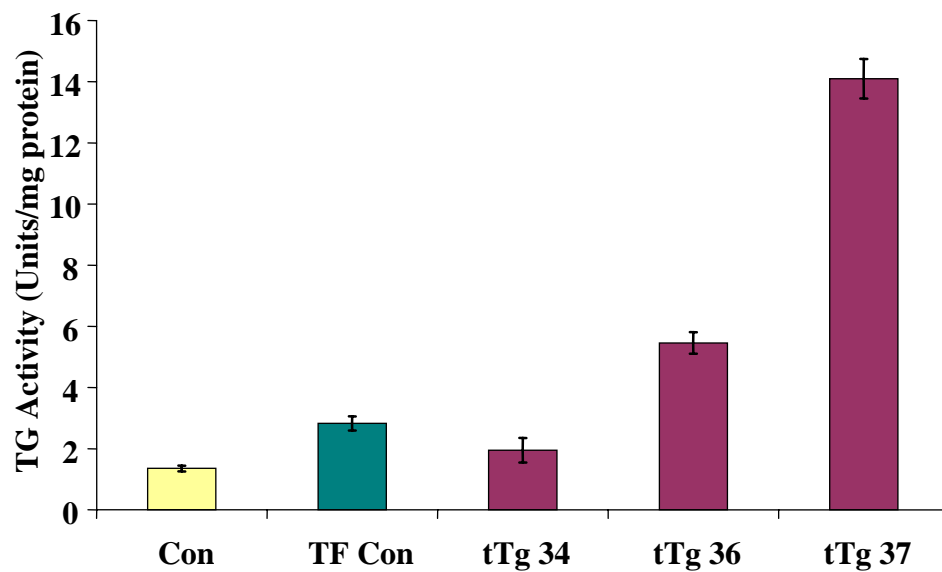
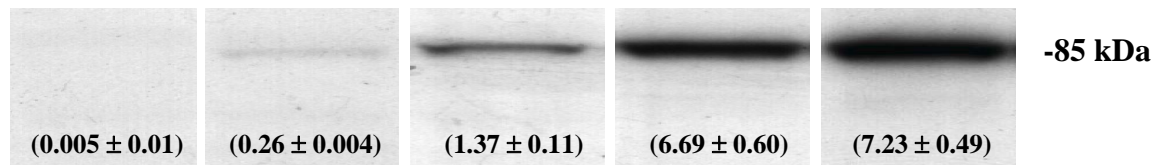


Figure 5.2 1097 cells were transfected with the pSG5-htg expression vector and the Nucleofection system as described in section 3.2.3. 28 clones were generated and screened for intracellular TG activity by the putrescine incorporation assay (a). Of the 28 clones, 15 showed increased TG activity (purple) compared to wild type (yellow) and transfection control cells (green). From these 15, 3 clones were selected (b) tTg 34, tTg 36 and tTg 37 that had 1.3, 5 and 14 times basal TG activity respectively. TG activity is expressed as nmols/hour/mg protein and represents mean \pm SEM from three separate experiments performed in triplicate.

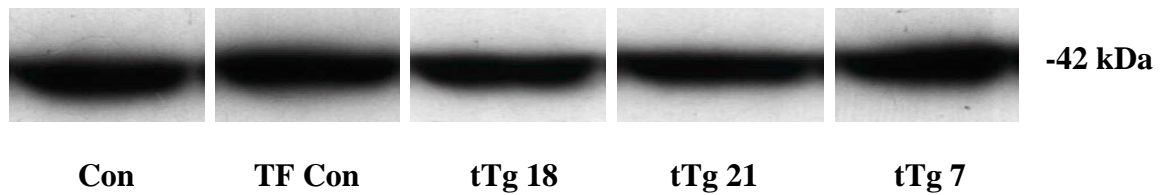
Figure 5.3 Western Blot Analysis of Selected Over-expressing Clones

a) OK Cell Clones

Tissue Transglutaminase

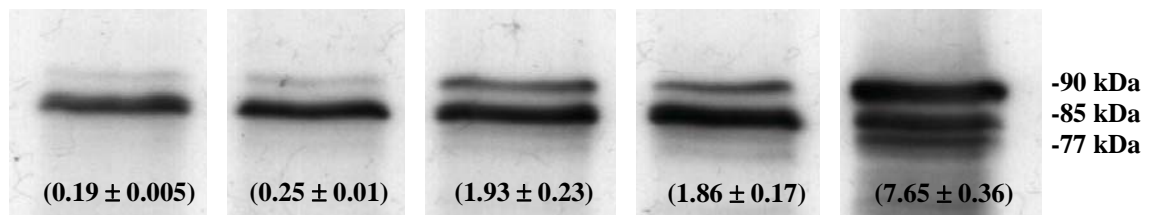


β -actin



b) 1097 Cell Clones

Tissue Transglutaminase



β -actin

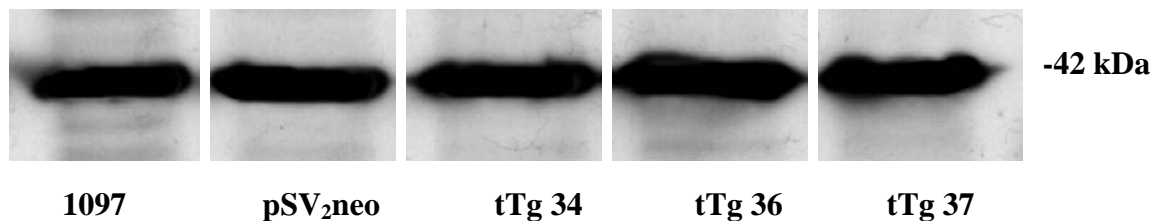


Figure 5.3 A volume equivalent to 20 μ g of protein from each cell homogenate was separated on a 10% (w/v) polyacrylamide gel, electrophoresed and blotted onto hybond C membrane as described in section 3.3.6. Western blots were immunoprobed for TG2 with 1:750 dilution of mouse monoclonal anti-TG2 antibody (TG100) and revealed by chemiluminescence as described in section 3.3.6.2. Values in parentheses indicate volume density measurements corrected for loading using β -actin.

5.2.3 TG2 mRNA expression

To determine whether increases in tissue transglutaminase expression were mRNA dependent, TG2 mRNA levels in transfected clones were examined by Northern blot analysis (figure 5.4). In both OK cell clones (figure 5.4a) and 1097 mesangial clones (figure 5.4b) there was an mRNA dependent increase in TG2 expression as indicated by increases in the 3.5 kb TG2 transcript. In the OK clones, densitometry analysis demonstrated a 1.5 fold, 3 fold and 4 fold increase in TG2 mRNA in clones tTg18, tTg21 and tTg7 respectively compared to RNA isolated from cells transfected with pCIneo alone. In 1097 cells, clones tTg34, tTg36 and tTg37 showed increases in TG2 mRNA of 4, 10 and 17 fold respectively compared to the transfection control.

5.2.4 Effect of TG2 expression on cell morphology

In order to determine if transfection of either OK cells or 1097 cells with the human TG2 gene had any effects on cell morphology, transfected cells were probed for TG2 by immunocytochemistry and their morphology studied using light microscopy. Figures 5.5 and 5.6 show representative micrographs (200 x magnification) of transfected OK and 1097 cell clones compared to wild type and transfection control cells. Interestingly, at low cell density, OK and clone tTg 21 cells showed a more spindle-like appearance however, as cells became more confluent no apparent difference in cell morphology was observed between wild type (fig 5.5A) and transfected OK cells (fig 5.5 B, C, D and E). Both maintained a typical cobblestone epithelial cell morphology and there did not appear to be an increase in cells showing morphological signs of apoptosis. Similarly, transfected 1097 cells (fig 5.6 B, C, D and E) showed no observable differences in cell morphology compared to wild type cells (fig 5.6 A).

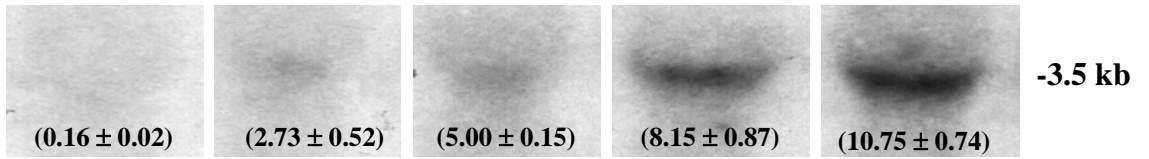
5.2.5 Growth characteristics of selected clones

The growth characteristics of both OK and 1097 transfected clones were determined by seeding a known cell number and counting attached cells at 24 hour intervals post seeding, using a haemocytometer. The log of the cell number was used to generate linear plots from which growth rates and cell doubling times were calculated (fig 5.7). No significant difference in growth rate was observed between OK clones tTg18, tTg21, tTg7 or pCIneo transfected cells compared to wild type OK cells (fig 5.7a). Doubling time for all cell clones was between 16-18 hours. Similarly, no significant difference in growth rate was observed between 1097 TG2 over-expressing clones compared to wild type cells (fig 5.7b).

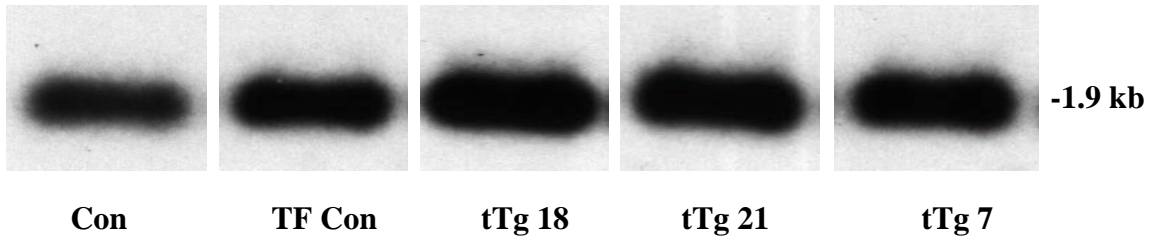
Figure 5.4 Northern Blot Analysis of Selected Over-expressing Clones

a) OK Cell Clones

Tissue Transglutaminase

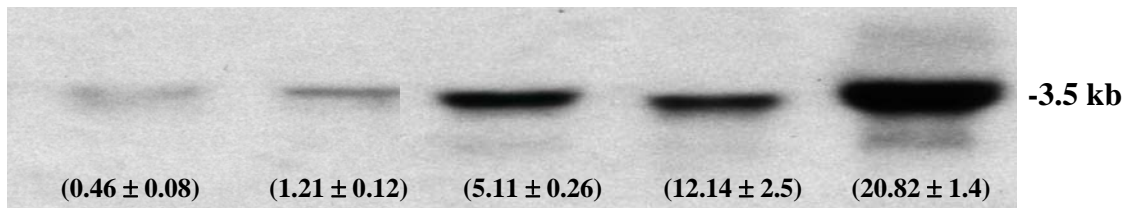


Cyclophilin



b) 1097 Cell Clones

Tissue Transglutaminase



Cyclophilin

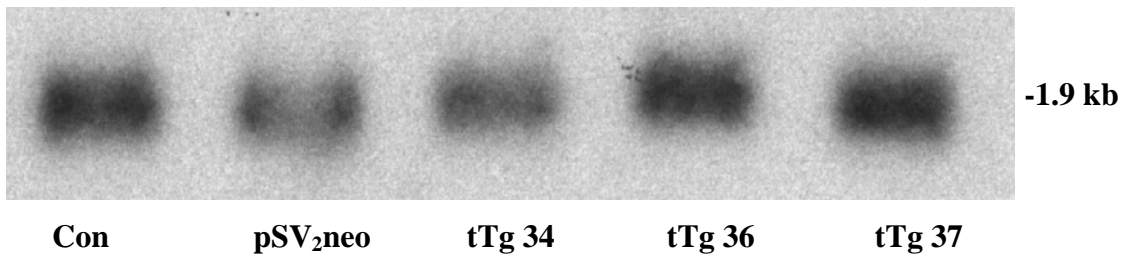


Figure 5.4 Total RNA extracted from OK (a) and 1097 cell clones (b) was separated on a 1.2% agarose/formaldehyde gel, blotted onto Hybond N membrane and probed with a random primed ³²P-dCTP labelled TG2-specific cDNA probe. Films were analysed by volume densitometry and transcript size determined by comparison to RNA molecular weight markers. Values in parentheses indicate volume densitometry measurements corrected for loading using the housekeeping gene cyclophilin.

Figure 5.5 Morphology of TG2 Over-expressing OK Tubular Cells

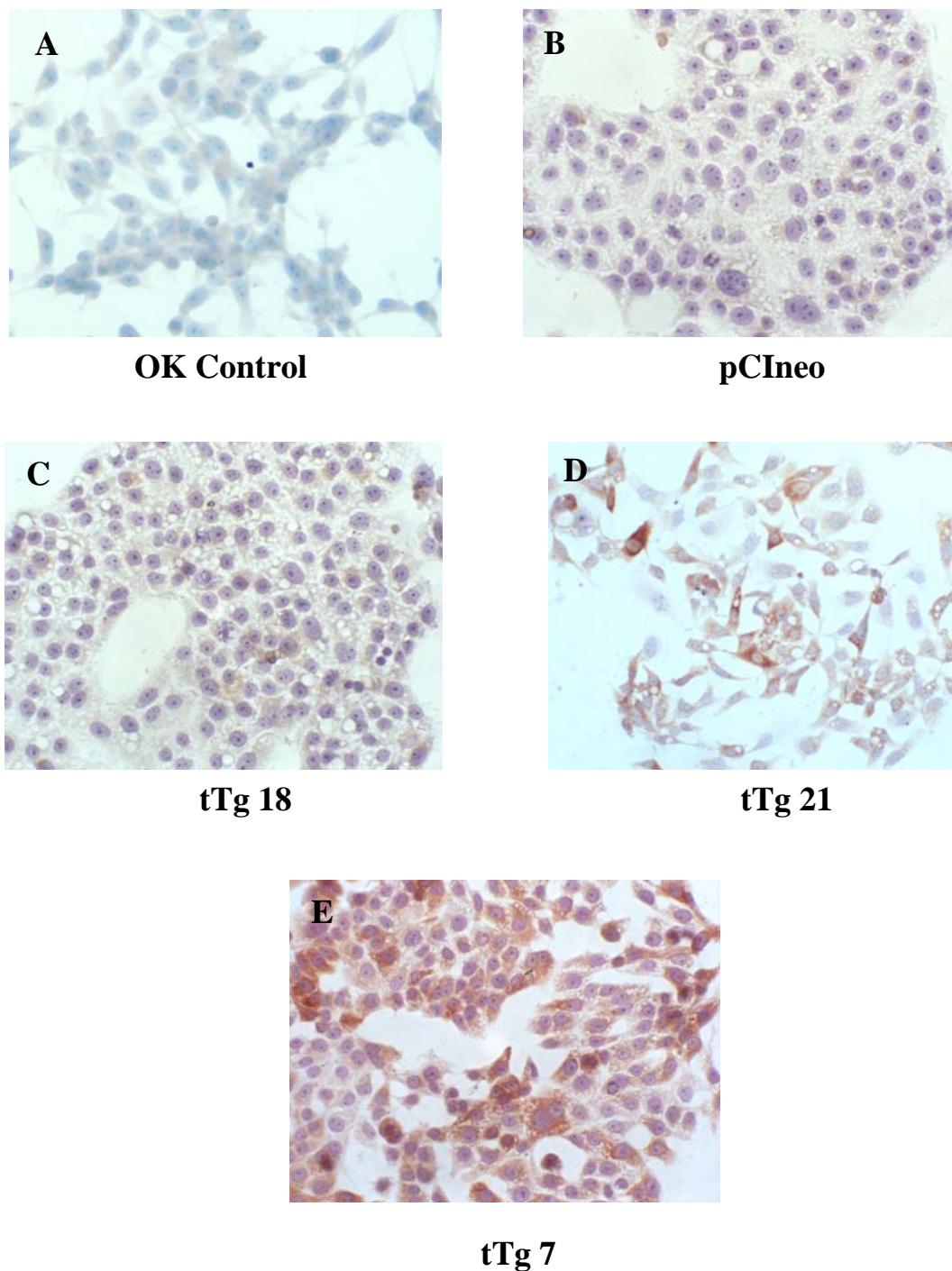


Figure 5.5 The morphology of TG2 over-expressing OK cell clones was analysed following immunocytochemical staining for TG2. Cells grown on coverslips were fixed in methanol, permeabilised and immunostained for TG2 with anti-TG2 monoclonal antibody (TG100) as described in section 3.3.7.4. Cells were visualised by light microscopy at 200 x magnification on an Olympus BH-2 microscope.

Figure 5.6 Morphology of TG2 Over-expressing 1097 Mesangial Cells

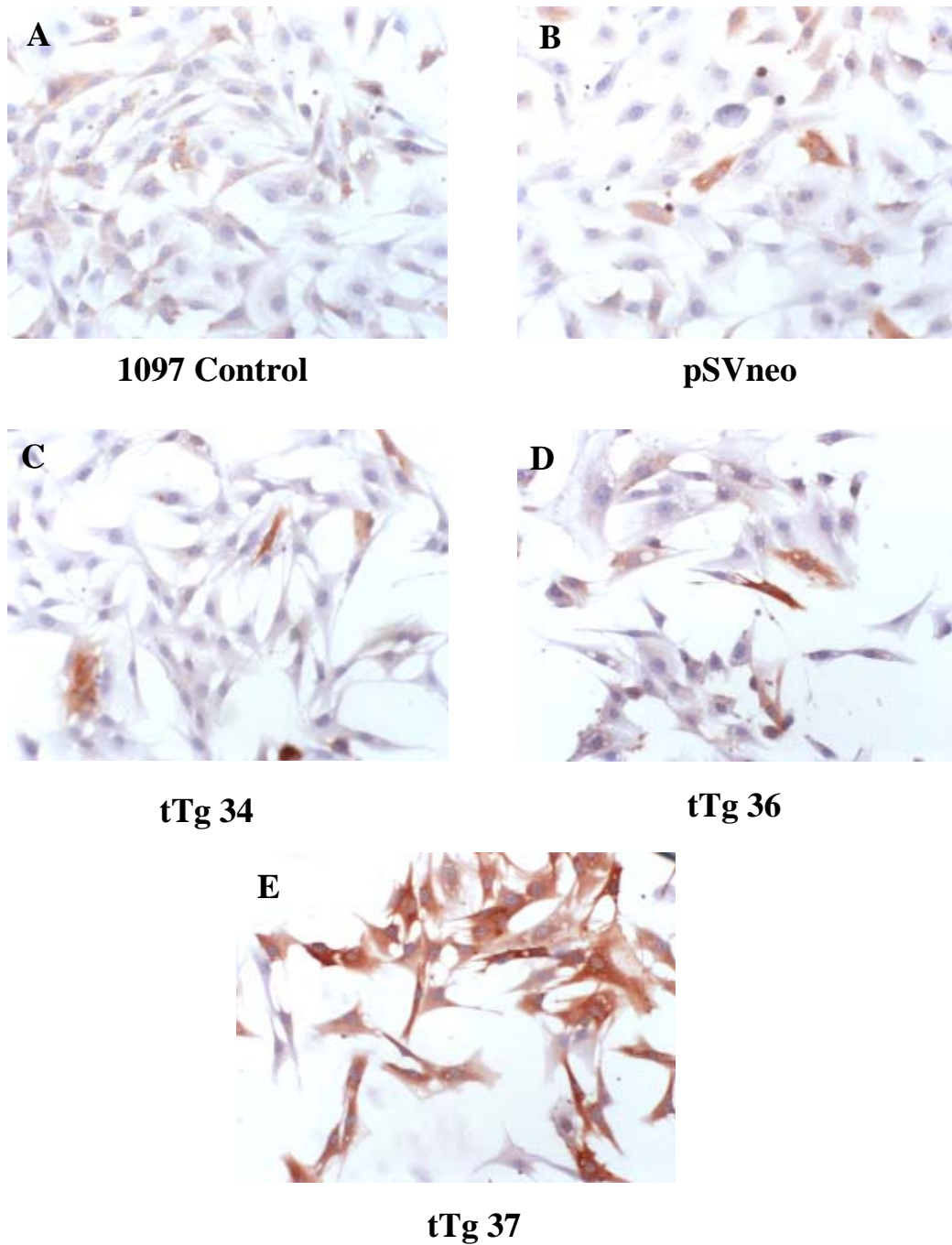
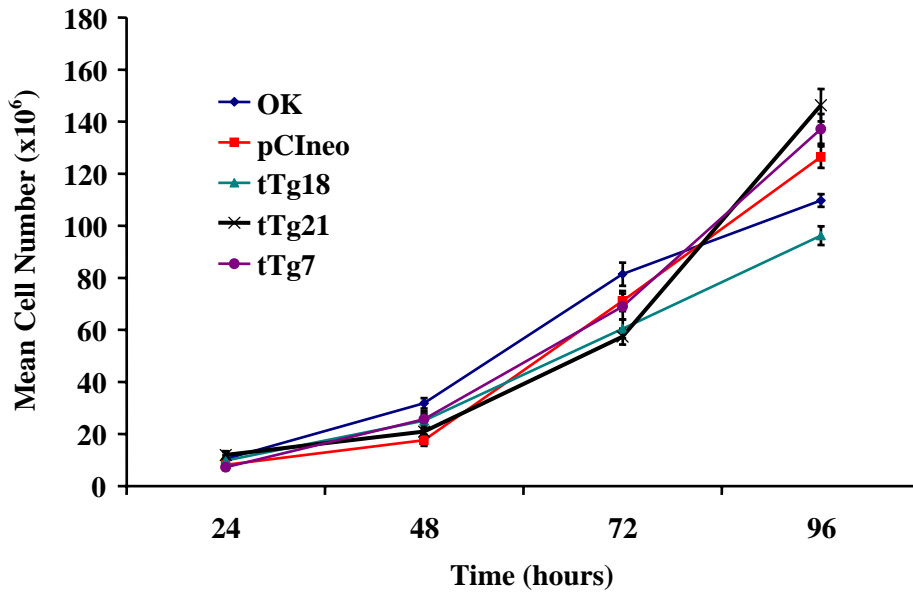


Figure 5.6 The morphology of TG2 over-expressing 1097 cell clones was analysed following immunocytochemical staining for TG2. Cells grown on coverslips were fixed in methanol, permeabilised and immunostained for TG2 with anti-TG2 monoclonal antibody (TG100) as described in section 3.3.7.4. Cells were visualised by light microscopy at 200 x magnification on an Olympus BH-2 microscope.

Figure 5.7 Growth Curves of Selected Over-expressing Cell Clones

a) OK Cell Clones



b) 1097 Cell Clones

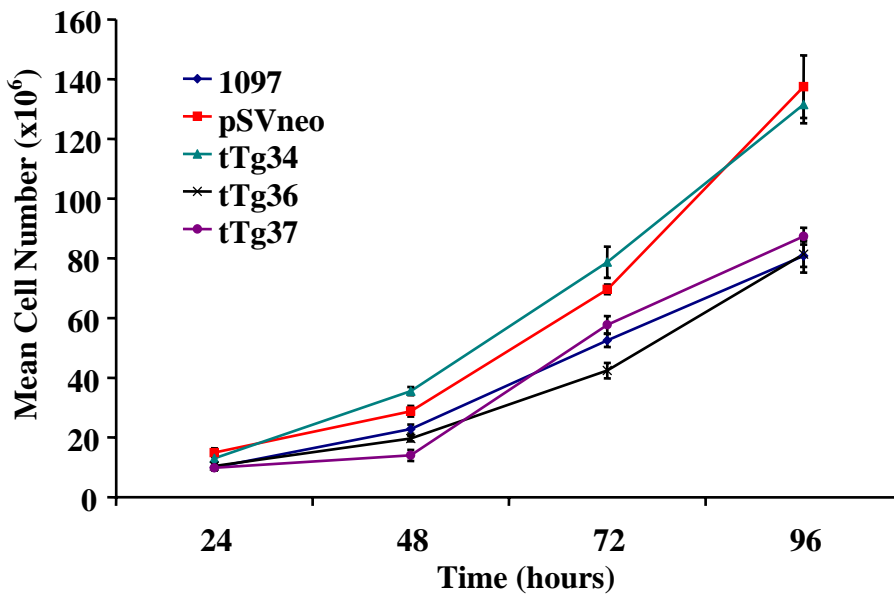


Figure 5.7 Cells were seeded at a density of 1×10^6 cells per flask. At 24, 48, 72 and 96 hours post seeding, cells were trypsinised and counted on a haemocytometer as described in section 3.2.5. Data represents the mean cell number of duplicate flasks \pm SEM

5.2.6 Extracellular TG2 expression

5.2.6.1 Extracellular TG activity

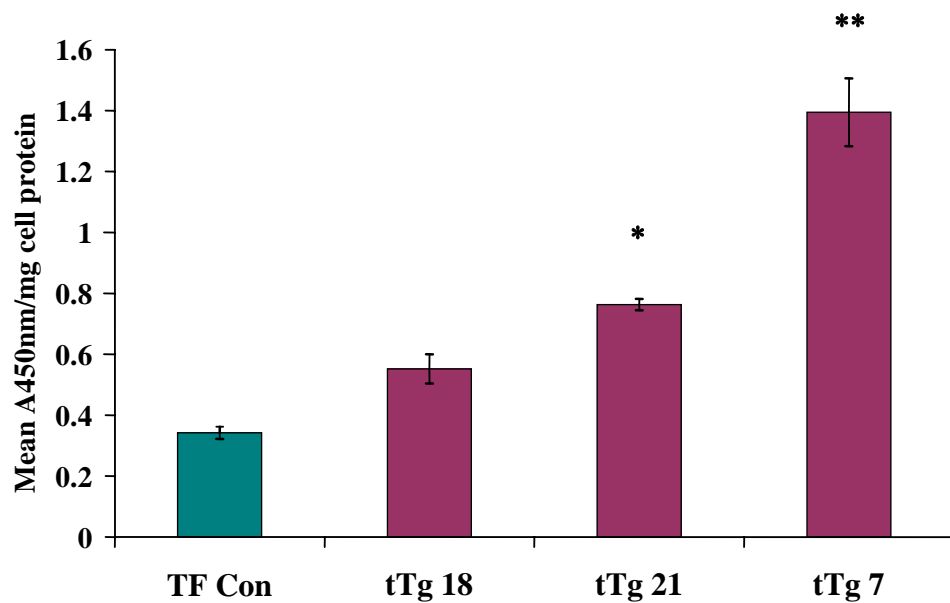
A cell ELISA which utilises the ability of active TG2 to incorporate the TG2 substrate biotin cadaverine into fibronectin was used to determine if increased TG2 expression resulted in changes in extracellular TG activity (fig 5.8). In all three TG2 over-expressing OK clones (fig 5.8a) an increase in TG2 expression produced a corresponding increase in extracellular TG activity (tTg21 $p < 0.01$ and tTg7, $p < 0.0001$; one way ANOVA with Bonferroni post hoc test). However, the magnitude of these increases was not as great as for intracellular activity being only 1.5 fold (tTg18), 2 fold (tTg21) and 4 fold (tTg7) that of the transfection control. In comparison, no significant changes in extracellular TG2 activity were observed in 1097 TG2 over-expressing clones (fig 5.8b).

5.2.6.2 Extracellular TG2 antigen

To establish whether increased intracellular expression of TG2 influenced the extracellular expression of TG2, a modified cell ELISA was used in which live cells were incubated with anti-TG2 antibody (CUB7402) and antigen-antibody binding revealed with HRP-conjugated anti-mouse IgG secondary antibody (fig 5.9). Again, in OK cells (fig 5.9a) increased intracellular TG2 expression resulted in a corresponding increase in extracellular antigen expression (tTg 18, $p < 0.05$; tTg 21 and tTg 7, $p < 0.01$; one way ANOVA with Bonferroni post hoc test). The magnitude of these changes also did not exactly match that of intracellular activity being increased by 3.8 fold (tTg18), 6.7 fold (tTg21) and 8.6 fold (tTg7) compared to the TF control. More significantly, increases in extracellular TG2 antigen were also much greater than that observed for extracellular activity. In 1097 cells, small increases in the extracellular expression of TG2 were observed in all three clones although this was not significant.

Figure 5.8 Extracellular TG Activity of Selected Over-expressing Clones

a) OK Cell Clones



b) 1097 Cell Clones

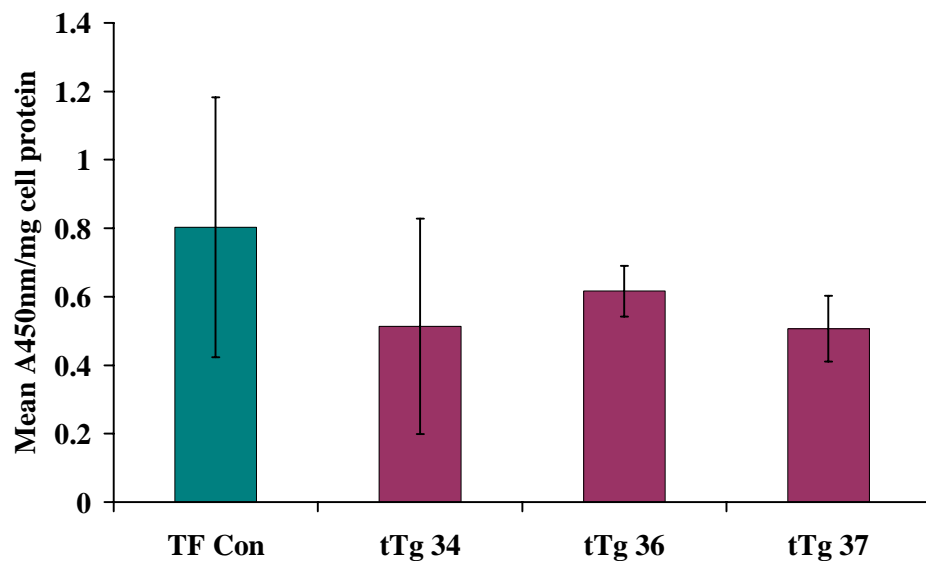
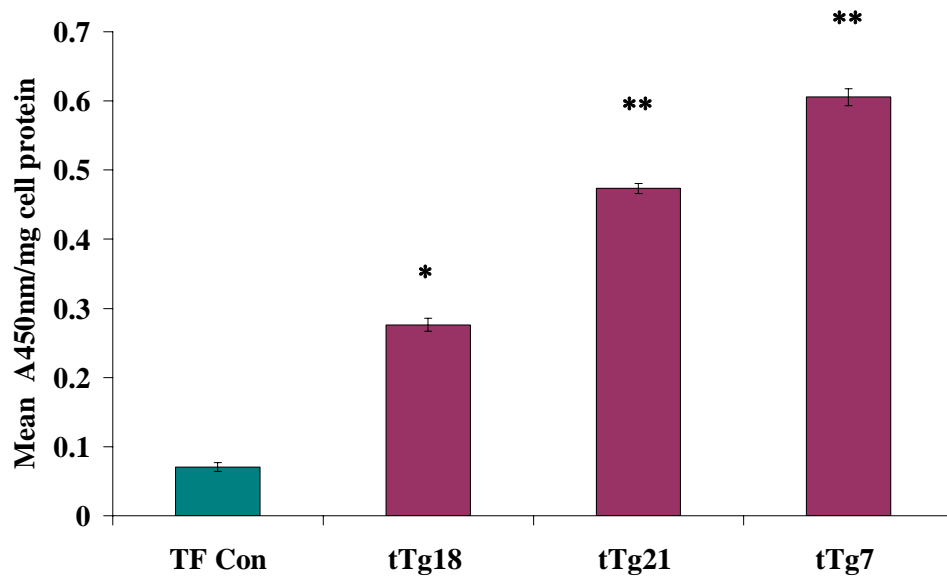


Figure 5.8 TG2 over-expressing clones from OK cells (a) and 1097 cells (b) were plated in 96 well plates coated with fibronectin, allowed to attach for 3 hours and analysed for extracellular TG activity using a cell ELISA which utilises the ability of active TG to incorporate biotin cadaverine into fibronectin (section 3.3.7.5). Values were corrected for deoxycholate solubilised cell protein. Data represents mean absorbance at 450nm/mg cell protein \pm SEM from three separate experiments, n=10 per experiment. *=p<0.01, **=p<0.0001 compared to the TF control by one way ANOVA with Bonferroni post hoc test.

Figure 5.9 Extracellular TG2 Antigen Levels of Selected Over-expressing Clones

a) OK Cell Clones



b) 1097 Cell Clones

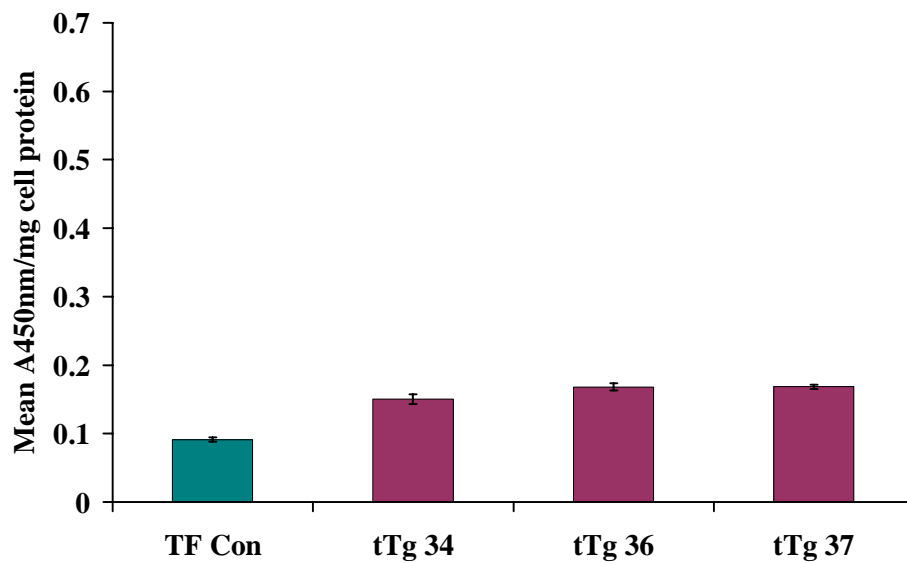


Figure 5.9 Extracellular TG2 antigen was determined by cell ELISA in which OK cell clones (a) or 1097 cell clones (b) were incubated overnight with anti-TG2 antibody (CUB7402) and revealed with 1:1000 anti-mouse HRP (section 3.3.7.6). Parallel plates were used for protein correction. All data represents mean absorbance at 450nm/mg cell protein \pm SEM from three separate experiments, n=10 per experiment. *= p<0.05, **=p<0.01 compared to the TF control by one way ANOVA with Bonferroni post hoc test.

5.3 Discussion

The increased expression of TG2 and its $\epsilon(\gamma\text{-glutamyl})$ lysine product by tubular and mesangial cells is an established event in the development of fibrosis (Johnson *et al.*, 1997; Johnson *et al.*, 1999; Johnson *et al.*, 2003b; Skill *et al.*, 2001). In order to investigate the role of elevated TG2 in the ECM changes associated with scarring, OK proximal tubular cells and 1097 mesangial cells were transfected with constitutive expression vectors containing the 3.3 kb human TG2 gene. A number of other groups have successfully used constitutive TG2 expression systems to study of the role of TG2 in cell-matrix interactions (Gentile *et al.*, 1992; Jones *et al.*, 1997). However, this is the first time that TG2 expression in renal cells has been modulated in this way.

Stable transfection of tubular and mesangial cell lines with TG2 resulted in the successful generation of 43 OK cell clones and 15 1097 mesangial cell clones possessing increased intracellular TG2 activity with respect to control cells. From these, three clones were selected from each cell line that had differing levels of expression. Interestingly, a difference in the intracellular TG activity of selected clones was observed at the initial screening and after the first few passages however, beyond this clones showed stable and elevated expression of TG2 for up to 15 passages post transfection. This initial drop in TG activity could be explained by previous studies that have demonstrated an increased susceptibility of cells expressing high levels of transglutaminase to undergo apoptosis (Verderio *et al.*, 1998). Thus cells expressing TG2 above a certain threshold may rapidly be deleted.

Given the stable expression of TG2 by transfected cells, a surprising finding was the apparent variation in immunocytochemical staining for TG2 within cells derived from the same clone, a finding which was evident in both tubular and mesangial cells. Whilst care was taken after transfection to select and pick colonies of cells that appeared to originate from a single cell, it cannot be ruled out that the selected clones are a heterogeneous population. However, studies of 3T3 fibroblasts stably transfected with constitutive expression vectors containing TG2 also show varying degrees of immunocytochemical staining for the enzyme despite being derived from individual colonies (Gentile *et al.*, 1992), suggesting that differences are not due to genetic heterogeneity. The variability in TG2 staining in 3T3 fibroblasts has been proposed to reflect differences in the degree to which the TG construct is expressed in individual cells (Gentile *et al.*, 1992) which may also be the case in stably transfected tubular and mesangial cells. Such heterogeneity may contribute to the viability of stable cell lines by preventing TG2 expression from reaching that which may promote cell

death. Given the apparent difference in expression by individual cells, establishing the purity of selected clones may therefore prove to be difficult.

A potential limitation of using stable TG2 over-expressing clones is that clones may be selected that are able to tolerate elevated TG2 by modifying associated pathways. A number of other studies have overcome this problem by using an inducible TG2 expression system in which TG2 is modulated by the presence or absence of tetracycline (tet on/off) (Balklava *et al.*, 2002; Piacentini *et al.*, 2002; Verderio *et al.*, 1999; Verderio *et al.*, 1998). This approach was initially attempted with both OK and 1097 cell lines but was abandoned due to problems with successfully transfecting these cells with the multiple vectors required for operation of the Tet system (data not shown) and because adequate control of TG2 expression by tetracycline was not achievable.

The selection of three clones from each cell line that had varying TG2 activity and correlating changes with matrix-associated $\epsilon(\gamma\text{-glutamyl lysine})$ crosslink was designed to minimise the problems associated with clonal variation. In addition, clones were characterised in terms of their growth rate and morphology to establish whether they showed cellular changes in response to TG2 modulation. The measurement of cell growth indicated no significant difference in growth rate between transfected and wild type cells. Similarly, a comparison of cell morphology between OK or 1097 cell clones and their respective control cells did not show any appreciable difference that might be attributable to increased TG2. This finding is contrary to previous studies of 3T3 fibroblasts and hamster fibrosarcoma cells in which cells show a more flattened and extended morphology in response to constitutive over-expression of TG2 (Gentile *et al.*, 1992; Johnson *et al.*, 1994). However, it is in keeping with studies utilising inducible expression of TG2 (Verderio *et al.*, 1998), in which cell morphology is unaltered in response to increased enzyme. A number of studies have demonstrated that changes in cell morphology in response to TG2 are associated with changes in adhesion to the substratum and the resistance to trypsinisation (Gentile *et al.*, 1992; Balklava *et al.*, 2002; Gaudry *et al.*, 1999a; Johnson *et al.*, 1994; Jones *et al.*, 1997). Surprisingly, visual inspection of the highest expressing clones from each cell line (M Fisher, personal observation) seemed to indicate increased resistance to trypsinisation suggesting that some change in morphology may have been expected.

Over-expression of TG2 also did not appear to increase the number of cells showing morphological signs of apoptosis. As suggested earlier, this may be because many of the cells susceptible to apoptosis as a result of extremely high levels of TG2 expression have already been deleted at early passage, leaving cells capable of sustaining the levels of TG2 reported

here. The ability of these remaining cells to tolerate high TG2 expression is likely to be due to the relative inactivity of the intracellular enzyme in intact cells under normal conditions of basal calcium (Verderio *et al.*, 1998).

Western and Northern blot analysis of selected clones demonstrated that elevated intracellular TG activity corresponded to increases in TG2 mRNA and was associated with increased TG2 protein expression. Interestingly, particularly in OK cells, the fold changes in mRNA were much lower than for TG2 protein expression. The discrepancy between the level of mRNA and protein expression in these cells suggests that TG2 may be subject to some form of post-transcriptional regulation that may affect its rate of translation or mRNA stability although little evidence for this is presented in the literature. In OK cells, increased TG2 protein expression was demonstrated by a rise in the presence of a single band at 85 kDa that represented full length TG2. In the 1097 cell line, both control and selected TG2 clones exhibited a band at 85kDa however, the highest expressing clone tTg 37 appeared to have a doublet band. An additional band was also observed at 90 kDa that was weakly detected in normal and transfection control cells and which increased in intensity in cells transfected with pSV₂neo + pSG5-htg, corresponding to increased TG activity.

The appearance of a smaller band in clone tTg37 cells may indicate the expression of a shorter isoform of TG2 as the result of alternative splicing. The presence of a slightly truncated isoform of TG2 has recently been described which would be consistent with this observation (Antonyak *et al.*, 2006) and interestingly, the Northern blot of clone tTg37 appears to show a slightly smaller band which would fit with the presence of an alternative transcript. The smaller band could also represent a proteolysed form of TG2 in this clone since the appearance of proteolytically cleaved TG2 is a common occurrence in the analysis of cell extracts (Griffin *et al.*, 2002). The identity of the additional 90 kDa band is uncertain given that the 85kDa band is consistent with the specificity of the monoclonal TG100 antibody for TG2. It may indicate the presence of a post-translationally modified form of TG2 that is increased in response to transfection. Interestingly, fatty acid acetylation of an intracellular pool of TG2 is thought to commonly occur which may dictate its association with the plasma membrane (Harsvalvi *et al.*, 1987). Modification of TG2 in mesangial cells following transfection could be significant in determining its localisation and may underlie the differences observed between tubular and mesangial cells in their processing of TG2.

Such differences were highlighted by the measurement of changes in the extracellular expression and activity of the enzyme. Tubular cell clones exhibited a corresponding significant increase in extracellular activity and expression in response to increasing

intracellular activity. An increase in extracellular TG2 is consistent with *in vivo* models of renal scarring in which an up-regulation of TG2 by tubular cells is associated with elevated levels of TG2 and crosslink in the peritubular space (Johnson *et al.*, 1999; Skill *et al.*, 2001). Numerous *in vitro* studies have also demonstrated a link between expression of TG2 and extracellular levels of the enzyme. For example, increased intracellular expression of TG2 in umbilical vein cells following transfection led to increased externalisation of TG2 (Gaudry *et al.*, 1999b). Similarly, induction of TG2 in 3T3 fibroblasts by stable transfection resulted in the appearance of an extracellular pool of the enzyme that localised to fibronectin (Verderio *et al.*, 1998). In OK tubular cells, glucose stimulated increases in TG2 expression and activity have been demonstrated to be associated with increased extracellular TG2 in the ECM and in culture media (Skill *et al.*, 2004). Finally, studies in human umbilical vein cells demonstrated that conversely, reduced TG2 was accompanied by a reduction in the amount of externalised TG2 enzyme (Jones *et al.*, 1997).

The presence of active extracellular TG2 in tubular cells clearly has important implications for its effects on the ECM. Significantly, previous studies have demonstrated that whilst both active and inactive forms of the enzyme are capable of being expressed at the cell surface, only active cell surface enzyme is deposited into the ECM (Balklava *et al.*, 2002).

In comparison to tubular cells, increased intracellular TG2 activity in mesangial cells did not result in an increase in either extracellular activity or expression of TG2. This is perhaps surprising given that high levels of extracellular TG2 and $\epsilon(\gamma\text{-glutamyl})$ lysine crosslink are found in the mesangium in diabetic nephropathy (Skill *et al.*, 2001). The reason for this differential cell surface expression of TG2 cannot be answered from the data generated here but suggests that tubular and mesangial cells have differently regulated export pathways that may underlie their differing functions. Such regulation may be closely related to ECM production since numerous studies have suggested a link between externalisation of TG2 and fibronectin (Akimov *et al.*, 2000; Gaudry *et al.*, 1999a; Verderio *et al.*, 1998).

The data presented in this chapter demonstrates for the first time the successful generation of stable TG2 over-expressing tubular and mesangial cell clones. These have been shown to be phenotypically normal but to differ in their extracellular expression and activity of TG2. In subsequent chapters, TG2 over-expressing tubular and mesangial cells will be utilised to investigate the effect of elevated levels of TG2 on the accumulation of ECM and further to determine whether this is associated with direct effects on the deposition and breakdown of mature ECM.

Chapter 6

Generation and Characterisation of Primary Tubular and Mesangial Cells from the TG2^{-/-} Knockout Mouse

6.1 Introduction

Chapter 5 described the generation and characterisation of stable OK and mesangial cell clones that show constitutive over-expression of TG2. Whilst providing a useful system in which to study the function of TG2 within the ECM, constitutive over-expression of TG2 may itself lead to phenotypic adaptations or clonal effects (Gentile *et al.*, 1992). A complementary *in vitro* approach would therefore be advantageous in providing confirmatory evidence for the role of TG2 in ECM accumulation.

To address this, tubular and mesangial cells have been isolated from the TG2 knockout (KO) mouse (De Laurenzi and Melino, 2001). In these animals, the targeted deletion of 1.2 kb of the TG2 gene from exon 5 to intron 6 by homologous recombination results in the abolition of the active site and the associated protein crosslinking activity (De Laurenzi and Melino, 2001). In spite of this, TG2^{-/-} mice show no phenotypic abnormality, develop normally and histological examination of their major organs appears normal. Study of these TG2-null cells will complement the over-expression studies by allowing the effect of a reduction in functional TG2 enzyme on the accumulation of ECM to be determined.

The TG2 knockout mouse model has previously been used to study the role of TG2 in the progression of renal scarring in the unilateral ureteral obstruction model (UUO) (Mohammed *et al.*, 2006). In this study, decreased TG2 activity was associated with a slowing down in the progression of tubulointerstitial scarring and glomerulosclerosis. Potentially the isolation and characterisation of TG2-null tubular and mesangial cells will shed light on the reason for this reduction in kidney scarring. This is a significant step since it will be the first time that isolated kidney cells from the TG2 KO mouse have been used in the study of TG2 action *in vitro*.

To isolate tubular and mesangial cells from TG2 knockout mice a modification of a technique described by (Takemoto *et al.*, 2002) will be utilised. Using this method retrograde perfusion of the mouse kidney with BSA-inactivated magnetic Dynabeads is performed, via cannulation of the abdominal aorta, allowing the separation of tubular and glomerular fractions. This technique relies on the physical size of the beads lodging in the glomerular tuft such that the glomeruli can be separated out magnetically and results in relatively pure cultures of tubular and mesangial cells.

In the present chapter, isolated TG2^{-/-} tubular and mesangial cells will be characterised in terms of their morphology and expression of epithelial and mesangial cell markers. The TG2 expression and activity will be determined by TG activity assay, Northern and Western

blotting. Immunofluorescence will be used to determine the level of $\epsilon(\gamma\text{-glutamyl})$ lysine crosslink within the ECM.

6.2 Results

6.2.1 Morphology of primary tubular and mesangial cells

Morphological analysis of tubular cells isolated from wild type (WT) and TG2^{-/-} mice (fig 6.1a and 6.1b) indicated that in general there was no difference in morphology between the two cell strains. Tubular cells were generally observed to have a rounded and flattened appearance that is typical of primary epithelial cells. However, wild type cells also had some areas in which the cells were more spindle-like in appearance which was not generally observed in TG2^{-/-} cells.

Mesangial cells isolated from WT and TG2^{-/-} mice (fig 6.1c and 6.1d) did not show any observable difference in their morphology. Both exhibited a typical spindle-shaped or stellate morphology similar to that of vascular smooth muscle cells.

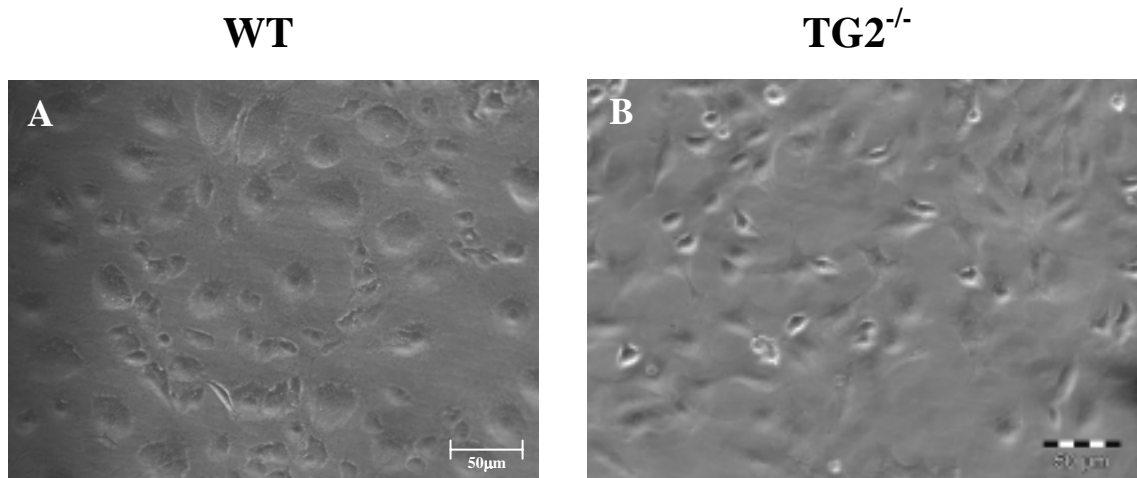
6.2.2 Cell markers

Immunofluorescent staining of tubular cells from WT and TG2^{-/-} mice for β -catenin and alpha smooth muscle actin (α -SMA) was used to establish the purity of tubular cell cultures (fig 6.2). β -catenin is a peripheral cytosolic protein involved in cell-cell interactions and expressed by tubular epithelial cells. α -SMA is a marker of myofibroblasts. At passage 1, over 98% of both WT and TG2^{-/-} were β -catenin positive and less than 1% were α -SMA positive indicating a mainly tubular epithelial culture. This decreased rapidly with passage and passage 1 cells were subsequently used experimentally.

To confirm the identity of WT and TG2^{-/-} mesangial cells, immunofluorescent staining was performed for fibroblast cell surface antigen, CD31 (endothelial adhesion molecule), vimentin (mesenchymal marker) and cytokeratin (epithelial marker). Both WT and TG2^{-/-} mesangial cells were negative for fibroblast antigen, CD31 and vimentin (fig 6.3a). When stained for cytokeratin, 3% of WT cells and 1% of TG2^{-/-} were found to be positive (figure 6.3b). This indicated a mainly mesangial culture with the presence of a small number of cells that could be either glomerular epithelial or glomerular endothelial cells.

Figure 6.1 Morphology of Wild-Type and TG2^{-/-} Tubular Epithelial and Mesangial Cells

a) Tubular Epithelial Cells



b) Mesangial Cells

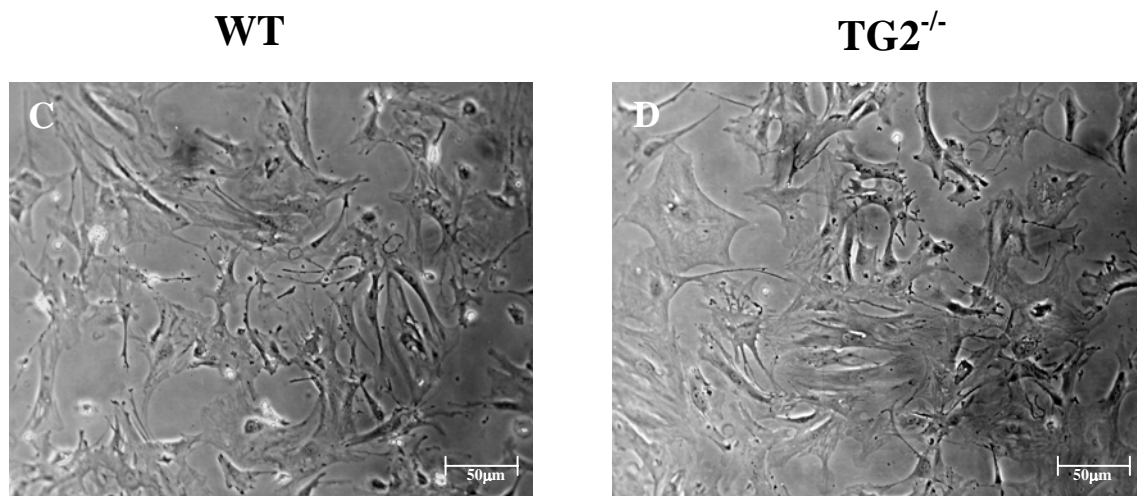


Figure 6.1 Representative micrographs of wild-type (WT) and TG2^{-/-} tubular epithelial cells (A and B) and wild-type and TG2^{-/-} mesangial cells (C and D) cultured following retrograde perfusion of kidneys with Dynabeads® and magnetic separation as described in sections 3.6.3.1 and 3.6.3.2. Cells were visualised on an Olympus BH-2 microscope and captured using a CC-12 digital camera at 400x magnification.

Figure 6.2 Immunofluorescent Characterisation of Primary Tubular Epithelial Cells

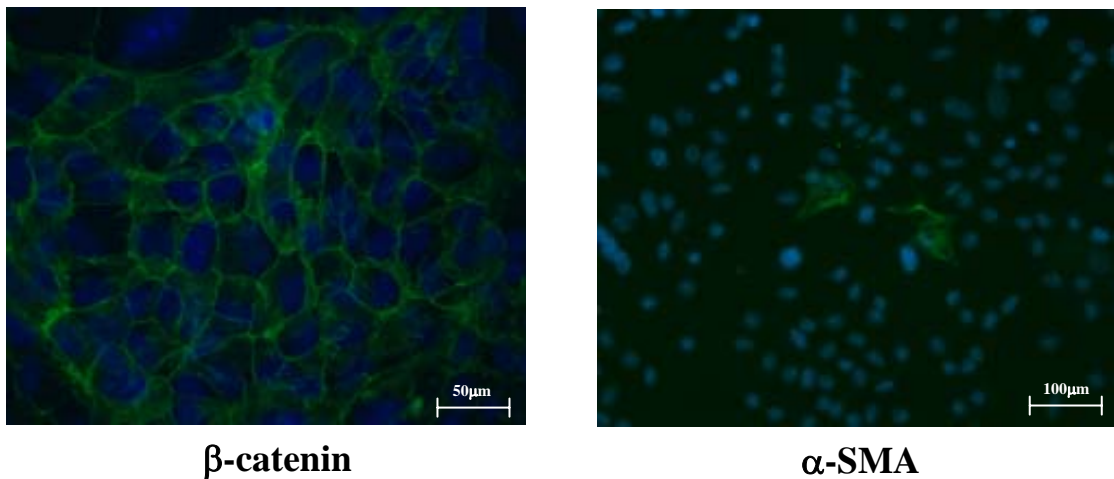


Figure 6.2 Representative photomicrographs of immunofluorescent staining for the tubular cell marker β -catenin (left) and the myofibroblast marker α -smooth muscle actin (α -SMA) (right) in primary tubular epithelial cells. Cells grown on coverslips were fixed in methanol, immunostained with mouse monoclonal anti- β -catenin and α -SMA and antibody binding revealed with anti-mouse FITC as described in section 3.1.8. Fluorescence was visualised using an Olympus BX61 microscope at 494nm with excitation at 518nm and cells captured using a CC-12 digital camera at 400x magnification (β catenin) and 200x magnification (α -SMA).

Figure 6.3 Immunofluorescent Characterisation of Primary Mesangial Cells

a) Cell Markers for Analysis of Mesangial Cells

Cell Marker	Cell Specificity	Mesangial Cell		Positive Control	
		WT	TG2 ^{-/-}		
Fibroblast Cell Surface Antigen	Fibroblast	Neg	Neg	NRK-49	++
CD31	Endothelial	Neg	Neg	HUVEC	++
Vimentin	Mesenchymal	Neg	Neg		
Cytokeratin	Epithelial	+ (2.7±1.1)	+ (0.9±0.5)	NRK-52E	++

b) Cytokeratin Positive Mesangial Cells

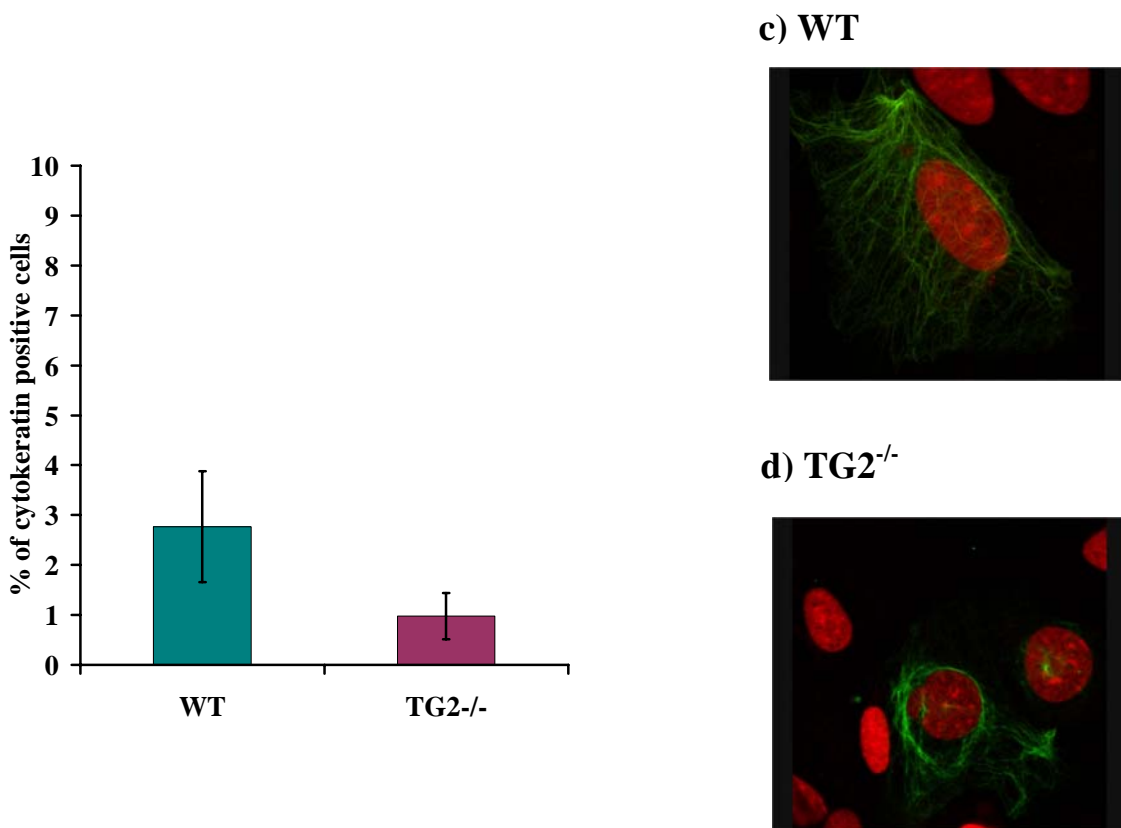


Figure 6.3 (a) Mesangial cells were identified by immunofluorescent staining for fibroblast, endothelial, mesenchymal and epithelial cell markers. Appropriate immortalised cell lines were used as a positive control. Neg = no staining, + = weakly positive, ++ = strongly positive. (b) The percentage of cytotkeratin positive cells in the mesangial cell population. (c) and (d) photomicrographs of cytotkeratin positive WT and TG2^{-/-} cells at 1000x magnification.

6.2.3 Transglutaminase activity

Measurement of TG activity in WT and TG2^{-/-} tubular cells (fig 6.4a) showed that TG2-null cells had a 99% reduction in TG activity compared to WT cells (0.9±0.43 nmols/hr vs 71.8±5.62 nmols/hr). However, TG2^{-/-} mesangial cells (fig 6.4b) only had a 50% reduction in TG activity compared to WT cells (15.5±0.9 nmols/hr vs 32.9±0.33 nmols/hr).

6.2.4 TG2 antigen

Immunoprobings of Western blots of tubular cell lysates with the monoclonal anti-TG2 antibody CUB7402 revealed the presence of an immunoreactive band at 85 kDa that was present in both WT and TG2^{-/-} cells (fig 6.5). Volume densitometry analysis showed that in TG2^{-/-} tubular cells there was a reduction in TG2 protein although this did not quite reach significance (p=0.06). Unfortunately, it was not possible to determine TG2 antigen levels in null mesangial cells due to problems with obtaining sufficient cells for analysis.

6.2.5 TG2 mRNA expression

TG2 mRNA expression was determined in homogenates from whole WT and TG2^{-/-} kidneys (fig 6.6). A 3.5 kb band corresponding to TG2 mRNA was detected in both WT and TG2 null kidneys. However, mRNA expression was reduced by 81% in TG2^{-/-} kidneys compared to WT (p<0.0001).

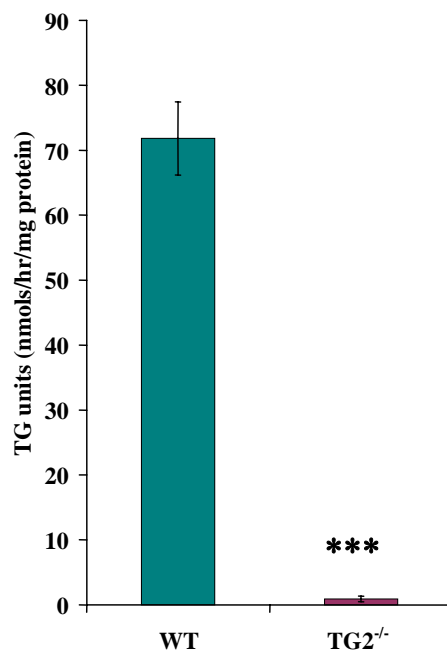
6.2.6 ε(γ-glutamyl) lysine crosslink levels

Immunofluorescence and multi-phase image analysis was used to assess the level of ε(γ-glutamyl) lysine crosslink in the ECM of WT and TG2^{-/-} tubular and mesangial cells (fig 6.7 and 6.8).

Analysis of TG2^{-/-} tubular ECM (fig 6.7) demonstrated a 6 fold reduction in crosslink levels compared to wild type ECM (p=0.05). In mesangial cells (fig 6.8), the level of crosslink was reduced by almost 3 fold in TG2^{-/-} ECM (p<0.05) compared to WT.

Figure 6.4 Transglutaminase Activity in WT and TG2^{-/-} Cells

a) Tubular Epithelial Cells



b) Mesangial Cells

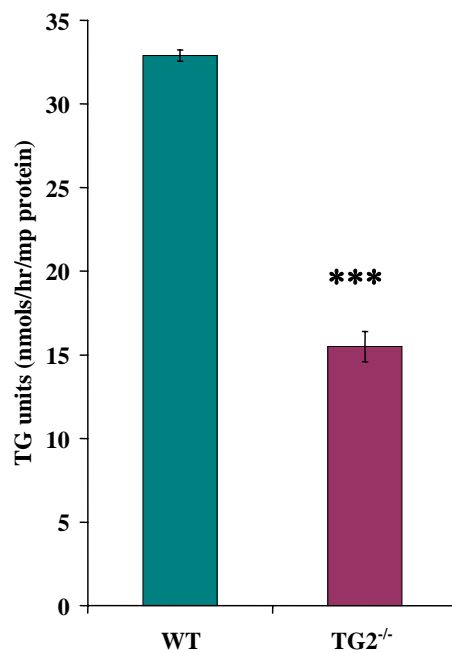
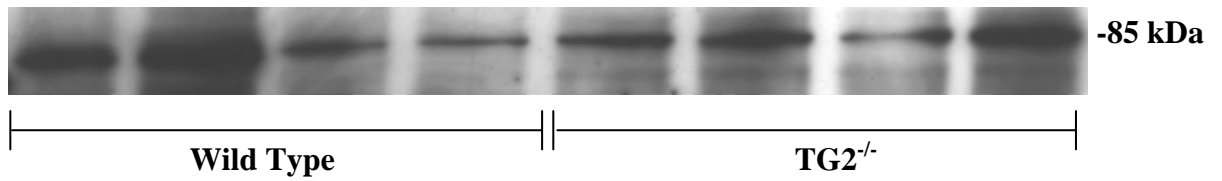


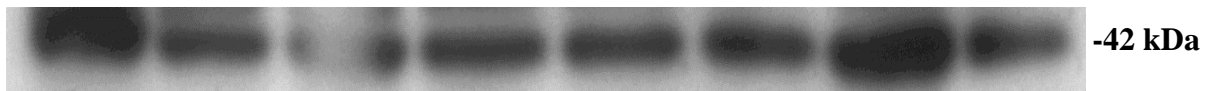
Figure 6.4 TG activity was determined in cell lysates from WT and TG2^{-/-} tubular epithelial (a) and mesangial cells (b) by the putrescine incorporation assay (section 3.3.7.1). TG activity is expressed as nmols/hour/mg protein and represents mean \pm SEM from 3 separate experiments performed in triplicate. ***= $p < 0.0001$ compared to wild type cells (students t test).

Figure 6.5 Western Blot for Tissue Transglutaminase in TG2^{-/-} Tubular Cells

a) Tissue Transglutaminase



b) β -actin



c) Volume Densitometry

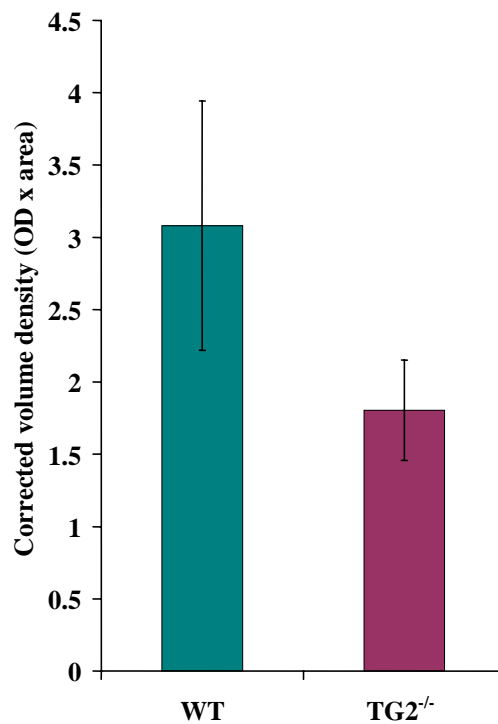
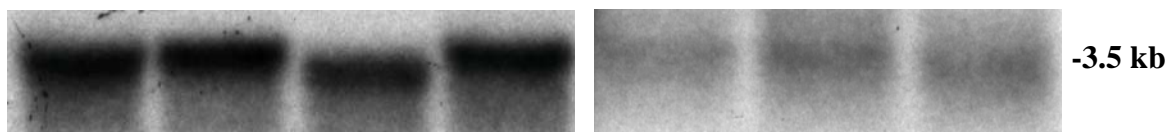


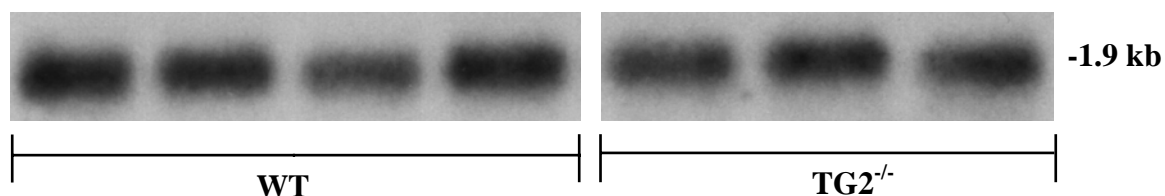
Figure 6.5 Cell lysates from WT and TG2^{-/-} tubular epithelial cells were separated on a 10% polyacrylamide gel and blotted onto a PVDF membrane (section 3.3.6). Western blots were immunoprobed for TG2 using monoclonal anti-TG2 antibody CUB7402 (a) and revealed by chemiluminescence (section 3.3.7.3). Repeat probing for β -actin was used as a loading control (b). Volume densitometry measurements were determined using Multi-Analyst version 3.2 and corrected for loading using β -actin (c). Data represents mean \pm SEM from 2 separate blots, n=4 samples per blot.

Figure 6.6 mRNA Expression (whole kidney)

a) Tissue Transglutaminase



b) Cyclophilin



c) Volume densitometry

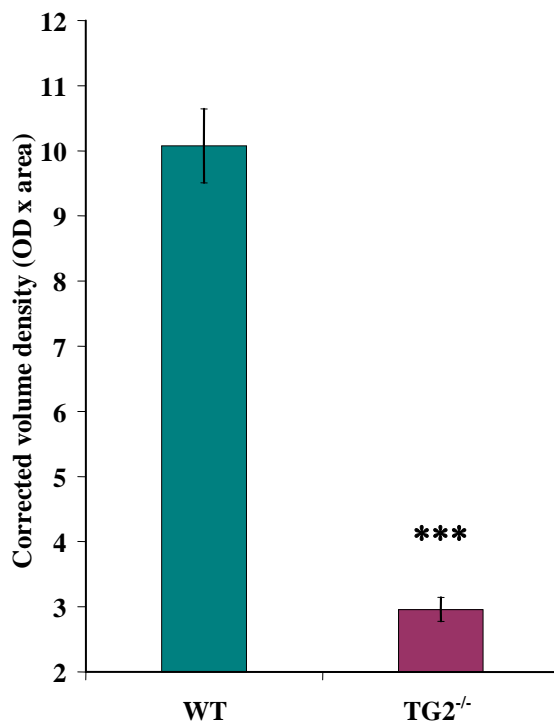
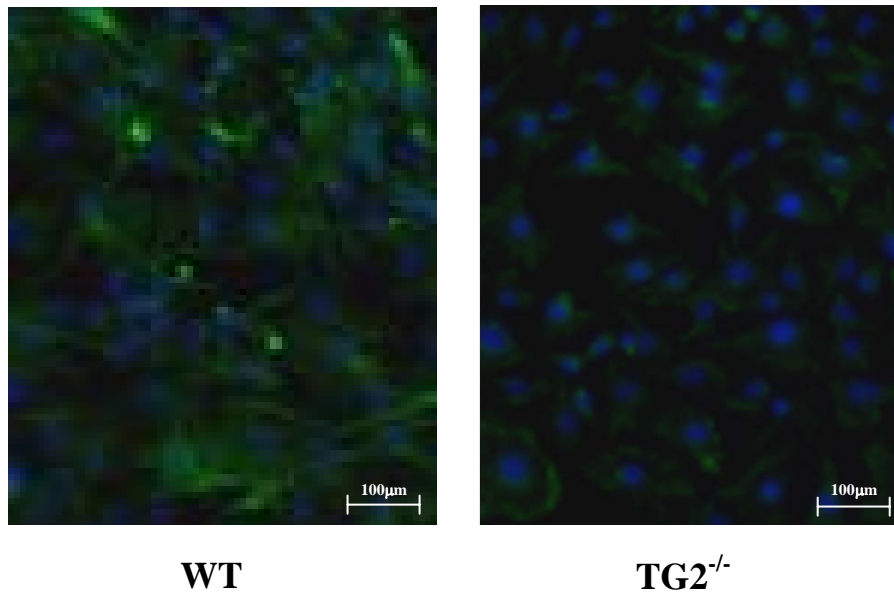


Figure 6.6 Kidneys from wild type and TG2^{-/-} mice were harvested, homogenised and the total RNA extracted using TRIzol™. RNA was subjected to Northern Blot analysis using a specific [³²P]-dCTP random primed cDNA probe for TG2 (a). Repeat probing with cyclophilin was used as a loading control (b). Volume densitometry analysis was performed using Multi-Analyst version 3.2™ (c). Data represents mean ± SEM from 2 separate blots, n=3-4 samples per blot. *** =p<0.0001 compared to wild type (students t test).

Figure 6.7 $\epsilon(\gamma\text{-glutamyl})$ lysine Crosslink Levels in $\text{TG2}^{-/-}$ Tubular ECM

a) Photomicrographs



b) Multi-phase Analysis

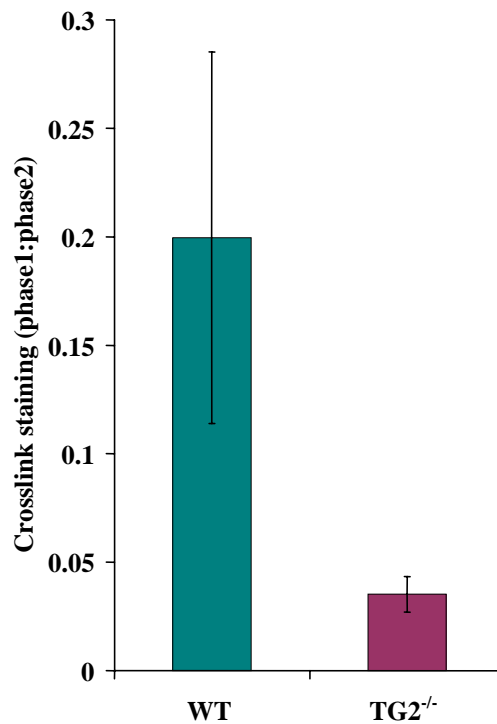
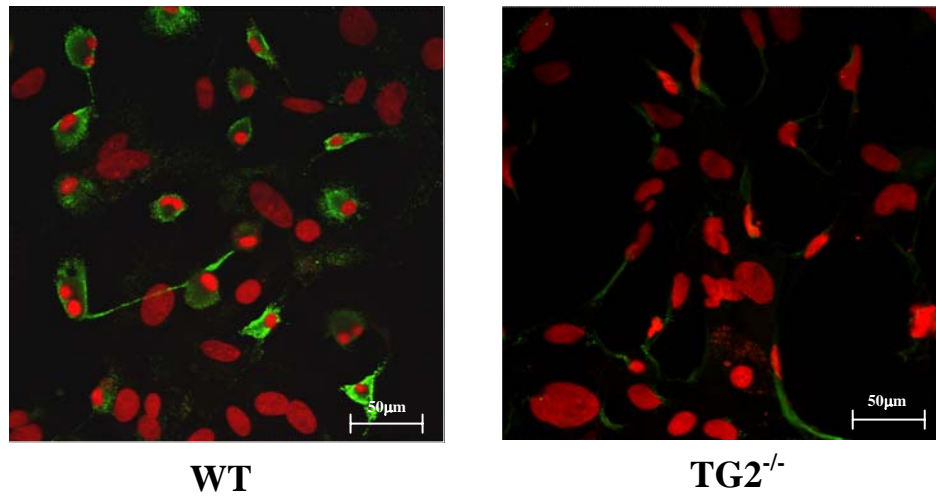


Figure 6.7 (a) Representative photomicrographs of WT (left) and $\text{TG2}^{-/-}$ tubular cells (right) immunostained with monoclonal anti $\epsilon(\gamma\text{-glutamyl})$ lysine antibody (200 x magnification). Quantification of staining was performed at 494nm (excitation at 518nm) using multi-phase image analysis (b) as described in section 3.5.2.6. Immunofluorescence was expressed as a ratio of crosslink (phase1): DAPI staining (phase2) to correct for cell number. Data represents mean \pm SEM of 10 random fields.

Figure 6.8 $\epsilon(\gamma\text{-glutamyl})$ lysine Crosslink Levels in $\text{TG2}^{-/-}$ Mesangial ECM

a) Photomicrographs



b) Semi-quantitative Analysis

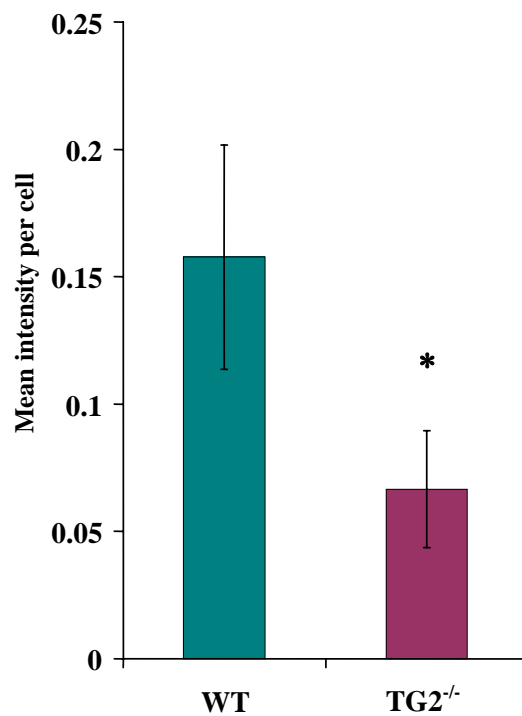


Figure 6.8 (a) Representative photomicrographs of WT (left) and $\text{TG2}^{-/-}$ tubular cells (right) immunostained with monoclonal anti $\epsilon(\gamma\text{-glutamyl})$ lysine antibody (400 x magnification). (b) Semi quantitation of staining was performed using confocal microscopy with excitation at 488nm. Data is expressed as the mean intensity of fluorescence per cell \pm SEM from at least 6 random fields. *= $p < 0.05$ compared to wild type cells (students t test).

6.3 Discussion

Tubular and mesangial cells from WT and TG2^{-/-} mice were successfully isolated by retrograde perfusion of the kidney with BSA-inactivated Dynabeads® and separated into relatively pure cell preparations by magnetic separation. Traditional methods of separating tubular and mesangial cells by the sieving of kidney tissue are problematic in the mouse due to the similar size of glomerular and tubular fragments and result in the low purity of mesangial cultures. Magnetic separation was successful in virtually eliminating the problems of tubular contamination to give mesangial cultures of comparative purity to those obtained by the originators of this technique (Takemoto *et al.*, 2002).

A significant problem that was encountered in performing the perfusion through the heart as originally described by Takemoto *et al.*, was the non-specific perfusion of other organs such as the liver which in turn resulted in relatively poor perfusion of the kidney. Despite increasing the concentration of beads in the perfusate several fold, it proved difficult by the original method to target sufficient quantities of beads to the kidney. The technique was improved significantly by performing the perfusion through the abdominal aorta which was tied above and below the renal artery such that the majority of the beads became lodged in the kidney.

Immunofluorescent staining revealed that primary mesangial cells were negative for fibroblast cell surface antigen and the endothelial marker CD31, indicating a relatively pure mesangial cell population. However, mesangial cells were also negative for the mesenchymal marker vimentin which was surprising given that these cells are smooth muscle-like cells of mesenchymal origin. The reason for the lack of vimentin staining is unclear and is unfortunately impossible to verify as the original staining data performed at Nottingham Trent University is unavailable. The lack of an appropriate control for vimentin, however, would suggest a problem with the vimentin antibody and may indicate that the staining did not work. A small number of cells were found to be cytokeratin positive which is likely to indicate the presence of contamination from glomerular epithelial cells as cytokeratin is known to be an epithelial cell marker. However, it is known that some mesangial cells in culture can also stain positive for cytokeratin making them difficult to distinguish (Mene, 2001).

WT and TG2^{-/-} tubular cells were 98% β -catenin positive and α -SMA negative at first passage indicating a mainly tubular culture. However, it was noted that the tubular cells rapidly lost the expression of epithelial cell markers with repeated passage such that by passage 3 they were predominantly β -catenin (and E-cadherin) negative. It is possible that the

trans-differentiation of epithelial cells to myofibroblasts is accountable for this loss of tubular phenotype however, *in vitro*, trans-differentiation of tubular cells normally results from exposure to high levels of TGF- β 1 (Fan *et al.*, 1999). It is more likely that culture of primary cells in the absence of collagen substratum underlies the change in cell phenotype although the loss of epithelial markers may also result from the inability of our primary epithelial cells to survive trypsinisation, allowing other cell types such as fibroblasts to flourish.

Morphological analysis of TG2^{-/-} cells showed no difference in cell morphology compared to WT cells. This is consistent with the original findings of De Laurenzi and Melino *in vivo* following disruption of TG2 (De Laurenzi and Melino, 2001) in which the major organs appeared normal and also with recent observations of the kidneys of TG2 null mice in the UUO model (Mohammed *et al.*, 2006).

A surprising finding was that whilst WT tubular and mesangial cells and indeed TG2^{-/-} tubular cells were able to attach in the absence of TG2, TG2^{-/-} mesangial cells required the addition of 50-100 μ g/ml of DTT-activated exogenous TG2 to successfully attach and grow. Since the expression of active TG2 at the cell surface appears to be important for attachment (Gentile *et al.*, 1992; Jones *et al.*, 1997) this suggests that the residual TG2 activity of TG2^{-/-} mesangial cells is not translocated to the cell surface. This would support the findings in TG2 over-expressing mesangial cells (Chapter 5) that show no increase in the cell surface trafficking of TG2 despite large increases in intracellular levels.

In comparison, TG2^{-/-} tubular cells may express an inactive extracellular TG2 that is in some way sufficient to facilitate attachment. Unfortunately, it was not possible to establish this by measuring the extracellular levels of TG2 in primary cells due to problems with establishing cultures in the 96 well plate format required for the assays. Alternatively, attachment of tubular cells may be TG2-independent and rely on the expression of other cell attachment factors such as integrins or cell adhesion molecules.

Western blot analysis of cell lysates from wild type and TG2^{-/-} tubular cells demonstrated the presence of an immunoreactive band at 85 kDa corresponding to TG2 that was present in both WT and TG2^{-/-} cells. This is consistent with recent Western blot analysis of kidney tissue from TG2^{-/-} mice in the study of the UUO model (Mohammed *et al.*, 2006) but a contradiction to the original findings of (De Laurenzi and Melino, 2001). The reason for this apparent discrepancy is unclear however, the presence of a band at 85 kDa in the TG2 knockout cells would appear to be consistent with a heterozygous genotype, suggesting that the animals are not pure knockouts. Whilst it is not entirely possible to rule out that these

animals are heterozygous for TG2 given that genotyping was not performed locally, it appears to be unlikely since the animals were genotyped by our close collaborators at Nottingham Trent University (E Verderio, personal communication), from whom we obtained the mice and demonstrated to be homozygous TG2^{-/-}. Genotyping of these mice was performed by PCR using one sense primer and two anti-sense primers: one directed to a sequence within the WT gene and one to the neomycin sequence of the targeting vector (see appendix). Homozygous knockout animals were distinguished by a single 372 bp band whilst heterozygous animals showed a band at 372 bp and a WT band at 252 bp. Interestingly, Western blot analysis by colleagues at Nottingham Trent University on tissue from these homozygous TG2^{-/-} mice also revealed the presence of an 85 kDa TG2 band (E Verderio personal communication, data not shown).

The improbability that these mice are heterozygous for TG2 suggests that an alternative explanation is required for the presence of immunoreactive TG2. Examination of the construct used to disrupt the TG2 gene may offer a clue to the existence of this band. Generation of the original TG2 knockouts by De Laurenzi and Melino resulted from the replacement of exons 5 and 6 with a targeting vector containing the neomycin resistance gene (fig 6.9). It is unclear from the original recombination whether the targeting vector also contained a stop codon in close proximity to the neomycin gene however, if this was the case, transcription would result in the expression of a slightly truncated protein lacking catalytic activity. Given that the binding site of the TG2 antibody (CUB7402) occurs in the proposed truncated region, then probing would fail to detect a TG2 band in these animals as demonstrated by De Laurenzi and Melino. It could be speculated that what is observed in the animals used in this study is the loss of such a stop codon through repeated breeding of the TG2 knockouts leading to read through and the generation of full length TG2 protein detectable by CUB7402.

The presence of a TG2 positive band in the TG2^{-/-} kidney lysates is almost certainly likely to represent the inactive form of the enzyme since generation of the knockout results from disruption of the active site of TG2 rather than deletion of the gene. This is supported by the measurement of TG activity in the TG2^{-/-} tubular cells which shows an almost total lack of TG activity. However TG2^{-/-} mesangial cells still retained half the TG activity of wild type cells. Little is known about the expression of other transglutaminase enzymes in mesangial cells apart from TG2 that may account for this TG activity. However a likely candidate is TG1 (keratinocyte TG) since this is expressed in the major organs of the TG2^{-/-} mouse in the absence of TG2 activity (De Laurenzi and Melino, 2001).

Figure 6.9 Proposed Gene Disruption of TG2 Used in the Generation of the TG2 Knockout Mouse

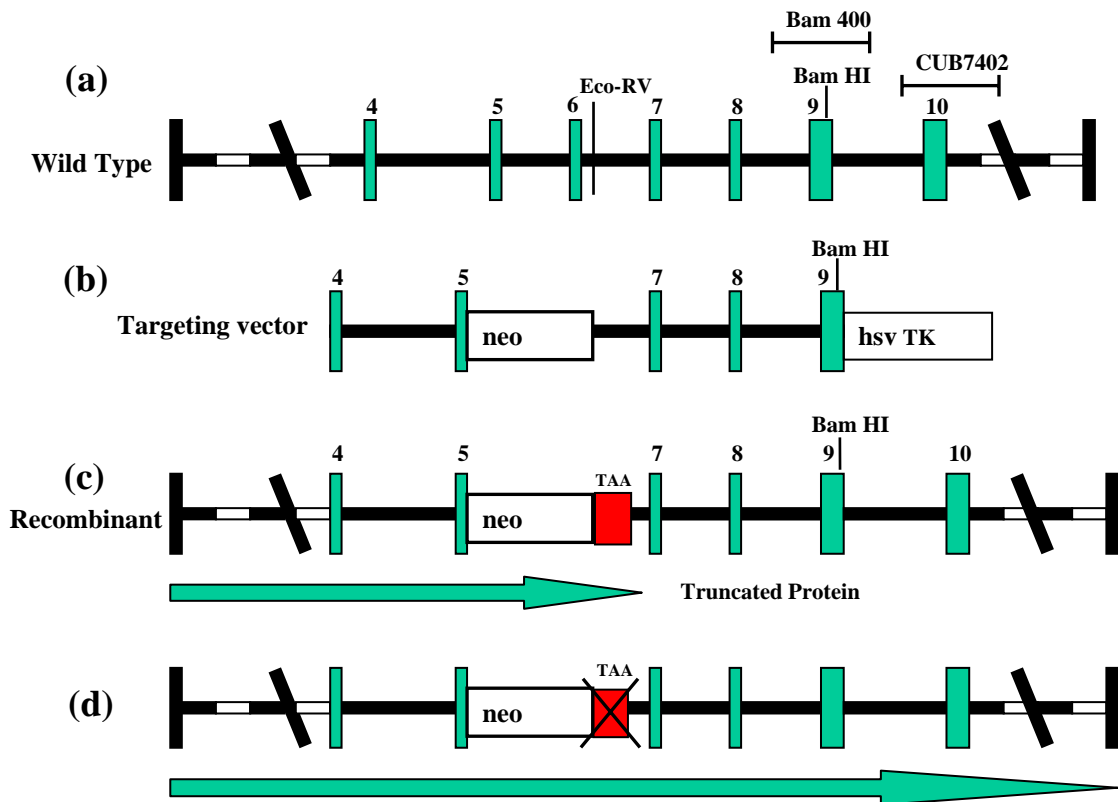


Figure 6.9 (a) Wild type TG2 gene from exon 4 to exon 10 showing the position of Eco-RV and BamHI sites and the binding sites of the Bam 400 cDNA probe (1240-1625 bp) and CUB7402 antibody (aa 447-478). (b) To perform targeted disruption of the TG2 gene a vector was generated by cloning an Eco/RV/BamHI genomic fragment containing intron 6 to exon 9 into the pPNT vector at the 5' end of the neomycin resistance gene followed by cloning of a PCR fragment from exon 4 to exon 5 into this vector. (c) Incorporation of this construct resulted in a recombinant TG2 gene in which 1.2kb comprising part of exon 5, exon 6 and intron 5 were deleted. It is speculated that the presence of a stop codon close to the neomycin gene would result in the transcription of an inactive and slightly truncated protein undetectable by CUB7402. It is further proposed that a subsequent loss of the stop codon through repeated breeding could result in transcription of full length TG2 protein to which CUB7402 would bind (d). Adapted from (De Laurenzi and Melino, 2001).

Given the presence of TG2 protein, perhaps a surprising finding is the almost total lack of TG2 mRNA expression in the TG2^{-/-} kidneys when analysed by Northern blotting. This may well be attributable to poor binding of the TG2 probe which targets the 385bp BamHI fragment of TG2 and may be affected by recombination with the targeting vector.

This chapter has demonstrated the successful isolation of relatively pure preparations of TG2^{-/-} tubular and mesangial cells that possess significantly reduced TG activity and $\epsilon(\gamma$ -glutamyl) lysine crosslink compared to wild type cells. These will be utilised in subsequent chapters to determine the effect of a loss of TG2 on the deposition and degradation pathways that contribute to the accumulation of matrix *in vitro*.

Chapter 7

Effect of Tissue Transglutaminase Modulation on Tubular Cell ECM

7.1 Introduction

Data presented in Chapter 5 demonstrated that tubular epithelial cells induced to over-express TG2 by stable transfection show elevated extracellular levels of the enzyme. Previous *in vivo* studies of renal disease have demonstrated that elevated levels of extracellular TG2, resulting from tubular cells, are associated with a parallel increase in ϵ (γ -glutamyl) lysine crosslinking within the ECM that correlates with the development of scarring (Johnson *et al.*, 1997; Johnson *et al.*, 1999). Such data suggests a link between increased TG2 expression and the accumulation of scar tissue.

The physiological role of TG2 crosslinking in the accumulation of excess ECM has yet to be fully established. Data so far suggests that TG2 may influence the ECM indirectly via the matrix storage and activation of the fibrogenic cytokine TGF- β 1 (Nunes *et al.*, 1997) or directly via effects on the deposition and breakdown of ECM proteins (Johnson *et al.*, 1997; Johnson *et al.*, 1999; Skill *et al.*, 2004). However, no conclusive evidence for either mechanism in the kidney has so far been presented.

Much of the evidence for a direct role of TG2 in matrix accumulation has come from the study of other cell systems in which TG2 has been modulated. For example, studies of Swiss 3T3 fibroblasts induced to over-express TG2 by transfection (Verderio *et al.*, 1998) have demonstrated that elevated TG2 and extracellular crosslinking contributes to the assembly and stabilisation of fibronectin fibrils. In human dermal fibroblasts cultured with exogenous TG2 (Gross *et al.*, 2003), an increase in TG2-mediated crosslinking promotes the increased deposition of ECM. In the kidney, the *in vitro* study of elevated glucose on TG2-induced ECM accumulation by proximal tubular cells (Skill *et al.*, 2004) has been investigated. This reveals a glucose-mediated increase in ECM associated TG2 activity and crosslinking that is paralleled by increased deposition of ECM and collagen.

It has also been suggested that TG2-mediated crosslinking of the ECM may influence the accumulation of matrix by increasing its resistance to the action of MMPs. So far, much of the data supporting this has come from the *in vitro* study of isolated collagen fibrils. For example, it has been demonstrated that the *in vitro* degradation of isolated collagen fibrils by MMP-1 is impeded in the presence of TG2 (Johnson *et al.*, 1999). Similarly, the *in vitro* study of dermal fibroblasts cultured with exogenous TG2, shows that increased TG2-mediated crosslinking of the ECM results in a decreased rate of matrix turnover, suggesting an effect on ECM breakdown (Gross *et al.*, 2003).

The data generated so far has led to the hypothesis that TG2 produced and exported by tubular cells, contributes to scarring directly by influencing both the deposition and degradation of ECM proteins, thus facilitating the accumulation of matrix. However, a major limitation of some of these studies is that they are not physiologically representative nor do they reflect the action of cell-synthesised TG2 on cell-generated matrix.

To address this, the effect of changes in cellular TG2 on the properties of mature ECM generated by both OK tubular cells induced to over-express TG2 by transfection (Chapter 5) and TG2-null tubular cells (Chapter 6) will be investigated.

The effect of modulating TG2 on the accumulation of matrix will be determined using the radio-labelling of deposited ECM with ³H-amino acids (total ECM) or ³H-proline (total collagen) and by hydroxyproline analysis (total collagen). Immunofluorescence will be used to characterise the composition of deposited ECM. Since a change in the rate of matrix deposition is the key contributor to the overall accumulation of matrix, this will be investigated by ³H-proline incorporation into deposited ECM in the presence of the MMP inhibitor Galardin. The role of TG2 in the resistance of the ECM to proteolytic degradation, so far only studied in isolated systems, will be determined by subjecting the ECM generated and deposited by tubular cells to degradation by a range of proteolytic enzymes including MMPs -1 and -2.

7.2 Results

7.2.1 Preliminary studies

The investigation into the effect of TG2 modulation on the properties of tubular cell-generated ECM required the design of a suitable *in vitro* model in which cell generated ECM could be radio-labelled, the cells removed effectively and the remaining labelled ECM recovered for analysis. For this, a number of preliminary experiments were performed to establish a suitable concentration of label, the washing regime required to minimise non-specific radioactivity and the most effective methods for cell removal and ECM recovery.

7.2.1.1 Optimum concentration of radiolabel

To determine the degree of ECM labelling with varying concentrations of proline label, OK cells were incubated for 72 hours with either 10, 100 or 300 μ Ci of $^3,^4$ H-proline or 50 μ Ci of 2,3,4,5 H-proline and the ECM label determined by scintillation counting (fig 7.1a). Labelling the ECM with 10 μ Ci of $^3,^4$ H proline gave a level of incorporation of around 2000dpm (disintegrations per minute)/well. Increasing the concentration of $^3,^4$ H-proline label from 10 μ Ci to 100 μ Ci and 300 μ Ci increased the level of ECM labelling by 4 and 7.5 fold respectively. Labelling of the ECM with 50 μ Ci of 2,3,4,5 H-proline was more efficient than labelling with 100 μ Ci of $^3,^4$ H proline. Since sufficient labelling was achieved with 10 μ Ci of $^3,^4$ H-proline, this was chosen for use in the radio labelling studies.

7.2.1.2 Removal of non-specific radioactivity

To minimise non-specific radioactivity resulting from radiolabel binding to the tissue culture plastic, a washing regime was required that would minimise this without removing the remaining ECM. To determine the number of washes required after the removal of cells, plates were washed with increasing volumes of PBS (10, 15, 20, 25 and 30ml) and a sample removed from each wash to determine the total dpm by scintillation counting (figure 7.1b). Wash 1 had a total dpm of around 3250 dpm that was reduced to around 600 dpm by wash 5. In comparison, the dpm of the remaining ECM was around 2000dpm/well. Since there was little difference in the dpm removed between wash 3 and 5, a washing regime of 3 washes with increasing volumes of PBS was used in the experimental model.

7.2.1.3 Cell removal

OK cells were labelled for 72 hours with 10 μ Ci of 3 H-proline and the cells removed with; 0.1% deoxycholate/PBS, 0.25% deoxycholate/PBS, 0.1% deoxycholate/Triton X-100 or 0.25M ammonium hydroxide for 10 mins at 37°C. The ease of cell removal with each agent

was determined visually and the dpm remaining in the ECM (after scraping) determined by scintillation counting (fig 7.2a). Ammonium hydroxide was the most effective cell removal agent and left the greatest amount of ECM behind (9690 dpm/10cm² plate). Both concentrations of deoxycholate showed similar effectiveness at removing the cells however, more ECM remained after treatment with 0.1% deoxycholate (8522 vs 8105 dpm). Removal of cells with 0.1% deoxycholate/Triton X-100 was equally as effective as the other agents but also removed more of the remaining ECM. The agent chosen for the experimental model was ammonium hydroxide.

7.2.1.4 ECM recovery

OK cells were cultured for 72 hours until confluent, the cells removed with 0.25M ammonium hydroxide, the ECM washed 5 times with increasing volumes of PBS and solubilised/precipitated for 1 hour at 37°C with either 2.5% SDS, 0.1M NaOH or 10% TCA (fig 7.2b). The solubilised/precipitated ECM was scraped and the protein concentration determined by the bicinchoninic acid assay as described in section 3.3.9.1.

The greatest ECM recovery was achieved with 2.5% SDS which yielded 0.18mg/ml of ECM protein/10cm² plate. Recovery of ECM with 0.1M NaOH was poor, only yielding 0.02mg/ml of ECM protein. Treatment with 10% TCA failed to precipitate the ECM and recovery was negligible. The agent used in the recovery of ECM in the experimental model was 2.5% SDS.

Figure 7.1 Determination of Labelling Protocol and Washing Regime for the ECM

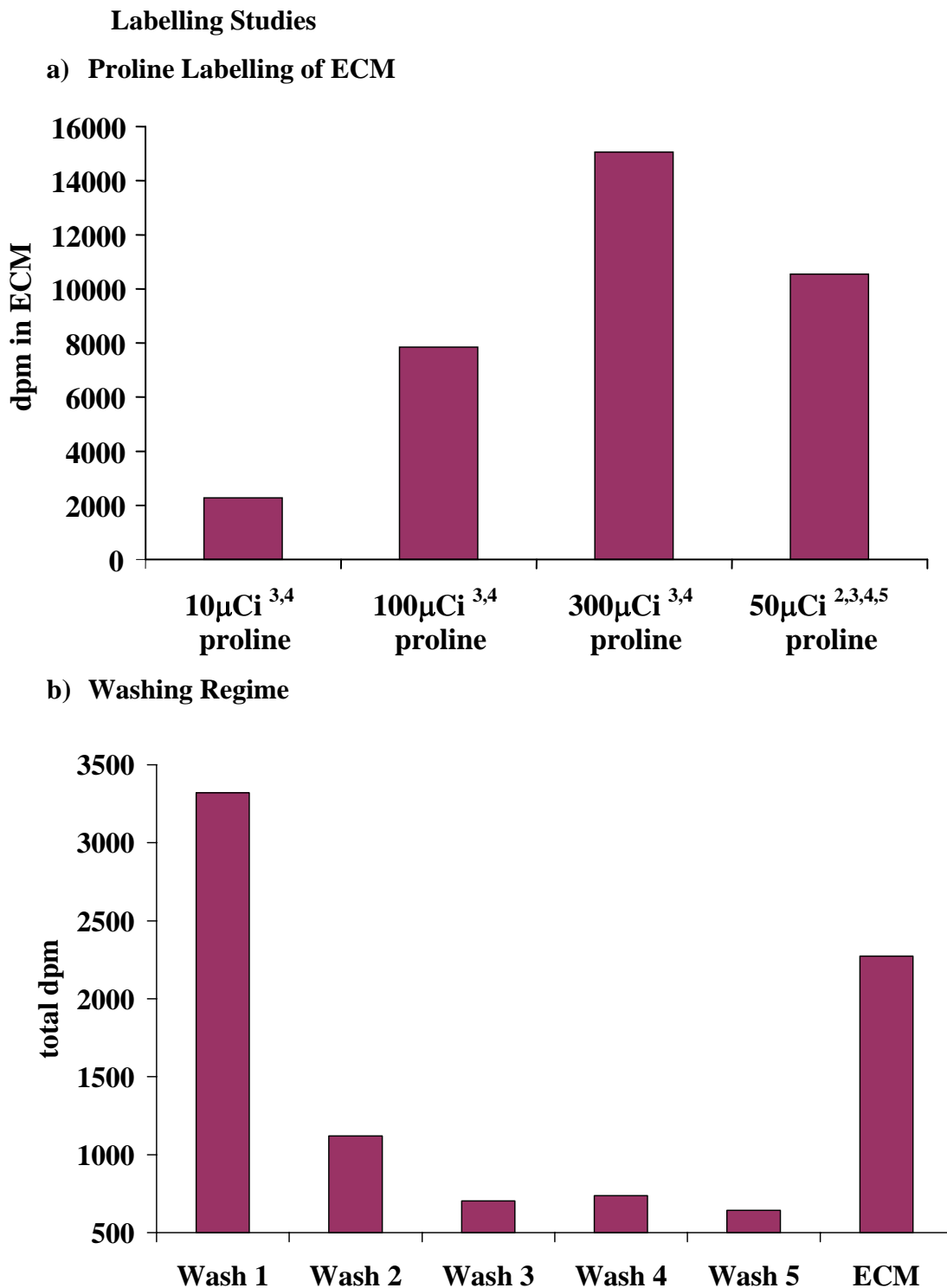
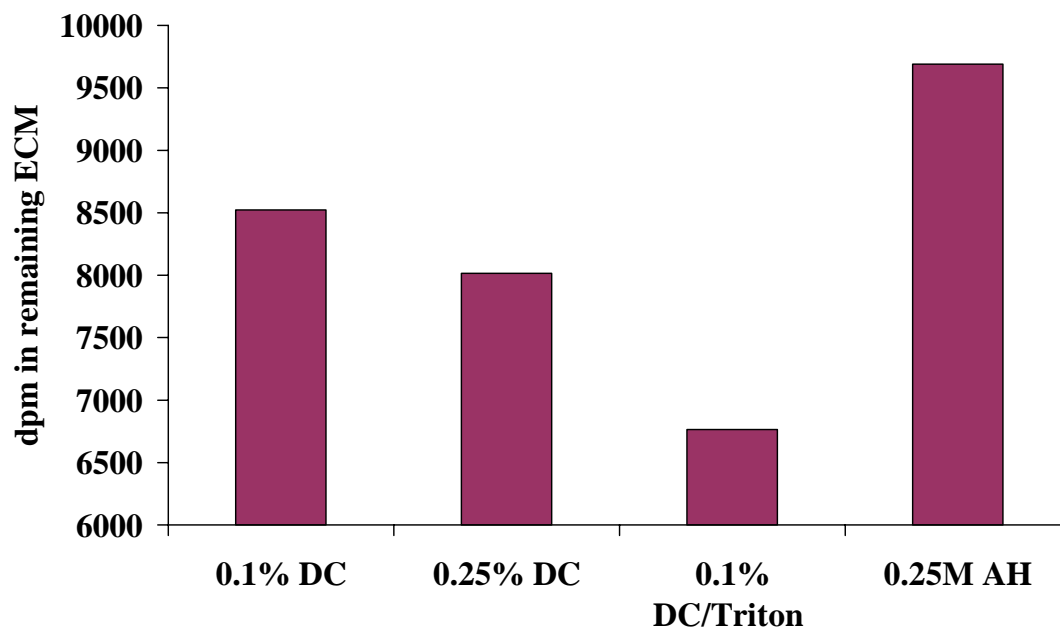


Figure 7.1 (a) OK cells were labelled for 72 hours with 10µCi, 100µCi or 300µCi of ^{3,4}H-proline or 50µCi of ^{2,3,4,5}H-proline, cells removed with 0.25M ammonium hydroxide, the ECM recovered by scraping and incorporated label measured by scintillation counting. (b) Following cell removal, plates were washed 5 times with increasing volumes of PBS (10, 15, 20, 25 and 30ml), a sample removed from each wash and the dpm determined by scintillation counting. Data is from a single experiment.

Figure 7.2 Evaluation of Cell Removal and ECM Recovery Agents for Use in the ECM

Labelling Studies.

a) Cell Removal



b) ECM Recovery

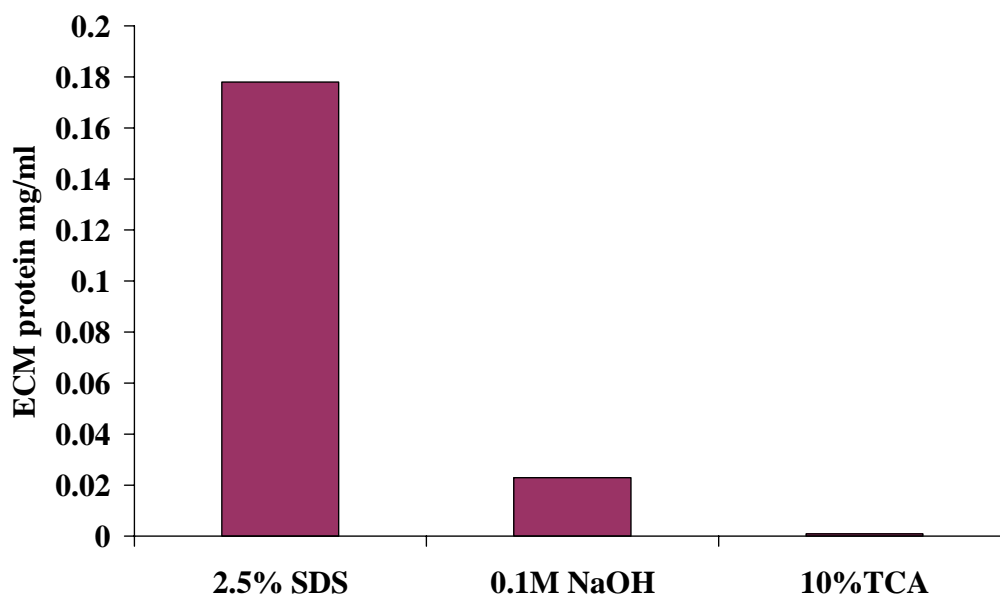


Figure 7.2 (a) OK Cells were cultured in the presence of 10 μ Ci of 3 H-proline for 72 hours. The ECM remaining after the removal of cells with 0.1% deoxycholate/PBS (0.1% DC), 0.25% deoxycholate/PBS, 0.1% deoxycholate/Triton X100 or 0.25M ammonium hydroxide (AH) was determined by scintillation counting. (b) The recovery of ECM by 2.5% SDS, 0.1M NaOH or 10% TCA was determined by the bicinchoninic acid assay as described in section 3.3.9.1. Data is from a single experiment.

7.2.2 Experimental data

7.2.2.1 Measurement of total deposited ECM

The non-specific incorporation of ³H-labelled amino acids into deposited ECM was used as a measure of any change in total ECM level in response to TG2 modulation. In TG2 over-expressing OK cells (fig 7.3a), no significant change in total deposited ECM was observed. To confirm these findings, deposited ECM was also quantified by the bicinchoninic acid assay (fig 7.3b). Again, despite a small increase in clone tTg21 ECM levels, overall there was no significant increase in total ECM.

In contrast, ³H-amino acid labelling of TG2^{-/-} ECM (fig 7.4) revealed a 17% reduction in total ECM (2.65 ± 1.82 dpm/mg protein) compared to wild type cells (3.18 ± 1.86 dpm/mg protein) although this did not achieve significance ($p=0.4$).

7.2.2.2 Measurement of total ECM collagen

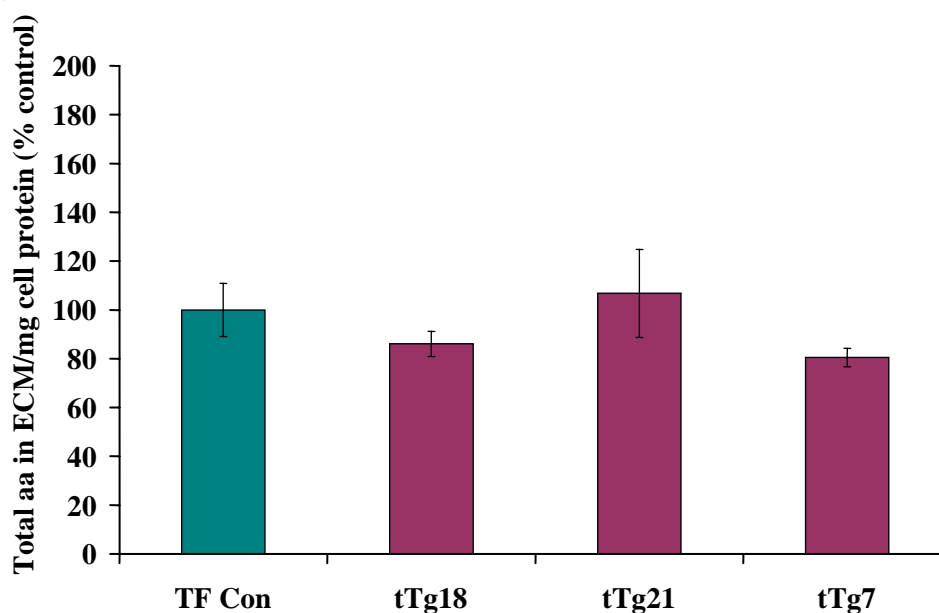
The incorporation of ³H-proline into deposited ECM was used as a measure of the total collagen content of the ECM. In TG2 over-expressing OK cells (fig 7.5a), increasing the intracellular TG activity to 5 fold that of the transfection control (clone tTg 21) increased ³H-proline incorporation by 37% (1673.944 ± 264.21 vs. 1240.754 ± 65.371 dpm/mg protein, $p<0.05$), while a 7 fold increase in TG activity (clone tTg7) caused an 186% increase in ³H-proline incorporation (2272.841 ± 405.85 vs. 1240.754 ± 65.371 dpm/mg protein, $p<0.05$).

Since ³H-proline may incorporate into non-collagenous proteins, ECM from over-expressing clone tTg7 was also subjected to hydroxyproline analysis by gas chromatography (fig 7.5b). Hydroxyproline content of tTg7 ECM was found to increase by 278% ($p<0.001$) compared to control.

In contrast, the collagen content of TG2^{-/-} tubular ECM as measured by ³H-proline labelling (fig 7.6a), was reduced by 26% compared to wild type ECM ($p<0.01$). This reduction in ECM collagen was confirmed by hydroxyproline analysis which demonstrated a 73% reduction ($p<0.001$) in hydroxyproline content (fig 7.6b).

Figure 7.3 Total ECM Levels in TG2 Over-expressing OK Cell Clone ECM

a) ³H Amino Acid Label



b) ECM protein by the Bicinchoninic Acid Assay

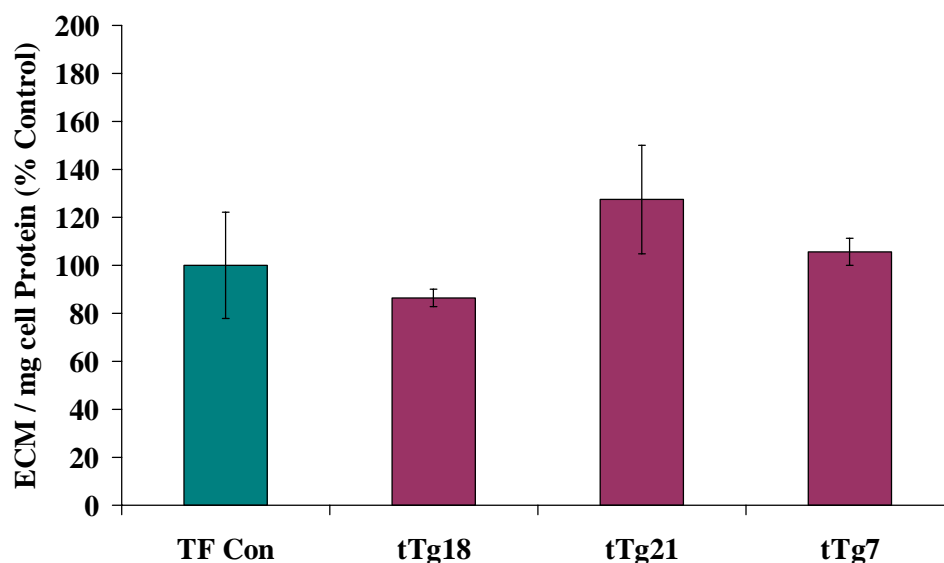


Figure 7.3 (a) Total ECM deposition in TG2 over-expressing OK cell clone ECM was determined by culture of clones for 72 hours in the presence of 20 μ Ci of ³H-amino acid mixture followed by recovery of the ECM as described in section 3.5.2.1. (b) Separate plates were analysed for total ECM protein by the bicinchoninic acid assay (section 3.3.9.1). Data represents mean values \pm SEM from 3 separate experiments performed in triplicate, corrected per mg of ammonium hydroxide-soluble cell protein and expressed as percentage of the control.

Figure 7.4 Total ECM Levels in WT and TG2^{-/-} Tubular ECM

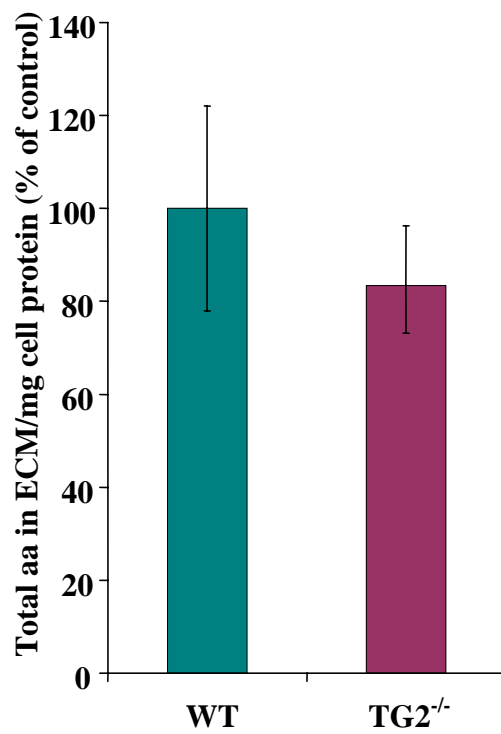
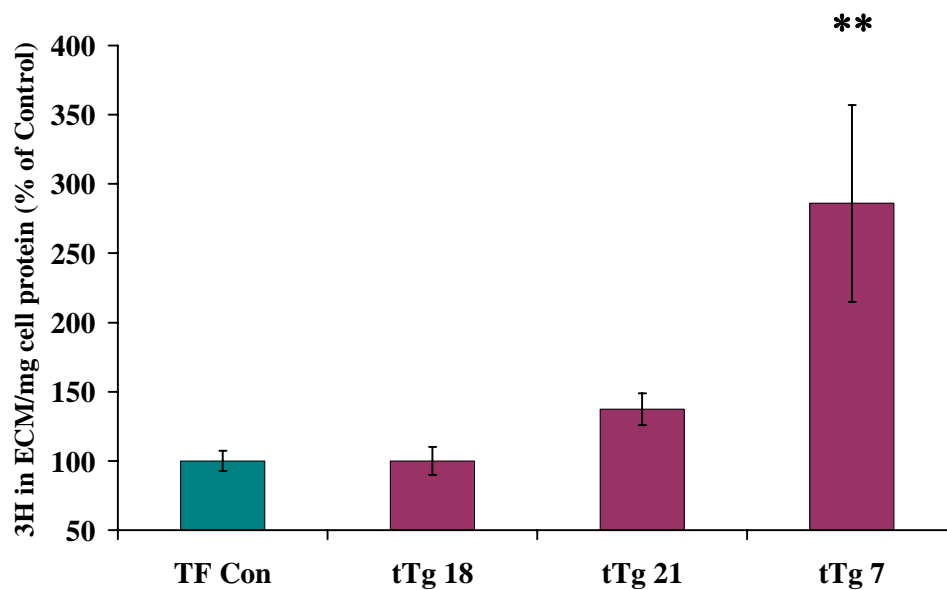


Figure 7.4 Total ECM deposition was determined in WT and TG2^{-/-} ECM by culture of primary cells for 72 hours in the presence of 20 μ Ci of ³H-amino acid mixture prior to recovery of the ECM and measurement of incorporated label by scintillation counting. Data represents mean ECM label \pm SEM from 3 separate experiments performed in duplicate, corrected per mg of ammonium hydroxide-soluble cell protein and expressed as percentage of the control.

Figure 7.5 Total ECM Collagen in TG2 Over-expressing OK Cell Clone ECM

a) ^3H -Proline Incorporation



b) Hydroxyproline Analysis

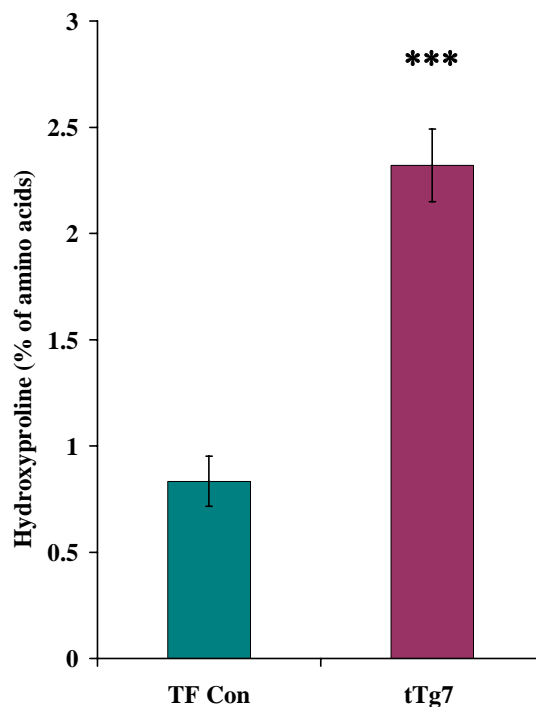
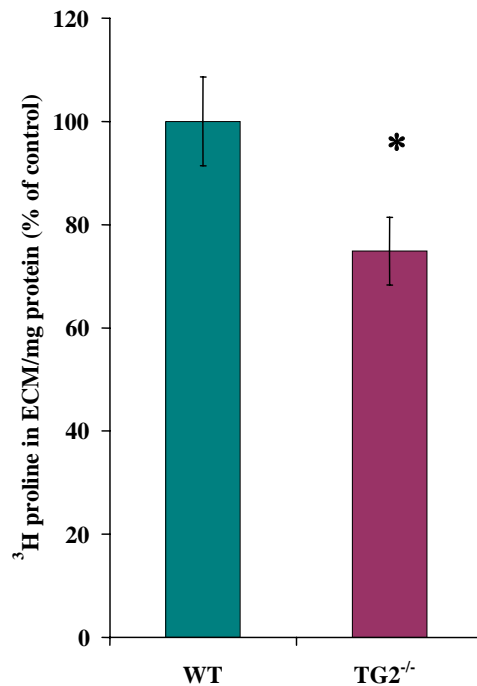


Figure 7.5 (a) Total ECM collagen was determined in TG2 over-expressing OK cell clone ECM by culture in the presence of $10\mu\text{Ci}$ ^3H -proline for 72 hours prior to recovery of the ECM and measurement of ^3H -proline labelling by scintillation counting (section 3.5.2.1). Data represents mean value \pm SEM from 3 separate experiments performed in triplicate, corrected per mg of cell protein and expressed as percentage of the control $**=p<0.01$ compared to transfection control by one way ANOVA with Bonferroni post hoc test (b) Levels of ECM collagen in clone tTg7 were confirmed by gas chromatography for hydroxyproline. Data represents mean \pm SEM from 3 separate plates and is expressed as percentage of amino acids. $***=p<0.001$ compared to transfection control (students t test).

Figure 7.6 Total ECM Collagen in WT and TG2^{-/-} Tubular ECM

a) ³H-Proline Incorporation



b) Hydroxyproline Analysis

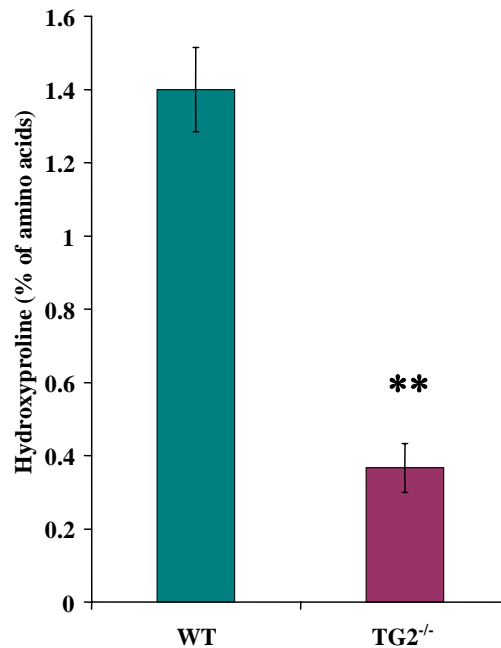


Figure 7.6 (a) Total ECM collagen was determined in WT and TG2^{-/-} ECM by culture in the presence of 10 μ Ci ³H-proline for 72 hours prior to recovery of the ECM as described previously. Data represents mean value \pm SEM from 3 separate experiments performed in duplicate, corrected per mg of cell protein and expressed as percentage of the control. (b) Levels of ECM collagen were confirmed by hydroxyproline analysis. Data represents mean \pm SEM from 3 separate plates and is expressed as percentage of amino acids. *=p<0.01, **=p<0.001 compared to wild type (students t test).

7.2.2.3 Analysis of collagen composition by immunofluorescence

Immunofluorescence was used to characterise which collagen types may contribute to the collagen composition of the ECM in response to TG2 modulation. Representative photomicrographs of the resultant staining are shown in fig 7.7.

In OK cells, changes in deposited collagens were characterised in the highest expressing clone tTg7. Collagens III and IV were just detectable in the ECM of normal OK cells (fig 7.7 panels A and B), but markedly elevated in clone tTg7 (fig 7.7 panels E and F). Multiphase image analysis (fig 7.8a) revealed a 96% increase in Collagen III ($p < 0.01$) and a 78% increase in Collagen IV ($p < 0.05$) in clone tTg7 ECM. Collagen I was barely detectable in either control or tTg7 (data not shown).

A comparison of WT (fig 7.7 panels I and J) and TG2^{-/-} ECM (fig 7.7 panels M and N) demonstrated strong reductions in both Collagen III and IV staining but not Collagen I (data not shown). Multiphase analysis of TG2^{-/-} ECM (fig 7.8b) demonstrated a 67% reduction in Collagen III and an 81% reduction in Collagen IV compared to WT ECM.

7.2.2.4 $\epsilon(\gamma\text{-glutamyl})$ lysine levels in the ECM

Immunofluorescent staining of the ECM for $\epsilon(\gamma\text{-glutamyl})$ lysine crosslink (fig 7.7 panels C, D, G, H, K, L, O and P) demonstrated a significant increase in the level of ECM associated crosslink in OK clone tTg7 ECM (+46%, $p < 0.01$) compared to control ECM (fig 7.7 panels C and G and fig 7.9a). The staining was observed to form a mesh like network of fibres that extended over the cell surface and into the ECM (fig 7.7 panels G and H).

TG2^{-/-} cells showed barely detectable levels of $\epsilon(\gamma\text{-glutamyl})$ lysine crosslink (fig 7.7 panels O and P and fig 7.9b) and the staining was mostly intracellular. In contrast, WT cells (panels K and L) showed a much greater degree of $\epsilon(\gamma\text{-glutamyl})$ lysine crosslink staining (+82%, $p = 0.05$) which extended beyond the cells and into the ECM.

Figure 7.7 Collagen Immunofluorescence

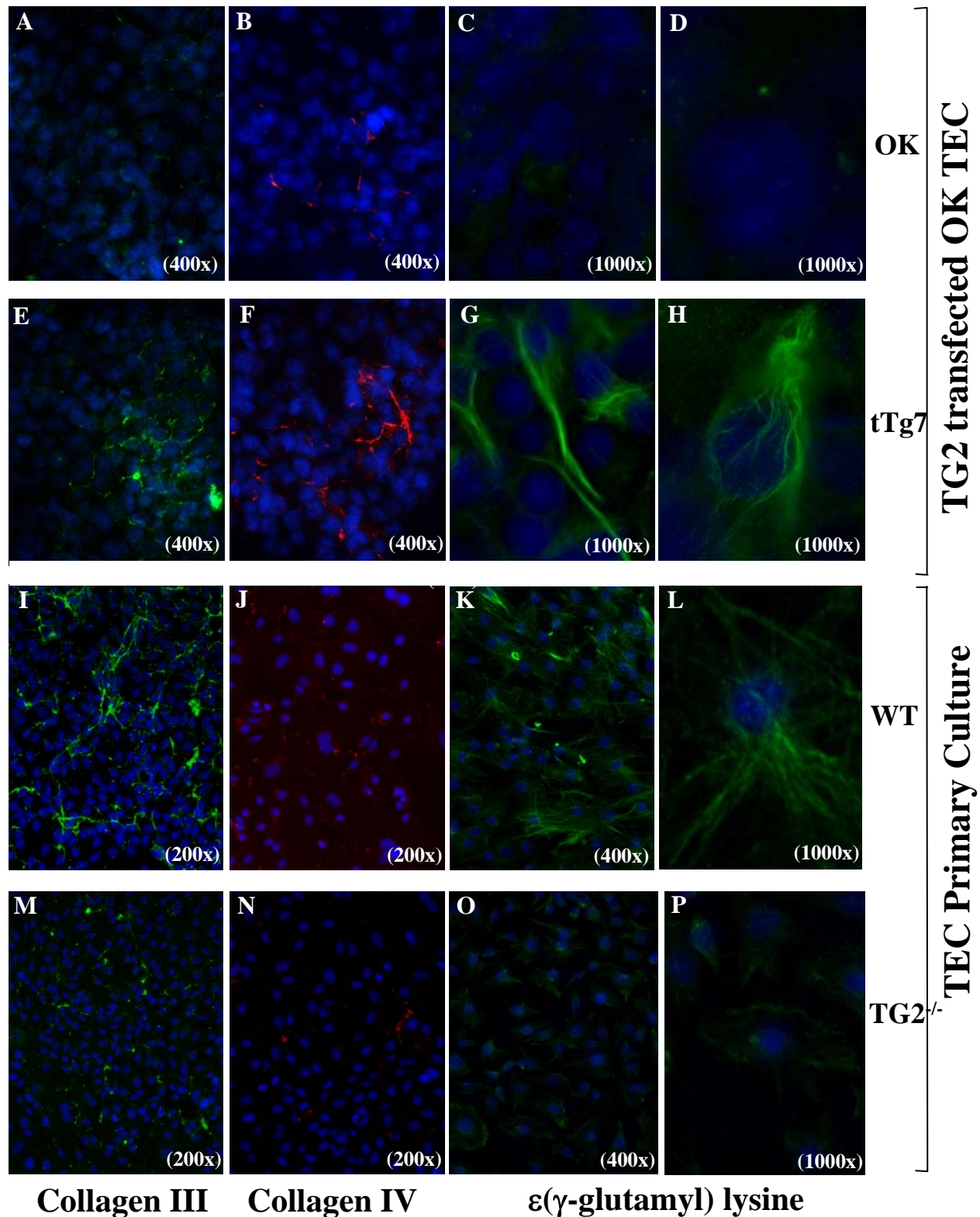
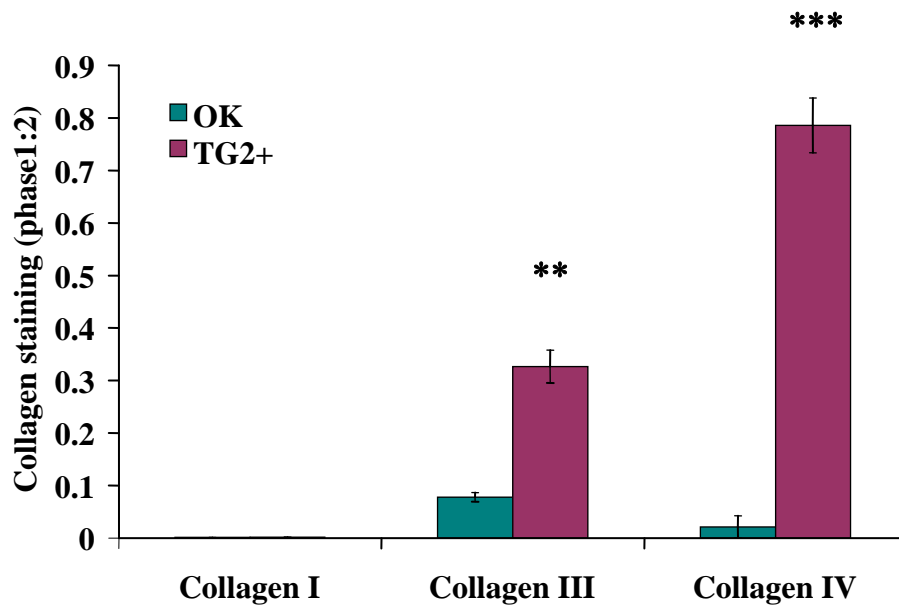


Figure 7.7 Representative photomicrographs of ECM from normal OK cells (panels A to D), over-expressing clone tTg7 (panels E to H), primary WT tubular cells (panels I to L) and TG2^{-/-} cells (panels M to P). ECM was probed with goat anti-collagen III polyclonal antibody and detected with anti-goat FITC (panels A, E, I and M) or rabbit anti-Collagen IV polyclonal and detected with anti-rabbit TRITC (panels B,F, J and N). Magnifications are shown in parentheses.

Figure 7.8 Multi-phase Image Analysis of Collagen Immunofluorescence

a) OK Over-expressing Clone tTg7 ECM



b) TG2^{-/-} Tubular ECM

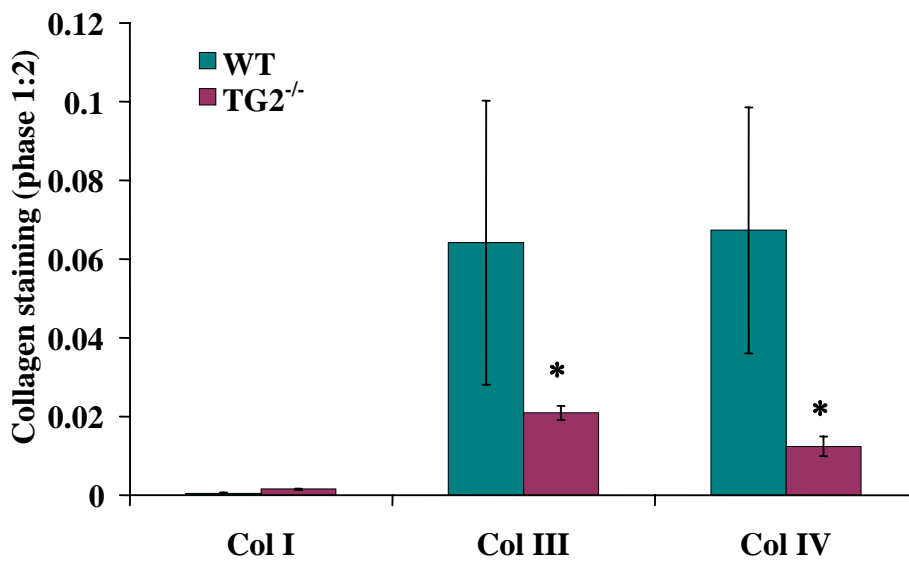
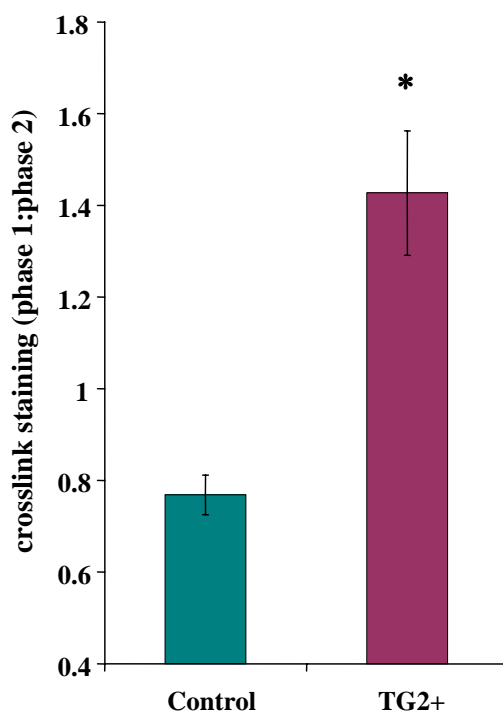


Figure 7.8 Collagen staining was determined in TG2 over-expressing OK clone tTg7 (a) and TG2^{-/-} (b) ECM by immunofluorescence and 10 random fields analysed by multiphase image analysis. Collagen immunofluorescence was expressed as a ratio of collagen (phase 1): DAPI staining (phase 2) to correct for cell number. Data represents mean ± SEM of 10 fields. *=p<0.05, **=p<0.001, ***=p<0.0001 compared to control (students t test).

Figure 7.9 Multi-phase Image Analysis of $\epsilon(\gamma\text{-glutamyl})$ lysine Crosslink

a) OK Over-expressing Clone tTg7 ECM



b) TG2^{-/-} Tubular ECM

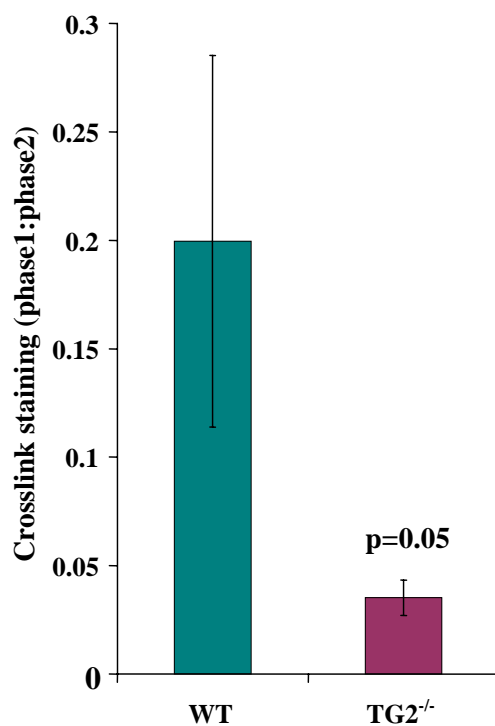


Figure 7.9 $\epsilon(\gamma\text{-glutamyl})$ lysine crosslink staining was determined in TG2 over-expressing OK clone tTg7 (a) and TG2^{-/-} (b) ECM by immunofluorescence and 10 random fields analysed by multi-phase image analysis. Immunofluorescence was expressed as a ratio of $\epsilon(\gamma\text{-glutamyl})$ lysine (phase 1): DAPI staining (phase 2) to correct for cell number. Data represents mean \pm SEM of 10 fields. *= $p < 0.01$ compared to control (students t test).

7.2.2.5 Collagen mRNA expression

To ascertain whether changes in the collagen composition of the ECM in response to TG2 modulation could be attributable to increased collagen expression, Northern blot analysis was used to determine the collagen mRNA expression profile of TG2 over-expressing OK cells and primary WT and TG2^{-/-} tubular cells (figs 7.10 to 7.13).

Interestingly, densitometric analysis of transfected OK cells indicated changes in collagen mRNA expression relative to un-transfected cells in response to transfection with the pCIneo vector alone. Decreases of 29.5% and 23.5% were observed in collagen I and IV mRNA expression (figs 7.10 and 7.12) in cells transfected with pCIneo compared to un-transfected cells. Conversely, collagen III mRNA expression as indicated by the presence of a 5.4 kb band, was increased by 82% ($p < 0.0001$; one way ANOVA with Bonferroni post hoc test) in pCIneo transfected cells. This was coupled with the appearance of a smaller unidentified band not present in either un-transfected or TG2 transfected cells.

In TG2 over-expressing OK cells, reductions were observed in the mRNA expression of collagens I, III and IV (fig 7.10, 7.11 and 7.12) compared to normal and transfection control OK cells. In the highest expressing clone tTg7, levels of collagen I and III mRNA were significantly reduced by 61.8% ($p < 0.05$; Bonferroni post hoc test) and 51.9% ($p < 0.0001$; Bonferroni post hoc test) respectively compared to the transfection control whilst a significant decrease in collagen IV expression of 43.5% ($p < 0.05$; Bonferroni post hoc test) was observed.

The changes in collagen mRNA expression were difficult to confirm in TG2 null tubular cells due to the small number of samples and variability in loading which influenced volume densitometry analysis. However, there appeared to be little overall change in collagen I and III mRNA expression in TG2^{-/-} cells (fig 7.13a and c) compared to WT although a small increase in collagen IV mRNA expression was indicated (fig 7.13b).

7.2.2.6 Collagen deposition rate

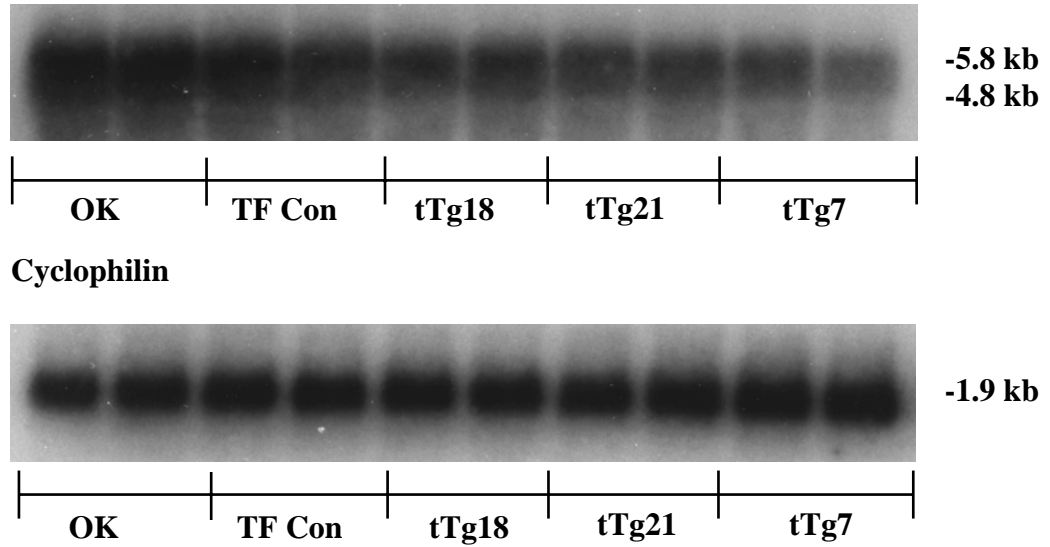
To determine whether TG2 modulation influenced the rate of collagen deposition, the ECM from TG2 over-expressing OK clone tTg7 (TG2+) and TG2 null tubular cells was labelled with ³H-proline in the presence of the MMP inhibitor Galardin (fig 7.14). Galardin is a recently developed broad spectrum peptidyl hydroxamate inhibitor that inhibits MMPs -1,-2,-3 and -9 (Grobelny *et al.*, 1992). In these cells, Galardin blocks over 95% of breakdown (unpublished observation) and was preferential to 1, 10 phenanthroline due to its lack of toxic effects on OK cells.

In OK cells, treatment with 10 μ M Galardin increased collagen deposition in both control and TG2+ ECM over 72 hours (fig 7.14a). However, the proportional increase in deposition of TG2+ ECM was double that of control ECM indicating that elevated TG2 influenced deposition rate.

Application of Galardin to primary tubular cells (fig 7.14b) resulted in an increase in ³H-proline incorporation into WT ECM of 15 dpm/mg protein compared to a 5 dpm increase in TG2^{-/-} generated ECM. This represented a 3 fold reduction in collagen deposition rate in the absence of TG2.

Figure 7.10 Collagen I mRNA Expression in TG2 Over-expressing OK Cells

**a) Northern blots
Collagen I**



b) Volume Densitometry

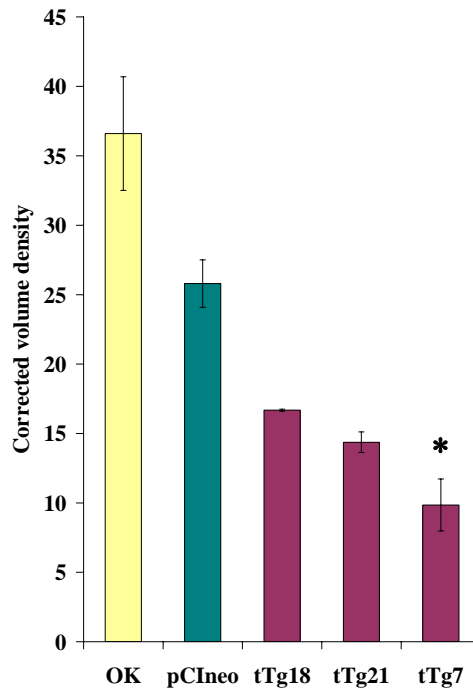
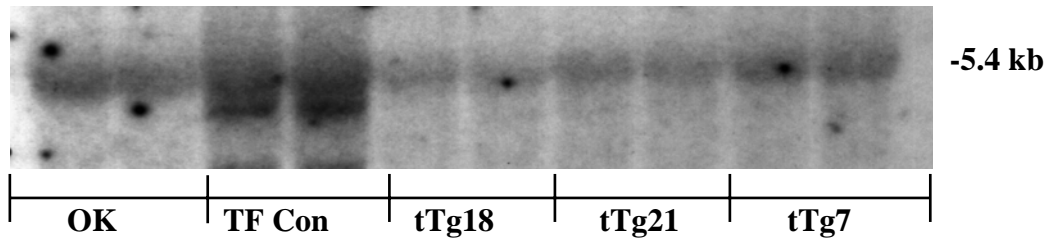


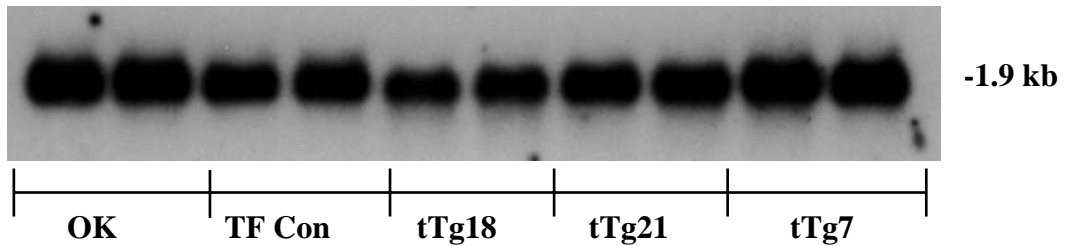
Figure 7.10 (a) TG2 over-expressing OK cells were harvested, total RNA extracted and subjected to Northern Blot analysis using a specific [³²P]-dCTP random primed cDNA probe for Collagen I (section 3.4.8). Repeat probing with cyclophilin was used as a loading control. (b) Volume densitometry analysis was performed using Multi-Analyst version 3.2TM. Data represents mean volume density \pm SEM from 2 separate blots, n=2 samples per blot, corrected for loading using cyclophilin. *=p<0.05 compared to transfection control cells (one way ANOVA with Bonferroni post hoc test).

Figure 7.11 Collagen III mRNA Expression in TG2 Over-expressing OK Cells

**a) Northern blots
Collagen III**



Cyclophilin



b) Volume densitometry

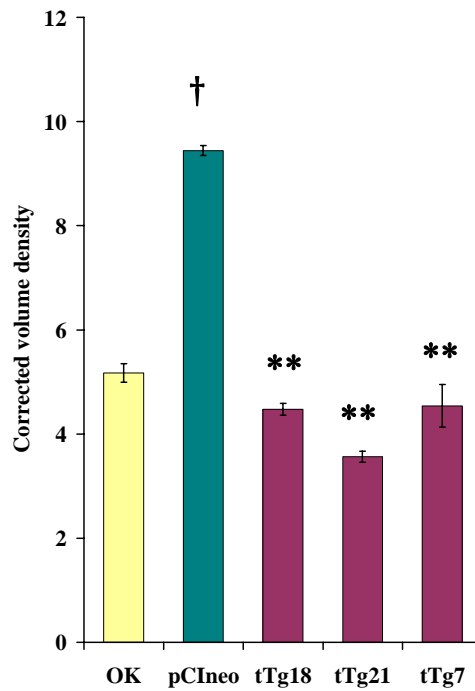
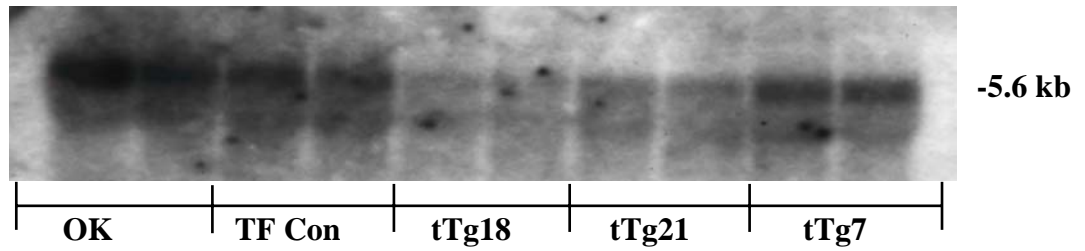


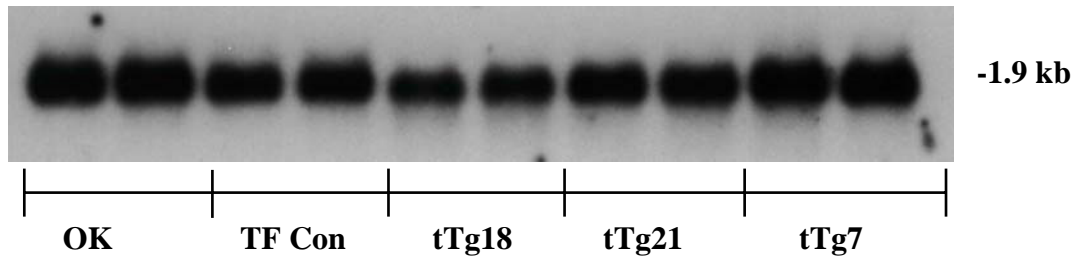
Figure 7.11 (a) TG2 over-expressing OK cells were harvested, total RNA extracted and subjected to Northern Blot analysis using a specific [³²P]-dCTP random primed cDNA probe for Collagen III. Repeat probing with cyclophilin was used as a loading control. (b) Volume densitometry analysis was performed using Multi-Analyst version 3.2™. Data represents mean volume density ± SEM from 2 separate blots, n=2 samples per blot, corrected for loading using cyclophilin. **=p<0.0001 compared to transfection control cells, † = p<0.0001 compared to un-transfected OK cells (one way ANOVA with Bonferroni post hoc test).

Figure 7.12 Collagen IV mRNA Expression in TG2 Over-expressing OK Cells

**a) Northern blots
Collagen IV**



Cyclophilin



b) Volume densitometry

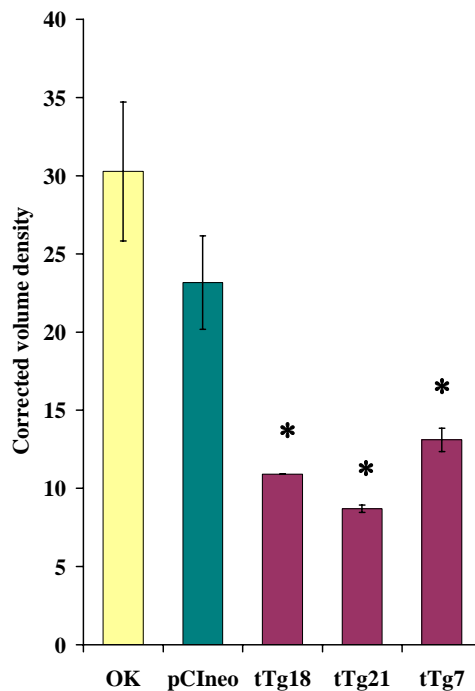


Figure 7.12 (a) TG2 over-expressing OK cells were harvested, total RNA extracted and subjected to Northern Blot analysis using a specific [³²P]-dCTP random primed cDNA probe for Collagen IV. Repeat probing with cyclophilin was used as a loading control. (b) Volume densitometry analysis was performed using Multi-Analyst version 3.2TM. Data represents mean volume density \pm SEM from 2 separate blots, n=2 samples per blot corrected for loading using cyclophilin. *=p<0.05 compared to transfection control cells (one way ANOVA with Bonferroni post hoc test).

Figure 7.13 Collagen mRNA Expression in WT and TG2^{-/-} Tubular Cells

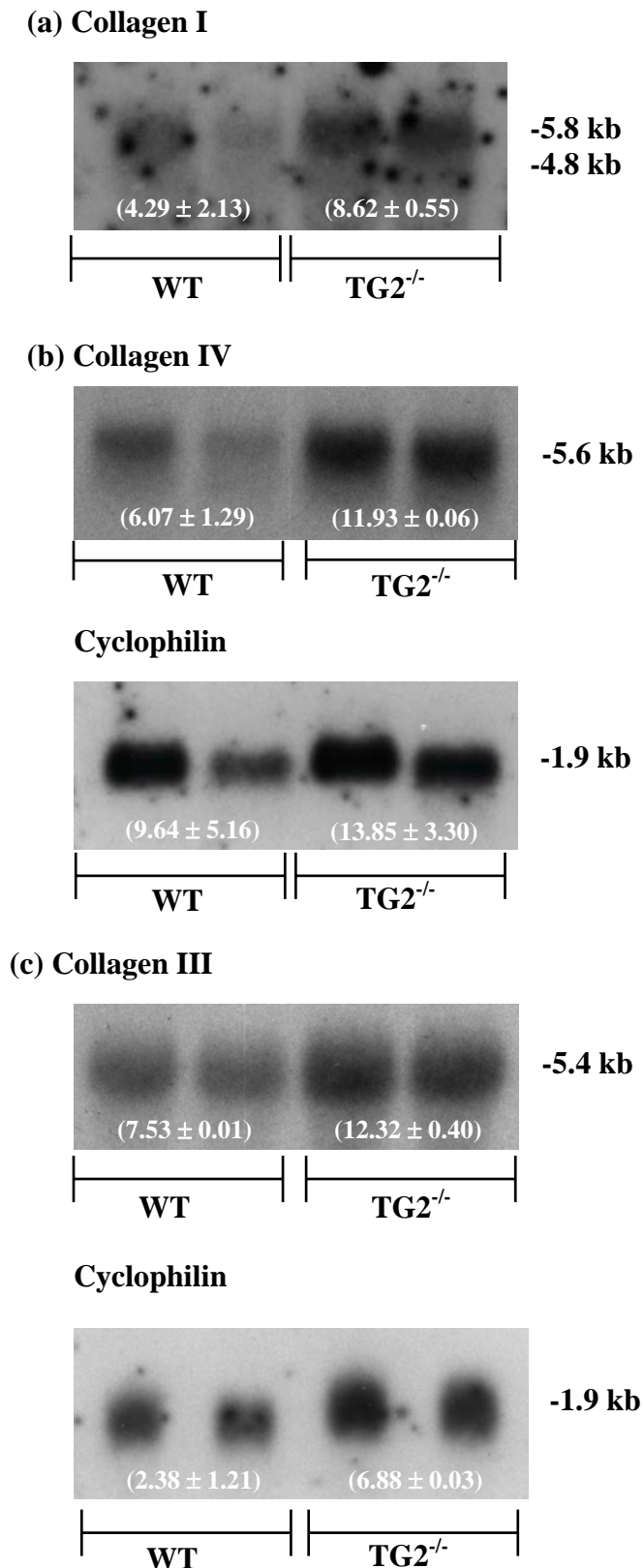
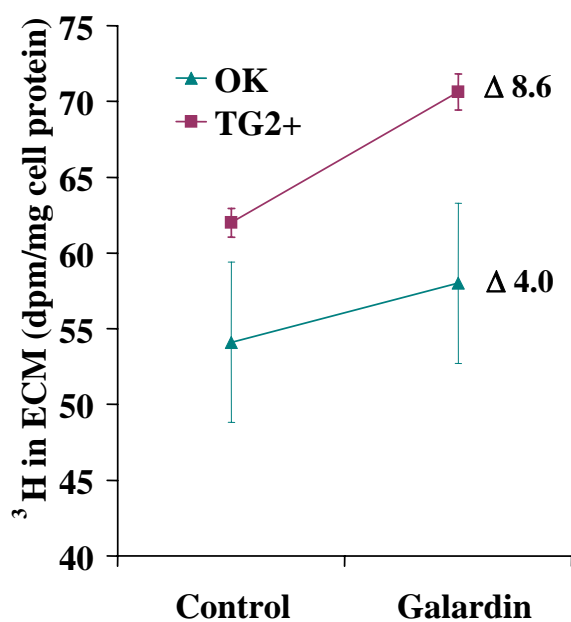


Figure 7.13 (a) WT and TG2^{-/-} primary tubular cells were harvested, total RNA extracted and subjected to Northern Blot analysis using specific [³²P]-dCTP random primed cDNA probes for collagen, I, III and IV. Repeat probing with cyclophilin was used as a loading control. Data in parentheses shows the mean volume densitometry value for each group.

Figure 7.14 ECM Deposition in the Presence of the MMP Inhibitor Galardin

a) OK Clone tTg7 ECM



b) TG2^{-/-} Tubular ECM

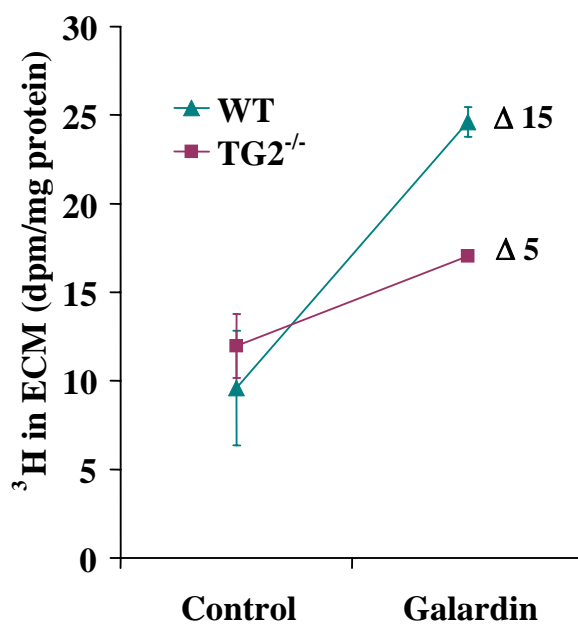


Figure 7.14 TG2 over-expressing OK cells (TG2+) and TG2^{-/-} tubular cells were labelled for 72 hours with 10 μ Ci of ³H-proline in the presence or absence of 10 μ M Galardin. ECM was recovered and label measured by scintillation counting. Data represents mean dpm/mg cellular protein \pm SEM from 3 separate experiments performed in duplicate.

7.2.2.7 mRNA expression of MMPs and TIMPs

Northern blotting was used to determine whether changes in TG2 expression had any feedback on the mRNA expression of matrix-degrading enzymes MMPs and their inhibitors TIMPs that in turn could affect the rate of ECM breakdown (figs 7.15 to 7.20). Quantitative analysis of MMP and TIMP mRNA expression was determined by volume densitometry with the exception of MMP-1 and TIMP-1 which were analysed by spot densitometry due to the poor quality of the blots and interference by high background signal.

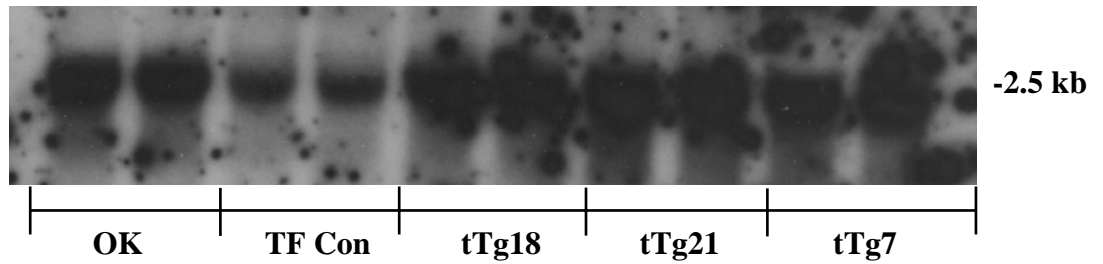
Densitometry analysis of transfected OK cells revealed that in a similar manner to collagen expression (section 7.2.2.5), transfection with the pCIneo vector alone also influenced the expression of MMPs and TIMPs relative to un-transfected OK cells. The mRNA expression of MMP-1, TIMP-1 and TIMP-3 (figs 7.15, 7.17 and 7.18) was reduced by 25% 12% and 54% respectively compared to un-transfected cells. In contrast, MMP-9 expression (fig 7.16) was increased by 39% ($p < 0.05$) in transfection control cells compared to normal. In TG2 over-expressing OK cells, spot densitometry indicated an increase in the mRNA expression of MMP-1 (fig 7.15) compared to the transfection control although this was not significant. Levels of TIMP-1 mRNA expression (fig 7.17) appeared relatively unchanged. TIMP-3 mRNA expression (fig 7.18) was shown to be increased as indicated by volume densitometry, with a 4.5 fold increase in clone tTg7 expression ($p < 0.01$) compared to the transfection control. MMP-9 mRNA expression (fig 7.16) was variable depending on the clone but was reduced by 25% in clone tTg7 ($p < 0.05$) compared to pCIneo. TIMP-2 was below the limit of detection and data is not shown.

The changes in MMP and TIMP mRNA expression in TG2 null tubular cells (figs 7.19 and 7.20) were difficult to interpret due to the poor quality of some blots and the considerable variability in loading both within and between groups. Examination of raw densitometric values indicated that mRNA expression of MMP-9, TIMP-1 and TIMP-2 was similar in WT and TG2^{-/-} cells. However, correction for loading using cyclophilin (data not shown) influenced these values such that MMP-9 appeared increased whilst TIMP-1 and TIMP-2 appeared decreased in TG2^{-/-} compared to WT. In comparison, TIMP-3 densitometric values were slightly higher in TG2^{-/-} cells although when corrected for loading, no change in TIMP-3 expression was observed. Volume density values of MMP-1 mRNA were unreliable due to the poor quality of the blot.

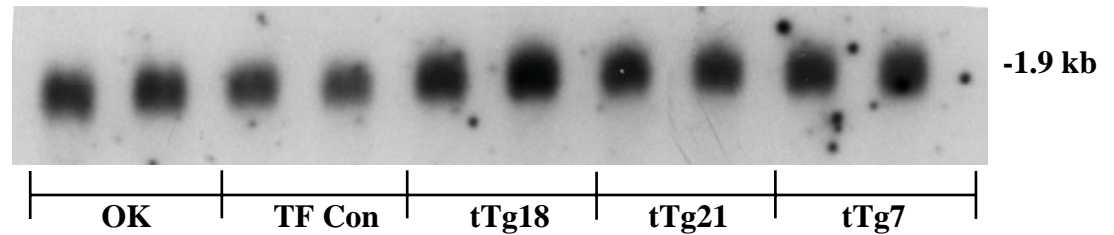
Figure 7.15 MMP-1 mRNA Expression in TG2 Over-expressing OK cells

a) Northern blots

MMP-1



Cyclophilin



b) Spot densitometry

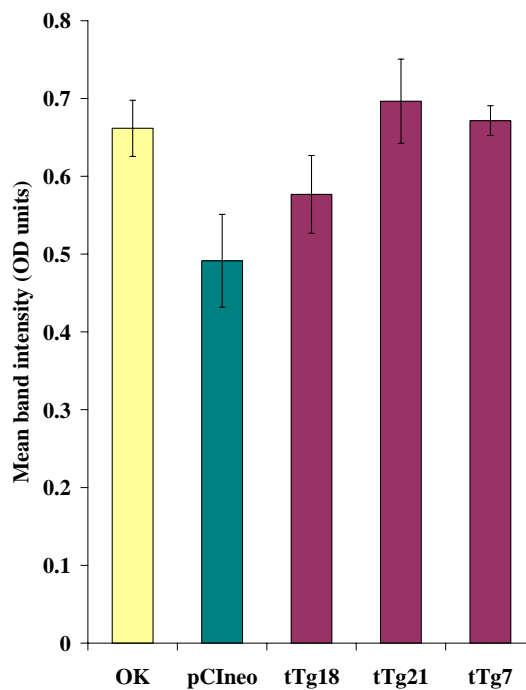
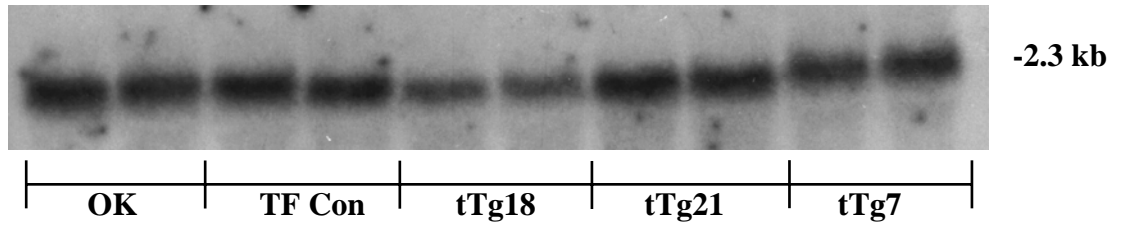


Figure 7.15 TG2 over-expressing OK tubular cells were harvested, total RNA extracted and subjected to Northern Blot analysis using a specific [³²P]-dCTP random primed cDNA probe for MMP-1. Repeat probing with cyclophilin was used as a loading control (a). Spot densitometry analysis was performed using Molecular Analyst version 4 software (b). Data represents mean optical density (OD) ± SEM from 2 separate blots, n=2 samples per blot corrected for loading using cyclophilin.

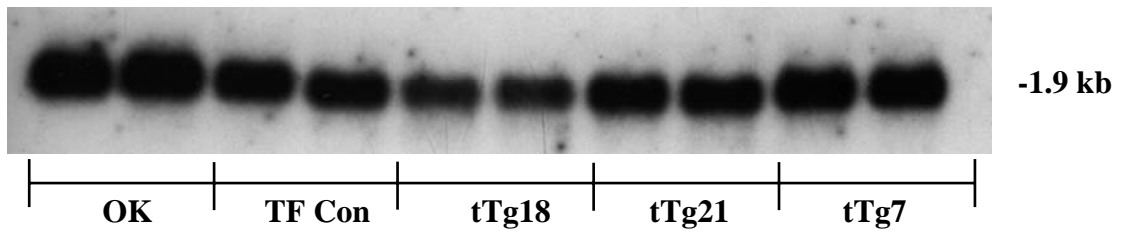
Figure 7.16 MMP-9 mRNA Expression in TG2 Over-expressing OK cells

a) Northern blots

MMP-9



Cyclophilin



b) Volume densitometry

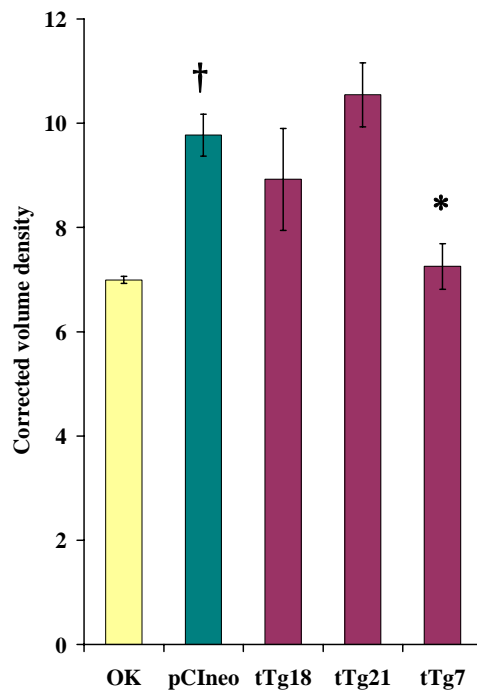
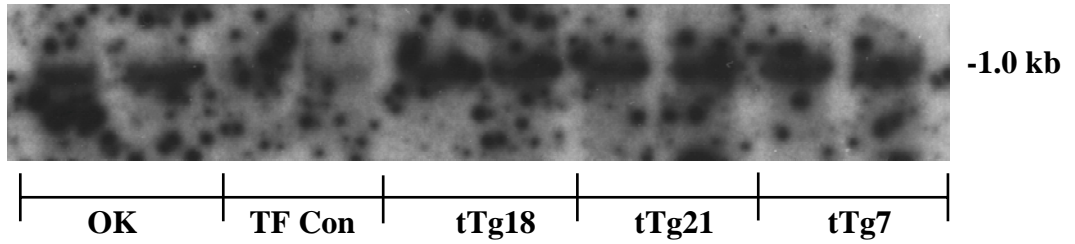


Figure 7.16 TG2 over-expressing OK tubular cells were harvested, total RNA extracted and subjected to Northern Blot analysis using a specific [³²P] dCTP random primed cDNA probe for MMP-9. Repeat probing with cyclophilin was used as a loading control (a). Volume densitometry analysis was performed using Multi-Analyst version 3.2™ (b). Data represents mean volume density ± SEM from 2 separate blots, n=2 samples per blot, corrected for loading using cyclophilin mRNA density. * = p<0.05 compared to transfection control cells, † = p<0.05 compared to un-transfected OK cells (one way ANOVA with Bonferroni post hoc test).

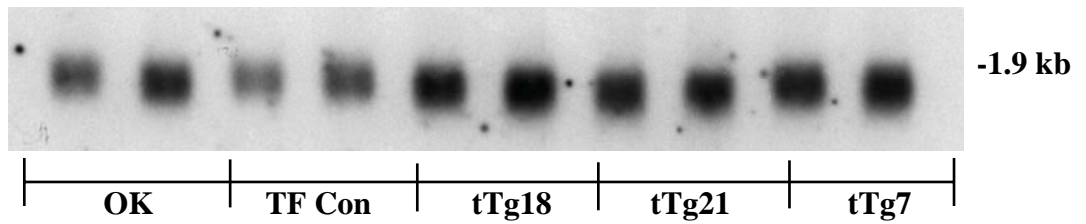
Figure 7.17 TIMP-1 mRNA Expression in TG2 Over-expressing OK cells

a) Northern blots

TIMP-1



Cyclophilin



b) Spot densitometry

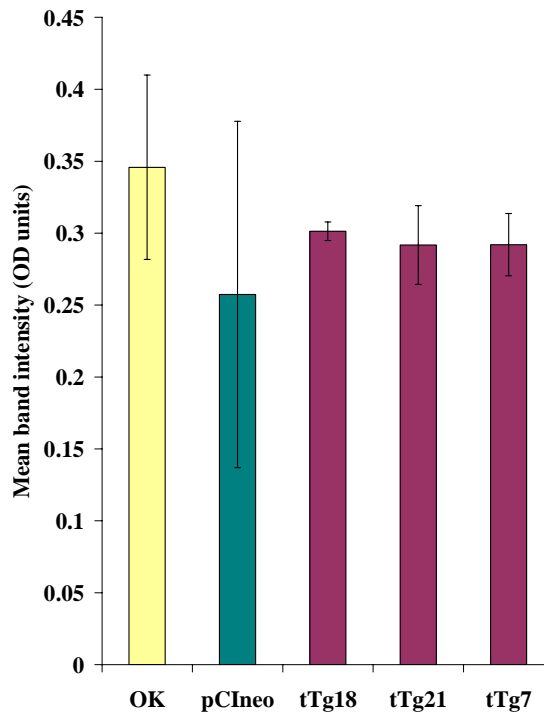
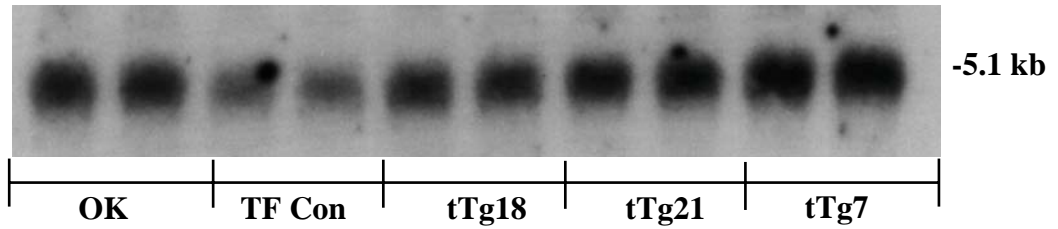


Figure 7.17 TG2 over-expressing OK tubular cells were harvested, total RNA extracted and subjected to Northern blot analysis using a specific [³²P] dCTP random primed cDNA probe for TIMP-1. Repeat probing with cyclophilin was used as a loading control (a). Spot densitometry analysis was performed using Molecular Analyst version 4 software (b). Data represents mean optical density (OD) ± SEM, from 2 separate blots, n=2 samples per blot, corrected for loading using cyclophilin mRNA density.

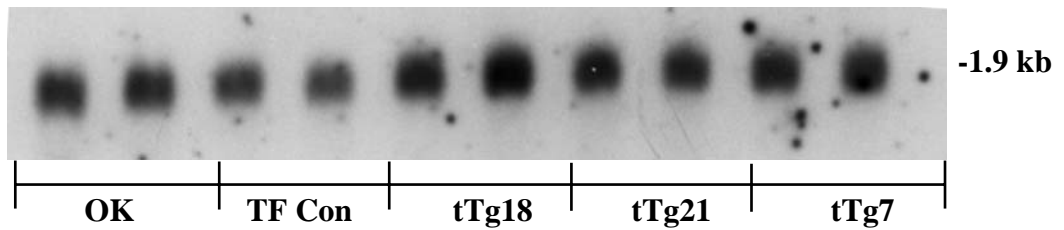
Figure 7.18 TIMP-3 mRNA Expression in TG2 Over-expressing OK cells

a) Northern blots

TIMP-3



Cyclophilin



b) Volume densitometry

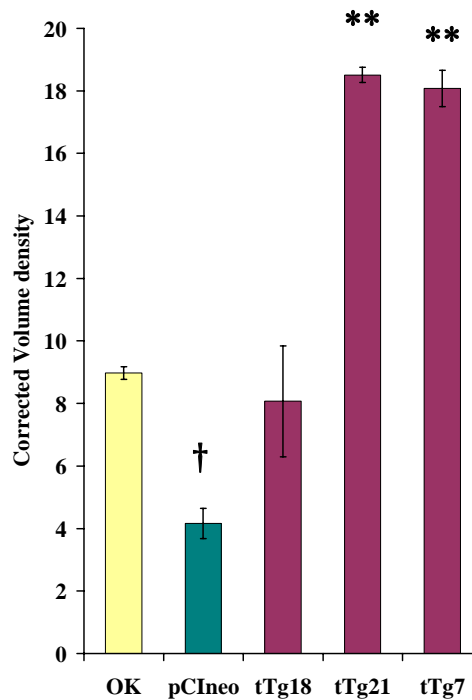
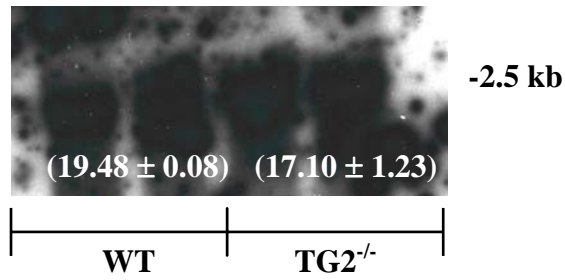


Figure 7.18 TG2 over-expressing OK tubular cells were harvested, total RNA extracted and subjected to Northern Blot analysis using a specific [³²P] dCTP random primed cDNA probe for TIMP-3. Repeat probing with cyclophilin was used as a loading control (a). Volume densitometry analysis was performed using Multi-Analyst version 3.2™ (b). Data represents mean volume density ± SEM, from 2 separate blots, n=2 samples per blot, corrected for loading using cyclophilin mRNA density. **=p<0.01 compared to transfection control cells, † = p<0.05 compared to un-transfected cells (one way ANOVA with Bonferroni post hoc test).

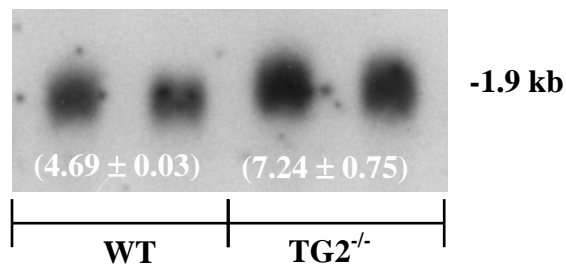
Figure 7.19 MMP-1 and MMP-9 mRNA Expression in WT and TG2^{-/-} Tubular Cells

Northern blots

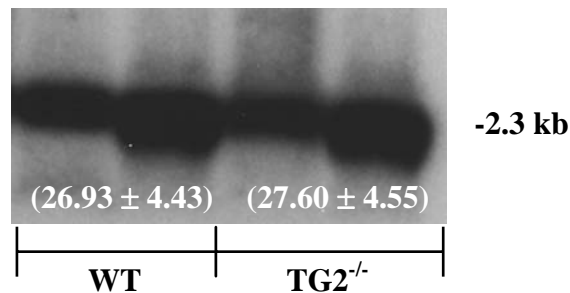
MMP-1



Cyclophilin



MMP-9



Cyclophilin

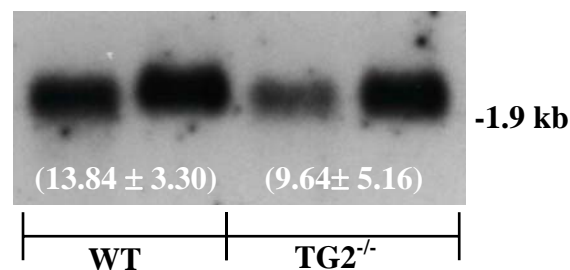


Figure 7.19 WT and TG2^{-/-} primary tubular cells were harvested, total RNA extracted and subjected to Northern Blot analysis using specific [³²P] dCTP random primed cDNA probes for MMP-1 and MMP-9. Repeat probing with cyclophilin was used as a loading control. Volume densitometry analysis was performed using Multi-Analyst version 3.2TM. Data in parentheses shows mean volume densitometry values ± SEM for each group.

Figure 7.20 TIMP-1, TIMP-2 and TIMP-3 mRNA Expression in WT and TG2^{-/-} Tubular Cells

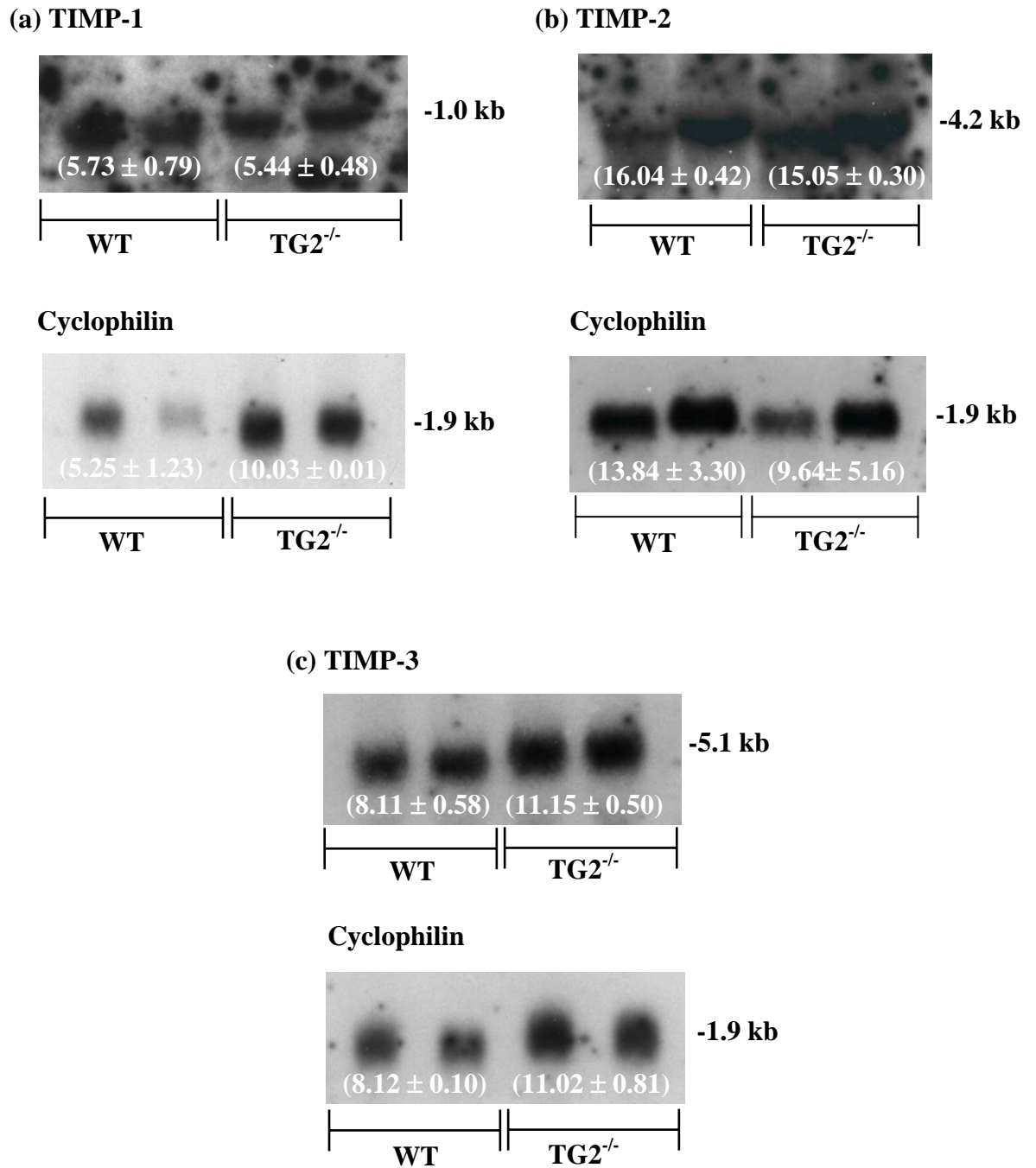


Figure 7.20 WT and TG2^{-/-} primary tubular cells were harvested, total RNA extracted and subjected to Northern Blot analysis using specific [³²P] dCTP random primed cDNA probes for TIMP-1, TIMP-2 and TIMP-3. Repeat probing with cyclophilin was used as a loading control. Volume densitometry analysis was performed using Multi-Analyst version 3.2TM. Data in parentheses shows mean volume densitometry values \pm SEM per group.

7.2.2.8 MMP activity of OK cells

7.2.2.8.1 Gelatin zymography of OK cell medium

To determine the MMP-1 and MMP-2 activity of normal OK cells, medium was isolated and subjected to gelatin zymography (fig 7.21a) and compared to controls of APMA activated human pro-MMP-1 and pro-MMP-2. OK cells appeared to show the presence of active MMP-2 as indicated by a band corresponding to 62kDa. Similarly, the presence of pro-MMP-1 and active MMP-1 was indicated by the presence of a doublet band at 52kDa and a single band at 42 kDa.

7.2.2.8.2 MMP activity of TG2 over-expressing OK cell medium

To determine if alterations in MMP and TIMP mRNA levels influenced overall MMP activity in TG2 over-expressing clones, conditioned medium from normal OK cells and clone tTg7 was tested against gelatin substrate using the EnzCheck assay system (fig 7.21b). A 53% reduction in MMP activity against gelatin was observed in tTg7 cells compared to wild type OK cells (0.023 vs 0.043 δ F1 units/hr).

7.2.2.9 Enzymatic degradation of tubular ECM

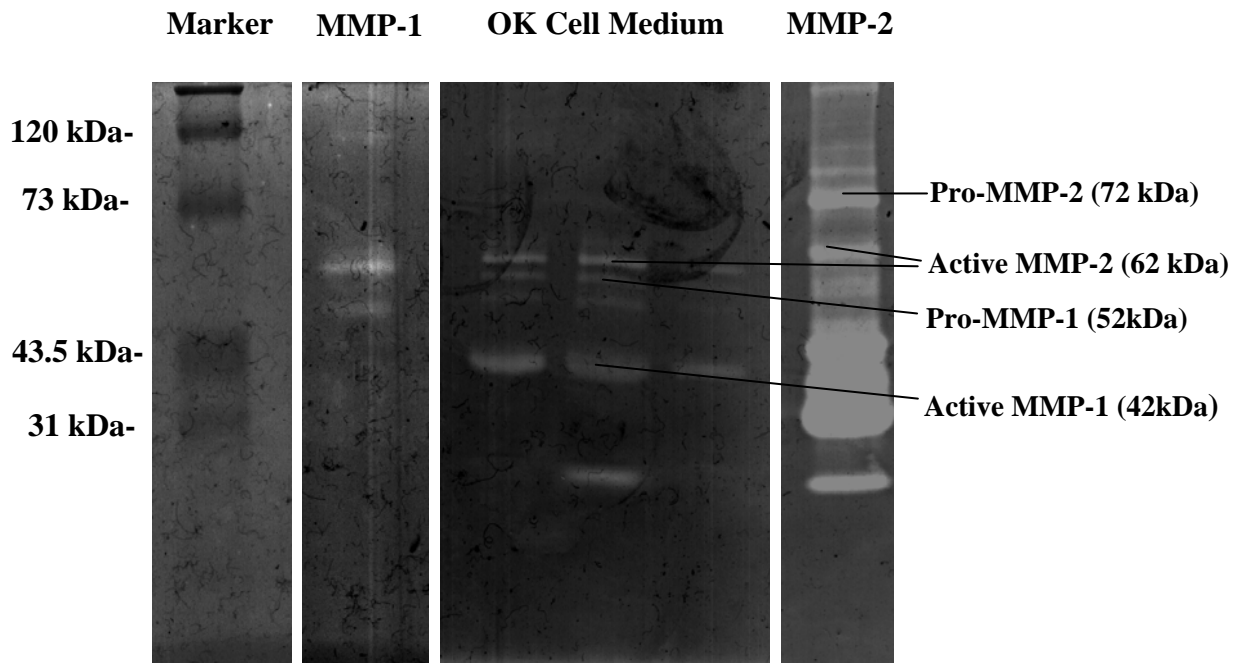
To establish whether mature ECM deposited by tubular cells could be successfully degraded, ECM from normal OK and clone tTg7 cells was subjected to treatment with a number of proteolytic enzymes.

For non-specific digestion of matrix proteins, the ECM was subjected to treatment with the proteolytic enzyme trypsin. The ECM was labelled for 72 hours with 3 H-proline followed by degradation of the ECM over a 20 minute time period with 5 μ g/ml trypsin (fig 7.22a). Both OK cell and clone tTg7 ECM was capable of being degraded by trypsin however, the ECM from clone tTg7 cells was found to be significantly more resistant to degradation by trypsin than control ECM ($p < 0.01$, students t test).

To develop a more physiologically relevant degradation assay, the ECM was degraded with bacterial collagenase from *Clostridium histolyticum* (fig 7.22b). This enzyme has previously been used in the study of collagen deposition (Eickelberg *et al.*, 1999; Nugent and Newman, 1989) and has the advantage of being collagen specific. Both control and tTg7 ECM was susceptible to degradation by this enzyme, however, degradation of tTg7 ECM with 0.01U/ml collagenase failed to show a significant difference in the rate of ECM breakdown compared to control ECM.

Figure 7.21 MMP Activity of OK Tubular Cells

a) Gelatin Zymograph of OK Cell Medium and Activated MMPs



b) Enzchek Assay

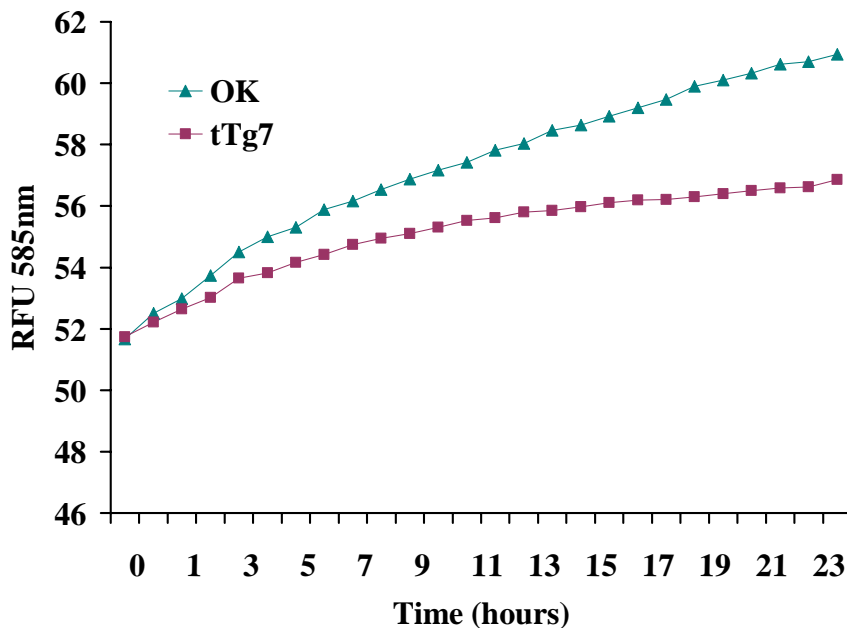


Figure 7.21 (a) 20µl of media isolated from normal OK cells was separated on a 10% polyacrylamide gel containing 1mg/ml of gelatin and analysed for MMP activity by gelatin zymography as described in section 3.5.4.3. Identification of bands was by reference to purified APMA-activated human pro-MMP1 and purified APMA-activated human pro-MMP-2 (Biogenesis, Poole, UK). Marker = Biorad kaleidoscope pre-stained standards. (b) Proteolytic activity was determined in 20µl of OK cell and clone tTg7 media against a DQ gelatin substrate using the Enzchek assay system as described in section 3.5.4.4. Data is expressed as relative fluorescent units at 585nm from a single experiment.

7.2.2.10 Degradation of tubular ECM with MMP-1 and MMP-2

To determine the ability of MMP-1 and MMP-2 to degrade cell synthesised and deposited tubular ECM, normal OK cell ECM was subjected to degradation by either 1µg/ml of APMA-activated pro-MMP-1, 1µg/ml of APMA-activated pro-MMP-2 or a combination of 1µg/ml MMP-1/MMP-2 (fig 7.23a). Control wells were incubated with MMP reaction buffer. Aliquots of the supernatant were scintillation counted and released radioactivity expressed as a percentage of the total ECM label.

Treatment of the ECM with either MMP-1 or MMP-2 alone was ineffective at degrading the matrix giving only 0.3% and 0.6% greater breakdown than the reaction buffer over the 24 hour time period. However, a combination of MMP-1 and MMP-2 was effective at degrading the ECM and gave double the breakdown achieved with either enzyme.

7.2.2.11 MMP-1/MMP-2 degradation of TG2 over-expressing and TG2 null tubular cell ECM

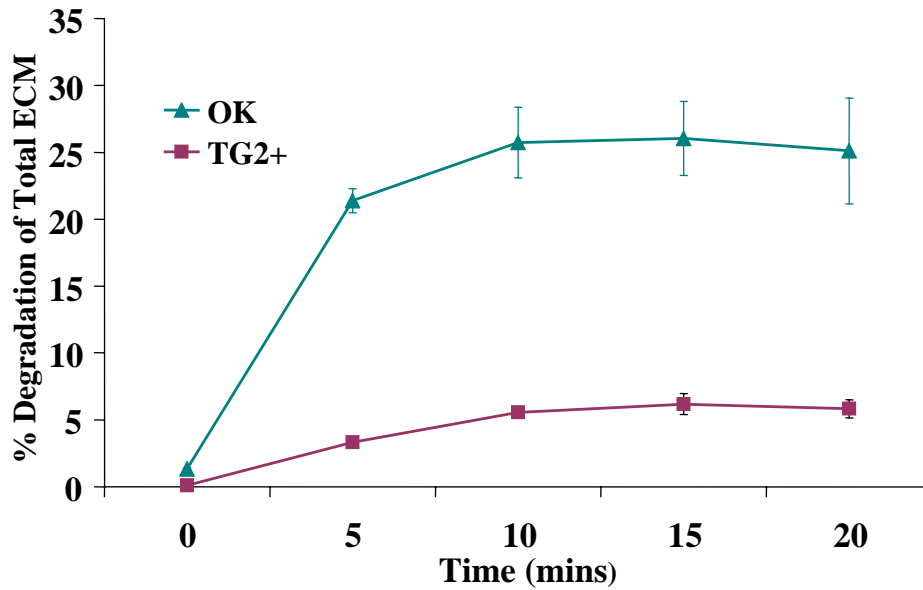
The degradation of tubular ECM by a combination of MMP-1 and MMP-2 was used to assess whether modulation of TG2 is able to influence the resistance of the ECM to MMP breakdown. Deposited tubular ECM previously labelled for 72 hours with ³H proline was degraded over 6 hours with a mixture of 1µg/ml MMP-1 and 1µg/ml MMP-2 (fig 7.23b).

Treatment of OK tTg7 clone ECM with MMP-1 and -2 (fig 7.23bi) reduced the percentage degradation of the ECM per hour from 2.3% as seen in OK cells to 1.1% indicating that tTg7 ECM was less susceptible to proteolytic decay than control cell ECM.

In contrast, the susceptibility of TG2^{-/-} ECM to MMP-1 and MMP-2 degradation was unchanged over the 6 hour time period (fig 7.23bii). However, TG2^{-/-} ECM was more readily degraded (2.86 v 3.61% per hour) for the first 30 mins after application of MMP-1 and 2.

Figure 7.22 Enzymatic Degradation of OK Clone tTg7 ECM

a) Degradation with 5 μ g/ml trypsin



b) Degradation with 0.01U/ml of collagenase from *Clostridium histolyticum*

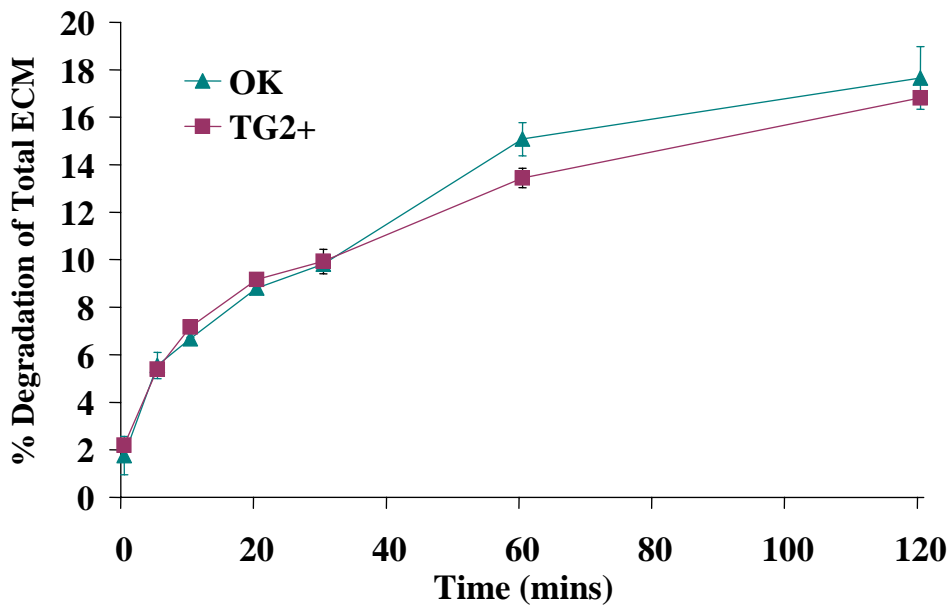
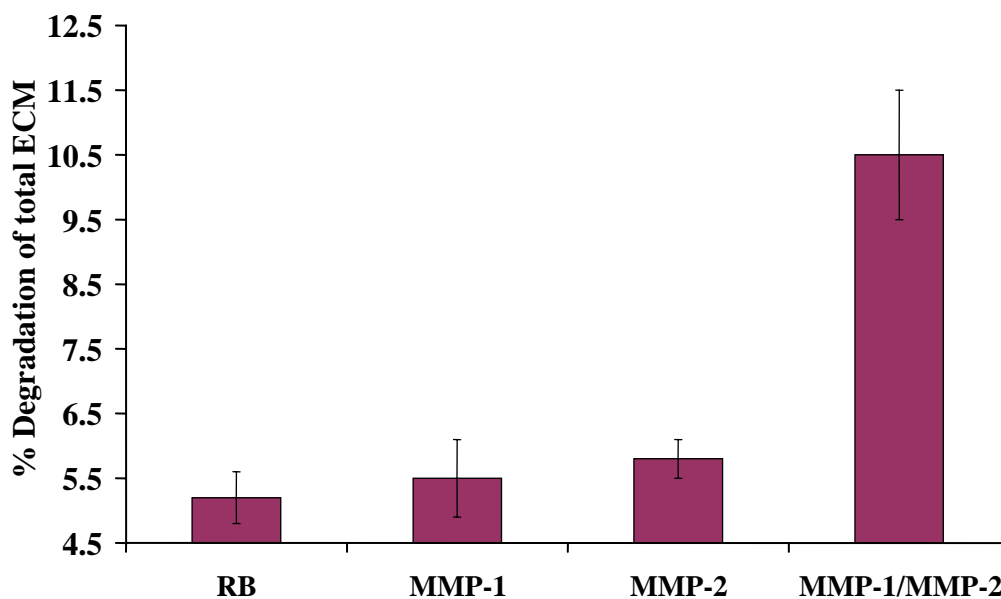


Figure 7.22 Cells were incubated with 10 μ Ci of 3 H-proline for 72 hours prior to degrading the ECM with 1ml of 0.01x trypsin-EDTA in PBS for up to 20 mins (a) or 0.01U/ml of collagenase from *Clostridium histolyticum* in PBS for up to 120 mins (b). 100 μ l samples were removed at 5 min (a) or 10 min intervals (b) and the amount of released label determined by scintillation counting (section 3.5.4.2). Data is expressed as the % degradation of total ECM label \pm SEM from 3 separate experiments performed in duplicate. All values were corrected for background degradation by PBS alone.

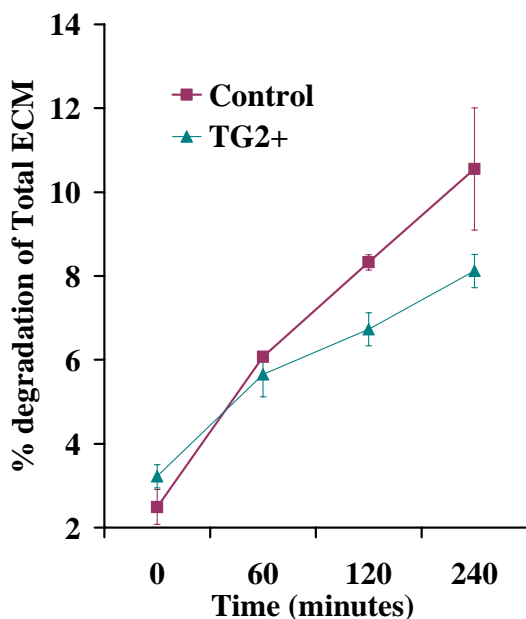
Figure 7.23 MMP Degradation of OK Cell Tubular ECM

a) Susceptibility of normal ECM to MMP breakdown



b) Combined MMP-1 and MMP-2 Degradation of Tubular Cell ECM

i) Clone tTg7 ECM



ii) TG2^{-/-} Tubular Cell ECM

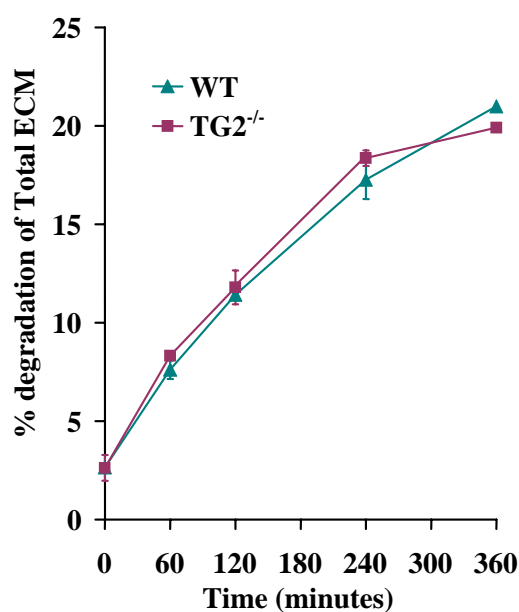


Figure 7.23 (a) OK cells were cultured for 72 hours with ³H-proline, the cells removed and the ECM degraded for 24 hours with either reaction buffer (RB), 1µg/ml APMA-activated MMP-1 alone, 1µg/ml MMP-2 alone or a combination of 1µg/ml MMP-1 and MMP-2 (section 3.5.4.2). (b) OK clone tTg7 ECM (i) and TG2^{-/-} tubular cell ECM (ii) was digested as previously with a combination of 1µg/ml of MMP-1 and 1µg/ml of MMP-2 for up to 24 hours. 50µl of supernatant was removed at 0, 30 and 60 and 120 mins and every 2 hours after that up to 24 hours. The percentage of total ECM degraded was determined by scintillation counting. Data represents mean ± SEM from 3 separate experiments performed in duplicate.

7.3 Discussion

Numerous studies have established that the accumulation of scar tissue in CKD is associated with the elevated expression of TG2 by tubular cells (Johnson *et al.*, 1997; Johnson *et al.*, 1999; Skill *et al.*, 2001). Previous data suggests that TG2 may play a direct role in the excess accumulation of ECM by influencing the deposition of available matrix proteins and their susceptibility to proteolytic breakdown (Johnson *et al.*, 1999). To investigate this, the properties of ECM generated and laid down by OK over-expressing tubular cells and primary tubular cells from the TG2 knockout mouse were examined.

Analysis of ECM levels demonstrated that elevating TG2 expression increased the level of ECM collagen but surprisingly did not affect the overall level of ECM, whilst a lack of TG2 reduced both total ECM and collagen levels. The changes in collagen are in support of previous data in glucose stimulated OK cells in which increased TG2 activity and ϵ (γ -glutamyl) lysine were associated with increased collagen that could be reduced by TG2 inhibition (Skill *et al.*, 2004). However, these changes were also associated with altered levels of total ECM attributable to increases in both fibronectin and collagen. Although an effect on the deposition of other ECM proteins such as fibronectin has not been investigated, it is likely that a compensatory reduction in non-collagenous components of the ECM contributes to the stable ECM levels observed here. Of relevance, it is compositional changes to the ECM that are often the first sign of early kidney disease with basement membranes having a higher interstitial collagen content. The qualitative change to the ECM in response to increased expression of TG2 demonstrated in this study, which favours the accumulation of collagen rich matrix would certainly support this.

Changes in ECM collagen were as a direct result of alterations in the levels of collagen III and IV in the ECM. Interestingly, neither OK tubular ECM nor that of primary tubular cells had significant levels of collagen I even when TG2 was elevated. This is in contrast to the *in vivo* situation where collagen I is increased markedly in disease (Floege *et al.*, 1992a; Johnson *et al.*, 2002; Mozes *et al.*, 1999; Uchio *et al.*, 1999). However, both OK cells and primary cells have detectable levels of collagen I mRNA. Given the suitability of collagen I as a TG2 substrate in other studies (Chau *et al.*, 2005), it seems reasonable to assume that if present in suitable quantities it would also be a good substrate for TG2. *In vivo*, the renal fibroblasts that surround tubular cells during the development of CKD generate significant amounts of collagen I that could easily become a substrate for tubular cell-derived TG2 (Müller and Rodemann, 1991; Rodemann and Müller, 1991).

Potentially increases in ECM collagen in response to TG2 modulation may reflect changes in mRNA-dependent collagen synthesis or the mRNA expression of MMPs and TIMPs and this was investigated by Northern blot analysis. An interesting observation was the apparent response of OK cells to transfection with the empty pCIneo vector which showed alterations in the mRNA expression of collagens and some MMPs and TIMPs compared to un-transfected cells. Given the random nature of vector integration into the genome at different chromosomal locations, it is likely that the observed mRNA changes in this clone reflect integration of pCIneo into regions that affect expression of these genes. In particular, the presence of the strong cytomegalovirus promoter in pCIneo may exert *trans* effects on endogenous promoters especially if integration of the vector occurs in close proximity (Hampf and Grossen 2007). Alternatively, the differential effects of pCIneo on collagen, MMP and TIMP expression relative to control cells may indicate that integration into endogenous DNA occurred within the regulatory region of a gene capable of influencing the expression of both collagen and matrix degrading enzymes such as Ets-1 (Trojanowski 2000).

Despite apparent changes in collagen mRNA expression in the transfection control which could have influenced the interpretation of data, TG2 over-expressing OK cells showed a consistent reduction in collagen I, III and IV mRNA expression compared to both pCIneo transfected and un-transfected OK cells, indicating that increased TG2 expression was associated with an overall reduction in collagen synthesis. Unfortunately, it was not possible to fully confirm whether opposing changes in collagen mRNA expression occurred in TG2 null cells given the variability in loading, which would have helped to reinforce this data and therefore further analysis is required. However, given that increases in the collagen content of the ECM were observed despite reductions in collagen synthesis suggests the potential importance of TG2 mediated post-translational crosslinking of available collagen to its accumulation.

The observed changes in the collagen content of the ECM in response to TG2 modulation may, of course, also be contributed to by alterations in the level of MMPs and TIMPs, which could affect the potential of the ECM to be degraded. Northern blot analysis was able to detect mRNA for MMP-1, MMP-9, TIMP-1 and TIMP-3 in TG2 modulated OK cells and also TIMP-2 in primary tubular cells however, the interpretation of this data was hindered by a high background signal especially for MMP-1 and TIMP-1 and the variation in loading in TG2 null cells. Elevated TG2 expression did appear to be associated with a small increase in MMP-1 and a much larger increase in TIMP-3 although not TIMP-1 and MMP-9 expression was variable, although reduced in clone tTg7. Opposing changes were suggested for some

MMPs and TIMPs in TG2 null cells if corrected for loading, with MMP-9 appearing to be increased and TIMP-1 and TIMP-3 decreased compared to WT cells. At best, this data suggests that some effect on MMP and TIMP expression may occur in response to TG2 modulation but the problems with the quantitation make it difficult to draw a definite conclusion as to the impact on the overall level of matrix degrading enzymes. Certainly, the measurement of MMP activity using fluorescein labelled gelatin suggests a reduction in MMP activity in tTg7 cells although the question still remains as to whether the collagen accumulation observed here is influenced in part by specific changes in MMP and TIMP expression which will probably require further clarification.

A feedback mechanism may exist that moderates the synthesis of collagens and possibly also ECM processing enzymes in the face of altered TG2 levels. Such feedback may not be a response to TG2 levels *per se* but may reflect the adaptation of tubular cells to the qualitative changes occurring in the ECM as a result of altered TG2 expression. Since integrins play a pivotal role in cell-ECM signalling, any adaptive change is likely to involve integrin binding which in turn may modulate ECM expression. It could be speculated that increased expression of integrins such as $\alpha1\beta1$ by tubular cells in response to the elevated collagen IV composition of the ECM could affect collagen synthesis given that it has been shown to negatively regulate collagen I expression at least (Heino 2000). However, any integrin-mediated effect on collagen synthesis in response to an altered collagen composition is also likely to involve changes in the expression of $\alpha2\beta1$, as this is known to be the major collagen receptor on epithelial cells (Heino 2000).

Alternatively, intracellular feedback on collagen synthesis may occur as a direct consequence of increased intracellular TG2 levels. It could be that elevated intracellular TG2 itself interacts with signalling pathways that are involved in the regulation of collagen synthesis. In support of this, TG2 has recently been identified as having intrinsic serine threonine kinase activity (Mishra *et al.*, 2007) and interestingly, studies on neuronal cells (Singh *et al.*, 2003) demonstrate that TG2 can activate a number of signalling pathways including ERK 1/2 and p38 MAP kinase that are also known to regulate collagen I expression (Ghosh 2002).

Since TG2 has been suggested to play a role in both ECM deposition and its susceptibility to MMP breakdown, a key part of this study was to investigate the effects of TG2 on these separate pathways. For these studies, a comparison was made between control OK cells and only the highest expressing OK cell clone tTg7. Whilst it would have been preferential to perform such experiments on all three over-expressing clones, this compromise

was required due to limitations of experimental cost and because the 7 fold increase in TG activity expressed by this clone is comparable to that observed per cell in CKD.

To determine whether TG2 was affecting collagen levels by influencing the rate of collagen deposition, labelling of the ECM with ³H-proline was performed in the presence of the MMP inhibitor Galardin. While tubular cells are known to produce other ECM proteases (Wagner *et al.*, 1996) blockage of MMP action in OK cell homogenates using the broad spectrum MMP inhibitor 1,10 phenanthroline, showed that more than 90% of all proteolytic action against various collagens could be blocked (data not shown). This indicates that most of the ECM clearance in this cell line is mediated by MMPs which gelatin zymography shows is predominantly due to MMPs -1 and -2. However, the toxic effects of 1,10 phenanthroline when used in cell cultures at the doses required meant that MMP inhibition by Galardin was more appropriate. Galardin is a specific, low toxicity MMP inhibitor that was originally developed as an inhibitor of human skin collagenase (Grobelny *et al.*, 1992) and blocks the action of MMP-1, -2, -3 and -9 (Grobelny *et al.*, 1992; Hao *et al.*, 1999). It was therefore ideally suited for use in these cell culture-based studies.

Using TG2 over expressing clone tTg7, a doubling of the rate of collagen deposition was seen over that in OK tubular cells, which was complemented by a 3 fold reduction in the deposition rate in TG2^{-/-} cells. Taken together, this data clearly shows that TG2 has a major influence on the deposition of available, soluble collagen molecules, and is in line with previous studies in human dermal fibroblasts cultured in the presence of exogenous TG2 (Gross *et al.*, 2003).

The mechanism of TG2 action on collagen deposition cannot be determined from the experiments performed here, although 2 areas are likely candidates. It is probable that TG2 is important in the stabilisation of newly synthesised and assembled collagen fibrils in the same manner as lysyl oxidase. Kleman and colleagues have previously described a TG2-mediated stabilisation process in a rhabdosarcoma cell line with collagens V and XI (Kleman *et al.*, 1995). Alternatively, TG2 may participate in the crosslinking of pre-assembled but immature collagen molecules into the matrix, a process that may lead to disorganised collagen fibril formation that is a characteristic feature of scar tissue.

In addition to an effect of TG2 on the rate of collagen deposition, TG2 was demonstrated to alter the susceptibility of the ECM to degradation. Firstly, the ability of the broad specificity serine protease trypsin and collagen-specific bacterial collagenase to effectively degrade WT OK cell ECM was demonstrated. In the case of trypsin this was perhaps surprising given that it is known to be ineffective at degrading mature fibrillar collagen

(Birkedal-Hansen *et al.*, 1985) which is the major ECM component in this matrix. The removal of cells with ammonium hydroxide may in some way alter the collagen structure in part enabling trypsin to effectively degrade it. A number of studies have certainly demonstrated that the chemical modification of collagen side chains has a significant impact on their ability to be proteolytically degraded by enzymes such as trypsin (Gratzer *et al.*, 2006). In particular, the modification of lysine and arginine residues is able to affect the amount and sites of trypsin cleavage (Gratzer *et al.*, 2004). Interestingly, degradation with trypsin revealed that clone tTg7 ECM was significantly more resistant to digestion than control ECM which would fit with these findings given that TG2 crosslinking occurs at lysine residues. Surprisingly, degradation of clone tTg7 ECM with collagenase was not significantly different to that of control ECM. This probably reflects the mechanism of bacterial collagenase action in which cleavage occurs at many sites along the collagen fibril rather than at specific target linkages that may be affected by TG2 crosslinking.

Degradation of the ECM with MMPs -1 and -2 demonstrated that tTg7 ECM also had an increased resistance to MMP breakdown. This is consistent with previous studies of the susceptibility of ECM to degradation using an *in vitro* degradation assay of isolated collagen fibrils which suggested that TG2 crosslinking caused resistance to degradation by MMP-1 (Johnson *et al.*, 1999). The data here clearly demonstrates that this is not an artefact of TG2 action on isolated collagen as matrix deposited by over expressing clone tTg7 showed about a 50% reduction in breakdown rate. However, there was surprisingly no difference in ECM breakdown rates between WT and TG2^{-/-} primary tubular ECM over a prolonged period, with an increase in breakdown in TG2^{-/-} ECM limited to the first 30 minutes after MMPs were applied. Although perhaps contradictory, it may simply indicate that TG2 crosslinking has to reach a threshold before it can influence proteolytic decay. If this threshold is not reached then removing more TG2 would theoretically have little or no effect as occurs after the first 30 minutes in these experiments. Understanding how TG2 action may influence the resistance to MMP breakdown is again beyond the scope of these experiments although it seems logical to assume that it must rely on changes in the level of crosslinking in the regions where MMPs act.

Previous work has suggested that much of the TG2 action in the extracellular environment could be through the activation of the large latent TGF- β 1 complex (Nunes *et al.*, 1997). A TG2-mediated increase in active TGF- β 1 could itself promote a pro-fibrotic condition by influencing the synthesis of numerous ECM proteins and TIMPs and causing a shut-down in TGF- β 1-responsive MMPs. Whilst there were certainly changes in collagen and

possibly MMP and TIMP expression, these were not the result of increased TGF- β activation in these cells as indicated by a lack of change in active TGF- β levels in response to TG2 modulation (Huang, 2006). This is in keeping with our previous studies in OK cells which show that glucose-stimulated ECM accumulation is TGF- β 1 independent (Skill *et al.*, 2004). The effects of TG2 on the deposition and breakdown properties of the ECM presented here must therefore result from a direct action of TG2 crosslinking and not via TGF- β -dependent mechanisms. Interestingly, it has been shown that tubular cells are unable to produce the large latent TGF β 1 complex (Ando *et al.*, 1995) with only the small latent complex being found; which TG2 will not affect. In this study, this has allowed the investigation of the direct action of TG2 without any potentially confounding effects of changes in TGF- β 1 activation.

The data presented in this chapter demonstrates for the first time that changes in tubular levels of TG2 directly affect the accumulation of ECM collagen by predominantly altering the rate of deposition but also by increasing the resistance of collagen to degradation by MMPs. This clearly identifies a critical role for TG2 in the regulation of the ECM and suggests a potentially pathological action when TG2 is raised in disease.

**The Role of Tissue Transglutaminase in
the Extracellular Matrix Changes
Associated With Kidney Scarring**

**Marie Fisher
Academic Nephrology Unit
School of Medicine and Biomedical Sciences
University of Sheffield**

Thesis submitted for the degree of Doctor of Philosophy

June 2007

Volume 2

Chapter 8

Effect of Tissue Transglutaminase Modulation on Mesangial Cell ECM

8.1 Introduction

In Chapter 7, it was demonstrated that TG2 modulation in tubular cells, which are the predominant cells to express TG2 in the scarred kidney, results in alterations in ECM homeostasis favouring the accumulation of tubular ECM.

However, in CKD progressive expansion of the tubulo-interstitial matrix is often paralleled by the expansion of the glomerular mesangium leading to glomerulosclerosis (Rosenblum, 1994). Studies on the streptozotocin model of diabetic nephropathy in which glomerulosclerosis is a significant feature, demonstrate that TG2 and its $\epsilon(\gamma\text{-glutamyl})$ lysine product were increased in the glomerular compartment and that both were found to be localised to the glomerular basement membrane and the mesangial matrix (Skill *et al.*, 2001). These increases were associated with a higher level of collagen crosslinking (Skill *et al.*, 2001). Such data suggests that TG2 may also play a role in influencing the ECM changes associated with glomerulosclerosis.

The precise cellular source of TG2 within the glomerulus has yet to be fully established although *in situ* hybridisation demonstrates that mesangial cells are capable of contributing to elevated glomerular levels of TG2 during glomerulosclerosis (Johnson *et al.*, 2003b). These perivascular pericyte-like cells are found in close association with the glomerular basement membrane and are important contributors to the synthesis and assembly of the mesangial matrix (Mene *et al.*, 1989). Similarly, cultured normal 1097 rat mesangial cells have been shown to express TG2 and there is some evidence to suggest that expression may be stimulated by cellular stress factors such as hypoxia (M Fisher, personal observation).

As the data presented in previous chapters demonstrates, it has been possible to over-express TG2 in mesangial cells by stable transfection. However, increasing the intracellular levels of TG2 does not correspond to an increase in the extracellular activity of the enzyme. This indicates that mesangial cells and tubular cells appear to behave differently in their handling of TG2, offering the opportunity to provide comparative data.

In the light of these findings, the aim of this chapter is to provide confirmatory evidence of the importance of extracellular localised TG2 in the modification of the ECM by using the same experimental techniques to investigate the accumulation of ECM in TG2 over-expressing mesangial cells and mesangial cells from the TG2 knockout mouse. Since there is a lack of extracellular TG2 in transfected mesangial cells, this will allow the determination of whether intra or extracellular TG2 is important in ECM accumulation. The use of TG2 knockout cells is even more crucial here given that removal of TG2 may be the only way to

influence extracellular TG2 levels in these cells.

8.2 Results

8.2.1 Measurement of total deposited ECM

Total deposited ECM levels were determined by measuring the incorporation of ³H-amino acids into the ECM (fig 8.1). In TG2 over-expressing 1097 mesangial cells (fig 8.1a), no significant change in total ECM levels was observed in response to an increase in TG2 expression. In contrast labelling of the ECM from TG2^{-/-} primary mesangial cells (fig 8.1b) demonstrated a 47% reduction in total ECM levels (p<0.05; students t test) compared to wild-type ECM.

8.2.2 Measurement of total ECM collagen

Changes in the total collagen content of mesangial ECM in response to TG2 modulation was measured by the incorporation of ³H-proline into deposited ECM (fig 8.2).

Increasing the TG2 expression in 1097 mesangial cells (fig 8.2a) resulted in a decrease in ³H-proline incorporation into the ECM of clone tTg34 and an increase in clone tTg36 (p=0.07) but no effect in clone tTg37. Taken together, this represented no overall change in the collagen content of the ECM. Unfortunately it was not possible to confirm this data by hydroxyproline analysis.

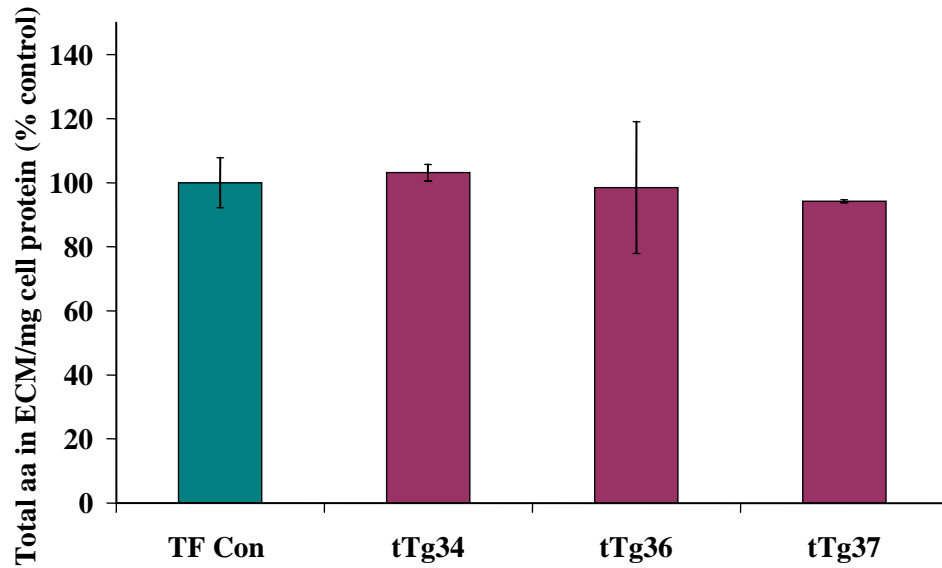
In TG2^{-/-} ECM (fig 8.2b), collagen levels were reduced by 55% (p<0.01; students t test) compared to wild-type ECM as measured by ³H-proline incorporation. This reduction was paralleled by 65.6% reduction in the hydroxyproline content of the ECM (p<0.01; students t test).

8.2.3 Total ECM collagen following electroporation

To determine whether a lack of increase in total collagen in the mesangial ECM in response to TG2 modulation reflected the absence of changes in extracellular TG activity, TG2 was released from 1097 clone tTg37 cells (as this was the highest TG2 expressing clone) by electroporation and levels of deposited collagen measured after 24 hours by ³H-proline incorporation (fig 8.3). Electroporation of clone tTg37 cells doubled the level of ECM collagen compared to non-electroporated tTg37 cells. This corresponded to an almost 2 fold increase in the level of extracellular TG2 as measured by biotin cadaverine incorporation (fig 8.4).

Figure 8.1 Total Mesangial Cell ECM Levels

a) 1097 TG2+ Mesangial Cell Clone ECM



b) TG2^{-/-} Mesangial ECM

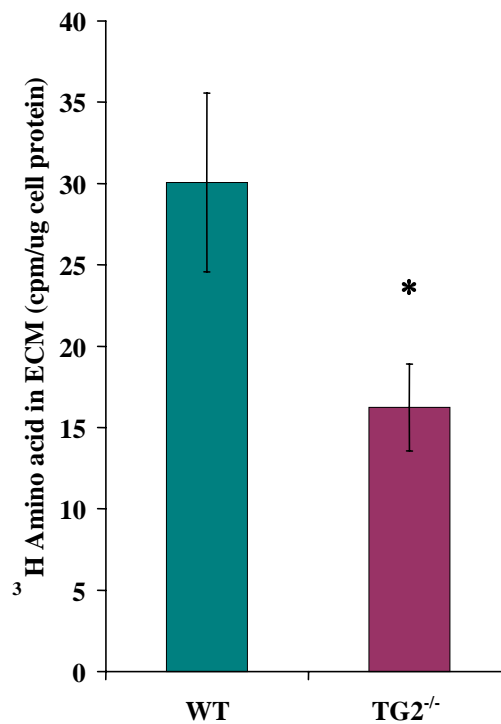
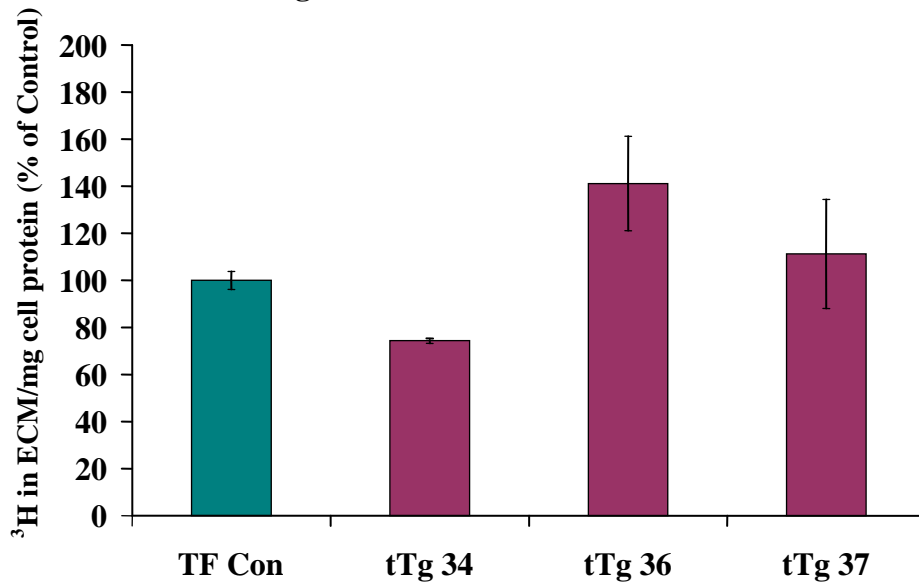


Figure 8.1 Total ECM deposition was determined by culturing 1097 TG2+ cell clones (a) and TG2^{-/-} mesangial cells (b) in the presence of 20 μ Ci of ³H-amino acid mixture for 72 hours prior to the recovery of the ECM (section 3.5.2.1). Data represents mean ECM label \pm SEM from 3 separate experiments performed in triplicate, corrected per μ g of ammonium hydroxide soluble cell protein. *= p <0.05 compared to wild-type (students t test).

Figure 8.2 Total Collagen in Mesangial Cell ECM

a) 1097 TG2+ Mesangial Cell Clone ECM



b) TG2^{-/-} mesangial ECM

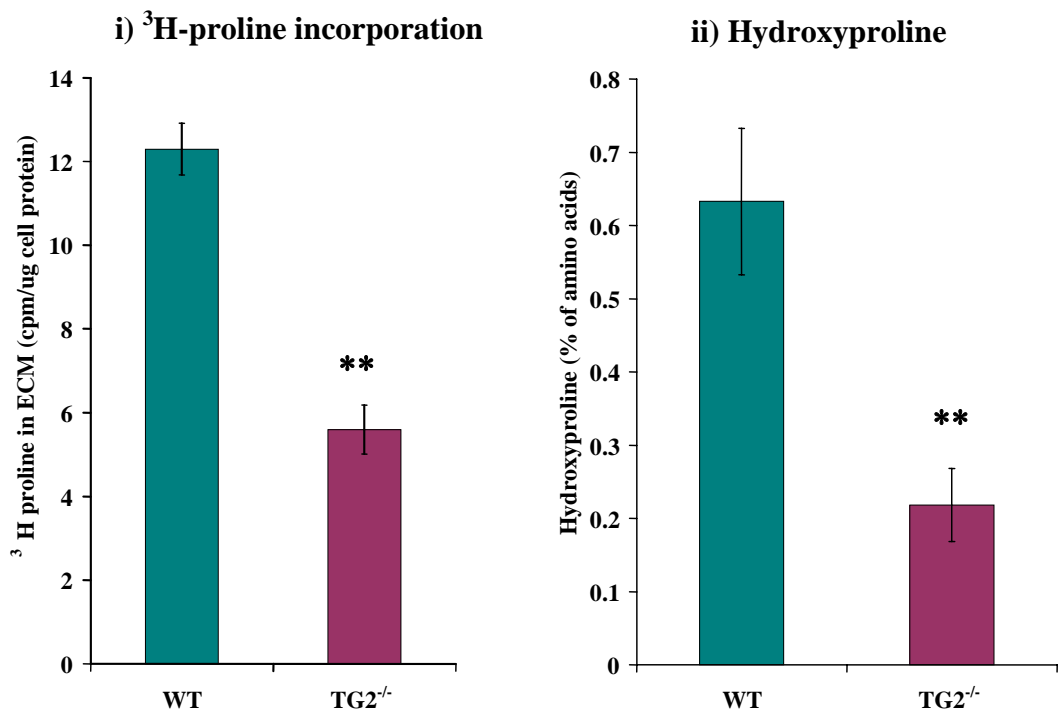


Figure 8.2 Collagen deposition into the ECM was determined by culturing 1097 TG2+ cell clones (a) and TG2^{-/-} mesangial cells (b) in the presence of 20 μ Ci of ³H-proline for 72 hours prior to the recovery of the ECM (section 3.5.2.1). Data represents mean ECM label \pm SEM from 2 separate experiments performed in triplicate, corrected per mg of ammonium hydroxide soluble cell protein. Collagen content of TG2^{-/-} ECM was confirmed by hydroxyproline analysis (bii) and expressed as a percentage of amino acids. n=3 samples per group. **=p<0.01 compared to wild-type (students t test).

Figure 8.3 Total Mesangial ECM Collagen Following Electroporation

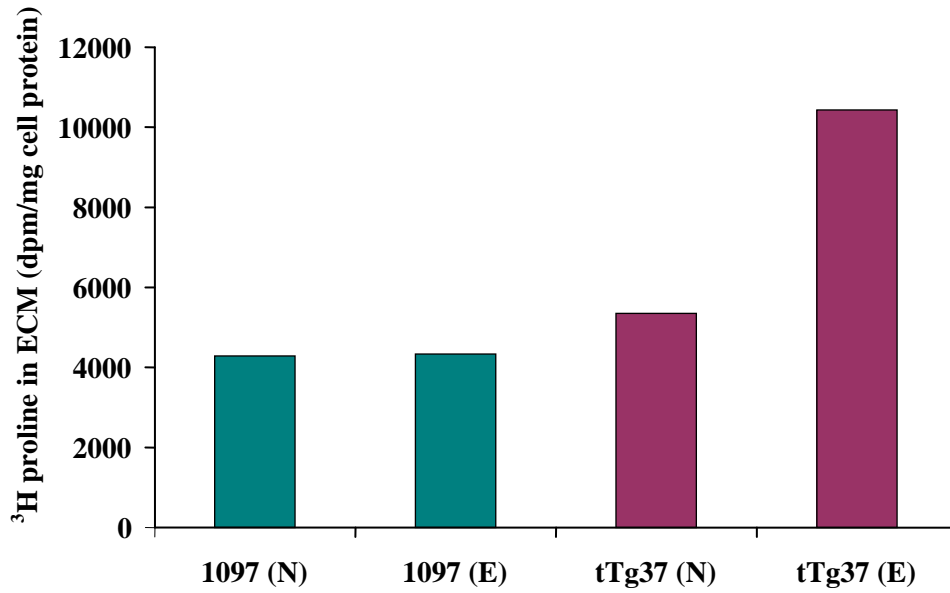


Figure 8.3 Un-transfected 1097 and clone tTg37 mesangial cells at a density of 2×10^6 were electroporated (E) using the Amaxa Nucleofector system (program T27) and solution V. Cells were plated and labelled for 24 hours with ³H-proline prior to the recovery of the ECM. No error bars are shown due to experiment only being performed once.

Figure 8.4 Extracellular TG Levels in Electroporated Mesangial Cells

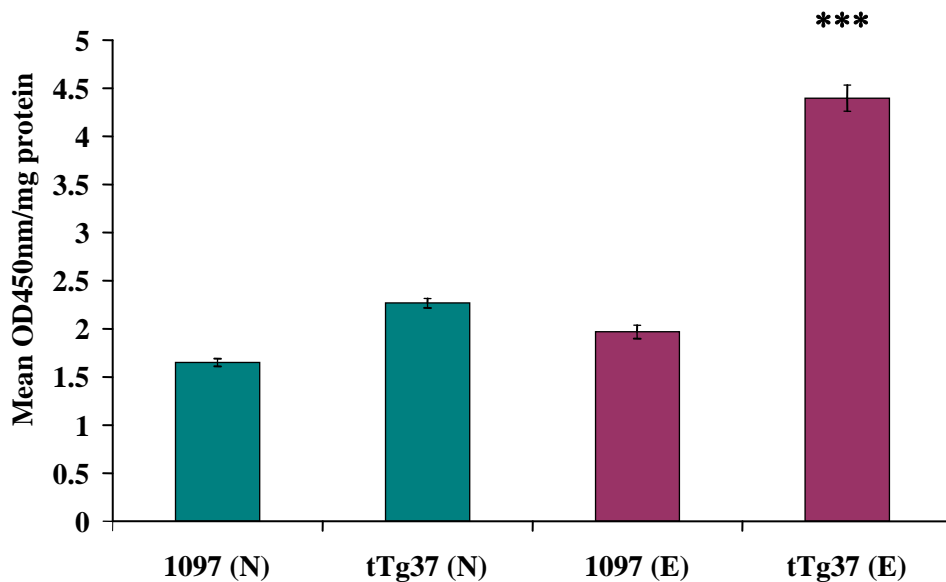


Figure 8.4 Un-transfected 1097 and clone tTg37 mesangial cells that had been electroporated (E) using the Amaxa Nucleofector system (program T27) and solution V were analysed for extracellular TG activity using the biotin cadaverine ELISA. Data represents mean \pm SEM, n=10 wells. ***=p<0.0001 compared to non-electroporated (N) tTg37 cells (students t test).

8.2.4 Collagen mRNA expression

Northern blot analysis was used to determine whether TG2 modulation had any effect on the mRNA expression of collagen (figs 8.5 to 8.8). TG2 over-expressing mesangial cells showed a reduction in collagen I (fig 8.5), III (fig 8.6) and IV expression (fig 8.7) compared to un-transfected 1097 cells and the pSVneo transfection control. In the case of collagen I and III, the reduction in mRNA expression became greater with increasing expression of TG2 such that clone tTg37 cells showed a 81% reduction in collagen I ($p < 0.01$; one way ANOVA with Bonferroni post hoc test) and a 94% reduction in collagen III ($p < 0.05$; Bonferroni post hoc test) compared to the pSVneo transfection control. In comparison, collagen IV mRNA expression remained fairly constant in all three clones demonstrating reductions of 61% (tTg34), 56% (tTg36) and 65% (tTg37) compared to pSVneo transfected cells ($p < 0.01$; Bonferroni post hoc test).

Analysis of WT and TG2^{-/-} mesangial cell collagen mRNA expression (fig 8.8) proved difficult due to problems with obtaining sufficient concentrations of primary cell RNA and only one sample from each group was analysed. Quantitation of mRNA expression by volume densitometry was therefore not possible due to the small sample size and the lack of discernible bands, in particular, for collagen I and III. However, collagen IV mRNA expression was distinguishable by the presence of a 5.6 kb band although this appeared relatively unchanged in TG2^{-/-} cells compared to WT.

Despite changes in collagen mRNA expression in TG2 over-expressing mesangial cells, little change in total ECM or total collagen deposition had been observed. As a result, it was felt that performing further analysis on the ECM of 1097 cells would not yield additional information. Therefore, the remainder of this chapter will focus on changes in the ECM of WT and TG2^{-/-} mesangial cells.

8.2.5 Collagen immunofluorescence of WT and TG2^{-/-} ECM

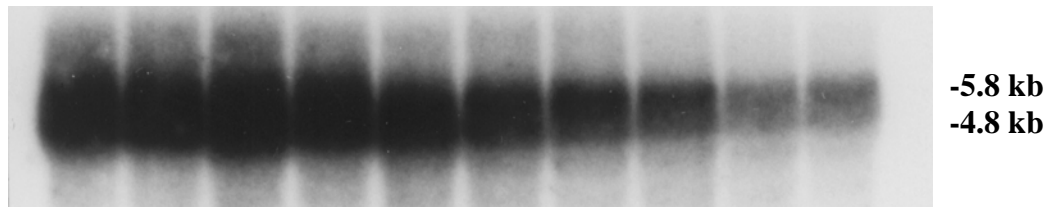
The collagen I, III and IV composition of WT and TG2^{-/-} ECM was analysed by immunofluorescence and confocal microscopy to determine if it was altered in response to a reduction in TG2 (fig 8.9 panels A to F and fig 8.10). Primary mesangial cells were found to be positive for collagen I, III and IV and interestingly much of the staining was intracellular (fig 8.9). Collagen I immunofluorescence was diffuse and found throughout WT and TG2^{-/-} cells with very little extracellular staining. Collagen I levels were increased in TG2^{-/-} mesangial cells compared to WT but this was not significant ($p = 0.19$).

Collagen III and IV staining was similar in intensity to that of collagen I in WT cells

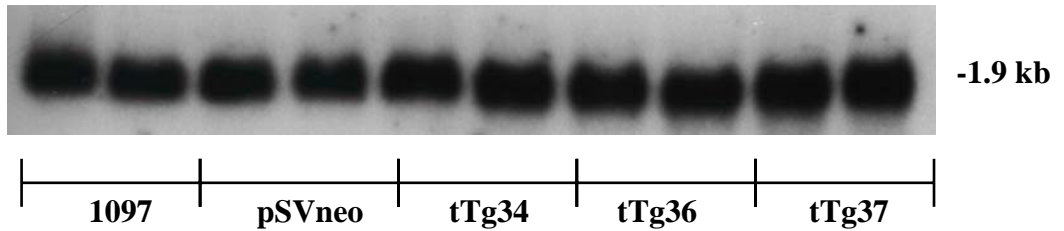
however, was much more intense than collagen I in TG2^{-/-} cells, in particular, collagen III which was indicated by strong immunofluorescence within the cell and as dense fibres between and beneath cells. Collagen IV had a similar distribution although staining was more diffuse than Collagen III. Again, collagen III and IV levels were significantly greater in TG2^{-/-} cells and ECM compared to wild type (p<0.001 and p<0.05 respectively) although much of these increases were due to changes in intracellular levels.

Figure 8.5 Collagen I mRNA Expression in TG2 Over-expressing Mesangial Cells

**a) Northern blots
Collagen I**



Cyclophilin



b) Volume densitometry

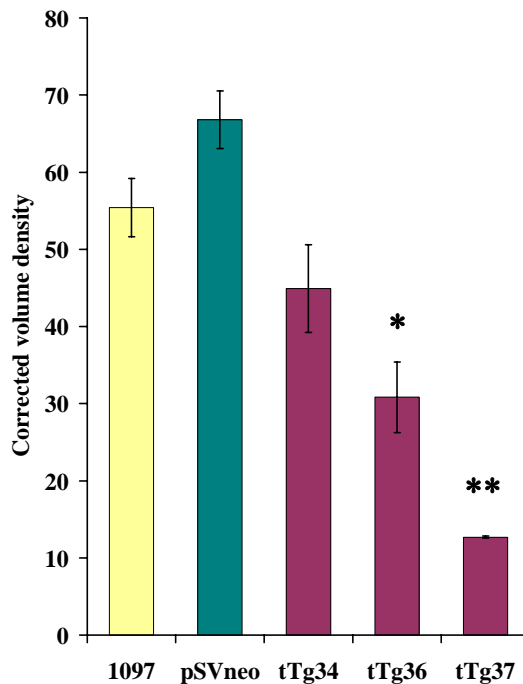
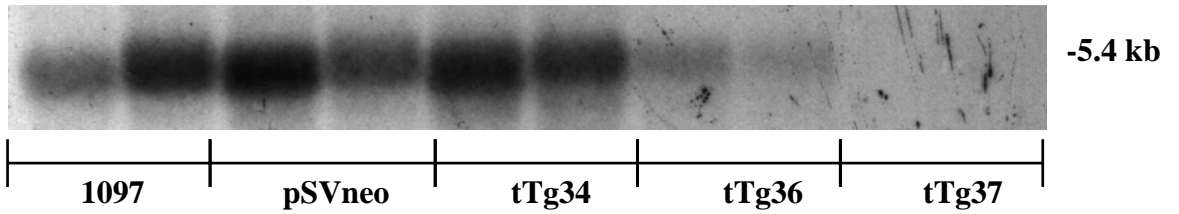


Figure 8.5 (a) TG2 over-expressing mesangial cells were harvested, total RNA extracted and subjected to Northern blot analysis using a specific [32 P]-dCTP random primed cDNA probe for Collagen I (section 3.4.8). Repeat probing with cyclophilin was used as a loading control. (b) Volume densitometry analysis was performed using Multi-Analyst version 3.2TM. Data represents mean volume density \pm SEM from 2 separate blots, n=2 samples per blot, corrected for loading using cyclophilin. *= $p < 0.05$, **= $p < 0.01$ compared to pSVneo (transfection control) cells (one way ANOVA with Bonferroni post hoc test).

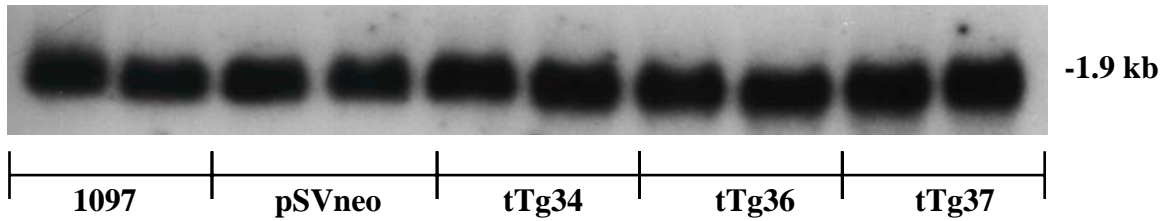
Figure 8.6 Collagen III mRNA Expression in TG2 Over-expressing Mesangial Cells

a) Northern blots

Collagen III



Cyclophilin



b) Volume densitometry

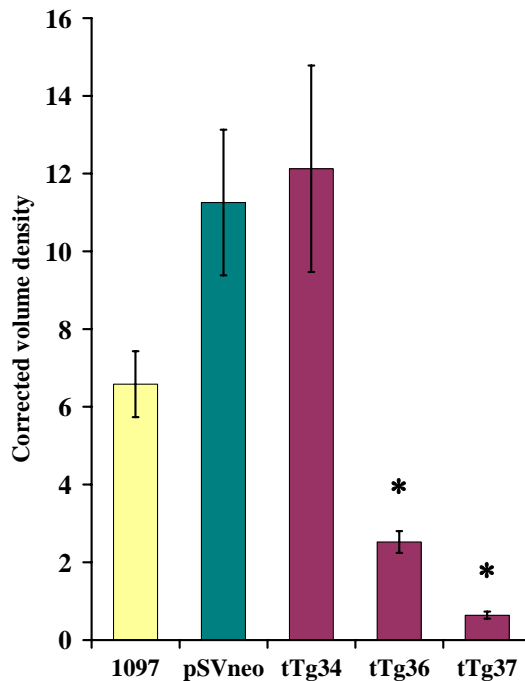
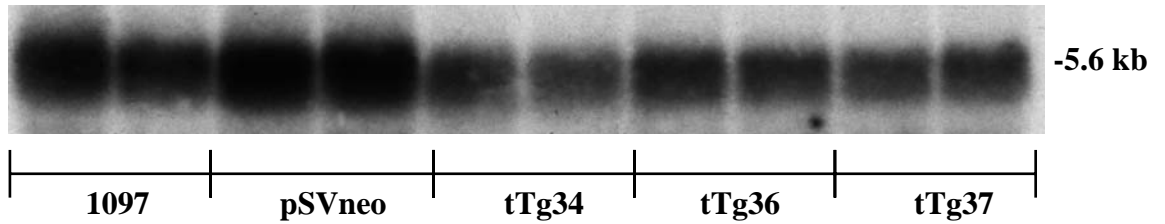


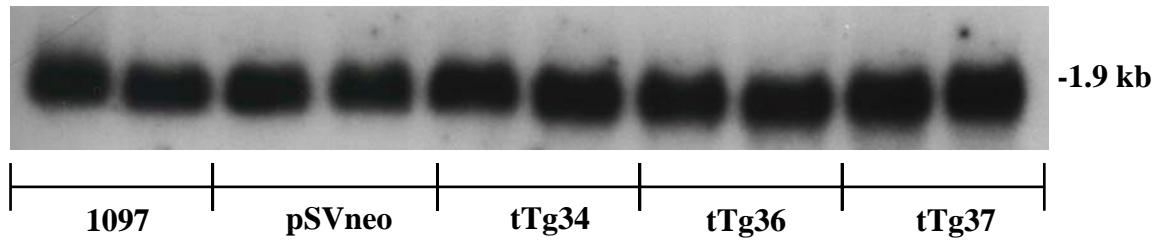
Figure 8.6 (a) TG2 over-expressing mesangial cells were harvested, total RNA extracted and subjected to Northern blot analysis using a specific [³²P]-dCTP random primed cDNA probe for Collagen III. Repeat probing with cyclophilin was used as a loading control. (b) Volume densitometry analysis was performed using Multi-Analyst version 3.2TM. Data represents mean volume density \pm SEM, from 2 separate blots, n=2 samples per blot, corrected for loading using cyclophilin. *=p<0.05 compared to pSVneo transfection control (one way ANOVA with Bonferroni post hoc test).

Figure 8.7 Collagen IV mRNA Expression in TG2 Over-expressing Mesangial Cells

**a) Northern blots
Collagen IV**



Cyclophilin



b) Volume densitometry

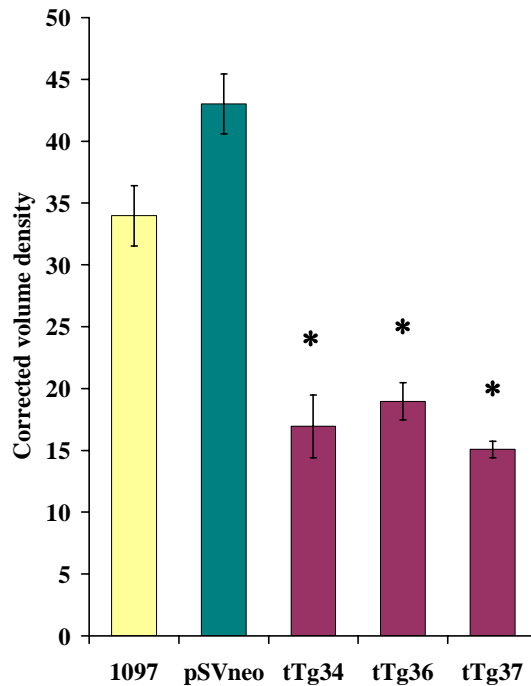
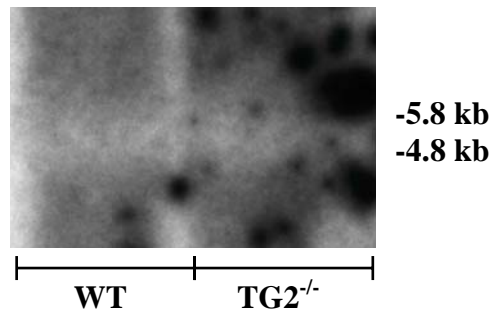


Figure 8.7 (a) TG2 over-expressing mesangial cells were harvested, total RNA extracted and subjected to Northern blot analysis using a specific [32 P]-dCTP random primed cDNA probe for Collagen IV. Repeat probing with cyclophilin was used as a loading control. (b) Volume densitometry analysis was performed using Multi-Analyst version 3.2TM. Data represents mean volume density \pm SEM from 2 separate blots, n=2 samples per blot, corrected for loading using cyclophilin. *=p<0.01 compared to pSVneo (one way ANOVA with Bonferroni post hoc test).

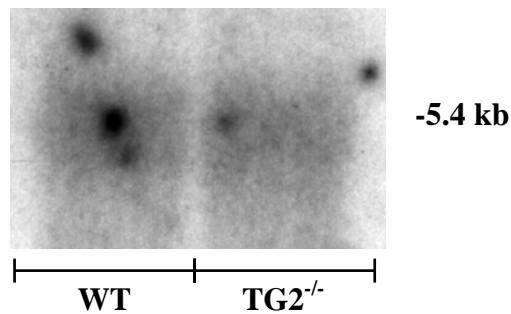
Figure 8.8 Collagen mRNA Expression in WT and TG2^{-/-} Mesangial Cells

Northern blots

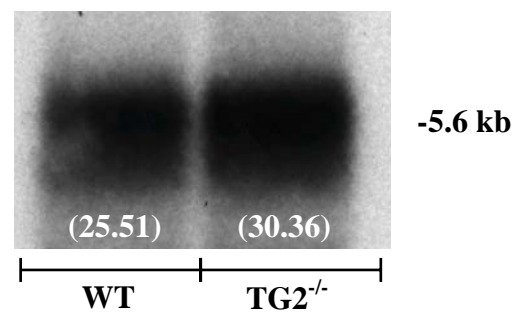
Collagen I



Collagen III



Collagen IV



Cyclophilin

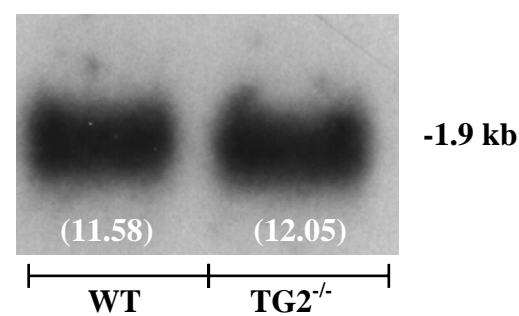


Figure 8.8 WT and TG2^{-/-} primary mesangial cells were harvested, total RNA extracted and subjected to Northern blot analysis using a specific [³²P] dCTP random primed cDNA probes for Collagen I, III and IV. Repeat probing with cyclophilin was used as a loading control. Data in parentheses shows uncorrected densitometric values for each band.

8.2.6 $\epsilon(\gamma\text{-glutamyl})$ lysine crosslink levels in WT and TG2^{-/-} ECM

$\epsilon(\gamma\text{-glutamyl})$ lysine crosslink levels were determined in WT and TG2^{-/-} mesangial cells by immunofluorescence and analysed by confocal microscopy (fig 8.9 panels G and H and fig 8.11).

WT cells showed a diffuse, punctuate intracellular pattern of crosslink staining that was brighter in rounded and spreading cells and in cellular projections. Staining was lower in TG2^{-/-} cells (-58%, $p < 0.05$) but prominent at the edge of cell islands.

8.2.7 Collagen deposition rate of WT and TG2^{-/-} ECM

Changes in deposition rate in response to a reduction in TG2 were determined by ³H proline incorporation in the presence of 10 μ M Galardin (fig 8.12). As expected, collagen deposition was significantly lower in TG2^{-/-} ECM compared to wild type ECM ($p < 0.01$). Application of Galardin resulted in an increase in collagen deposition of 6.5 dpm/ μ g cellular protein in wild type ECM ($p < 0.05$) compared to 3.7 dpm/ μ g protein in TG2^{-/-} ECM ($p < 0.01$) representing a 2 fold decline in collagen deposition.

8.2.7 ECM degradation rate

The degradation of wild type and TG2^{-/-} ECM with 1 μ g/ml of MMP-1 and 1 μ g/ml MMP-2 for 6 hours was used to assess the difference in ECM degradation rate (fig 8.13). WT and TG2^{-/-} ECM showed a linear degradation of the ECM over the 6 hour time period and surprisingly, no significant difference in ECM degradation rates was observed.

Figure 8.9 Collagen and $\epsilon(\gamma\text{-glutamyl})$ lysine Immunofluorescence

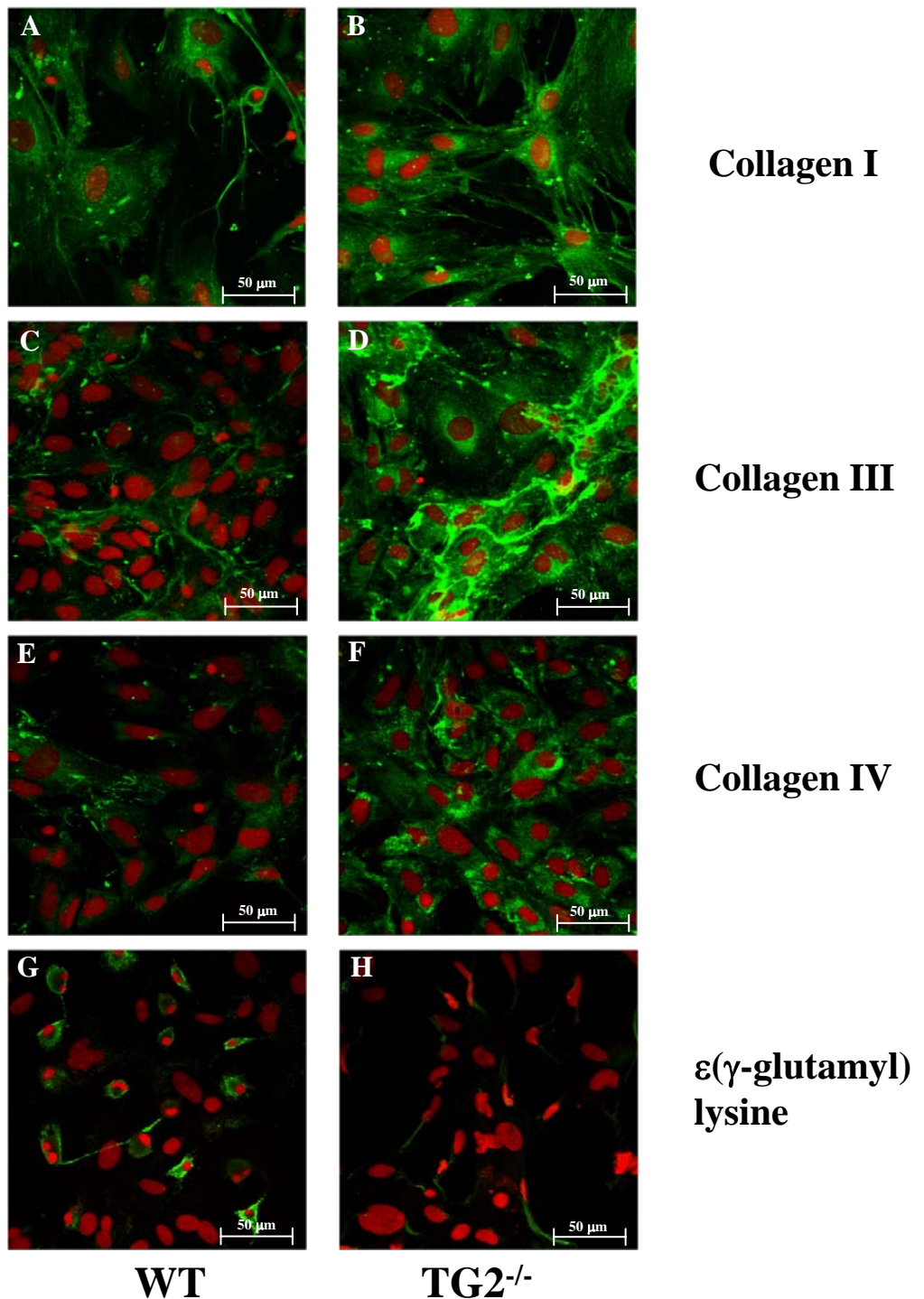


Figure 8.9 Representative photomicrographs of WT (Panels A, C, E and G) and TG2^{-/-} mesangial cells (panels B, D, F and H) immunoprobed for collagen and $\epsilon(\gamma\text{-glutamyl})$ lysine crosslink. Cells were fixed and immunoprobed with mouse monoclonal collagen I (A, B), goat polyclonal collagen III (C,D), goat polyclonal collagen IV (E,F) and mouse monoclonal $\epsilon(\gamma\text{-glutamyl})$ lysine antibody (G,H) and revealed with FITC secondary. Cells were mounted in medium containing propidium iodide and are shown at 400 x magnification.

Figure 8.10 Semi-quantitative Analysis of Collagen Immunofluorescence

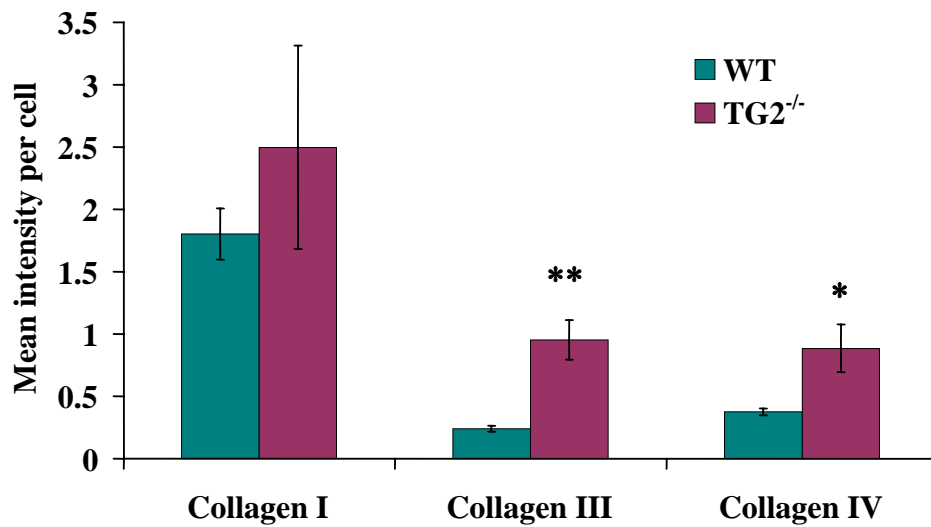


Figure 8.10 Collagen staining was determined in WT and TG2^{-/-} mesangial ECM by immunofluorescence. Semi-quantitation of staining was performed using confocal microscopy with excitation at 488nm. Data is expressed as the mean intensity of fluorescence per cell \pm SEM from at least 6 random fields.. *= $p < 0.05$, **= $p < 0.001$ compared to WT (students t test).

Figure 8.11 $\epsilon(\gamma$ -glutamyl) lysine Crosslink Levels

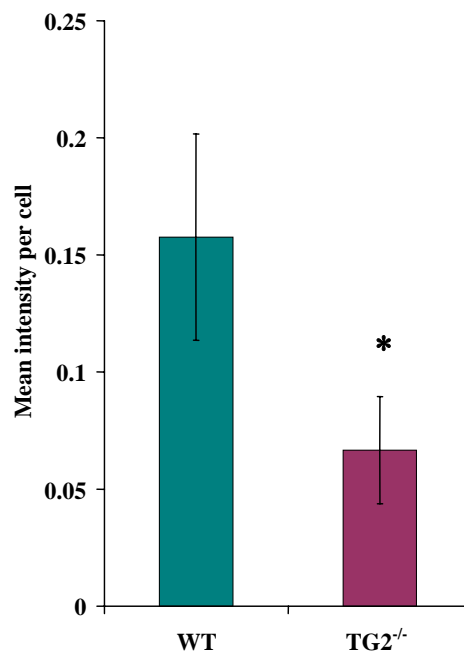


Figure 8.11 $\epsilon(\gamma$ -glutamyl) lysine crosslink staining was determined in WT and TG2^{-/-} mesangial cells by immunofluorescence and at least 6 random fields analysed by confocal microscopy (section 3.3.8.1). Fluorescence was semi-quantitated and expressed as mean intensity per cell \pm SEM. *= $p < 0.05$ compared to WT (students t test).

Figure 8.12 ECM Deposition in the presence of the MMP Inhibitor Galardin

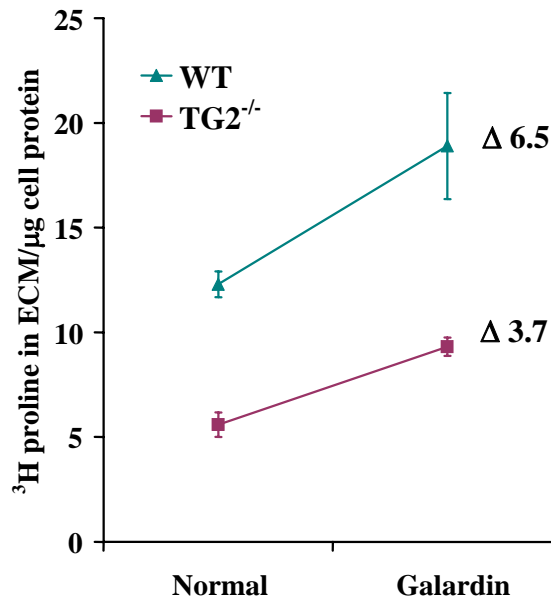


Figure 8.12 WT and TG2^{-/-} mesangial cells were labelled for 72 hours with 10μCi of ³H-proline in the presence or absence of 10μM Galardin (section 3.5.3.1). The ECM was recovered and label measured by scintillation counting. Data represents mean dpm/μg cellular protein ± SEM from 3 separate experiments performed in duplicate.

Figure 8.13 Combined MMP-1 and MMP-2 Degradation of WT and TG2^{-/-} Mesangial ECM

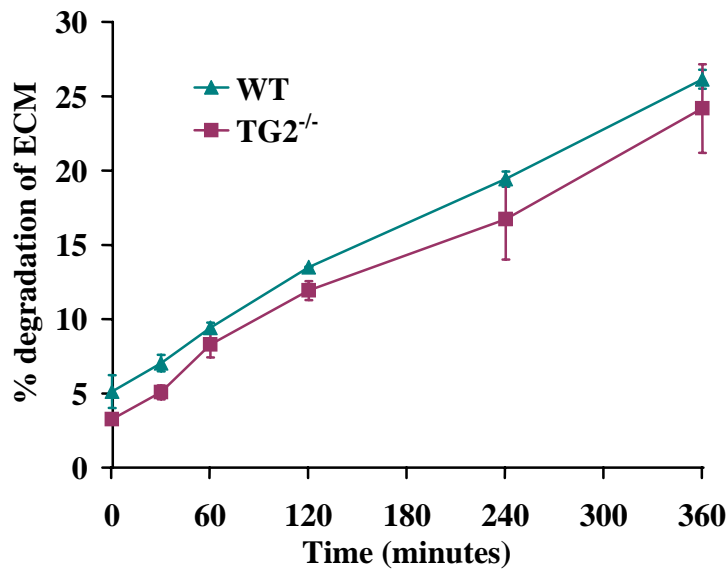


Figure 8.13 WT and TG2^{-/-} mesangial ECM was labelled with 10μCi of ³H-proline for 72 hours prior to digestion with a combination of 1μg/ml of MMP-1 and 1μg/ml of MMP-2 for up to 24 hours (section 3.5.4.2). 50μl of supernatant was removed at 0, 30 and 60 minutes and then 2 hourly intervals up to 6 hours. Released label was measured by scintillation counting. Data represents mean percentage of total ECM degraded ± SEM from 2 separate experiments performed in duplicate.

8.3 Discussion

Numerous studies have suggested a role for TG2-mediated crosslinking in the expansion of the mesangial matrix that is associated with the development of glomerulosclerosis (El Nahas *et al.*, 2004; Johnson *et al.*, 2004; Johnson *et al.*, 2003b; Skill *et al.*, 2001). Evidence presented in Chapter 7 indicates that in tubular cells, TG2 has a direct effect on the accumulation of ECM by facilitating the increased deposition of collagen coupled with an increased resistance of the ECM to MMP breakdown. Such effects appear to be attributable to increased extracellular levels of TG2. In order to corroborate the importance of extracellular TG2 in the accumulation of mesangial matrix, this chapter investigated changes in ECM metabolism in TG2 over-expressing mesangial cells that do not export TG2 and complemented this with the study of TG2 null-mesangial cell ECM.

As anticipated, total ECM level and ECM collagen content was unaltered in TG2 over-expressing mesangial cells despite large increases in intracellular TG2 levels. The known retention of TG2 by these cells coupled with this lack of ECM change suggests a direct link between TG2 export and the ECM and indicates that TG2 must be outside the cell in order to affect the ECM. This was further investigated by electroporating clone tTg37 mesangial cells and comparing the level of ECM collagen to that of non-electroporated cells. While this was clearly an artificial method of releasing the enzyme and not representative of controlled export, it successfully demonstrated a link between extracellular levels of TG2 and collagen accumulation in these cells. Such data implies that if these cells could be induced to traffic TG2 to the extracellular environment, this would indeed cause changes in ECM levels as seen in tubular cells. Unfortunately, it was not possible to take these investigations further due to the extensive degree of cell death after prolonged culture once electroporated. Alternative methods of releasing TG2 from mesangial cells that do not affect cell viability, coupled with more extensive analysis of changes in ECM levels in response to TG2 release are required to fully establish the potential of TG2 to affect mesangial matrix accumulation.

In an attempt to provide some confirmatory evidence of the importance of extracellular TG2 in the modification of mesangial ECM and given the tight control of TG2 export by transfected mesangial cells, further investigation into the effect of TG2 on ECM metabolism was performed on mesangial cells isolated from the TG2 knockout mouse. TG2-null mesangial cells were found to have lower ECM levels and to deposit less ECM collagen than wild type cells. This reduction in total ECM and collagen is consistent with the observations in TG2 null tubular cells. In contrast to TG2 transfected mesangial cells however, changes in ECM levels were associated with lower levels of both extracellular TG2 and $\epsilon(\gamma\text{-glutamyl})$

lysine crosslink in the ECM. Reductions in extracellular TG2 in null mesangial cells may reflect their inability to produce the active enzyme. The generation of the TG2 knockout by the targeted deletion of exons 5 and 6 results in the loss of the active site (De Laurenzi and Melino, 2001). Previous studies have shown that the presence of the intact active site Cys²⁷⁷ is important for secretion and deposition of the enzyme into the matrix (Balklava *et al.*, 2002). Clearly, disruption of this site may have crucial consequences for its export. In the case of TG2 over-expressing mesangial cells however, it is likely that export is subject to additional regulation given that they produce large amounts of the active enzyme intracellularly.

The reduction in total ECM and collagen demonstrated in TG2^{-/-} mesangial cells may have been an indirect consequence of alterations in the TGF- β 1 pathway however, the percentage of active TGF- β 1 in TG2^{-/-} mesangial cells has been shown to be unchanged as is the case in TG2^{-/-} tubular cells (Huang, 2006). This further strengthens the hypothesis that TG2-mediated changes in the ECM represent direct effects on ECM metabolism rather than via the up-regulation of TGF- β 1.

In tubular cells, changes in ECM collagen were as a direct result of alterations in the levels of collagen III and IV in the ECM (Chapter 7, section 7.2.2.3); therefore changes in the same collagen types were investigated in primary mesangial cells. Immunofluorescence for collagen I was also included since mesangial cells in culture are also known to make this collagen type. Primary mesangial cells were positive for collagen I, III and IV, which is consistent with the observations of other groups that have studied collagen production by cultured mesangial cells (Ishimura *et al.*, 1989). In keeping with these previous studies, semi-quantitative analysis of immunofluorescence indicated that collagen I was the predominant collagen type although this was perhaps surprising given the intensity of collagen III and IV staining in some sections. This apparent discrepancy may reflect inconsistencies in the number of cells analysed per field such that greater numbers of cells in collagen III and IV stained sections lowered the mean intensity of staining per cell.

The production of interstitial collagens I and III by mesangial cells *in vivo* represents an activated phenotype that is associated with the expression of α -SMA (Couser and Johnson, 1994). Primary mesangial cells cultured on plastic have been demonstrated to undergo some degree of de-differentiation and phenotypic transformation such that they show myofibroblastic characteristics (Mene, 2001) and this may well be the case here.

Interestingly, the localisation of all three collagens was found to be mainly intracellular. This is in keeping with observations in cultured rat mesangial cells that show an intracellular

localisation of collagen until they reach confluency at which time extracellular deposition of collagen occurs at cell-to-cell contact (Ishimura *et al.*, 1989). The data provided by the immunofluorescence therefore represents changes in intracellular collagen and does not provide information about the composition of deposited ECM which is where we believe TG2 exerts its influence. It does however show increases in collagen I, III and IV immunofluorescence in TG2^{-/-} mesangial cells compared to wild type cells although it was not possible to determine whether these changes are mRNA dependent. This data may suggest a mechanism to explain the reduction in total collagen observed in these cells whereby more collagen is retained by TG2^{-/-} cells rather than being deposited into the ECM. TG2^{-/-} mesangial cells certainly deposit less collagen and at a slower rate than wild type cells as indicated by labelling of the ECM in the presence of Galardin.

Despite the influence of TG2 on the susceptibility of tubular ECM to degradation, TG2-null tubular cells did not show any difference in their ECM degradation rates (Chapter 7, section 7.2.2.11). Likewise, there was no significant difference in degradation rates between wild-type and TG2^{-/-} mesangial ECM. As in TG2-null tubular ECM, this data suggests that a minimum level of TG2 crosslinking is required within the ECM above which degradation could be altered. Thus an increase in TG2 as seen in over-expressing cells would equate with an increase in crosslink above the minimum requirement, subsequently increasing the resistance to breakdown. Conversely, a reduction in TG2 from basal levels as seen in TG2 null cells, where a minimum level of crosslink is maintained, would have little effect on degradation.

The data presented in this chapter suggests that there are tightly controlled mechanisms governing TG2 export in mesangial cells. However, when released, mesangial derived TG2 is capable of influencing the deposition of collagen and therefore the accumulation of ECM. This data serves to support the hypothesis that TG2 plays a direct role in the accumulation of ECM via its effects on ECM metabolism.

Chapter 9

Effect of Transglutaminase Inhibition on Disease Progression in the Subtotal Nephrectomy (SNx) Model of Renal Scarring

9.1 Introduction

Evidence presented in the preceding chapters has highlighted the contribution of TG2-mediated crosslinking within the ECM to the accumulation of matrix via its direct action on the deposition of collagen and the resistance of the ECM to the action of MMPs. A strategy that inhibits the crosslinking activity of TG2 may therefore be effective in preventing the accumulation of ECM that is associated with progressive kidney disease and represent a potential therapeutic avenue.

To investigate this, two site-specific inhibitors of TG have been developed: NTU283 (1, dimethyl-2[oxopropyl] thio] imidazolium) a compound previously synthesised as a Factor XIIIa inhibitor (Syntex, 1990) and NTU281 a synthetic CBZ-glutaminy glycine analogue (N-benzyloxycarbonyl-L-phenylalanyl-6-dimethylsulphonium-5-oxo-Lnorleucine) (Griffin M, 2004) that are both non-competitive irreversible inhibitors of TG activity.

The specific properties and action of these inhibitors for *in vivo* application and specifically on renal TG activity has yet to be established. To address this, firstly, *in vitro* characterisation of the inhibitors will be performed to test their stability and their ability to inhibit renal TG activity. The potential of the inhibitors to cross the cell membrane (cell solubility) will be tested on tubular epithelial cells in culture. Dose response studies will then be performed in rats subjected to 5/6th nephrectomy to establish a suitable *in vivo* dose to inhibit increased renal TG activity resulting from disease.

Subsequently, the intra-renal delivery of these inhibitors to rats subjected to SNx from the onset of renal injury will be used to establish whether TG inhibition can prevent progressive experimental scarring and thus preserve kidney function. Levels of TG activity will be correlated with the degree of kidney scarring and function at 1 week, 1 month and 3 months post nephrectomy. Changes in the level of ECM proteins will be determined by immunohistochemistry, coupled with multiphase image analysis and changes in the mRNA expression of ECM proteins determined by Northern blot analysis.

9.2 Results

9.2.1 Pilot data

9.2.1.1 Effectiveness of TG inhibitors

Pre-incubation of tissue homogenates from SNx animals with 100 μ M of inhibitors NTU283 and NTU281 was used to determine inhibition of renal TG activity (fig 9.1). The 100 μ M concentration was based on dose-response experiments performed on cell sonicates at Nottingham Trent University (R. Jones, personal communication). Pre-incubation with either inhibitor was highly effective at reducing TG activity levels. NTU283 reduced TG activity by 80% ($p < 0.05$) and NTU281 by 40%.

9.2.1.2 Cellular uptake of TG inhibitors in vitro

The influence of TG2 inhibitors on intracellular TG activity was used to assess their cellular uptake. Rat tubular epithelial cells were incubated with 100 μ M of NTU283 or NTU281 for 24 hours prior to assay for TG activity (fig 9.2). Treatment with NTU283 reduced intracellular TG activity by more than 50% ($p < 0.05$) however, treatment with NTU281 had no effect on intracellular levels. This demonstrates the ability of NTU283 but not NTU281 to transverse the cell membrane.

9.2.1.3 Inhibitor stability study

The intra-renal delivery of inhibitors by osmotic mini-pump requires inhibitors to be stable at 37°C for at least one month. The temperature stability of NTU283 and NTU281 was therefore assessed by pre-incubation of inhibitors that had been stored at -80°C or 37°C for 7, 14, 21 or 28 days, with tissue homogenates from SNx animals. Pre-incubation with NTU283 stored at -80°C (fig 9.3a) reduced TG activity by 80% at day 7 ($p < 0.01$) and maintained a similar level of inhibition at later time points of between 65-70% ($p < 0.01$). Treatment with inhibitor stored at 37°C (fig 9.3a) gave 80% inhibition of TG activity at day 7 ($p < 0.01$) with some loss of inhibition at later time points although inhibition remained stable at 45% ($p < 0.01$). Pre-incubation with NTU281 stored at -80°C (fig 9.3b) gave a 60% reduction in TG activity at day 7 ($p < 0.05$) that lessened to 20% at day 14 and 40% at 21-28 days ($p < 0.05$). Storage at 37°C had no effect on the level of inhibition at day 7 (60%) compared to -80°C storage and inhibition also remained similar to that of the -80°C stored enzyme at later time points (30-40%).

9.2.1.4 Inhibitor dose response curve *in vivo*

An inhibitor dose response curve was constructed by measuring the inhibition of TG activity in the kidney once homogenised using the ^{14}C -putrescine incorporation assay. This was carried out on kidneys recovered from SNx animals treated for 7 days with 1mM, 10mM or 50mM of NTU283 or NTU281 (3 animals per group) and a suitable Ki_{50} determined for the continuous one month infusion of inhibitor (fig 9.4). Treatment with inhibitor NTU283 produced a progressive inhibition of TG activity with increasing dose that was greater than 50% at 50mM (purple line). Treatment with NTU281 failed to produce a significant reduction in TG activity with only 20% inhibition at 50mM dose.

9.2.1.5 One month inhibitor pilot study-50mM dose

A pilot study was performed in which inhibition of TG activity was determined in animals treated with a continuous infusion of 50mM of NTU283 or NTU281 for one month. Treatment for one month with inhibitor NTU283 produced a greater than 50% inhibition of TG activity ($p < 0.01$) as measured by putrescine incorporation (fig 9.5a).

Inhibition of TG activity by NTU281 was measured by *in situ* activity assay due to its low cell permeability and thus its inability to deactivate intracellular TG (fig 9.5b). The *in situ* TG activity assay more accurately measures extracellular TG activity. Using this, a significant reduction in *in situ* TG activity following treatment with NTU281 ($p < 0.01$) of over 75% was demonstrated. In comparison, only 30% inhibition of *in situ* activity was observed with NTU283.

Figure 9.1 Effectiveness of TG Inhibitors

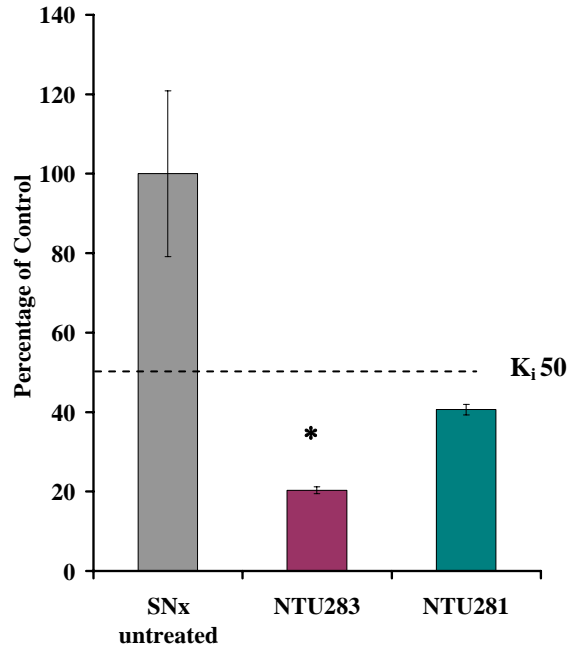


Figure 9.1 Tissue homogenates from animals subjected to SNx were pre-incubated with 100 μ M of inhibitor NTU283 or NTU281. TG activity was measured by the putrescine incorporation assay as described in section 3.3.7.1. Data represents mean \pm SEM from 3 separate experiments performed in triplicate and is expressed as percentage of untreated SNx. *=p<0.05 compared to untreated SNx.

Figure 9.2 Cellular Uptake of TG Inhibitors *in vitro*

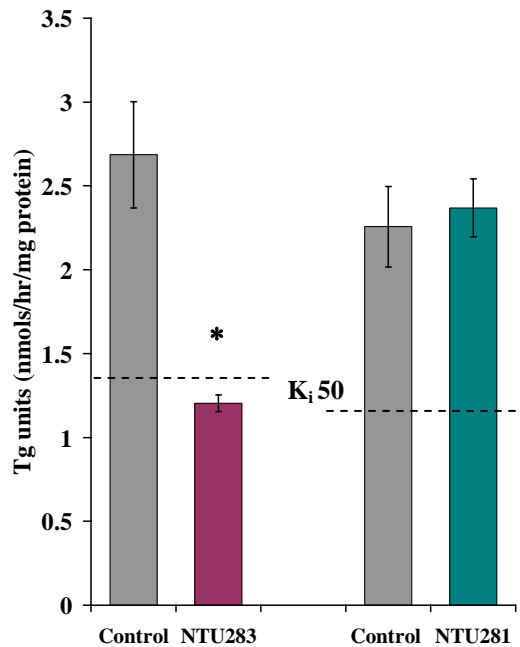


Figure 9.2 Rat proximal tubular epithelial cells (RPT) were treated for 24 hours with 100 μ M final concentration of inhibitor NTU283 or NTU281. Cells were sonicated and intracellular TG activity determined by the putrescine incorporation assay. TG activity is expressed as nmols/hour/mg protein and represents mean \pm SEM from 3 separate experiments performed in triplicate. *=p<0.01 compared to control (students t test).

Figure 9.3 One Month Inhibitor Stability Study

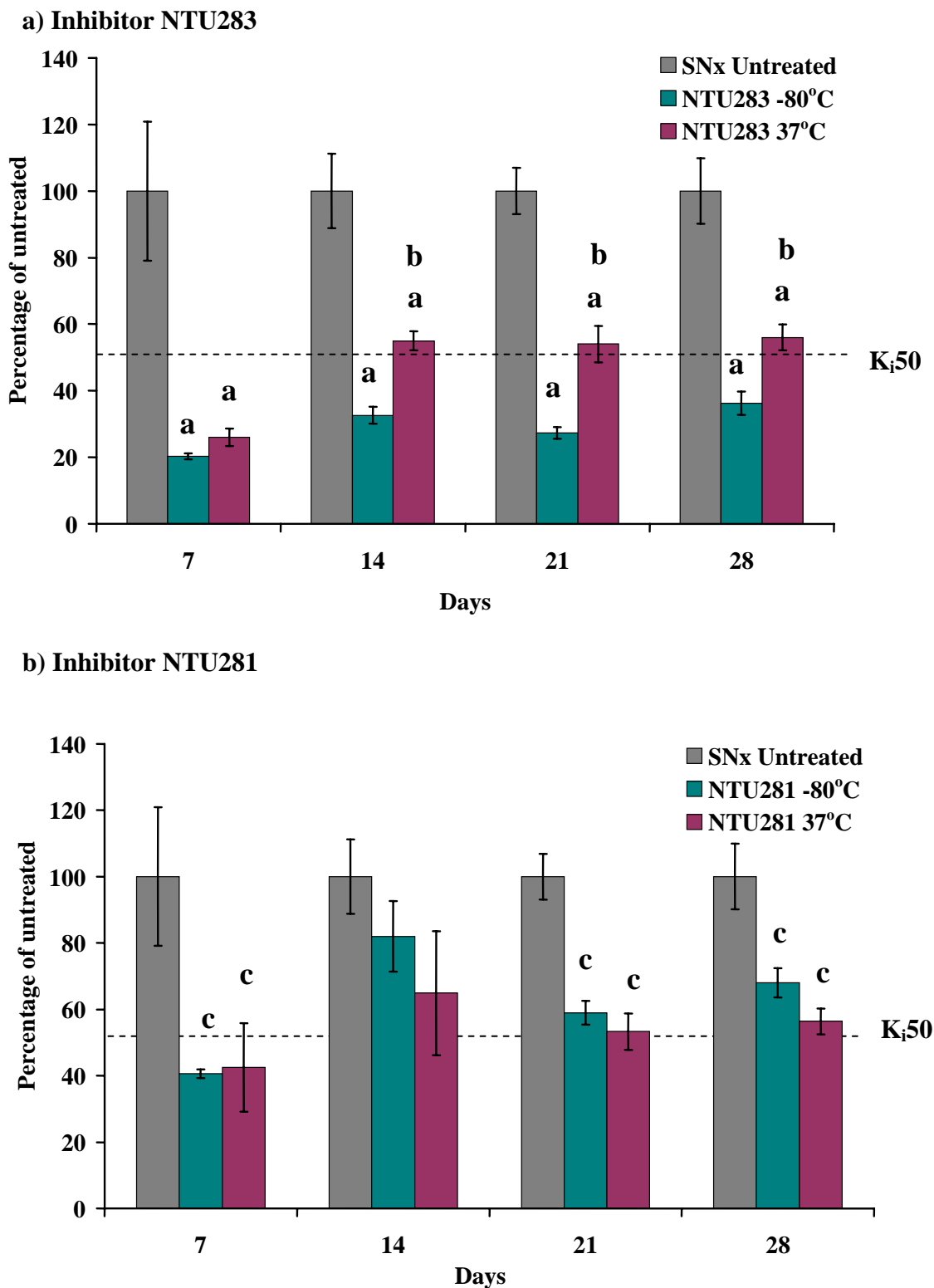


Figure 9.3 Inhibitors NTU283 (a) and NTU281 (b) were stored at either -80°C or 37°C for 7, 14, 21 and 28 days. At each time point, inhibitors were tested for TG inhibition by incubation of $100\mu\text{M}$ of inhibitor with tissue homogenate for 5 mins at 37°C prior to analysis of TG activity by the putrescine incorporation assay. Data represents mean TG units (nmols/hr/mg protein) \pm SEM from 3 separate experiments performed in triplicate and is expressed as percentage of untreated control. Statistical difference determined by one way ANOVA with Bonferroni post hoc test. a= $p < 0.01$ compared to untreated control; b= $p < 0.01$ compared to inhibitor stored at -80°C ; c= $p < 0.05$ compared to untreated control.

Figure 9.4 One Week Inhibitor Dose Response Curve

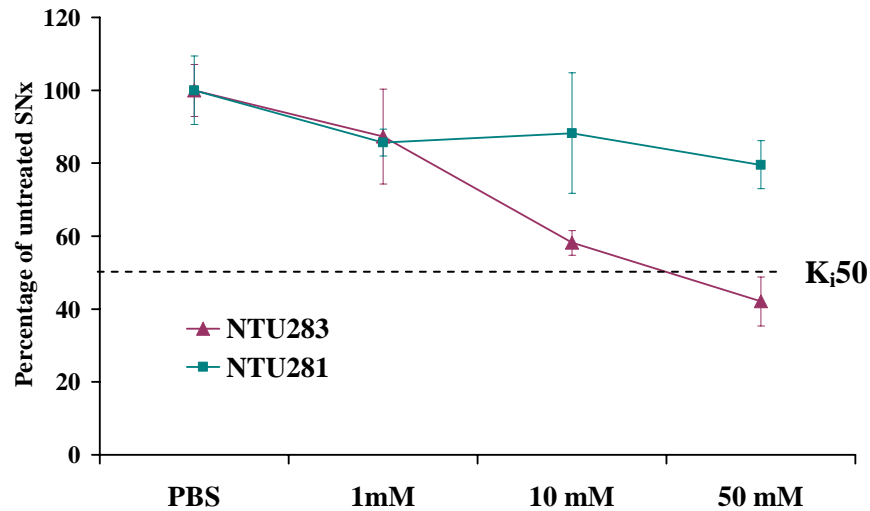


Figure 9.4 Subtotal nephrectomised rats were treated for 7 days with a continuous infusion of inhibitor NTU283 or NTU281 at 1mM, 10mM or 50mM concentration. Kidney tissue was harvested and TG activity determined by putrescine incorporation assay. Data represents mean TG units (nmols/hr/mg protein) \pm SEM from 3 separate experiments, n=4 samples per experimental group and is expressed as percentage of untreated control.

Figure 9.5 Transglutaminase Activity One Month Study at 50mM

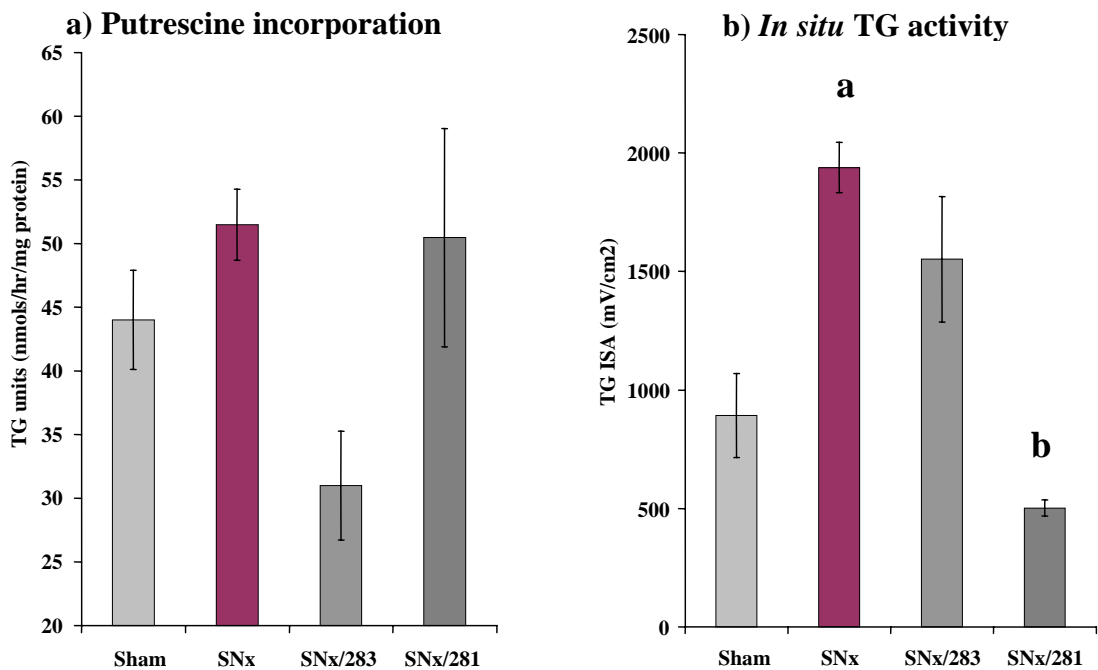


Figure 9.5 Rats subjected to SNx were treated with a continuous infusion of NTU283 and NTU281 at 50mM dose. (a) TG activity was determined in tissue homogenates by the putrescine incorporation assay. (b) *In situ* TG activity was determined on cryostat sections incubated with fluorescein (FITC) cadaverine, incorporation revealed with anti-FITC monoclonal and visualised with goat anti-mouse Cy5-conjugated antibody (section 3.3.7.2). Sections were visualised by confocal microscopy. Semi-quantitation of activity was obtained using the mean Cy5 emissions per field (mV/cm^2) from at least ten 200x magnification fields. a= $p < 0.01$ compared to sham-operated control, b= $p < 0.01$ compared to SNx (one way ANOVA with Bonferroni post hoc test).

9.2.2 Three month TG inhibitor SNx study

9.2.2.1 General observations

Animals treated with inhibitors NTU281 or NTU283 showed no obvious phenotypic changes compared to control animals. SNx animals treated with TG inhibitors gained body weight at a slightly greater rate than untreated animals, but this only achieved significance for NTU281 at day 84 ($p < 0.05$ compared to SNx) and was less than sham-operated controls (table 9.1). Measurement of heart (creatinine kinase, CK) and liver enzymes (alanine aminotransferase ALT, aspartate aminotransferase, AST) demonstrated significant decreases in CK and ALT with inhibitor treatment at day 7 ($p < 0.05$ compared to sham and SNx respectively) and increases in AST and CK with NTU283 at day 28 although these did not reach significance. By 84 days post-SNx no adverse effects of TG inhibition on heart or liver function was observed (table 9.2). Analysis of blood clot strength as measured by solubility in 5M urea indicated that fibrin crosslinking by Factor XIIIa was not affected.

9.2.2.2 Assessment of renal function

Kidney function was assessed by creatinine clearance (table 9.1 and fig 9.6a) which is a measure of glomerular filtration rate (GFR). At 7 days post-SNx, creatinine clearance was reduced by 50% in SNx-treated animals compared to sham. The creatinine clearance increased slightly in this group over the next month in response to compensatory renal growth, but fell sharply between 28 and 84 days as the remnant kidney progressively scarred. Comparable reductions in creatinine clearance were observed in NTU283 and NTU281 treated animals up to 28 days post-SNx due to a reduction in renal mass. After this point, inhibitor-treated animals maintained their renal function at just over 50% of control in comparison to the untreated animals where renal function fell below 20% of control levels.

Proteinuria (table 9.1 and fig 9.6b) and albuminuria (table 9.1 and fig 9.6c) were used as a measure of glomerular leakage and damage. Surprisingly, maintenance of renal function was independent of an improvement in proteinuria with NTU283 although NTU281 caused a slight reduction in proteinuria by 84 days post-SNx. Albuminuria was reasonably consistent between untreated SNx and inhibitor-treated groups over the first month but significantly reduced by NTU283 and NTU281 treatment at 84 days post-SNx ($p < 0.01$ and $p < 0.05$ respectively).

Table 9.1 Three Month TG2 Inhibitor SNx Study Renal Function Data

Days Post SNx	Body Wt (g)	Kidney Wt (g)	CrCl (ml/min)	Proteinuria (mg/24 hr)	Albuminuria (mg/24hr)
⁷ Sham	320±14.1	1.07±0.07	1.16±0.67	68.3±9.5	2.88±0.54
⁷ SNx	313±11.5	1.51±0.12 ^a	0.61±.35 ^a	128.3±0.5 ^b	27.85±9.01 ^a
⁷ SNx + 283	287.6±17.7	1.47±0.09 ^a	0.54±0.31 ^a	109.5±17.5 ^b	29.29±6.00 ^a
⁷ SNx + 281	290.6±20.6	1.54±0.03 ^a	0.63±0.36 ^a	136.8.5±8.1 ^b	20.52±3.26 ^a
²⁸ Sham	349.0±17.0	1.08±0.01	1.32±0.29	118.7±27.1	8.42±1.75
²⁸ SNx	354.3±18.2	1.61±0.09 ^a	0.91±0.12	299.9±77.9 ^b	47.20±19.62
²⁸ SNx + 283	320.3±24.8	1.79±0.07 ^a	0.76±0.06	448.5±50.8 ^{bc}	21.07±11.34
²⁸ SNx + 281	332.0±3.2	1.91±0.28 ^a	0.86±0.13	240.6±42.9	41.55±10.54
⁸⁴ Sham	513.2±6.7	1.37±0.03	1.72±0.18	129.6±14.6	3.48±0.91
⁸⁴ SNx	433.2±28 ^a	3.22±0.25 ^a	0.37±0.18 ^b	672±121.7 ^b	294±83.22 ^b
⁸⁴ SNx + 283	449±20.0 ^a	3.07±0.29 ^a	0.86±0.05 ^c	835.7±83.4 ^b	112.58±37.26 ^{ad}
⁸⁴ SNx + 281	408±9.4 ^c	2.94±0.13 ^a	0.93±0.10 ^c	503.4±57 ^b	87.34±31.51 ^{ac}

Table 9.2 Three Month TG2 Inhibitor SNx Study Toxicity Data

Days Post SNx	AST (Units/l)	ALT (Units/l)	CK (Units/l)	24h clot stability
⁷ Sham	88±2.64	69.7±3.33	277.33±22.19	N/a
⁷ SNx	89.6±2.03	71±6.08	242.66±31.5	N/a
⁷ SNx + 283	78.3±7.31	49.6±2.84 ^{ac}	157±34.38 ^a	N/a
⁷ SNx + 281	88±1.0	51±1.0 ^{ac}	192.66±18.21 ^a	N/a
²⁸ Sham	70.33±8.09	71.66±7.22	154±24.26	N/a
²⁸ SNx	71.33±5.36	66.66±4.70	152±17.57	N/a
²⁸ SNx + 283	90.66±1.20	61.66±8.09	220.66±18.85	N/a
²⁸ SNx + 281	82±4.73	63.33±0.88	306±82.02	N/a
⁸⁴ Sham	88±15.26	81.8±10.6	225±38.9	stable
⁸⁴ SNx	74.6±19.0	58.6±12.8	161.6±56.1	stable
⁸⁴ SNx + 283	73.8±9.4	56±9.1	171.4±67.6	stable
⁸⁴ SNx + 281	88±7.8	55±5.7	95.4±11.3	stable

Tables 9.1 and 9.2 Body weights, kidney weights, parameters of renal function and toxicity measurements were performed on samples collected immediately prior to termination at 7, 28 and 84 days post-SNx. Creatinine clearance (CrCl), aspartate aminotransferase (AST), alanine aminotransferase (ALT) and creatine kinase (CK) were measured in serum obtained from the heart. Proteinuria was measured in 24 hour urine samples. Clot stability was determined in blood samples treated with 5M urea. With the exception of clot stability all data represents mean ± SEM, n=5-6 animals for each experimental group per time point. Statistical difference determined by one way ANOVA with Bonferroni post hoc test. a=p<0.05, b=p<0.01 compared to sham, c=p<0.05, d=p<0.01 compared to untreated SNx.

Figure 9.6 Changes in Renal Function Markers

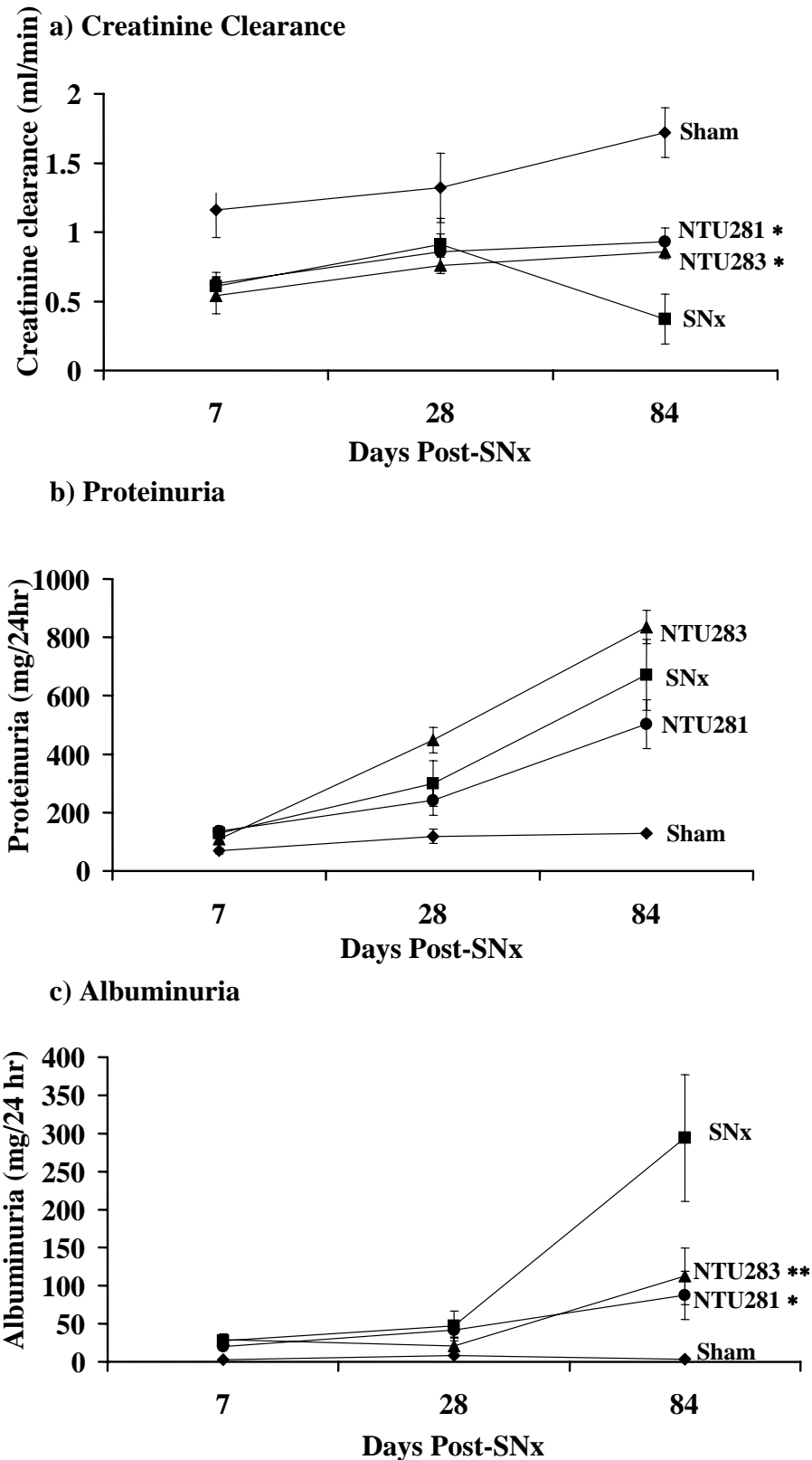


Figure 9.6 Kidney function was assessed by measuring creatinine clearance (a). Proteinuria (b) and albuminuria (c) were used as a determinant of glomerular leakage. All tests were performed on serum or urine obtained at 24, 48 and 84 days post-SNx. Data represents mean values \pm SEM, n=5-6 animals for each experimental group per time point. Statistical difference determined by one way ANOVA with Bonferroni post hoc test. *=p<0.05, **=p<0.01 compared to untreated SNx at 84 days.

9.2.2.3 Quantification of renal scarring

Analysis of renal scarring was performed on Masson's Trichrome-stained paraffin-embedded sections using multiphase image analysis (section 3.5.2.6).

All animals subjected to SNx developed progressive scarring leading to significant glomerulosclerosis and advanced tubulointerstitial fibrosis by 84 days post-nephrectomy (figure 9.7 and 9.8). Scarring was associated with extensive flattening of the tubular epithelium resulting in significant tubular atrophy. Animals treated with NTU283 and NTU281 showed less advanced disease throughout the remnant kidney with the exception of rat 11 that had areas of heavily scarred tissue.

Analysis of the renal histology of inhibitor-treated animals revealed some degree of abnormality compared to normal animals. Most had areas of slightly thickened tubular basement membrane and some had an enlarged tubular lumen, although minimal tubular atrophy was seen. A visible reduction in the number of interstitial cells (both inflammatory and non-inflammatory) was noted in both treated groups.

Assessment of changes in renal scarring by multiphase analysis (fig 9.9) indicated that at 7 days post-SNx, animals treated with NTU283 showed slightly elevated levels of glomerular and tubulointerstitial scarring compared to untreated SNx animals ($p < 0.01$). Likewise, tubulointerstitial scarring was also slightly elevated in the NTU281 treated group ($p < 0.05$). At day 28, comparable levels of scarring were demonstrated in all groups with the exception of NTU283 which showed a slight but significant increase in glomerulosclerosis ($p < 0.01$). By 84 days post-SNx, untreated animals showed 4 fold increases in glomerulosclerosis and tubulointerstitial scarring ($p < 0.001$ compared to sham). Treatment with both inhibitors significantly reduced this level of scarring. Glomerulosclerosis was reduced by 48% ($p < 0.01$) in NTU283 treated animals and by 60% ($p < 0.05$) in the NTU281 treated group whilst tubulointerstitial scarring was reduced by 60% ($p < 0.01$) and 74% ($p < 0.01$) respectively.

Figure 9.7 Representative Photomicrographs of Masson's Trichrome Staining

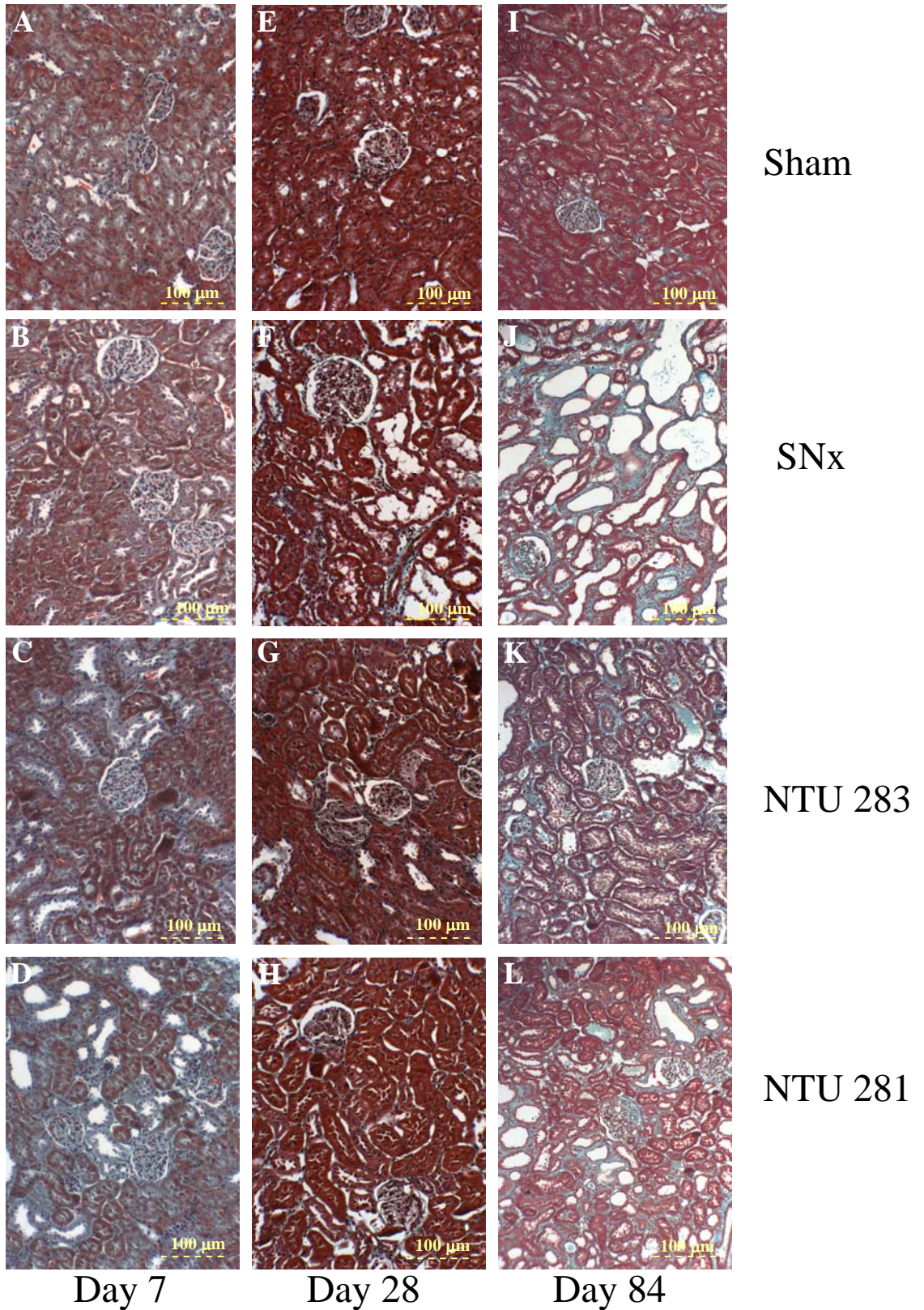


Figure 9.7 Representative Masson's Trichrome-stained sections from sham-operated (A, E, I), SNx (B,F,J), NTU283 treated (C,G,K) and NTU281 treated animals (D,H,L). Assessment of scarring was made at 7 days (A to D), 28 days, (E to H) and 84 days post-SNx (I to L). Photomicrographs are at 100x magnification.

Figure 9.8 Glomerulosclerosis and Tubulointerstitial Fibrosis at 84 Days Post-SNx

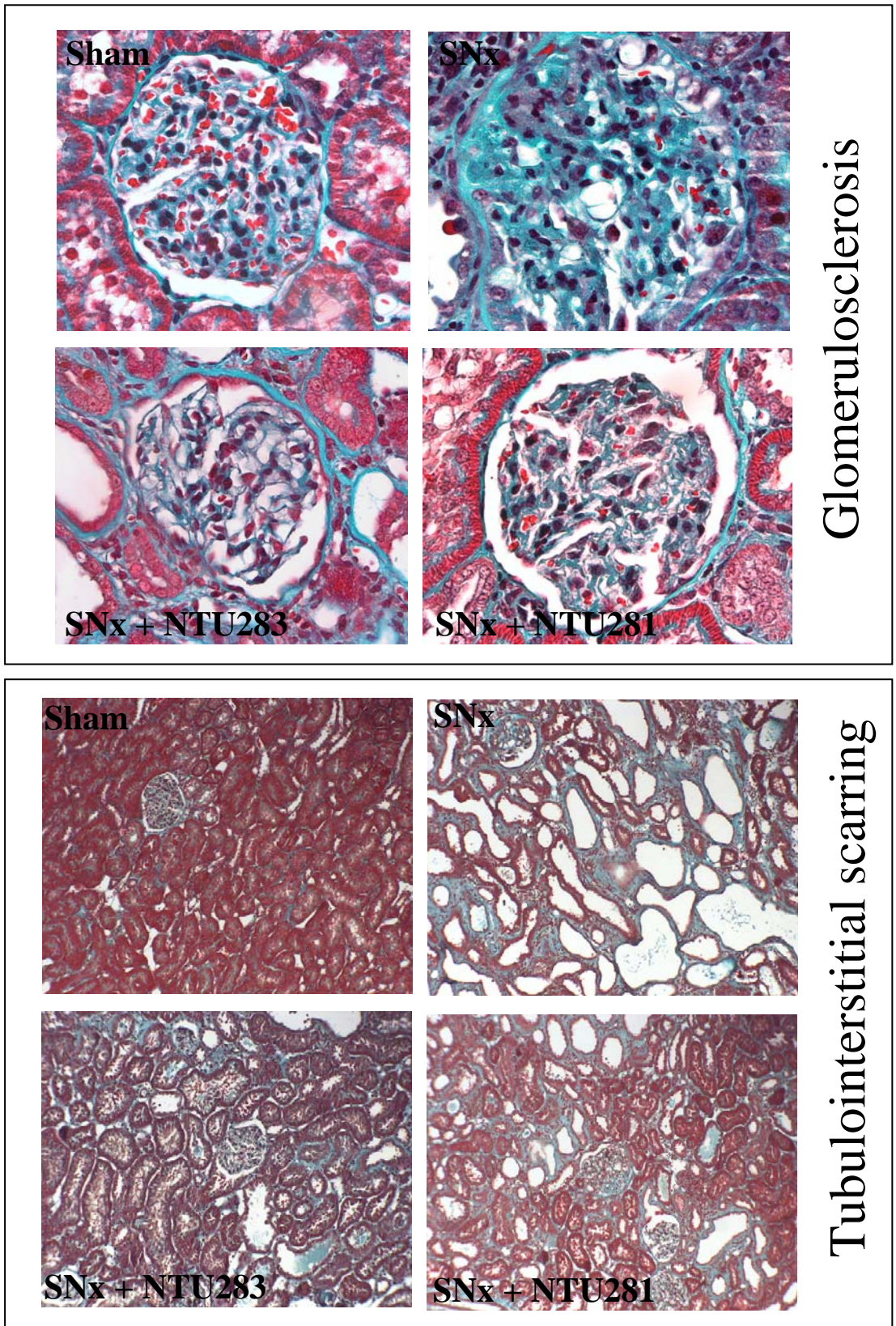
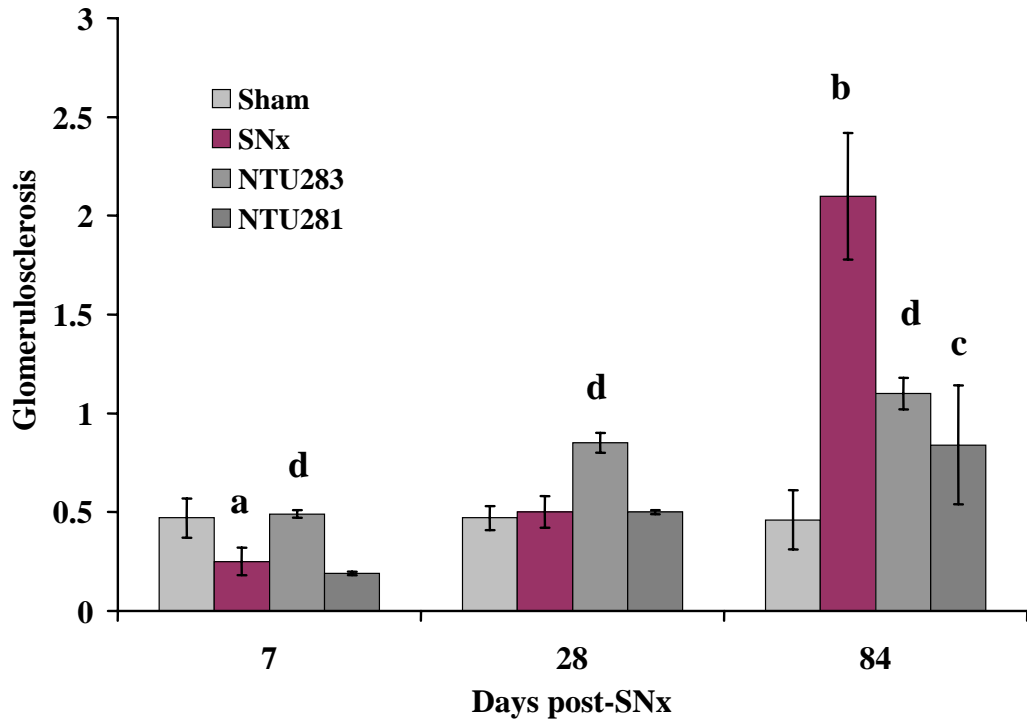


Figure 9.8 Representative Masson's Trichrome staining of glomeruli (top panel) and tubulointerstitium (bottom panel) from control (sham), SNx, NTU283 and NTU281 treated animals at day 84 post-SNx. Glomeruli are at 400 x magnification, tubulointerstitium is at 200 x magnification.

Figure 9.9 Assessment of Renal Scarring by Multi-phase Image Analysis

a) Glomerulosclerosis



b) Tubulointerstitial scarring

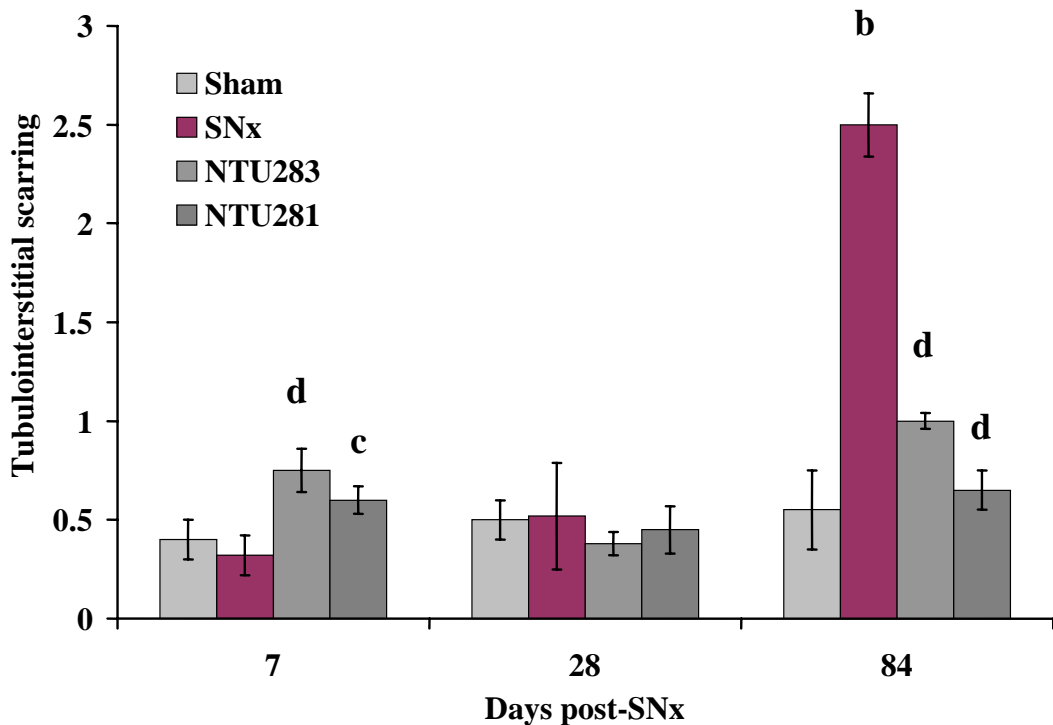


Figure 9.9 The level of glomerulosclerosis (a) and tubulointerstitial scarring (b) was assessed by multi-phase image analysis of Masson's Trichrome-stained sections using 3 phases as described in section 3.5.2.6. 10 glomeruli (400x magnification) or 10 cortical fields (100x magnification) were analysed for each animal on at least 3 sections. Statistical difference determined by one way ANOVA with Bonferroni post hoc test. a=p<0.05, b=p<0.001 compared to sham; c=p<0.05, d=p<0.01 compared to untreated SNx.

9.2.2.4 Inhibition of TG activity

Changes in overall renal TG activity were measured in remnant kidney homogenates at day 7, 28 and 84 post-SNx by the putrescine incorporation assay (fig 9.10).

TG activity was elevated in the SNx group at day 7, day 28 and day 84 compared to sham-operated animals and increased by 100% over the 84 day period. Treatment with inhibitor NTU283 reduced TG activity by 40% to below that of sham-operated animals at day 7 ($p < 0.01$ compared to SNx) and to control levels by day 28. At 84 days, activity in NTU283 treated animals rose to just over half that of untreated SNx animals ($p < 0.05$). NTU281 was ineffective at inhibiting overall TG activity at day 7 but gave similar levels of TG inhibition to that of NTU283 at both day 28 and day 84 ($p < 0.05$).

NTU281 has a low potential to cross the cell membrane and therefore its inhibitory activity is more accurately measured using a TG *in situ* activity assay optimised for measuring extracellular TG activity. Using this assay, extracellular TG activity was more than 4 fold greater in remnant kidneys of SNx animals when compared to controls (fig 9.11). Inhibitor NTU281 prevented any increase in extracellular TG activity up to 28 days (fig 9.11b) and reduced the elevated level in SNx animals at 84 days by more than 60%.

9.2.2.5 Inhibition of $\epsilon(\gamma\text{-glutamyl})$ lysine crosslink

To determine how effective TG inhibition was over a prolonged treatment period, measurement of its end product, $\epsilon(\gamma\text{-glutamyl})$ lysine was performed. Levels of $\epsilon(\gamma\text{-glutamyl})$ lysine crosslink were quantified at 84 days post-SNx by cation exchange chromatography following exhaustive proteolytic digestion (fig 9.12). SNx animals had a 7 fold increase in crosslink compared to sham animals ($p < 0.01$). Treatment with either NTU283 or NTU281 was effective at inhibiting this increase and at day 84 $\epsilon(\gamma\text{-glutamyl})$ lysine crosslink levels were not significantly higher than control animals with either inhibitor.

Figure 9.10 Changes in Transglutaminase Activity

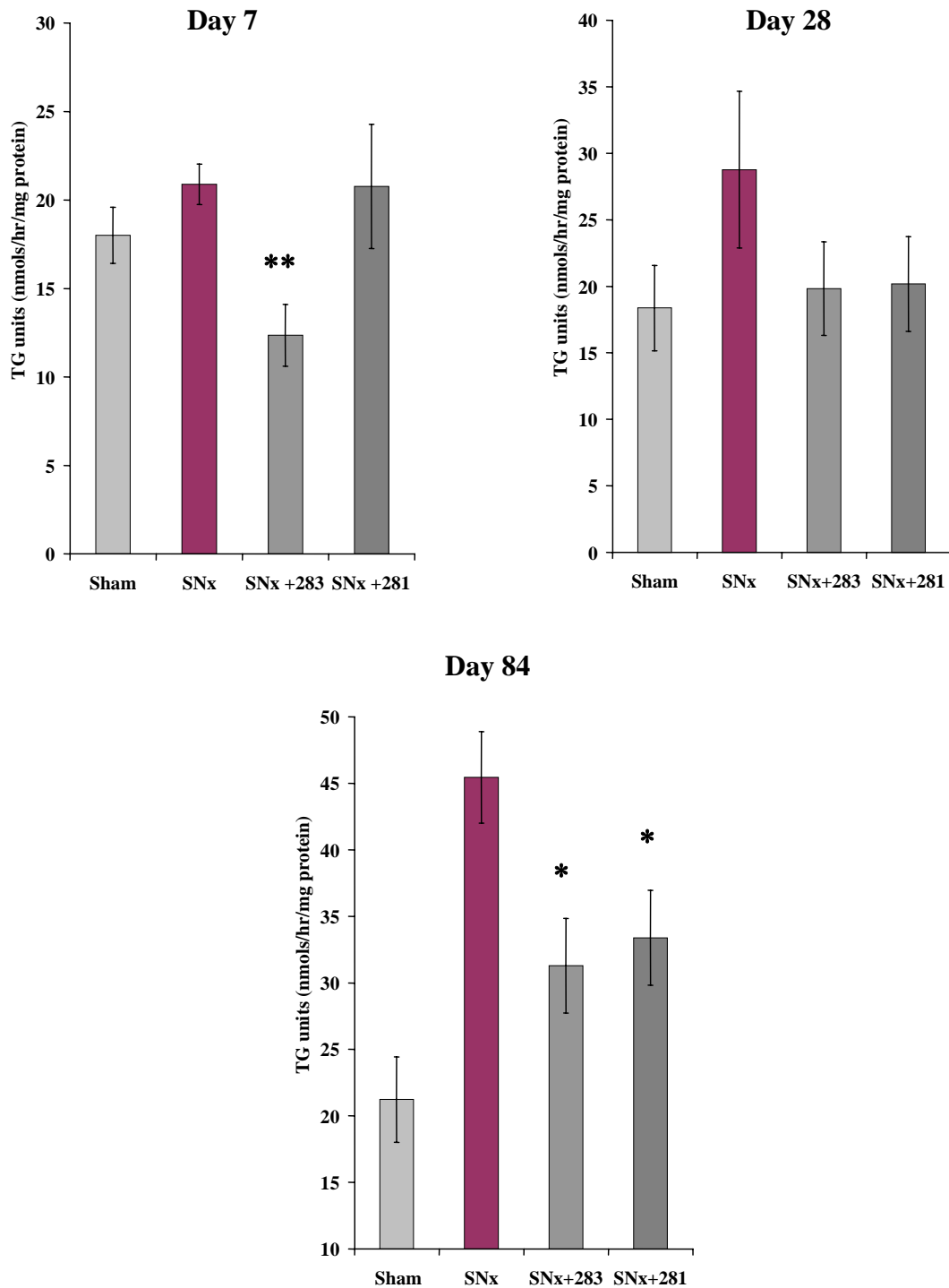
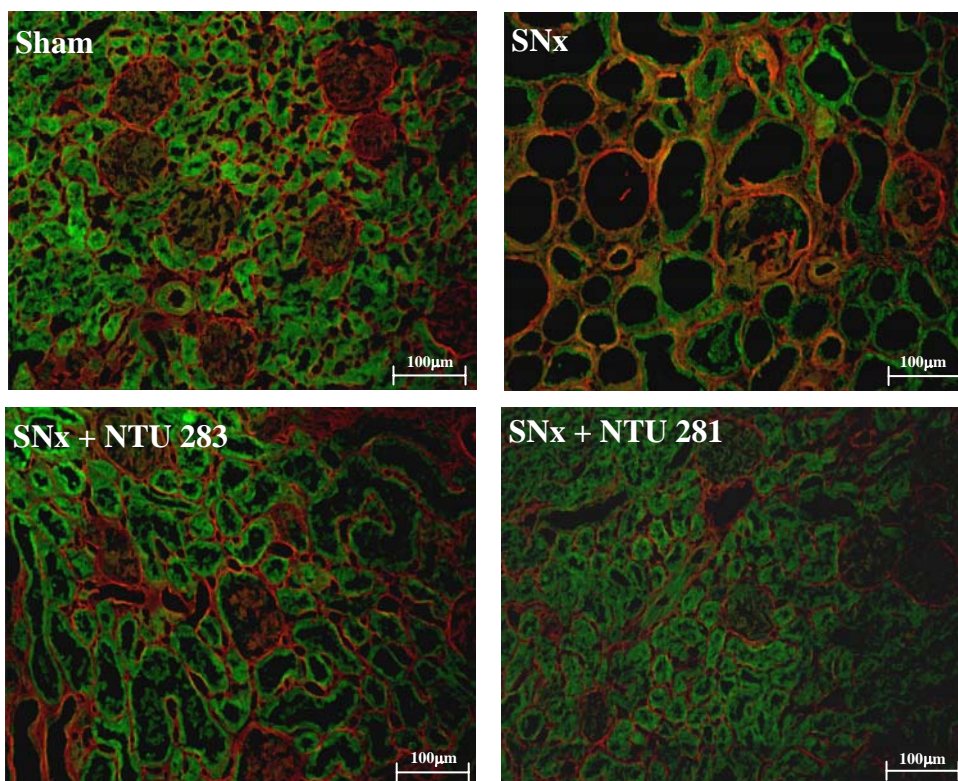


Figure 9.10 Transglutaminase activity was determined in remnant kidney homogenates at day 7, day 28 and day 84 post SNx by the putrescine incorporation assay. TG activity is expressed as mean nmols/hr/mg protein \pm SEM from 3 separate assays, n=5-6 per experimental group per time point. *= $p < 0.05$, **= $p < 0.01$ compared to untreated SNx by one way ANOVA with Bonferroni post hoc test.

Figure 9.11 TG *in situ* Activity

a) Photomicrographs



b) Semi-quantitation of fluorescence

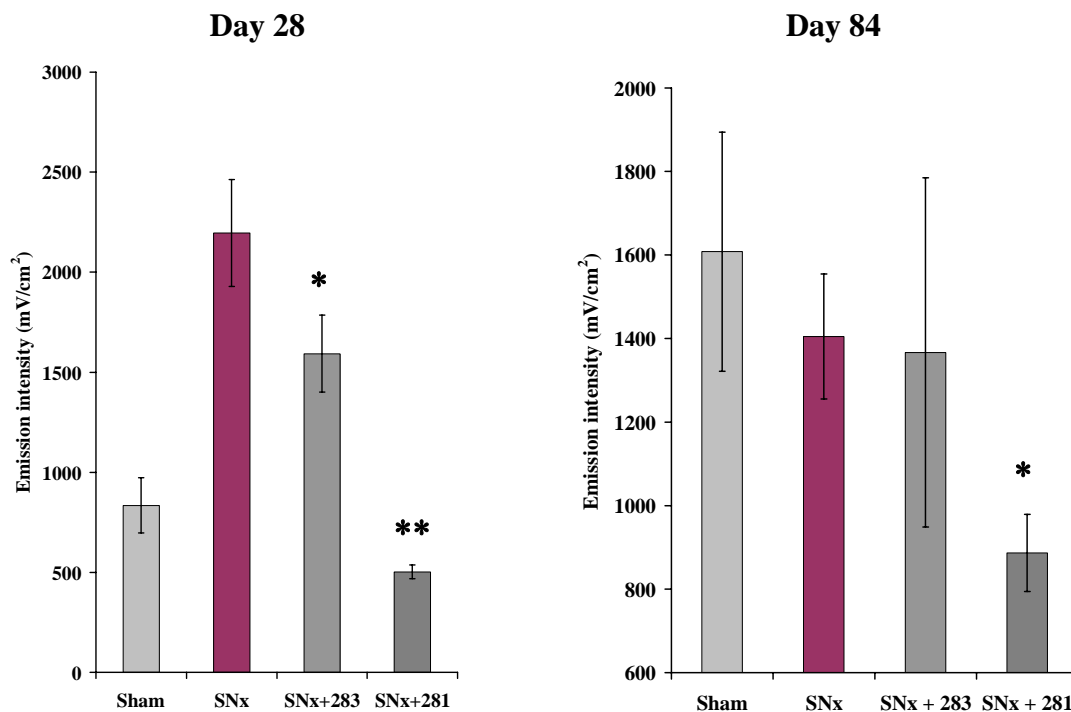


Figure 9.11 TG *in situ* activity was determined by fluorescein cadaverine incorporation and visualised by confocal microscopy as described in section 3.3.7.2. Representative sections are shown at 84 days post-SNx (200 x magnification) with red emissions indicating TG activity (top). Semi-quantitation of activity at 28 and 84 days post-SNx was obtained using the mean Cy5 emissions per field (mV/cm²) from n=10 fields. *= $p < 0.05$, **= $p < 0.01$ compared to untreated SNx by one way ANOVA with Bonferroni post hoc test.

Figure 9.12 $\epsilon(\gamma\text{-glutamyl})$ Lysine Crosslink at 84 Days Post-SNx

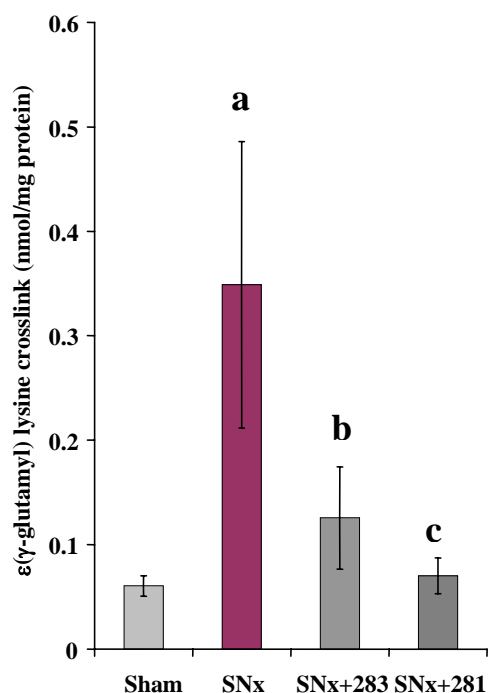


Figure 9.12 $\epsilon(\gamma\text{-glutamyl})$ lysine crosslink was measured following exhaustive proteolytic digestion by cation exchange chromatography on an amino acid analyser as described in section 3.3.8.2. Data represents mean \pm SEM from 3 separate experiments performed in duplicate, $n=5-6$ per experimental group. $a=p<0.01$ compared to sham, $b=p<0.05$, $c=p<0.01$ compared to untreated SNx (one way ANOVA with Bonferroni post hoc test).

Figure 9.13 Total Collagen Levels at Day 84 by Hydroxyproline Analysis

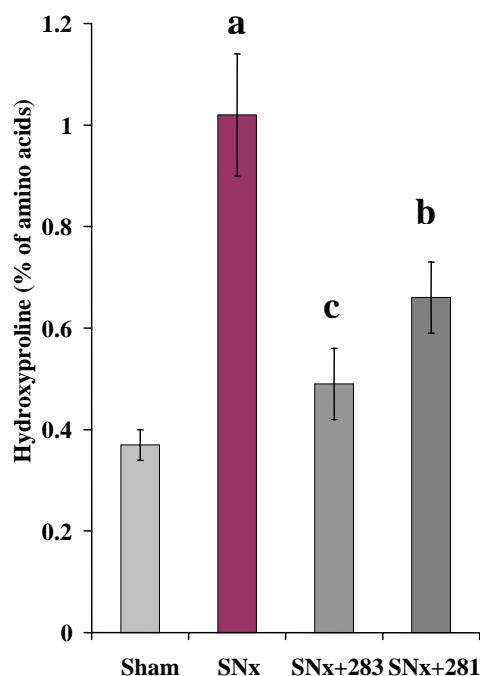


Figure 9.13 Total collagen levels were determined by measurement of hydroxyproline in kidney tissue at 84 days post-SNx by derivatisation with 7-chloro-4-nitrobenz-2-oxa-1,3-diazole and separation by gas liquid chromatography (section 3.5.2.2). Data is expressed as a percentage of total amino acids and represents mean values \pm SEM, $n=5-6$ per experimental group. $a=p<0.001$ compared to sham. $b=p<0.05$, $c=p<0.01$ compared to untreated SNx (one way ANOVA with Bonferroni post hoc test).

9.2.2.6 Total collagen levels

Measurement of hydroxyproline content as determined by gas liquid chromatography (GLC) was used as a measure of whole kidney collagen. At 84 days post-SNx (fig 9.13) levels of hydroxyproline were increased by 275% in untreated SNx kidneys compared to control ($p < 0.001$). In comparison, the hydroxyproline levels in remnant kidneys treated with TG inhibitors increased by only 33% with NTU281 (not significantly different from sham-operated controls), and by 78% with NTU283.

9.2.2.7 Immunohistochemical analysis of ECM

To gain a more specific insight into which particular ECM components were altered during the progressive scarring of remnant kidneys and whether they were affected by TG inhibition, immunohistochemistry was performed on cryostat (collagen I) and paraffin-embedded sections (collagen III, IV and fibronectin). Staining was quantified by multiphase analysis as described in section 3.5.2.6.

9.2.2.7.1 Collagen I

In sham-operated animals, some light staining for collagen I was localised to the tubulo-interstitium with very little glomerular staining and remained constant over the 84 days (fig 9.14). SNx animals showed a small increase in interstitial collagen I at day 7 that became more widespread at day 28 and day 84. This was accompanied at the latter time point by extensive collagen I staining in the mesangial matrix of sclerotic glomeruli. Multi-phase image analysis (fig 9.15) revealed that by day 84, collagen I was significantly increased in this group compared to sham ($p < 0.05$). Both NTU283 and NTU281-treated groups showed a similar distribution of collagen I staining to that of SNx at 7 and 28 days but by day 84 the increase in collagen I had been significantly reduced to less than a fifth that of SNx animals ($p < 0.05$ and $p = 0.05$ respectively).

9.2.2.7.2 Collagen III

Sham-operated animals showed a peri-tubular distribution of collagen III that did not significantly increase over the 84 day time course (figure 9.16). In SNx animals, this distribution was elevated slightly at day 7 compared to sham and significantly so at day 84 ($p < 0.05$) with extensive interstitial collagen accumulation. In contrast to collagen I however, there was little glomerular collagen III staining. Treatment with both inhibitors increased collagen III at day 7 (NTU281 treated, $p < 0.05$) compared to SNx but had little effect at day 28 (figure 9.17). However, by day 84, collagen III levels had been reduced in the NTU283 treated group by 50% compared to SNx ($p < 0.05$) although the decrease with NTU281

treatment did not reach significance.

9.2.2.7.3 Collagen IV

Sham-operated animals showed a linear distribution of collagen IV staining along the tubular and glomerular basement membranes, the pattern of which remained relatively constant throughout the time course. Only at 84 days did SNx-treated animals demonstrate elevated collagen IV levels compared to sham-operated animals (figure 9.18). This was characterised by increased collagen IV immunostain in the interstitium and peri-glomerular area which was extensive by day 84. Treatment with inhibitor NTU283 failed to reduce this elevated collagen IV (figure 9.19) however, treatment with NTU281 was able to lower collagen IV relative to SNx at 84 days although it did not reach significance.

9.2.2.7.4 Fibronectin

Sham operated animals showed fibronectin immunoreactivity in the cytoplasm of both distal and proximal tubular cells that appeared to localise to the luminal surface (figure 9.20) However, in contrast to previous studies in SNx rats (Floege *et al.*, 1992a; Okuda *et al.*, 1992) there was little or no fibronectin staining in glomeruli. The cytoplasmic fibronectin staining was elevated in SNx animals at day 7 and significantly so at day 84 ($p < 0.05$) compared to sham (figure 9.21). Treatment with inhibitor NTU283 had little effect on this at the early time points but by day 84 had reduced staining by 45% compared to untreated SNx animals ($p < 0.05$). Treatment with NTU281 surprisingly increased fibronectin staining at day 7 ($p < 0.05$) and day 28 ($p < 0.05$) compared to both sham and SNx but was almost as effective at reducing fibronectin at day 84 as inhibitor NTU283.

Figure 9.14 Representative Photomicrographs of Collagen I Immunohistochemistry

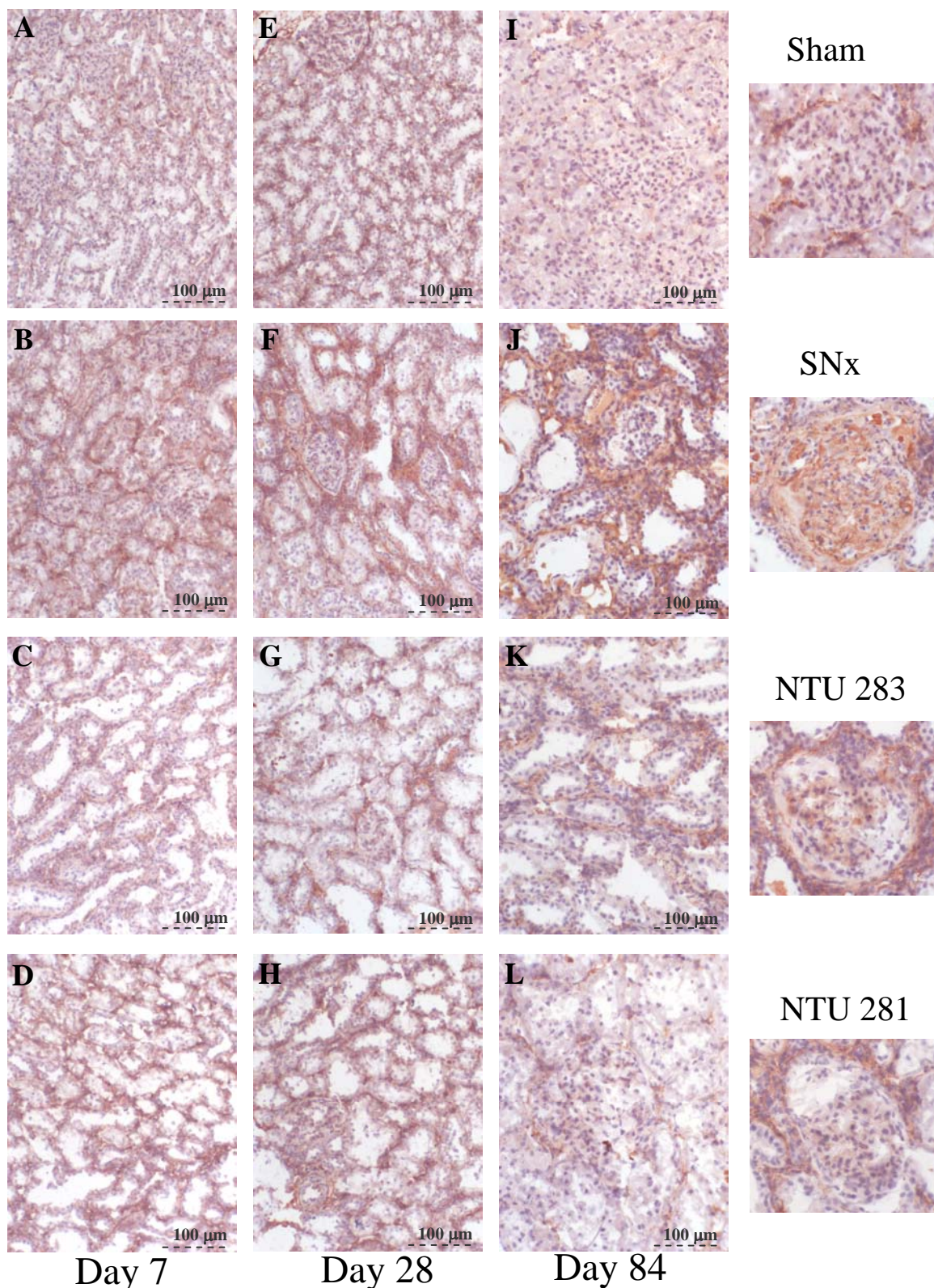


Figure 9.14 Representative Collagen I stained cryostat sections (left) from sham-operated (A, E, I), SNx (B,F,J), NTU283 treated (C,G,K) and NTU281 treated animals (D,H,L). The degree of staining was analysed at 7 days (A to D), 28 days, (E to H) and 84 days post-SNx (I to L). Photomicrographs of glomerular staining are shown (right) at day 84. Tubulointerstitial sections are at 100x magnification, glomeruli are at 400 x magnification.

Figure 9.15 Multi-phase Image Analysis of Collagen I Immunohistochemistry

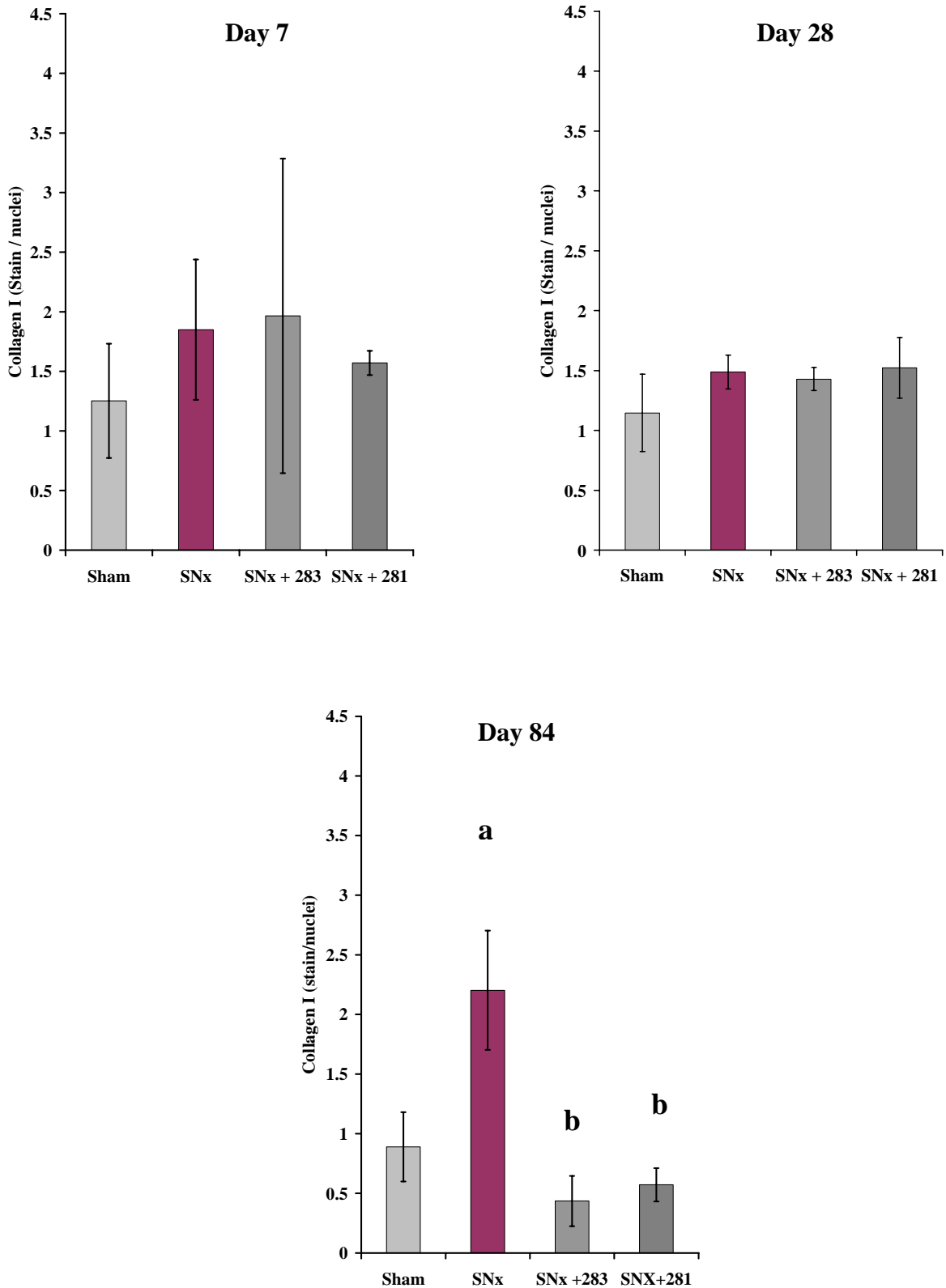


Figure 9.15 Cryostat sections from kidneys harvested at 7, 28 and 84 days post-SNx were immunoprobed with 1:50 goat anti-collagen I antibody as described in section 3.5.2.5. Staining was quantified by multi-phase image analysis (section 3.5.2.6). Data represents mean percentage area (stain:nuclei) \pm SEM from 10 sections analysed per animal, n=5-6 animals per group. a=p<0.05 compared to sham, b=p<0.05 compared to SNx (one way ANOVA with Bonferroni post hoc test).

Figure 9.16 Representative Photomicrographs of Collagen III Immunohistochemistry

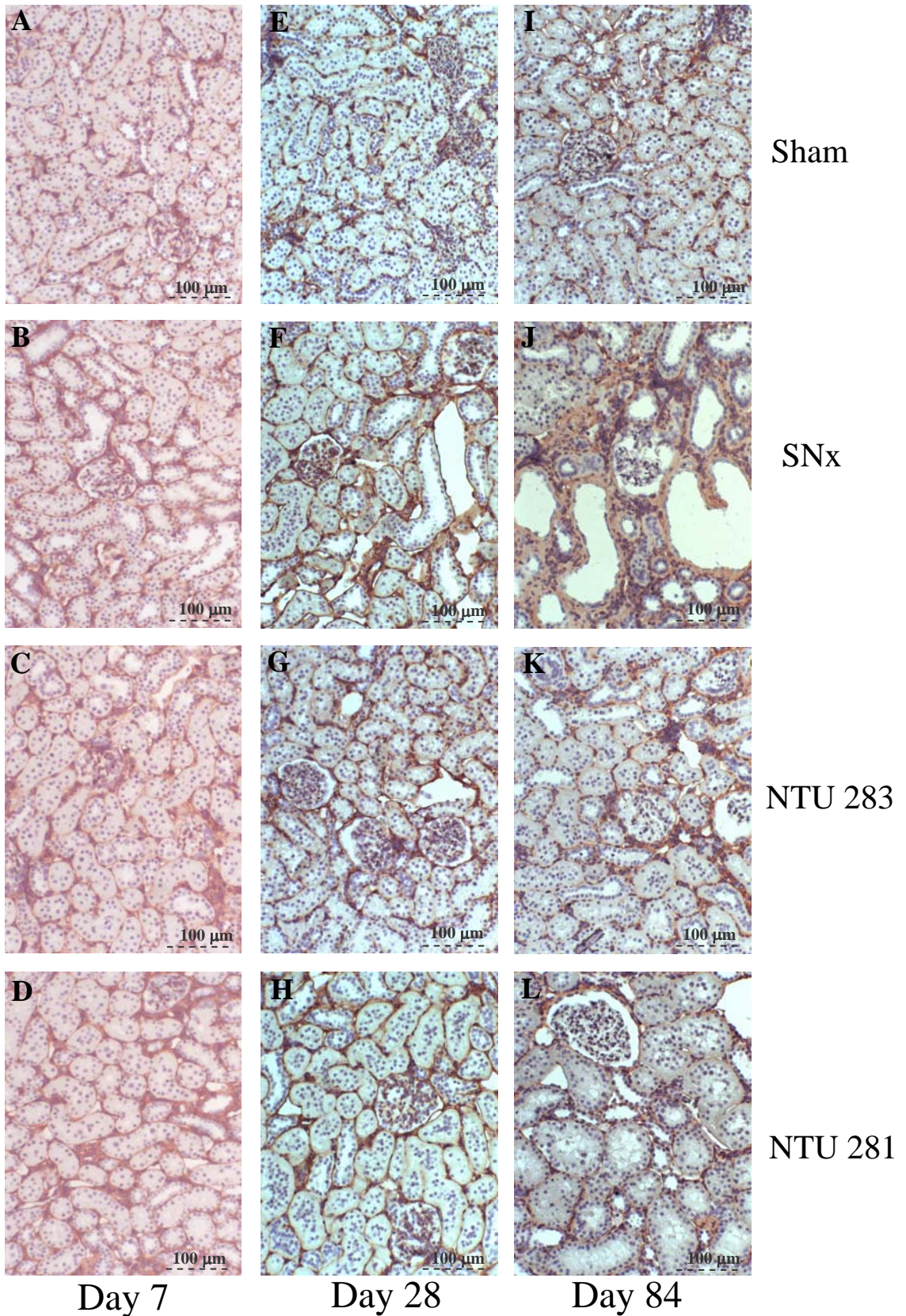


Figure 9.16 Representative Collagen III stained paraffin sections from sham-operated (A, E, I), SNx (B,F,J), NTU283 treated (C,G,K) and NTU281 treated animals (D,H,L). The degree of staining was analysed at 7 days (A to D), 28 days, (E to H) and 84 days post-SNx (I to L). Photomicrographs are at 100x magnification.

Figure 9.17 Multi-phase Analysis of Collagen III Immunohistochemistry

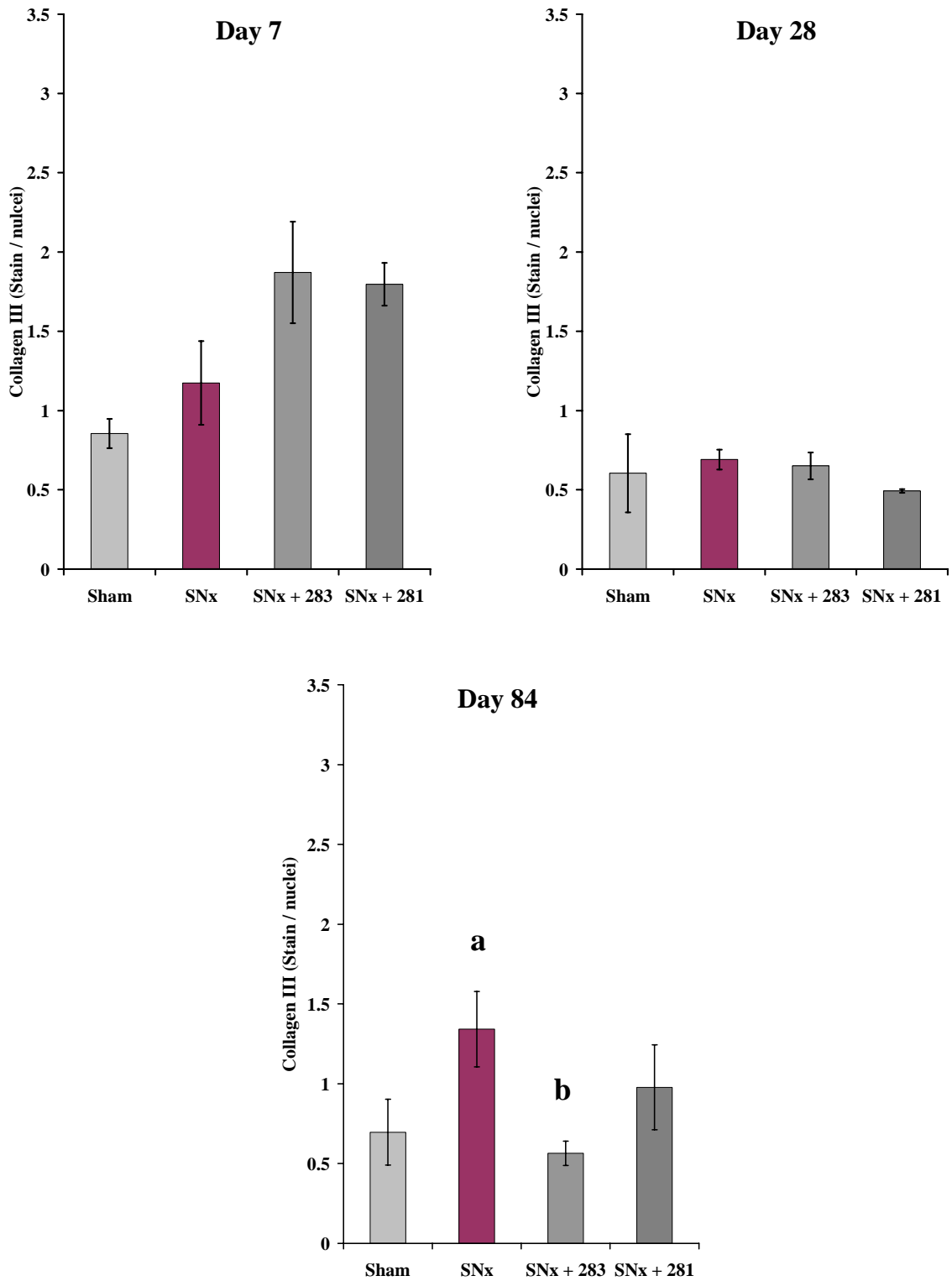


Figure 9.17 Paraffin-embedded sections from kidneys harvested at 7, 28 and 84 days post-SNx were immunoprobed with 1:10 rabbit anti-collagen III antibody as described in section 3.5.2.4 Staining was quantified by multi-phase image analysis. Data represents mean \pm SEM from 10 sections analysed per animal, $n=5-6$ animals per group. $a=p<0.05$ compared to sham, $b=p<0.05$ compared to untreated SNx (one way ANOVA with Bonferroni post hoc test).

Figure 9.18 Representative Photomicrographs of Collagen IV Immunohistochemistry

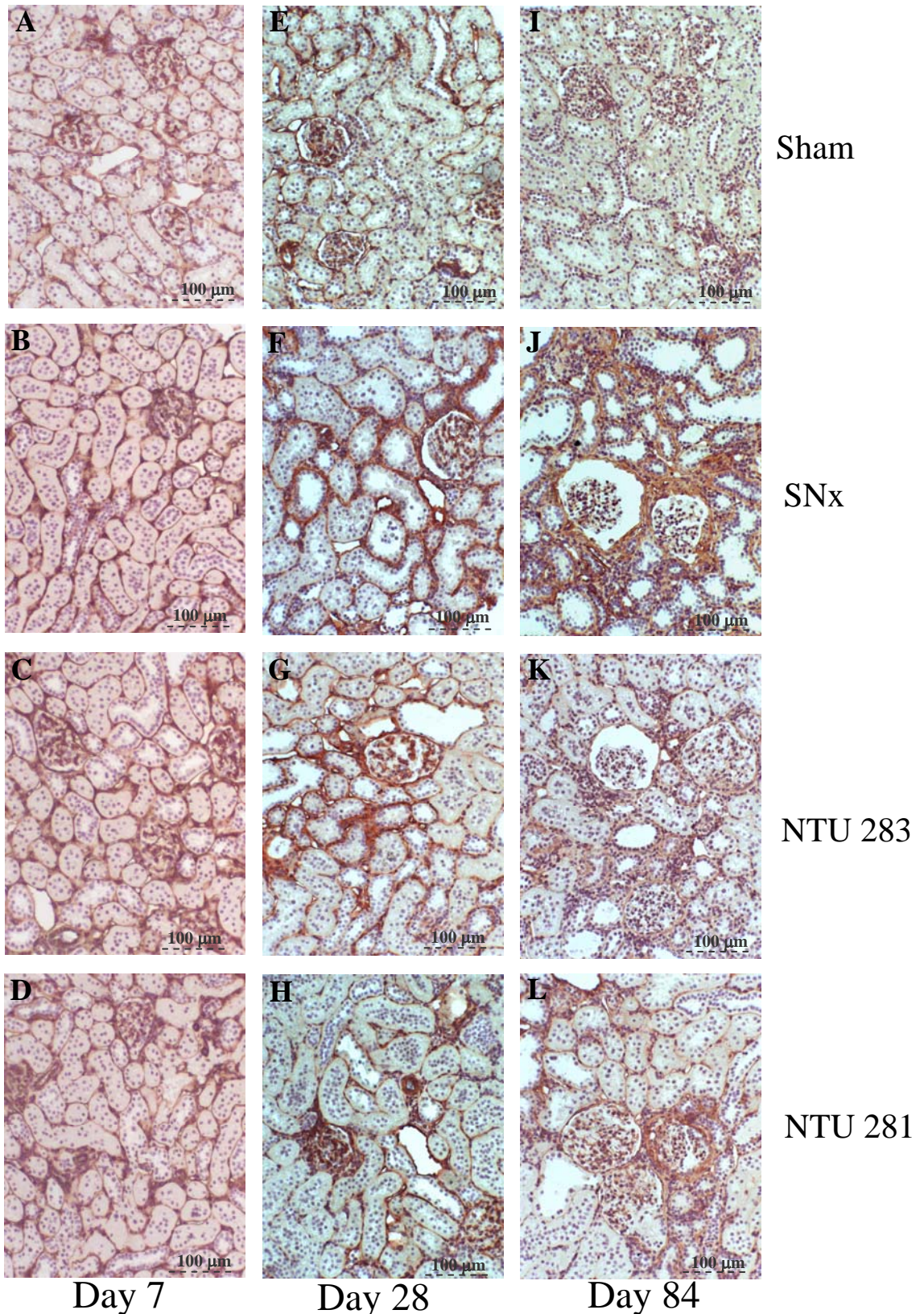


Figure 9.18 Representative Collagen IV stained paraffin sections from sham-operated (A, E, I), SNx (B,F,J), NTU283 treated (C,G,K) and NTU281 treated animals (D,H,L). The degree of staining was analysed at 7 days (A to D), 28 days, (E to H) and 84 days post-SNx (I to L). Photomicrographs are at 100x magnification.

Figure 9.19 Multi-phase Analysis of Collagen IV Immunohistochemistry

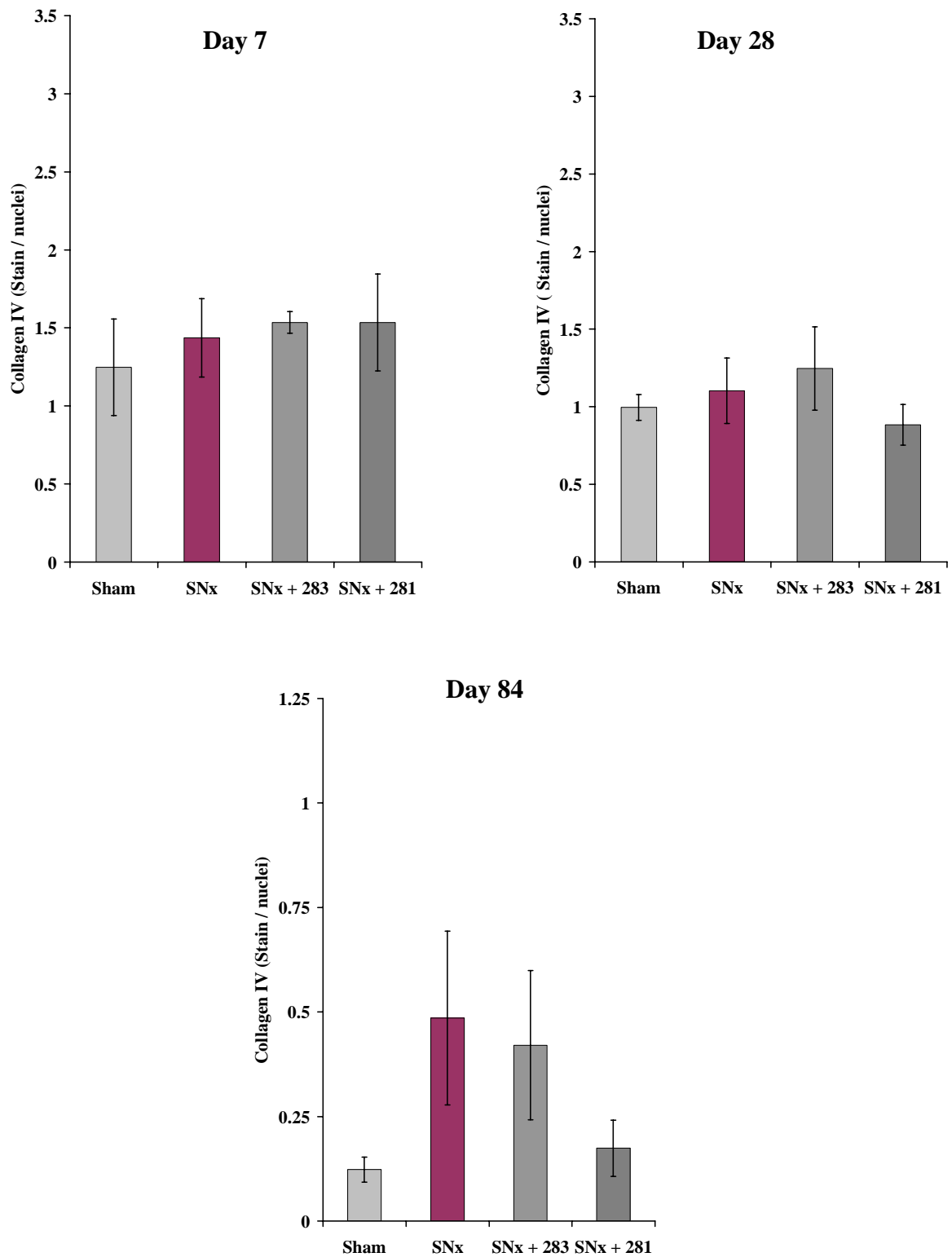


Figure 9.19 Paraffin-embedded sections from kidneys harvested at 7, 28 and 84 days post-SNx were immunoprobed with 1:35 rabbit anti-collagen IV antibody as described in section 3.5.2.4 and staining quantified by multi-phase image analysis. Data represents mean \pm SEM from 10 sections analysed per animal, n=5-6 animals per group.

Figure 9.20 Representative Photomicrographs of Fibronectin Immunohistochemistry

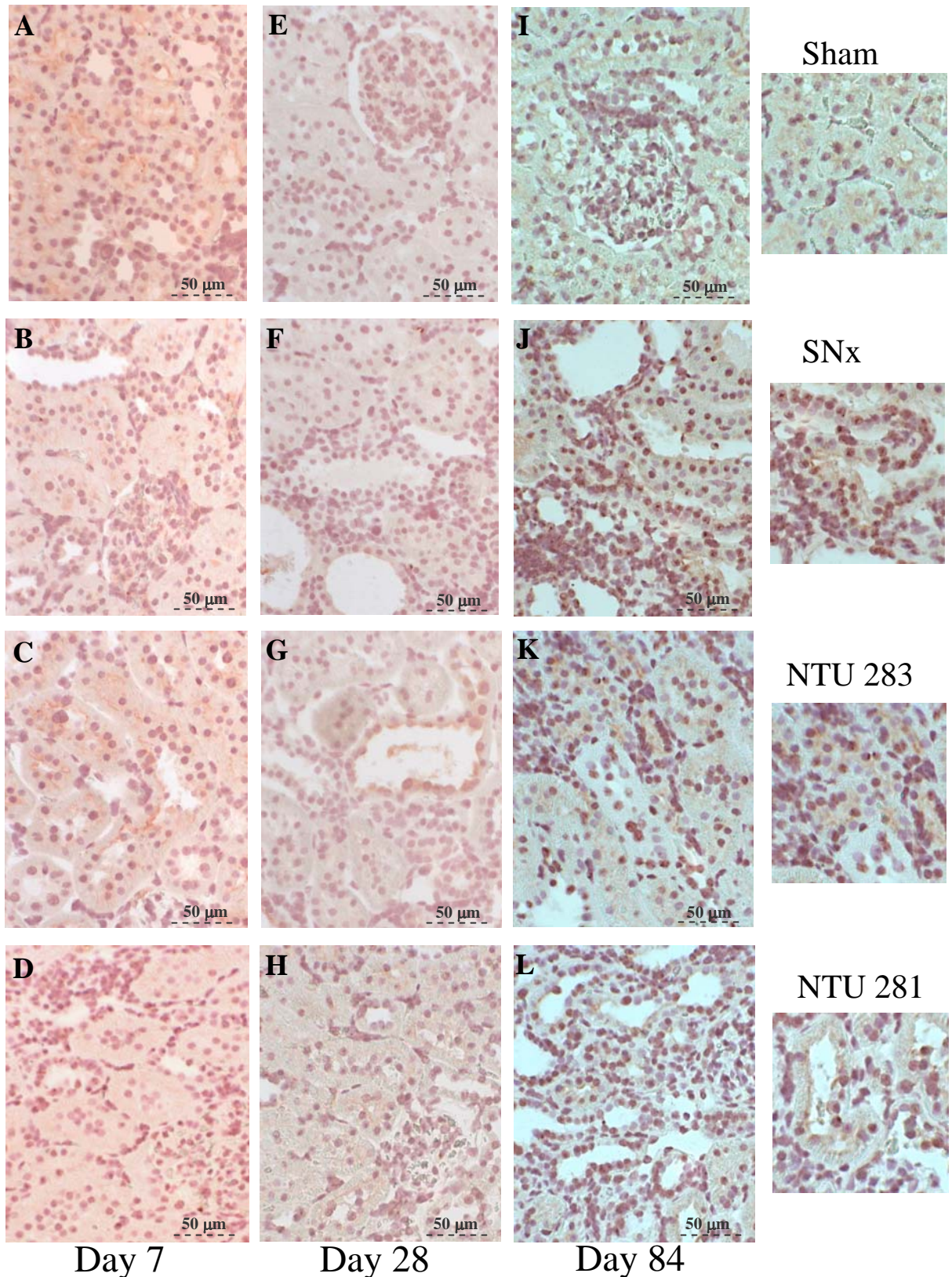


Figure 9.20 Representative fibronectin stained paraffin sections from sham-operated (A, E, I), SNx (B,F,J), NTU283 treated (C,G,K) and NTU281 treated animals (D,H,L). The degree of staining was analysed at 7 days (A to D), 28 days, (E to H) and 84 days post-SNx (I to L). Main panels (left) are at 200x magnification. Right panels show representative staining at 400x magnification.

Figure 9.21 Multi-phase Analysis of Fibronectin Immunohistochemistry

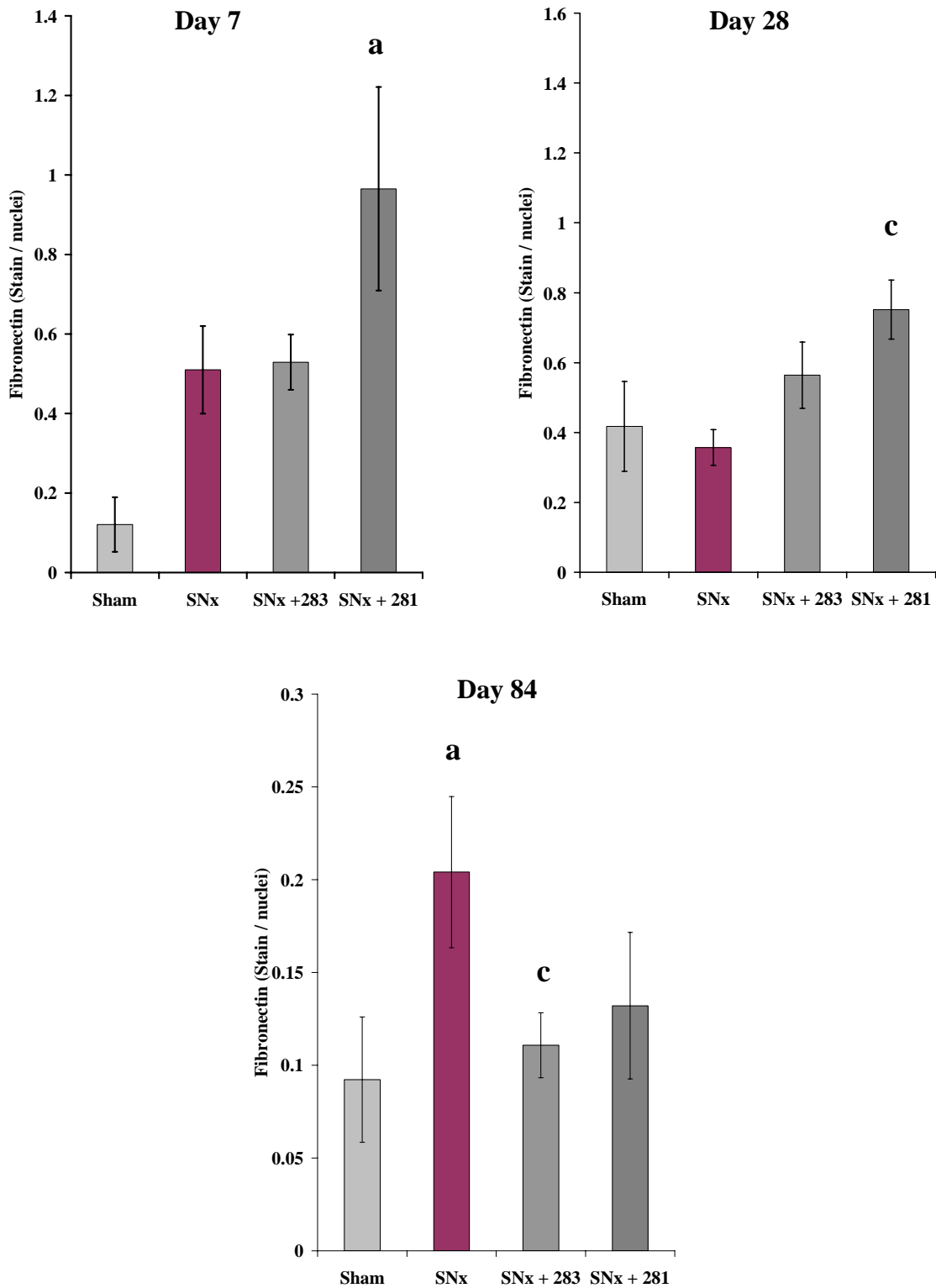


Figure 9.21 Paraffin-embedded sections from kidneys harvested at 7, 28 and 84 days post-SNx were immunoprobed with 1:50 mouse monoclonal anti-fibronectin antibody as described in section 3.5.2.4. Staining was quantified by multi-phase image analysis. Data represents mean \pm SEM from 10 sections analysed per animal, $n=5-6$ animals per group. $a=p<0.05$, $b<0.01$ compared to sham, $c=p<0.05$ compared to SNx (one way ANOVA with Bonferroni post hoc test).

9.2.2.8 mRNA expression of ECM components

To ascertain whether TG inhibitors were affecting the post-translational processing of ECM components alone rather than acting via non-specific effects on their expression or by negative feedback, mRNA levels of major ECM components and processing enzymes were measured at 84 days post-SNx by Northern blot analysis (fig 9.22).

Unfortunately, visual inspection of the blots revealed a high degree of RNA degradation with considerable variability in signal between experimental groups and samples within the same group. As a consequence, quantitation of Northern blots by densitometric analysis was not possible and blots were interpreted visually. Gross increases in the mRNA expression of collagen I and III (fig 9.22a and b) were apparent in 2 of the 4 SNx samples compared to sham. Treatment with NTU283 appeared to further increase collagen I and III mRNA expression in 2 samples although expression was not detectable in the other 2 samples nor in the NTU281 treated group. Changes in fibronectin and MMP-1 mRNA expression (fig 9.22 c and d) were impossible to interpret as discrete bands were not distinguishable. TIMP-1 mRNA expression appeared increased in 3 out of 4 SNx samples compared to sham (fig 9.22 e). Treatment with NTU283 appeared to have little effect on TIMP-1 mRNA expression however, TIMP-1 appeared to be decreased in response to NTU281 treatment especially when cyclophilin loading was compared.

9.2.2.9 Interstitial cells

9.2.2.9.1 Myofibroblasts

Immunohistochemistry for α -SMA was used as a marker for myofibroblasts (figures 9.23 and 9.24).

At day 7, the distribution of α -SMA staining in all groups was mainly confined to the vascular walls of the renal arteries and arterioles and to isolated cells within the interstitium. Staining was increased slightly in SNx and more so in inhibitor NTU283 treated animals. NTU281 treatment significantly increased α -SMA staining ($p < 0.05$) compared to that of sham operated and SNx animals.

At day 28, α -SMA staining appeared in the peri-glomerular region of SNx and inhibitor treated kidneys whilst the distribution in sham-operated kidneys remained predominantly interstitial. Treatment with either inhibitor NTU283 or NTU281 reduced α -SMA compared to sham and SNx although these changes were not significant.

By day 84, some glomerular staining was observed in sham-operated animals. This was

significantly increased in SNx animals ($p < 0.01$) with extensive peri-glomerular staining and in some cases accumulation of α -SMA positive cells within the mesangium. Treatment with either inhibitor failed to significantly reduce this accumulation.

9.2.2.9.2 Monocyte/macrophages

The degree of monocyte/macrophage infiltration was assessed by immunohistochemistry for the monocyte marker ED1 (CD68 in humans) (figures 9.25 and 9.26).

ED1 staining of sham-operated kidneys highlighted the occasional positive cell in both the tubulointerstitium and glomerulus (fig 9.25). In advanced disease, the staining in these areas was far more intense indicating the presence of far more cells of monocytic origin. Multi-phase image analysis (fig 9.26) showed that at day 7, ED1-positive staining was increased in untreated SNx animals compared to sham-operated animals. Similar elevated levels of ED1 were observed in inhibitor-treated groups.

At day 28, both inhibitors elevated ED1-positive staining to levels much greater than SNx alone. A 5 fold increase in ED1 staining due to SNx was increased to 21 and 13 fold control levels when treated with NTU283 ($p < 0.05$) and NTU281 respectively.

By day 84, levels of ED1 staining were comparable in untreated SNx and NTU283 treated animals however, staining was reduced with NTU281 treatment (not significant).

9.2.2.10 Correlation analysis

Across all time points the level of tubulointerstitial scarring (Masson's Trichrome staining) correlated well with ϵ (γ -glutamyl) lysine crosslink levels ($r = 0.72$, $p < 0.001$). However, while TG *in situ* activity correlated well with both tubulointerstitial scarring and crosslink up to 28 days ($r = 0.75$, $p < 0.01$), the reduction in the level of inhibition seen by 84 days resulted in a poor association at this later time point ($r = 0.22$, not significant). Crosslink levels also correlated ($p < 0.05$) with collagen I ($r = 0.53$), collagen IV ($r = 0.51$) and collagen III ($r = 0.34$) when measured individually. Measurements of collagen by hydroxyproline revealed a better association with immunoreactive collagen I ($r = 0.49$, $p < 0.01$), than either collagen III ($r = 0.34$, $p < 0.05$) or IV ($r = 0.33$, $p < 0.05$). Creatinine clearance correlated inversely with scarring ($r = -0.6$, $p < 0.01$) and particularly collagen III ($r = -0.73$, $p < 0.001$), with a weaker link to crosslink ($r = -0.35$, $p < 0.05$). ED1 staining showed no correlation to crosslink levels even when NTU283 data was excluded ($r = 1.1$, NS), although there was good association with scarring ($r = 0.62$, $p < 0.01$)

Figure 9.22 mRNA Expression of Collagens, Fibronectin, MMP-1 and TIMP-1

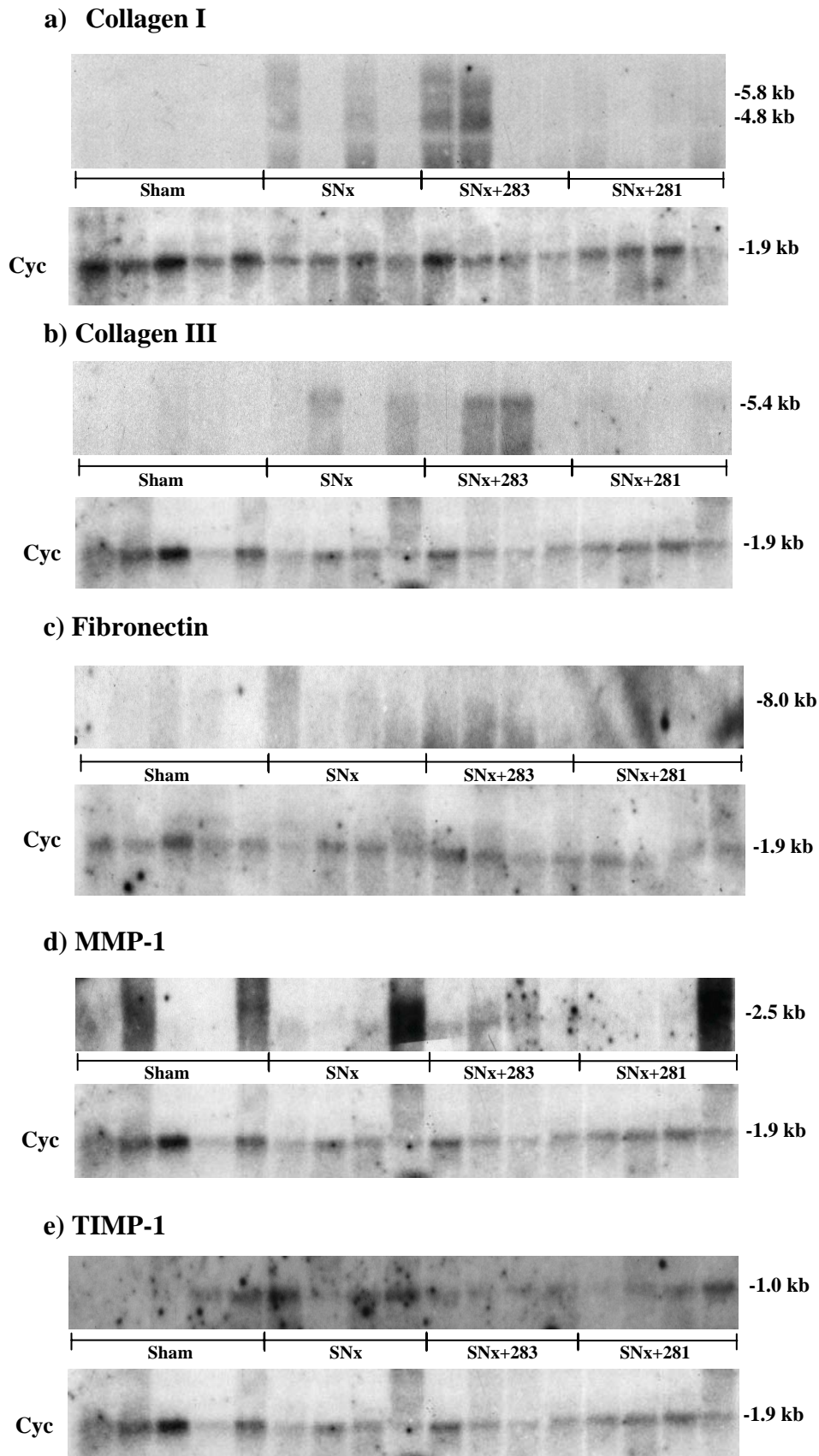


Figure 9.22 Representative Northern blots probed using specific [32 P] dCTP random primed cDNA probes for collagen I (a) collagen III (b), fibronectin (c), MMP-1 (d) and TIMP-1 (e) at 84 days post-SNx. Repeat probing for cyclophilin (cyc) was used as a loading control. n=4-5 animals per experimental group.

Figure 9.23 Representative Photomicrographs of α -SMA Immunohistochemistry

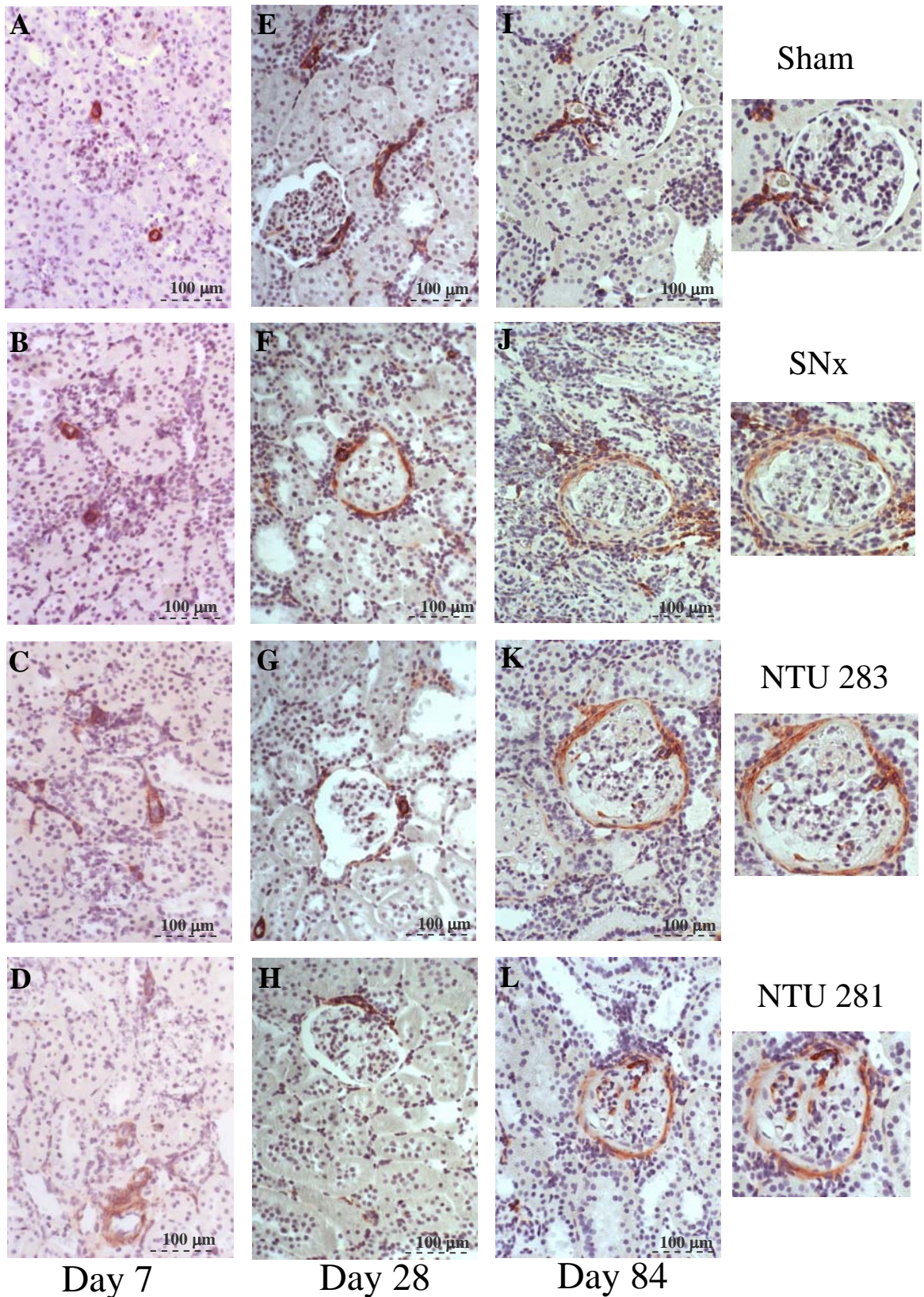


Figure 9.23 Representative α -SMA stained paraffin sections from sham-operated (A, E, I), SNx (B,F,J), NTU283 treated (C,G,K) and NTU281 treated animals (D,H,L). The degree of staining was analysed at 7 days (A to D), 28 days, (E to H) and 84 days post-SNx (I to L). Main photomicrographs are at 100x magnification, glomeruli are at 400x magnification.

Figure 9.24 Multi-phase Analysis of α -SMA Immunohistochemistry

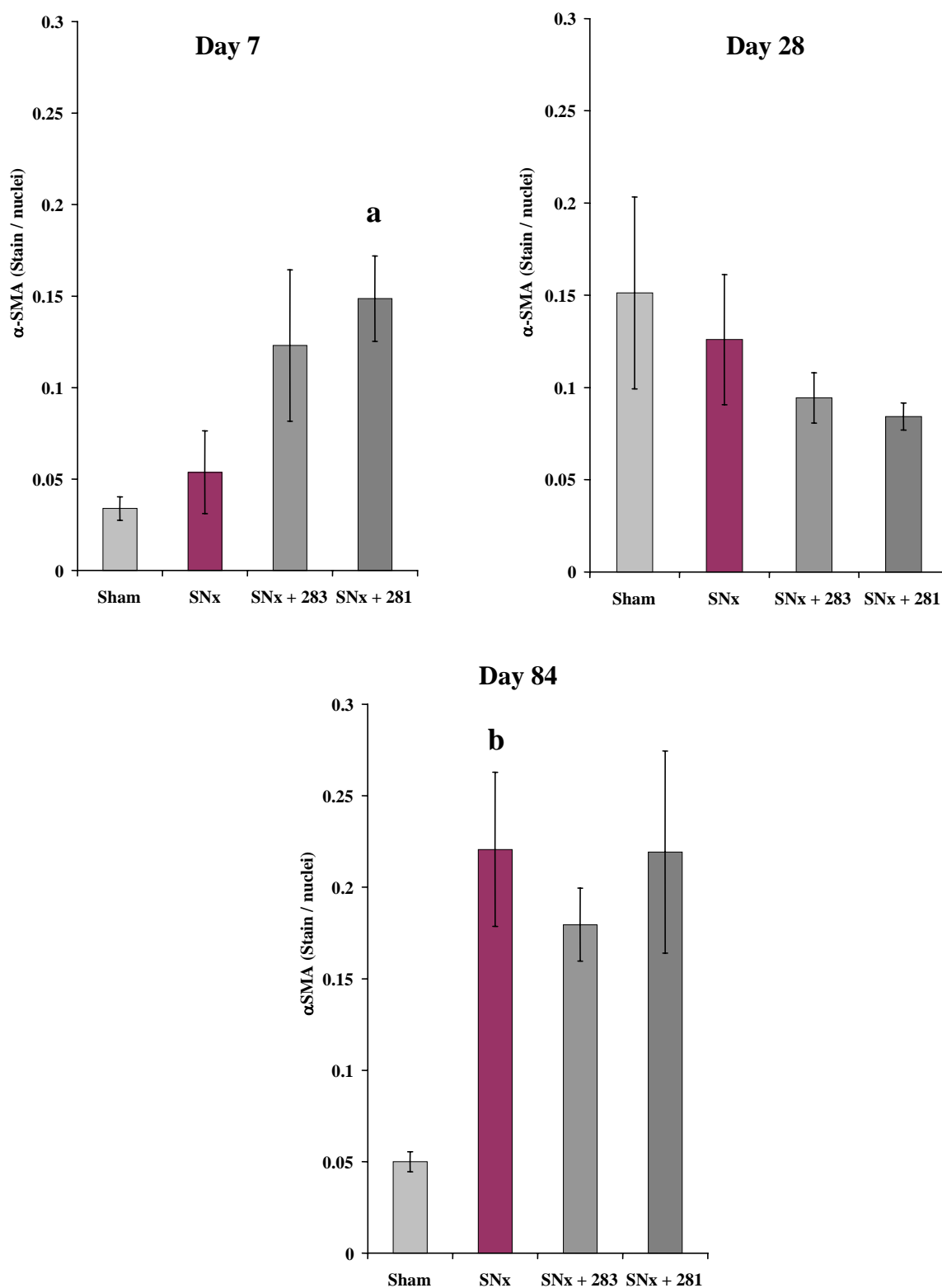


Figure 9.24 Paraffin-embedded sections from kidneys harvested at 7, 28 and 84 days post-SNx were immunoprobed with 1:100 mouse anti α -SMA antibody as described in section 3.5.2.4. Staining was quantified by multi-phase image analysis. Data represents mean \pm SEM from 10 sections analysed per animal, n=5-6 animals per group. a=p<0.05 compared to untreated SNx., b=p<0.01 compared to sham (one way ANOVA with Bonferroni post hoc test).

Figure 9.25 Representative Photomicrographs of ED1 Immunohistochemistry

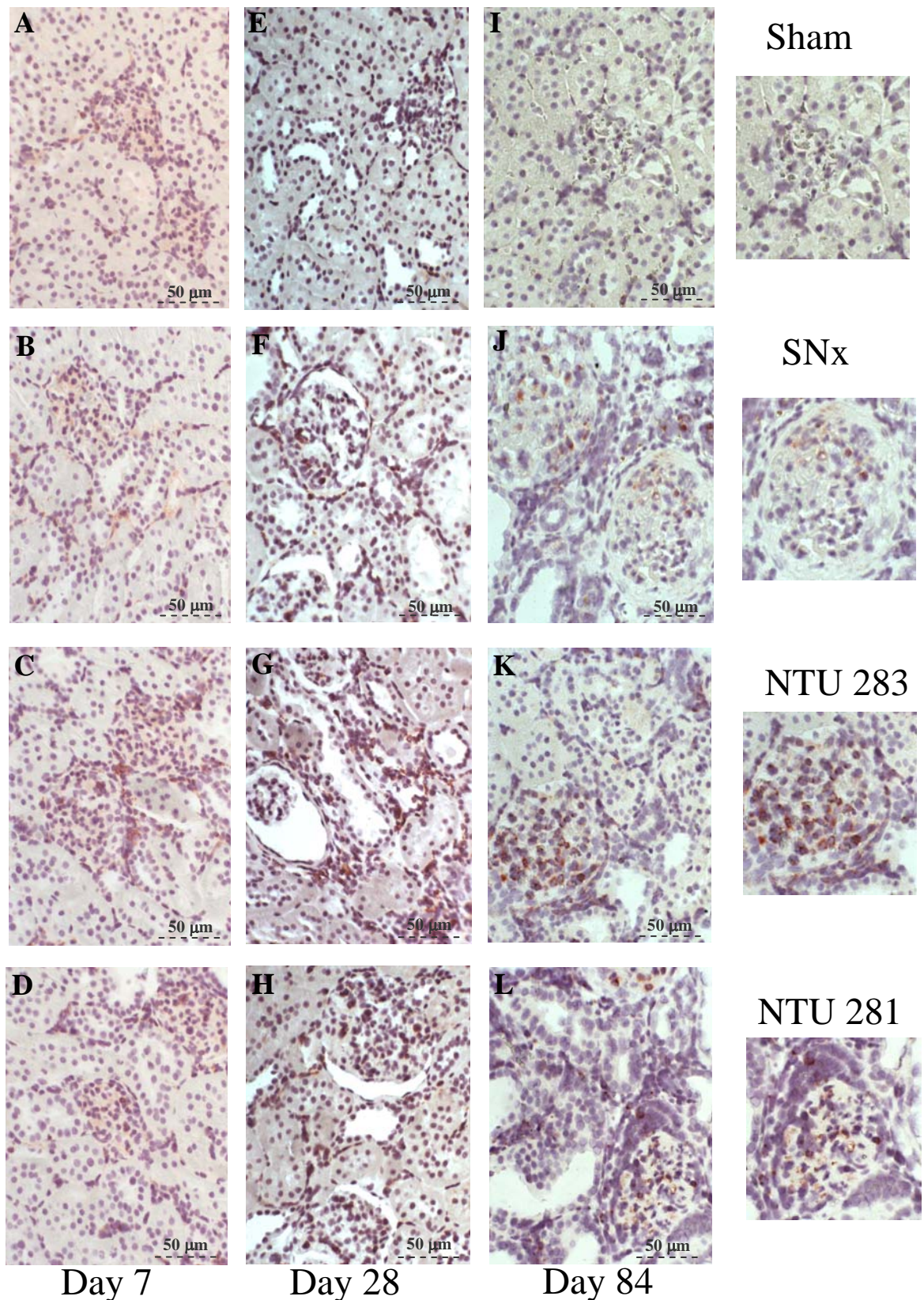


Figure 9.25 Representative ED1 (CD68) stained paraffin sections from sham-operated (A, E, I), SNx (B,F,J), NTU283 treated (C,G,K) and NTU281 treated animals (D,H,L). The degree of staining was analysed at 7 days (A to D), 28 days, (E to H) and 84 days post-SNx (I to L). Main panels (left) are at 200x magnification. Right panels show representative staining at 400x magnification

Figure 9.26 Multi-phase Analysis of ED1 (CD68) Immunohistochemistry

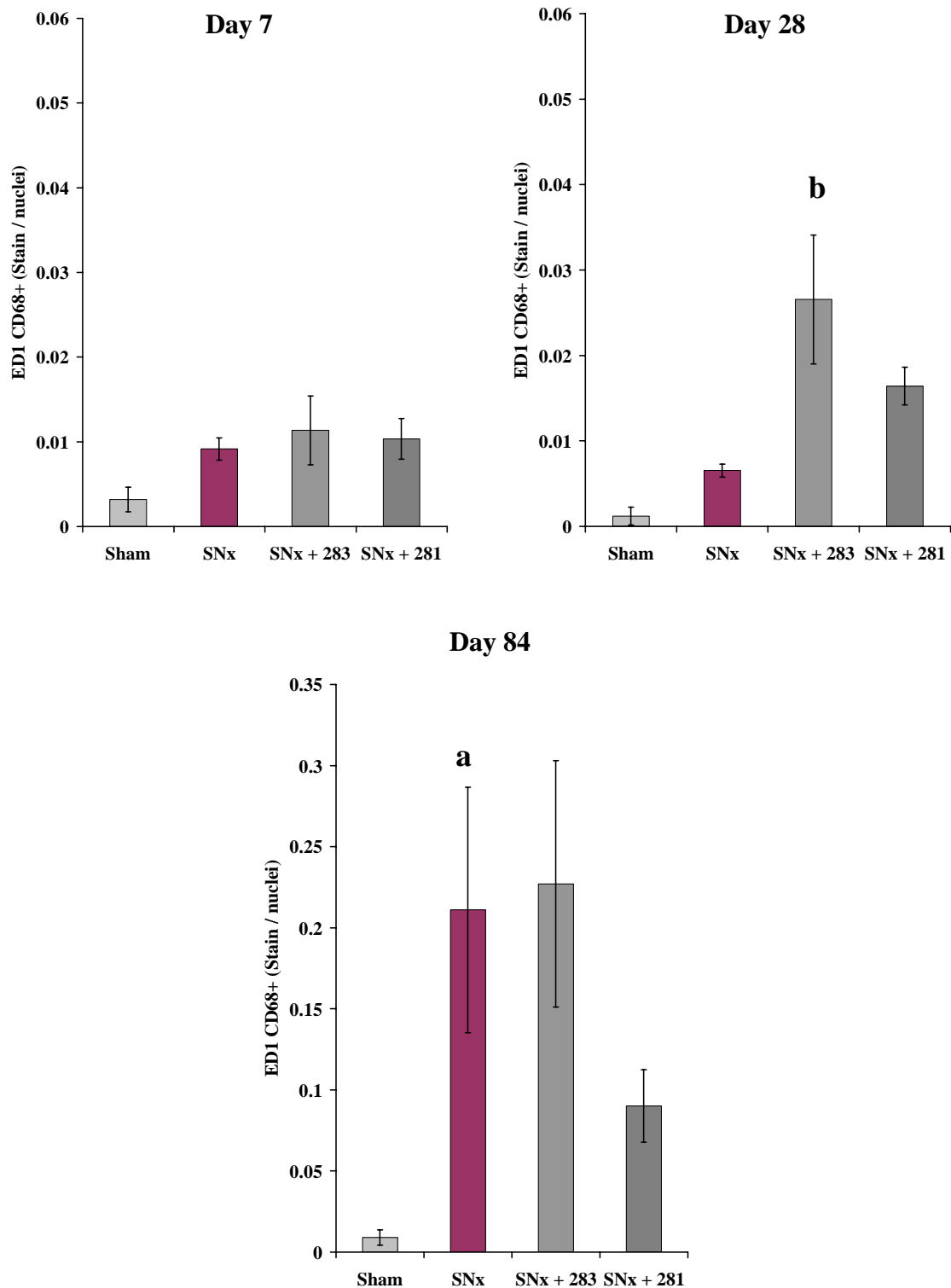


Figure 9.26 ED1 (CD68) stained paraffin-embedded sections from kidneys harvested at 7, 28 and 84 days post-SNx were immunoprobed with 1:50 mouse monoclonal anti-ED1 antibody as described in section 3.5.2.4. Staining was quantified by multi-phase image analysis. Data represents mean \pm SEM from 10 sections analysed per animal, n=5-6 animals per group. a=p<0.05 compared to sham, b=p<0.05 compared to untreated SNx (one way ANOVA with Bonferroni post hoc test).

9.3 Discussion

Despite many advances in our understanding of the factors that contribute to the development of kidney scarring there remains no effective therapeutic strategy to prevent its progression. Previous studies using the 5/6th nephrectomy model of experimental kidney scarring coupled with the mechanistic data presented in the preceding chapters has highlighted the contribution of TG2-mediated crosslinking within the ECM to the accumulation of matrix. Such data suggests that the targeted inhibition of TG2 enzyme activity may be effective in preventing the accumulation of ECM that is associated with progressive kidney disease.

In this chapter, the specific properties of two inhibitors of TG activity NTU283 (1, dimethyl-2[oxopropyl] thio] imidazolium) and NTU281 (N-benzyloxycarbonyl-L-phenylalanyl-6-dimethylsulphonium-5-oxo-L-norleucine) have been characterised in terms of their action against renal TG. Both inhibitors contain a dimethylsulfonium group that has previously been shown to interact with cysteine residues including Cys²⁷⁷ within the active site via an acetylation reaction (figure 9.27) leading to non-competitive and irreversible inhibition of the enzyme (Fround, 1994).

Data obtained from the pilot studies demonstrated that both inhibitors were highly effective at inhibiting renal TG activity when applied to a kidney homogenate and that this inhibition remained effective after storage at either -80°C or 37°C . Interestingly, there were notable differences in the cellular uptake of the two inhibitors when administered to rat tubular epithelial cells in culture. NTU283 was highly cell soluble and readily entered the intracellular compartment. In contrast, NTU281 was much less able to transfer across the cell membrane and its action was therefore limited to the extracellular compartment. Such a difference is significant in determining whether total (intracellular and extracellular) inhibition or extracellular TG inhibition alone is sufficient to impede the action of TG2.

The dose response data over a 7 day period indicated that NTU283 inhibited TG activity in a dose-dependent manner with a K_{i50} of 25mM. Similar results were obtained when the *in situ* TG activity (a measure of extracellular activity) was determined in response to NTU281. However, a pilot study for one month at 25mM dose of NTU281 failed to produce inhibition of TG activity *in vivo* (data not shown). It is likely that this lack of inhibition was attributable to an increase in renal mass in response to ablation that diluted the effects of the inhibitor at this dose. Compensatory renal growth is known to be an early event following 5/6th nephrectomy and this was evident in the kidneys removed at termination in this study.

Figure 9.27 Mechanism of Inhibition by Site-Specific Thioimidazole Inhibitors

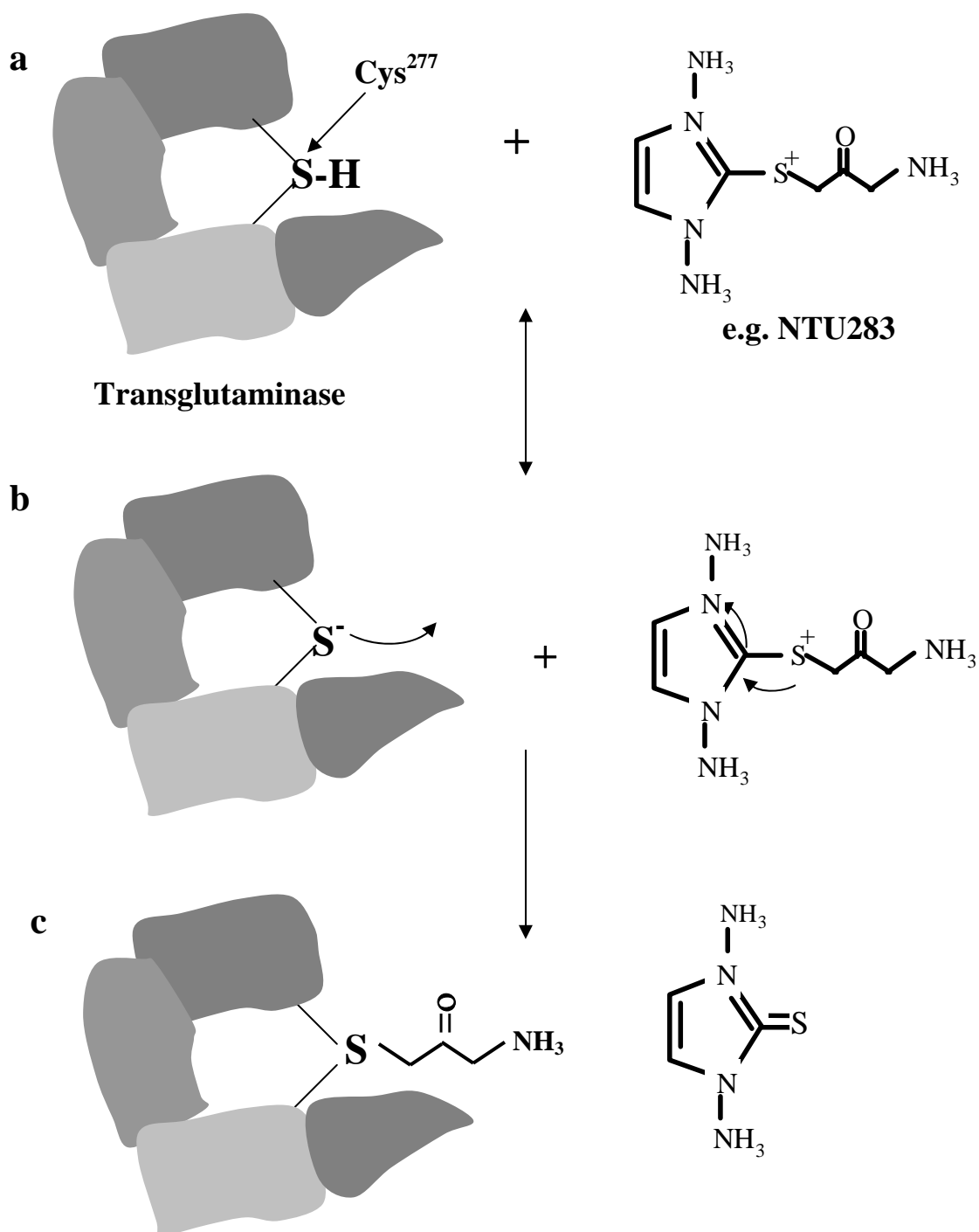


Figure 9.27 The mechanism of inactivation by thioimidazole compounds has been determined from the study of Factor XIIIa inhibition (Fround, 1994). Kinetic analysis demonstrates that the enzyme initially forms a reversible complex with inhibitor prior to irreversible modification of the enzyme. Inhibition involves the irreversible acetylation of the thiol group (b) contained within the active site cysteine which renders the thiol group unreactive towards its glutamyl and amine substrates (c).

As a consequence it was necessary to repeat the pilot dosing studies at a 50mM dose over 28 days so that the level of inhibition could be checked once the bulk of the compensatory growth had occurred. Application of NTU283 and NTU281 at 50mM for 1 month to SNx animals demonstrated that at this dose both inhibitors were effective at inhibiting TG activity in a disease model over a 28 day experimental period. Whilst it would have been preferential to increase the dose for the second and third pump replacements to compensate for the slight loss in TG inhibition at 84 days, the crosslink analysis showed an almost complete prevention in the build up of $\epsilon(\gamma\text{-glutamyl})$ lysine indicating that the level of inhibition was sufficient over the 3 month SNx study.

The level of TG inhibition achieved by NTU281 and NTU283, in rats subjected to 5/6th nephrectomy (SNx), over the 3 months from the onset of renal injury, resulted in reduced levels of glomerular and interstitial scarring and fibrosis indicating that TG2 inhibition was effective in preventing progressive scarring. It is not clear why at 7 days post-SNx levels of scarring, in particular in the interstitium, were elevated in inhibitor treated animals compared to SNx and sham. This continued to be the case in the glomeruli of NTU283-treated animals at day 28. It may be explained by localised scarring in response to insertion of the cannula that by day 84 had become resolved. There is some evidence from previous pilot studies using mini-pumps primed with PBS that cannulation itself can cause small areas of scarring. An alternative explanation may be that the elevated staining is a result of limitations in the Masson's Trichrome staining technique which has previously been demonstrated to give false positive staining under certain conditions such as oedema or excess lipids (Abo-Zenah *et al.*, 2002), however, a similar change was seen in Collagen III immunohistochemistry suggesting that Collagen III changes may be the cause of increased Masson's Trichrome staining. This early increase in collagens in response to TG inhibition is consistent with the changes observed in other animal models (Huang, 2006) and would fit with the *in vitro* observations described in previous chapters indicating some feedback between TG and collagen levels. Thus the early changes may reflect transient changes in immature collagens in response to TG inhibition that are lost as scarring begins to develop.

Assessment of renal function as measured by creatinine clearance showed that renal function was maintained in response to inhibitor treatment and did not progressively decline over the 84 days. Surprisingly, the reduction in scarring was not matched with a corresponding reduction in proteinuria with only NTU281 moderating proteinuria slightly (-30%). This is confusing given that both inhibitors were seen to improve glomerulosclerosis in this model and that similar application of NTU281 to rats with streptozotocin-induced

diabetic nephropathy resulted in a greater than 50% reduction in proteinuria (Huang, 2006), both suggesting that a more significant effect on proteinuria might have been expected. It has been proposed however, that albuminuria is a more accurate indicator of renal disease and specifically of glomerulosclerosis than measurement of total urinary protein (Shihabi *et al.*, 1991). This may be partly due to its increased specificity and the exclusion of proteins or contaminants that may adversely influence proteinuric data. When albuminuria was determined in urines from the 3 month SNx study, interestingly, a significant reduction in albumin was demonstrated by 84 days in both NTU283 and NTU281 treated groups which would be consistent with an improvement in scarring. Such a finding makes the lack of reduction in proteinuria in response to inhibitor treatment difficult to reconcile. It could be speculated that the selective effect of inhibitor treatment on albuminuria reflects a protective influence on the charge selectivity of the glomerular capillary wall, an important restrictive force in the passage of albumin through the glomerular membrane (D'Amico and Bazzi 2003). The continued presence of proteinuria suggests that a similar effect is not extended to the maintenance of size selectivity. The loss of this would allow continual, elevated leakage of larger molecular weight proteins into the urine which could contribute to proteinuria. It cannot be ruled out however, that this improvement in albuminuria is as a result of a reduction in blood pressure in response to TG inhibition, in what is a hypertensive model of chronic kidney disease. Several studies have demonstrated that the control of hypertension is important in the reduction of albuminuria and therefore in slowing the progression of CKD (Cantarovich and Rangoonwala, 2003; Pavan *et al.*, 2003; Rossing *et al.*, 1994; Viberti and Chaturvedi, 1997). A potential criticism of this investigation is that blood pressure monitoring was not performed and this would have provided useful information as to any potential effects of TG inhibition on hypertension.

As indicated by the Masson's Trichrome data, inhibition of TG2 was associated with an overall reduction in total collagen by day 84 as determined by gas liquid chromatography for hydroxyproline. This was attributable to a reduction in the accumulation of interstitial collagens I and III in response to both inhibitors but only NTU281 had an effect on Collagen IV levels. The discrepancy between the action of the inhibitors on collagen IV may reflect differences in their intra-renal concentration and distribution, thus determining any effect on the tubular basement membrane. The extracellular levels of NTU281 are likely to be higher than NTU283, due to its poor transfer across the cell membrane which limits its action to the extracellular compartment.

TG inhibition was also associated with a reduction in fibronectin accumulation by 84

days, which is perhaps not surprising given the importance of fibronectin as a TG substrate as well as its involvement as a major component of the kidney scar (Eddy 2000a). However, this was in spite of apparent increases in fibronectin in the inhibitor-treated groups at the early time points. Deposition of fibronectin is known to be an early event in scar tissue formation (Eddy 2000a) and it is likely that increased fibronectin levels are a reflection of the kidney response to SNx which may have been further elevated in inhibitor-treated animals in response to cannulation.

Analysis of the mRNA expression of major ECM proteins involved in the scarring process as well as MMP-1 and TIMP-1, proved difficult due to the poor quality of the RNA and subsequent variability of the Northern blots. Collagen I and III mRNA expression appeared to be increased in some SNx samples whilst others remained comparable to untreated levels. A similar discrepancy in collagen expression was observed in NTU283 treated animals whilst a lack of discrete bands made changes in fibronectin and MMP-1 expression impossible to distinguish. A definite conclusion as to the effect of TG inhibition on ECM protein mRNA levels was therefore not able to be drawn from the data presented here. However, data presented in previous chapters indicates that the actions of TG2 on the accumulation of matrix are via the post-translational modification of ECM components rather than through effects on ECM synthesis perhaps suggesting that TG inhibition should have had little effect on ECM mRNA levels. Previous cell culture studies utilising NTU283 in an *in vitro* model of hyperglycaemia certainly support this, given that glucose induced ECM accumulation was significantly reduced in the absence of changes in ECM protein mRNA levels (Skill *et al.*, 2004).

A very interesting observation was an obvious reduction in interstitial cell number in inhibitor treated groups by the end of the time-course. However, immunohistochemistry for α -SMA (a myofibroblast marker) indicated a similar level of staining in the treated and untreated groups. Likewise, ED1 staining for monocytic cells also remained high when treated with NTU283 although treatment with NTU281 reduced the number of ED1-positive cells by 84 days. Such data suggests that the reduction in interstitial cell number seen in advanced disease is mainly attributable to interstitial cell types not identified by either α -SMA or ED1 staining. Clearly, fibroblasts are a likely candidate since they are the pivotal interstitial cell type involved in renal scarring and are not for the most part α -SMA positive (Zeisberg *et al.*, 2000). Staining for fibroblast specific markers such as FSP-1 (Strutz *et al.*, 1995) would have been useful in elucidating their role in this study. Similarly, infiltrating lymphocytes may also be responsible for changes in interstitial cell numbers. B and T lymphocytes are known to be

important contributors to the inflammatory response in renal scarring (Zheng *et al.*, 2005). The reduction in ED1-positive cells at the later time point by NTU281 may be due to an inhibitory effect on a number of inflammatory events that TG2 has been shown to participate in including the migration of monocytes (Akimov and Belkin, 2001b) or through inhibition of TG2-mediated changes in phospholipase A2 activity (Cordella-Miele *et al.*, 1990).

Surprisingly, the strong reduction in monocytic cells observed at day 84 post-SNx, was in sharp contrast to the significant increase in ED1-positive staining observed with both inhibitors at day 28. The contribution of TG2 inhibitors to promoting an inflammatory response is unclear. However, studies using TG2 knockout mice suggest that inflammatory infiltration is associated with a reduced rate of clearance of apoptotic macrophages (Szondy *et al.*, 2003). It is also feasible that at earlier time points, infiltrating cells are more readily able to access and migrate through the tissue, a process that may be compromised in advanced disease due to increased TG2 crosslinking and scarring of the ECM.

An important question to be addressed in this study is the specificity of the two inhibitors when administered *in vivo* given the similar structures of the eight TG enzymes so far characterised (Lorand and Graham, 2003). It is likely that both NTU281 and 283 are capable of inhibiting all TGs although probably with varying potencies. In the extracellular compartment of the kidney, only Factor XIIIa and TG2 are known to be present and would therefore be the principle targets, especially for NTU281 given that it is retained in the extracellular environment. Whilst the main target of inhibition in this study appears to be TG2, any effects on Factor XIIIa cannot be ruled out especially in the initial stages of wound repair although the enzyme is less likely to be important in the later stages of ECM deposition (Verderio *et al.*, 2005). Clearly, an assessment of changes in Factor XIIIa in renal scarring would be beneficial in determining such effects.

The equal effectiveness of NTU281 and NTU283 indicates that their principle inhibitory actions are extracellular. The poor cell solubility of NTU281 would certainly limit any potential non specific effects on other intracellular TG or thiol-containing enzymes, however, the potential of NTU283 to affect intracellular targets apart from TG2 cannot be dismissed given its known ability to inhibit other TG isotypes. Clearly, any potential inhibitory action of these thioimidazole compounds on other enzyme systems and their side-effects require further investigation in the development of an anti-TG therapy.

The data presented in this chapter demonstrates that the treatment of remnant kidneys with non competitive inhibitors of TG activity is able to prevent progressive kidney

remodelling and scarring whilst maintaining kidney function. Such data confirms the importance of TG2 in disease progression and strongly supports the further development of anti-TG therapies based on the more effective inhibitor NTU281 with improved TG isoform specificity.

Chapter 10

General Discussion

Extensive studies have established a clear link between TG2 mediated protein crosslinking via the $\epsilon(\gamma\text{-glutamyl})$ lysine iso-dipeptide and the progression of kidney disease and renal insufficiency in experimental models and in human disease (El Nahas *et al.*, 2004; Johnson *et al.*, 2004; Johnson *et al.*, 2003b; Johnson *et al.*, 1997; Johnson *et al.*, 1999; Skill *et al.*, 2001; Skill *et al.*, 2004). The up-regulation and release of TG2 into the extracellular compartment is considered to be an important event in the advancement of the disease. However, previous studies have yet to establish whether elevated TG2 and $\epsilon(\gamma\text{-glutamyl})$ lysine crosslinking are crucial in driving renal disease or whether they are merely accompanying factors. In addition, the initiating stimuli for TG2 and the subsequent contribution of TG2 to the pathological changes associated with disease progression remains largely speculative.

The principle aims of this thesis were to investigate the possible pathways by which TG2 is up-regulated in tubular epithelial cells and to identify the mechanisms by which it may contribute to the accumulation of ECM during kidney scarring. The ultimate aim was to ascertain whether the targeted inhibition of TG2 was effective at preventing ECM accumulation, not only to determine whether TG2 has a driving role in disease development but also to potentially offer a target for therapeutic intervention.

In order to determine potential regulators of TG2 in tubular epithelial cells, Chapter 4 explored the effect of a range of pro-fibrogenic stimuli on TG2 expression. This data revealed that whilst growth factors and cytokines appeared to have little effect on TG2 expression, tubular cells were seen to up-regulate TG2 in response to both hypoxia and acidosis, two factors associated with causing tubular stress and injury. Interestingly, previous studies of TG2 expression in OK tubular cells have demonstrated an up-regulation of TG2 in response to elevated glucose (Skill *et al.*, 2004), which is also a potent stimulus for tubular damage. Evidence appears to be emerging therefore that the tubular expression of TG2 may primarily be controlled by mechanisms that are responsive to metabolic stress.

Whilst these factors have the potential to induce TG2 by independent mechanisms it is tempting to speculate that their influence on TG2 expression may result from the activation of common pathways (illustrated in figure 10.1). Hypoxia and elevated glucose are both known stimulators of the protein kinase C pathway (Bunn and Poyton, 1996; Ha and Kim, 1999; Koya and King, 1998) which has been implicated in the induction of TG2 in other cell types such as peritoneal macrophages (Ishii and Ui, 1994). Protein kinase C activation may therefore be one mechanism regulating TG2 expression in tubular cells in response to these

factors. In addition, hypoxia and elevated glucose have been shown to be capable of activating the stress responsive transcription factor NF- κ B (Evans *et al.*, 2002; Koong *et al.*, 1994; Michiels *et al.*, 2002). For example, in human proximal tubular cells, hypoxia induced activation of NF- κ B is partially responsible for induction of PAI-1 expression (Li *et al.*, 2005). Elevated glucose has been shown to increase NF- κ B activity in a whole host of cell types including vascular smooth muscle cells (Golovchenko *et al.*, 2000; Ramana *et al.*, 2004), endothelial cells (Chen *et al.*, 2003) and lens epithelial cells (Ramana *et al.*, 2003). In tubular cells, elevated glucose and the associated production of advanced glycation end products have been demonstrated to induce IL-6 secretion via the activation of NF- κ B (Morcos *et al.*, 2002). Similarly, acidosis may indirectly activate NF- κ B through the generation of ROS (Rustom *et al.*, 2003). Significantly, the TG2 promoter is known to possess a binding site for NF- κ B (Kuncio *et al.*, 1998) and interestingly, up-regulation of TG2 mediated by activation of the NF- κ B pathway has been implicated in liver disease (Kuncio *et al.*, 1998; Mirza *et al.*, 1997). Such data suggests that activation of the NF- κ B pathway may have the potential to play a role in the induction of TG2 in tubular cells in response to stress factors. Clearly, further work utilising inhibitors of either protein kinase C such as Calphostin-C or inhibitors of NF- κ B such as pyrrolidine-dithiocarbamate would be beneficial in deciphering the potential role of these pathways in stress mediated TG2 expression.

In addition to the possible activation of protein kinase C and NF- κ B mediated pathways, it is likely that a critical player in any crosstalk between the responses to stress factors is HIF-1 α . In tubular cells, hypoxia regulates a number of pro-fibrogenic genes such as collagen I, MMP-2 and TIMP-1 some of which are direct targets for HIF-1 α (Norman *et al.*, 1999). Elevated glucose is also capable of influencing gene expression via the HIF-HRE pathway. For example, in cultured proximal tubular cells, elevated glucose is able to reduce hypoxia-induced VEGF expression via changes in HIF-HRE activation (Katavetin *et al.*, 2006). In addition, acidosis has the potential to modulate HIF-1 via its neutralising effects on the function of Von Hippel Lindau tumour suppressor protein and the degradation of HIF-1 (Mekhail *et al.*, 2004).

Analysis of the nucleotide sequence of the human TG2 gene promoter (M Fisher, personal observation) reveals the presence of three sites containing the 5'CGTG 3' HIF-1 binding core sequence suggesting the potential of TG2 as a HIF-1 target gene, at least in humans. The recent identification of TG2 as a von Hippel-Lindau repressible gene and its

ability to be regulated by oxygen in renal carcinoma cells (Wykoff *et al.*, 2000) may further suggest the involvement of HIF-1 dependent pathways in TG2 induction.

Figure 10.1 Possible Mechanisms of TG2 Induction in Tubular Epithelial Cells

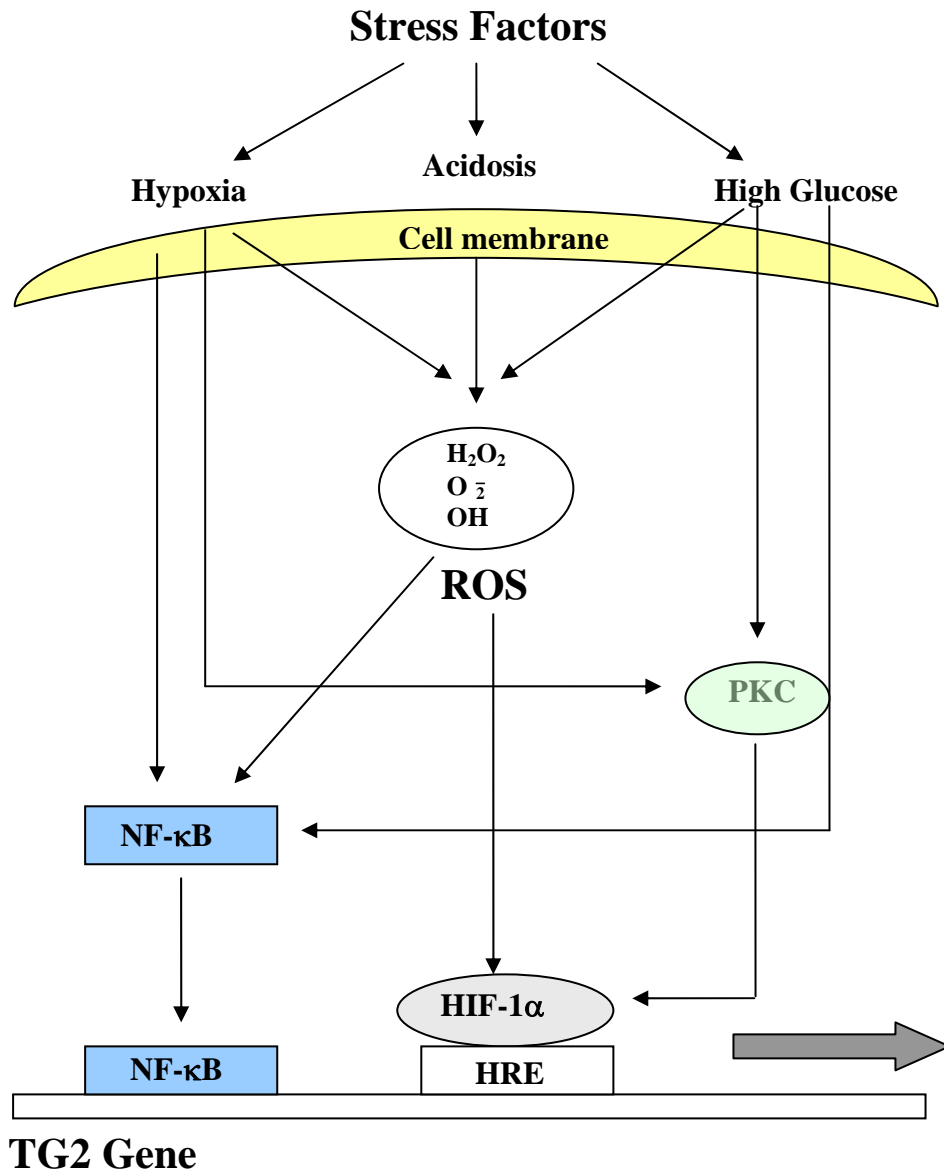


Figure 10.1 Up-regulation of TG2 occurs in response to hypoxia, acidosis and elevated glucose all of which are cellular stress factors that contribute to tubular injury. The response of tubular cells to stress may be mediated by activation of a number of signalling pathways, some of which are common to more than one stress factor. Hypoxia and elevated glucose can both stimulate the activation of protein kinase C (PKC), and the transcription factor NF-κB whilst hypoxia, glucose and acidosis all increase the generation of ROS that may be upstream regulators of HIF-1α as well as further stimulators of NF-κB. Protein kinase C also transmits signals through HIF-1. An NF-κB binding site and putative hypoxia response elements (HREs) are present on the TG2 promoter.

The mechanisms by which stress factors modulate gene expression via HIF-1 remain largely speculative. However, recent studies suggest that oxidative stress may be a key upstream event in the modulation of HIF-1. In proximal tubular cells, the effects of elevated glucose on the HIF-HRE pathway appear to be mediated by oxidative stress as indicated by an amelioration of these effects by antioxidants (Katavetin *et al.*, 2006). Hypoxia has been proposed to contribute to oxidative stress through inhibition of mitochondrial electron transport leading to changes in redox status and the increased generation of ROS (Agani *et al.*, 2000; Chandel *et al.*, 2000). These are thought to act as second messengers that contribute to the stabilisation of HIF-1 α and subsequently influence gene transcription (Chandel *et al.*, 2000). In support of this, exposure of HEK293 kidney cells to hypoxia results in increased mitochondrial ROS production (Mansfield *et al.*, 2004) although an effect on HIF-1 is not demonstrated. Acidosis has also been demonstrated to contribute to oxidative stress through the generation of ROS. For example in LLC-PK1 tubular cells, acidosis increases generation of ROS reportedly leading to tubular injury (Rustom *et al.*, 2003). The ability of cellular stress factors to influence ROS production suggests the stimulation of common oxidative pathways of which one significant downstream event may be the induction of TG2. Given the reported involvement of ROS in progressive scarring (Ha and Lee, 2003), the induction of such an enzyme with the potential to influence matrix remodelling may provide a significant link between these events. Clearly, the increased expression of TG2 in an environment of tubular stress resulting from low oxygen, elevated glucose or metabolic acidosis could represent an important additional pro-fibrogenic pathway.

It is possible that other cellular stress factors associated with tubular injury and fibrogenesis, may elicit some of their pro-fibrogenic effects through the increased expression of TG2. Of particular interest is proteinuria that leads to abnormal protein reabsorption by tubular cells and subsequent tubular damage (Zoja *et al.*, 2004). A key component of proteinuric urine is albumin and this has been demonstrated in a number of studies to stimulate the accumulation of ECM proteins by proximal tubular cells (Stephan *et al.*, 2004; Wohlfarth *et al.*, 2003). It is possible that the effects of albumin on ECM accumulation may partly be elicited through the induction and release of TG2. The effect of albumin on TG2 activity has recently been investigated by co-workers using an *in vitro* model of protein overload in NRK-52E proximal tubular cells (Huang, 2006). However, interestingly, whilst concentrations of albumin of 1mg/ml produced small increases in TG2 activity, higher concentrations of albumin of up to 30mg/ml had no effect or even reduced TG2 over a 96 hour time period. The reason for this lack of induction is unclear and is perhaps surprising

given that these studies were performed using whole bovine serum albumin containing fatty acids which have been reported to be responsible for much of the injurious effects of albumin on tubular cells (Arici *et al.*, 2002; Ishola *et al.*, 2006; Kamijo *et al.*, 2002; Thomas and Schreiner, 1993).

Whatever the mechanism of stress factor-induced TG2 expression it appears unlikely that it is mediated through growth factor stimulation. A number of previous studies have demonstrated the induction of growth factors and cytokines by stress factors such as hypoxia and glucose that would have the potential to modulate TG2 expression in tubular cells. Most importantly, these include TGF- β 1 (Fraser *et al.*, 2003; Orphanides *et al.*, 1997; Rocco *et al.*, 1992). However, in OK cells there appears to be little change in TG2 expression in response to TGF- β 1 stimulation. Similarly, NRK-52E cells show only small increases in TG2 expression and activity following TGF- β 1 treatment (E. Parker, personal communication). Certainly, OK cells possess the ability to respond to TGF- β 1 as indicated by regulation of collagen and TIMP-1 expression (TS Johnson, personal communication). However, previous studies of glucose-stimulated TG2 expression and activity in OK cells (Skill *et al.*, 2004) demonstrate that increases in TG2 are TGF- β 1-independent.

Previous studies have highlighted the importance of TG2 translocation from the intracellular to extracellular environment in the progression of fibrosis (Johnson *et al.*, 1999; Skill *et al.*, 2001). Chapter 5 presented the characterisation of tubular and mesangial cells stably transfected to constitutively over-express TG2, part of which involved the measurement of extracellular TG2 levels. A surprising finding was the clear difference between the tubular and mesangial cell handling of increased intracellular TG2 levels and the subsequent effect on TG2 export. Tubular cells showed corresponding increases in both extracellular TG enzyme activity and cell surface TG2 protein expression in response to elevated intracellular enzyme levels. In contrast, mesangial cells failed to demonstrate changes in their extracellular TG levels despite comparable increases in intracellular TG2 expression. It is likely that the release of TG2 by mesangial cells is subject to additional regulation by factors that operate independently of intracellular TG2 levels.

The export of TG2 by mesangial cells may only occur under conditions of cell stress or damage akin to those observed during the course of renal disease and not represented in these studies. Elevated levels of TG2 expression and externalisation of TG2 into the glomerular compartment are certainly a feature of early experimental diabetic nephropathy (Skill *et al.*, 2001) suggesting that mesangial cells have the potential to release TG2 during the course of

this disease. However, mesangial cells *in vivo* would have been exposed to a range of stimuli associated with diabetic nephropathy that could have activated the export of TG2 and which are not present *in vitro*. It appears unlikely that export is regulated by hyperglycaemia itself however, as exposure of 1097 mesangial cells to elevated glucose fails to affect extracellular TG2 levels despite an increase in TG2 expression (M Fisher, data not shown). It is possible that physical pressures placed on mesangial cells as a consequence of haemodynamic changes *in vivo* such as mechanical stretch and shear stress may result in TG2 release. Mesangial cells subjected to mechanical stress are known to increase the secretion of a number of ECM proteins including collagen, FN and laminin (Yasuda *et al.*, 1996) as well as growth factors such as VEGF and TGF- β 1 (Gruden *et al.*, 1997; Riser *et al.*, 1996) and may well secrete TG2. Mechanical forces are thought to influence protein secretion mainly via the increased stimulation of exocytotic pathways (Apodaca, 2002). For example, mechanical stress can stimulate cytoskeletal re-organisation which in turn may affect membrane tension and alter membrane traffic (Apodaca, 2002). In addition, cells may respond to mechanical stress by altering integrin expression in turn stimulating focal adhesion kinase (FAK). The interaction of FAK with a number of other cytoplasmic proteins can modulate signalling pathways such as Rho that again regulate the cytoskeleton and may affect protein trafficking (Katsumi *et al.*, 2004). Mechanical stress may also lead to the release of proteins via temporary disruptions to the plasma membrane (Janmey and Weitz, 2004). Whether mechanical stress is involved in the release of TG2 remains to be determined although preliminary studies on the effect of mechanical stretch on 1097 cells suggests that TG2 activity at least is unaffected (Huang, 2006).

Whatever the factors are that initiate the release of TG2 from mesangial cells, it is evident from previous studies that extracellular levels of TG2 are a consequence of controlled and regulated export (Gaudry *et al.*, 1999a; Verderio *et al.*, 1998). The mechanisms by which this may occur are the subject of much speculation given that TG2 has features of a cytoplasmic protein such as N-acetylation and a lack of glycosylation and significantly, lacks an N-terminal leader sequence required for secretion via the conventional ER/Golgi route (Ikura *et al.*, 1988; Ikura *et al.*, 1989). Interestingly, studies of other proteins lacking an N-terminal signal peptide such as lectin suggest that the differentiation status of the cell may be an important factor for export (Cooper and Barondes, 1990). Thus, a change in the physiological status of mesangial cells *in vivo* to a myofibroblastic phenotype coupled with an increased expression of TG2 may favour its export. Studies on the export of TG2 however, suggest that externalisation of this enzyme may be reliant on its association with FN and/or

integrins. It is well established that TG2 is a FN-binding protein and that TG2 is found tightly associated with FN at the cell surface (Akimov and Belkin, 2001a; Akimov *et al.*, 2000; Gaudry *et al.*, 1999a; Upchurch *et al.*, 1987; Verderio *et al.*, 1998). Interestingly, truncation of TG2 such that the N-terminal FN-binding domain is absent prevents its cell surface localisation suggesting the importance of the TG2-FN association in TG2 export (Gaudry *et al.*, 1999a). In parallel studies, TG2 has been demonstrated to co-localise with several $\beta 1$ and $\beta 3$ integrins at the cell surface and to act as an integrin-associated co-receptor for FN (Akimov *et al.*, 2000). Interestingly, in these studies, integrin-TG2 complexes appear to be formed inside the cell and accumulate on the cell surface. Truncation of the integrin binding domain of TG2 prevents such integrin-TG2 interaction and subsequently TG2 is not externalised (Akimov *et al.*, 2000). Both studies raise the possibility that translocation of TG2 is determined by intracellular interactions with FN and/or integrins that may act as carriers of TG2 to the cell surface. Thus, in mesangial cells, export of TG2 may be closely linked to changes in FN deposition into the ECM or alterations in the expression of integrins. An increase in FN deposition is a key feature of the glomerulosclerosis that accompanies the development of renal disease (Floege *et al.*, 1992a; Funabiki *et al.*, 1990; Okuda *et al.*, 1992). Similarly, an increase in the expression of $\beta 1$ integrins by activated mesangial cells is observed (Kuhara *et al.*, 1997), in particular $\alpha 1\beta 1$ and $\alpha 5\beta 1$, both of which are able to associate with TG2 (Akimov *et al.*, 2000). Clearly further work is required to dissect the mechanisms that control the export of TG2 by mesangial cells. Current technology that allows the fluorescent tagging of proteins could be useful in tracking the movement of TG2 protein. In addition, mutation of the TG2 protein could provide useful information regarding which critical sites within TG2 are required for export.

In contrast to mesangial cells, tubular externalisation of TG2 appears to be closely related to synthesis and *in vitro* is not dependent on the presence of factors that cause tubular damage. The release of TG2 may constitute an important cell survival response in the face of increasing enzyme levels. It is known that excessive accumulation of TG2 within tubular cells in experimental renal disease can lead to their death through extensive intracellular crosslinking in the absence of apoptosis (Johnson *et al.*, 1997). *In vivo* such an event is likely to be dependent upon the influx of calcium into the cell as a result of tubular damage possibly resulting from ischaemic injury and oxidative stress (Chi *et al.*, 1995; Parkinson *et al.*, 1996; Swann *et al.*, 1991; Ueda and Shah, 1992). The continual release of TG2 may be an attempt by tubular cells to keep intracellular levels below that which would be potentially detrimental to them. On the other hand, increased externalisation of TG2 in response to elevated

intracellular levels may be involved in stabilising the ECM by affecting deposition and breakdown which *in vivo* would initially help to maintain tissue integrity but later contribute to fibrosis.

To determine if this was the case, Chapter 7 investigated whether over-expression of TG2 in tubular cells could influence the accumulation of ECM through effects on deposition and breakdown. The data presented clearly demonstrates that increased intracellular and extracellular levels of TG2 resulting from over-expression of the enzyme are associated with elevated levels of collagen within the ECM. Interestingly, this occurs despite apparent reductions in collagen synthesis and probably MMP activity which would presumably result in a balanced ECM clearance. The increases in ECM collagen in response to TG2 are likely, therefore, to result from direct effects on the stabilisation of collagen matrix. Previous studies have demonstrated that TG2-mediated stabilisation of the matrix can cause a pathological increase in collagen deposition (Gross *et al.*, 2003; Skill *et al.*, 2004). Consistent with this, studies performed here with the MMP inhibitor Galardin show that TG2 modulation in tubular cells alters the rate of collagen deposition. A major influence of the TG2 released by tubular cells during progressive disease on the accumulation of ECM therefore appears to be in promoting collagen deposition.

A study of the crosslinking action of TG2 on collagen V and XI in rhabdosarcoma cells suggests that TG2 participates in the stabilisation of newly synthesised and assembled collagen fibrils (figure 10.2) in a similar manner to lysyl oxidase-catalysed pyridinoline crosslinking (Kleman *et al.*, 1995). In these collagens, TG crosslinking sites are thought to be contained within the highly homologous N-telopeptide and pro-peptide domains with crosslinking occurring as part of the maturation of collagen fibrils. Similar sites have been identified in the N-pro-peptide regions of collagen III (Bowness *et al.*, 1987). Previous *in vitro* studies demonstrate that crosslinking of isolated collagen III by TG2 increases both the rate and amount of collagen III fibril formation presumably by acting on these regions (Skill *et al.*, 2004). A similar mechanism is probably important in modifying the rate at which collagen is deposited by tubular cells. The coupling of TG2 to FN at the cell surface would help to facilitate this role by localising the enzyme to areas where fibril formation may occur. It cannot be excluded however, that TG2 may be able to crosslink soluble, free pre-assembled collagen molecules in either an immature or mature form into the matrix.

Such an action would probably contribute to haphazard orientation and organisation of collagen fibrils within the expanding matrix. Similarly, TG2 may crosslink more mature and

Figure 10.2 Proposed Effects of TG2 on Collagen Accumulation in the Tubular ECM

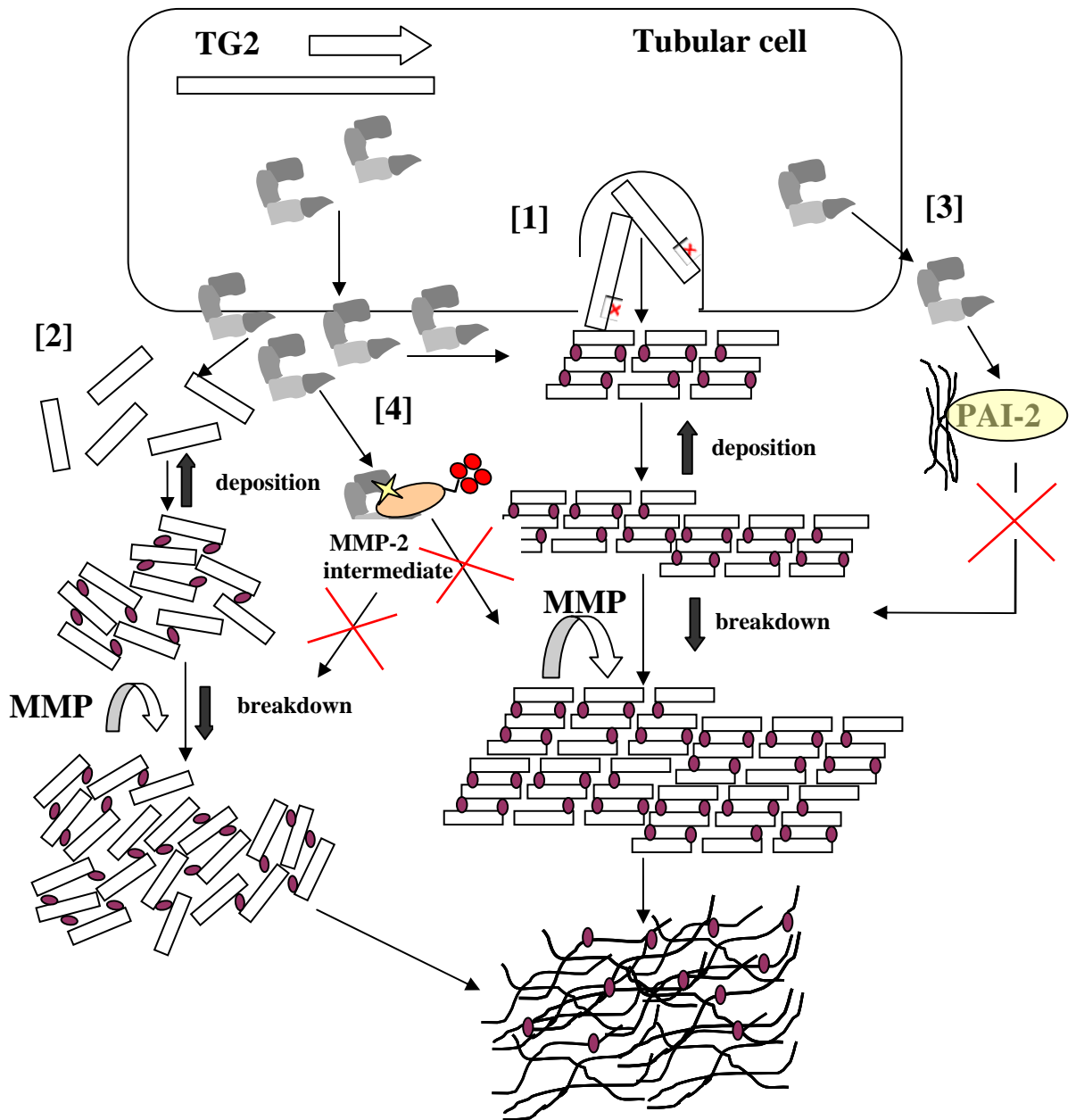


Figure 10.2 TG2 up-regulated and externalised by tubular epithelial cells could promote collagen accumulation by a number of mechanisms. [1] TG2 could crosslink newly synthesised collagen as part of fibril formation leading to increased deposition into the matrix and a reduced susceptibility to proteolytic degradation. [2] TG2 could also crosslink free and as yet unassembled collagen molecules leading to disorganised collagen accumulation. [3] TG2 may also further reduce breakdown of collagen by recruiting PAI-2 to the matrix, preventing plasminogen activation as well as to bind to the activation intermediate of MMP-2 [4] potentially reducing its activation.

established matrix thus promoting its continued deposition. However, it appears unlikely that the latter is a mechanism favoured by tubular cells given that TG *in situ* activity studies on cryostat tissue from scarred kidneys show that increased extracellular TG2 activity is exclusively observed in the peri-tubular region and not widely distributed across the tubulointerstitium (Johnson *et al.*, 1999). This indicates that established, mature ECM is a less favourable substrate and suggests that the predominant stabilising role of TG2 is in the deposition of newly synthesised matrix.

The ability of TG2 to influence the deposition of collagen into tubular ECM was paralleled by its effect on the susceptibility of the tubular matrix to degradation by MMPs. Degradation studies performed using MMP-1 and -2 demonstrate that matrix laid down by over-expressing clone tTg7 is in fact 50% more resistant to MMP breakdown than that deposited by non-transfected OK cells. This is an important observation since TG2 has only previously been demonstrated to affect the resistance of isolated ECM substrates *in vitro* (Johnson *et al.*, 1999) and not complex ECM generated and deposited by tubular cells. Given that the MMPs are major regulators of ECM degradation both in the glomerulus and the tubulointerstitium (Lenz *et al.*, 2000) any qualitative change to the ECM as a result of TG2 crosslinking, rendering it more resistant to MMP action is likely to have a significant effect on the accumulation of matrix. This is in addition to an already pro-fibrogenic environment in which reductions in MMP activity are likely to contribute to scarring (Catania *et al.*, 2007). Previous studies demonstrate that whilst MMP-1 and MMP-2 mRNA and active enzyme are elevated in renal disease (Johnson *et al.*, 2002), this is counteracted by increases in TIMP-1 and TIMP-2 expression and subsequently MMP activity is reduced. Similarly in this study (Chapter 7), any elevations in MMP-1 mRNA may be negated by corresponding increases in TIMP-1 although this was not fully established. Thus, any reduced breakdown of the ECM during renal disease is likely to be the culmination of altered MMP activity coupled with qualitative changes in the ECM mediated by TG2 crosslinking.

Any direct influence of TG2 on the resistance of the ECM to MMP breakdown must rely on changes in the level of crosslinking in the regions where MMPs act. MMP cleavage of triple helical collagen I, II and III, is known to occur after Gly-Ile or Gly-Leu bonds at residues 772-773 located three quarters away from the N-terminus in the helical region (Aimes and Quigley, 1995; Fields, 1991; Miller *et al.*, 1976). Studies of collagen I crosslinking by TG2 *in vitro*, show that the ratio of $\epsilon(\gamma$ glutamyl) lysine crosslink to collagen monomer is high (Collighan *et al.*, 2004). It is likely that high levels of crosslink both within and between fibrils in the helical region would affect the ability of MMPs to cleave.

Similarly, enhanced fibril stabilisation by TG2 crosslinking in the N- and C-terminal regions of collagen could also affect their solubilisation by MMPs given that initial MMP binding is thought to occur in these regions (Welgus *et al.*, 1981). TG2 crosslinking may also interfere with MMP binding by preventing unwinding and destabilisation of the fibrillar structure. Evidence suggests that localised unravelling of the helical structure at MMP cleavage sites is a prerequisite for MMP binding and proteolysis (Tam *et al.*, 2004).

As well as direct effects on MMP binding and cleavage, it may be speculated that the interaction of TG2 with the MMPs themselves could contribute to a reduced rate of breakdown. Interestingly TG2 has been shown to preferentially associate with the activation intermediate of MMP-2 decreasing the rate of its maturation (Belkin *et al.*, 2004). Whilst this is thought to protect TG2 against proteolysis by MMP-2, it may also impact on the levels of active MMP-2 available for matrix degradation.

The stabilising influence of TG2 on the ECM is likely to extend to a reduced susceptibility to breakdown by other remodelling enzymes such as those of the plasminogen activator system. In addition to MMPs, a significant proportion of matrix turnover in the kidney is attributable to enzymes of the plasminogen system (Eddy, 1996). TG2 has the potential to influence breakdown by these enzymes not only by the direct crosslinking of ECM substrates but also indirectly by crosslinking regulatory proteins. For example, TG2 is known to participate in the crosslinking of PAI-2 to fibrinogen contributing to stabilisation of the fibrin clot (Ritchie *et al.*, 2000). In this case, crosslinking of PAI-2 allows the molecule to be directed to the fibrin strands where PAI-2 can function as an inhibitor of fibrinolysis. It could be speculated that TG2-mediated crosslinking of PAI-2 into the ECM would have a similar effect in inhibiting plasminogen-mediated proteolysis. Clearly, in the *in vivo* situation the influence of TG2 on ECM degradation is reliant on a reduced susceptibility to all ECM degrading enzymes, not just those of the MMP system. Further work is required to identify the role of TG2-mediated crosslinking in the resistance of tubular ECM to breakdown by enzymes other than MMPs.

The ability of TG2 to stabilise the ECM and thus influence its deposition and breakdown may also have the potential to contribute to a reduced remodelling of mesangial matrix as indicated by data presented in Chapter 8. This data demonstrates that whilst there is a tight regulation of mesangial cell TG2 export, once the enzyme is released by mesangial cells following electroporation, it is able to act by similar mechanisms to influence the deposition of mesangial matrix. The collagen deposited by mesangial cells subjected to

electroporation is seemingly affected by TG2-mediated crosslinking in a similar way to that deposited by tubular cells, as indicated by increased collagen levels. Clearly, as previously discussed, the role of mesangial cell-derived TG2 in modulating the glomerular matrix in disease is dependent on the mechanisms required to promote TG2 release by mesangial cells.

The known role of TG2 in the activation of TGF- β 1, through recruitment and crosslinking of the large latent TGF- β 1 binding protein (LTBP-1) to the ECM (Nunes *et al.*, 1997; Verderio *et al.*, 1999) suggests that TG2 may additionally influence the ECM via indirect effects on TGF- β 1. However, it appears increasingly unlikely that changes in TGF- β 1 activation are a mechanism for TG2 action on the tubular ECM given the data presented in other studies (Huang, 2006; Skill *et al.*, 2004). TG2 may still be important for recruitment of LTBP-1, since the addition of exogenous LTBP-1 to OK tubular cells that lack LTBP-1 results in increased latent TGF- β 1 incorporation into the ECM (Huang, 2006). However, once recruited, the activation and subsequent matrix stimulating effect of TGF- β 1 is likely to be dependent on other activating factors such as thrombospondin-1.

Taken together, the *in vitro* data presented here provides strong evidence to support a direct role for TG2-mediated crosslinking in the accumulation of ECM collagen via its effects on the deposition of collagen molecules as well as the rate at which they are degraded. This physiological function of TG2 in disease progression would represent a significant contributory pathway in an already pro-fibrotic environment of increased matrix synthesis and reduced proteolytic activity. The increased stabilisation of tubular matrix by TG2-mediated crosslinking not only has direct implications for the scarring process but may also influence the behaviour of tubular cells through qualitative changes to the ECM. These findings are important not only in providing greater understanding of the role of TG2 in the ECM changes associated with renal scarring but also its potential role in other scarring diseases in which TG2 levels are elevated such as liver fibrosis and atherosclerosis (Mirza *et al.*, 1997; Bowness *et al.*, 1989; Bowness *et al.*, 1990; Bowness *et al.*, 1994). Clearly, an understanding of the mechanisms by which TG2 affects the accumulation of matrix is important in opening up new therapeutic avenues for the prevention of progressive scarring.

The potential of TG2 as a target for therapeutic intervention in kidney scarring was investigated in Chapter 9 by the application of two site-specific TG inhibitors to rats subjected to 5/6th subtotal nephrectomy. The key question to be addressed by this study was whether the inhibition of TG2 could reduce or prevent the development of kidney scarring and thus maintain tissue architecture and function by interfering with TG2-mediated matrix

accumulation. The data clearly demonstrates that inhibiting the crosslinking action of TG2 from the onset of disease is effective at reducing both tubulointerstitial and glomerular scarring whilst preserving kidney function as indicated by creatinine clearance. Further, the prevention of progressive scarring is as a direct result of inhibiting the TG2-mediated accumulation of interstitial collagens which is strongly supportive of a direct role for TG2 in the scarring process. In keeping with the findings here, inhibition of TG2 has also recently been demonstrated to attenuate the progressive scarring associated with streptozotocin-induced diabetic nephropathy in rats, by similar mechanisms (Huang, 2006).

The direct effect of TG2 inhibition on the accumulation of ECM and thus the progression of scarring was paralleled by a number of unexpected findings most notably a significant reduction in inflammation in advanced disease. This suggests that the true potential of TG2 inhibition in the prevention of scarring may not purely rely on its ability to prevent excessive stabilisation of the ECM. Certainly, the multi-functional nature of TG2 implicates it in a number of other processes that may be relevant to scarring. In the case of reduced inflammation the apparent effects of NTU283 are probably directed at interstitial cell types other than myofibroblasts and monocytes such as lymphocytes whereas NTU281 appears to specifically affect cells of monocytic origin. It is unclear how TG2 inhibition may produce such anti-inflammatory effects although a possible explanation may be that it is able to hinder the extravasation and migration of inflammatory cells. Studies performed on T cells for example, suggest that TG2 is required for the trans-endothelial migration of lymphocytes (Mohan *et al.*, 2003). Similarly, significant work by Belkin's group demonstrates the importance of integrin-associated cell surface TG2 in monocyte migration (Akimov and Belkin, 2001b). However, this is attributable to interactions between TG2 and the gelatin-binding domain of FN and does not involve the transamidating function of TG2 making it unlikely to be directly affected by TG2 inhibition. It is possible that the interaction of TG2 inhibitors with the enzyme could physically hinder its association with FN and/or integrins which would probably have an impact on migration. Presumably, this would have to occur at the cell surface, given the poor cell solubility of NTU281.

An alternative explanation for this reduced inflammation is that TG2 inhibition is having a significant effect on the inflammatory response through an influence on phospholipase A₂ activation. It has been reported that TG2 enhances the activation of phospholipase A₂ via the formation of intra-molecular iso-peptide bonds or polyamination (Cordella-Miele *et al.*, 1990). Since the phospholipase A₂ catalyzed release of arachidonic acid from the cell membrane is an important step in the synthesis of inflammatory eicosanoids, TG2 inhibition

may reduce inflammation by interfering with this pathway. Interestingly, inhibition of TG2 by recombinant peptides in a guinea pig model of allergic conjunctivitis has been demonstrated to reduce inflammation via inhibition of phospholipase A₂ activity (Sohn *et al.*, 2003).

The influence of TG2 inhibition on the progression of renal disease may extend to a number of additional pro-fibrogenic events that are beyond the scope of this thesis (figure 10.3). For example, a recent *in vitro* study suggests a link between elevated levels of TG2 and tubular cells undergoing EMT (Parker *et al.*, 2006). In that study, NRK-52E cells with high levels of TG2 demonstrated a loss of epithelial cell markers but the acquisition of fibroblast characteristics. Whilst a causal role for TG2 in EMT has yet to be established such data raises the possibility that in addition to direct effects on the ECM, TG2 may participate in the generation of a pro-fibrogenic phenotype. In particular, an increase in TG2-mediated crosslinking of collagen I leading to its increased deposition could be a trigger for EMT *in vivo* given that collagen I promotes tubular cell trans-differentiation (Zeisberg *et al.*, 2001). Increased TGF- β 1 activation may also contribute to EMT although this is an unlikely mechanism of any TG2 action on EMT in this model given that levels of TGF- β are unaffected. If TG2 does participate in EMT, its inhibition and thus the maintenance of a tubular phenotype could clearly have profound implications for the prevention of scar formation.

A potentially pro-fibrogenic effect of TG2 in renal disease and one that has not been investigated in this study is a reduction in tubular cell survival. Previous studies in the subtotal nephrectomy model indicate that TG2 may contribute to tubular atrophy through a novel form of cell death (Johnson *et al.*, 1997). Tubular cells expressing high levels of intracellular TG2 are lost through extensive crosslinking of their intracellular proteins in a process that appears to be independent of apoptosis. Whilst the principle inhibitory effects of both NTU283 and NTU281 on TG2-mediated crosslinking appear to be extracellular, the ability of NTU283 to cross the cell membrane suggests that it could have a supplementary action against intracellular TG2. As such, the prevention of scarring by NTU283 could result from a dual protective effect against ECM accumulation and the death of tubular cells by TG2- dependent mechanisms.

In contrast, other studies have demonstrated that TG2 may protect cells from undergoing apoptosis under conditions of cell stress via the interaction of cell surface TG2 with FN and RGD-independent cell adhesion (Verderio *et al.*, 2003). Whether such mechanisms operate

Figure 10.3 Proposed Mechanisms of Tubular Cell TG2 Action in Kidney Scarring

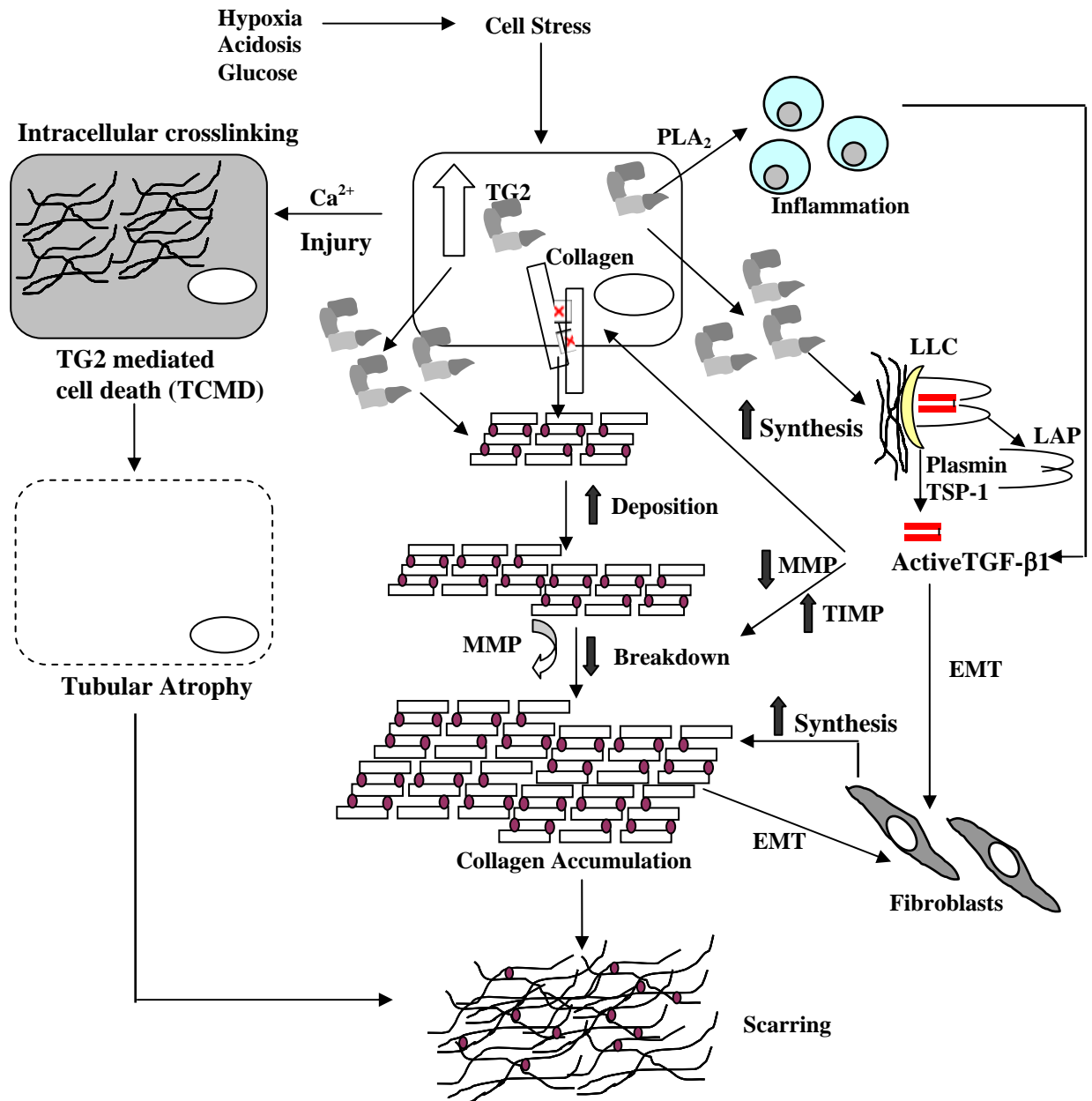


Figure 10.3 TG2 is up-regulated by tubular epithelial cells in response to cellular stress resulting in externalisation of the enzyme into the matrix. Further injury to tubular cells causes them to die due to extensive crosslinking of their intracellular proteins which contributes to tubular atrophy. Once TG2 is increased in the matrix, it can crosslink newly synthesised collagen, leading to its increased deposition and reduced susceptibility to proteolytic degradation, thereby promoting its accumulation. Extracellular TG2 can also recruit TGF- β 1 by crosslinking the large latent TGF- β 1 complex (LLC) to the matrix, making it available for activation by thrombospondin-1 (TSP-1) and plasmin. TGF- β 1 can further contribute to collagen accumulation by promoting increased synthesis and by modulating the expression of MMPs and TIMPs as well as stimulating EMT into myofibroblasts. Myofibroblasts themselves contribute to matrix synthesis which further promotes collagen accumulation and EMT. TG2 can also influence inflammation through activation of phospholipase A₂ (PLA₂)

during renal disease has not been investigated, however, it is unlikely that TG2 inhibition would influence this process given that TG2-FN interaction occurs independently of the transamidating activity of the enzyme which these inhibitors are designed to block.

Whilst the principle target of TG2 inhibition is the direct prevention of collagen accumulation, by interfering with ECM deposition and expansion in the diseased kidney, it is clear that any potential additional effects of treatment with TG2 inhibitors on inflammation, EMT or cell death *in vivo* could broaden their beneficial protective role in preventing progressive scarring.

The development of TG2 inhibition as an effective clinical therapy for progressive kidney scarring will be dependent on the resolution of a number of critical issues. In particular, the effectiveness of TG2 inhibition at reversing the progression of established kidney disease must be considered since this is more relevant to the clinical situation in which many patients present with advanced disease. Further studies whereby TG2 inhibitors are administered to animals showing mild, moderate or severe scarring will be required to resolve this question.

An additional important consideration to be addressed must be the most effective mode of inhibitor delivery for use in the clinical setting. In the present *in vivo* rat study, application of inhibitors was achieved using implantable pumps. Whilst these offer the advantage of direct delivery into the kidney, ensuring effective and consistent inhibition, their distinct disadvantage is that they require replacement. Not only would this be inconvenient for the patient but in the rat study, repeated placement of pumps in the same area resulted in inadequate wound healing and infection. Intravenous, subcutaneous or oral administration of inhibitors all represent feasible options for delivery. One option currently being considered is the incorporation of the TG2 inhibitors into a slow release resin for subcutaneous implantation in a similar manner to that of insulin implants.

The long-term systemic administration of TG2 inhibitors in itself raises issues of potential side effects of which the current data is limited. The broad inhibitory capabilities of both inhibitors against TGs other than TG2 may produce as yet unpredicted systemic effects on additional TG mediated pathways. Inhibition of important TG subtypes such as Factor XIIIa, TG1 (keratinocyte TG) or TG3 (epidermal TG) could potentially have implications for blood clotting and maintenance of normal epidermal barrier function. Indeed, recent data obtained from the study of an *in vitro* tissue engineered model of human skin suggest that sufficient doses of NTU283 are able to promote keratinocyte hyperproliferation and

parakeratosis (Harrison *et al.*, 2007). The limited data presented in this study indicates that localised delivery of NTU283 does not have an effect on systemic Factor XIIIa as indicated by normal levels of fibrin crosslinking although this is certainly due to a minimal circulating concentration of the inhibitor. Given that NTU283 was originally developed as an anti-thrombotic agent against Factor XIIIa, it remains to be determined whether any effects are observed when this inhibitor is administered via systemic routes. Clearly, more extensive data is required to establish the deleterious effects of long-term systemic application of these compounds which will be critical in determining their suitability for clinical use.

The success of TG2 inhibition as an effective clinical therapy will almost certainly be dependent on its comparison to existing regimes aimed at slowing the progression of chronic kidney disease. Of these, ACE (angiotensin converting enzyme) inhibition and angiotensin receptor blockade are widely reported to be advantageous in slowing the progression of CKD due to dual effects on hypertension and proteinuria (Cantarovich and Rangoonwala, 2003; Wolf and Ritz, 2005). Whether TG2 inhibition can offer an effective alternative to these therapies or whether a multi-targeted approach is required to successfully impede the progression of scarring remains to be determined.

Whilst there are a several important issues that still need to be addressed, the data presented in Chapter 9 provides compelling evidence for the potential of TG2 inhibition as an effective anti-scarring therapy with wider application for the treatment of a number of fibrotic conditions in which TG2 has been implicated (Griffin *et al.*, 1979; Mirza *et al.*, 1997, Bowness *et al.*, 1989; Bowness *et al.*, 1990; Bowness *et al.*, 1994).

In conclusion, the data presented in this thesis has given a significant insight into the regulation of TG2 expression and export and the role of TG2 in the extracellular matrix changes associated with kidney scarring. The *in vitro* investigations have highlighted the possible mechanisms by which TG2 may contribute to the expansion of the ECM. Finally, and perhaps most importantly, the application of TG inhibitors *in vivo* has demonstrated that TG2 may represent a potential therapeutic target for the treatment of kidney scarring and disease.

Chapter 11

References

- Abbate, M., Zoja, C., Morigi, M., Rottoli, D., Angioletti, S., Tomasoni, S., Zanchi, C., Longaretti, L., Donadelli, R. and Remuzzi, G.** (2002). Transforming growth factor-beta1 is up-regulated by podocytes in response to excess intraglomerular passage of proteins: a central pathway in progressive glomerulosclerosis. *Am J Pathol.* **161**, 2179-93.
- Abo-Zenah, H., Katsoudas, S., Wild, G., de Takats, D., Shortland, J., Brown, C. B. and El Nahas, A. M.** (2002). Early human renal allograft fibrosis: cellular mediators. *Nephron.* **91**, 112-9.
- Abou-Samra, A. B., Goldsmith, P. K., Xie, L. Y., Juppner, H., Spiegel, A. M. and Segre, G. V.** (1994). Down-regulation of parathyroid (PTH)/PTH-related peptide receptor immunoreactivity and PTH binding in opossum kidney cells by PTH and dexamethasone. *Endocrinology.* **135**, 2588-94.
- Adams, J. C.** (2001). Thrombospondins: multifunctional regulators of cell interactions. *Annu Rev Cell Dev Biol.* **17**, 25-51.
- Adolph, K. W.** (1999). Relative abundance of thrombospondin 2 and thrombospondin 3 mRNAs in human tissues. *Biochem Biophys Res Commun.* **258**, 792-6.
- Aeschlimann, D., Kaupp, O. and Paulsson, M.** (1995). Transglutaminase-catalyzed matrix cross-linking in differentiating cartilage: identification of osteonectin as a major glutaminyl substrate. *J Cell Biol.* **129**, 881-92.
- Aeschlimann, D. and Paulsson, M.** (1991). Cross-linking of laminin-nidogen complexes by tissue transglutaminase. A novel mechanism for basement membrane stabilization. *J Biol Chem.* **266**, 15308-17.
- Aeschlimann, D., Paulsson, M. and Mann, K.** (1992). Identification of Gln726 in nidogen as the amine acceptor in transglutaminase-catalyzed cross-linking of laminin-nidogen complexes. *J Biol Chem.* **267**, 11316-21.
- Aeschlimann, D. and Thomazy, V.** (2000). Protein crosslinking in assembly and remodelling of extracellular matrices: the role of transglutaminases. *Connect Tissue Res.* **41**, 1-27.
- Agani, F. H., Pichiule, P., Chavez, J. C. and LaManna, J. C.** (2000). The role of mitochondria in the regulation of hypoxia-inducible factor 1 expression during hypoxia. *J Biol Chem.* **275**, 35863-7.
- Agarwal, R.** (2005). Hypertension in chronic kidney disease and dialysis: pathophysiology and management. *Cardiol Clin.* **23**, 237-48.
- Agrez, M., Gu, X., Turton, J., Meldrum, C., Niu, J., Antalis, T. and Howard, E. W.** (1999). The alpha v beta 6 integrin induces gelatinase B secretion in colon cancer cells. *Int J Cancer.* **81**, 90-7.
- Aimes, R. T. and Quigley, J. P.** (1995). Matrix metalloproteinase-2 is an interstitial collagenase. Inhibitor-free enzyme catalyzes the cleavage of collagen fibrils and soluble native type I collagen generating the specific 3/4- and 1/4-length fragments. *J Biol Chem.* **270**, 5872-6.

- Akimov, S. S. and Belkin, A. M.** (2001a). Cell-surface transglutaminase promotes fibronectin assembly via interaction with the gelatin-binding domain of fibronectin: a role in TGFbeta-dependent matrix deposition. *J Cell Sci.* **114**, 2989-3000.
- Akimov, S. S. and Belkin, A. M.** (2001b). Cell surface tissue transglutaminase is involved in adhesion and migration of monocytic cells on fibronectin. *Blood.* **98**, 1567-76.
- Akimov, S. S., Krylov, D., Fleischman, L. F. and Belkin, A. M.** (2000). Tissue transglutaminase is an integrin-binding adhesion coreceptor for fibronectin. *J Cell Biol.* **148**, 825-38.
- Alexopoulos, E., Seron, D., Hartley, R. B., Nolasco, F. and Cameron, J. S.** (1989). Immune mechanisms in idiopathic membranous nephropathy: the role of the interstitial infiltrates. *Am J Kidney Dis.* **13**, 404-12.
- Alfrey, A. C.** (1994). Role of iron and oxygen radicals in the progression of chronic renal failure. *Am J Kidney Dis.* **23**, 183-7.
- Allen, D. A., Harwood, S., Varaganam, M., Raftery, M. J., Yaqoob, M. M., Hsieh, T. J., Zhang, S. L., Filep, J. G., Tang, S. S., Ingelfinger, J. R. et al.** (2003). High glucose stimulates angiotensinogen gene expression via reactive oxygen species generation in rat kidney proximal tubular cells. *FASEB J.* **17**, 908-10.
- Alonso, J., Mampaso, F., Martin, A., Palacios, I. and Egido, J.** (1999). Changes in the pattern of fibronectin mRNA alternative splicing in acute experimental mesangioproliferative nephritis. *Lab Invest.* **79**, 185-94.
- Alpers, C. E., Seifert, R. A., Hudkins, K. L., Johnson, R. J. and Bowen-Pope, D. F.** (1992). Developmental patterns of PDGF B-chain, PDGF-receptor, and alpha-actin expression in human glomerulogenesis. *Kidney Int.* **42**, 390-9.
- Alvestrand A and P, S.** (1997). The Uraemic Syndrome. In *Nephrology*, (eds Jamison R. L., and Wilkinson R.), pp. 467-477: Chapman and Hall Medical.
- Anderson, S.** (1989). Antihypertensive therapy and the progression of renal disease. *J Hypertens Suppl.* **7**, S39-42.
- Anderson, S., Meyer, T. W., Rennke, H. G. and Brenner, B. M.** (1985). Control of glomerular hypertension limits glomerular injury in rats with reduced renal mass. *J Clin Invest.* **76**, 612-9.
- Ando, T., Okuda, S., Tamaki, K., Yoshitomi, K. and Fujishima, M.** (1995). Localization of transforming growth factor-beta and latent transforming growth factor-beta binding protein in rat kidney. *Kidney Int.* **47**, 733-9.
- Angles-Cano, E., Rondeau, E., Delarue, F., Hagege, J., Sultan, Y. and Sraer, J. D.** (1985). Identification and cellular localization of plasminogen activators from human glomeruli. *Thromb Haemost.* **54**, 688-92.
- Antonyak, M. A., Jansen, J. M., Miller, A.M., Ly, T. K., Endo, M. and Cerione, R. A.** (2006) Two isoforms of tissue transglutaminase mediate opposing cellular fates. *Proc Natl Acad Sci U.S.A.* **103**, 18609-14.

- Apodaca, G.** (2002). Modulation of membrane traffic by mechanical stimuli. *Am J Physiol Renal Physiol.* **282**, F179-90.
- Arici, M., Brown, J., Williams, M., Harris, K. P., Walls, J. and Brunskill, N. J.** (2002). Fatty acids carried on albumin modulate proximal tubular cell fibronectin production: a role for protein kinase C. *Nephrol Dial Transplant.* **17**, 1751-7.
- Auld, G. C., Ritchie, H., Robbie, L. A. and Booth, N. A.** (2001). Thrombin upregulates tissue transglutaminase in endothelial cells: a potential role for tissue transglutaminase in stability of atherosclerotic plaque. *Arterioscler Thromb Vasc Biol.* **21**, 1689-94.
- Bailey, N. C. and Kelly, C. J.** (1997). Nephritogenic T cells use granzyme C as a cytotoxic mediator. *Eur J Immunol.* **27**, 2302-9.
- Balklava, Z., Verderio, E., Collighan, R., Gross, S., Adams, J. and Griffin, M.** (2002). Analysis of tissue transglutaminase function in the migration of Swiss 3T3 fibroblasts: the active-state conformation of the enzyme does not affect cell motility but is important for its secretion. *J Biol Chem.* **277**, 16567-75.
- Ballestar, E. and Franco, L.** (1997). Use of the transglutaminase reaction to study the dissociation of histone N-terminal tails from DNA in nucleosome core particles. *Biochemistry.* **36**, 5963-9.
- Bandyopadhyay, R. S., Phelan, M. and Faller, D. V.** (1995). Hypoxia induces AP-1-regulated genes and AP-1 transcription factor binding in human endothelial and other cell types. *Biochim Biophys Acta.* **1264**, 72-8.
- Barasch, J., Yang, J., Qiao, J., Tempst, P., Erdjument-Bromage, H., Leung, W. and Oliver, J. A.** (1999). Tissue inhibitor of metalloproteinase-2 stimulates mesenchymal growth and regulates epithelial branching during morphogenesis of the rat metanephros. *J Clin Invest.* **103**, 1299-307.
- Baricos, W. H., Cortez, S. L., Deboisblanc, M. and Xin, S.** (1999). Transforming growth factor-beta is a potent inhibitor of extracellular matrix degradation by cultured human mesangial cells. *J Am Soc Nephrol.* **10**, 790-5.
- Baricos, W. H., Cortez, S. L., el-Dahr, S. S. and Schnaper, H. W.** (1995). ECM degradation by cultured human mesangial cells is mediated by a PA/plasmin/MMP-2 cascade. *Kidney Int.* **47**, 1039-47.
- Barnes, R. N., Bungay, P. J., Elliott, B. M., Walton, P. L. and Griffin, M.** (1985). Alterations in the distribution and activity of transglutaminase during tumour growth and metastasis. *Carcinogenesis.* **6**, 459-63.
- Basnakian, A. G., Ueda, N., Kaushal, G. P., Mikhailova, M. V. and Shah, S. V.** (2002). DNase I-like endonuclease in rat kidney cortex that is activated during ischemia/reperfusion injury. *J Am Soc Nephrol.* **13**, 1000-7.
- Bassuk, J. A. and Berg, R. A.** (1989). Protein disulphide isomerase, a multifunctional endoplasmic reticulum protein. *Matrix.* **9**, 244-58.

- Bassuk, J. A., Pichler, R., Rothmier, J. D., Pippen, J., Gordon, K., Meek, R. L., Bradshaw, A. D., Lombardi, D., Strandjord, T. P., Reed, M. et al.** (2000). Induction of TGF-beta1 by the matricellular protein SPARC in a rat model of glomerulonephritis. *Kidney Int.* **57**, 117-28.
- Battegay, E. J., Raines, E. W., Seifert, R. A., Bowen-Pope, D. F. and Ross, R.** (1990). TGF-beta induces bimodal proliferation of connective tissue cells via complex control of an autocrine PDGF loop. *Cell.* **63**, 515-24.
- Baud, L. and Ardaillou, R.** (1993). Involvement of reactive oxygen species in kidney damage. *Br Med Bull.* **49**, 621-9.
- Baylis, A. L.** (1997). Glomerular Filtration. In *Nephrology*, (eds. Jamison R. L., Wilkinson, R.), pp. 23-33: Chapman and Hall.
- Beck, K., Hunter, I. and Engel, J.** (1990). Structure and function of laminin: anatomy of a multidomain glycoprotein. *FASEB J.* **4**, 148-60.
- Becker, J. W., Marcy, A. I., Rokosz, L. L., Axel, M. G., Burbaum, J. J., Fitzgerald, P. M., Cameron, P. M., Esser, C. K., Haggmann, W. K., Hermes, J. D. et al.** (1995). Stromelysin-1: three-dimensional structure of the inhibited catalytic domain and of the C-truncated proenzyme. *Protein Sci.* **4**, 1966-76.
- Begg, G. E., Carrington, L., Stokes, P. H., Matthews, J. M., Wouters, M. A., Husain, A., Lorand, L., Iismaa, S. E. and Graham, R. M.** (2006a). Mechanism of allosteric regulation of transglutaminase 2 by GTP. *Proc Natl Acad Sci U S A.* **103**, 19683-8.
- Begg, G. E., Holman, S. R., Stokes, P. H., Matthews, J. M., Graham, R. M. and Iismaa, S. E.** (2006b). Mutation of a critical arginine in the GTP-binding site of transglutaminase 2 disinhibits intracellular cross-linking activity. *J Biol Chem.* **281**, 12603-9.
- Belkin, A. M., Zemskov, E. A., Hang, J., Akimov, S. S., Sikora, S. and Strongin, A. Y.** (2004). Cell-surface-associated tissue transglutaminase is a target of MMP-2 proteolysis. *Biochemistry.* **43**, 11760-9.
- Bender, B. L., Jaffe, R., Carlin, B. and Chung, A. E.** (1981). Immunolocalization of entactin, a sulfated basement membrane component, in rodent tissues, and comparison with GP-2 (laminin). *Am J Pathol.* **103**, 419-26.
- Benyon, R. J. and Bond, J. S.** (1994). Proteolytic enzymes: a practical approach (Ed. Hames B. D.) Oxford University Press.
- Bergamini, C. M.** (1988). GTP modulates calcium binding and cation-induced conformational changes in erythrocyte transglutaminase. *FEBS Lett.* **239**, 255-8.
- Bergamini, C. M., Signorini, M., Barbato, R., Menabo, R., Di Lisa, F., Gorza, L. and Beninati, S.** (1995). Transglutaminase-catalyzed polymerization of troponin in vitro. *Biochem Biophys Res Commun.* **206**, 201-6.
- Bergers, G., Brekken, R., McMahon, G., Vu, T. H., Itoh, T., Tamaki, K., Tanzawa, K., Thorpe, P., Itohara, S., Werb, Z. et al.** (2000). Matrix metalloproteinase-9 triggers the angiogenic switch during carcinogenesis. *Nat Cell Biol.* **2**, 737-44.

- Bergstein, J. M., Riley, M. and Bang, N. U.** (1988). Analysis of the plasminogen activator activity of the human glomerulus. *Kidney Int.* **33**, 868-74.
- Bernassola, F., Rossi, A. and Melino, G.** (1999). Regulation of transglutaminases by nitric oxide. *Ann N Y Acad Sci.* **887**, 83-91.
- Birckbichler, P. J., Orr, G. R., Conway, E. and Patterson, M. K., Jr.** (1977). Transglutaminase activity in normal and transformed cells. *Cancer Res.* **37**, 1340-4.
- Birckbichler, P. J., Orr, G. R., Patterson, M. K., Jr., Conway, E. and Carter, H. A.** (1981). Increase in proliferative markers after inhibition of transglutaminase. *Proc Natl Acad Sci U S A.* **78**, 5005-8.
- Birckbichler, P. J., Orr, G. R., Patterson, M. K., Jr., Conway, E., Carter, H. A. and Maxwell, M. D.** (1983). Enhanced transglutaminase activity in transformed human lung fibroblast cells after exposure to sodium butyrate. *Biochim Biophys Acta.* **763**, 27-34.
- Birckbichler, P. J. and Patterson, M. K., Jr.** (1978). Cellular transglutaminase, growth, and transformation. *Ann N Y Acad Sci.* **312**, 354-65.
- Birk, D. E. and Trelstad, R. L.** (1984). Extracellular compartments in matrix morphogenesis: collagen fibril, bundle, and lamellar formation by corneal fibroblasts. *J Cell Biol.* **99**, 2024-33.
- Birk, D. E. and Trelstad, R. L.** (1986). Extracellular compartments in tendon morphogenesis: collagen fibril, bundle, and macroaggregate formation. *J Cell Biol.* **103**, 231-40.
- Birkedal-Hansen, H., Taylor, R. E., Bhowan, A. S., Katz, J., Lin, H. Y. and Wells, B. R.** (1985). Cleavage of bovine skin type III collagen by proteolytic enzymes. Relative resistance of the fibrillar form. *J Biol Chem.* **260**, 16411-7.
- Blasi, F. and Carmeliet, P.** (2002). uPAR: a versatile signalling orchestrator. *Nat Rev Mol Cell Biol.* **3**, 932-43.
- Bode, W., Gomis-Ruth, F. X. and Stockler, W.** (1993). Astacins, serralysins, snake venom and matrix metalloproteinases exhibit identical zinc-binding environments (HEXXHXXGXXH and Met-turn) and topologies and should be grouped into a common family, the 'metzincins'. *FEBS Lett.* **331**, 134-40.
- Bohle, A., Mackensen-Haen, S. and Wehrmann, M.** (1996). Significance of postglomerular capillaries in the pathogenesis of chronic renal failure. *Kidney Blood Press Res.* **19**, 191-5.
- Boros, S., Ahrman, E., Wunderink, L., Kamps, B., de Jong, W. W., Boelens, W. C. and Emanuelsson, C. S.** (2006). Site-specific transamidation and deamidation of the small heat-shock protein Hsp20 by tissue transglutaminase. *Proteins.* **62**, 1044-52.
- Boros, S., Kamps, B., Wunderink, L., de Bruijn, W., de Jong, W. W. and Boelens, W. C.** (2004). Transglutaminase catalyzes differential crosslinking of small heat shock proteins and amyloid-beta. *FEBS Lett.* **576**, 57-62.
- Bosman, F. T. and Stamenkovic, I.** (2003). Functional structure and composition of the extracellular matrix. *J Pathol.* **200**, 423-8.

- Boudreau, N. J. and Jones, P. L.** (1999). Extracellular matrix and integrin signalling: the shape of things to come. *Biochem J.* **339**, 481-8.
- Bowness, J. M., Folk, J. E. and Timpl, R.** (1987). Identification of a substrate site for liver transglutaminase on the aminopropeptide of type III collagen. *J Biol Chem.* **262**, 1022-4.
- Bowness, J. M. and Tarr, A. H.** (1990). Lipoprotein binding of crosslinked type III collagen aminopropeptide and fractions of its antigen in blood. *Biochem Biophys Res Commun.* **170**, 519-25.
- Bowness, J. M., Tarr, A. H. and Wiebe, R. I.** (1989). Transglutaminase-catalysed cross-linking: a potential mechanism for the interaction of fibrinogen, low density lipoprotein and arterial type III procollagen. *Thromb Res.* **54**, 357-67.
- Bowness, J. M., Venditti, M., Tarr, A. H. and Taylor, J. R.** (1994). Increase in epsilon(gamma-glutamyl)lysine crosslinks in atherosclerotic aortas. *Atherosclerosis.* **111**, 247-53.
- Brady, H. R.** (1994). Leukocyte adhesion molecules and kidney diseases. *Kidney Int.* **45**, 1285-300.
- Brenner, B. M.** (1985). Nephron adaptation to renal injury or ablation. *Am J Physiol Renal Physiol.* **249**, F324-37.
- Brenner, B. M., Meyer, T. W. and Hostetter, T. H.** (1982). Dietary protein intake and the progressive nature of kidney disease: the role of hemodynamically mediated glomerular injury in the pathogenesis of progressive glomerular sclerosis in aging, renal ablation, and intrinsic renal disease. *N Engl J Med.* **307**, 652-9.
- Brown, P. A., Wilson, H. M., Reid, F. J., Booth, N. A., Simpson, J. G., Morrison, L., Power, D. A. and Haites, N. E.** (1994). Urokinase-plasminogen activator is synthesized in vitro by human glomerular epithelial cells but not by mesangial cells. *Kidney Int.* **45**, 43-7.
- Bultmann, H., Santas, A. J. and Peters, D. M.** (1998). Fibronectin fibrillogenesis involves the heparin II binding domain of fibronectin. *J Biol Chem.* **273**, 2601-9.
- Bunn, H. F. and Poyton, R. O.** (1996). Oxygen sensing and molecular adaptation to hypoxia. *Physiol Rev.* **76**, 839-85.
- Butler, S. J. and Landon, M.** (1981). Transglutaminase-catalysed incorporation of putrescine into denatured cytochrome. Preparation of a mono-substituted derivative reactive with cytochrome c oxidase. *Biochim Biophys Acta.* **670**, 214-21.
- Caenazzo, C., Garbisa, S., Onisto, M., Zampieri, M., Baggio, B. and Gambaro, G.** (1997). Effect of glucose and heparin on mesangial alpha 1(IV)COLL and MMP-2/TIMP-2 mRNA expression. *Nephrol Dial Transplant.* **12**, 443-8.
- Cai, G., Chen, X., Fu, B. and Lu, Y.** (2005). Activation of gelatinases by fibrin is PA/plasmin system-dependent in human glomerular endothelial cells. *Mol Cell Biochem.* **277**, 171-9.

- Campisi, A., Caccamo, D., Li Volti, G., Curro, M., Parisi, G., Avola, R., Vanella, A. and Ientile, R.** (2004). Glutamate-evoked redox state alterations are involved in tissue transglutaminase upregulation in primary astrocyte cultures. *FEBS Lett.* **578**, 80-4.
- Cantarovich, F. and Rangoonwala, B.** (2003). Therapeutic effects of angiotensin II inhibition or blockade on the progression of chronic renal disease. *Int J Clin Pract.* **57**, 801-22.
- Carome, M. A., Striker, L. J., Peten, E. P., Moore, J., Yang, C. W., Stetler-Stevenson, W. G. and Striker, G. E.** (1993). Human glomeruli express TIMP-1 mRNA and TIMP-2 protein and mRNA. *Am J Physiol.* **264**, F923-9.
- Casadio, R., Polverini, E., Mariani, P., Spinozzi, F., Carsughi, F., Fontana, A., Polverino de Laureto, P., Matteucci, G. and Bergamini, C. M.** (1999). The structural basis for the regulation of tissue transglutaminase by calcium ions. *Eur J Biochem.* **262**, 672-9.
- Catania, J. M., Chen, G. and Parrish, A. R.** (2007). Role of matrix metalloproteinases in renal pathophysiology. *Am J Physiol Renal Physiol.* **3**, F905-11.
- Cattell, V.** (2002). Nitric oxide and glomerulonephritis. *Kidney Int.* **61**, 816-21.
- Chakraborti, S., Mandal, M., Das, S., Mandal, A. and Chakraborti, T.** (2003). Regulation of matrix metalloproteinases: an overview. *Mol Cell Biochem.* **253**, 269-85.
- Chakravarti, S., Magnuson, T., Lass, J. H., Jepson, K. J., La Mantia, C. and Corral, H.** (1998) Lumican regulates collagen fibril assembly: skin fragility and corneal opacity in the absence of lumican. *J Cell Biol.* **141**, 1277-86
- Chana, R. S., Wheeler, D. C., Thomas, G. J., Williams, J. D. and Davies, M.** (2000). Low-density lipoprotein stimulates mesangial cell proteoglycan and hyaluronan synthesis. *Nephrol Dial Transplant.* **15**, 167-72.
- Chandel, N. S., McClintock, D. S., Feliciano, C. E., Wood, T. M., Melendez, J. A., Rodriguez, A. M. and Schumacker, P. T.** (2000). Reactive oxygen species generated at mitochondrial complex III stabilize hypoxia-inducible factor-1 α during hypoxia: a mechanism of O₂ sensing. *J Biol Chem.* **275**, 25130-8.
- Chau, D. Y., Collighan, R. J., Verderio, E. A., Addy, V. L. and Griffin, M.** (2005). The cellular response to transglutaminase-cross-linked collagen. *Biomaterials.* **26**, 6518-29.
- Chen, H. and Mosher, D. F.** (1996). Formation of sodium dodecyl sulfate-stable fibronectin multimers. Failure to detect products of thiol-disulfide exchange in cyanogen bromide or limited acid digests of stabilized matrix fibronectin. *J Biol Chem.* **271**, 9084-9.
- Chen, J. S. and Mehta, K.** (1999). Tissue transglutaminase: an enzyme with a split personality. *Int J Biochem Cell Biol.* **31**, 817-36.
- Chen, S., Lin, F., Iismaa, S., Lee, K. N., Birckbichler, P. J. and Graham, R. M.** (1996). Alpha₁-adrenergic receptor signaling via Gh is subtype specific and independent of its transglutaminase activity. *J Biol Chem.* **271**, 32385-91.

- Chen, S., Mukherjee, S., Chakraborty, C. and Chakrabarti, S.** (2003). High glucose-induced, endothelin-dependent fibronectin synthesis is mediated via NF-kappa B and AP-1. *Am J Physiol Cell Physiol.* **284**, C263-72.
- Chen, S. J., Artlett, C. M., Jimenez, S. A. and Varga, J.** (1998). Modulation of human alpha1(I) procollagen gene activity by interaction with Sp1 and Sp3 transcription factors in vitro. *Gene.* **215**, 101-10.
- Chen, S. J., Yuan, W., Mori, Y., Levenson, A., Trojanowska, M. and Varga, J.** (1999). Stimulation of type I collagen transcription in human skin fibroblasts by TGF-beta: involvement of Smad 3. *J Invest Dermatol.* **112**, 49-57.
- Chen, Y., Blom, I. E., Sa, S., Goldschmeding, R., Abraham, D. J. and Leask, A.** (2002). CTGF expression in mesangial cells: involvement of SMADs, MAP kinase, and PKC. *Kidney Int.* **62**, 1149-59.
- Cheng, Y. S., Champlaud, M. F., Burgeson, R. E., Marinkovich, M. P. and Yurchenco, P. D.** (1997). Self-assembly of laminin isoforms. *J Biol Chem.* **272**, 31525-32.
- Chi, W. M., Berezsky, I. K., Smith, M. W. and Trump, B. F.** (1995). Changes in $[Ca^{2+}]_i$ in cultured rat proximal tubular epithelium: an in vitro model for renal ischemia. *Biochim Biophys Acta.* **1243**, 513-20.
- Chien, S., Li, S. and Shyy, Y. J.** (1998). Effects of mechanical forces on signal transduction and gene expression in endothelial cells. *Hypertension.* **31**, 162-9.
- Chiocca, E. A., Davies, P. J. and Stein, J. P.** (1988). The molecular basis of retinoic acid action. Transcriptional regulation of tissue transglutaminase gene expression in macrophages. *J Biol Chem.* **263**, 11584-9.
- Chiocca, E. A., Davies, P. J. and Stein, J. P.** (1989). Regulation of tissue transglutaminase gene expression as a molecular model for retinoid effects on proliferation and differentiation. *J Cell Biochem.* **39**, 293-304.
- Christopher, R. A., Kowalczyk, A. P. and McKeown-Longo, P. J.** (1997). Localization of fibronectin matrix assembly sites on fibroblasts and endothelial cells. *J Cell Sci.* **110**, 569-81.
- Chung, L., Dinakarbandian, D., Yoshida, N., Lauer-Fields, J. L., Fields, G. B., Visse, R. and Nagase, H.** (2004). Collagenase unwinds triple-helical collagen prior to peptide bond hydrolysis. *EMBO J.* **23**, 3020-30.
- Clark, E. C., Nath, K. A., Hostetter, M. K. and Hostetter, T. H.** (1991). Role of ammonia in progressive interstitial nephritis. *Am J Kidney Dis.* **17**, 15-9.
- Clark, I. M. and Cawston, T. E.** (1989). Fragments of human fibroblast collagenase. Purification and characterization. *Biochem J.* **263**, 201-6.
- Clayton, A., Thomas, J., Thomas, G. J., Davies, M. and Steadman, R.** (2001). Cell surface heparan sulfate proteoglycans control the response of renal interstitial fibroblasts to fibroblast growth factor-2. *Kidney Int.* **59**, 2084-94.

- Clement, S., Velasco, P. T., Murthy, S. N., Wilson, J. H., Lukas, T. J., Goldman, R. D. and Lorand, L.** (1998). The intermediate filament protein, vimentin, in the lens is a target for cross-linking by transglutaminase. *J Biol Chem.* **273**, 7604-9.
- Cohen, I. and Anderson, B.** (1987). Immunochemical characterization of the transglutaminase-catalyzed polymer of activated platelets. *Thromb Res.* **47**, 409-16.
- Coimbra, T. M., Carvalho, J., Fattori, A., Da Silva, C. G. and Lachat, J. J.** (1996). Transforming growth factor-beta production during the development of renal fibrosis in rats with subtotal renal ablation. *Int J Exp Pathol.* **77**, 167-73.
- Collighan, R., Clara, S., Li, X., Parry, J. and Griffin, M.** (2004). Transglutaminases as tanning agents for the leather industry. *J. Am Leather Chemists Ass.* **99**, 293-298.
- Colognato, H., Winkelmann, D. A. and Yurchenco, P. D.** (1999). Laminin polymerization induces a receptor-cytoskeleton network. *J Cell Biol.* **145**, 619-31.
- Combe, C., Burton, C. J., Dufourco, P., Weston, S., Horsburgh, T., Walls, J. and Harris, K. P.** (1997). Hypoxia induces intercellular adhesion molecule-1 on cultured human tubular cells. *Kidney Int.* **51**, 1703-9.
- Cook, T. F., Burke, J. S., Bergman, K. D., Quinn, C. O., Jeffrey, J. J. and Partridge, N. C.** (1994). Cloning and regulation of rat tissue inhibitor of metalloproteinases-2 in osteoblastic cells. *Arch Biochem Biophys.* **311**, 313-20.
- Cooper, A. J., Wang, J., Pasternack, R., Fuchsbauer, H. L., Sheu, R. K. and Blass, J. P.** (2000). Lysine-rich histone (H1) is a lysyl substrate of tissue transglutaminase: possible involvement of transglutaminase in the formation of nuclear aggregates in (CAG)(n)/Q(n) expansion diseases. *Dev Neurosci.* **22**, 404-17.
- Cooper, D. N. and Barondes, S. H.** (1990). Evidence for export of a muscle lectin from cytosol to extracellular matrix and for a novel secretory mechanism. *J Cell Biol.* **110**, 1681-91.
- Cordella-Miele, E., Miele, L. and Mukherjee, A. B.** (1990). A novel transglutaminase-mediated post-translational modification of phospholipase A2 dramatically increases its catalytic activity. *J Biol Chem.* **265**, 17180-8.
- Couser, W. G. and Johnson, R. J.** (1994). Mechanisms of progressive renal disease in glomerulonephritis. *Am J Kidney Dis.* **23**, 193-8.
- Coussens, L. M., Fingleton, B. and Matrisian, L. M.** (2002). Matrix metalloproteinase inhibitors and cancer: trials and tribulations. *Science.* **295**, 2387-92.
- Coussons, P. J., Price, N. C., Kelly, S. M., Smith, B. and Sawyer, L.** (1992). Factors that govern the specificity of transglutaminase-catalysed modification of proteins and peptides. *Biochem J.* **282**, 929-30.
- Dallas, S. L., Rosser, J. L., Mundy, G. R. and Bonewald, L. F.** (2002) Proteolysis of latent transforming growth factor- β (TGF- β)- binding protein-1 by osteoclasts. *J Biol Chem.* **277**, 21352-60.

- Dangelo, M., Sarment, D. P., Billings, P. C. and Pacifici, M.** (2001) Activation of transforming growth factor beta in chondrocytes undergoing endochondrial ossification. *J Bone Miner Res.* **16**, 2339-47.
- Danielson, K. G., Baribault, H., Holmes, D. F., Graham, H., Kadler, K. E. and Iozzo R. V.** (1997) Targeted disruption of decorin leads to abnormal collagen morphology and skin fragility. *J. Cell Biol.* **136**, 729-43.
- D'Amico, G. and Bazzi, C.** (2003) Pathophysiology of proteinuria. *Kidney Int.* **63**, 809-25.
- D'Ardenne, A. J., Burns, J., Sykes, B. C. and Kirkpatrick, P.** (1983). Comparative distribution of fibronectin and type III collagen in normal human tissues. *J Pathol.* **141**, 55-69.
- Davies, M., Hughes, K. T. and Thomas, G. J.** (1980). Evidence that kidney lysosomal proteinases degrade the collagen of glomerular basement membrane. *Ren Physiol.* **3**, 116-9.
- Davies, M., Martin, J., Thomas, G. J. and Lovett, D. H.** (1992). Proteinases and glomerular matrix turnover. *Kidney Int.* **41**, 671-8.
- Davies, P. J., Chiocca, E. A. and Stein, J. P.** (1988). Retinoid-regulated expression of tissue transglutaminase in normal and leukemic myeloid cells. *Adv Exp Med Biol.* **231**, 63-71.
- De Laurenzi, V. and Melino, G.** (2001). Gene disruption of tissue transglutaminase. *Mol Cell Biol.* **21**, 148-55.
- Delany, A. M., Jeffrey, J. J., Rydziel, S. and Canalis, E.** (1995). Cortisol increases interstitial collagenase expression in osteoblasts by post-transcriptional mechanisms. *J Biol Chem.* **270**, 26607-12.
- Derrick, N. and Laki, K.** (1966). Enzymatic labelling of actin and tropomyosin with 14 C-labelled putrescine. *Biochem Biophys Res Commun.* **22**, 82-8.
- Diamond, J. R., Levinson, M., Kreisberg, R. and Ricardo, S. D.** (1997). Increased expression of decorin in experimental hydronephrosis. *Kidney Int.* **51**, 1133-9.
- Dieterich, W., Ehnis, T., Bauer, M., Donner, P., Volta, U., Riecken, E. O. and Schuppan, D.** (1997). Identification of tissue transglutaminase as the autoantigen of coeliac disease. *Nat Med.* **3**, 797-801.
- Dobashi, K., Ghosh, B., Orak, J. K., Singh, I. and Singh, A. K.** (2000). Kidney ischemia-reperfusion: modulation of antioxidant defenses. *Mol Cell Biochem.* **205**, 1-11.
- Douthwaite, J. A., Johnson, T. S., Haylor, J. L., Watson, P. and El Nahas, A. M.** (1999). Effects of transforming growth factor-beta1 on renal extracellular matrix components and their regulating proteins. *J Am Soc Nephrol.* **10**, 2109-19.
- Dumin, J. A., Dickeson, S. K., Stricker, T. P., Bhattacharyya-Pakrasi, M., Roby, J. D., Santoro, S. A. and Parks, W. C.** (2001). Pro-collagenase-1 (matrix metalloproteinase-1) binds the alpha(2)beta(1) integrin upon release from keratinocytes migrating on type I collagen. *J Biol Chem.* **276**, 29368-74.

- Eckardt, K. U., Bernhardt, W. M., Weidemann, A., Warnecke, C., Rosenberger, C., Wiesener, M. S. and Willam, C.** (2005). Role of hypoxia in the pathogenesis of renal disease. *Kidney Int Suppl.* **99**, S46-51.
- Eddy, A. A.** (1989). Interstitial nephritis induced by protein-overload proteinuria. *Am J Pathol.* **135**, 719-33.
- Eddy, A. A.** (1996). Molecular insights into renal interstitial fibrosis. *J Am Soc Nephrol.* **7**, 2495-508.
- Eddy, A. A.** (2000a). Molecular basis of renal fibrosis. *Pediatr Nephrol.* **15**, 290-301.
- Eddy, A. A. and Giachelli, C. M.** (1995). Renal expression of genes that promote interstitial inflammation and fibrosis in rats with protein-overload proteinuria. *Kidney Int.* **47**, 1546-57.
- Eddy, A. A., Kim, H., Lopez-Guisa, J., Oda, T. and Soloway, P.D.** (2000b) Interstitial fibrosis in mice with overload proteinuria: deficiency of TIMP-1 is not effective. *Kidney Int.* **58**, 618-28.
- Edwards, D. R., Leco, K. J., Beaudry, P. P., Atadja, P. W., Veillette, C. and Riabowol, K. T.** (1996). Differential effects of transforming growth factor-beta 1 on the expression of matrix metalloproteinases and tissue inhibitors of metalloproteinases in young and old human fibroblasts. *Exp Gerontol.* **31**, 207-23.
- Edwards, D. R., Murphy, G., Reynolds, J. J., Whitham, S. E., Docherty, A. J., Angel, P. and Heath, J. K.** (1987). Transforming growth factor beta modulates the expression of collagenase and metalloproteinase inhibitor. *EMBO J.* **6**, 1899-904.
- Edwards, R. M.** (1983). Segmental effects of norepinephrine and angiotensin II on isolated renal microvessels. *Am J Physiol.* **244**, F526-34.
- Eickelberg, O., Centrella, M., Reiss, M., Kashgarian, M. and Wells, R. G.** (2002). Betaglycan inhibits TGF-beta signaling by preventing type I-type II receptor complex formation. Glycosaminoglycan modifications alter betaglycan function. *J Biol Chem.* **277**, 823-9.
- Eickelberg, O., Kohler, E., Reichenberger, F., Bertschin, S., Woodtli, T., Erne, P., Perruchoud, A. P. and Roth, M.** (1999). Extracellular matrix deposition by primary human lung fibroblasts in response to TGF-beta1 and TGF-beta3. *Am J Physiol.* **276**, L814-24.
- El-Nahas, A. M.** (2003). Plasticity of kidney cells: role in kidney remodeling and scarring. *Kidney Int.* **64**, 1553-63.
- El-Nahas, A. M., Paraskevakou, H., Zoob, S., Rees, A. J. and Evans, D. J.** (1983). Effect of dietary protein restriction on the development of renal failure after subtotal nephrectomy in rats. *Clin Sci (Colch).* **65**, 399-406.
- El Nahas, A. M.** (1995). Pathways to renal fibrosis. *Exp Nephrol.* **3**, 71-5.
- El Nahas, A. M., Abo-Zenah, H., Skill, N. J., Bex, S., Wild, G., Griffin, M. and Johnson, T. S.** (2004). Elevated epsilon-(gamma-glutamyl)lysine in human diabetic nephropathy results from increased expression and cellular release of tissue transglutaminase. *Nephron Clin Pract.* **97**, 108-17.

- El Nahas, A. M., Muchaneta-Kubara, E. C., Essawy, M. and Soylemezoglu, O.** (1997). Renal fibrosis: insights into pathogenesis and treatment. *Int J Biochem Cell Biol.* **29**, 55-62.
- Eligula, L., Chuang, L., Phillips, M. L., Segura, K. and Muhlrud, A.** (1998). Transglutaminase induced crosslinking between subdomain 2 of G-actin and the 636-642 lysine rich loop of myosin subfragment 1. *J. Biophys.* **74**, 953-963.
- Endo, K., Takino, T., Miyamori, H., Kinsen, H., Yoshizaki, T., Furukawa, M. and Sato, H.** (2003) Cleavage of syndecan-1 by membrane type matrix metalloproteinase-1 stimulates cell migration. *J Biol Chem.* **278**, 40764-70.
- Engelmyer, E., van Goor, H., Edwards, D. R. and Diamond, J. R.** (1995). Differential mRNA expression of renal cortical tissue inhibitor of metalloproteinase-1, -2, and -3 in experimental hydronephrosis. *J Am Soc Nephrol.* **5**, 1675-83.
- Esposito, C. and Caputo, I.** (2005). Mammalian transglutaminases. Identification of substrates as a key to physiological function and physiopathological relevance. *FEBS J.* **272**, 615-31.
- Essawy, M., Soylemezoglu, O., Muchaneta-Kubara, E. C., Shortland, J., Brown, C. B. and El Nahas, A. M.** (1997). Myofibroblasts and the progression of diabetic nephropathy. *Nephrol Dial Transplant.* **12**, 43-50.
- Evans, J. L., Goldfine, I. D., Maddux, B. A. and Grodsky, G. M.** (2002). Oxidative stress and stress-activated signaling pathways: a unifying hypothesis of type 2 diabetes. *Endocr Rev.* **23**, 599-622.
- Ezura, Y., Chakravarti, S., Oldberg, A., Chervoneva, I. and Birk, D. E.** (2000) Differential expression of lumican and fibromodulin regulate collagen fibrillogenesis in developing mouse tendons. *J Cell Biol.* **151**, 779-88
- Falanga, V., Martin, T. A., Takagi, H., Kirsner, R. S., Helfman, T., Pardes, J. and Ochoa, M. S.** (1993). Low oxygen tension increases mRNA levels of alpha 1 (I) procollagen in human dermal fibroblasts. *J Cell Physiol.* **157**, 408-12.
- Fan, J. M., Ng, Y. Y., Hill, P. A., Nikolic-Paterson, D. J., Mu, W., Atkins, R. C. and Lan, H. Y.** (1999). Transforming growth factor-beta regulates tubular epithelial-myofibroblast transdifferentiation in vitro. *Kidney Int.* **56**, 1455-67.
- Fawcett, J. and Rabkin, R.** (1995). The processing of insulin-like growth factor-I (IGF-I) by a cultured kidney cell line is altered by IGF-binding protein-3. *Endocrinol.* **136**, 1340-7.
- Feng, J. F., Readon, M., Yadav, S. P. and Im, M. J.** (1999). Calreticulin down-regulates both GTP binding and transglutaminase activities of transglutaminase II. *Biochemistry.* **38**, 10743-9.
- Feng, L., Tang, W. W., Loskutoff, D. J. and Wilson, C. B.** (1993). Dysfunction of glomerular fibrinolysis in experimental antiglomerular basement membrane antibody glomerulonephritis. *J Am Soc Nephrol.* **3**, 1753-64.
- Fesus, L.** (1998). Transglutaminase-catalyzed protein cross-linking in the molecular program of apoptosis and its relationship to neuronal processes. *Cell Mol Neurobiol.* **18**, 683-94.

- Fesus, L., Horvath, A. and Harsfalvi, J.** (1983). Interaction between tissue transglutaminase and phospholipid vesicles. *FEBS Lett.* **155**, 1-5.
- Fesus, L., Nagy, L., Basilion, J. P. and Davies, P. J.** (1991). Retinoic acid receptor transcripts in human umbilical vein endothelial cells. *Biochem Biophys Res Commun.* **179**, 32-8.
- Fesus, L., Thomazy, V. and Falus, A.** (1987). Induction and activation of tissue transglutaminase during programmed cell death. *FEBS Lett.* **224**, 104-8.
- Fields, G. B.** (1991). A model for interstitial collagen catabolism by mammalian collagenases. *J Theor Biol.* **153**, 585-602.
- Fine, L. G., Bandyopadhyay, D. and Norman, J. T.** (2000). Is there a common mechanism for the progression of different types of renal diseases other than proteinuria? Towards the unifying theme of chronic hypoxia. *Kidney Int Suppl.* **57**, S22-6.
- Fine, L. G., Orphanides, C. and Norman, J. T.** (1998). Progressive renal disease: the chronic hypoxia hypothesis. *Kidney Int Suppl.* **65**, S74-8.
- Fischer, E., Mougenot, B., Callard, P., Ronco, P. and Rossert, J.** (2000). Abnormal expression of glomerular basement membrane laminins in membranous glomerulonephritis. *Nephrol Dial Transplant.* **15**, 1956-64.
- Fitzgerald, M. L., Wang, Z., Park, P. W., Murphy, G. and Bernfield M.** (2000) Shedding of syndecan-1 and -4 ectodomains is regulated by multiple signalling pathways and mediated by a timp-3 sensitive metalloproteinase. *J Cell Biol.* **148**, 811-24.
- Floege, J., Alpers, C. E., Burns, M. W., Pritzl, P., Gordon, K., Couser, W. G. and Johnson, R. J.** (1992a). Glomerular cells, extracellular matrix accumulation, and the development of glomerulosclerosis in the remnant kidney model. *Lab Invest.* **66**, 485-97.
- Floege, J., Burns, M. W., Alpers, C. E., Yoshimura, A., Pritzl, P., Gordon, K., Seifert, R. A., Bowen-Pope, D. F., Couser, W. G. and Johnson, R. J.** (1992b). Glomerular cell proliferation and PDGF expression precede glomerulosclerosis in the remnant kidney model. *Kidney Int.* **41**, 297-309.
- Floege, J., Johnson, R. J., Gordon, K., Iida, H., Pritzl, P., Yoshimura, A., Campbell, C., Alpers, C. E. and Couser, W. G.** (1991). Increased synthesis of extracellular matrix in mesangial proliferative nephritis. *Kidney Int.* **40**, 477-88.
- Floege, J., Johnson, R. J., Gordon, K., Yoshimura, A., Campbell, C., Iruela-Arispe, L., Alpers, C. E. and Couser, W. G.** (1992c). Altered glomerular extracellular matrix synthesis in experimental membranous nephropathy. *Kidney Int.* **42**, 573-85.
- Fogerty, F. J., Akiyama, S. K., Yamada, K. M. and Mosher, D. F.** (1990). Inhibition of binding of fibronectin to matrix assembly sites by anti-integrin (alpha 5 beta 1) antibodies. *J Cell Biol.* **111**, 699-708.
- Folk, J. E.** (1983). Mechanism and basis for specificity of transglutaminase-catalyzed epsilon-(gamma-glutamyl) lysine bond formation. *Adv Enzymol Relat Areas Mol Biol.* **54**, 1-56.

- Fox, B. A., Yee, V. C., Pedersen, L. C., Le Trong, I., Bishop, P. D., Stenkamp, R. E. and Teller, D. C.** (1999). Identification of the calcium binding site and a novel ytterbium site in blood coagulation factor XIII by x-ray crystallography. *J Biol Chem.* **274**, 4917-23.
- Francki, A., Bradshaw, A. D., Bassuk, J. A., Howe, C. C., Couser, W. G. and Sage, E. H.** (1999). SPARC regulates the expression of collagen type I and transforming growth factor-beta1 in mesangial cells. *J Biol Chem.* **274**, 32145-52.
- Francki, A., McClure, T. D., Brekken, R. A., Motamed, K., Murri, C., Wang, T. and Sage, E. H.** (2004). SPARC regulates TGF-beta1-dependent signaling in primary glomerular mesangial cells. *J Cell Biochem.* **91**, 915-25.
- Fraser, D., Brunskill, N., Ito, T. and Phillips, A.** (2003). Long-term exposure of proximal tubular epithelial cells to glucose induces transforming growth factor-beta 1 synthesis via an autocrine PDGF loop. *Am J Pathol.* **163**, 2565-74.
- Fround, K. F., K. Doshi, and S. Gaul.** (1994). Transglutaminase inhibition by 2-[(2-oxopropyl) 10] Imidazolium Derivatives: Mechanism of Factor IIIa Inactivation. *Biochemistry.* **33**, 10109-10119.
- Fukui, M., Nakamura, T., Ebihara, I., Makita, Y., Osada, S., Tomino, Y. and Koide, H.** (1994). Effects of enalapril on endothelin-1 and growth factor gene expression in diabetic rat glomeruli. *J Lab Clin Med.* **123**, 763-8.
- Funabiki, K., Horikoshi, S., Tomino, Y., Nagai, Y. and Koide, H.** (1990). Immunohistochemical analysis of extracellular components in the glomerular sclerosis of patients with glomerulonephritis. *Clin Nephrol.* **34**, 239-46.
- Gard, D. L. and Lazarides, E.** (1979). Specific fluorescent labeling of chicken myofibril Z-line proteins catalyzed by guinea pig liver transglutaminase. *J Cell Biol.* **81**, 336-47.
- Gates, R. E.** (1991). Elimination of interfering substances in the presence of detergent in the bicinchoninic acid protein assay. *Anal Biochem.* **196**, 290-5.
- Gaudry, C. A., Verderio, E., Aeschlimann, D., Cox, A., Smith, C. and Griffin, M.** (1999a). Cell surface localization of tissue transglutaminase is dependent on a fibronectin-binding site in its N-terminal beta-sandwich domain. *J Biol Chem.* **274**, 30707-14.
- Gaudry, C. A., Verderio, E., Jones, R. A., Smith, C. and Griffin, M.** (1999b). Tissue transglutaminase is an important player at the surface of human endothelial cells: evidence for its externalization and its colocalization with the beta(1) integrin. *Exp Cell Res.* **252**, 104-13.
- Gekle, M., Knaus, P., Nielsen, R., Mildenerger, S., Freudinger, R., Wohlfarth, V., Sauvant, C. and Christensen, E. I.** (2003). Transforming growth factor-beta1 reduces megalin- and cubilin-mediated endocytosis of albumin in proximal-tubule-derived opossum kidney cells. *J Physiol.* **552**, 471-81.
- Gentile, V., Saydak, M., Chiocca, E. A., Akande, O., Birckbichler, P. J., Lee, K. N., Stein, J. P. and Davies, P. J.** (1991). Isolation and characterization of cDNA clones to mouse macrophage and human endothelial cell tissue transglutaminases. *J Biol Chem.* **266**, 478-83.

- Gentile, V., Thomazy, V., Piacentini, M., Fesus, L. and Davies, P. J.** (1992). Expression of tissue transglutaminase in Balb-C 3T3 fibroblasts: effects on cellular morphology and adhesion. *J Cell Biol.* **119**, 463-74.
- George, M. D., Vollberg, T. M., Floyd, E. E., Stein, J. P. and Jetten, A. M.** (1990). Regulation of transglutaminase type II by transforming growth factor-beta 1 in normal and transformed human epidermal keratinocytes. *J Biol Chem.* **265**, 11098-104.
- Ghosh, A. K.** (2002). Factors involved in the regulation of type I collagen gene expression: implication in fibrosis. *Exp Biol Med (Maywood).* **227**, 301-14.
- Giannelli, G., Falk-Marzillier, J., Schiraldi, O., Stetler-Stevenson, W. G. and Quaranta, V.** (1997). Induction of cell migration by matrix metalloprotease-2 cleavage of laminin-5. *Science.* **277**, 225-8.
- Glass, W. F., 2nd, Kreisberg, J. I. and Troyer, D. A.** (1993). Two-chain urokinase, receptor, and type 1 inhibitor in cultured human mesangial cells. *Am J Physiol Renal Physiol.* **264**, F532-9.
- Gleadle, J. M., Ebert, B. L., Firth, J. D. and Ratcliffe, P. J.** (1995). Regulation of angiogenic growth factor expression by hypoxia, transition metals, and chelating agents. *Am J Physiol Cell Physiol.* **268**, C1362-8.
- Gohring, W., Sasaki, T., Heldin, C. H. and Timpl, R.** (1998). Mapping of the binding of platelet-derived growth factor to distinct domains of the basement membrane proteins BM-40 and perlecan and distinction from the BM-40 collagen-binding epitope. *Eur J Biochem.* **255**, 60-6.
- Goldberg, H., Helaakoski, T., Garrett, L. A., Karsenty, G., Pellegrino, A., Lozano, G., Maity, S. and de Crombrughe, B.** (1992). Tissue-specific expression of the mouse alpha 2(I) collagen promoter. Studies in transgenic mice and in tissue culture cells. *J Biol Chem.* **267**, 19622-30.
- Goldberg, M. A., Dunning, S. P. and Bunn, H. F.** (1988). Regulation of the erythropoietin gene: evidence that the oxygen sensor is a heme protein. *Science.* **242**, 1412-5.
- Golovchenko, I., Goalstone, M. L., Watson, P., Brownlee, M. and Draznin, B.** (2000). Hyperinsulinemia enhances transcriptional activity of nuclear factor-kappaB induced by angiotensin II, hyperglycemia, and advanced glycosylation end products in vascular smooth muscle cells. *Circ Res.* **87**, 746-52.
- Gomez, D. E., Alonso, D. F., Yoshiji, H. and Thorgeirsson, U. P.** (1997). Tissue inhibitors of metalloproteinases: structure, regulation and biological functions. *Eur J Cell Biol.* **74**, 111-22.
- Gomis-Ruth, F. X., Gohlke, U., Betz, M., Knauper, V., Murphy, G., Lopez-Otin, C. and Bode, W.** (1996). The helping hand of collagenase-3 (MMP-13): 2.7 Å crystal structure of its C-terminal haemopexin-like domain. *J Mol Biol.* **264**, 556-66.
- Gomis-Ruth, F. X., Maskos, K., Betz, M., Bergner, A., Huber, R., Suzuki, K., Yoshida, N., Nagase, H., Brew, K., Bourenkov, G. P. et al.** (1997). Mechanism of inhibition of the human matrix metalloproteinase stromelysin-1 by TIMP-1. *Nature.* **389**, 77-81.

- Goumenos, D., Tsomi, K., Iatrou, C., Oldroyd, S., Sungur, A., Papaioannides, D., Moustakas, G., Ziroyannis, P., Mountokalakis, T. and El Nahas, A. M.** (1998). Myofibroblasts and the progression of crescentic glomerulonephritis. *Nephrol Dial Transplant*. **13**, 1652-61.
- Goumenos, D. S., Tsamandas, A. C., Oldroyd, S., Sotsiou, F., Tsakas, S., Petropoulou, C., Bonikos, D., El Nahas, A. M. and Vlachojannis, J. G.** (2001). Transforming growth factor-beta(1) and myofibroblasts: a potential pathway towards renal scarring in human glomerular disease. *Nephron*. **87**, 240-8.
- Grams, F., Crimmin, M., Hinnes, L., Huxley, P., Pieper, M., Tschesche, H. and Bode, W.** (1995). Structure determination and analysis of human neutrophil collagenase complexed with a hydroxamate inhibitor. *Biochemistry*. **34**, 14012-20.
- Gratzer, P. F., Santerre, J. P. and Lee, J. M.** (2004). Modulation of collagen proteolysis by chemical modification of amino acid side-chains in acellularized arteries. *Biomaterials*. **25**, 2081-94.
- Gratzer, P. F., Santerre, J. P. and Lee, J. M.** (2006). The effect of chemical modification of amino acid side-chains on collagen degradation by enzymes. *J Biomed Mater Res B Appl Biomater*. **21**, 21.
- Greenberg, C., Birckbichler, P. and Rice, R.** (1991). Transglutaminases: Multifunctional enzymes that stabilise tissues. *FEBS Lett* **5**, 3071-3077.
- Greiber, S., Kramer-Guth, A., Pavenstadt, H., Gutenkunst, M., Schollmeyer, P. and Wanner, C.** (1996). Effects of lipoprotein(a) on mesangial cell proliferation and viability. *Nephrol Dial Transplant*. **11**, 778-85.
- Grenard, P., Bresson-Hadni, S., El Alaoui, S., Chevallier, M., Vuitton, D. A. and Ricard-Blum, S.** (2001). Transglutaminase-mediated cross-linking is involved in the stabilization of extracellular matrix in human liver fibrosis. *J Hepatol*. **35**, 367-75.
- Griffin, K. A., Picken, M. and Bidani, A. K.** (1994). Radiotelemetric BP monitoring, antihypertensives and glomeruloprotection in remnant kidney model. *Kidney Int*. **46**, 1010-8.
- Griffin, M., Casadio, R. and Bergamini, C. M.** (2002). Transglutaminases: nature's biological glues. *Biochem J*. **368**, 377-96.
- Griffin M, C. I. G., and Saint. R.,** (2004). Novel Compounds and Methods of Using The Same. In *International Publication Number WO 2004/113363*, pp. PCT/GB2004/002569. GB Patent.
- Griffin, M., Smith, L. L. and Wynne, J.** (1979). Changes in transglutaminase activity in an experimental model of pulmonary fibrosis induced by paraquat. *Br J Exp Pathol*. **60**, 653-61.
- Griffin, M. and Wilson, J.** (1984). Detection of epsilon(gamma-glutamyl) lysine. *Mol Cell Biochem*. **58**, 37-49.
- Grobelny, D., Poncz, L. and Galardy, R. E.** (1992). Inhibition of human skin fibroblast collagenase, thermolysin, and *Pseudomonas aeruginosa* elastase by peptide hydroxamic acids. *Biochemistry*. **31**, 7152-4.

- Groenen, P. J., Bloemendal, H. and de Jong, W. W.** (1992). The carboxy-terminal lysine of alpha B-crystallin is an amine-donor substrate for tissue transglutaminase. *Eur J Biochem.* **205**, 671-4.
- Groenen, P. J., Smulders, R. H., Peters, R. F., Grootjans, J. J., van den Ijssel, P. R., Bloemendal, H. and de Jong, W. W.** (1994). The amine-donor substrate specificity of tissue-type transglutaminase. Influence of amino acid residues flanking the amine-donor lysine residue. *Eur J Biochem.* **220**, 795-9.
- Groffen, A.J., Hop, F. W., Tryggvason, K., Dijkman, H., Assman, K. J., Veerkamp, J. H., Monnens, L.A. and Van den Heival, L. P.** (1997) Evidence for the existence of multiple heparin sulphate proteoglycans in the human glomerular basement membrane and mesangial matrix. *Eur J Biochem.* **247**, 175-82.
- Groffen, A. J., Ruegg, M. A., Dijkman, H., van de Velden, T. J., Buskens, C. A., van den Born, J., Assmann, K. J., Monnens, L. A., Veerkamp, J. H. and van den Heuvel, L. P.** (1998). Agrin is a major heparan sulfate proteoglycan in the human glomerular basement membrane. *J Histochem Cytochem.* **46**, 19-27.
- Groffen, A. J., Veerkamp, J. H., Monnens, L. A. and van den Heuvel, L. P.** (1999). Recent insights into the structure and functions of heparan sulfate proteoglycans in the human glomerular basement membrane. *Nephrol Dial Transplant.* **14**, 2119-29.
- Grootjans, J. J., Groenen, P. J. and de Jong, W. W.** (1995). Substrate requirements for transglutaminases. Influence of the amino acid residue preceding the amine donor lysine in a native protein. *J Biol Chem.* **270**, 22855-8.
- Gross, S. R., Balklava, Z. and Griffin, M.** (2003). Importance of tissue transglutaminase in repair of extracellular matrices and cell death of dermal fibroblasts after exposure to a solarium ultraviolet A source. *J Invest Dermatol.* **121**, 412-23.
- Gruden, G., Thomas, S., Burt, D., Lane, S., Chusney, G., Sacks, S. and Viberti, G.** (1997). Mechanical stretch induces vascular permeability factor in human mesangial cells: mechanisms of signal transduction. *Proc Natl Acad Sci U S A.* **94**, 12112-6.
- Gu, Z., Kaul, M., Yan, B., Kridel, S. J., Cui, J., Strongin, A., Smith, J. W., Liddington, R. C. and Lipton, S. A.** (2002). S-nitrosylation of matrix metalloproteinases: signaling pathway to neuronal cell death. *Science.* **297**, 1186-90.
- Ha, H. and Kim, K. H.** (1999). Pathogenesis of diabetic nephropathy: the role of oxidative stress and protein kinase C. *Diabetes Res Clin Pract.* **45**, 147-51.
- Ha, H. and Lee, H. B.** (2000). Reactive oxygen species as glucose signaling molecules in mesangial cells cultured under high glucose. *Kidney Int Suppl.* **77**, S19-25.
- Ha, H. and Lee, H. B.** (2003). Reactive oxygen species and matrix remodeling in diabetic kidney. *J Am Soc Nephrol.* **14**, S246-9.
- Haase, V. H.** (2006). Hypoxia-inducible factors in the kidney. *Am J Physiol Renal Physiol.* **291**, F271-81.

- Haberstroh, U., Zahner, G., Disser, M., Thaiss, F., Wolf, G. and Stahl, R. A.** (1993). TGF-beta stimulates rat mesangial cell proliferation in culture: role of PDGF beta-receptor expression. *Am J Physiol Renal Physiol.* **264**, F199-205.
- Haddad, J. J.** (2002). Redox regulation of pro-inflammatory cytokines and IkappaB-alpha/NF-kappaB nuclear translocation and activation. *Biochem Biophys Res Commun.* **296**, 847-56.
- Hahn-Dantona, E., Ruiz, J. F., Bornstein, P. and Strickland, D. K.** (2001). The low density lipoprotein receptor-related protein modulates levels of matrix metalloproteinase 9 (MMP-9) by mediating its cellular catabolism. *J Biol Chem.* **276**, 15498-503.
- Hajjar, K. A. and Acharya, S. S.** (2000). Annexin II and regulation of cell surface fibrinolysis. *Ann N Y Acad Sci.* **902**, 265-71.
- Hallmann, R., Horn, N., Selg, M., Wendler, O., Pausch, F. and Sorokin, L. M.** (2005). Expression and function of laminins in the embryonic and mature vasculature. *Physiol Rev.* **85**, 979-1000.
- Hamano, K., Iwano, M., Akai, Y., Sato, H., Kubo, A., Nishitani, Y., Uyama, H., Yoshida, Y., Miyazaki, M., Shiiki, H. et al.** (2002). Expression of glomerular plasminogen activator inhibitor type 1 in glomerulonephritis. *Am J Kidney Dis.* **39**, 695-705.
- Hampf, M. and Gossen, M.** (2007) Promoter crosstalk effects on gene expression. *J. Mol Biol.* **365**, 911-20.
- Hangai, M., Kitaya, N., Xu, J., Chan, C. K., Kim, J. J., Werb, Z., Ryan, S. J. and Brooks, P. C.** (2002). Matrix metalloproteinase-9-dependent exposure of a cryptic migratory control site in collagen is required before retinal angiogenesis. *Am J Pathol.* **161**, 1429-37.
- Hanrahan, D.** (1983). Studies and transformation of Escherichia coli with plasmids. *J Mol Biol.* **166**, 557-562.
- Hao, J. L., Nagano, T., Nakamura, M., Kumagai, N., Mishima, H. and Nishida, T.** (1999). Effect of galardin on collagen degradation by Pseudomonas aeruginosa. *Exp Eye Res.* **69**, 595-601.
- Haralson, M. A., Jacobson, H. R. and Hoover, R. L.** (1987). Collagen polymorphism in cultured rat kidney mesangial cells. *Lab Invest.* **57**, 513-23.
- Haroon, Z. A., Lai, T. S., Hettasch, J. M., Lindberg, R. A., Dewhirst, M. W. and Greenberg, C. S.** (1999). Tissue transglutaminase is expressed as a host response to tumor invasion and inhibits tumor growth. *Lab Invest.* **79**, 1679-86.
- Harris, D. C., Chan, L. and Schrier, R. W.** (1988). Remnant kidney hypermetabolism and progression of chronic renal failure. *Am J Physiol Renal Physiol.* **254**, F267-76.
- Harris, D. C., Tay, Y. C., Chen, J., Chen, L. and Nankivell, B. J.** (1995). Mechanisms of iron-induced proximal tubule injury in rat remnant kidney. *Am J Physiol Renal Physiol.* **269**, F218-24.
- Harris, R. C. and Neilson, E. G.** (2006). Toward a unified theory of renal progression. *Annu Rev Med.* **57**, 365-80.

- Harrison, C. A., Layton, C. M., Hau, Z., Bullock, A. J., Johnson, T. S. and Macneil, S.** (2007). Transglutaminase inhibitors induce hyperproliferation and parakeratosis in tissue-engineered skin. *Br J Dermatol.* **156**, 247-57.
- Harsfalvi, J., Arato, G. and Fesus, L.** (1987). Lipids associated with tissue transglutaminase. *Biochim Biophys Acta.* **923**, 42-5.
- Hartwig, S., Hu, M. C., Cella, C., Piscione, T., Filmus, J. and Rosenblum, N. D.** (2005). Glypican-3 modulates inhibitory Bmp2-Smad signaling to control renal development in vivo. *Mech Dev.* **122**, 928-38.
- Hasselaar, P. and Sage, E. H.** (1992). SPARC antagonizes the effect of basic fibroblast growth factor on the migration of bovine aortic endothelial cells. *J Cell Biochem.* **49**, 272-83.
- Heino, J.** (2000) The collagen receptor integrins have distinct ligand recognition and signalling functions. *Matrix Biol.* **19**, 319-23.
- Henry, M. D. and Campbell, K. P.** (1998). A role for dystroglycan in basement membrane assembly. *Cell.* **95**, 859-70.
- Henry, M. D., Satz, J. S., Brakebusch, C., Costell, M., Gustafsson, E., Fassler, R. and Campbell, K. P.** (2001). Distinct roles for dystroglycan, beta1 integrin and perlecan in cell surface laminin organization. *J Cell Sci.* **114**, 1137-44.
- Heremans, A., van der Schueren, B., de Cock, B., Paulsson, M., Cassiman, J. J., van den Berghe, H. and David, G.** (1989). Matrix-associated heparan sulfate proteoglycan: core protein-specific monoclonal antibodies decorate the pericellular matrix of connective tissue cells and the stromal side of basement membranes. *J Cell Biol.* **109**, 3199-211.
- Hertig, A., Berrou, J., Allory, Y., Breton, L., Commo, F., Costa De Beauregard, M. A., Carmeliet, P. and Rondeau, E.** (2003). Type 1 plasminogen activator inhibitor deficiency aggravates the course of experimental glomerulonephritis through overactivation of transforming growth factor beta. *FASEB J.* **17**, 1904-6.
- Hidalgo, M. and Eckhardt, S. G.** (2001). Development of matrix metalloproteinase inhibitors in cancer therapy. *J Natl Cancer Inst.* **93**, 178-93.
- Higashi, S. and Miyazaki, K.** (1999). Reactive site-modified tissue inhibitor of metalloproteinases-2 inhibits the cell-mediated activation of progelatinase A. *J Biol Chem.* **274**, 10497-504.
- Hildebrand, A., Romaris, M., Rasmussen, L. M., Heinegard, D., Twardzik, D. R., Border, W. A. and Ruoslahti, E.** (1994). Interaction of the small interstitial proteoglycans biglycan, decorin and fibromodulin with transforming growth factor beta. *Biochem J.* **302**, 527-34.
- Hocking, D. C., Sottile, J., Reho, T., Fassler, R. and McKeown-Longo, P. J.** (1999). Inhibition of fibronectin matrix assembly by the heparin-binding domain of vitronectin. *J Biol Chem.* **274**, 27257-64.
- Holland, P. W., Harper, S. J., McVey, J. H. and Hogan, B. L.** (1987). In vivo expression of mRNA for the Ca⁺⁺-binding protein SPARC (osteonectin) revealed by in situ hybridization. *J Cell Biol.* **105**, 473-82.

- Hostetter, T. H., Olson, J. L., Rennke, H. G., Venkatachalam, M. A. and Brenner, B. M.** (1981). Hyperfiltration in remnant nephrons: a potentially adverse response to renal ablation. *Am J Physiol Renal Physiol.* **241**, F85-93.
- Hsieh, T. J., Zhang, S. L., Filep, J. G., Tang, S. S., Ingelfinger, J. R. and Chan, J. S.** (2002). High glucose stimulates angiotensinogen gene expression via reactive oxygen species generation in rat kidney proximal tubular cells. *Endocrinol.* **143**, 2975-85.
- Hu, K., Yang, J., Tanaka, S., Gonias, S. L., Mars, W. M. and Liu, Y.** (2006). Tissue-type plasminogen activator acts as a cytokine that triggers intracellular signal transduction and induces matrix metalloproteinase-9 gene expression. *J Biol Chem.* **281**, 2120-7.
- Hu, Q. and Maity, S. N.** (2000). Stable expression of a dominant negative mutant of CCAAT binding factor/NF-Y in mouse fibroblast cells resulting in retardation of cell growth and inhibition of transcription of various cellular genes. *J Biol Chem.* **275**, 4435-44.
- Huang, L.** (2006). Transglutaminase inhibition in experimental diabetic nephropathy : the role of tissue transglutaminase in latent TGF-beta activation and transglutaminase mediated cell death. *Ph.D thesis*: University of Sheffield.
- Huang, L. E., Gu, J., Schau, M. and Bunn, H. F.** (1998). Regulation of hypoxia-inducible factor 1alpha is mediated by an O₂-dependent degradation domain via the ubiquitin-proteasome pathway. *Proc Natl Acad Sci U S A.* **95**, 7987-92.
- Hughes, P. E., Renshaw, M. W., Pfaff, M., Forsyth, J., Keivens, V. M., Schwartz, M. A. and Ginsberg, M. H.** (1997). Suppression of integrin activation: a novel function of a Ras/Raf-initiated MAP kinase pathway. *Cell.* **88**, 521-30.
- Hugo, C., Kang, D. H. and Johnson, R. J.** (2002). Sustained expression of thrombospondin-1 is associated with the development of glomerular and tubulointerstitial fibrosis in the remnant kidney model. *Nephron.* **90**, 460-70.
- Hui, W., Rowan, A. D. and Cawston, T.** (2001). Modulation of the expression of matrix metalloproteinase and tissue inhibitors of metalloproteinases by TGF-beta1 and IGF-1 in primary human articular and bovine nasal chondrocytes stimulated with TNF-alpha. *Cytokine.* **16**, 31-5.
- Hwang, K. C., Gray, C. D., Sivasubramanian, N. and Im, M. J.** (1995). Interaction site of GTP binding Gh (transglutaminase II) with phospholipase C. *J Biol Chem.* **270**, 27058-62.
- Ichinose, A., Fujikawa, K. and Suyama, T.** (1986). The activation of pro-urokinase by plasma kallikrein and its inactivation by thrombin. *J Biol Chem.* **261**, 3486-9.
- Ichinose, A., Kisiel, W. and Fujikawa, K.** (1984). Proteolytic activation of tissue plasminogen activator by plasma and tissue enzymes. *FEBS Lett.* **175**, 412-8.
- Ihn, H., Ohnishi, K., Tamaki, T., LeRoy, E. C. and Trojanowska, M.** (1996). Transcriptional regulation of the human alpha2(I) collagen gene. Combined action of upstream stimulatory and inhibitory cis-acting elements. *J Biol Chem.* **271**, 26717-23.
- Iismaa, S. E.** (2002). Structure and function of tissue transglutaminase. *Minerva Biotechnologica.* **14**, 113-119.

- Iismaa, S. E., Wu, M. J., Nanda, N., Church, W. B. and Graham, R. M.** (2000). GTP binding and signaling by Gh/transglutaminase II involves distinct residues in a unique GTP-binding pocket. *J Biol Chem.* **275**, 18259-65.
- Ikura, K., Kita, K., Fujita, I., Hashimoto, H. and Kawabata, N.** (1998). Identification of amine acceptor protein substrates of transglutaminase in liver extracts: use of 5-(biotinamido) pentylamine as a probe. *Arch Biochem Biophys.* **356**, 280-6.
- Ikura, K., Nasu, T., Yokota, H., Tsuchiya, Y., Sasaki, R. and Chiba, H.** (1988). Amino acid sequence of guinea pig liver transglutaminase from its cDNA sequence. *Biochemistry.* **27**, 2898-905.
- Ikura, K., Shinagawa, R., Suto, N. and Sasaki, R.** (1994). Increase caused by interleukin-6 in promoter activity of guinea pig liver transglutaminase gene. *Biosci Biotechnol Biochem.* **58**, 1540-1.
- Ikura, K., Yokota, H., Sasaki, R. and Chiba, H.** (1989). Determination of amino- and carboxyl-terminal sequences of guinea pig liver transglutaminase: evidence for amino-terminal processing. *Biochemistry.* **28**, 2344-8.
- Im, M. J., Russell, M. A. and Feng, J. F.** (1997). Transglutaminase II: a new class of GTP-binding protein with new biological functions. *Cell Signal.* **9**, 477-82.
- Imai, K., Hiramatsu, A., Fukushima, D., Pierschbacher, M. D. and Okada, Y.** (1997). Degradation of decorin by matrix metalloproteinases: identification of the cleavage sites, kinetic analyses and transforming growth factor-beta1 release. *Biochem J.* **322**, 809-14.
- Imig, J. D. and Incho, E. W.** (2002). Adaptations of the renal microcirculation to hypertension. *Microcirculation.* **9**, 315-28.
- Iredale, J. P., Benyon, R. C., Arthur, M. J., Ferris, W. F., Alcolado, R., Winwood, P. J., Clark, N. and Murphy, G.** (1996). Tissue inhibitor of metalloproteinase-1 messenger RNA expression is enhanced relative to interstitial collagenase messenger RNA in experimental liver injury and fibrosis. *Hepatology.* **24**, 176-84.
- Ishidoya, S., Morrissey, J., McCracken, R. and Klahr, S.** (1996). Delayed treatment with enalapril halts tubulointerstitial fibrosis in rats with obstructive nephropathy. *Kidney Int.* **49**, 1110-9.
- Ishii, I. and Ui, M.** (1994). Retinoic acid-induced gene expression of tissue transglutaminase via protein kinase C-dependent pathway in mouse peritoneal macrophages. *J Biochem (Tokyo).* **115**, 1197-202.
- Ishimura, E., Sterzel, R. B., Budde, K. and Kashgarian, M.** (1989). Formation of extracellular matrix by cultured rat mesangial cells. *Am J Pathol.* **134**, 843-55.
- Ishola, D. A., Jr., Post, J. A., van Timmeren, M. M., Bakker, S. J., Goldschmeding, R., Koomans, H. A., Braam, B. and Joles, J. A.** (2006). Albumin-bound fatty acids induce mitochondrial oxidant stress and impair antioxidant responses in proximal tubular cells. *Kidney Int.* **70**, 724-31.
- Iwai, N., Shimoike, H. and Kinoshita, M.** (1995). Genes up-regulated in hypertrophied ventricle. *Biochem Biophys Res Commun.* **209**, 527-34.

- Iwamoto, T., Nakashima, Y. and Sueishi, K.** (1990). Secretion of plasminogen activator and its inhibitor by glomerular epithelial cells. *Kidney Int.* **37**, 1466-76.
- Jackson, B., Debrevi, L., Cubela, R., Whitty, M. and Johnston, C. I.** (1986). Preservation of renal function in the rat remnant kidney model of chronic renal failure by blood pressure reduction. *Clin Exp Pharmacol Physiol.* **13**, 319-23.
- Jacobsen, P., Rossing, K., Tarnow, L., Rossing, P., Mallet, C., Poirier, O., Cambien, F. and Parving, H. H.** (1999). Progression of diabetic nephropathy in normotensive type 1 diabetic patients. *Kidney Int Suppl.* **71**, S101-5.
- Jakobsen, E. and Godal, H. C.** (1974). Simple, semiquantitative test for partial factor XIII (FSF) deficiency. *Scand J Haematol.* **12**, 366-8.
- Jalalah, S. M., Furness, P. N., Barker, G., Thomas, M., Hall, L. L., Bicknell, G. R., Shaw, J. A. and Pringle, J. H.** (2000). Inactive matrix metalloproteinase 2 is a normal constituent of human glomerular basement membrane. An immuno-electron microscopic study. *J Pathol.* **191**, 61-6.
- Janmey, P. A. and Weitz, D. A.** (2004). Dealing with mechanics: mechanisms of force transduction in cells. *Trends Biochem Sci.* **29**, 364-70.
- Jarusiripipat, C., Shapiro, J. I., Chan, L. and Schrier, R. W.** (1991). Reduction of remnant nephron hypermetabolism by protein restriction. *Am J Kidney Dis.* **18**, 367-74.
- Jeong, J. M., Murthy, S. N., Radek, J. T. and Lorand, L.** (1995). The fibronectin-binding domain of transglutaminase. *J Biol Chem.* **270**, 5654-8.
- Jimenez, S. A., Varga, J., Olsen, A., Li, L., Diaz, A., Herhal, J. and Koch, J.** (1994). Functional analysis of human alpha 1(I) procollagen gene promoter. Differential activity in collagen-producing and -nonproducing cells and response to transforming growth factor beta 1. *J Biol Chem.* **269**, 12684-91.
- Jinde, K., Nikolic-Paterson, D. J., Huang, X. R., Sakai, H., Kurokawa, K., Atkins, R. C. and Lan, H. Y.** (2001). Tubular phenotypic change in progressive tubulointerstitial fibrosis in human glomerulonephritis. *Am J Kidney Dis.* **38**, 761-9.
- John, R., Webb, M., Young, A. and Stevens, P. E.** (2004). Unreferred chronic kidney disease: a longitudinal study. *Am J Kidney Dis.* **43**, 825-35.
- Johnson, K. A., van Etten, D., Nanda, N., Graham, R. M. and Terkeltaub, R. A.** (2003a). Distinct transglutaminase 2-independent and transglutaminase 2-dependent pathways mediate articular chondrocyte hypertrophy. *J Biol Chem.* **278**, 18824-32.
- Johnson, R. J., Floege, J., Yoshimura, A., Iida, H., Couser, W. G. and Alpers, C. E.** (1992). The activated mesangial cell: a glomerular "myofibroblast"? *J Am Soc Nephrol.* **2**, S190-7.
- Johnson, T. S., Abo-Zenah, H., Skill, J. N., Bex, S., Wild, G., Brown, C. B., Griffin, M. and El Nahas, A. M.** (2004). Tissue transglutaminase: a mediator and predictor of chronic allograft nephropathy? *Transplantation.* **77**, 1667-75.

- Johnson, T. S., El-Koraie, A. F., Skill, N. J., Baddour, N. M., El Nahas, A. M., Njloma, M., Adam, A. G. and Griffin, M.** (2003b). Tissue transglutaminase and the progression of human renal scarring. *J Am Soc Nephrol.* **14**, 2052-62.
- Johnson, T. S., Griffin, M., Thomas, G. L., Skill, J., Cox, A., Yang, B., Nicholas, B., Birckbichler, P. J., Muchaneta-Kubara, C. and El Nahas, A. M.** (1997). The role of transglutaminase in the rat subtotal nephrectomy model of renal fibrosis. *J Clin Invest.* **99**, 2950-60.
- Johnson, T. S., Haylor, J. L., Thomas, G. L., Fisher, M. and El Nahas, A. M.** (2002). Matrix metalloproteinases and their inhibitors in experimental renal scarring. *Exp Nephrol.* **10**, 182-95.
- Johnson, T. S., Knight, C. R., el-Alaoui, S., Mian, S., Rees, R. C., Gentile, V., Davies, P. J. and Griffin, M.** (1994). Transfection of tissue transglutaminase into a highly malignant hamster fibrosarcoma leads to a reduced incidence of primary tumour growth. *Oncogene.* **9**, 2935-42.
- Johnson, T. S., Scholfield, C. I., Parry, J. and Griffin, M.** (1998). Induction of tissue transglutaminase by dexamethasone: its correlation to receptor number and transglutaminase-mediated cell death in a series of malignant hamster fibrosarcomas. *Biochem J.* **331**, 105-12.
- Johnson, T. S., Skill, N. J., El Nahas, A. M., Oldroyd, S. D., Thomas, G. L., Douthwaite, J. A., Haylor, J. L. and Griffin, M.** (1999). Transglutaminase transcription and antigen translocation in experimental renal scarring. *J Am Soc Nephrol.* **10**, 2146-57.
- Jones, C. L.** (1996). Matrix degradation in renal disease. *Nephrology.* **2**, 13-23.
- Jones, C. L., Buch, S., Post, M., McCulloch, L., Liu, E. and Eddy, A. A.** (1991). Pathogenesis of interstitial fibrosis in chronic purine aminonucleoside nephrosis. *Kidney Int.* **40**, 1020-31.
- Jones, R. A., Nicholas, B., Mian, S., Davies, P. J. and Griffin, M.** (1997). Reduced expression of tissue transglutaminase in a human endothelial cell line leads to changes in cell spreading, cell adhesion and reduced polymerisation of fibronectin. *J Cell Sci.* **110**, 2461-72.
- Jozic, D., Bourenkov, G., Lim, N. H., Visse, R., Nagase, H., Bode, W. and Maskos, K.** (2005). X-ray structure of human proMMP-1: new insights into procollagenase activation and collagen binding. *J Biol Chem.* **280**, 9578-85.
- Junaid, A., Rosenberg, M. E. and Hostetter, T. H.** (1997). Interaction of angiotensin II and TGF-beta 1 in the rat remnant kidney. *J Am Soc Nephrol.* **8**, 1732-8.
- Kaartinen, M. T., Pirhonen, A., Linnala-Kankkunen, A. and Maenpaa, P. H.** (1997). Transglutaminase-catalyzed cross-linking of osteopontin is inhibited by osteocalcin. *J Biol Chem.* **272**, 22736-41.
- Kagan, H. M. and Li, W.** (2003). Lysyl oxidase: properties, specificity, and biological roles inside and outside of the cell. *J Cell Biochem.* **88**, 660-72.
- Kallio, P. J., Wilson, W. J., O'Brien, S., Makino, Y. and Poellinger, L.** (1999). Regulation of the hypoxia-inducible transcription factor 1alpha by the ubiquitin-proteasome pathway. *J Biol Chem.* **274**, 6519-25.

- Kamanna, V. S.** (2002). Low density lipoproteins and mitogenic signal transduction processes: role in the pathogenesis of renal disease. *Histol Histopathol.* **17**, 497-505.
- Kamihagi, K., Katayama, M., Ouchi, R. and Kato, I.** (1994). Osteonectin/SPARC regulates cellular secretion rates of fibronectin and laminin extracellular matrix proteins. *Biochem Biophys Res Commun.* **200**, 423-8.
- Kamijo, A., Kimura, K., Sugaya, T., Yamanouchi, M., Hase, H., Kaneko, T., Hirata, Y., Goto, A., Fujita, T. and Omata, M.** (2002). Urinary free fatty acids bound to albumin aggravate tubulointerstitial damage. *Kidney Int.* **62**, 1628-37.
- Kanalas, J. J.** (1995). Analysis of the plasminogen system on rat glomerular epithelial cells. *Exp Cell Res.* **218**, 561-6.
- Kang, D. H., Hughes, J., Mazzali, M., Schreiner, G. F. and Johnson, R. J.** (2001). Impaired angiogenesis in the remnant kidney model: II. Vascular endothelial growth factor administration reduces renal fibrosis and stabilizes renal function. *J Am Soc Nephrol.* **12**, 1448-57.
- Karakurum, M., Shreeniwas, R., Chen, J., Pinsky, D., Yan, S. D., Anderson, M., Sunouchi, K., Major, J., Hamilton, T., Kuwabara, K. et al.** (1994). Hypoxic induction of interleukin-8 gene expression in human endothelial cells. *J Clin Invest.* **93**, 1564-70.
- Katavetin, P., Miyata, T., Inagi, R., Tanaka, T., Sassa, R., Ingelfinger, J. R., Fujita, T. and Nangaku, M.** (2006). High glucose blunts vascular endothelial growth factor response to hypoxia via the oxidative stress-regulated hypoxia-inducible factor/hypoxia-responsible element pathway. *J Am Soc Nephrol.* **17**, 1405-13.
- Kato, S., Nakagawa, N., Yano, Y., Satoh, K., Kohno, H. and Ohkubo, Y.** (1996). Transglutaminase induced by epidermal growth factor negatively regulates the growth signal in primary cultured hepatocytes. *Biochem J.* **313**, 305-9.
- Kato, T., Takahashi, K., Klahr, S., Reyes, A. A. and Badr, K. F.** (1994). Dietary supplementation with L-arginine ameliorates glomerular hypertension in rats with subtotal nephrectomy. *J Am Soc Nephrol.* **4**, 1690-4.
- Katsumi, A., Orr, A. W., Tzima, E. and Schwartz, M. A.** (2004). Integrins in mechanotransduction. *J Biol Chem.* **279**, 12001-4.
- Kawano, T., Morimoto, K. and Uemura, Y.** (1970). Partial purification and properties of urokinase inhibitor from human placenta. *J Biochem (Tokyo).* **67**, 333-42.
- Kazes, I., Delarue, F., Hagege, J., Bouzahir-Sima, L., Rondeau, E., Sraer, J. D. and Nguyen, G.** (1998). Soluble latent membrane-type 1 matrix metalloprotease secreted by human mesangial cells is activated by urokinase. *Kidney Int.* **54**, 1976-84.
- Kenichi, M., Masanobu, M., Takehiko, K., Shoko, T., Akira, F., Katsushige, A., Takashi, H., Yoshiyuki, O. and Shigeru, K.** (2004). Renal synthesis of urokinase type-plasminogen activator, its receptor, and plasminogen activator inhibitor-1 in diabetic nephropathy in rats: modulation by angiotensin-converting-enzyme inhibitor. *J Lab Clin Med.* **144**, 69-77.

- Kim, H., Oda, T., Lopez-Guisa, J., Wing, D., Edwards, D. R., Soloway, P. D. and Eddy, A. A.** (2001) Timp-1 deficiency does not attenuate interstitial fibrosis in obstructive nephropathy. *J Am Soc Nephrol.* **12**, 736-48.
- Kim, H. S., Shang, T., Chen, Z., Pflugfelder, S. C. and Li, D. Q.** (2004). TGF-beta1 stimulates production of gelatinase (MMP-9), collagenases (MMP-1, -13) and stromelysins (MMP-3, -10, -11) by human corneal epithelial cells. *Exp Eye Res.* **79**, 263-74.
- Kim, Y. K., Lee, S. K., Ha, M. S., Woo, J. S. and Jung, J. S.** (2002). Differential role of reactive oxygen species in chemical hypoxia-induced cell injury in opossum kidney cells and rabbit renal cortical slices. *Exp Nephrol.* **10**, 275-84.
- Kitching, A. R., Kong, Y. Z., Huang, X. R., Davenport, P., Edgton, K. L., Carmeliet, P., Holdsworth, S. R. and Tipping, P. G.** (2003). Plasminogen activator inhibitor-1 is a significant determinant of renal injury in experimental crescentic glomerulonephritis. *J Am Soc Nephrol.* **14**, 1487-95.
- Klahr, S., Levey, A. S., Beck, G. J., Caggiula, A. W., Hunsicker, L., Kusek, J. W. and Striker, G.** (1994). The effects of dietary protein restriction and blood-pressure control on the progression of chronic renal disease. Modification of Diet in Renal Disease Study Group. *N Engl J Med.* **330**, 877-84.
- Klahr, S. and Morrissey, J. J.** (2000). The role of vasoactive compounds, growth factors and cytokines in the progression of renal disease. *Kidney Int Suppl.* **75**, S7-14.
- Klahr, S., Schreiner, G. and Ichikawa, I.** (1988). The progression of renal disease. *N Engl J Med.* **318**, 1657-66.
- Klein, G., Langegger, M., Timpl, R. and Ekblom, P.** (1988). Role of laminin A chain in the development of epithelial cell polarity. *Cell.* **55**, 331-41.
- Kleman, J. P., Aeschlimann, D., Paulsson, M. and van der Rest, M.** (1995). Transglutaminase-catalyzed cross-linking of fibrils of collagen V/XI in A204 rhabdomyosarcoma cells. *Biochemistry.* **34**, 13768-75.
- Kliem, V., Johnson, R. J., Alpers, C. E., Yoshimura, A., Couser, W. G., Koch, K. M. and Floege, J.** (1996). Mechanisms involved in the pathogenesis of tubulointerstitial fibrosis in 5/6-nephrectomized rats. *Kidney Int.* **49**, 666-78.
- Knauper, V., Cowell, S., Smith, B., Lopez-Otin, C., O'Shea, M., Morris, H., Zardi, L. and Murphy, G.** (1997). The role of the C-terminal domain of human collagenase-3 (MMP-13) in the activation of procollagenase-3, substrate specificity, and tissue inhibitor of metalloproteinase interaction. *J Biol Chem.* **272**, 7608-16.
- Knauper, V., Lopez-Otin, C., Smith, B., Knight, G. and Murphy, G.** (1996). Biochemical characterization of human collagenase-3. *J Biol Chem.* **271**, 1544-50.
- Knauper, V., Osthus, A., DeClerck, Y. A., Langley, K. E., Blaser, J. and Tschesche, H.** (1993). Fragmentation of human polymorphonuclear-leucocyte collagenase. *Biochem J.* **291**, 847-54.
- Knowlden, J., Martin, J., Davies, M. and Williams, J. D.** (1995). Metalloproteinase generation by human glomerular epithelial cells. *Kidney Int.* **47**, 1682-9.

- Koide, H., Nakamura, T., Ebihara, I. and Tomino, Y.** (1997). Effect of unilateral nephrectomy on gene expression of metalloproteinases and their inhibitors. *Nephron*. **75**, 479-83.
- Koong, A. C., Chen, E. Y. and Giaccia, A. J.** (1994). Hypoxia causes the activation of nuclear factor kappa B through the phosphorylation of I kappa B alpha on tyrosine residues. *Cancer Res*. **54**, 1425-30.
- Kootstra, C. J., Bergijk, E. C., Veninga, A., Prins, F. A., de Heer, E., Abrahamson, D. R. and Bruijn, J. A.** (1995). Qualitative alterations in laminin expression in experimental lupus nephritis. *Am J Pathol*. **147**, 476-88.
- Kopp, J. B., Bianco, P., Young, M. F., Termine, J. D. and Robey, P. G.** (1992). Renal tubular epithelial cells express osteonectin in vivo and in vitro. *Kidney Int*. **41**, 56-64.
- Kornblihtt, A. R., Pesce, C. G., Alonso, C. R., Cramer, P., Srebrow, A., Werbajh, S. and Muro, A. F.** (1996). The fibronectin gene as a model for splicing and transcription studies. *FASEB J*. **10**, 248-57.
- Kouba, D. J., Nakano, H., Nishiyama, T., Kang, J., Uitto, J. and Mauviel, A.** (2001). Tumor necrosis factor-alpha induces distinctive NF-kappa B signaling within human dermal fibroblasts. *J Biol Chem*. **276**, 6214-24.
- Koury, S. T. and Koury, M. J.** (1993). Erythropoietin production by the kidney. *Semin Nephrol*. **13**, 78-86.
- Koya, D. and King, G. L.** (1998). Protein kinase C activation and the development of diabetic complications. *Diabetes*. **47**, 859-66.
- Kozyraki, R., Fyfe, J., Verroust, P. J., Jacobsen, C., Dautry-Varsat, A., Gburek, J., Willnow, T. E., Christensen, E. I. and Moestrup, S. K.** (2001). Megalin-dependent cubilin-mediated endocytosis is a major pathway for the apical uptake of transferrin in polarized epithelia. *Proc Natl Acad Sci U S A*. **98**, 12491-6.
- Kramer, A. B., Ricardo, S. D., Kelly, D. J., Waanders, F., van Goor, H. and Navis, G.** (2005). Modulation of osteopontin in proteinuria-induced renal interstitial fibrosis. *J Pathol*. **207**, 483-92.
- Kraut, J. A. and Kurtz, I.** (2005) Metabolic acidosis of CKD: diagnosis, clinical characteristics and treatment. *Am J Kidney Dis*. **45**, 978-93.
- Kribben, A., Herget-Rosenthal, S., Lange, B., Michel, M. C. and Philipp, T.** (1998). Stimulation of mitogen activated protein kinase and cellular proliferation in renal proximal tubular cells. *Ren Fail*. **20**, 229-34.
- Kristensen, P., Eriksen, J. and Dano, K.** (1991). Localization of urokinase-type plasminogen activator messenger RNA in the normal mouse by in situ hybridization. *J Histochem Cytochem*. **39**, 341-9.
- Kriz, W., Elger, M., Lemley, K. V. and Sakai, T.** (1990). Mesangial cell-glomerular basement membrane connections counteract glomerular capillary and mesangium expansion. *Am J Nephrol*. **10**, 4-13.

- Kuhara, T., Kagami, S. and Kuroda, Y.** (1997). Expression of beta 1-integrins on activated mesangial cells in human glomerulonephritis. *J Am Soc Nephrol.* **8**, 1679-87.
- Kuncio, G. S., Tsyganskaya, M., Zhu, J., Liu, S. L., Nagy, L., Thomazy, V., Davies, P. J. and Zern, M. A.** (1998). TNF-alpha modulates expression of the tissue transglutaminase gene in liver cells. *Am J Physiol Gastrointest Liver Physiol.* **274**, G240-5.
- Kupprion, C., Motamed, K. and Sage, E. H.** (1998). SPARC (BM-40, osteonectin) inhibits the mitogenic effect of vascular endothelial growth factor on microvascular endothelial cells. *J Biol Chem.* **273**, 29635-40.
- Kurkinen, M., Condon, M. R., Blumberg, B., Barlow, D. P., Quinones, S., Saus, J. and Pihlajaniemi, T.** (1987). Extensive homology between the carboxyl-terminal peptides of mouse alpha 1(IV) and alpha 2(IV) collagen. *J Biol Chem.* **262**, 8496-9.
- Kuroda, M., Sasamura, H., Kobayashi, E., Shimizu-Hirota, R., Nakazato, Y., Hayashi, M. and Saruta, T.** (2004). Glomerular expression of biglycan and decorin and urinary levels of decorin in primary glomerular disease. *Clin Nephrol.* **61**, 7-16.
- Laemmli, U. K.** (1970). Cleavage of structural proteins during the assembly of the head of bacteriophage T4. *Nature.* **227**, 680-5.
- Lai, T. S., Hausladen, A., Slaughter, T. F., Eu, J. P., Stamler, J. S. and Greenberg, C. S.** (2001). Calcium regulates S-nitrosylation, denitrosylation, and activity of tissue transglutaminase. *Biochemistry.* **40**, 4904-10.
- Langenbach, K. J. and Sottile, J.** (1999). Identification of protein-disulfide isomerase activity in fibronectin. *J Biol Chem.* **274**, 7032-8.
- Langham, R. G., Kelly, D. J., Maguire, J., Dowling, J. P., Gilbert, R. E. and Thomson, N. M.** (2003). Over-expression of platelet-derived growth factor in human diabetic nephropathy. *Nephrol Dial Transplant.* **18**, 1392-6.
- Langholz, O., Rockel, D., Mauch, C., Kozłowska, E., Bank, I., Krieg, T. and Eckes, B.** (1995). Collagen and collagenase gene expression in three-dimensional collagen lattices are differentially regulated by alpha 1 beta 1 and alpha 2 beta 1 integrins. *J Cell Biol.* **131**, 1903-15.
- Larsson, L. I., Skriver, L., Nielsen, L. S., Grondahl-Hansen, J., Kristensen, P. and Dano, K.** (1984). Distribution of urokinase-type plasminogen activator immunoreactivity in the mouse. *J Cell Biol.* **98**, 894-903.
- Lauer-Fields, J. L., Juska, D. and Fields, G. B.** (2002). Matrix metalloproteinases and collagen catabolism. *Biopolymers.* **66**, 19-32.
- Lauer-Fields, J. L., Tuzinski, K. A., Shimokawa, K., Nagase, H. and Fields, G. B.** (2000). Hydrolysis of triple-helical collagen peptide models by matrix metalloproteinases. *J Biol Chem.* **275**, 13282-90.
- Lawler, J. and Hynes, R. O.** (1986). The structure of human thrombospondin, an adhesive glycoprotein with multiple calcium-binding sites and homologies with several different proteins. *J Cell Biol.* **103**, 1635-48.

- Leblond, C. P. and Inoue, S.** (1989). Structure, composition, and assembly of basement membrane. *Am J Anat.* **185**, 367-90.
- Lechuga, C. G., Hernandez-Nazara, Z. H., Dominguez Rosales, J. A., Morris, E. R., Rincon, A. R., Rivas-Estilla, A. M., Esteban-Gamboa, A. and Rojkind, M.** (2004). TGF-beta1 modulates matrix metalloproteinase-13 expression in hepatic stellate cells by complex mechanisms involving p38MAPK, PI3-kinase, AKT, and p70S6k. *Am J Physiol Gastrointest Liver Physiol.* **287**, G974-87.
- Lee, H. S., Park, S. Y., Moon, K. C., Hong, H. K., Song, C. Y. and Hong, S. Y.** (2001). mRNA expression of urokinase and plasminogen activator inhibitor-1 in human crescentic glomerulonephritis. *Histopathology.* **39**, 203-9.
- Lee, K. N., Birckbichler, P. J., Patterson, M. K., Jr., Conway, E. and Maxwell, M.** (1987). Induction of cellular transglutaminase biosynthesis by sodium butyrate. *Biochim Biophys Acta.* **928**, 22-8.
- Lee, K. N., Maxwell, M. D., Patterson, M. K., Jr., Birckbichler, P. J. and Conway, E.** (1992). Identification of transglutaminase substrates in HT29 colon cancer cells: use of 5-(biotinamido)pentylamine as a transglutaminase-specific probe. *Biochim Biophys Acta.* **1136**, 12-6.
- Lee, L. K., Meyer, T. W., Pollock, A. S. and Lovett, D. H.** (1995). Endothelial cell injury initiates glomerular sclerosis in the rat remnant kidney. *J Clin Invest.* **96**, 953-64.
- Leehey, D. J., Song, R. H., Alavi, N. and Singh, A. K.** (1995). Decreased degradative enzymes in mesangial cells cultured in high glucose media. *Diabetes.* **44**, 929-35.
- Lelongt, B., Legallicier, B., Piedagnel, R. and Ronco, P. M.** (2001). Do matrix metalloproteinases MMP-2 and MMP-9 (gelatinases) play a role in renal development, physiology and glomerular diseases? *Curr Opin Nephrol Hypertens.* **10**, 7-12.
- Lelongt, B., Trugnan, G., Murphy, G. and Ronco, P. M.** (1997). Matrix metalloproteinases MMP2 and MMP9 are produced in early stages of kidney morphogenesis but only MMP9 is required for renal organogenesis in vitro. *J Cell Biol.* **136**, 1363-73.
- Lemley, K. V. and Kriz, W.** (1991). Anatomy of the renal interstitium. *Kidney Int.* **39**, 370-81.
- Lenz, O., Elliot, S. J. and Stetler-Stevenson, W. G.** (2000). Matrix metalloproteinases in renal development and disease. *J Am Soc Nephrol.* **11**, 574-81.
- Leonard, M. O., Cottell, D. C., Godson, C., Brady, H. R. and Taylor, C. T.** (2003). The role of HIF-1 alpha in transcriptional regulation of the proximal tubular epithelial cell response to hypoxia. *J Biol Chem.* **278**, 40296-304.
- Lesort, M., Tucholski, J., Miller, M. L. and Johnson, G. V.** (2000). Tissue transglutaminase: a possible role in neurodegenerative diseases. *Prog Neurobiol.* **61**, 439-63.
- Leszczynski, D., Zhao, Y., Luokkamaki, M. and Foegh, M. L.** (1994). Apoptosis of vascular smooth muscle cells. Protein kinase C and oncoprotein Bcl-2 are involved in regulation of apoptosis in non-transformed rat vascular smooth muscle cells. *Am J Pathol.* **145**, 1265-70.

- Levey, A. S., Coresh, J., Balk, E., Kausz, A. T., Levin, A., Steffes, M. W., Hogg, R. J., Perrone, R. D., Lau, J. and Eknoyan, G.** (2003). National Kidney Foundation practice guidelines for chronic kidney disease: evaluation, classification, and stratification. *Ann Intern Med.* **139**, 137-47.
- Li, X., Kimura, H., Hirota, K., Kasuno, K., Torii, K., Okada, T., Kurooka, H., Yokota, Y. and Yoshida, H.** (2005). Synergistic effect of hypoxia and TNF-alpha on production of PAI-1 in human proximal renal tubular cells. *Kidney Int.* **68**, 569-83.
- Liu, S., Cerione, R. A. and Clardy, J.** (2002). Structural basis for the guanine nucleotide-binding activity of tissue transglutaminase and its regulation of transamidation activity. *Proc Natl Acad Sci U S A.* **99**, 2743-7.
- Liu, Y., Centracchio, J. N., Lin, L., Sun, A. M. and Dworkin, L. D.** (1998). Constitutive expression of HGF modulates renal epithelial cell phenotype and induces c-met and fibronectin expression. *Exp Cell Res.* **242**, 174-85.
- Locatelli, F., Canaud, B., Eckardt, K. U., Stenvinkel, P., Wanner, C. and Zoccali, C.** (2003). Oxidative stress in end-stage renal disease: an emerging threat to patient outcome. *Nephrol Dial Transplant.* **18**, 1272-80.
- Lochter, A., Galosy, S., Muschler, J., Freedman, N., Werb, Z. and Bissell, M. J.** (1997). Matrix metalloproteinase stromelysin-1 triggers a cascade of molecular alterations that leads to stable epithelial-to-mesenchymal conversion and a premalignant phenotype in mammary epithelial cells. *J Cell Biol.* **139**, 1861-72.
- Lorand, L., Campbell-Wilkes, L. K. and Cooperstein, L.** (1972). A filter paper assay for transamidating enzymes using radioactive amine substrates. *Anal Biochem.* **50**, 623-31.
- Lorand, L. and Conrad, S. M.** (1984). Transglutaminases. *Mol Cell Biochem.* **58**, 9-35.
- Lorand, L. and Graham, R. M.** (2003). Transglutaminases: crosslinking enzymes with pleiotropic functions. *Nat Rev Mol Cell Biol.* **4**, 140-56.
- Lorand, L., Parameswaran, K. N. and Velasco, P. T.** (1991). Sorting-out of acceptor-donor relationships in the transglutaminase-catalyzed cross-linking of crystallins by the enzyme-directed labeling of potential sites. *Proc Natl Acad Sci U S A.* **88**, 82-3.
- Loskutoff, D. J. and Edgington, T. E.** (1977). Synthesis of a fibrinolytic activator and inhibitor by endothelial cells. *Proc Natl Acad Sci U S A.* **74**, 3903-7.
- Lowry, O. H., Rosebrough, N. J., Farr, A. L. and Randall, R. J.** (1951). Protein measurement with the Folin phenol reagent. *J Biol Chem.* **193**, 265-75.
- Lu, S. and Davies, P. J.** (1997). Regulation of the expression of the tissue transglutaminase gene by DNA methylation. *Proc Natl Acad Sci U S A.* **94**, 4692-7.
- Lu, S., Saydak, M., Gentile, V., Stein, J. P. and Davies, P. J.** (1995). Isolation and characterization of the human tissue transglutaminase gene promoter. *J Biol Chem.* **270**, 9748-56.
- Lukashev, M. E. and Werb, Z.** (1998). ECM signalling: orchestrating cell behaviour and misbehaviour. *Trends Cell Biol.* **8**, 437-41.

- Lysaght, M. J.** (2002). Maintenance dialysis population dynamics: current trends and long-term implications. *J Am Soc Nephrol.* **13**, S37-40.
- Maeda, S., Dean, D. D., Gomez, R., Schwartz, Z. and Boyan, B. D.** (2002) The first stage of transforming growth factor beta 1 activation is release of the large latent complex from the extracellular matrix of growth plate chondrocytes by matrix vesicle Stromolysin-1 (MMP-3) *Calcif Tissue Int.* **70**, 54-65.
- Main, I. W. and Atkins, R. C.** (1995). The role of T-cells in inflammatory kidney disease. *Curr Opin Nephrol Hypertens.* **4**, 354-8.
- Maity, S. N., Golumbek, P. T., Karsenty, G. and de Crombrughe, B.** (1988). Selective activation of transcription by a novel CCAAT binding factor. *Science.* **241**, 582-5.
- Malemud, C. J.** (2006). Matrix metalloproteinases (MMPs) in health and disease: an overview. *Front Biosci.* **11**, 1696-701.
- Malliaros, J., Holdsworth, S. R., Wojta, J., Erlich, J. and Tipping, P. G.** (1993). Glomerular fibrinolytic activity in anti-GBM glomerulonephritis in rabbits. *Kidney Int.* **44**, 557-64.
- Malyankar, U. M., Almeida, M., Johnson, R. J., Pichler, R. H. and Giachelli, C. M.** (1997). Osteopontin regulation in cultured rat renal epithelial cells. *Kidney Int.* **51**, 1766-73.
- Mansfield, K. D., Simon, M. C. and Keith, B.** (2004). Hypoxic reduction in cellular glutathione levels requires mitochondrial reactive oxygen species. *J Appl Physiol.* **97**, 1358-66.
- Mariani, P., Carsughi, F., Spinozzi, F., Romanzetti, S., Meier, G., Casadio, R. and Bergamini, C. M.** (2000). Ligand-induced conformational changes in tissue transglutaminase: Monte Carlo analysis of small-angle scattering data. *Biophys J.* **78**, 3240-51.
- Marti, H. P., McNeil, L., Davies, M., Martin, J. and Lovett, D. H.** (1993). Homology cloning of rat 72 kDa type IV collagenase: cytokine and second-messenger inducibility in glomerular mesangial cells. *Biochem J.* **291**, 441-6.
- Martin, J., Knowlden, J., Davies, M. and Williams, J. D.** (1994). Identification and independent regulation of human mesangial cell metalloproteinases. *Kidney Int.* **46**, 877-85.
- Martin, J., Steadman, R., Knowlden, J., Williams, J. and Davies, M.** (1998). Differential regulation of matrix metalloproteinases and their inhibitors in human glomerular epithelial cells in vitro. *J Am Soc Nephrol.* **9**, 1629-37.
- Martinez, J., Chalupowicz, D. G., Roush, R. K., Sheth, A. and Barsigian, C.** (1994). Transglutaminase-mediated processing of fibronectin by endothelial cell monolayers. *Biochemistry.* **33**, 2538-45.
- Massague, J.** (2000). How cells read TGF-beta signals. *Nat Rev Mol Cell Biol.* **1**, 169-78.
- Matrisian, L. M.** (1994). Matrix metalloproteinase gene expression. *Ann N Y Acad Sci.* **732**, 42-50.

- Matsuda, M., Shikata, K., Makino, H., Sugimoto, H., Ota, K., Akiyama, K., Hirata, K. and Ota, Z.** (1997). Gene expression of PDGF and PDGF receptor in various forms of glomerulonephritis. *Am J Nephrol.* **17**, 25-31.
- McGregor, B., Colon, S., Mutin, M., Chignier, E., Zech, P. and McGregor, J.** (1994). Thrombospondin in human glomerulopathies. A marker of inflammation and early fibrosis. *Am J Pathol.* **144**, 1281-7.
- McKeown-Longo, P. J. and Mosher, D. F.** (1983). Binding of plasma fibronectin to cell layers of human skin fibroblasts. *J Cell Biol.* **97**, 466-72.
- McLennan, S. V., Martell, S. Y. and Yue, D. K.** (2000). High glucose concentration inhibits the expression of membrane type metalloproteinase by mesangial cells: possible role in mesangium accumulation. *Diabetologia.* **43**, 642-8.
- Mekhail, K., Gunaratnam, L., Bonicalzi, M. E. and Lee, S.** (2004). HIF activation by pH-dependent nucleolar sequestration of VHL. *Nat Cell Biol.* **6**, 642-7.
- Melino, G., Annicchiarico-Petruzzelli, M., Piredda, L., Candi, E., Gentile, V., Davies, P. J. and Piacentini, M.** (1994). Tissue transglutaminase and apoptosis: sense and antisense transfection studies with human neuroblastoma cells. *Mol Cell Biol* **14**, 6584-96.
- Melino, G. and Piacentini, M.** (1998). 'Tissue' transglutaminase in cell death: a downstream or a multifunctional upstream effector? *FEBS Lett.* **430**, 59-63.
- Mene, P.** (2001). Mesangial cell cultures. *J Nephrol.* **14**, 198-203.
- Mene, P., Simonson, M. S. and Dunn, M. J.** (1989). Physiology of the mesangial cell. *Physiol Rev.* **69**, 1347-424.
- Mezzano, S., Aros, C., Droguett, A., Burgos, M. E., Ardiles, L., Flores, C., Schneider, H., Ruiz-Ortega, M. and Egido, J.** (2004). NF-kappaB activation and overexpression of regulated genes in human diabetic nephropathy. *Nephrol Dial Transplant.* **19**, 2505-12.
- Mezzano, S. A., Barria, M., Droguett, M. A., Burgos, M. E., Ardiles, L. G., Flores, C. and Egido, J.** (2001). Tubular NF-kappaB and AP-1 activation in human proteinuric renal disease. *Kidney Int.* **60**, 1366-77.
- Mian, S., el Alaoui, S., Lawry, J., Gentile, V., Davies, P. J. and Griffin, M.** (1995). The importance of the GTP-binding protein tissue transglutaminase in the regulation of cell cycle progression. *FEBS Lett.* **370**, 27-31.
- Michiels, C., Minet, E., Mottet, D. and Raes, M.** (2002). Regulation of gene expression by oxygen: NF-kappaB and HIF-1, two extremes. *Free Radic Biol Med.* **33**, 1231-42.
- Miller, E. J., Harris, E. D., Jr., Chung, E., Finch, J. E., Jr., McCroskery, P. A. and Butler, W. T.** (1976). Cleavage of Type II and III collagens with mammalian collagenase: site of cleavage and primary structure at the NH₂-terminal portion of the smaller fragment released from both collagens. *Biochemistry.* **15**, 787-92.
- Miner, J. H.** (1999). Renal basement membrane components. *Kidney Int.* **56**, 2016-24.

- Miner, J. H., Patton, B. L., Lentz, S. I., Gilbert, D. J., Snider, W. D., Jenkins, N. A., Copeland, N. G. and Sanes, J. R.** (1997). The laminin alpha chains: expression, developmental transitions, and chromosomal locations of alpha1-5, identification of heterotrimeric laminins 8-11, and cloning of a novel alpha3 isoform. *J Cell Biol.* **137**, 685-701.
- Ming, M., Chan, W., Wang, T. T., Roberts, K. D., Bouvier, M., Lachance, S., Carriere, S. and Chan, J. S.** (1996). beta-Adrenoceptors and dexamethasone synergistically stimulate the expression of the angiotensinogen gene in opossum kidney cells. *Kidney Int.* **50**, 94-101.
- Minto, A. W., Fogel, M. A., Natori, Y., O'Meara, Y. M., Abrahamson, D. R., Smith, B. and Salant, D. J.** (1993). Expression of type I collagen mRNA in glomeruli of rats with passive Heymann nephritis. *Kidney Int.* **43**, 121-7.
- Mirza, A., Liu, S. L., Frizell, E., Zhu, J., Maddukuri, S., Martinez, J., Davies, P., Schwarting, R., Norton, P. and Zern, M. A.** (1997). A role for tissue transglutaminase in hepatic injury and fibrogenesis, and its regulation by NF-kappaB. *Am J Physiol Gastrointest Liver Physiol.* **272**, G281-8.
- Mishra, S., Melino, G. and Murphy, L. J.** (2007). Transglutaminase 2 kinase activity facilitates protein kinase A induced phosphorylation of retinoblastoma protein. *J Biol Chem.* **282**, 10108-15.
- Mizutani, M., Yuzawa, Y., Maruyama, I., Sakamoto, N. and Matsuo, S.** (1993). Glomerular localization of thrombomodulin in human glomerulonephritis. *Lab Invest.* **69**, 193-202.
- Mohammed, N. B., Haylor, J. L., Hau, Z., El Nahas, A. M., Griffin, M. and Johnson, T. S.** (2006). Knockout of Transglutaminase Type 2 Slows the Development of Kidney Scarring in the Mouse UUO Model. *Oral presentation Renal Association*. Harrogate, UK.
- Mohan, K., Pinto, D. and Issekutz, T. B.** (2003). Identification of tissue transglutaminase as a novel molecule involved in human CD8+ T cell transendothelial migration. *J Immunol.* **171**, 3179-86.
- Mondorf, U. F., Piiper, A., Herrero, M., Olbrich, H. G., Bender, M., Gross, W., Scheuermann, E. and Geiger, H.** (1999). Lipoprotein(a) stimulates growth of human mesangial cells and induces activation of phospholipase C via pertussis toxin-sensitive G proteins. *Kidney Int.* **55**, 1359-66.
- Morcos, M., Sayed, A. A., Bierhaus, A., Yard, B., Waldherr, R., Merz, W., Kloeting, I., Schleicher, E., Mentz, S., Abd el Baki, R. F. et al.** (2002). Activation of tubular epithelial cells in diabetic nephropathy. *Diabetes.* **51**, 3532-44.
- Morigi, M., Macconi, D., Zoja, C., Donadelli, R., Buelli, S., Zanchi, C., Ghilardi, M. and Remuzzi, G.** (2002). Protein overload-induced NF-kappaB activation in proximal tubular cells requires H₂O₂ through a PKC-dependent pathway. *J Am Soc Nephrol.* **13**, 1179-89.
- Morwenna, S. and Ratcliffe, P.** (1997). Mammalian oxygen sensing and hypoxia inducible factor-1. *Int J Biochem Cell Biol.* **29**, 1419-32.
- Mosher, D. F.** (1984). Cross-linking of fibronectin to collagenous proteins. *Mol Cell Biochem.* **58**, 63-8.

- Mozes, M. M., Bottinger, E. P., Jacot, T. A. and Kopp, J. B.** (1999). Renal expression of fibrotic matrix proteins and of transforming growth factor-beta (TGF-beta) isoforms in TGF-beta transgenic mice. *J Am Soc Nephrol.* **10**, 271-80.
- Mu, D., Cambier, S., Fjellbirkeland, L., Baron, J. L., Munger, J. S., Kawakatsu, H., Sheppard, D., Broaddus, V. C. and Nishimura, S. L.** (2002) The integrin $\alpha\beta 8$ mediates epithelial homeostasis through MT1-MMP dependent activation of TGF- $\beta 1$. *J Cell Biol.* **157**, 493-507.
- Muchaneta-Kubara, E. C. and El Nahas, A. M.** (1997). Myofibroblast phenotypes expression in experimental renal scarring. *Nephrol Dial Transplant.* **12**, 904-15.
- Muchaneta-Kubara, E. C., Sayed-Ahmed, N. and el Nahas, A. M.** (1995). Subtotal nephrectomy: a mosaic of growth factors. *Nephrol Dial Transplant* **10**, 320-7.
- Muller, G. A. and Rodemann, H. P.** (1991). Characterization of human renal fibroblasts in health and disease: I. Immunophenotyping of cultured tubular epithelial cells and fibroblasts derived from kidneys with histologically proven interstitial fibrosis. *Am J Kidney Dis.* **17**, 680-3.
- Murdoch, A. D., Liu, B., Schwarting, R., Tuan, R. S. and Iozzo, R. V.** (1994). Widespread expression of perlecan proteoglycan in basement membranes and extracellular matrices of human tissues as detected by a novel monoclonal antibody against domain III and by in situ hybridization. *J Histochem Cytochem.* **42**, 239-49.
- Murtaugh, M. P., Arend, W. P. and Davies, P. J.** (1984). Induction of tissue transglutaminase in human peripheral blood monocytes. *J Exp Med.* **159**, 114-25.
- Murtaugh, M. P., Dennison, O., Stein, J. P. and Davies, P. J.** (1986). Retinoic acid-induced gene expression in normal and leukemic myeloid cells. *J Exp Med.* **163**, 1325-30.
- Murthy, S. N., Iismaa, S., Begg, G., Freymann, D. M., Graham, R. M. and Lorand, L.** (2002). Conserved tryptophan in the core domain of transglutaminase is essential for catalytic activity. *Proc Natl Acad Sci U S A.* **99**, 2738-42.
- Murthy, S. N., Wilson, J. H., Lukas, T. J., Kuret, J. and Lorand, L.** (1998). Cross-linking sites of the human tau protein, probed by reactions with human transglutaminase. *J Neurochem.* **71**, 2607-14.
- Myllyharju, J.** (2003). Prolyl 4-hydroxylases, the key enzymes of collagen biosynthesis. *Matrix Biol.* **22**, 15-24.
- Myllyharju, J. and Kivirikko, K. I.** (2001). Collagens and collagen-related diseases. *Ann Med.* **33**, 7-21.
- Myllyharju, J. and Kivirikko, K. I.** (2004). Collagens, modifying enzymes and their mutations in humans, flies and worms. *Trends Genet.* **20**, 33-43.
- Nadeau, O. W., Traxler, K. W. and Carlson, G. M.** (1998). Zero-length crosslinking of the beta subunit of phosphorylase kinase to the N-terminal half of its regulatory alpha subunit. *Biochem Biophys Res Commun.* **251**, 637-41.

- Nagamine, Y., Medcalf, R. L. and Munoz-Canoves, P.** (2005). Transcriptional and posttranscriptional regulation of the plasminogen activator system. *Thromb Haemost.* **93**, 661-75.
- Nagase, H.** (1997). Activation mechanisms of matrix metalloproteinases. *Biol Chem.* **378**, 151-60.
- Nagase, H. and Woessner, J. F., Jr.** (1999). Matrix metalloproteinases. *J Biol Chem.* **274**, 21491-4.
- Nagy, L., Saydak, M., Shipley, N., Lu, S., Basilion, J. P., Yan, Z. H., Syka, P., Chandraratna, R. A., Stein, J. P., Heyman, R. A. et al.** (1996). Identification and characterization of a versatile retinoid response element (retinoic acid receptor response element-retinoid X receptor response element) in the mouse tissue transglutaminase gene promoter. *J Biol Chem.* **271**, 4355-65.
- Nagy, L., Thomazy, V. A., Shipley, G. L., Fesus, L., Lamph, W., Heyman, R. A., Chandraratna, R. A. and Davies, P. J.** (1995). Activation of retinoid X receptors induces apoptosis in HL-60 cell lines. *Mol Cell Biol.* **15**, 3540-51.
- Nakabeppu, Y., Sakumi, K., Sakamoto, K., Tsuchimoto, D., Tsuzuki, T. and Nakatsu, Y.** (2006). Mutagenesis and carcinogenesis caused by the oxidation of nucleic acids. *Biol Chem.* **387**, 373-9.
- Nakagawa, T., Lan, H. Y., Zhu, H. J., Kang, D. H., Schreiner, G. F. and Johnson, R. J.** (2004) Differential regulation of VEGF by TGF-beta and hypoxia in rat proximal tubular cells. *Am J Physiol Renal Physiol.* **287**, F658-64.
- Nakai, A., Satoh, M., Hirayoshi, K. and Nagata, K.** (1992). Involvement of the stress protein HSP47 in procollagen processing in the endoplasmic reticulum. *J Cell Biol.* **117**, 903-14.
- Nakamura, M., Yamabe, H., Osawa, H., Nakamura, N., Shimada, M., Kumasaka, R., Murakami, R., Fujita, T., Osanai, T. and Okumura, K.** (2006). Hypoxic conditions stimulate the production of angiogenin and vascular endothelial growth factor by human renal proximal tubular epithelial cells in culture. *Nephrol Dial Transplant* **6**, 1489-95.
- Nakamura, T., Fukui, M., Ebihara, I., Osada, S., Tomino, Y. and Koide, H.** (1994). Abnormal gene expression of matrix metalloproteinases and their inhibitor in glomeruli from diabetic rats. *Ren Physiol Biochem.* **17**, 316-25.
- Nakaoka, H., Perez, D. M., Baek, K. J., Das, T., Husain, A., Misono, K., Im, M. J. and Graham, R. M.** (1994). Gh: a GTP-binding protein with transglutaminase activity and receptor signaling function. *Science* **264**, 1593-6.
- Nanda, N., Iismaa, S. E., Copeland, N. G., Gilbert, D. J., Jenkins, N., Graham, R. M. and Sutrave, P.** (1999). Organization and chromosomal mapping of mouse Gh/tissue transglutaminase gene (Tgm2). *Arch Biochem Biophys.* **366**, 151-6.
- Nath, K. A., Croatt, A. J. and Hostetter, T. H.** (1990). Oxygen consumption and oxidant stress in surviving nephrons. *Am J Physiol Renal Physiol.* **258**, F1354-62.

- Neame, P. J., Kay, C. J., McQuillan, D.J., Beales, M. P. and Hassall, J. R.** (2000). Independent modulation of collagen fibrillogenesis by decorin and lumican. *Cell Mol Life Sci.* **57**, 859-63.
- Nemes, Z., Jr., Adany, R., Balazs, M., Boross, P. and Fesus, L.** (1997). Identification of cytoplasmic actin as an abundant glutaminyl substrate for tissue transglutaminase in HL-60 and U937 cells undergoing apoptosis. *J Biol Chem.* **272**, 20577-83.
- Ng, Y. Y., Fan, J. M., Mu, W., Nikolic-Paterson, D. J., Yang, W. C., Huang, T. P., Atkins, R. C. and Lan, H. Y.** (1999). Glomerular epithelial-myofibroblast transdifferentiation in the evolution of glomerular crescent formation. *Nephrol Dial Transplant.* **14**, 2860-72.
- Ng, Y. Y., Huang, T. P., Yang, W. C., Chen, Z. P., Yang, A. H., Mu, W., Nikolic-Paterson, D. J., Atkins, R. C. and Lan, H. Y.** (1998). Tubular epithelial-myofibroblast transdifferentiation in progressive tubulointerstitial fibrosis in 5/6 nephrectomized rats. *Kidney Int.* **54**, 864-76.
- Nicholas, B., Smethurst, P., Verderio, E., Jones, R. and Griffin, M.** (2003). Cross-linking of cellular proteins by tissue transglutaminase during necrotic cell death: a mechanism for maintaining tissue integrity. *Biochem J.* **371**, 413-22.
- Nikolic-Paterson, D. J., Lan, H. Y., Hill, P. A. and Atkins, R. C.** (1994). Macrophages in renal injury. *Kidney Int Suppl.* **45**, S79-82.
- Noakes, P. G., Miner, J. H., Gautam, M., Cunningham, J. M., Sanes, J. R. and Merlie, J. P.** (1995). The renal glomerulus of mice lacking α -laminin/laminin beta 2: nephrosis despite molecular compensation by laminin beta 1. *Nat Genet.* **10**, 400-6.
- Noe, V., Fingleton, B., Jacobs, K., Crawford, H. C., Vermeulen, S., Steelant, W., Bruyneel, E., Matrisian, L. M. and Mareel, M.** (2001). Release of an invasion promoter E-cadherin fragment by matrilysin and stromelysin-1. *J Cell Sci.* **114**, 111-118.
- Norman, J. T., Clark, I. M. and Garcia, P. L.** (2000). Hypoxia promotes fibrogenesis in human renal fibroblasts. *Kidney Int.* **58**, 2351-66.
- Norman, J. T., Gatti, L., Wilson, P. D. and Lewis, M.** (1995). Matrix metalloproteinases and tissue inhibitor of matrix metalloproteinases expression by tubular epithelia and interstitial fibroblasts in the normal kidney and in fibrosis. *Exp Nephrol.* **3**, 88-9.
- Norman, J. T. and Lewis, M. P.** (1996). Matrix metalloproteinases (MMPs) in renal fibrosis. *Kidney Int Suppl.* **54**, S61-3.
- Norman, J. T., Orphanides, C., Garcia, P. and Fine, L. G.** (1999). Hypoxia-induced changes in extracellular matrix metabolism in renal cells. *Exp Nephrol.* **7**, 463-9.
- Nugent, M. A. and Newman, M. J.** (1989). Inhibition of normal rat kidney cell growth by transforming growth factor-beta is mediated by collagen. *J Biol Chem.* **264**, 18060-7.
- Nunes, I., Gleizes, P. E., Metz, C. N. and Rifkin, D. B.** (1997). Latent transforming growth factor-beta binding protein domains involved in activation and transglutaminase-dependent cross-linking of latent transforming growth factor-beta. *J Cell Biol.* **136**, 1151-63.

- Oda, T., Jung, Y. O., Kim, H. S., Cai, X., Lopez-Guisa, J. H., Ikeda, Y. and Eddy A. A.** (2005) PAI-1 deficiency attenuates the fibrogenic response to ureteral obstruction. *Kidney Int.* **76**, 2502-3.
- Ohashi, R., Kitamura, H. and Yamanaka, N.** (2000). Peritubular capillary injury during the progression of experimental glomerulonephritis in rats. *J Am Soc Nephrol.* **11**, 47-56.
- Ohashi, R., Shimizu, A., Masuda, Y., Kitamura, H., Ishizaki, M., Sugisaki, Y. and Yamanaka, N.** (2002). Peritubular capillary regression during the progression of experimental obstructive nephropathy. *J Am Soc Nephrol.* **13**, 1795-805.
- Ohuchi, E., Imai, K., Fujii, Y., Sato, H., Seiki, M. and Okada, Y.** (1997). Membrane type 1 matrix metalloproteinase digests interstitial collagens and other extracellular matrix macromolecules. *J Biol Chem.* **272**, 2446-51.
- Okada, H., Kikuta, T., Kobayashi, T., Inoue, T., Kanno, Y., Takigawa, M., Sugaya, T., Kopp, J. B. and Suzuki, H.** (2005). Connective tissue growth factor expressed in tubular epithelium plays a pivotal role in renal fibrogenesis. *J Am Soc Nephrol.* **16**, 133-43.
- Okada, M., Takemura, T., Murakami, K., Hino, S. and Yoshioka, K.** (1996). Expression of tenascin in normal and diseased human kidneys. *Nippon Jinzo Gakkai Shi.* **38**, 213-9.
- Okuda, S., Kanai, H., Tamaki, K., Onoyama, K. and Fujishima, M.** (1992). Synthesis of fibronectin by isolated glomeruli from nephrectomized hypertensive rats. *Nephron.* **61**, 456-63.
- Oliverio, S., Amendola, A., Rodolfo, C., Spinedi, A. and Piacentini, M.** (1999). Inhibition of "tissue" transglutaminase increases cell survival by preventing apoptosis. *J Biol Chem.* **274**, 34123-8.
- Ong, A. C., Jowett, T. P., Firth, J. D., Burton, S., Karet, F. E. and Fine, L. G.** (1995). An endothelin-1 mediated autocrine growth loop involved in human renal tubular regeneration. *Kidney Int.* **48**, 390-401.
- Orphanides, C., Fine, L. G. and Norman, J. T.** (1997). Hypoxia stimulates proximal tubular cell matrix production via a TGF-beta1-independent mechanism. *Kidney Int.* **52**, 637-47.
- Ota, K., Stetler-Stevenson, W. G., Yang, Q., Kumar, A., Wada, J., Kashihara, N., Wallner, E. I. and Kanwar, Y. S.** (1998). Cloning of murine membrane-type-1-matrix metalloproteinase (MT-1-MMP) and its metanephric developmental regulation with respect to MMP-2 and its inhibitor. *Kidney Int.* **54**, 131-42.
- Overall, C. M., Wrana, J. L. and Sodek, J.** (1991). Transcriptional and post-transcriptional regulation of 72-kDa gelatinase/type IV collagenase by transforming growth factor-beta 1 in human fibroblasts. Comparisons with collagenase and tissue inhibitor of matrix metalloproteinase gene expression. *J Biol Chem.* **266**, 14064-71.
- Pankov, R. and Yamada, K. M.** (2002). Fibronectin at a glance. *J Cell Sci.* **115**, 3861-3.
- Parameswaran, K. N., Cheng, X. F., Chen, E. C., Velasco, P. T., Wilson, J. H. and Lorand, L.** (1997). Hydrolysis of gamma:epsilon isopeptides by cytosolic transglutaminases and by coagulation factor XIIIa. *J Biol Chem.* **272**, 10311-7.

- Park, J. E., Keller, G. A. and Ferrara, N.** (1993). The vascular endothelial growth factor (VEGF) isoforms: differential deposition into the subepithelial extracellular matrix and bioactivity of extracellular matrix-bound VEGF. *Mol Biol Cell*. **4**, 1317-26.
- Parker, E., Sun, T., Johnson, T. S. and El Nahas A. M.** (2006). Upregulation of tissue transglutaminase in transforming growth factor beta induced epithelial mesenchymal transdifferentiation in rat tubular epithelial cells. *Renal Association Conference*, poster RA6236. Harrogate.
- Parkinson, N. A., James, A. F. and Hendry, B. M.** (1996). Actions of endothelin-1 on calcium homeostasis in Madin-Darby canine kidney tubule cells. *Nephrol Dial Transplant*. **11**, 1532-7.
- Patterson, M. L., Atkinson, S. J., Knauper, V. and Murphy, G.** (2001). Specific collagenolysis by gelatinase A, MMP-2, is determined by the hemopexin domain and not the fibronectin-like domain. *FEBS Lett*. **503**, 158-62.
- Pavan, M. V., Ghini, B., Castro, M. and Lopes de Faria, J. B.** (2003). Prevention of hypertension attenuates albuminuria and renal expression of fibronectin in diabetic spontaneously hypertensive rats. *Am J Nephrology*. **23**, 422-428.
- Pedersen, L. C., Yee, V. C., Bishop, P. D., Le Trong, I., Teller, D. C. and Stenkamp, R. E.** (1994). Transglutaminase factor XIII uses proteinase-like catalytic triad to crosslink macromolecules. *Protein Sci*. **3**, 1131-5.
- Peppin, G. J. and Weiss, S. J.** (1986). Activation of the endogenous metalloproteinase, gelatinase, by triggered human neutrophils. *Proc Natl Acad Sci U S A*. **83**, 4322-6.
- Petitclerc, E., Stromblad, S., von Schalscha, T. L., Mitjans, F., Piulats, J., Montgomery, A. M., Cheresch, D. A. and Brooks, P. C.** (1999). Integrin alpha(v)beta3 promotes M21 melanoma growth in human skin by regulating tumor cell survival. *Cancer Res*. **59**, 2724-30.
- Piacentini, M. and Autuori, F.** (1994). Immunohistochemical localization of tissue transglutaminase and Bcl-2 in rat uterine tissues during embryo implantation and post-partum involution. *Differentiation*. **57**, 51-61.
- Piacentini, M., Ceru, M. P., Dini, L., Di Rao, M., Piredda, L., Thomazy, V., Davies, P. J. and Fesus, L.** (1992). In vivo and in vitro induction of 'tissue' transglutaminase in rat hepatocytes by retinoic acid. *Biochim Biophys Acta*. **1135**, 171-9.
- Piacentini, M., Farrace, M. G., Piredda, L., Matarrese, P., Ciccocanti, F., Falasca, L., Rodolfo, C., Giammarioli, A. M., Verderio, E., Griffin, M. et al.** (2002). Transglutaminase overexpression sensitizes neuronal cell lines to apoptosis by increasing mitochondrial membrane potential and cellular oxidative stress. *J Neurochem*. **81**, 1061-72.
- Pichler, R. H., Bassuk, J. A., Hugo, C., Reed, M. J., Eng, E., Gordon, K. L., Pippin, J., Alpers, C. E., Couser, W. G., Sage, E. H. et al.** (1996a). SPARC is expressed by mesangial cells in experimental mesangial proliferative nephritis and inhibits platelet-derived-growth-factor-mediated mesangial cell proliferation in vitro. *Am J Pathol*. **148**, 1153-67.
- Pichler, R. H., Hugo, C., Shankland, S. J., Reed, M. J., Bassuk, J. A., Andoh, T. F., Lombardi, D. M., Schwartz, S. M., Bennett, W. M., Alpers, C. E. et al.** (1996b). SPARC is expressed in renal interstitial fibrosis and in renal vascular injury. *Kidney Int*. **50**, 1978-89.

- Piedagnel, R., Murphy, G., Ronco, P. M. and Lelongt, B.** (1999). Matrix metalloproteinase 2 (MMP2) and MMP9 are produced by kidney collecting duct principal cells but are differentially regulated by SV40 large-T, arginine vasopressin, and epidermal growth factor. *J Biol Chem.* **274**, 1614-20.
- Ploetz, C., Zychband, E. I., Birk, D. E. and Trelstad, R. L.** (1991). Collagen fibril assembly and deposition in the developing dermis: segmental deposition in extracellular compartments *J Struct Biol.* **106**, 73-81.
- Powell, W. C., Fingleton, B., Wilson, C. L., Boothby, M. and Matrisian, L. M.** (1999). The metalloproteinase matrilysin proteolytically generates active soluble Fas ligand and potentiates epithelial cell apoptosis. *Curr Biol.* **9**, 1441-7.
- Prockop, D. J. and Kivirikko, K. I.** (1995). Collagens: molecular biology, diseases, and potentials for therapy. *Annu Rev Biochem.* **64**, 403-34.
- Prockop, D. J., Sieron, A. L. and Li, S. W.** (1998). Procollagen N-proteinase and procollagen C-proteinase. Two unusual metalloproteinases that are essential for procollagen processing probably have important roles in development and cell signaling. *Matrix Biol.* **16**, 399-408.
- Pruna, A., Peyri, N., Berard, M. and Boffia, M. C.** (1997) Thrombomodulin is synthesised by human mesangial cells. *Kidney Int.* **51**, 687-93.
- Purkerson, M. L., Joist, J. H., Yates, J. and Klahr, S.** (1987). Role of hypertension and coagulation in the progressive glomerulopathy of rats with subtotal renal ablation. *Miner Electrolyte Metab.* **13**, 370-6.
- Pyke, C., Kristensen, P., Ostergaard, P. B., Oturai, P. S. and Romer, J.** (1997). Proteoglycan expression in the normal rat kidney. *Nephron.* **77**, 461-70.
- Qi, W., Twigg, S., Chen, X., Polhill, T. S., Poronnik, P., Gilbert, R. E. and Pollock, C. A.** (2005). Integrated actions of transforming growth factor-beta1 and connective tissue growth factor in renal fibrosis. *Am J Physiol Renal Physiol.* **288**, F800-9.
- Quan, G., Choi, J. Y., Lee, D. S. and Lee, S. C.** (2005). TGF-beta1 up-regulates transglutaminase two and fibronectin in dermal fibroblasts: a possible mechanism for the stabilization of tissue inflammation. *Arch Dermatol Res.* **297**, 84-90.
- Quinn, C. O., Scott, D. K., Brinckerhoff, C. E., Matrisian, L. M., Jeffrey, J. J. and Partridge, N. C.** (1990). Rat collagenase. Cloning, amino acid sequence comparison, and parathyroid hormone regulation in osteoblastic cells. *J Biol Chem.* **265**, 22342-7.
- Raats, C. J., Bakker, M. A., Hoch, W., Tamboer, W. P., Groffen, A. J., van den Heuvel, L. P., Berden, J. H. and van den Born, J.** (1998). Differential expression of agrin in renal basement membranes as revealed by domain-specific antibodies. *J Biol Chem.* **273**, 17832-8.
- Radek, J. T., Jeong, J. M., Murthy, S. N., Ingham, K. C. and Lorand, L.** (1993). Affinity of human erythrocyte transglutaminase for a 42-kDa gelatin-binding fragment of human plasma fibronectin. *Proc Natl Acad Sci U S A.* **90**, 3152-6.

- Raines, E. W., Lane, T. F., Iruela-Arispe, M. L., Ross, R. and Sage, E. H.** (1992). The extracellular glycoprotein SPARC interacts with platelet-derived growth factor (PDGF)-AB and -BB and inhibits the binding of PDGF to its receptors. *Proc Natl Acad Sci U S A.* **89**, 1281-5.
- Ramana, K. V., Friedrich, B., Bhatnagar, A. and Srivastava, S. K.** (2003). Aldose reductase mediates cytotoxic signals of hyperglycemia and TNF-alpha in human lens epithelial cells. *FASEB J.* **17**, 315-7.
- Ramana, K. V., Friedrich, B., Srivastava, S., Bhatnagar, A. and Srivastava, S. K.** (2004). Activation of nuclear factor-kappaB by hyperglycemia in vascular smooth muscle cells is regulated by aldose reductase. *Diabetes.* **53**, 2910-20.
- Ramirez, F., Tanaka, S. and Bou-Gharios, G.** (2006). Transcriptional regulation of the human alpha2(I) collagen gene (COL1A2), an informative model system to study fibrotic diseases. *Matrix Biol.* **25**, 365-72.
- Raugi, G. J. and Lovett, D. H.** (1987). Thrombospondin secretion by cultured human glomerular mesangial cells. *Am J Pathol.* **129**, 364-72.
- Razzaque, M. S., Koji, T., Horita, Y., Nishihara, M., Harada, T., Nakane, P. K. and Taguchi, T.** (1995). Synthesis of type III collagen and type IV collagen by tubular epithelial cells in diabetic nephropathy. *Pathol Res Pract.* **191**, 1099-104.
- Reckelhoff, J. F., Tygart, V. L., Mitias, M. M. and Walcott, J. L.** (1993). STZ-induced diabetes results in decreased activity of glomerular cathepsin and metalloprotease in rats. *Diabetes.* **42**, 1425-32.
- Reckelhoff, J. F., Tygart, V. L., Racusen, L. C. and Dzielak, D. J.** (1994). Glomerular metalloprotease activity in streptozotocin- treated rats and in spontaneously diabetic rats (BB/DP). *Life Sci.* **55**, 941-50.
- Remacle, A. G., Rozanov, D. V., Fugere, M., Day, R. and Strongin, A. Y.** (2006). Furin regulates the intracellular activation and the uptake rate of cell surface-associated MT1-MMP. *Oncogene.* **25**, 5648-55.
- Remuzzi, G. and Bertani, T.** (1998). Pathophysiology of progressive nephropathies. *N Engl J Med.* **339**, 1448-56.
- Reponen, P., Leivo, I., Sahlberg, C., Apte, S. S., Olsen, B. R., Thesleff, I. and Tryggvason, K.** (1995). 92-kDa type IV collagenase and TIMP-3, but not 72-kDa type IV collagenase or TIMP-1 or TIMP-2, are highly expressed during mouse embryo implantation. *Dev Dyn.* **202**, 388-96.
- Rerolle, J. P., Hertig, A., Nguyen, G., Sraer, J. D. and Rondeau, E. P.** (2000). Plasminogen activator inhibitor type 1 is a potential target in renal fibrogenesis. *Kidney Int.* **58**, 1841-50.
- Reunanen, N., Westermarck, J., Hakkinen, L., Holmstrom, T. H., Elo, I., Eriksson, J. E. and Kahari, V. M.** (1998). Enhancement of fibroblast collagenase (matrix metalloproteinase-1) gene expression by ceramide is mediated by extracellular signal-regulated and stress-activated protein kinase pathways. *J Biol Chem.* **273**, 5137-45.

- Riches, D. W., Chan, E. D. and Winston, B. W.** (1996). TNF-alpha-induced regulation and signalling in macrophages. *Immunobiology*. **195**, 477-90.
- Rifkin, B. R., Vernillo, A. T. and Golub, L. M.** (1993). Blocking periodontal disease progression by inhibiting tissue-destructive enzymes: a potential therapeutic role for tetracyclines and their chemically-modified analogs. *J Periodontol*. **64**, 819-27.
- Riikonen, T., Westermarck, J., Koivisto, L., Broberg, A., Kahari, V. M. and Heino, J.** (1995). Integrin alpha 2 beta 1 is a positive regulator of collagenase (MMP-1) and collagen alpha 1(I) gene expression. *J Biol Chem*. **270**, 13548-52.
- Riser, B. L., Cortes, P., Heilig, C., Grondin, J., Ladson-Wofford, S., Patterson, D. and Narins, R. G.** (1996). Cyclic stretching force selectively up-regulates transforming growth factor-beta isoforms in cultured rat mesangial cells. *Am J Pathol*. **148**, 1915-23.
- Riser, B. L., Ladson-Wofford, S., Sharba, A., Cortes, P., Drake, K., Guerin, C. J., Yee, J., Choi, M. E., Segarini, P. R. and Narins, R. G.** (1999). TGF-beta receptor expression and binding in rat mesangial cells: modulation by glucose and cyclic mechanical strain. *Kidney Int*. **56**, 428-39.
- Ritchie, H., Lawrie, L. C., Crombie, P. W., Mosesson, M. W. and Booth, N. A.** (2000). Cross-linking of plasminogen activator inhibitor 2 and alpha 2-antiplasmin to fibrin(ogen). *J Biol Chem*. **275**, 24915-20.
- Ritter, S. J. and Davies, P. J.** (1998). Identification of a transforming growth factor-beta1/bone morphogenetic protein 4 (TGF-beta1/BMP4) response element within the mouse tissue transglutaminase gene promoter. *J Biol Chem*. **273**, 12798-806.
- Rocco, M. V., Chen, Y., Goldfarb, S. and Ziyadeh, F. N.** (1992). Elevated glucose stimulates TGF-beta gene expression and bioactivity in proximal tubule. *Kidney Int*. **41**, 107-14.
- Rodemann, H. P. and Muller, G. A.** (1991). Characterization of human renal fibroblasts in health and disease: II. In vitro growth, differentiation, and collagen synthesis of fibroblasts from kidneys with interstitial fibrosis. *Am J Kidney Dis*. **17**, 684-6.
- Roderick, P., Nicholson, T., Armitage, A., Mehta, R., Mullee, M., Gerard, K., Drey, N., Feest, T., Greenwood, R., Lamping, D. et al.** (2005). An evaluation of the costs, effectiveness and quality of renal replacement therapy provision in renal satellite units in England and Wales. *Health Technol Assess*. **9**, 1-178.
- Rodolfo, C., Mormone, E., Matarrese, P., Ciccocanti, F., Farrace, M. G., Garofano, E., Piredda, L., Fimia, G. M., Malorni, W. and Piacentini, M.** (2004). Tissue transglutaminase is a multifunctional BH3-only protein. *J Biol Chem*. **279**, 54783-92.
- Rondeau, E., Mougenot, B., Lacave, R., Peraldi, M. N., Kruihof, E. K. and Sraer, J. D.** (1990). Plasminogen activator inhibitor 1 in renal fibrin deposits of human nephropathies. *Clin Nephrol*. **33**, 55-60.
- Rosenblum, N. D.** (1994). The mesangial matrix in the normal and sclerotic glomerulus. *Kidney Int Suppl*. **45**, S73-7.

- Rossert, J., Terraz, C. and Dupont, S.** (2000). Regulation of type I collagen genes expression. *Nephrol Dial Transplant.* **15**, 66-8.
- Rossing, P., Hommel, E., Smidt, U. M. and Parving, H. H.** (1994). Reduction in albuminuria predicts diminished progression in diabetic nephropathy. *Kidney Int Suppl.* **45**, S145-9.
- Rovin, B. H. and Tan, L. C.** (1993). LDL stimulates mesangial fibronectin production and chemoattractant expression. *Kidney Int.* **43**, 218-25.
- Rovin, B. H., Wurst, E. and Kohan, D. E.** (1990). Production of reactive oxygen species by tubular epithelial cells in culture. *Kidney Int.* **37**, 1509-14.
- Ruiz-Ortega, M., Gomez-Garre, D., Alcazar, R., Palacios, I., Bustos, C., Gonzalez, S., Plaza, J. J., Gonzalez, E. and Egido, J.** (1994). Involvement of angiotensin II and endothelin in matrix protein production and renal sclerosis. *J Hypertens Suppl.* **12**, S51-8.
- Ruoslahti, E.** (1996). RGD and other recognition sequences for integrins. *Annu Rev Cell Dev Biol.* **12**, 697-715.
- Rustom, R., Maltby, P., Grime, J. S., Hughes, A., Costigan, M., Shenkin, A., Critchley, M. and Bone, J. M.** (1998). Tubular peptide hypermetabolism and urinary ammonia in chronic renal failure in man: a maladaptive response? *Nephron.* **79**, 306-11.
- Rustom, R., Wang, B., McArdle, F., Shalamanova, L., Alexander, J., McArdle, A., Thomas, C. E., Bone, J. M., Shenkin, A. and Jackson, M. J.** (2003). Oxidative stress in a novel model of chronic acidosis in LLC-PK1 cells. *Nephron Exp Nephrol.* **95**, e13-23.
- Sady, S. P., Goyal, M., Thomas, P. E., Wharram, B. L. and Wiggins, R. C.** (1995). Fibronectin mRNA in the developing glomerular crescent in rabbit anti-glomerular basement membrane disease. *J Am Soc Nephrol.* **5**, 2087-90.
- Saffarian, S., Collier, I. E., Marmer, B. L., Elson, E. L. and Goldberg, G.** (2004). Interstitial collagenase is a Brownian ratchet driven by proteolysis of collagen. *Science.* **306**, 108-11.
- Sage, E. H. and Bornstein, P.** (1991). Extracellular proteins that modulate cell-matrix interactions. SPARC, tenascin, and thrombospondin. *J Biol Chem* **266**, 14831-4.
- Sage, H., Vernon, R. B., Decker, J., Funk, S. and Iruela-Arispe, M. L.** (1989a). Distribution of the calcium-binding protein SPARC in tissues of embryonic and adult mice. *J Histochem Cytochem.* **37**, 819-29.
- Sage, H., Vernon, R. B., Funk, S. E., Everitt, E. A. and Angello, J.** (1989b). SPARC, a secreted protein associated with cellular proliferation, inhibits cell spreading in vitro and exhibits Ca²⁺-dependent binding to the extracellular matrix. *J Cell Biol.* **109**, 341-56.
- Sahai, A., Mei, C., Pattison, T. A. and Tannen, R. L.** (1997a). Chronic hypoxia induces proliferation of cultured mesangial cells: role of calcium and protein kinase C. *Am J Physiol.* **273**, F954-60.

- Sahai, A., Mei, C., Zavosh, A. and Tannen, R. L.** (1997b). Chronic hypoxia induces LLC-PK1 cell proliferation and dedifferentiation by the activation of protein kinase C. *Am J Physiol.* **272**, F809-15.
- Saitta, B., Gaidarova, S., Cicchillitti, L. and Jimenez, S. A.** (2000). CCAAT binding transcription factor binds and regulates human COL1A1 promoter activity in human dermal fibroblasts: demonstration of increased binding in systemic sclerosis fibroblasts. *Arthritis Rheum.* **43**, 2219-29.
- Sakai, M., Tsukada, T. and Harris, R. C.** (2001) Oxidant stress activates AP-1 and heparin-binding epidermal growth factor-like growth factor transcription in renal epithelial cells. *Exp Nephrol.* **9**, 28-39.
- Sane, D. C., Moser, T. L., Pippen, A. M., Parker, C. J., Achyuthan, K. E. and Greenberg, C. S.** (1988). Vitronectin is a substrate for transglutaminases. *Biochem Biophys Res Commun.* **157**, 115-20.
- Sappino, A. P., Huarte, J., Vassalli, J. D. and Belin, D.** (1991). Sites of synthesis of urokinase and tissue-type plasminogen activators in the murine kidney. *J Clin Invest.* **87**, 962-70.
- Sarnak, M. J.** (2003). Cardiovascular complications in chronic kidney disease. *Am J Kidney Dis.* **41**, 11-7.
- Sasaki, A., Naganuma, H., Satoh, E., Kawataki, T., Amagasaki, K. and Nukui, H.** (2001). Participation of thrombospondin-1 in the activation of latent transforming growth factor-beta in malignant glioma cells. *Neurol Med Chir (Tokyo).* **41**, 253-8; discussion 258-9.
- Sauvant, C., Holzinger, H. and Gekle, M.** (2001). Modulation of the basolateral and apical step of transepithelial organic anion secretion in proximal tubular opossum kidney cells. Acute effects of epidermal growth factor and mitogen-activated protein kinase. *J Biol Chem.* **276**, 14695-703.
- Sauvant, C., Holzinger, H. and Gekle, M.** (2002). Short-term regulation of basolateral organic anion uptake in proximal tubular OK cells: EGF acts via MAPK, PLA(2), and COX1. *J Am Soc Nephrol.* **13**, 1981-91.
- Savage, C. O.** (1994). The biology of the glomerulus: endothelial cells. *Kidney Int.* **45**, 314-9.
- Schaefer, L., Grone, H. J., Raslik, I., Robenek, H., Ugorcakova, J., Budny, S., Schaefer, R. M. and Kresse, H.** (2000). Small proteoglycans of normal adult human kidney: distinct expression patterns of decorin, biglycan, fibromodulin, and lumican. *Kidney Int.* **58**, 1557-68.
- Schaefer, L., Han, X., August, C., Matzkies, F., Lorenz, T. and Schaefer, R. M.** (1997). Differential regulation of glomerular gelatinase B (MMP-9) and tissue inhibitor of metalloproteinase-1 (TIMP-1) in obese Zucker rats. *Diabetologia.* **40**, 1035-43.
- Schaefer, L., Raslik, I., Grone, H. J., Schonherr, E., Macakova, K., Ugorcakova, J., Budny, S., Schaefer, R. M. and Kresse, H.** (2001). Small proteoglycans in human diabetic nephropathy: discrepancy between glomerular expression and protein accumulation of decorin, biglycan, lumican, and fibromodulin. *FASEB J.* **15**, 559-61.

- Schiffer, M., Schiffer, L. E., Gupta, A., Shaw, A. S., Roberts, I. S., Mundel, P. and Bottinger, E. P.** (2002). Inhibitory smads and tgf-Beta signaling in glomerular cells. *J Am Soc Nephrol.* **13**, 2657-66.
- Schittny, J. C., Paulsson, M., Vallan, C., Burri, P. H., Kedei, N. and Aeschlimann, D.** (1997). Protein cross-linking mediated by tissue transglutaminase correlates with the maturation of extracellular matrices during lung development. *Am J Respir Cell Mol Biol.* **17**, 334-43.
- Schittny, J. C. and Yurchenco, P. D.** (1990). Terminal short arm domains of basement membrane laminin are critical for its self-assembly. *J Cell Biol.* **110**, 825-32.
- Schor, S. L., Ellis, I. R., Jones, S. J., Baillie, R., Seneviratne, K., Clausen, J., Motegi, K., Vojtesek, B., Kankova, K., Furrie, E. et al.** (2003). Migration-stimulating factor: a genetically truncated onco-fetal fibronectin isoform expressed by carcinoma and tumor-associated stromal cells. *Cancer Res.* **63**, 8827-36.
- Schreck, R., Albermann, K. and Baeuerle, P. A.** (1992). Nuclear factor kappa B: an oxidative stress-responsive transcription factor of eukaryotic cells (a review). *Free Radic Res Commun.* **17**, 221-37.
- Schultz-Cherry, S., Lawler, J. and Murphy-Ullrich, J. E.** (1994). The type 1 repeats of thrombospondin 1 activate latent transforming growth factor-beta. *J Biol Chem.* **269**, 26783-8.
- Schwartz, E., Goldfischer, S., Coltoff-Schiller, B. and Blumenfeld, O. O.** (1985). Extracellular matrix microfibrils are composed of core proteins coated with fibronectin. *J Histochem Cytochem.* **33**, 268-74.
- Schwarzbauer, J. E. and Sechler, J. L.** (1999). Fibronectin fibrillogenesis: a paradigm for extracellular matrix assembly. *Curr Opin Cell Biol.* **11**, 622-7.
- Schwarzbauer, J. E., Tamkun, J. W., Lemischka, I. R. and Hynes, R. O.** (1983). Three different fibronectin mRNAs arise by alternative splicing within the coding region. *Cell.* **35**, 421-31.
- Schweda, F., Blumberg, F. C., Schweda, A., Nabel, C., Holmer, S. R., Riegger, G. A., Pfeifer, M. and Kramer, B. K.** (2000). Effects of chronic hypoxia on renal PDGF-A, PDGF-B, and VEGF gene expression in rats. *Nephron.* **86**, 161-6.
- Sean Eardley, K. and Cockwell, P.** (2005). Macrophages and progressive tubulointerstitial disease. *Kidney Int.* **68**, 437-55.
- Sechler, J. L., Corbett, S. A., Wenk, M. B. and Schwarzbauer, J. E.** (1998). Modulation of cell-extracellular matrix interactions. *Ann N Y Acad Sci.* **857**, 143-54.
- Sechler, J. L., Cumiskey, A. M., Gazzola, D. M. and Schwarzbauer, J. E.** (2000). A novel RGD-independent fibronectin assembly pathway initiated by alpha4beta1 integrin binding to the alternatively spliced V region. *J Cell Sci.* **113**, 1491-8.
- Sechler, J. L., Takada, Y. and Schwarzbauer, J. E.** (1996). Altered rate of fibronectin matrix assembly by deletion of the first type III repeats. *J Cell Biol.* **134**, 573-83.

- Selbi, W., de la Motte, C., Hascall, V. and Phillips, A.** (2004). BMP-7 modulates hyaluronan-mediated proximal tubular cell-monocyte interaction. *J Am Soc Nephrol.* **15**, 1199-211.
- Selbi, W., de la Motte, C. A., Hascall, V. C., Day, A. J., Bowen, T. and Phillips, A. O.** (2006). Characterization of hyaluronan cable structure and function in renal proximal tubular epithelial cells. *Kidney Int.* **70**, 1287-95.
- Semenza, G. L.** (1998). Hypoxia-inducible factor 1: master regulator of O₂ homeostasis. *Curr Opin Genet Dev.* **8**, 588-94.
- Semenza, G. L.** (1999). Regulation of mammalian O₂ homeostasis by hypoxia-inducible factor 1. *Annu Rev Cell Dev Biol.* **15**, 551-78.
- Shah, S. V.** (2004). Oxidants and iron in chronic kidney disease. *Kidney Int Suppl.* **91**, S50-5.
- Shah, S. V., Baricos, W. H. and Basci, A.** (1987). Degradation of human glomerular basement membrane by stimulated neutrophils. Activation of a metalloproteinase(s) by reactive oxygen metabolites. *J Clin Invest.* **79**, 25-31.
- Shankavaram, U. T., DeWitt, D. L., Funk, S. E., Sage, E. H. and Wahl, L. M.** (1997). Regulation of human monocyte matrix metalloproteinases by SPARC. *J Cell Physiol.* **173**, 327-34.
- Shihabi, Z. K., Konen, J. C. and O'Connor, M. L.** (1991). Albuminuria vs urinary total protein for detecting chronic renal disorders. *Clin Chem.* **37**, 621-4.
- Shimada, J., Suzuki, Y., Kim, S. J., Wang, P. C., Matsumura, M. and Kojima, S.** (2001). Transactivation via RAR/RXR-Sp1 interaction: characterization of binding between Sp1 and GC box motif. *Mol Endocrinol.* **15**, 1677-92.
- Shreeniwas, R., Koga, S., Karakurum, M., Pinsky, D., Kaiser, E., Brett, J., Wolitzky, B. A., Norton, C., Plocinski, J., Benjamin, W. et al.** (1992). Hypoxia-mediated induction of endothelial cell interleukin-1 alpha. An autocrine mechanism promoting expression of leukocyte adhesion molecules on the vessel surface. *J Clin Invest.* **90**, 2333-9.
- Shweiki, D., Itin, A., Soffer, D. and Keshet, E.** (1992). Vascular endothelial growth factor induced by hypoxia may mediate hypoxia-initiated angiogenesis. *Nature.* **359**, 843-5.
- Simkevich, C. P., Thompson, J. P., Poppleton, H. and Raghov, R.** (1992). The transcriptional tissue specificity of the human pro alpha 1 (I) collagen gene is determined by a negative cis-regulatory element in the promoter. *Biochem J.* **286**, 179-85.
- Simons, J. L., Provoost, A. P., Anderson, S., Rennke, H. G., Troy, J. L. and Brenner, B. M.** (1994). Modulation of glomerular hypertension defines susceptibility to progressive glomerular injury. *Kidney Int.* **46**, 396-404.
- Singh, R., Song, R. H., Alavi, N., Pegoraro, A. A., Singh, A. K. and Leehey, D. J.** (2001a). High glucose decreases matrix metalloproteinase-2 activity in rat mesangial cells via transforming growth factor-beta1. *Exp Nephrol.* **9**, 249-57.

- Singh, U. S., Erickson, J. W. and Cerione, R. A.** (1995). Identification and biochemical characterization of an 80 kilodalton GTP-binding/transglutaminase from rabbit liver nuclei. *Biochemistry*. **34**, 15863-71.
- Singh, U. S., Kunar, M. T., Kao, Y. L. and Baker, K. M.** (2001b). Role of transglutaminase II in retinoic acid-induced activation of RhoA-associated kinase-2. *EMBO J.* **20**, 2413-23.
- Singh, U. S., Pan, J., Kao, Y. L., Joshi, S., Young, K. L. and Baker, K. M.** (2003). Tissue transglutaminase mediates activation of RhoA and MAP kinase pathways during retinoic acid-induced neuronal differentiation of SH-SY5Y cells. *J Biol Chem.* **278**, 371-9.
- Skill, N.J.** (2001) Tissue transglutaminase in human and experimental diabetic nephropathy. *Ph.D thesis*. Nottingham Trent University.
- Skill, N. J., Griffin, M., El Nahas, A. M., Sanai, T., Haylor, J. L., Fisher, M., Jamie, M. F., Mould, N. N. and Johnson, T. S.** (2001). Increases in renal epsilon-(gamma-glutamyl)-lysine crosslinks result from compartment-specific changes in tissue transglutaminase in early experimental diabetic nephropathy: pathologic implications. *Lab Invest.* **81**, 705-16.
- Skill, N. J., Johnson, T. S., Coutts, I. G., Saint, R. E., Fisher, M., Huang, L., El Nahas, A. M., Collighan, R. J., Griffin, M., Abo-Zenah, H. et al.** (2004). Inhibition of transglutaminase activity reduces extracellular matrix accumulation induced by high glucose levels in proximal tubular epithelial cells. *J Biol Chem.* **279**, 47754-62.
- Slife, C. W., Dorsett, M. D., Bouquett, G. T., Register, A., Taylor, E. and Conroy, S.** (1985). Subcellular localization of a membrane-associated transglutaminase activity in rat liver. *Arch Biochem Biophys.* **241**, 329-36.
- Small, K., Feng, J. F., Lorenz, J., Donnelly, E. T., Yu, A., Im, M. J., Dorn, G. W., 2nd and Liggett, S. B.** (1999). Cardiac specific overexpression of transglutaminase II (G(h)) results in a unique hypertrophy phenotype independent of phospholipase C activation. *J Biol Chem.* **274**, 21291-6.
- Smith, G. N., Jr., Mickler, E. A., Hasty, K. A. and Brandt, K. D.** (1999). Specificity of inhibition of matrix metalloproteinase activity by doxycycline: relationship to structure of the enzyme. *Arthritis Rheum.* **42**, 1140-6.
- Sodhi, C. P., Battle, D. and Sahai, A.** (2000). Osteopontin mediates hypoxia-induced proliferation of cultured mesangial cells: role of PKC and p38 MAPK. *Kidney Int.* **58**, 691-700.
- Sohn, J., Kim, T. I., Yoon, Y. H., Kim, J. Y. and Kim, S. Y.** (2003). Novel transglutaminase inhibitors reverse the inflammation of allergic conjunctivitis. *J Clin Invest.* **111**, 121-8.
- Sorokin, L. M., Conzelmann, S., Ekblom, P., Battaglia, C., Aumailley, M. and Timpl, R.** (1992). Monoclonal antibodies against laminin A chain fragment E3 and their effects on binding to cells and proteoglycan and on kidney development. *Exp Cell Res.* **201**, 137-44.
- Sorsa, T., Ding, Y., Salo, T., Lauhio, A., Teronen, O., Ingman, T., Ohtani, H., Andoh, N., Takeha, S. and Konttinen, Y. T.** (1994). Effects of tetracyclines on neutrophil, gingival, and salivary collagenases. A functional and western-blot assessment with special reference to their cellular sources in periodontal diseases. *Ann N Y Acad Sci.* **732**, 112-31.

- Springman, E. B., Angleton, E. L., Birkedal-Hansen, H. and Van Wart, H. E.** (1990). Multiple modes of activation of latent human fibroblast collagenase: evidence for the role of a Cys73 active-site zinc complex in latency and a "cysteine switch" mechanism for activation. *Proc Natl Acad Sci U S A.* **87**, 364-8.
- Stack, M. S., Itoh, Y., Young, T. N. and Nagase, H.** (1996). Fluorescence quenching studies of matrix metalloproteinases (MMPs): evidence for structural rearrangement of the proMMP-2/TIMP-2 complex upon mercurial activation. *Arch Biochem Biophys.* **333**, 163-9.
- Steer, D. L., Shah, M. M., Bush, K. T., Stuart, R. O., Sampogna, R. V., Meyer, T. N., Schwesinger, C., Bai, X., Esko, J. D. and Nigam, S. K.** (2004). Regulation of ureteric bud branching morphogenesis by sulfated proteoglycans in the developing kidney. *Dev Biol.* **272**, 310-27.
- Stephan, J. P., Mao, W., Filvaroff, E., Cai, L., Rabkin, R. and Pan, G.** (2004). Albumin stimulates the accumulation of extracellular matrix in renal tubular epithelial cells. *Am J Nephrol.* **24**, 14-9.
- Stephens, D. J. and Pepperkok, R.** (2002). Imaging of procollagen transport reveals COPI-dependent cargo sorting during ER-to-Golgi transport in mammalian cells. *J Cell Sci.* **115**, 1149-60.
- Stokes, M. B., Holler, S., Cui, Y., Hudkins, K. L., Eitner, F., Fogo, A. and Alpers, C. E.** (2000). Expression of decorin, biglycan, and collagen type I in human renal fibrosing disease. *Kidney Int.* **57**, 487-98.
- Stokes, M. B., Hudkins, K. L., Zaharia, V., Taneda, S. and Alpers, C. E.** (2001). Up-regulation of extracellular matrix proteoglycans and collagen type I in human crescentic glomerulonephritis. *Kidney Int.* **59**, 532-42.
- Strutz, F., Okada, H., Lo, C. W., Danoff, T., Carone, R. L., Tomaszewski, J. E. and Neilson, E. G.** (1995) Identification and characterisation of the fibroblast marker FSP-1. *J Cell Biol.* **130**, 393-405.
- Strutz, F., Zeisberg, M., Hemmerlein, B., Sattler, B., Hummel, K., Becker, V. and Muller, G. A.** (2000). Basic fibroblast growth factor expression is increased in human renal fibrogenesis and may mediate autocrine fibroblast proliferation. *Kidney Int.* **57**, 1521-38.
- Strutz, F., Zeisberg, M., Renziehausen, A., Raschke, B., Becker, V., van Kooten, C. and Muller, G.** (2001). TGF-beta 1 induces proliferation in human renal fibroblasts via induction of basic fibroblast growth factor (FGF-2). *Kidney Int.* **59**, 579-92.
- Suto, N., Ikura, K. and Sasaki, R.** (1993). Expression induced by interleukin-6 of tissue-type transglutaminase in human hepatoblastoma HepG2 cells. *J Biol Chem.* **268**, 7469-73.
- Svennson, L., Aszodi, A., Reinhart, F. P., Fassler, R., Heinegard, D. and Oldberg, A.** (1999) Fibromodulin null mice have abnormal collagen fibrils, tissue organisation and altered lumican deposition in tendon. *J Biol Chem.* **274**, 9636-47.
- Swann, J. D., Smith, M. W., Phelps, P. C., Maki, A., Berezesky, I. K. and Trump, B. F.** (1991). Oxidative injury induces influx-dependent changes in intracellular calcium homeostasis. *Toxicol Pathol.* **19**, 128-37.

- Syntex.** (1990). 3,5 substituted 4,5-dihydroisoxazoles as transglutaminase inhibitors. *US Patent 4 912*, 120.
- Szondy, Z., Sarang, Z., Molnar, P., Nemeth, T., Piacentini, M., Mastroberardino, P. G., Falasca, L., Aeschlimann, D., Kovacs, J., Kiss, I. et al.** (2003). Transglutaminase 2^{-/-} mice reveal a phagocytosis-associated crosstalk between macrophages and apoptotic cells. *Proc Natl Acad Sci U S A.* **100**, 7812-7.
- Taal, M. W., Omer, S. A., Nadim, M. K. and Mackenzie, H. S.** (2000). Cellular and molecular mediators in common pathway mechanisms of chronic renal disease progression. *Curr Opin Nephrol Hypertens.* **9**, 323-31.
- Tada, H., Kawai, H., Ishii, H., Nomura, K., Urayama, T. and Isogai, S.** (1995). Thrombospondin modulates adhesion, proliferation and production of extracellular matrix in mesangial cells. *Tohoku J Exp Med.* **177**, 293-302.
- Taipale, J. and Keski-Oja, J.** (1997). Growth factors in the extracellular matrix. *FASEB J.* **11**, 51-9.
- Takahra, T., Smart, D. E., Oakley, F. and Mann, D. A.** (2004). Induction of myofibroblast MMP-9 transcription in three-dimensional collagen I gel cultures: regulation by NF-kappaB, AP-1 and Sp1. *Int J Biochem Cell Biol.* **36**, 353-63.
- Takemoto, M., Asker, N., Gerhardt, H., Lundkvist, A., Johansson, B. R., Saito, Y. and Betsholtz, C.** (2002). A new method for large scale isolation of kidney glomeruli from mice. *Am J Pathol.* **161**, 799-805.
- Tam, E. M., Moore, T. R., Butler, G. S. and Overall, C. M.** (2004). Characterization of the distinct collagen binding, helicase and cleavage mechanisms of matrix metalloproteinase 2 and 14 (gelatinase A and MT1-MMP): the differential roles of the MMP hemopexin c domains and the MMP-2 fibronectin type II modules in collagen triple helicase activities. *J Biol Chem.* **279**, 43336-44.
- Tamaki, T., Ohnishi, K., Hartl, C., LeRoy, E. C. and Trojanowska, M.** (1995). Characterization of a GC-rich region containing Sp1 binding site(s) as a constitutive responsive element of the alpha 2(I) collagen gene in human fibroblasts. *J Biol Chem.* **270**, 4299-304.
- Tanney, D. C., Feng, L., Pollock, A. S. and Lovett, D. H.** (1998). Regulated expression of matrix metalloproteinases and TIMP in nephrogenesis. *Dev Dyn.* **213**, 121-9.
- Taraboletti, G., Morigi, M., Figliuzzi, M., Giavazzi, R., Zoja, C. and Remuzzi, G.** (1992). Thrombospondin induces glomerular mesangial cell adhesion and migration. *Lab Invest.* **67**, 566-71.
- Thomas, M. E. and Schreiner, G. F.** (1993). Contribution of proteinuria to progressive renal injury: consequences of tubular uptake of fatty acid bearing albumin. *Am J Nephrol.* **13**, 385-98.
- Thomazy, V. A. and Davies, P. J.** (1999). Expression of tissue transglutaminase in the developing chicken limb is associated both with apoptosis and endochondral ossification. *Cell Death Differ.* **6**, 146-54.

- Thompson, J. P., Simkevich, C. P., Holness, M. A., Kang, A. H. and Raghow, R.** (1991). In vitro methylation of the promoter and enhancer of Pro alpha 1(I) collagen gene leads to its transcriptional inactivation. *J Biol Chem.* **266**, 2549-56.
- Throckmorton, D. C., Brogden, A. P., Min, B., Rasmussen, H. and Kashgarian, M.** (1995). PDGF and TGF-beta mediate collagen production by mesangial cells exposed to advanced glycosylation end products. *Kidney Int.* **48**, 111-7.
- Timpl, R. and Brown, J. C.** (1996). Supramolecular assembly of basement membranes. *Bioessays.* **18**, 123-32.
- Torbohm, I., Schonermack, M., Wingen, A. M., Berger, B., Rother, K. and Hansch, G. M.** (1990). C5b-8 and C5b-9 modulate the collagen release of human glomerular epithelial cells. *Kidney Int.* **37**, 1098-104.
- Torigoe, T., Izumi, H., Yoshida, Y., Ishiguchi, H., Okamoto, T., Itoh, H. and Kohno, K.** (2003). Low pH enhances Sp1 DNA binding activity and interaction with TBP. *Nucleic Acids Res.* **31**, 4523-30.
- Troeberg, L., Tanaka, M., Wait, R., Shi, Y. E., Brew, K. and Nagase, H.** (2002). E. coli expression of TIMP-4 and comparative kinetic studies with TIMP-1 and TIMP-2: insights into the interactions of TIMPs and matrix metalloproteinase 2 (gelatinase A). *Biochemistry.* **41**, 15025-35.
- Trojanowski, M.** (2000) Ets factors and regulation of the extracellular matrix. *Oncogene.* **19**, 6464-71.
- Truong, L. D., Foster, S. V., Barrios, R., D'Agati, V., Verani, R. R., Gonzalez, J. M. and Suki, W. N.** (1996). Tenascin is an ubiquitous extracellular matrix protein of human renal interstitium in normal and pathologic conditions. *Nephron.* **72**, 579-86.
- Truong, L. D., Majesky, M. W., Pindur, J., Barrios, R., D'Agati, V., Lechago, J., Suki, W. and Majesky, M.** (1994a). Tenascin is synthesized and secreted by rat mesangial cells in culture and is present in extracellular matrix in human glomerular diseases. *J Am Soc Nephrol.* **4**, 1771-7.
- Truong, L. D., Pindur, J., Barrios, R., D'Agati, V., Lechago, J., Suki, W. and Majesky, M.** (1994b). Tenascin is an important component of the glomerular extracellular matrix in normal and pathologic conditions. *Kidney Int.* **45**, 201-10.
- Tucholski, J., Kuret, J. and Johnson, G. V.** (1999). Tau is modified by tissue transglutaminase in situ: possible functional and metabolic effects of polyamination. *J Neurochem.* **73**, 1871-80.
- Turner, P. M. and Lorand, L.** (1989). Complexation of fibronectin with tissue transglutaminase. *Biochemistry.* **28**, 628-35.
- Tyrrell, D. J., Sale, W. S. and Slife, C. W.** (1986). Localization of a liver transglutaminase and a large molecular weight transglutaminase substrate to a distinct plasma membrane domain. *J Biol Chem.* **261**, 14833-6.

- Uchio, K., Manabe, N., Kinoshita, A., Tamura, K., Miyamoto, M., Ogura, A., Yamamoto, Y. and Miyamoto, H.** (1999). Abnormalities of extracellular matrices and transforming growth factor beta1 localization in the kidney of the hereditary nephrotic mice (ICGN strain). *J Vet Med Sci.* **61**, 769-76.
- Ueda, N. and Shah, S. V.** (1992). Role of intracellular calcium in hydrogen peroxide-induced renal tubular cell injury. *Am J Physiol Renal Physiol.* **263**, F214-21.
- Uehara, G., Suzuki, D., Toyoda, M., Umezono, T. and Sakai, H.** (2004). Glomerular expression of platelet-derived growth factor (PDGF)-A, -B chain and PDGF receptor-alpha, -beta in human diabetic nephropathy. *Clin Exp Nephrol.* **8**, 36-42.
- Upchurch, H. F., Conway, E., Patterson, M. K., Birckbichler, P. J. and Maxwell, M. D.** (1987). Cellular transglutaminase has affinity for extracellular matrix. *In Vitro Cell Dev Biol.* **23**, 795-800.
- Uria, J. A., Ferrando, A. A., Velasco, G., Freije, J. M. and Lopez-Otin, C.** (1994). Structure and expression in breast tumors of human TIMP-3, a new member of the metalloproteinase inhibitor family. *Cancer Res.* **54**, 2091-4.
- Van den Steen, P. E., Dubois, B., Nelissen, I., Rudd, P. M., Dwek, R. A. and Opdenakker, G.** (2002). Biochemistry and molecular biology of gelatinase B or matrix metalloproteinase-9 (MMP-9). *Crit Rev Biochem Mol Biol.* **37**, 375-536.
- Van Vliet, A., Baelde, H. J., Vleming, L. J., de Heer, E. and Bruijn, J. A.** (2001). Distribution of fibronectin isoforms in human renal disease. *J Pathol.* **193**, 256-62.
- Van Wart, H. E. and Birkedal-Hansen, H.** (1990). The cysteine switch: a principle of regulation of metalloproteinase activity with potential applicability to the entire matrix metalloproteinase gene family. *Proc Natl Acad Sci U S A.* **87**, 5578-82.
- Vassalli, J. D., Sappino, A. P. and Belin, D.** (1991). The plasminogen activator/plasmin system. *J Clin Invest.* **88**, 1067-72.
- Verderio, E., Gaudry, C., Gross, S., Smith, C., Downes, S. and Griffin, M.** (1999). Regulation of cell surface tissue transglutaminase: effects on matrix storage of latent transforming growth factor-beta binding protein-1. *J Histochem Cytochem.* **47**, 1417-32.
- Verderio, E., Nicholas, B., Gross, S. and Griffin, M.** (1998). Regulated expression of tissue transglutaminase in Swiss 3T3 fibroblasts: effects on the processing of fibronectin, cell attachment, and cell death. *Exp Cell Res.* **239**, 119-38.
- Verderio, E. A., Johnson, T. S. and Griffin, M.** (2005). Transglutaminases in wound healing and inflammation. *Prog Exp Tumor Res.* **38**, 89-114.
- Verderio, E. A., Telci, D., Okoye, A., Melino, G. and Griffin, M.** (2003). A novel RGD-independent cell adhesion pathway mediated by fibronectin-bound tissue transglutaminase rescues cells from anoikis. *J Biol Chem.* **278**, 42604-14.
- Verrecchia, F. and Mauviel, A.** (2004). TGF-beta and TNF-alpha: antagonistic cytokines controlling type I collagen gene expression. *Cell Signal.* **16**, 873-80.

- Viberti, G. and Chaturvedi, N.** (1997). Angiotensin converting enzyme inhibitors in diabetic patients with microalbuminuria or normoalbuminuria. *Kidney Int Suppl.* **63**, S32-5.
- Vincenti, M. P., White, L. A., Schroen, D. J., Benbow, U. and Brinckerhoff, C. E.** (1996). Regulating expression of the gene for matrix metalloproteinase-1 (collagenase): mechanisms that control enzyme activity, transcription, and mRNA stability. *Crit Rev Eukaryot Gene Expr.* **6**, 391-411.
- Virolainen, P., Perala, M., Vuorio, E. and Aro, H. T.** (1995). Expression of matrix genes during incorporation of cancellous bone allografts and autografts. *Clin Orthop Relat Res.* **317**, 263-72.
- Vo, H. P., Lee, M. K. and Crowe, D. L.** (1998). alpha2beta1 integrin signaling via the mitogen activated protein kinase pathway modulates retinoic acid-dependent tumor cell invasion and transcriptional downregulation of matrix metalloproteinase 9 activity. *Int J Oncol.* **13**, 1127-34.
- Vuorio, T., Makela, J. K., Kahari, V. M. and Vuorio, E.** (1987). Coordinated regulation of type I and type III collagen production and mRNA levels of pro alpha 1(I) and pro alpha 2(I) collagen in cultured morphea fibroblasts. *Arch Dermatol Res.* **279**, 154-60.
- Wagner, S. N., Atkinson, M. J., Wagner, C., Hofler, H., Schmitt, M. and Wilhelm, O.** (1996). Sites of urokinase-type plasminogen activator expression and distribution of its receptor in the normal human kidney. *Histochem Cell Biol.* **105**, 53-60.
- Wang, D. R., Sato, M., Sato, T., Kojima, N., Higashi, N. and Senoo, H.** (2004). Regulation of matrix metallo-proteinase expression by extracellular matrix components in cultured hepatic stellate cells. *Comp Hepatol.* **3**, S20.
- Wang, G. L., Jiang, B. H., Rue, E. A. and Semenza, G. L.** (1995). Hypoxia-inducible factor 1 is a basic-helix-loop-helix-PAS heterodimer regulated by cellular O₂ tension. *Proc Natl Acad Sci U S A.* **92**, 5510-4.
- Wang, G. L. and Semenza, G. L.** (1993). General involvement of hypoxia-inducible factor 1 in transcriptional response to hypoxia. *Proc Natl Acad Sci U S A.* **90**, 4304-8.
- Wang, G. L. and Semenza, G. L.** (1995). Purification and characterization of hypoxia-inducible factor 1. *J Biol Chem.* **270**, 1230-7.
- Wang, X., Martindale, J. L., Liu, Y. and Holbrook, N. J.** (1998). The cellular response to oxidative stress: influences of mitogen-activated protein kinase signalling pathways on cell survival. *Biochem J.* **333**, 291-300.
- Wang, Y., Chen, J., Chen, L., Tay, Y. C., Rangan, G. K. and Harris, D. C.** (1997). Induction of monocyte chemoattractant protein-1 in proximal tubule cells by urinary protein. *J Am Soc Nephrol.* **8**, 1537-45.
- Welge-Lussen, U., May, C. A. and Lutjen-Drecoll, E.** (2000). Induction of tissue transglutaminase in the trabecular meshwork by TGF-beta1 and TGF-beta2. *Invest Ophthalmol Vis Sci.* **41**, 2229-38.
- Welgus, H. G., Jeffrey, J. J. and Eisen, A. Z.** (1981). The collagen substrate specificity of human skin fibroblast collagenase. *J Biol Chem.* **256**, 9511-5.

- Wennerberg, K., Lohikangas, L., Gullberg, D., Pfaff, M., Johansson, S. and Fassler, R.** (1996). Beta 1 integrin-dependent and -independent polymerization of fibronectin. *J Cell Biol* **132**, 227-38.
- Werb, Z.** (1997). ECM and cell surface proteolysis: regulating cellular ecology. *Cell*. **91**, 439-42.
- Wesson, L. G.** (1989). Compensatory growth and other growth responses of the kidney. *Nephron*. **51**, 149-84.
- Westermarck, J., Holmstrom, T., Ahonen, M., Eriksson, J. E. and Kahari, V. M.** (1998). Enhancement of fibroblast collagenase-1 (MMP-1) gene expression by tumor promoter okadaic acid is mediated by stress-activated protein kinases Jun N-terminal kinase and p38. *Matrix Biol*. **17**, 547-57.
- Wheeler, D. C. and Chana, R. S.** (1993). Interactions between lipoproteins, glomerular cells and matrix. *Miner Electrolyte Metab.* **19**, 149-64.
- Wheeler, D. C., Persaud, J. W., Fernando, R., Sweny, P., Varghese, Z. and Moorhead, J. F.** (1990). Effects of low-density lipoproteins on mesangial cell growth and viability in vitro. *Nephrol Dial Transplant*. **5**, 185-91.
- White, L. A., Mitchell, T. I. and Brinckerhoff, C. E.** (2000). Transforming growth factor beta inhibitory element in the rabbit matrix metalloproteinase-1 (collagenase-1) gene functions as a repressor of constitutive transcription. *Biochim Biophys Acta*. **1490**, 259-68.
- Wierzbicka-Patynowski, I. and Schwarzbauer, J. E.** (2002). Regulatory role for SRC and phosphatidylinositol 3-kinase in initiation of fibronectin matrix assembly. *J Biol Chem*. **277**, 19703-8.
- Wierzbicka-Patynowski, I. and Schwarzbauer, J. E.** (2003). The ins and outs of fibronectin matrix assembly. *J Cell Sci*. **116**, 3269-76.
- Wilson, H. M., Haites, N. E., Reid, F. J. and Booth, N. A.** (1996). Interleukin-1 beta up-regulates the plasminogen activator/plasmin system in human mesangial cells. *Kidney Int*. **49**, 1097-104.
- Wilson, H. M., Reid, F. J., Brown, P. A., Power, D. A., Haites, N. E. and Booth, N. A.** (1993). Effect of transforming growth factor-beta 1 on plasminogen activators and plasminogen activator inhibitor-1 in renal glomerular cells. *Exp Nephrol*. **1**, 343-50.
- Wing, A. J. and Jones, E.** (2000). Epidemiology of end stage renal failure: a global perspective. In *Mechanisms and Management of Chronic Renal Failure*, (ed. A. M. El Nahas), pp. 1-19: Oxford University Press.
- Wingfield, P. T., Sax, J. K., Stahl, S. J., Kaufman, J., Palmer, I., Chung, V., Corcoran, M. L., Kleiner, D. E. and Stetler-Stevenson, W. G.** (1999). Biophysical and functional characterization of full-length, recombinant human tissue inhibitor of metalloproteinases-2 (TIMP-2) produced in *Escherichia coli*. Comparison of wild type and amino-terminal alanine appended variant with implications for the mechanism of TIMP functions. *J Biol Chem*. **274**, 21362-8.

- Wohlfarth, V., Drumm, K., Mildenerger, S., Freudinger, R. and Gekle, M.** (2003). Protein uptake disturbs collagen homeostasis in proximal tubule-derived cells. *Kidney Int Suppl.* **84**, S103-9.
- Wolf, G. and Ritz, E.** (2005). Combination therapy with ACE inhibitors and angiotensin II receptor blockers to halt progression of chronic renal disease: pathophysiology and indications. *Kidney Int.* **67**, 799-812.
- Wolf, G., Schroeder, R., Ziyadeh, F. N. and Stahl, R. A.** (2004). Albumin up-regulates the type II transforming growth factor-beta receptor in cultured proximal tubular cells. *Kidney Int.* **66**, 1849-58.
- Wright, E. J., McCaffrey, T. A., Robertson, A. P., Vaughan, E. D., Jr. and Felsen, D.** (1996). Chronic unilateral ureteral obstruction is associated with interstitial fibrosis and tubular expression of transforming growth factor-beta. *Lab Invest.* **74**, 528-37.
- Wu, C., Hughes, P. E., Ginsberg, M. H. and McDonald, J. A.** (1996). Identification of a new biological function for the integrin alpha v beta 3: initiation of fibronectin matrix assembly. *Cell Adhes Commun.* **4**, 149-58.
- Wu, K., Setty, S., Mauer, S. M., Killen, P., Nagase, H., Michael, A. F. and Tsilibary, E. C.** (1997). Altered kidney matrix gene expression in early stages of experimental diabetes. *Acta Anat (Basel).* **158**, 155-65.
- Wung, B. S., Cheng, J. J., Chao, Y. J., Lin, J., Shyy, Y. J. and Wang, D. L.** (1996). Cyclical strain increases monocyte chemotactic protein-1 secretion in human endothelial cells. *Am J Physiol Heart and Circulat Physiol.* **270**, H1462-8.
- Wykoff, C. C., Pugh, C. W., Maxwell, P. H., Harris, A. L. and Ratcliffe, P. J.** (2000). Identification of novel hypoxia dependent and independent target genes of the von Hippel-Lindau (VHL) tumour suppressor by mRNA differential expression profiling. *Oncogene.* **19**, 6297-305.
- Xie, B., Laouar, A. and Huberman, E.** (1998). Fibronectin-mediated cell adhesion is required for induction of 92-kDa type IV collagenase/gelatinase (MMP-9) gene expression during macrophage differentiation. The signaling role of protein kinase C-beta. *J Biol Chem.* **273**, 11576-82.
- Xu, J., Rodriguez, D., Petitclerc, E., Kim, J. J., Hangai, M., Moon, Y. S., Davis, G. E. and Brooks, P. C.** (2001). Proteolytic exposure of a cryptic site within collagen type IV is required for angiogenesis and tumor growth in vivo. *J Cell Biol.* **154**, 1069-79.
- Xue, J. L., Ma, J. Z., Louis, T. A. and Collins, A. J.** (2001). Forecast of the number of patients with end-stage renal disease in the United States to the year 2010. *J Am Soc Nephrol.* **12**, 2753-8.
- Yamada, H., Saito, F., Fukuta-ohi, H., Zhang, D., Hase, A., Arai, K., Okuyama, A., Maekawa, R., Shimizu, T. and Matsumura, K.** (2001) Processing of beta dystroglycan by matrix metalloproteinase disrupts the link between the extracellular matrix and cell membrane via the dystroglycan complex. *Hum Mol Genet.* **15**, 1563-9.

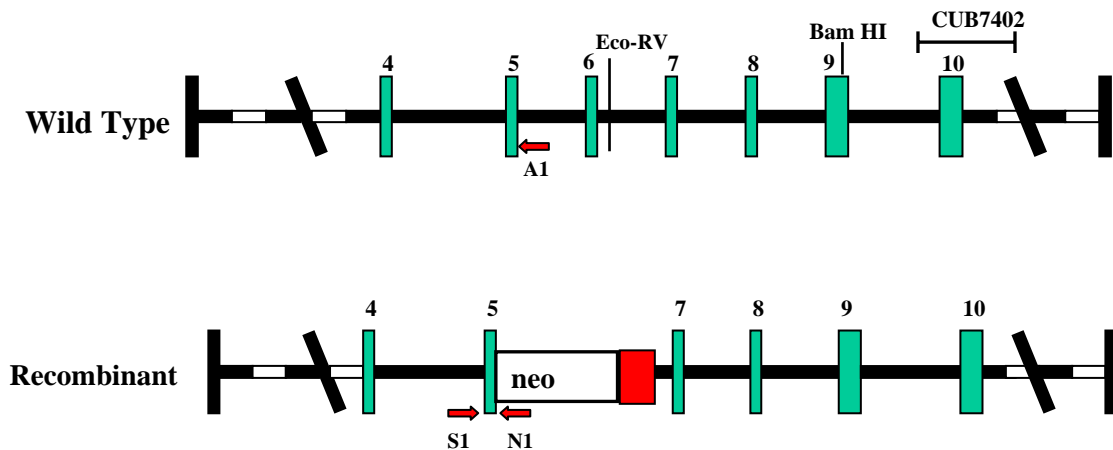
- Yamamoto, T., Nakamura, T., Noble, N. A., Ruoslahti, E. and Border, W. A.** (1993). Expression of transforming growth factor beta is elevated in human and experimental diabetic nephropathy. *Proc Natl Acad Sci U S A.* **90**, 1814-8.
- Yamamoto, T., Noble, N. A., Miller, D. E. and Border, W. A.** (1994). Sustained expression of TGF-beta 1 underlies development of progressive kidney fibrosis. *Kidney Int* **45**, 916-27.
- Yan, S. F., Tritto, I., Pinsky, D., Liao, H., Huang, J., Fuller, G., Brett, J., May, L. and Stern, D.** (1995). Induction of interleukin 6 (IL-6) by hypoxia in vascular cells. Central role of the binding site for nuclear factor-IL-6. *J Biol Chem.* **270**, 11463-71.
- Yang, J., Shultz, R. W., Mars, W. M., Wegner, R. E., Li, Y., Dai, C., Nejak, K. and Liu, Y.** (2002). Disruption of tissue-type plasminogen activator gene in mice reduces renal interstitial fibrosis in obstructive nephropathy. *J Clin Invest.* **110**, 1525-38.
- Yang, J. T. and Hynes, R. O.** (1996). Fibronectin receptor functions in embryonic cells deficient in alpha 5 beta 1 integrin can be replaced by alpha V integrins. *Mol Biol Cell.* **7**, 1737-48.
- Yard, B. A., Chorianopoulos, E., Herr, D. and van der Woude, F. J.** (2001). Regulation of endothelin-1 and transforming growth factor-beta1 production in cultured proximal tubular cells by albumin and heparan sulphate glycosaminoglycans. *Nephrol Dial Transplant.* **16**, 1769-75.
- Yasuda, T., Kondo, S., Homma, T. and Harris, R. C.** (1996). Regulation of extracellular matrix by mechanical stress in rat glomerular mesangial cells. *J Clin Invest.* **98**, 1991-2000.
- Yasunari, K., Watanabe, T. and Nakamura, M.** (2006). Reactive oxygen species formation by polymorphonuclear cells and mononuclear cells as a risk factor of cardiovascular diseases. *Curr Pharm Biotechnol.* **7**, 73-80.
- Yee, V. C., Le Trong, I., Bishop, P. D., Pedersen, L. C., Stenkamp, R. E. and Teller, D. C.** (1996). Structure and function studies of factor XIIIa by x-ray crystallography. *Semin Thromb Hemost.* **22**, 377-84.
- Yee, V. C., Pedersen, L. C., Le Trong, I., Bishop, P. D., Stenkamp, R. E. and Teller, D. C.** (1994). Three-dimensional structure of a transglutaminase: human blood coagulation factor XIII. *Proc Natl Acad Sci U S A.* **91**, 7296-300.
- Yokoi, H., Sugawara, A., Mukoyama, M., Mori, K., Makino, H., Suganami, T., Nagae, T., Yahata, K., Fujinaga, Y., Tanaka, I. et al.** (2001). Role of connective tissue growth factor in profibrotic action of transforming growth factor-beta: a potential target for preventing renal fibrosis. *Am J Kidney Dis.* **38**, S134-8.
- Yoshioka, T., Bills, T., Moore-Jarrett, T., Greene, H. L., Burr, I. M. and Ichikawa, I.** (1990). Role of intrinsic antioxidant enzymes in renal oxidant injury. *Kidney Int.* **38**, 282-8.
- Yurchenco, P. D. and Cheng, Y. S.** (1993). Self-assembly and calcium-binding sites in laminin. A three-arm interaction model. *J Biol Chem.* **268**, 17286-99.
- Yu, Q. and Stamenkovic, I.** (2000) Cell surface localised matrix metalloproteinase 9 proteolytically activates TGFβ and promotes tumour invasion and angiogenesis. *Genes Dev.* **14**, 163-76.

- Zager, R. A., Sacks, B. M., Burkhart, K. M. and Williams, A. C.** (1999). Plasma membrane phospholipid integrity and orientation during hypoxic and toxic proximal tubular attack. *Kidney Int.* **56**, 104-17.
- Zandi-Nejad, K., Eddy, A. A., Glassock, R. J. and Brenner, B. M.** (2004). Why is proteinuria an ominous biomarker of progressive kidney disease? *Kidney Int Suppl.* **92**, S76-89.
- Zeisberg, M., Bonner, G., Maeshima, Y., Colorado, P., Muller, G. A., Strutz, F. and Kalluri, R.** (2001). Renal fibrosis: collagen composition and assembly regulates epithelial-mesenchymal transdifferentiation. *Am J Pathol.* **159**, 1313-21.
- Zeisberg, M., Khurana, M., Rao, V. H., Cosgrove, D., Rougier, J. P., Werner, M. C., Shield, C. F., Werb, Z. and Kalluri, R.** (2006) Stage-specific action of matrix metalloproteinases influences progressive hereditary kidney disease. *PLoS Med.* **3**, e100.
- Zeisberg, M., Strutz, F. and Muller, G. A.** (2000). Role of fibroblast activation in inducing interstitial fibrosis. *J Nephrol.* **13**, S111-20.
- Zhang, G., Moorhead, P. J. and El Nahas, A. M.** (1995a). Myofibroblasts and the progression of experimental glomerulonephritis. *Exp Nephrol.* **3**, 308-18.
- Zhang, L. X., Mills, K. J., Dawson, M. I., Collins, S. J. and Jetten, A. M.** (1995b). Evidence for the involvement of retinoic acid receptor RAR alpha-dependent signaling pathway in the induction of tissue transglutaminase and apoptosis by retinoids. *J Biol Chem.* **270**, 6022-9.
- Zhang, W., Ou, J., Inagaki, Y., Greenwel, P. and Ramirez, F.** (2000). Synergistic cooperation between Sp1 and Smad3/Smad4 mediates transforming growth factor beta1 stimulation of alpha 2(I)-collagen (COL1A2) transcription. *J Biol Chem.* **275**, 39237-45.
- Zhang, X., Yamashita, M., Uetsuki, H. and Kakehi, Y.** (2002). Angiogenesis in renal cell carcinoma: Evaluation of microvessel density, vascular endothelial growth factor and matrix metalloproteinases. *Int J Urol.* **9**, 509-14.
- Zheng, G., Wang, Y., Mahajan, D., Qin, X., Wang, Y., Wang, Y., Alexander, S. I. and Harris, D. C.** (2005) The role of tubulointerstitial inflammation. *Kidney Int.* **94**, S96-100.
- Zhu, H. and Bunn, H. F.** (2001). Signal transduction. How do cells sense oxygen? *Science.* **292**, 449-51.
- Zoja, C., Benigni, A. and Remuzzi, G.** (2004). Cellular responses to protein overload: key event in renal disease progression. *Curr Opin Nephrol Hypertens.* **13**, 31-7.
- Zoja, C., Morigi, M., Figliuzzi, M., Bruzzi, I., Oldroyd, S., Benigni, A., Ronco, P. and Remuzzi, G.** (1995). Proximal tubular cell synthesis and secretion of endothelin-1 on challenge with albumin and other proteins. *Am J Kidney Dis.* **26**, 934-41.

Appendix

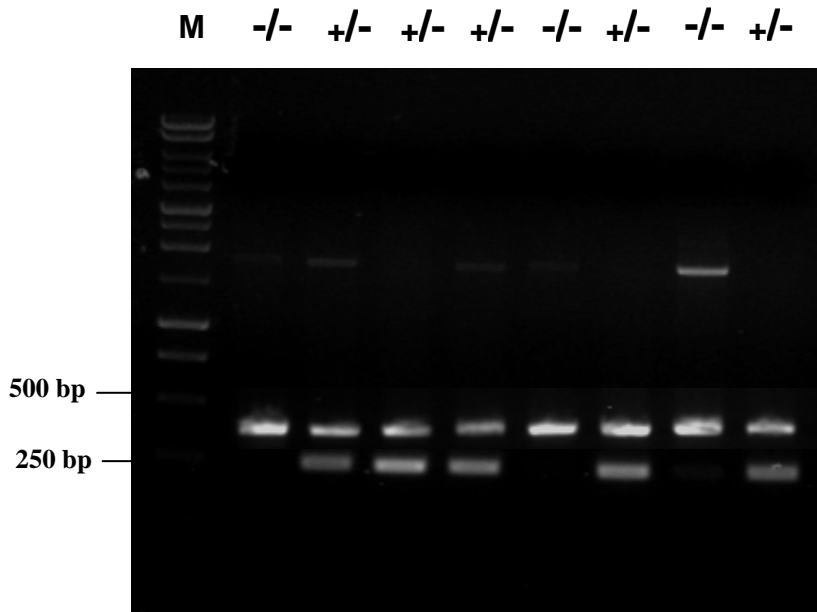
Genotyping of TG2 Knockout mice

(a) PCR primers and their position



A1 = 5' TCCTGACCTGAGTCCTCGTC 3'
 N1 = 5' ACGAGACTAGTGAGACGTGC 3'
 S1 = 5' TACTCCAGCTTCCTGTTCTG 3'

b) PCR screening of mouse genotype



(a) Genotyping of TG2 knockout mice was performed at Nottingham Trent University using three primers as described in (De Laurenzi and Melino 2001). Two antisense primers were used: one directed to a sequence within intron 5 (A1) of the TG2 gene which is deleted in knockout alleles and the second targeted to the neomycin resistance gene (N1). The sense primer (S1) was directed to a sequence in intron 4 present in both wild-type and knockout alleles. (b) Representative agarose gel obtained from the PCR screening of mouse genotype. Wild type (+/+) animals were distinguished by the presence of a single band at 252bp (non shown). Homozygous TG2 knockouts (-/-) were distinguished by the presence of a single band at 372bp (lanes 1, 5 and 7). Heterozygous (+/-) animals showed the presence of both bands (lanes 2, 3, 4, 6 and 8). Homozygous animals were subsequently supplied to Sheffield University for the isolation of primary tubular and mesangial cells (section 3.6.3.2 and Chapter 6).